Annual Report

2012 – 2013

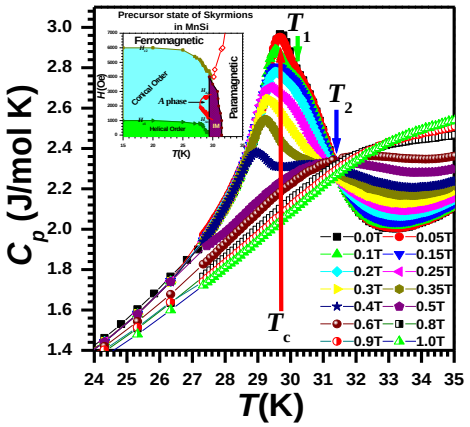

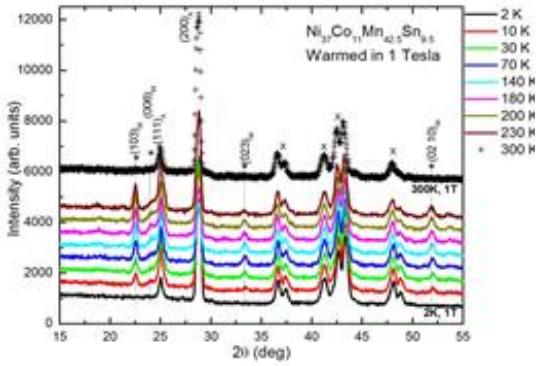

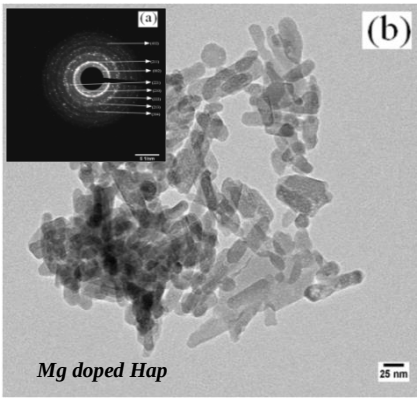

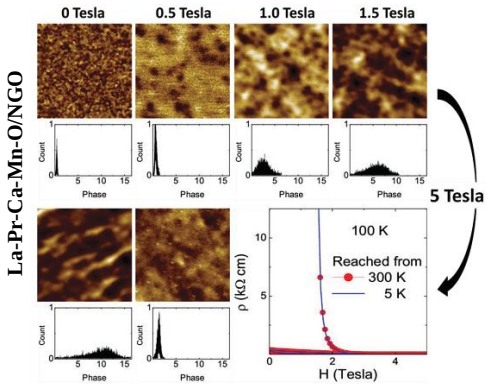

UGC-DAE CONSORTIUM FOR SCIENTIFIC RESEARCH

University Campus, Khandwa Road, Indore 452001

UGC-DAE CONSORTIUM FOR SCIENTIFIC RESEARCH

(An Autonomous Institution of UGC)

Annual Report

2012 – 2013

University Campus, Khandwa Road, Indore 452001

www.csr.res.in

UGC – DAE CONSORTIUM FOR SCIENT IFIC RESEARCH

Head Office

Director: Dr. Praveen Chaddah
UGC-DAE CSR
University campus, Khandwa Road
Indore (M. P.) 452 001
Tel: 0731 2463945, 2463913, 2762267
Fax: 0731 2462294
E-mail: director@csr.res.in

Contact Information

Indore Centre

Centre-Director: Prof. Ajay Gupta
UGC-DAE CSR, Indore Centre
University campus, Khandwa Road
Indore (M. P.) 452 001
Tel: 0731 2472200, 2463913, 2762267
Fax: 0731 2465437, 2462294
E-mail: agupta@csr.res.in /
cd_indore@csr.res.in

Kolkata Centre

Centre-Director: Dr. Ajit Kumar Sinha
UGC-DAE CSR, Kolkata Centre
3/LB8, plot 8, Bidhan Nagar
Kolkata 700 091
Tel: 033 23351866, 23358035, 23356542
Fax: 033 23356543, 23357008
E-mail: aks@delta.res.in

Mumbai Centre

Centre-Director: Dr. V. Siruguri
UGC-DAE CSR, Mumbai Centre
R-5 Shed, Bhabha Atomic Research Centre
Trombay, Mumbai 400085
Tel: 022 25505327, 25594930
Fax: 022 25505402
E-mail: siruguri@csr.res.in

Kalpakkam Node

Scientist in-Charge: Dr. G. Amarendra
UGC-DAE CSR, Kalpakkam Node
Via Kokilamedu Gate,
Kokilamedu-603 104, T.N
Tel: 044-2748 0500 Ext. 21918 or 21919(off)
E-mail: ga@csr.res.in

CONTENTS

1	Director's Report	01
2	Collaborative Research using DAE and CSR facilities	07
	2.1 Collaborative Research at Dhruva Reactor, BARC	07
	2.2 Collaborative Research at VECC, TIFR	24
	2.3 Photoelectron spectroscopy on INDUS-1 and other facilities of RRCAT	44
	2.4 Collaborative Research using in-house facilities at Indore Centre	46
	2.5 Collaborative Research using in-house facilities at Kolkata Centre	63
	2.6 Collaborative Research using in-house facilities at Mumbai Centre	72
	2.7 Collaborative Research using in-house facilities at Kalpakkam Node	73
3	In-house Research activities	78
	3.1 Research activities at Indore Centre (Bulk magnetic materials and oxides; Thin films and multilayers; Nanomaterials; Other studies)	78
	3.2 Research activities at Kolkata Centre (Trace element studies; Condensed matter studies; Chemical sciences and radiochemistry; Nuclear structure; Radiation biology)	109
	3.3 Research activities at Mumbai Centre (Neutron scattering studies; X-ray diffraction; Dielectric studies; Other studies)	124
	3.4 Research activities at Kalpakkam Node	139
4	New Facilities Acquired / Developed	144
5	Publications in Journals	151
6	Presentations in Conferences/Symposia	168
7	Workshops and Seminars organized by UGC-DAE CSR	173
8	Theses and Student Projects	182
9	Seminar/Workshop/Lectures delivered by UGC-DAE CSR Scientists	185
10	Other Activities	188
11	List of Collaborative Research Schemes	194
12	Utilisation of in-house facilities of UGC-DAE CSR : User List	202
13	General information on staff position	233
14	Specializations and research facilities of our Scientists/Engineers	234
15	List of staff	237
16	Committees	240

1. Director's Report

The UGC-DAE Consortium for Scientific Research has been providing cutting-edge facilities for experimental research, in condensed matter physics and in accelerator-based sciences, to researchers from the university system. In addition to providing access to the unique big-science facilities like the Dhruva Neutron Facility at BARC, the Indus Synchrotrons at RRCAT, the accelerators at VECC, the Pelletrons at TIFR and at IOP, utilization of the experimental research facilities set up in close collaboration with IGCAR at our laboratories in the Node at Kalpakkam has been growing and the first journal publications have appeared. The utilization of the LTHM (low temperature and high magnetic field) diffraction beamline we built on Dhruva reactor is impressive, as is also that of the photoemission spectroscopy beamline we built on Indus-1 synchrotron. The Kolkata Centre continues to help nuclear physicists in the utilization of the VECC facilities with our expertise and our vigorous outreach efforts, and its activities in radiation biology and radiation chemistry continue, alongwith radiation-induced synthesis of nanoparticles. We are commissioning many new facilities in our laboratories, as described elsewhere in this report. These additions are a continuing process, as we strive to stay at the forefront.

We continue the tradition of providing statistical indicators in the next few pages as a reminder and check on our sustained commitment and conscious efforts to reach out across the country. The awareness workshops and thematic meetings we organized to this end are described in the report. The report also describes research work of our users from the value-added access to the big-science facilities of DAE, and from the utilization of the state-of-art experimental facilities in our own laboratories. The report also describes the in-house research activities of our scientists, as they compete internationally. The primary check on research output is the journal publications; these are listed and are reassuring. The citations we get are reasonable. We are conscious about citations and impact factors, but look beyond numbers to see whether the research output makes an impact on the work of other well-established research groups internationally.

Our laboratory facilities are utilized by the best (e.g. IISc, IITs), and we enthusiastically provide them to researchers from new and from less-endowed universities. Being ourselves an emerging byline away from metro-cities, we have a lot of empathy with the latter category. Over the last few years we have encountered a special problem that we think will be encountered by emerging bylines in our universities as they respond to the call for creating more knowledge.

Two separate themes of research pursued with our LTHM facilities have faced the issue of various leading groups from France, Germany, Japan, and USA, publishing in leading journals while denying our scientists appropriate credit. In almost all cases some correction was forthcoming from the publishers, but the limitations of the corrections are also obvious. The need for focusing, and 'exploding' research on our keywords, and the use of pre-print repositories, provided us some succour. Such incidents are bound to grow as our emerging bylines create new knowledge; our experiences could provide a starting point for debate.

I thank Dr. T. Shripathi for compiling and editing this report.

Praveen Chaddah

Distribution of Universities/Institutions' users for in-house facilities and Collaborative Research Schemes of CSR

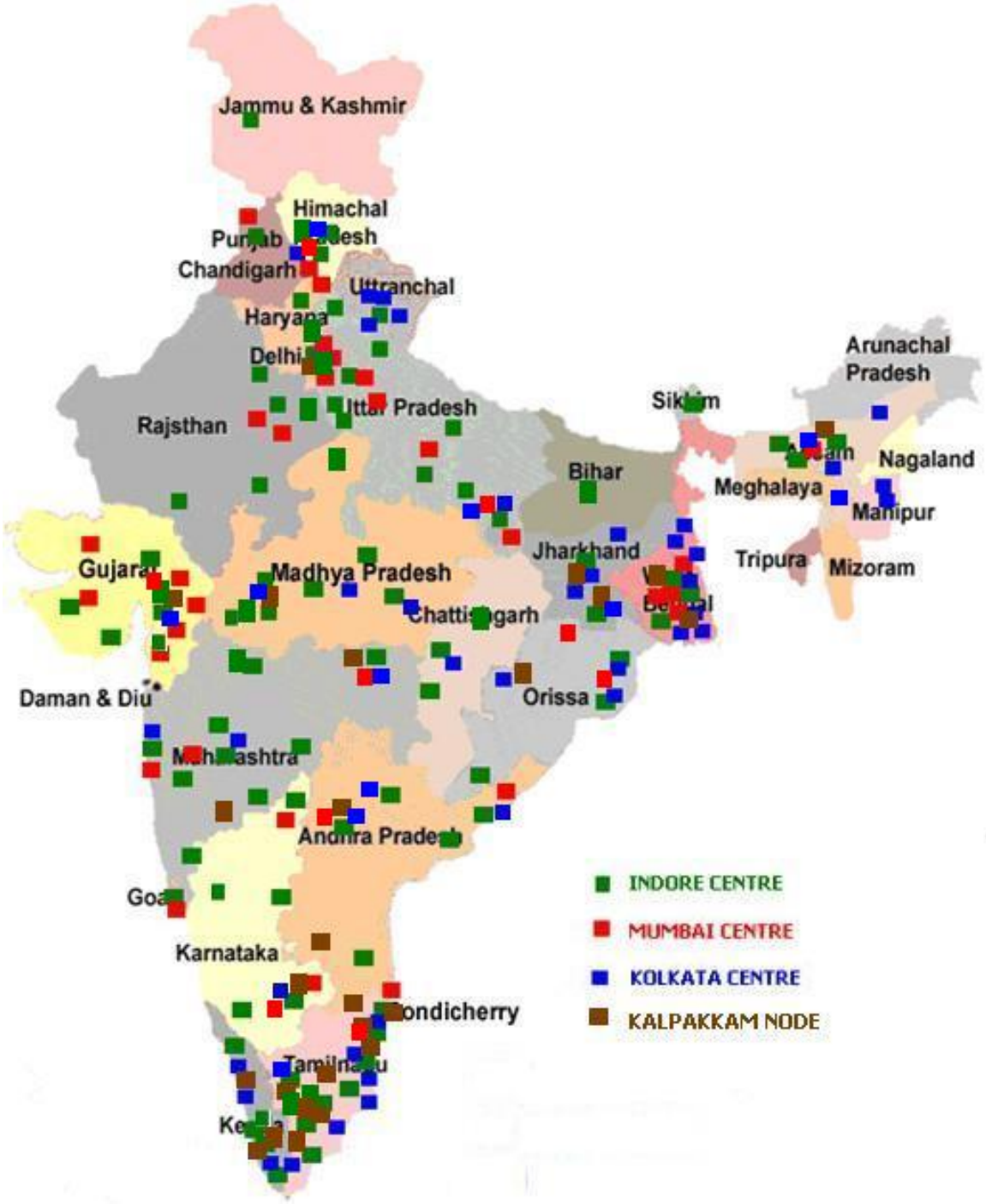

Number of Universities/Institutions participating in UGC-DAE CSR Programmes

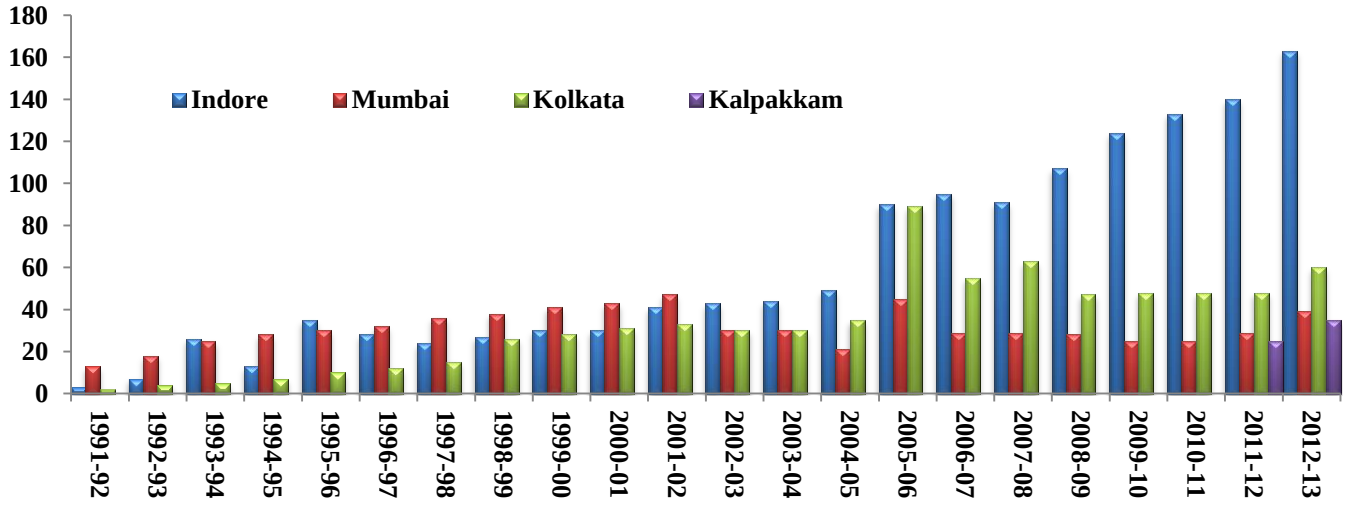

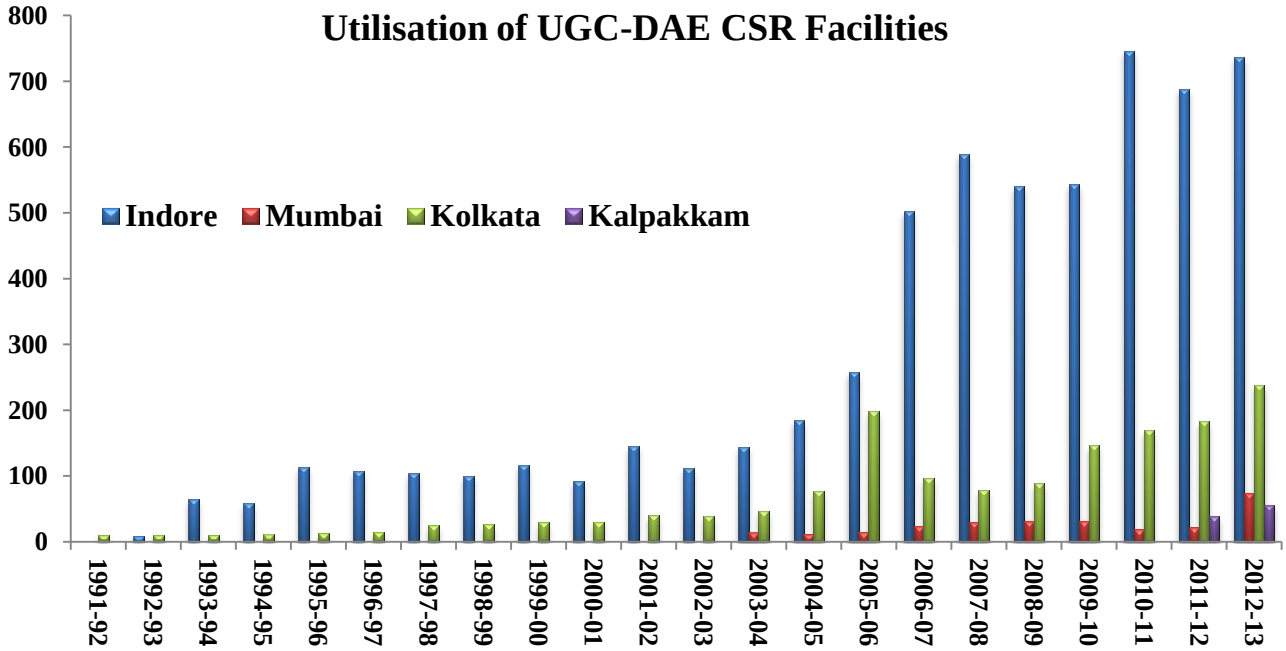

Collaborative Research Schemes sponsored by UGC-DAE CSR

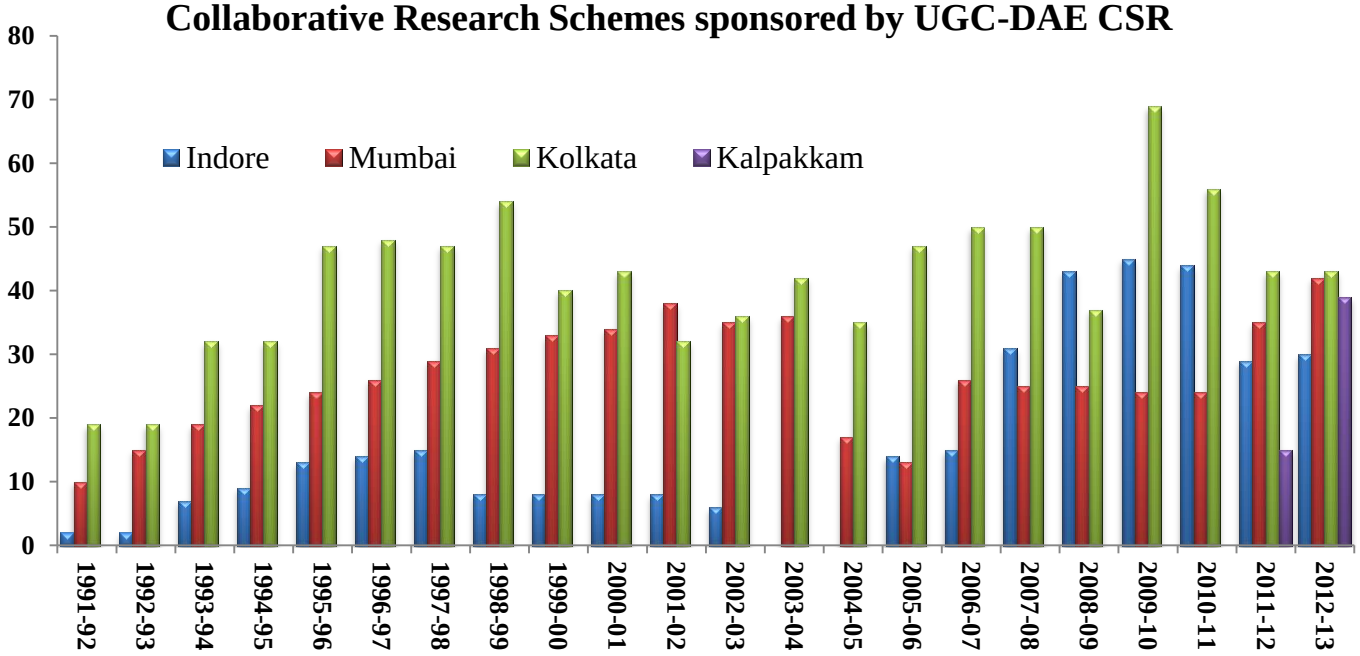

In-house and Collaborative Research Publications of UGC-DAE CSR

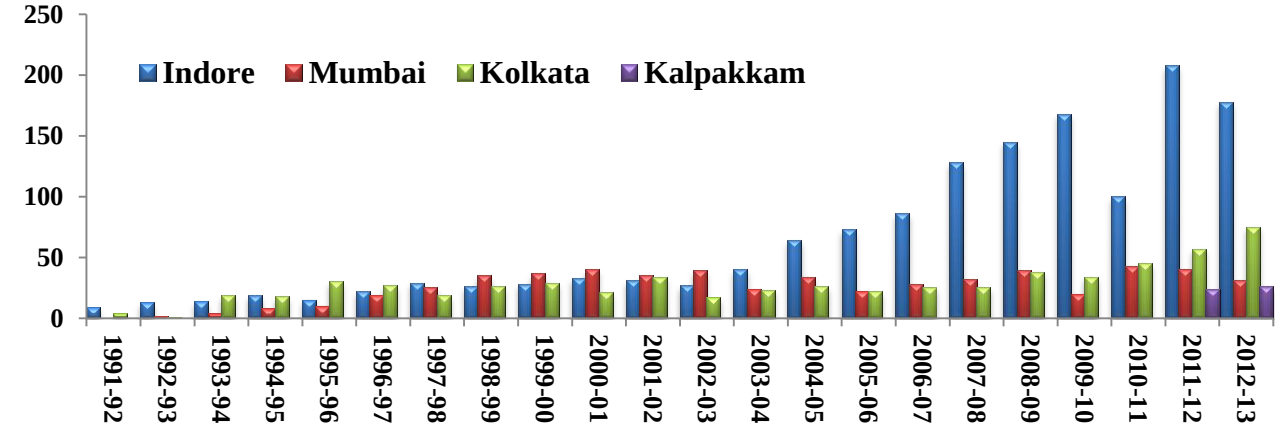

2. Collaborative Research using DAE and CSR facilities

2.1. Collaborative Research Schemes at Dhruva Reactor, BARC, Mumbai

Since January 2013, 42 projects under the collaborative research schemes (CRS) are being supported. Among these projects the area of research interest spans small angle neutron scattering, neutron powder diffraction, and applications of neutron activation analysis. During the year, seven projects were closed after completion. The annual project review meeting was held on October 4-5, 2012 and besides reviewing the progress of various ongoing projects, 9 new projects were sanctioned after peer-review and presentations by the principal investigators, out of which 7 projects got underway. There are 13 projects sanctioned on the CSR diffractometer.

The results obtained from some of the ongoing CRS are described below.

2.1.1. Magnetic ground state of bulk $Co_{0.3}Zn_{0.7}Fe_2O_4$ spinel ferrite using neutron diffraction, magnetization and ac-susceptibility studies

The systems having the magnetic dilution below percolation threshold exhibits finite magnetic clusters in an infinite magnetic network.

In the present study, the bulk spinel compound $Co_{0.3}Zn_{0.7}Fe_2O_4$ has been prepared by wet chemical route method. At macroscopic level, the compound exhibits magnetic in-homogeneity, below the site percolation threshold for the ferrimagnetic ordering, due to the concentration of magnetic ion at a tetrahedral site. Various physical property studies were carried out unravel the magnetic ground state of this system. In the temperature dependent neutron diffraction experiments, a diffused scattering signal is observed below the magnetic peak (1 1 1) at a Q value of ~ 1.29 $Å^{-1}$. The appearance of the diffused scattering peak indicates the presence of a finite magnetic cluster with infinite magnetic network. The diffused scattering signal intensity decreases with increases in magnetic field at T = 10 K.

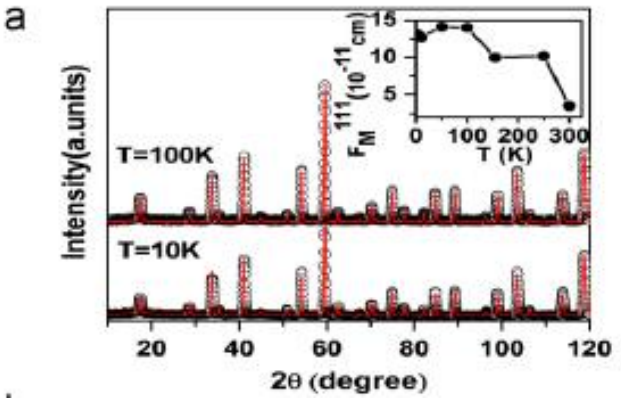

Fig. 1 *Rietveld refinement of the neutron diffraction patterns recorded at 100 and 10 K respectively. The inset of the figure shows the variation of the structure factor of the (1 1 1) peak.*

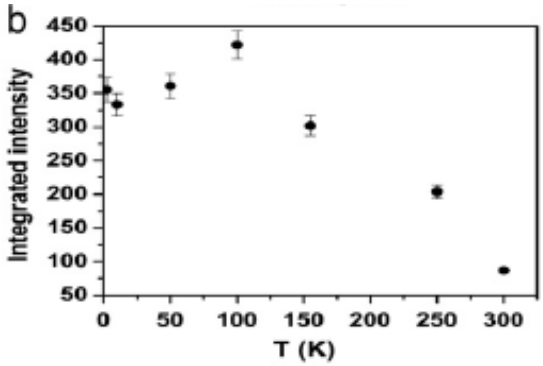

Fig. 2 *Variation of the integrated intensity of the (1 1 1) peak as a function of temperature.*

The *ac* susceptibility measurement exhibits three peak behavior in χ' and χ" indicating the presence of finite magnetic clusters and cluster–cluster interaction in the system. The absence of magnetic (2 0 0) peak in neutron diffraction at 2 K and bifurcation of zero field and field cooled magnetization indicate the phase transition from uniaxial random ferromagnetic (URF) phase to semi spin glass or canted random ferromagnetic (CRF) phase in the system with temperature.

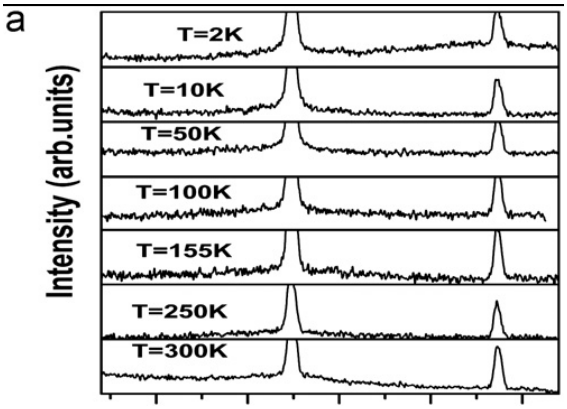

Fig. 3 *Diffuse signal below the (1 1 1) Bragg peak observed in the neutron diffraction patterns at different temperatures.*

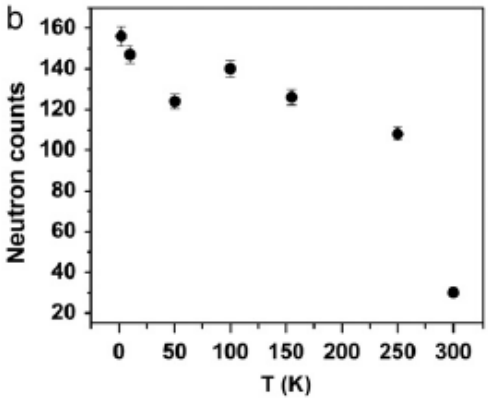

Fig. 4 *The variation in the diffuse scattering intensity with respect to temperature.*

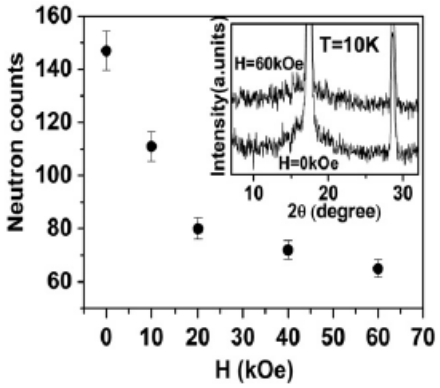

Fig. 5 *Variation of the diffuse scattering intensity below the (1 1 1) peak observed in neutron diffraction patterns is plotted as a function of applied magnetic field. Inset shows the Bragg peaks at 10 K in H = 0 and 60 kOe respectively.*

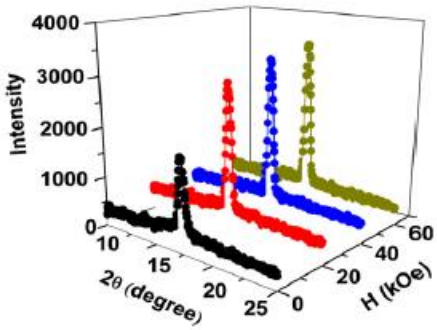

Fig. 6 *Changes in the (1 1 1) Bragg peak intensity at T = 10 K under different applied magnetic fields.*

The appearance of diffuse scattering in neutron diffraction experiments below 50 K clearly manifests the presence of strong interaction between the clusters and that the clusters are randomly oriented, which can be inferred from the decrease of the intensity of magnetic peak (1 1 1) as a function of decreasing temperature below 100 K.

Application of external magnetic field during neutron diffraction experiments results in orientation of some of the clusters in the direction of the infinite network, which can be observed by the increase of the intensity of the Bragg peak. Since the change in intensity is very small, it can be said that the system is strongly (magnetically) disordered.

Harshida Parmar and R. V. Upadhyay (CHARUSAT, Changa); S. Rayaprol, V. Siruguri

2.1.2. Synthesis, Structure and Magnetic studies on $Pb(Fe_{2/3}W_{1/3})O_3$-$Pb(Fe_{1/2}Nb_{1/2})O_3$ Multiferroic systems

The perovskite $Pb(Fe_{2/3}W_{1/3})O_3$ (PFW) ; $Pb(Fe_{1/2}Nb_{1/2})O_3$ (PFN) multiferroic systems are the prospective materials for various applications. In these multiferroics the magnetic (d^5) Fe^{3+} ions and non-magnetic (d^0) Nb^{5+} and W^{6+} ions share the B site of the $A(B^IB^{II})O^3$ perovskite structure. The (d^5) ion in the BO_6 octahedral sites leads to ferromagnetic order while the (d^0) ions in similar lattice position provide ferroelectric order. This class of materials would offer a large application potential for new devices taking advantage of two coupled degrees of freedom based on local off-centered distortion and electron spin. The major applications of multiferroic materials are in spintronic devices, functional sensors, and multistate memory devices. The choice of such materials is very much limited due to inherent lack of simultaneous ferroelectric and ferromagnetic orders in a single phase material at room temperature (RT).

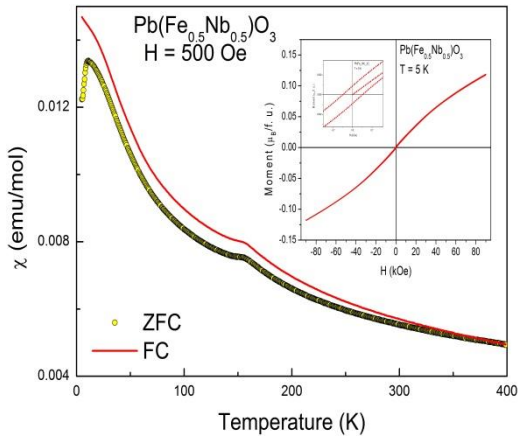

Fig. 7 *Magnetic susceptibility and magnetization (at 5K) for $Pb(Fe_{1/2}Nb_{1/2})O_3$ sample.*

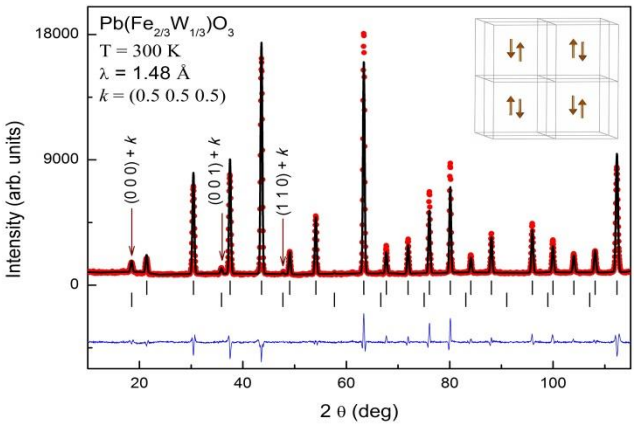

Fig. 8 *Rietveld refinement of room temperature ND pattern of $Pb(Fe_{2/3}W_{1/3})O_3$ for chemical and magnetic structure. Arrangement of spins in magnetic cells is shown in the inset.*

In our earlier work, the magneto-electric coupling on PFN was studied through temperature dependent dielectric and neutron diffraction studies across the magnetic Neel temperature showing an anomaly at 143 K. In continuation with earlier work, we did magnetization studies on PFN and the room temperature Neutron diffraction studies on (PFW_{1-x}-PFN_x) solid solution. The zero field cooled (ZFC) and the field cooled (FC)

magnetizations measured between 5 and 400 K at 500 Oe for PFN is shown in Fig. 7, the M-H curve for PFN taken at 5 K is shown as an inset. The FC curve shows a magnetization increase with decreasing temperature and has a huge increment below 200 K. The ZFC curve showed a sharp cusp around 150 K, almost the same temperature where the dielectric anomaly was observed (in our earlier work), and significant splitting of the ZFC and FC curves had occurred at 250 K. This splitting reveals a spin-glass-like transition, similar to that reported for PFN. Comparing the low temperature and the high temperature M-H curve indicate that the anti-ferromagnetic ordering below Neél temperature and a weak ferromagnetism at RT.

Few compositions of (PFW_{1-x}-PFN_x) solid solutions were synthesized (x = 0, 0.2, 0.4, 0.6, 0.8 and 1,) and room temperature (RT) neutron diffraction (ND) studies were carried out. The T_N for pure PFN is 143 K while for PFW it is well above RT. Fig. 8 shows the Rietveld refinement of PFW neutron diffraction data at RT. The appearance of additional peaks in PFW at 2θ =18.38, 35.82 and 47.68 indicates the AFM state of PFW at RT. Fig. 9 shows the room temperature ND data for the compositions with x (PFN) =0.2, 0.4, 0.6 and 0.8. With increase in the PFN content in the solid solution the intensity of the magnetic peaks decreases indicating the decrease in the magnetic ordering at RT. For the compositions x = 0.8 and 1 the magnetic peaks are not seen since the onset of magnetic ordering is below RT.

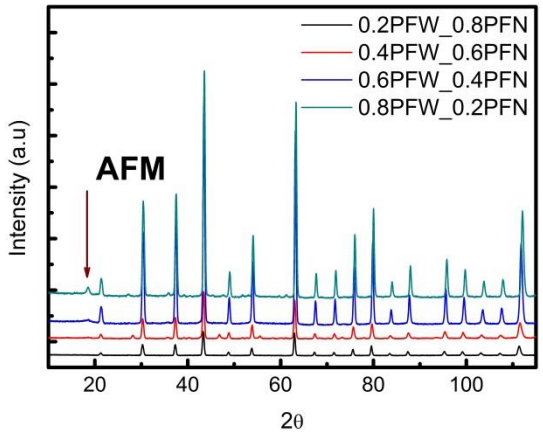

Fig. 9 *Room temperature neutron diffraction data for PFW-PFN solid solutions with different compositions. The vertical arrow indicates the AFM peak.*

S. Matteppanavar and Basavaraj Angadi (Bangalore University, Bengaluru); S. Rayaprol

2.1.3. High-Q neutron diffraction studies on Lead silicate glasses

The PbO-SiO_2 system is a very popular glass in our daily life as “crystal glass” and it has numerous industrial applications, e.g., as optical glasses, in radiation shielding etc. This system forms glasses over a wide composition range, up to 90 mol % PbO, and the glasses can be easily prepared by using the conventional melt-quench technique. The structure of PbO-SiO_2 glasses has been widely studied by diffraction measurements, and spectroscopic measurements. It is also well known that PbO is classified to network modifiers and to intermediates between network formers and network modifiers. Neutron diffraction measurements have revealed large amounts of free volume which is not found in other binary silicate glasses.

However, substantial structural questions still remain to understand the wide glass forming range because a three-dimensional model for the structure is missing: (i) How is the structure governed by SiO_4 tetrahedra and PbO_3 and/or PbO_4 polyhedra? (ii) What is the substantial structural role of PbO as an

intermediate? In an attempt to shed light onto these questions and explain the glass forming ability of PbO-SiO_2 glasses, we reveal details of the glass structure by the use of a combination of x-ray and neutron- diffraction measurements, with the aid of MCGR technique.

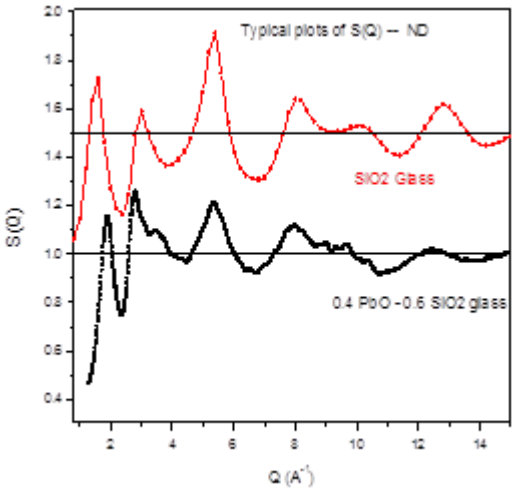

Fig.1

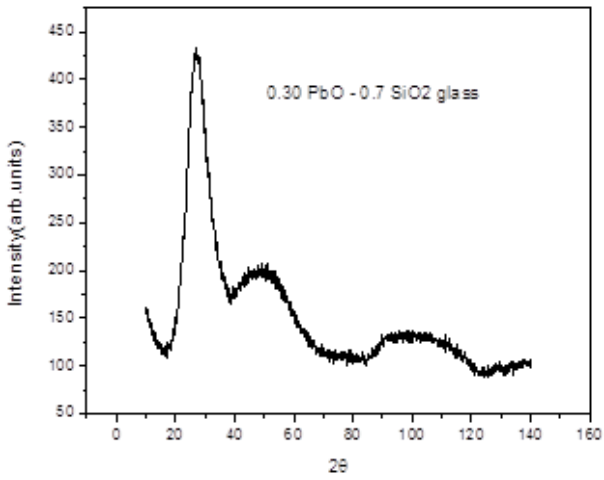

Fig.2

Table 1:

Sr. No.	x	Density (g/cc)	Mol. Vol. (cc/mol)	DTA	Microhardness (Gpa)	Lower wavelength cut off (nm)
1.	35.69	7.05	23.40	345 461 482	2.885	404
2.	40	6.65	23.75	350 450 485	3.412	381
3.	50	6.07	23.33	370 520 570	3.712	365
4.	60	5.22	24.01	440 -- --	4.109	358
5.	70	4.29	25.41	640 -- --	4.427	342

Neutron diffraction measurements have been carried out on High-Q diffractometer and the data is analyzed using MCGR technique. As x increases from 0 to 0.65 Si-O distance goes from 1.61Å to 1.63Å. Pb-O distance is found to have 2 distances around 2.3Å and 2.7Å corresponding to PbO_3 and PbO_4 units in the network. O-O distance is about 2.65Å is a collection of O-O distances from SiO_4, PbO_3 and PbO_4 units. Also from SEM measurements we find that this glass has lead rich and silica rich phases and quite unique as both

phases are glassy. The observed high free volume in this glass by earlier study can be explained on the basis of these concentration fluctuations between these 2 phases. We are doing a 3D modeling study to understand this system further.

M.S. Jogad and Rashmi M. Jogad (Gulbarga University, Gulbarga) and P. S. R. Krishna (BARC)

2.1.4. Interaction between Serum Albumins and Drugs

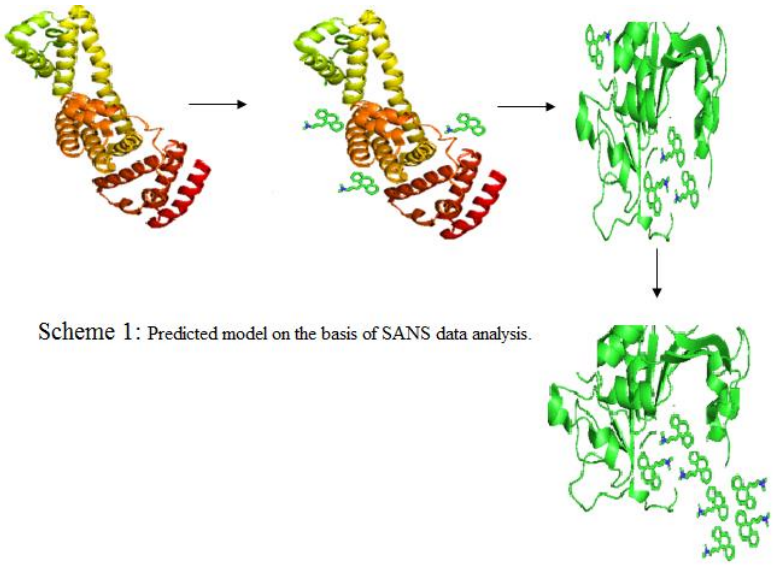

Fig. 1 *Scheme 1: predicted model on the basis of SANS data analysis.*

The interactions between serum albumins (HSA/BSA) and amphiphilic drugs have been studied by using spectroscopic (UV-visible, Fluorescence, Circular Dichroism) and small angle scattering (SANS) techniques. The spectroscopic results show occurrence of interactions whereas the analysis of SANS data indicates unfolding of proteins in the presence of low concentration of drugs which is believed to be the opening of the globular protein structure into a random coil Gaussian conformation of the unfolded polypeptide chain. At higher drug concentrations, there is appearance of correlation peaks in SANS profiles of serum-drug complexes indicating the presence of repulsive intermicellar interaction between the positively charged drug micelles. Hence, the protein-drug complexes have been assumed as micelle-like clusters of drug randomly distributed along the unfolded polypeptide chain. Based on these results a model is proposed (Scheme1).

Kabir-ud-din (Aligarh Muslim University, Aligarh) and V. K. Aswal (BARC)

2.1.5. Studies on Core-Shell Structured Metal Oxide / PANI Nanocomposites

Polyaniline was synthesized by In- Situ chemical polymerization of aniline in the presence of hydrochloric acid as a catalyst and ammonium-peroxydisulphate as an oxidant. The Titania nanoparticles have been hydrothermally synthesized with standard experimental procedure by Titanium tetrachloride ($TiCl_4$). Finally the PANI/TiO_2 nano-composite is synthesized by addition of TiO2 nanoparticles (40 wt %) at the time of Polyaniline synthesis. Morphology of these particles are studied with various experimental techniques like

X-ray diffraction (XRD), Scanning electron microscope (SEM) and Small angle neutron scattering (SANS) on Dhruva reactor BARC Mumbai.

In SANS experiment intensity of scattered neutrons I(Q) is measured as a function of the scattering vector Q = ($4\pi Sin\theta/\lambda$). The radius of gyration (R_g) is obtained by application of the Guinier equation (1) to the scattered intensities. R_g of PANI, TiO_2 and their composite are estimated as 18.42 nm, 30.05nm and 6.58nm respectively.

$$(Q)= I(o)\exp [(-Q^2 (R_g^2) /3] \quad \ldots\ldots\ldots\ldots\ldots (1)$$

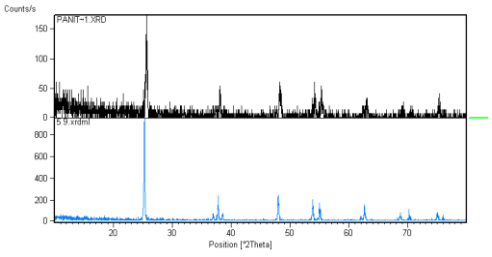

Fig. 13 *XRD of PANI/TiO_2 Nano composite and TiO_2.*

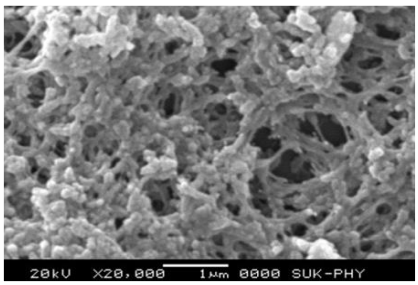

Fig. 14 *SEM Image of PANI/TiO_2 Nanocomposite*

These results indicate that size reduction is taking place due to composite formation which can be attributed to the strong core-shell formation between TiO2 and polyaniline. The surface fractal dimension (Ds) of these particles have been calculated by using the equation

$$\ln I(Q) = \ln I_o - \alpha \ln Q \quad \ldots\ldots\ldots\ldots\ldots\ldots\ldots (2)$$

where 'α' is a constant and the surface fractal dimension Ds = 6-α. This surface fractal dimension indicates the surface morphology. The SANS results indicate that polyaniline, TiO_2 and their composite fractal dimensions are 2.65, 2.31 and 2.82 respectively. These results indicate that the composite surface is more rough compare to the PANI and TiO_2.

N. Narsimulu (Osmania University, Hyderabad) and D. Sen (BARC)

2.1.6. Self-assembly of Stimuli Responsive Amphiphilic Block Copolymers

We have done earlier preliminary studies on PNIPAM-PDMPA31. Similar studies were carried out on PNIPAM-PDMPA66 to characterize core-shell micelles by using spectral (Turbidimetric, NMR) and scattering techniques (Dynamic light scattering (DLS)). In dilute aqueous solutions, the copolymer molecules self-assemble into nano-sized core-shell micelles with PNIPAM core as a function of temperature and salt. We also study invert micellization structure i.e. PDMPA as a core in the presence of SDS.

We have carried out experiments on linear and star type POE-POP-POE triblock copolymer commonly known as Pluronic®, Pluronic® R and Tetronic® which form core-shell aggregates known as micelles. P103, P104 and P104 (with ~ same mass) were investigated in presence of p-hydroxy benzoic acid PHBA and its sodium salt. PHBA (antioxidant) has very little solubility in water. When this antioxidant was added to pluronic solution, it facilitates in the micellization process and leads to sphere to ellipsoidal transition. The intensity in

the SANS plot moved towards the lower Q region. Supportive studies were carried out using DLS, viscometry and cloud point measurements.

Mehul Khimani, Pratap Bahadur (V. N. South Gujarat University, Surat) and V. K. Aswal (BARC)

2.1.7. SANS Investigation of the Silicon Rubber Membranes

One of the best entity for removal of volatile organic pollutant from water, poly(dimethylsiloxane) (PDMS) based membranes from two types of initial precursor 'hydroxyl terminated poly (dimethylsiloxane) macromers' of lower and higher viscosity was thoroughly investigated using SANS, GPC, ESI-MS,LC-APCI-MS, NMR, cross-linking density and performance measurements. The viscous nature of the precursors were found to be due to interaction among the homologous macromolecular units which otherwise were very thin solution in dilute systems below 20 % (w/w). SANS data from dilute 10-20 % (w/w) solutions of the both precursors in CDCl3 revealed that the macromolecular structure size were only about 10-12 Å Rg in agreement with their mass values of 1-3 kDa from LC-APCI-MS data.

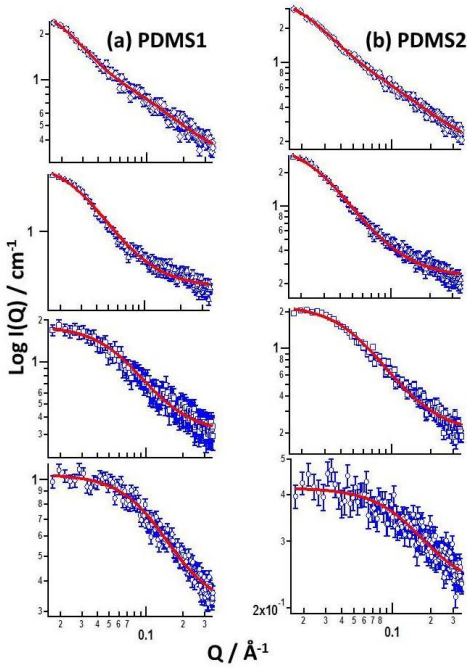

Fig. 15 *Similar SANS profiles of membranes obtained from 2 different precursors.*

In both the cases, the macromolecular structure sizes were increased by two to three-folds due to the cross-linking in the liquid state and exhibited Gaussian chain statistics which on evaporation of the solvent, were condensed to the formation of the membranes of cross-linked network structure. Both the membranes on equilibrium swelling in $CDCl_3$ solvent again showed the scattering signatures of Gaussian chain statistics implying a large inter-chain spacing between the macromolecular units on swelling so that the chain segments can freely rotate along the main chain, implying a high degree of chain mobility. Their structural similarities were further confirmed by similar performance in separation of volatile organic from water.

Puyam S. Singh (CSIR-CSMCRI, Bhavnagar) and V. K. Aswal (BARC)

2.1.8. Modification of Attractive and Repulsive Interactions among Proteins in Solution due to the Presence of mono-, di- and tri-valent ions

Bovine serum albumins, at physiological pH, shows a short-range attraction and in addition a long-range electrostatic repulsion among them. These interactions are modified in presence of different counterions. Small angle neutron scattering study shows that for the equal ionic strength, the interactions are largely modified by

the tri-valent (Fe^{3+}) and di-valent (Ni^{2+}) ions and comparatively less by the mono-valent (Na^{+}) ions. The effect is nearly similar for the di- and tri-valent ions in comparison with the mono-valent one. SANS profiles and the fitted curves by using two-Yukawa potential model are shown in Fig. 16a. An oblate form factor of dimensions ≈ 9Å × 39Å × 39Å was used to fit the SANS data and the corresponding structure factors are shown in Fig. 16b. The strength of the attractive and repulsive interactions depends strongly on the type of the dissolved ions and salt concentrations.

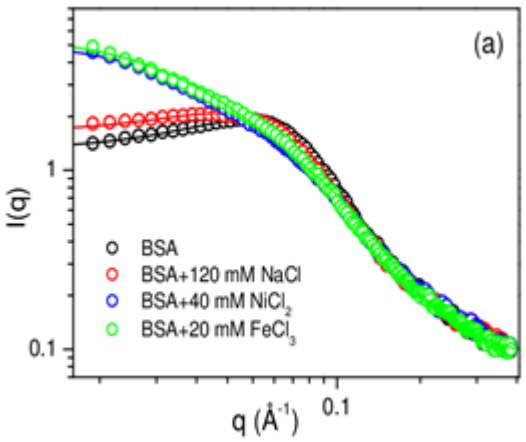

Fig. 16(a) *SANS data (open circle) and fitted curves (solid line) for 10 wt% BSA in aqueous solution at pD 7.0 and in presence of salts having equal ionic strength, i.e., 120, 40 and 20 mM NaCl, $NiCl_2$ and $FeCl_3$ respectively.*

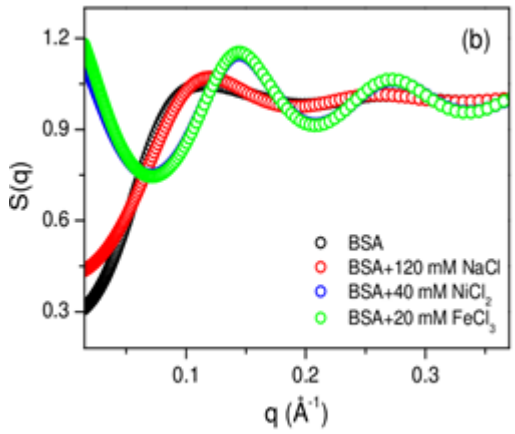

Fig. 16(b) *Interparticle structure factor, S(q), extracted from the fitting using two-Yukawa potential models.*

Sarathi Kundu (IASST, Guwahati), Kaushik Das (IASST), and V. K. Aswal (BARC)

2.1.9. Stimuli Responsive Solution Behavior of Surfactants: A SANS Study

Non-ionic surfactant solution on heating beyond a certain temperature gets cloudy and phase separate on standing. The phenomenon is known as Clouding Phenomenon and the temperature is known as Cloud Point (CP). This phenomenon is rare in ionic surfactant solutions, but recently we have shown that clouding can occur in ionic surfactants too. Various anionic surfactants: tetra-n-butyl ammonium dodecylsulfate (TBADS), tetra-n-butylammonium dodecyl benzene sulfonate (TBADBS), tetra-n-butyl ammonium sulfonato myristic acid methyl ester (TBAMES), tetra-n-butyl phosphonium dodecylsulfate (TBPDS) and tetra-n-butylphophonium dodecyl benzene sulfonate (TBPDBS), are synthesized and their clouding behavior have been studied with and without inorganic salts.

Small Angle Neutron Scattering (SANS) has been used to study the morphological changes when the solution is heated toward CP. It has been found that two morphologies are present in the solution when it approaches the CP. The percentages of individual micellar fraction and that of giant aggregates below and above the CP have been obtained by SANS data and were further confirmed by NMR and DLS data. The

micellar fractions can be tuned by increasing the temperature, [salt] and nature of salt (Figure). Interestingly; the data showed a micellar growth on heating which is an unusual behavior for ionic surfactant solutions. Effect of addition of various inorganic salts (NaCl, $Mg(NO_3)_2$ and $Al(NO_3)_3$) has also been studied on the CP and the growth in ionic surfactants. It was observed that the judicious selection of an inorganic salt can tune the CP, morphology and growth (or disintegration) in either way.

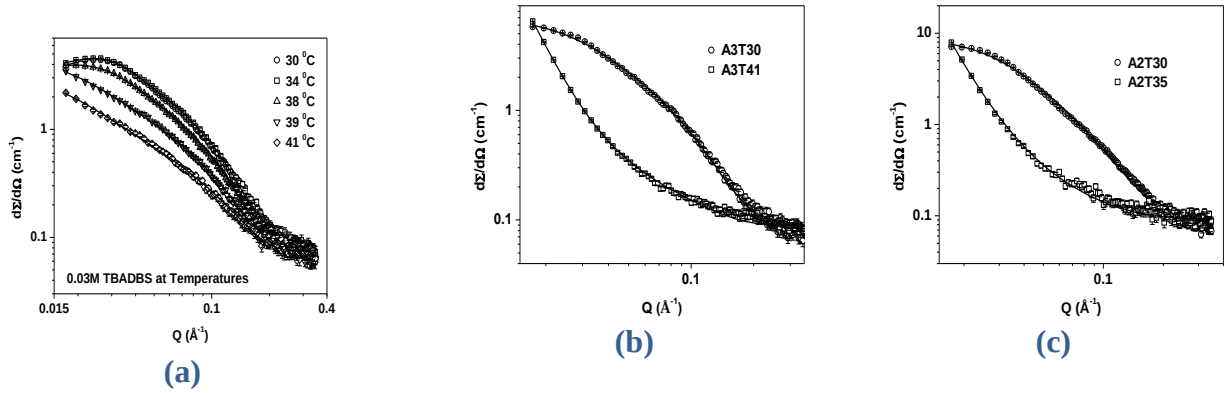

Fig. 17 *SANS data of a) 30mM TBADBS, b) 30mM TBADBS in presence of 1.0mM $Mg(NO_3)_2$ and c) 30mM TBADBS in presence of 0.5mM $Al(NO_3)_3$ at different temperatures.*

Sanjeev Kumar (M. S. University, Baroda) and V. K. Aswal (BARC)

2.1.10. Ionic Liquid Induced Sphere-to-Ribbon Transition in the Block Copolymer Mediated Synthesis of Silver Nanoparticles

Spherical silver nanoparticles (AgNPs) with size ~20 nm have been synthesized from an aqueous $AgNO_3$ solution using the amphiphilic block copolymer, Pluronic P123 (EO_{20}–PO_{70}–EO_{20}), under ambient conditions without the use of any other reducing agents.

The size of the AgNPs was highly dependent on the size and geometry of the micelles of the block copolymer. As synthesized AgNPs were characterize by UV-Vis spectroscopy, Transmission Electron Microscopy (TEM) and Dynamic Light Scattering (DLS).

The addition of an ionic liquid (IL), N-alkyl pyridinium dodecyl sulphate, $C_nP_yD_s$, where n = 4, 6, 8, induced a sphere-to-ribbon (cylindrical) transition of the AgNPs. We observed that the presence of ILs reduces the equilibrium time as well as acting as a shape directing agent. The micelles of P123 and ILs in aqueous solution were characterized by Small Angle Neutron Scattering (SANS) and DLS methods. The size and shape of the AgNPs correlate with the geometry of micelles of the amphiphilic block copolymer and ILs in aqueous solution.

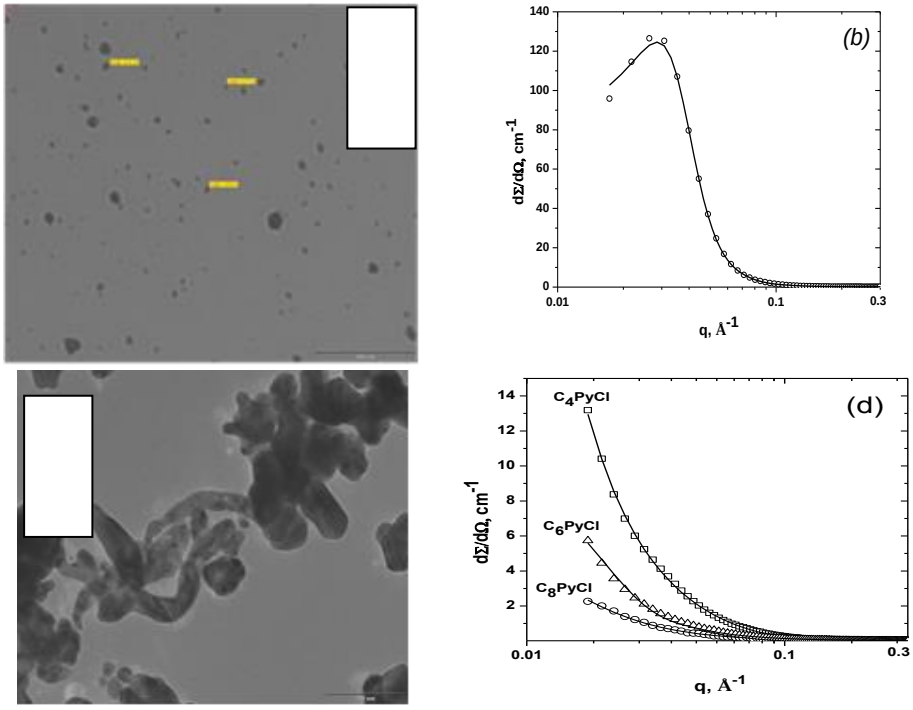

Fig. 1 *TEM image of AgNPs synthesized (a) using P123 (as reducing agent and without IL) and (c) using P123 (with C_8PyDs IL), (b) SANS data of 10% (w/v) P123 in aqueous solution, and (d) 0.05% (w/v) ILs in aqueous solution at 30^{o}C.*

Saurabh S. Soni, Rohit L. Vekariya (S. P. University, V. V. Nagar) and V. K. Aswal (BARC)

2.1.11. Study of Trace Elements in Kidney Stones Using Neutron Activation Analysis

A urinary stone is a hard, crystalline mineral material formed within the kidney or urinary tract. Urinary stones are typically classified by their location and their chemical composition. Kidney stone disease which is expected to affect one in eight persons in his or her life time is one of the commonest diseases plaguing mankind. The patient suffering from such a disease is under severe pain and is unable to pass urine for days as a result of stones formed inside the body which blocks the passage of the urine through kidney, thereby bringing its functioning to a halt. The stone precipitation process is still not properly understood. It is postulated that trace elements present in kidney stones too play an important role in the stone formation process. During the present period of the project the concentrations of trace element, namely Zn, Sr, Co, Fe, Cr, Sc, Se, Na and Mn were determined using Instrument Neutron Activation Analysis (INAA) in four kidney stones collected from different patients, three of which were calcium oxalate type and one was uric acid type. The quantification of Calcium was done by using Energy Dispersive X-Ray Fluorescence (EDXRF) technique.

For INAA, samples were irradiated in Tray rod facility of Dhruva reactor, Mumbai and pneumatic fast transfer system (PFTS) of KAMINI reactor, Kalpakkam. Radioactive assay was carried out using high purity germanium detector coupled to 8k channel analyzer. For EDXRF measurements, powdered samples were mixed thoroughly with cellulose powder in agate mortar and pelletized by a hydraulic press. Measurements were made using Jordan Valley, EX-3600 M EDXRF spectrometer. The mean concentrations of different trace elements obtained by INAA along with the concentration of Ca determined by EDXRF are shown in Table 1. The concentrations of trace elements in general were found to be higher in calcium oxalate stones when

compared to the uric stone and significant positive correlation was observed in the concentrations of Ca with Sr and Zn.

Table 2: Concentrations (mg kg^{-1}) of elements in Kidney stone samples by INAA

Element	KS-2	KS-3	KS-8	KS-10
Zn	217 ± 12	6.8 ± 0.7	60.3 ± 5.1	38.3 ± 2.2
Sr	47.9 ± 2.1	BDL	35.9 ± 1.7	37.2 ± 2.1
Na	1843 ± 44	1019 ± 33	1986 ± 25	1799 ± 64
Mn	1.44 ± 0.12	0.63 ± 0.08	1.80 ± 0.14	0.37 ± 0.05
Fe	36.1 ± 2.7	18.2 ± 1.3	26.2 ± 2.5	38.8 ± 2.1
Cr	0.31 ± 0.03	0.08 ± 0.01	0.29 ± 0.03	0.27 ± 0.03
Se	1.18 ± 0.11	0.39 ± 0.05	2.29 ± 0.18	1.08 ± 0.17
Co#	31 ± 2	12 ± 1	102 ± 6	10 ± 1
Sc#	1.2 ± 0.2	BDL	1.3 ± 0.1	2.6 ± 0.2
Ca (%)*	23.28 ± 1.13	0.33 ± 0.06	21.52 ± 1.52	22.17 ± 1.91

* by EDXRF; # indicates μg kg^{-1} (ppb)

Alok Srivastava, B. Vasisht, P. Aggarwal (Punjab University, Chandigarh), A. V. R. Reddy, K. K. Swain, R. Acharya (BARC), and Uttam Mete (PGIMER, Chandigarh)

2.1.12. SANS and Dielectric Spectroscopy Studies of Chitosan – Gold Nanocomposites

Biodegradable polymer has wide applications in bio-medical and energy related fields. Chitosan is one of the important polysaccharides with several advantages including biocompatibility, nontoxic and electrolytic properties. In this work gold nanocomposites were prepared upon chitosan without any reducing and stabilizing agents – a green method. The chitosan – gold nanocomposites films have been prepared using solution casting method. For this 1wt% chitosan solution was prepared in 1.5 wt% acetic acid. To this $HAuCl_4.3H_2O$ was added to make 1 mM Au. The solution was mixed and poured in a dish. The as obtained films are shown in Fig 1. The films were analyzed using Small Angle Neutron Scattering (SANS), FESEM, XRD and Dielectric spectroscopy. SANS has been used to determine size and distribution of gold nanoparticles in chitosan matrix (Fig 2). The size of the gold nanoparticle was found to be around 6-10 nm. FESEM shows that the gold particles were found to be homogenously dispersed in the chitosan matrix. The size of the particles as determined by FESEM was ~ 10 nm. XRD measurements for the chitosan-gold nanocomposite showed peaks for gold. The dielectric relaxation behaviors of the films were examined using broad band dielectric spectroscopy in the frequency range 1 mHz to 1 MHz. The relaxation positions for chitosan – gold nanocomposite was different from that of chitosan film. It was also observed that the relaxation frequency was higher for chitosan – gold nanocomposite than for chitosan films alone. These results indicate that the presence

of gold nanoparticles affect the dynamics of the polymers. This work has potential applications in the field of energy materials and biomedical engineering.

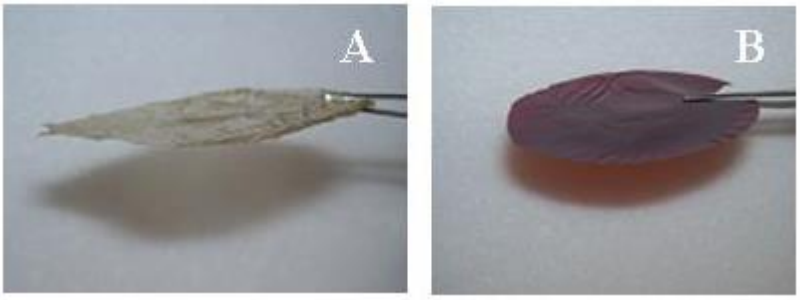

***Fig 1**. A) Chitosan film and B) Chitosan – gold nanocomposite film*

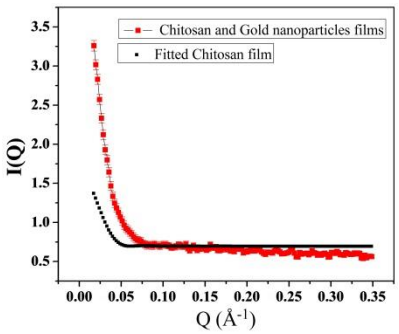

***Fig. 2.** SANS for the Chitosan – gold nanocomposite.*

Radha Perumal Ramasamy, S. N. Suraiya Begum (Anna University, Chennai), and V. K. Aswal (BARC)

2.1.13. Influence of Doping on Multiferroic $YbMnO_3$

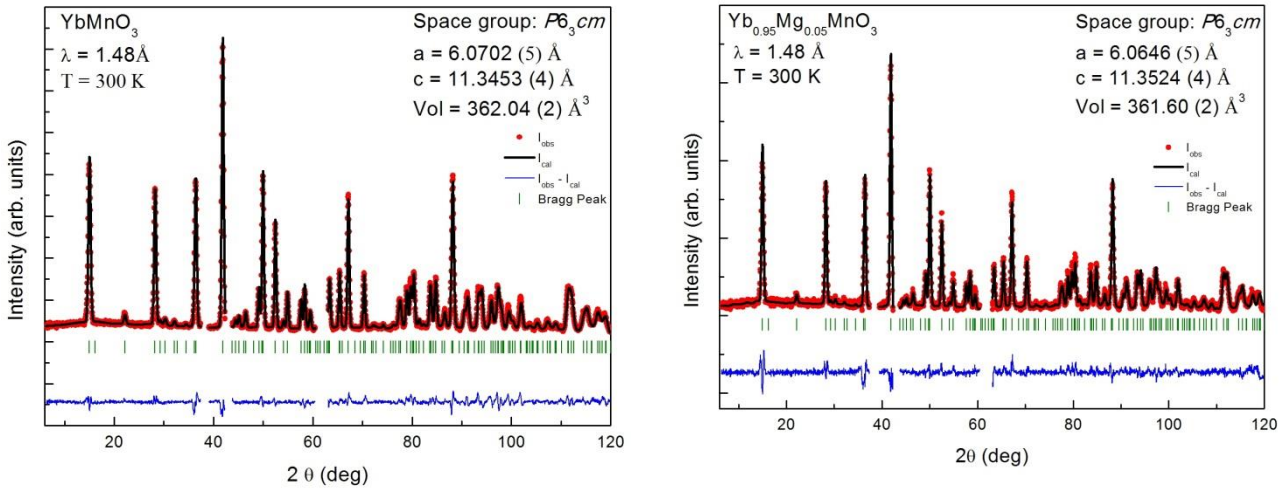

***Fig. 1.** Room temperature ND patterns of $YbMnO_3$ and $Yb_{0.95}Mg_{0.05}MnO_3$ samples refined using Rietveld method.*

To study the aspect of influence of doping in $YbMnO_3$ in detail, a series of polycrystalline samples of $Yb_{1-x}Mg_xMnO_3$ (x = 0 to 0.50) were synthesized by the standard solid state reaction technique. XRD patterns showed no impurity peaks, thus confirming that Mg is being substituted for Yb in the above samples. Room temperature (RT) Neutron diffraction (ND) measurements were carried on powder samples at a wavelength of 1.48Å a using the facility of UGC-DAE CSR beam line in Dhruva, BARC. ND patterns were analyzed using Rietveld method and the refinement of crystal structure was carried out using the FULLPROF program. From the analysis of the data, it is observed that Mg doping ($0<x<0.5$) at Yb site in$YbMnO_3$ is achieved without any change in the crystal structure. Fig. 1 shows the room temperature ND patterns for x = 0.0 and 0.05 samples.

The lattice parameter *c* increases on doping 5% Mg at Yb site, whereas the lattice parameter *a* decreases with increase in the level of doping. The changes in Mn-O bond lengths and O-Mn-O bond-angles are expected to modify the buckling in the rare-earth plane and, in turn, tilt the MnO_5 polyhedron.

$YbMnO_3$ is a rare earth hexagonal magneto electric multiferroic material possessing its own interesting properties. We would like to understand properties of doped $YbMnO_3$, as very limited information on the effect of doping on $YbMnO_3$ is available in the literature. Hence the present work is to study the influence of Mg doping on the properties of $YbMnO_3$ material. It is expected that Mg will replace Yb sites. The dopant chosen is Mg^{2+} since the ionic radius of Mg^{2+} (0.890 Å) is smaller than that of Yb^{3+} (0.985 Å) by ~9.5% and therefore, it is expected to go to Yb^{3+} site preferentially. Distortions in the structure are likely to take place to accommodate the smaller cation. These distortions will directly affect the ferroelectric polarization properties of the system. The addition of Mg^{2+} ion in $YbMnO_3$ introduces corresponding stoichiometric amount of Mn^{4+} ion ($Yb_{1-x}Mg_xMn_{1-x}^{3+}Mn_x^{4+}O_3$). The mixed valence state of Mn^{3+}/Mn^{4+} will affect the magnetic and transport properties. Further, this may also lead to oxygen vacancy defects and the migration of these defects at different temperatures will influence the dielectric and ferroelectric properties.

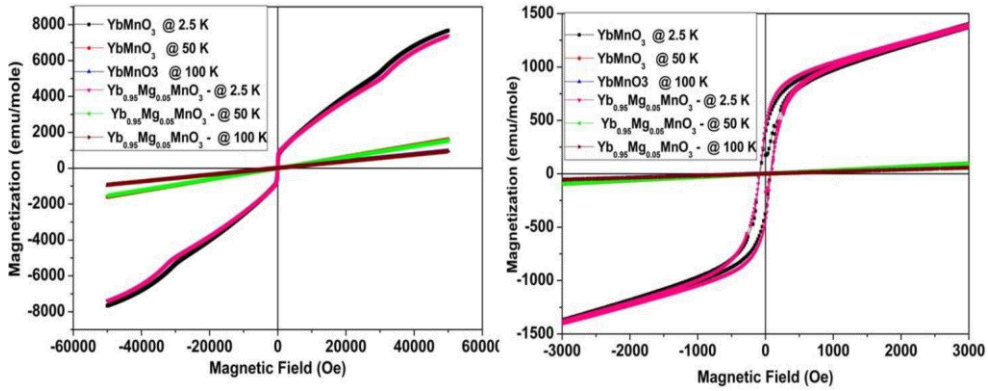

Fig 1. *M vs. H curves of $Yb_{1-x}Mg_xMnO_3$ (x = 0.00 and 0.05) measured at 2.5 K, 50 K and 100 K. b) Enlarged view of M vs. H graph of $Yb_{1-x}Mg_xMnO_3$ (x = 0.00 and 0.05).*

Magnetization (M) vs. Field (H) plots were obtained at 100 K, which is above the Neél temperature, T_N, of the sample, is observed to be linear indicating the paramagnetic behavior of samples. M vs. H plot obtained at a temperature of 50 K, which is below T_N of the sample, is linear indicating the antiferromagnetic nature. Hysteresis or saturation of magnetization was not observed due to the expected anti-ferromagnetic behavior of samples at these temperatures. However, the M vs. H plot obtained at 2.5 K exhibited hysteresis with no saturation (Fig. 22). Detailed analysis of the Neutron Diffraction and magnetization measurements is to be carried out and other measurements like heat capacity etc. are being planned on these samples.

B. Sattibabu, M. Sundararaman, A. K. Bhatnagar (University of Hyderabad); S. Rayaprol and V. Siruguri

2.1.14. Structure-Property relations in R_2TGe_3 (*R* = rare earth, *T* = transition metal) Compounds

The intermetallic compounds having general formula, R_2TGe_3 (*R* = rare earth and *T* = transition metal) have been studied for their structural and physical properties. Valence fluctuation in metals like cerium and

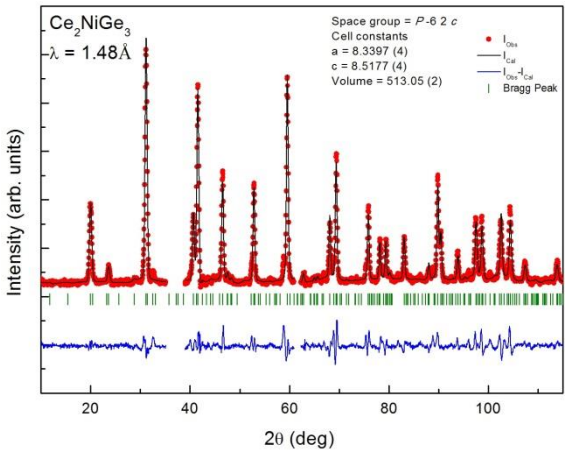

Fig. 1. *Neutron diffraction pattern of powdered sample of Ce_2NiGe_3 at room temperature.*

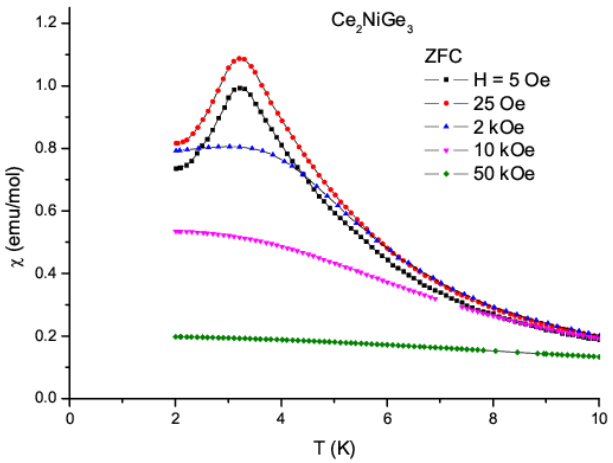

Fig. 2. *Magnetic susceptibility for Ce_2NiGe_3 measured under different applied dc fields.*

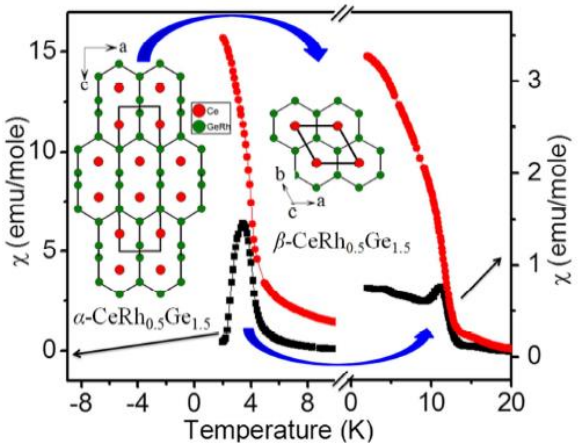

Fig. 3 *Two polymorphs of the new intermetallic compound $CeRh_{0.5}Ge_{1.5}$ was synthesized by arc melting using different synthetic strategies. α-$CeRh_{0.5}Ge_{1.5}$ is a tetragonal system crystallizing in the α-$ThSi_2$ structure type and β-$CeRh_{0.5}Ge_{1.5}$ is a hexagonal system, crystallizing in the AlB_2 structure type. The magnetic measurements of both $CeRh_{0.5}Ge_{1.5}$ phases suggest a possible spin glass behavior at low temperatures, due to randomness in the system with multiple magnetic transitions.*

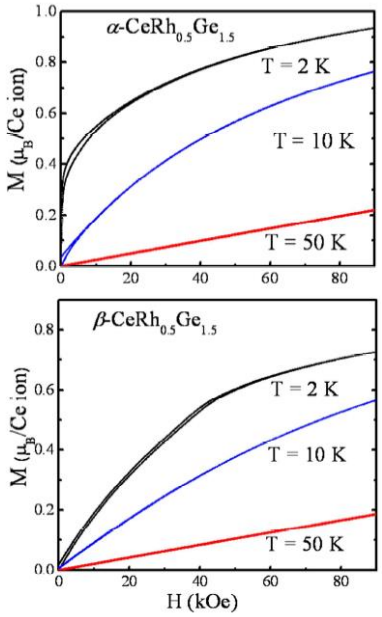

Fig. 4 *Magnetization measured as a function of ramping fields for two polymorphs of $CeRh_{0.5}Ge_{1.5}$ compound at various temperatures is shown here.*

ytterbium, where electrons or holes play a significant role in fluctuation between magnetic [$Ce^{3+}(4f^1)$, $Yb^{3+}(4f^{13})$] and nonmagnetic [$Ce^{4+}(4f^0)$,$Yb^{2+}(4f^{14})$] states makes the compounds more interesting as some of the compounds exhibit heavy Fermion behavior, superconductivity, Kondo anomalies, and spin glass behavior. Neutron diffraction experiments of these interesting compounds are expected to give insight into nuclear (crystalline) and magnetic structure, which will be important in understanding the structure-property correlations in these compounds. We have synthesized few compounds of this series, with a general formula of Ce_2TGe_3 (T = Rh, Ni, Pd, Pt, Co) and Yb_2AuGe_3.

In Figs. 1 and 2, the room temperature neutron diffraction pattern and magnetic properties of Ce_2NiGe_3 are shown. The compound crystallizes in a hexagonal unit cell. Detailed studies on these interesting compounds are currently under progress.

In Figs. 3 and 4, two polymorphs of Ce-Rh-Ge are shown along with their crystallographic structure and magnetic susceptibility behavior. Magnetization measured as a function of field is also shown in a separate figure.

An interesting observation made during the course of the Ce-Rh-Ge sample preparation was that depending upon the starting material and preparatory conditions, the compound exhibits two structure types. The low field magnetic susceptibility figure clearly exhibits the differences in the magnetic ordering temperatures and low field magnetization behavior. This study thus provides a convincing evidence of strong structure-property correlations in these strongly correlated electron systems.

Deepti Kalsi, Sebastian C. Peter (JNCASR, Bengaluru); S. Rayaprol

2.1.15. Synthesis and characterization of intermetallic compounds HoCoNi and Ce_4Ge_3

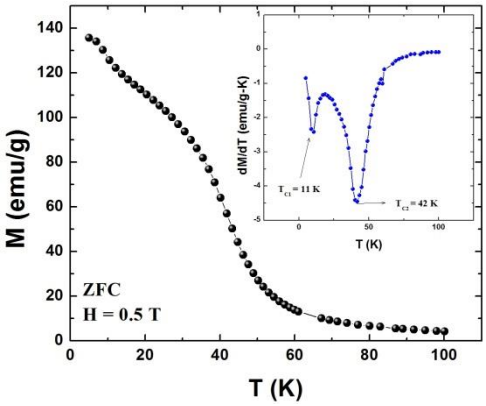

Fig. 1. *Magnetization (M) vs. temperature (T) of HoCoNi. Inset shows dM/dT with respect to temperature.*

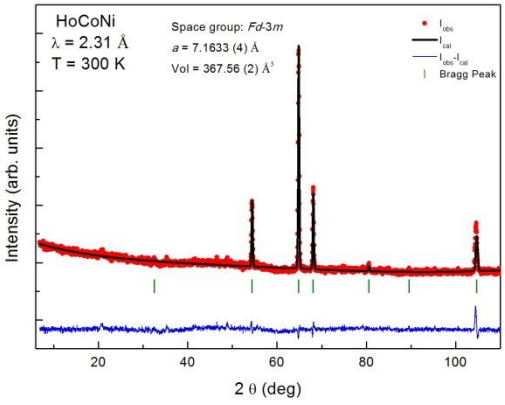

Fig. 2. *Room temperature neutron diffraction pattern of HoCoNi, refined using Rietveld method.*

Room temperature powder X ray diffraction data of HoCoNi compound confirm that it is in single phase, having $MgCu_2$ type cubic Laves phase structure as the parent compound $HoCo_2$ (Space group $Fd\bar{3}m$, No. 227). The EDAX results confirm the at.% composition of elements Ho:Co:Ni close to 1:1:1 ratio. Temperature variation of magnetization of HoCoNi compound, measured in 0.5 T field in ZFC and FC

conditions shows a transition from paramagnetic to ferromagnetic state at ~ 42 K (T_C). An additional transition has been observed at low temperature below T_C and it could be due to spin reorientation. Room temperature neutron diffraction pattern of HoCoNi has been obtained (wavelength 2.31 Å). We plan to do low temperature neutron diffraction experiments to understand about the magnetic transitions in this material.

Powder neutron diffraction pattern of Ce_4Ge_3 at room temperature corresponds to the X-ray diffraction finding that this sample has cubic, Th_3P_4-type structure. We plan to study low temperature magnetic structure of this compound, in the presence of applied magnetic fields in order to understand the nature of the metamagnetic transition observed at 2 K.

R. Nirmala (IIT-Madras); S. Rayaprol and V. Siruguri

2.1.16. Small angle neutron scattering for probing segmented morphology in polyurethane foams synthesized from castor oil

Small angle neutron scattering is used as the primary tool to probe the morphology of the segmented polymeric phase in polyurethane foams synthesized from castor oil. Fourier transform infrared spectroscopy (FTIR), Differential Scanning Calorimetry (DSC) and Atomic forced microscopy (AFM) are used as complementary techniques. The polyurea hard segment shows aggregation with increasing concentration of castor oil. This is shown by the gradually loosing periodicity of nano-scaled hard domains, dispersed in soft polyol segment as indicated by the gradual decrease in scattering intensity. AFM measurements give a ratifying visual description of the phase separation which supports the neutron scattering data.

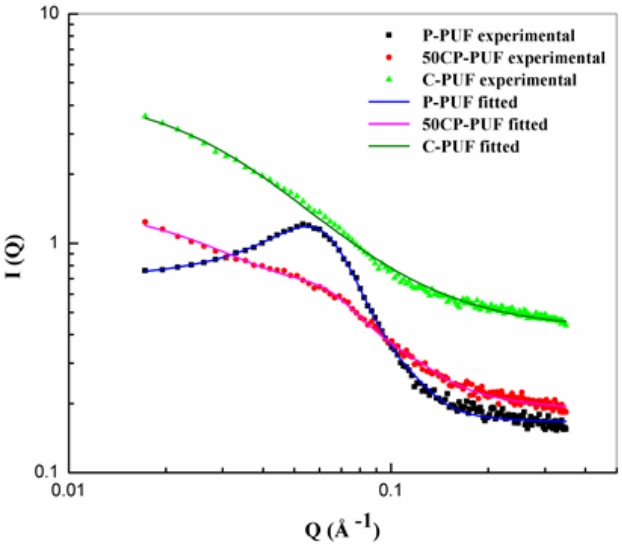

Fig. 1. *Neutron scattering from foams*

G. Harikrishnan (IIT-Kharagpur) and V.K. Aswal (BARC)

2.2. Collaborative Research at VECC, TIFR

2.2.1. Experimental study of the rotational band structure in ^{113}Sb

The odd-mass Sb (Z = 51) nuclei display diverse modes of excitations. While the low-energy states are mostly spherical and vibrational in nature, the ones at high energy have sizable collectivity. The level structures of these nuclei indicate a variety of rich structural information.

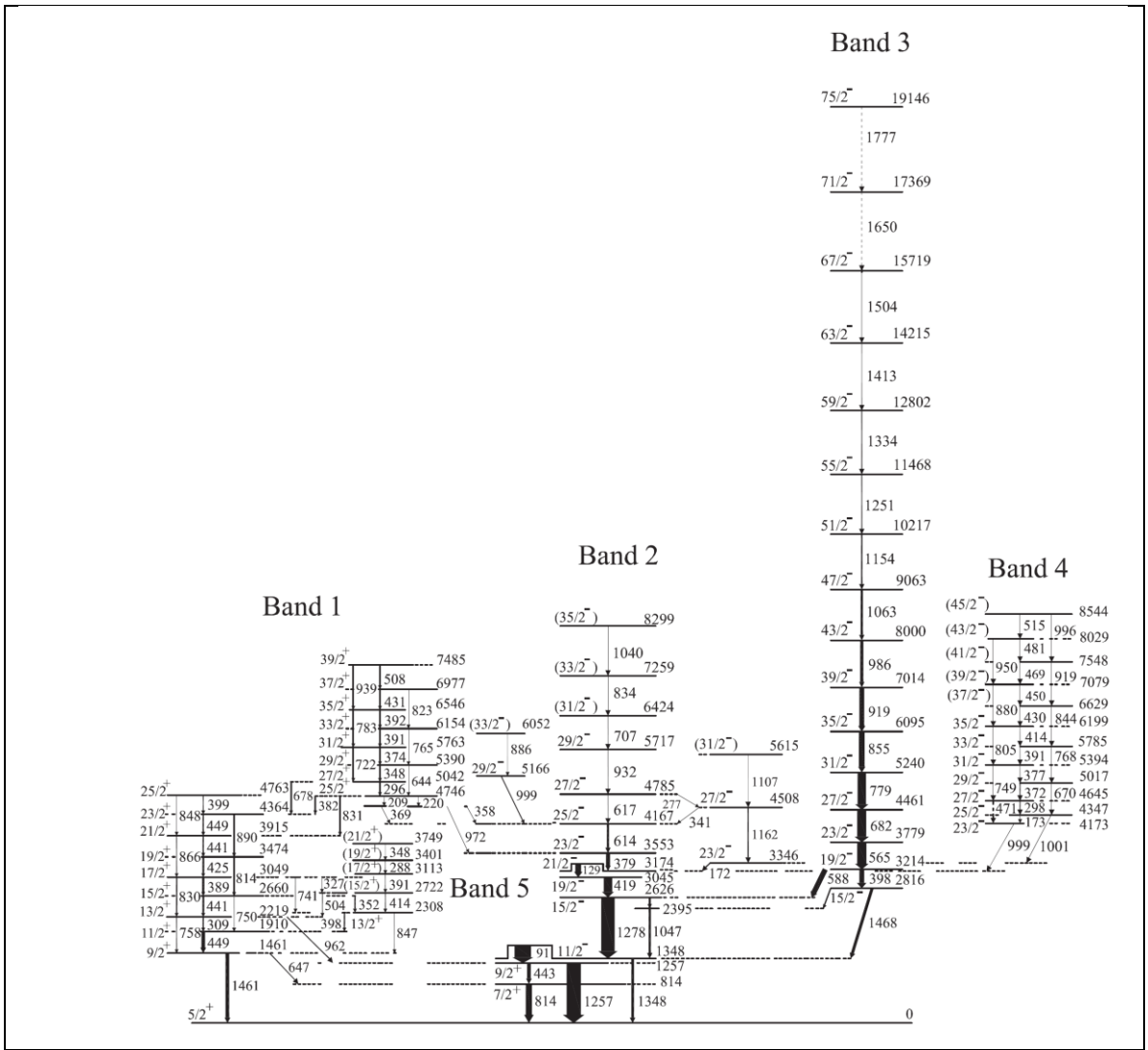

Level scheme of ^{113}Sb from present investigation

Excited states of ^{113}Sb, were populated in the ^{100}Mo(^{19}F, 6n□) reaction at a beam energy of 105 MeV, have been using the INGA at IUAC. Doppler Shift Attenuation Method (DSAM) was used to extract the level lifetimes of quite a few states in the two □I = 1 bands in this nucleus and has yielded unqiue information on the

underlying configurations in this nucleus. The level scheme of ^{113}Sb as deduced from the present investigation is presented in the figure below :

The investigation of rotational bands in ^{113}Sb has resulted in the extension of previously reported two strongly coupled high-*K* bands & several new sequences have been established. The transitions probabilities as deduced from the lifetime measurements indicate a plausible termination of bands at high spins in a non-collective oblate state.

S. Ganguly (Chandernagore College); M. K. Pradhan, P. Banerjee(SINP); H. P Sharma (VECC); S. Muralithar , R. P. Singh, R. K. Bhowmik (IUAC)

2.2.2. An effective Nuclear Model: from Nuclear Matter to Finite Nuclei

The primary objective was to construct a suitable finite range effective interaction that could be effectively used in nuclear calculations starting from finite nuclei to nuclear matter under extreme conditions of density, asymmetry and temperature. The finite range effective interaction was chosen as the starting point. The interaction is given by,

$$v_{eff}(\vec{r}) = t_0(1+x_0P_\sigma)\delta(\vec{r}) + \frac{1}{6}t_3(1+x_3P_\sigma)\left[\frac{\rho(\vec{R})}{1+b\rho(\vec{R})}\right]^\gamma \delta(\vec{r}) + (W + BP_\sigma - HP_\tau - MP_\sigma P_\tau)f(r) \qquad (1)$$

where, $f(r)$ is the functional form of a short range interaction of conventional form such as Yukawa, Gaussian or exponential and is specified by a single parameter α, the range of the interaction. The remaining symbols in Eqn. (1) have their usual meaning.

The Hartree-Fock (HF) calculation of finite nuclei with this simple effective interaction has been successfully carried out. The calculations using a Yukawa form for the potential have also been successful. Finally the Hartree-Fock (HF) calculation of finite nucleus with our simple finite range effective interaction (SEI) having Gaussian form factor has been successfully implemented. The formalism used here is the Density Functional Theory (DFT) where the energy density of the nucleus can be expressed in the local quantities, namely, the density, kinetic energy density and spin density and the other various contributions too have been worked out. Attempts are underway to include deformation effects, pairing etc in this formalism.

T R Routray, M M. Bhuyan, S.K.Tripathy, B.B.Dash, B.Behera (Sambalpur University): S K Patra (IOP): X. Vinas (University of Barcelona); D N Basu (VECC)

2.2.3. Magnetic Rotational Bands crossing and role of proton and neutron orbitals in Magnetic Rotation (MR) phenomena near A = 135 region.

The nuclei near A ~135 with the neutron number approaching towards N = 82 shell closure show shape driving effect at high spins with moderate deformation and display a variety of interesting phenomenon such as shape co-existence, Magnetic Rotation (MR) bands and MR band crossing. Nilsson diagram indicates that there are several positive parity states originating from g7/2, d5/2, d3/2 and s1/2 orbitals and a negative parity state originating from h11/2. For N = 78 odd-Z isotones, some of the dipole bands have been interpreted as Magnetic Rotation bands and possible MR band crossing has been reported in few cases. However, in contrast to its isotones, 135La has not been explored for the phenomena of MR. Therefore the present study was focussed on the investigation of the high spin states in this nucleus.

The high spin states in ^{135}La were populated by the reaction ^{128}Te (^{11}B, 4n) ^{135}La using a ^{11}B beam of 50.5 MeV from the pelletron accelerator at the Tata Institute of Fundamental Research (TIFR), Mumbai. This experiment was performed recently during the current INGA campaign at TIFR, Mumbai. . The level scheme of ^{135}La obtained from the presentwork as shown in the figure was constructed on the basis of a detailed analysis of the γ -ray intensity considerations and coincidence relationships obtained fromγ -γ and γ -γ -γ analysis. The present work besides verifying the previously reported levels also identified new levels.

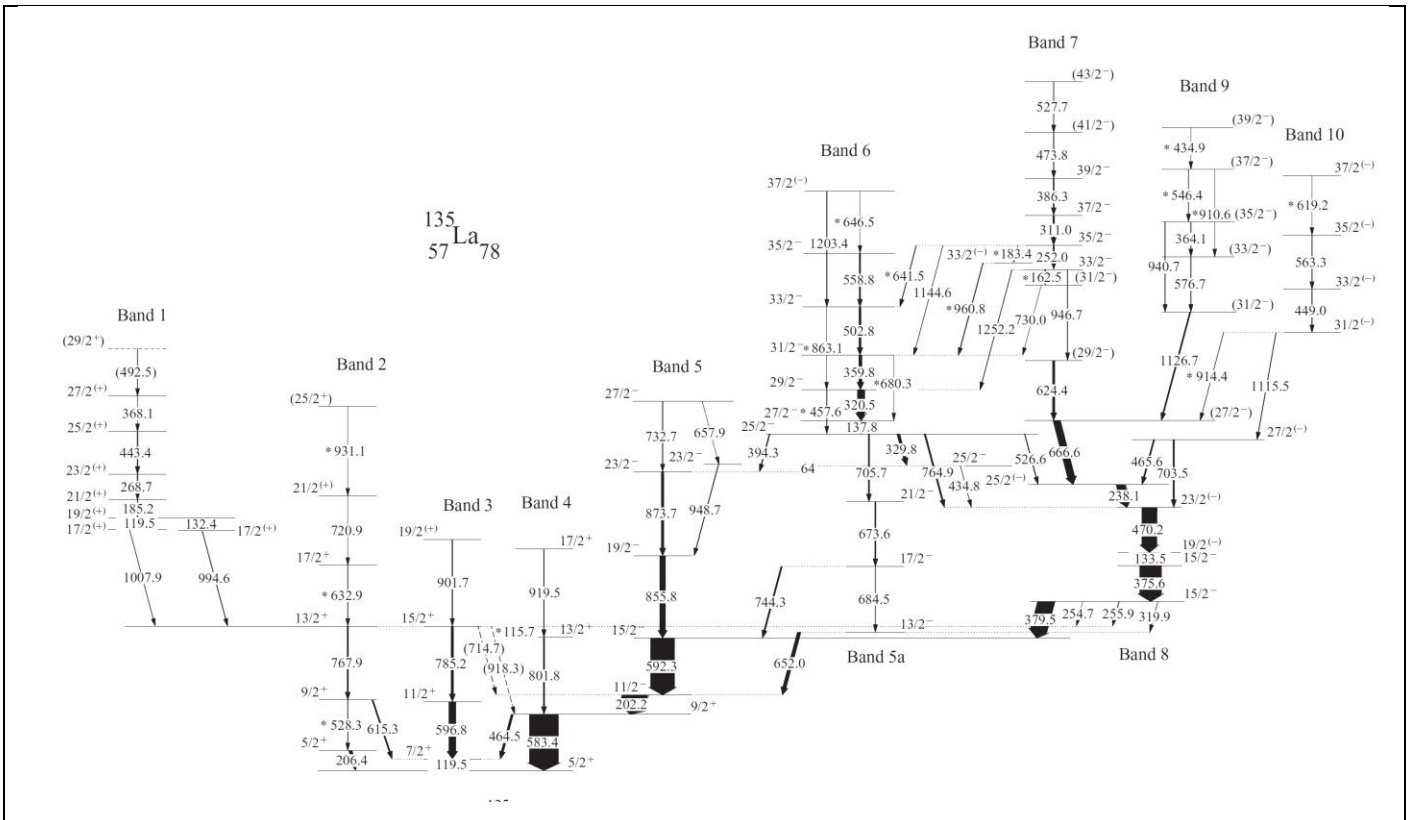

Level scheme of ^{135}La from the present investigation

A comparison with the theoretical models indicate that (i) the positive parity band (ΔI = 2) has been established and identified as a decoupled band ; (ii) two negative parity dipole bands have been observed and interpreted in

the framework of Tilted Axis Cranking model and configurations have been assigned to them. Lifetime measurements are essential to support the confirmation of the MR nature of the bands.

Ritika Garg, S. Kumar, Mansi Saxena, Savi Goyal, Davinder Siwal, Sunil Kalkal, S. Verma, S. Mandal, R. Singh, S. C. Pancholi (University of Delhi); R. Palit(TIFR); Deepika Choudhury, A. K. Jain (IIT Roorkee); S. S. Ghugre (UGC-DAE CSR,KC); G. Mukherjee (VECC); R. Kumar, S. Muralithar, R. K. Bhowmik and R. P. Singh (IUAC)

2.2.4. Nuclear structure effects on breakup and multi-nucleon transfer reactions.

Elastic scattering reactions are the simplest of all nuclear reactions. Precise measurements of the elastic angular distributions determine parameters of the real and imaginary parts of the nuclear interaction potential. From systematic analysis of elastic scattering measurements involving tightly bound nuclei, the so called "threshold anomaly" (TA) has been observed in a number of systems. In an earlier work, it has been observed that in heavy ion induced reactions, the projectile structure plays an important role. Particularly, in case of scattering of loosely bound projectiles a different type energy dependence from that of TA is observed, which has been known as `breakup threshold anomaly' (BTA). In case of BTA, a repulsive real dynamical potential is generated due to couplings of breakup channels to the elastic scattering. There are some contradictory observations regarding BTA. For ^{7}Li + ^{208}Pb, TA has been observed, whereas for ^{6}Li + ^{209}Bi, the BTA has been observed. Therefore, more measurements involving heavy targets and weakly bound projectile are essential to understand the systematics of TA and BTA, and motivated us to under take investigation of elastic scattering for ^{7}Li + ^{232}Th

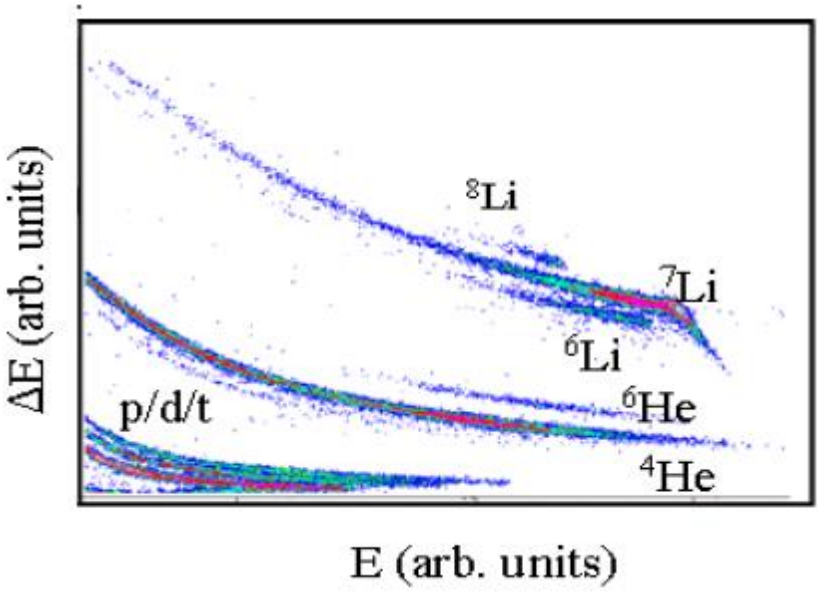

Typical ΔE Vs E spectrum for ^{7}Li + ^{232}Th system at θ lab= 60°.

The experiment was performed using ^{7}Li beam from BARC-TIFR Pelletron facility, Mumbai, India. the elastically scattered ^{7}Li ions were detected by four silicon surface barrier detectors in ΔE-E telescopic arrangements. Two monitor detectors with thickness around 300 μm were used for absolute normalization and beam monitoring. The elastic scattering angular distribution measurements were carried out for different beam energies covering a wide range from 24 to 44 MeV.

The optical model analysis of the elastic scattering data were performed using the SNOOPY8Q code. The best fitted optical model parameters show significant energy dependence, which is characteristic feature of the elastic scattering.

The experimental data have also been analyzed using the optical model with a phenomenological ECIS code potential. The preliminary analysis is indicative of (i) For the ^{6}Li +^{232}Th system the behaviour of the imaginary part of the phenomenological potential as a function of energy indicates the presence of the breakup threshold anomaly., (Ii) for the ^{7}Li + ^{232}Thsystem the behaviour of the corresponding parts of the potential as a function of energy is consistent with a situation close to the ordinary threshold anomaly observed in tightly bound nuclei.

Shradha Dubey, S. Mukherjee, D. Patel, N. N. Deshmukh, S. Appannababu, S. Mukherjee, (M. S. University of Baroda); Y.K. Gupta, G. Prajapati, V. V. Desai, B. N. Joshi, L.S. Danu, S.Mukhopadhyay, B.V. John, B.K. Nayak, D. C. Biswas (BARC)

2.2.5. Effect of projectile spin on fission fragment angular distribution for the system ^{13}C,^{14}N+^{238}U.

Fission fragment angular distribution measurements for ^{6,7}Li + ^{235,238}U systems were carried out using the 14 UD BARC-TIFR pelletron accelerator facility at Mumbai. Beam (^{6,7}Li) energies between 28 to 42 MeV in the step of 2 MeV have been used. Targets of ^{235,238}U of thickness ~280 μg/cm^2 were prepared by electro deposition on 750 μg/cm^2 Al foil as backing. The FFs were detected using five ΔE-E silicon surface barrier detectors of thickness 12-15 μ-m and 300 μm respectively. Two Si surface barrier detectors, kept at forward angles were used as monitor for absolute normalization of fission cross sections. Three telescopes (with ΔE ~50 μm and E~ 1000 μm) were also placed around the grazing angles to catch the light charged particles (with Z=1,2,3) in coincidence with the fission fragments to estimate the contribution from breakup induced fissions.

The angular distribution at each energy has been fitted with the expression given by Vandenbosch to obtain the value of fission fragment angular anisotropy by taking the ratio of differential cross section at 180^{o} to 90^{o}, i.e., W(180^{0})/W(90^{0}). It was observed that the FF anisotropies for ^{6,7}Li+^{238}U are consistent with the ones measured earlier by Freieselben *et al.*. It was found that the FF anisotropy values for ^{6,7}Li+^{238}U are larger compared to ^{6,7}Li+^{235}U at near barrier energies. This is possibly due to the difference in ground state spin of the two targets. The larger g.s. spin of 235U (7/2) broadens the k_0-distribution that results in reduced FF angular anisotropy ($A=1+\langle I^2\rangle/4k_0^2$).

It was also observed that the anisotropies of fission fragments from ^{7}Li fission are larger compared to ^{6}Li fission. This is probably due to the differences in the neutron-fission competition which favors later-chance

fission for the system formed with ^{7}Li. The anisotropy ratio, W(180^{0})/W(90^{0}), as a function of the bombarding energy for ^{6,7}Li+^{238}U shows structure which again seems to be connected with neutron-fission competition.

The elastic scattering of the ^{7}Li+^{159}Tb, ^{232}Th systems was investigated through very precise and complete angular distribution at energies from below the coulomb barrier to approximately twice this value. We have also derived the total reaction cross section for this system in order to investigate the role of BU (Break Up) on total reaction cross section. The comparison of these results with the earlier measurements using spherical targets would give some information on the Breakup Threshold Anomaly BTA.

The predicted values of anisotropy by SSP Model were found to reproduce the experimental anisotropies for ^{6,7}Li+^{235}U. However, for ^{6,7}Li+^{238}U systems, the SSPM calculations are on an average smaller than the experimental anisotropies. These calculations do not include the effect of (i) target g.s. spin and (ii) projectile breakup.

Total fission cross section for a particular energy was obtained by integrating the measured FF angular distributions with respect to angles. The angle integrated fission cross sections for ^{6}Li at low bombarding energies were found to be larger than those of ^{7}Li induced fission. This could be understood in terms of larger contribution of breakup fragment induced fission for ^{6}Li than ^{7}Li due to smaller breakup threshold of the former compared to the latter.

N L Singh, A Parihari(M. S. University of Baroda); S Santra, K Mahata, P. K. Rath, K. Ramchandran, B. K Nayak, A. Pal, R. Chakrabarti, S Kailas (BARC); Sushil K Sharma(TIFR)

2.2.6. Reverse micelle mediated room temperature synthesis of highly luminescent rare earth phosphate nanoparticles

Trivalent lanthanide ions display fascinating optical properties. The discovery of the corresponding elements and their fist industrial uses were intimately linked to their optical properties. This relationship has been kept alive until today when many high-technology applications of lanthanide-containing materials such as energy -saving lighting devices, displays, optical fibers and amplifiers, lasers, responsive luminescent stains for biomedical analyses and *in cellulo* sensing and imaging heavily rely on the brilliant and pure-color emission of lanthanide ions. Ln^{3+}-doped lanthanide orthophosphate have been applied in light-emitting devices, laser hosts, catalysts and as markers for biomolecules, such as Ln^{3+}-doped LnPO4 colloidal nanoparticles synthesized in boiling organic solvent exhibited multicolor emission had a strong potential application in biosensors. Herein, we have investigated synthesis of highly luminescent lanthanide doped rare earth phosphate nanoparticles using reverse micellar approach at room temperature.

Nanostructured lanthanum phosphates has been prepared by using AOT/n-heptane reverse micelle at room temperature. Aqueous solution of Lanthanum nitrate hexahydrate ($La(NO_3)_3$.6H2O) and Sodium di-hydrogen phosphate (NaH_2PO_4), each of strength 0.05 M were used as precursors during the synthesis. Two reverse micelles were made individually enclosing aqueous solution of lanthanum nitrate and Sodium di-hydrogen phosphate at different ω and were then mixed together and subjected to rapid mechanical stirring at 1000 rpm for three hours. The reverse micelles present in the organic phase move around in the entire volume

of the organic phase in a random Brownian motion and hence, collide with each other. In consequence of continuous coalescence and decoalescence process, the content of the water pools of the two reverse micelles was distributed evenly over the entire droplet population and reaction could occur inside the droplets. As a consequence, nanostructured lanthanum phosphates were formed. Doping concentration of rare earth ions, Ce^{3+} and Tb^{3+} were kept at 0.05 M for both and maximum of 33% (by vol) doping were maintained throughout the synthesis process.

S. Chall, S. C. Bhattacharya (Jadavpur Univ); S. and A. Saha

2.2.7. Radiation Induced Synthesis of Metal Clusters: Effect of Dose Rate and LET

The noble metal nanoparticles become marvelous as a consequence of their extensive catalytic, electro catalytic, biosensing, and magnetic properties. A range of physical and chemical methods have been utilized to prepare nanomaterials and several of these are anchored by the use of a structure–directing template. We used "soft" templates of swollen liquid crystals (SLC) in preparation of nanomaterials using radiation chemical tool. The Swollen liquid crystals (SLC) using the cationic/anionic surfactant were synthesized by dissolving CTAB/SDS in water containing various noble metal salts. The reductions of doped mesophases were carried out with ^{60}Co gamma source at Department of chemistry University of Pune/UGC-DAE-CSR Kolkata. A homogenous black gel was destabilized using isopropyl alcohol and nanostructures were extracted by centrifugation and then dried in oven at 60^{o} C. We observe dose dependent formation of porous nanostructures within the soft template.

The characterization was done by using UV-Vis spectrophotometer. It is clear that radiation chemical techniquee can be effectively used for the reduction of metal precursor in the SLC template (Fig.1) The DLS data shows the size of 3-4 nm due to interconnected network of nanowires. This interconnected network was proved by TEM analysis which shows that the network of nanowires aggregated into a ball shaped domain with 50-100 nm diameter. (Fig.2)

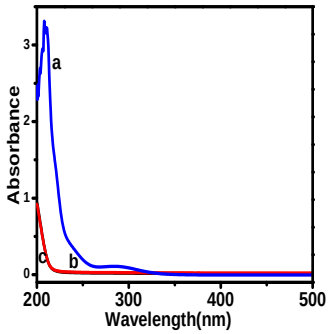

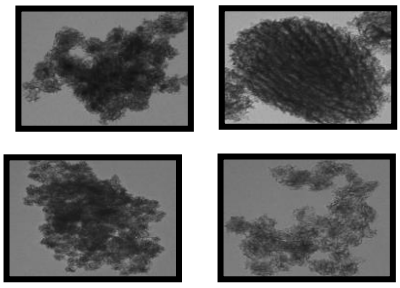

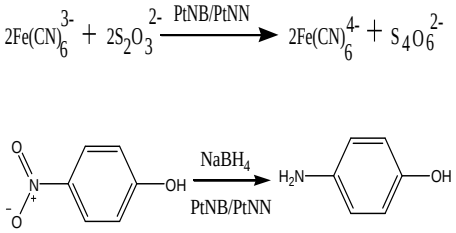

Fig. 1 Fig.2 Fig.3

These synthesized nanomaterials were effectively used to study the a) Catalytic reduction of p-Nitro phenol (PNP) to p-Amino phenol (PAP), b) Catalytic electron transfer reaction between hexacyanoferrate (III) and Thiosulfate anion, c) Catalytic application in Suzuki reaction. Kinetics of these reactions (Fig.3) was studied in

detail. In conclusion we have successfully synthesized the porous nanostructures by radiation chemical techniques and applied these nanostructures in various catalytic reactions.

A. Kalekar (Pune University); G. Sharma (Pune University;) A. Saha

2.2.8. Radiation Induced Modification of DNA and Some Pyrimidine Nucleosides and Nucleotides

Radiation chemical studies of 2'-deoxythymidine (2'-DT) were carried out in the initial stage. In the case of reaction of hydrated electron, more than 90% of the parent compound was disappeared within an absorbed dose of 1 kGy. The extent of degradation in the case of irradiated samples were determined by HPLC. In order to get more information about the details of transformation products, LC-MS analysis was carried out on an HPLC coupled with a single quadruple mass spectrometer (Waters). Presence of thymine in irradiated samples were confirmed by the results obtained from LC-MS analysis in both positive and negative ionization mode. However we didn't get the information of any other products in the case of hydrated electron reaction of 2'-DT. Sulfate radical and superoxide radical was also found to cause damage in the parent compound.

Free radical chemistry of some pharmaceutically active molecules (example - methylxanthine drugs) having structural similarity with purine bases can also give rise to valuable mechanistic insights in to DNA damage/repair. Hence pulse radiolysis studies were carried out on theophylline (T), structural analogue of purine, with different oxidizing radicals ($^{\bullet}OH$, $SO_4^{\bullet-}$ and $N_3^{\bullet}$). The bimolecular rate constant of theophylline with different oxidizing radicals were found to be > 10^9 $M^{-1}S^{-1}$, that is near diffusion controlled. From the transient spectrum, we conclude that the primary path of theophylline on its reaction with $^{\bullet}OH$ was addition at C8 followed by addition at C4, which leads to two different hydroxyl radical adduct radicals. However, specific one electron oxidants such as $SO_4^{\bullet-}$ and $N_3^{\bullet}$ generate radical cation of theophylline. Oxide radical anion ($O^{\bullet-}$), widely known to undergo hydrogen abstraction reaction, generates two different hydrogen abstracted radical species (obtained from transient intermediate spectrum as well as bimolecular rate determination) and hence hydrogen abstraction at both methyl side chains of theophylline was very plausible. However more end product studies are required for probing a complete transformation mechanism.

Other than these work, we have also investigated the degradation (induced by $^{\bullet}OH$) of some model pollutants (fensulfothion, a widely used soil insecticide and nematicide). From the transient absorption spectra, different intermediate species generated in the reaction were determined. About 20 stable transformation products were identified by UPLC-MS/MS analysis. The major reaction of $^{\bullet}OH$ with fensulfothion was determined as one electron oxidation at sulfur atom in the side chain leading to the formation of sulfur centered radical cation followed by hydroxyl radical addition at both of the ipso positions. However, a very low TOC reduction is observed in this case even though a complete transformation of the parent compound is obtained. The data obtained was very much helpful for probing a complete degradation mechanism of fensulfothion and similar compounds. This work is currently accepted in *Chemosphere*.

S. K. Mathews, C.T. Aravindkumar (Mahatma Gandhi University); A. Saha

2.2.9. Study of Effect of Radiation on the Metalloid/ Oxide Incorporated Polymeric High Temperature Resistive Flexible Nano-Composite Thin Films for Microelectronics Application

Films of polymers Polycarbonate (PC) and Polysulfone (PS) (Virgin or pure) and Composites films of these incorporating metalloid (Fe) and Oxide (TiO_2) have been prepared. The effects of gamma irradiation on various metalloid/oxide incorporated flims have been studied with UV-vis and FTIR spectroscopy. FT-IR spectra of Pure PS and TiO_2 incorporated PS have been obtained and being analyzed. FT-IR spectra of Pure PS and Fe incorporated PS have been obtained and being analyzed. DSC measurement have been undertaken in limited number of samples of Pure PC and Fe incorporated PC the variation in T_g and thermal properties due to palm leaf incorporation in different amount are being analyzed. Microhardness studies have been performed on prepared fly ash reinforced polymethyl methacralate (PMMA) composite matrices to monitor elastic and plastic behavior of the films.

Arunendra Kumar Patel, R. Bajpai, J.M.Keller (Rani Durgavati University); A. Saha

2.2.10. Comprehensive study on radiation induced metal tolerance in fungi

Environmental contaminations through discharge of heavy metals are causing an alarming situation in recent years. Along with heavy metal pollution, lignocellulosic wastes added an extra pollution load to the society. For proper abatement of heavy metal pollution, most of chemical and physical treatment procedures are not only costly but also less effective. As such, bioremediation is now attaining more focus and considered as an effective tool for abatement of metal pollution for its low cost and high efficacy. Among different microorganisms fungi are considered as potential bio-remediators due to their higher surface to volume ratio. At the same time fungi are important source of lingo- cellulosic waste degradation enzymes (like cellulase and amylase).

Irradiation treatment is one of the effective strain improving method in fungi. Cordeiro et al., (1995) reported that exposure to gamma showed maximum potential to induce mutation in fungi (*Metarhizium anisopliae)* than that of UV or other chemical mutagens. In this study attempts have been made to establish the potential of gamma in modulating metal tolerance as well as enzyme activity.

50 fungal strains were isolated from soils near garbage dump site of Dhapa, Kolkata, among which four sensitive and tolerant strains (two *Aspergillus sp* and two *Penicillium sp*) were selected for further experiments depending on MIC values against Cd, Zn and Pb. Gamma exposed group of *A.niger* showed 1.5 times and *A terreus* showed 1.12 times more zinc tolerance than the unirradiated ones which are reflected in terms of their change in CFU (colony forming unit), mycelial accumulation and removal potential. Similarly gamma irradiated group of *A.terreus* shown 1.6 times more cadmium tolerance than unirradiated counterparts while for *Penicillium cyclopium*, it is 1.2 times. Flow cytometric determination of metallothionein revealed that with zinc and cadmium treatment, metallothionein expression has been increased with respect to control (isolated from soil), further enhancement occurred with gamma dose. It may be concluded that low doses of gamma radiation has the potential to increase metallo-resistance by means of enhancement of metallothionein expression in fungi. Gamma radiation causes dose dependent linear response in modulation of fungal amylase and cellulase

activity under heavy metal stress and is metal specific. e,g maximum increase in activity of amylase and cellulase activity was noted in the range of 80Gy - 100Gy in case of Pb while against Zn the effective dose was 100 Gy for *A.niger*.

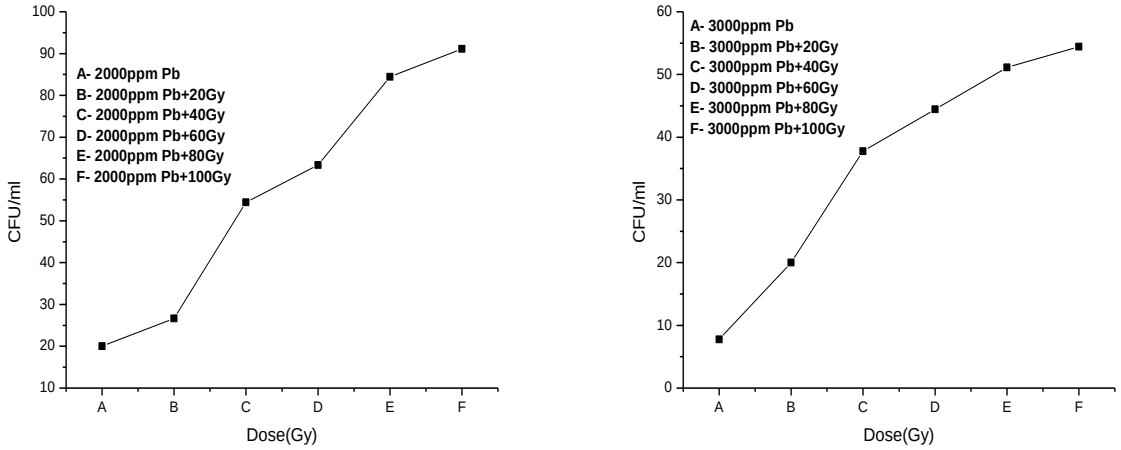

Fig 1- Colony forming unit of irradiated Aspergillus niger with different doses of gamma rays and grown in medium enriched with different conc. of Pb. [n=6].

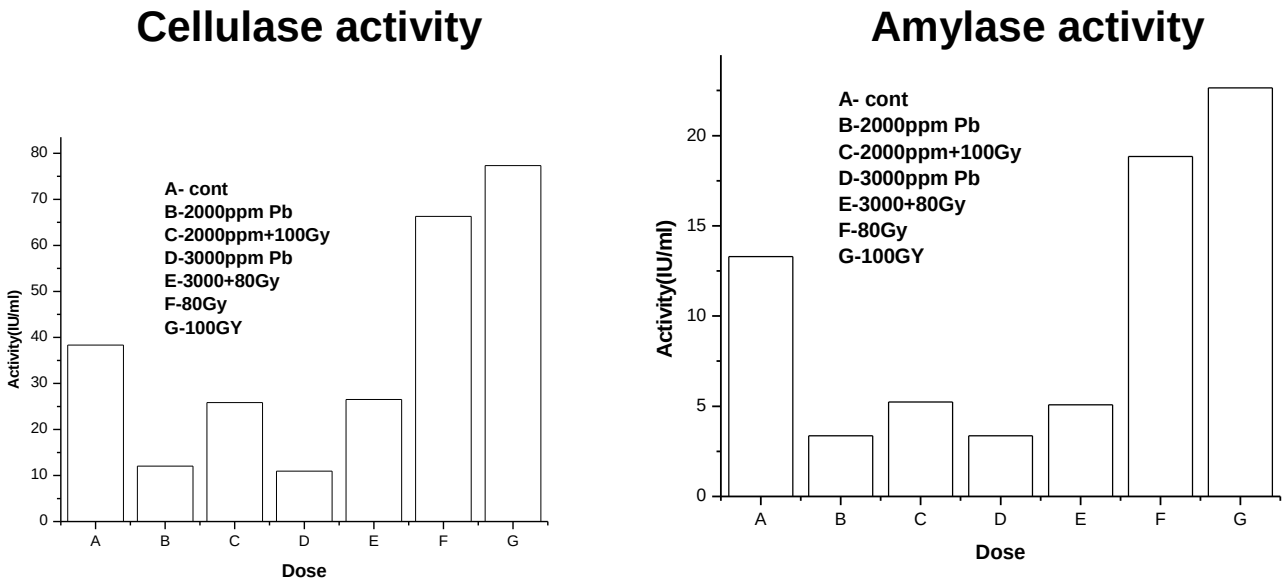

Fig-2 Amylase and Cellulase activity of A.niger under individual lead, gamma stress and under combined stress w.r.t control

Dipanwita Das, S.C.Santra (Kalyani University); Anindita Chakraborty

2.2.11. Radiation Induced Alterations in DNA, RNA and Polyamine level in plants

Aim of this study to understand the stress-induced changes in metallothionein expression in *Plantago ovata*. Seedling injury, chlorophyll and proline content were estimated to study the stress response in *P.ovata* following exposure to gamma irradiation and cadmium chloride. Effects of these stress inducible agents on metallothionein gene and protein expression were further investigated using PCR, RT-PCR, immunocytochemistry and flow cytometry. Both the stresses increased seedling injury and proline content but decreased chlorophyll content. These genes namely *PoMT1*, *PoMT2* and *PoMT3* were isolated, sequenced and characterized. Expression of these three genes was found to alter in a dose dependent and tissue specific manner in both the cases. The results were in agreement with the observations of immunocytochemistry and FACS analysis of metallothionein protein. Results indicated differential gene expression upon exposure to different agents imparting oxidative stress. It is conjectured that the redox balance is maintained by altered gene expression. Metallothionein increase in dose dependent manner indicates maintenance of cellular homeostasis.

Nirmalya Ghoshal, Sarmistha Raychaudhuri (Calcutta University); Anindita Chakraborty

2.2.12. Arsenic induced genotoxicity and modulation of trace elements in mammalian cells

Arsenic (As), a Group I human carcinogen, is the major source of ground water contamination all over the world. The permissible limit of As, set by World Health Organization (WHO) is 10 parts per billion (ppb). However, in many countries including India and Bangladesh, people are consuming As through drinking water at much higher level. Up to 50 ppm of As is reported in many states in the USA. The Swiss albino mice were treated with different concentrations of Arsenic trioxide (As_2O_3) both orally (adlibitum) and through itraperitoneal (i.p) injection. For i.p injection the doses were 2mg/kg body weight and 4mg/kg body weight and for oral administration the doses used, were 0.4mg/L(ppm), 0.8 ppm, 2ppm and 4ppm for one month duration. At the end of the treatment period, tissues (liver, kidney, spleen and skin) were dissected out, blotted properly, lyophilized and grounded in an agate mortar. The tissue samples were analyzed by Xenemetrix EX-3600 ED-XRF system. The modulation of the trace element profile was then checked by comparing with the control. For a number of elements (Copper, Manganese, Iron, Potassium, Sulphur), differential modulatory effect with low (0.4 mg/L) and high dose (4mg/L) exposure for short and long time period (15 days, 1 month) was observed. In this preliminary study we observed that Arsenic (As) exposure in male Swiss albino mice for one month and 15 days through drinking water can modulate the trace element profile in different tissues. A total of 10 elements were recorded in As-untreated and treated mice by Energy Dispersive X-ray Fluorescence (EDXRF) study. The pattern of modulation of elements was not uniform but tissue specific.

Further experiments were done with selected doses of BSO i.e., 50 mg/kg bw (body weight) and 100 mg/kg bw, 10 hours prior to sacrifice and one dose of BSO i.e., BSO 200mg/kg bw one hour prior to colchicine injection. For combined treatment of BSO and arsenic 200mg/kg bw of BSO was used dose and arsenic doses were 4mg/kg As_2O_3 and 8mg/kg As_2O_3.

Based on the results obtained from the FACS study showing interesting trend in arsenic treated mice bone marrow and spleen cells with apoptotic induction clearly evidenced in the spleen of arsenic treated mice (detailed in previous years report), this year western blot analysis and Rt-PCR of Nrf2 were performed with the BSO treated and arsenic treated mice. Whole cell protein extracts and western blot analysis were performed and the total RNA Extraction and RT-PCR Analysis were performed in liver tissue.Our results showed that 0.4ppm, 2ppm, 4ppm arsenic trioxide treatment through drinking water for 30 days and 90 days induction of heat shock protein70, together with modulation of trace elements, Cellular Nrf2 protein level and mRNA level increased in all treatment groups. Keap1 protein as well as mRNA level decreased concomitantly in arsenic treated mice

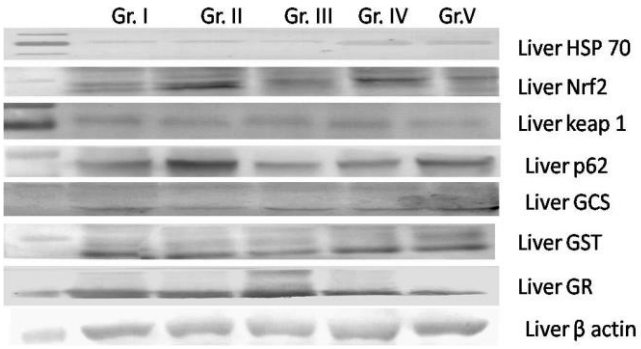

Fig. Western blotting of the Hsp 70, Nrf2, Keap1, p62, GCS, GST and GR protein profile of liver of mice treated with different doses of As_2O_3(Group I:Untreated animals (Control), Group II: 0.4 ppm As_2O_3 treated through drinking water for 30 days, Group III: 2 ppm As_2O_3treated through drinking water for 30 days, Group IV: 4 ppm As_2O_3 treated through drinking water for 30 days, Group V: 4 ppm As_2O_3 treated through drinking water for 90 days)

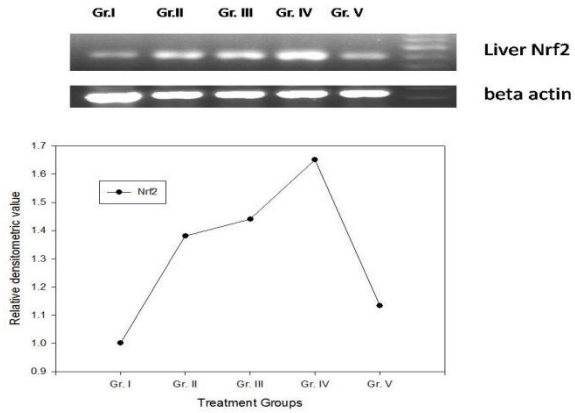

Fig. RT PCR and densitometric analysis of the Nrf2, of liver of mice treated with different doses of As_2O_3 (Group I: Untreated animals (Control), Group II: 0.4 ppm As_2O_3 treated through drinking water for 30 days, Group III: 2 ppm As_2O_3treated through drinking water for 30 days, Group IV: 4 ppm As_2O_3 treated through drinking water for 30 days, Group V: 4 ppm As_2O_3 treated through drinking water for 90 days)

Hoechst 33342 Staining in hepatocytes:

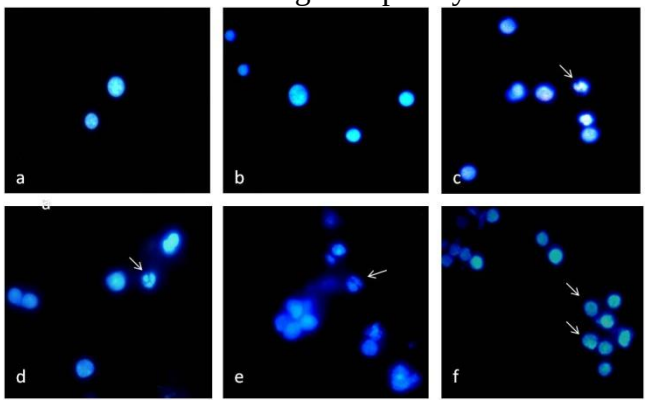

Fig. Mouse hepatocytes showing apoptosis (arrow) by Hoechst 33342 staining ; control (a and b), after 30 days arsenic trioxide treatment with different doses 0.4ppm (c), 2ppm (d), 4ppm (e) and 90 days arsenic trioxide treatment with the dose of 4ppm (f).

Anshuman Chatterjee, Ritu (Viswabharati); M.Sudarshan, Anindita Chakraborty (UGC-DAE CSR KC)

2.2.13. Studies on trace element distribution and their role in salt stress adaptation in halophytic plants of mangrove vegetation of West Bengal

Trace elements mostly present in the sediment, in the mixture zone of fresh water and salt water, is accumulated in plants and animals through usual uptake and assimilation process and play a crucial role in salt stress adaptation of mangrove vegetation. Due to rapid deposition of trace metal from water phase to sediment in the saline environment, the bioavailability of trace metals in mangrove vegetated deltas are fairly high and thus uptake of trace elements is very significant in mangrove plants. This work attempts to study the distribution and localization of trace elements in in salt tolerant plants of Sundarban, West Bengal and the interaction among mangrove plant pigments, leaf element and water salinity.

Three mangrove plants (*Avicennia officinales, Excoecaria agallocha and Acanthus illicifolious*) were selected for sampling. Plants parts (leaf, stem and roots) were collected from five sampling sites (Canning, Hemnagar, Chemaguri, Jharkhali and Henry islands). Water and Surface sediment sample were also collected from the same sampling sites and were analyzed in the trace elemental lab, UGC DAE CSR, Kolkata Centre, India.

Samples were freezedried in Vortis Freezedrier, homogenized by agate mortar and made into pellets (1 mm thick and 13 mm diameter) using a tabletop KBR pelletizer . Three replicates were made for each sampling site. The elemental analysis was carried out using a Xenemetrix EDXRF spectrometer.

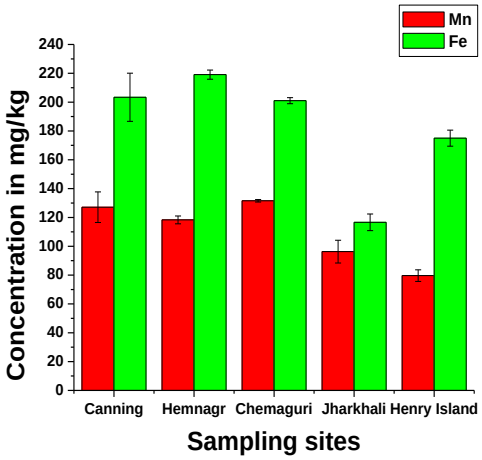

Leaf Elemental (Mn, Fe)
Concentration in *Avicennia officinales*

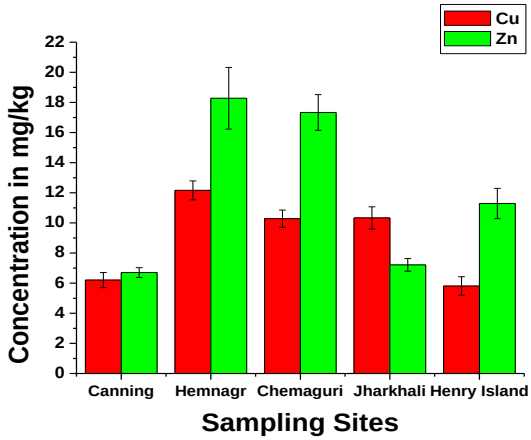

Leaf Elemental (Cu, Zn)
Concentration in *Avicennia officinales*

Elements like Mg, P, S, K, Ca, Mn, Fe, Cu, Zn. Mg, P, S, K and Ca were detected in the different plant parts *A. officinales from most of the sampling sites* showed highest conc.of a few elements in the lef as compared to the root and bark excepting that from Hemnagar where max conc was noted in stem bark while the same palnt showed max conc of elements in root when collected from Henry island. Leaf of the plants collected from Canning and Hemnagar reflected similar trend of elemental concentration(Mg<P<S<K<Ca) (Fe>Mn>Zn>Cu) while Jharkhali and Henry island followed same trend (K>Ca>Mg>S>P) (Mn>Fe>Zn>Cu).

However there was no similarity in such trend in case of stem bark or root in case of Mg, P,S,K, Ca. On the other ahnd Fe,Mn,Zn,Cu in the stem bark showed similar trend in Canning,Henry Island Hemnagar and Jharkhali followed same trend (Fe>Mn>Zn>Cu).

Elemental concentration of Surface sedmint sample in Premonsoon Season:

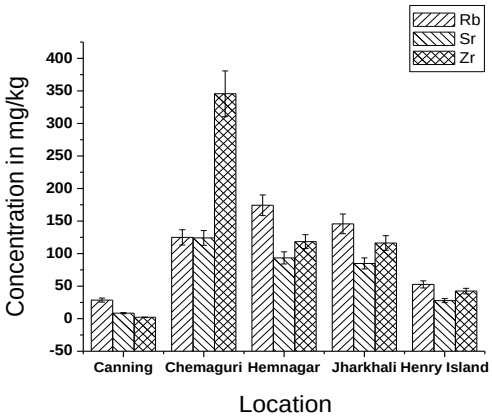

Elemental concentration of Surface sediment sample in Premonsoon Season:

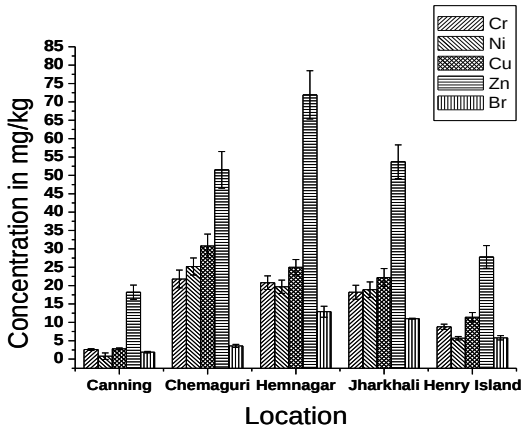

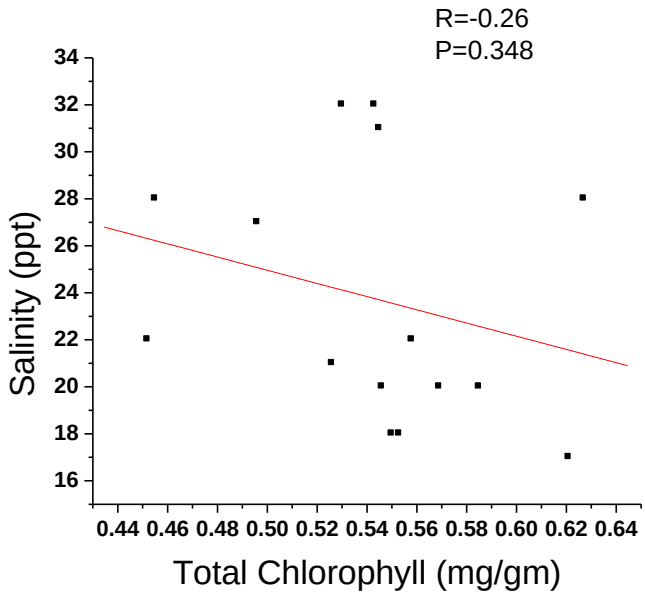

Excoecaria agallocha

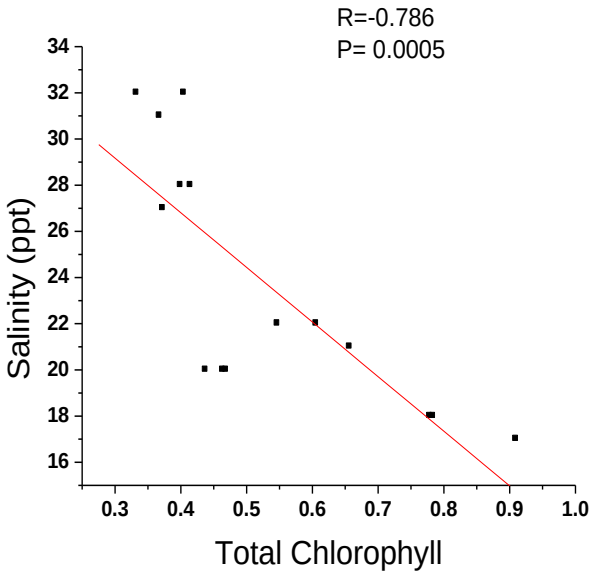

Avicennia officinales

Several elements were detected, like- Al, Si, K, Ca, Ti, V, Cr, Mn, Fe, Ni, Cu, Zn, Br, Sr, Rb, Zr in surface sediment, Fe concentration was observed to be higher than all other elements. Concof Cr, Cu, Ni and Zn were like Zn>Cu>Cr>Ni in all four study sites wheras Rb, Sr, Zr, reflected the trend Rb>Zr>Sr in Hemnagar, Jharkhali and Henry Island except Canning.

Significant difference between Chlorophyll a was noted in *Excoecaria sp*., *Avicennia sp* and *Acanthus sp.* collected from different sites. Total Chlorophyll, Chlorophyll a was negatively correlated with water salinity in *Avicennia sp.and Excoecaria sp*. Decrease in ratio of Chlorophyll a and b indicates chlorophyll a is the sensitive component of photosynthetic pigments.

S. Bhar, S.C. Santra, (University of Kalyani); Anindita Chakraborty and M. Sudarshan

2.2.14. Developing a laboratory scale biofilm based metal removal system using heavy metal tolerant radioresistant marine coastal microbes

Marine microbes play an important role in the cycle of sea-water matter, the objective was to isolate heavy metal accumulating radio tolerant bacteria from marine coastal region. It would ensure screening out potential microbes which can survive under extreme conditions and at the same time bears the efficiency of heavy metal accumulation in order to detoxify the environment.

Lead is a common contaminant of water body, the source of which is mainly from battery industry. It leads to various problems in human health. In adults, lead is linked to reproductive and nervous system problems, high blood pressure, kidney damage, memory and concentration difficulties and, in high amounts, coma, convulsions and death. At particular risk are children who may suffer from brain or nervous system damage, behavioral and learning problems and slowed growth.

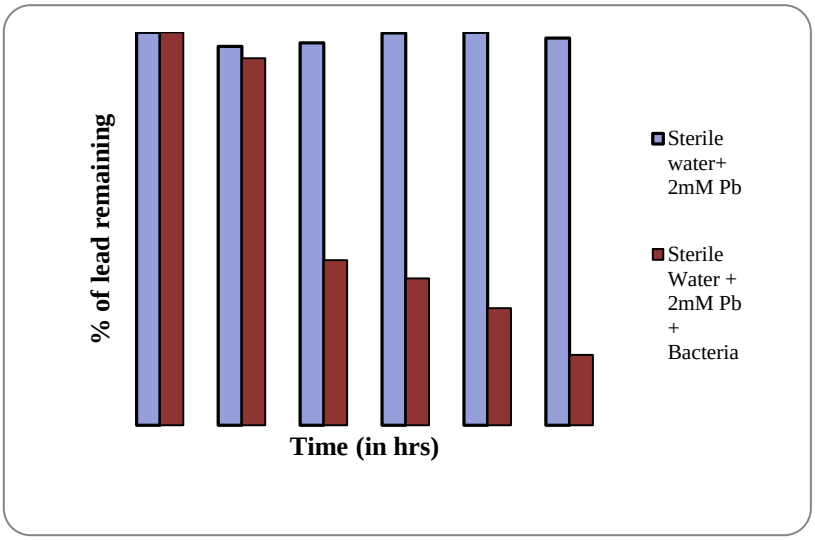

Fig. 1.a. *Representing the efficiency of lead removal by immobilized consortium supplemented with 2mM $Pb(NO_3)_2$. It was found that the concentration of lead in sterile water supplemented with 2mM $Pb(NO_3)_2$ remained almost same, but it gradually decreased with time in another set where consortium was inoculated. After 6 hours of incubation more than 50% of $Pb(NO_3)_2$ was removed and at 48^{th} hour the efficiency of removal reached to 82.06%.*

Significant amount of intracellular lead accumulation was found among all of the isolates. Therefore, a bioremedial package was developed which would help to reduce the lead concentration from the contaminant water body.

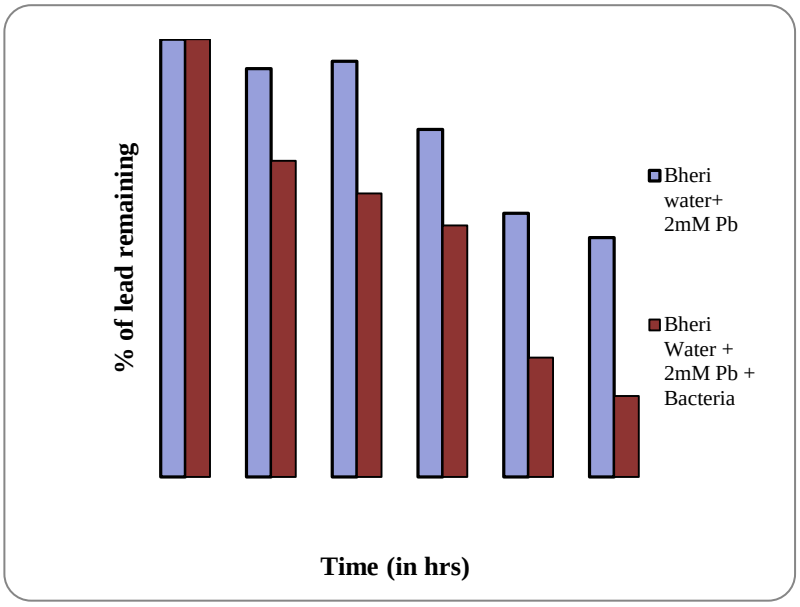

Fig. 1.b. *Representing the efficiency of lead removal by immobilized consortium from water body contaminated with heavy metal like lead. Two sets of unsterilized Bheri water was supplemented with 2mM $Pb(NO_3)_2$. In one set no immobilized consortium was added, where in first 6 hours no significant reduction was found. After 12^{th} and 48^{th} hours 20.62% and 45.35% reduction was observed. But when consortium was added in another set, the removal of lead increased to 42.56% and 81.52% of $Pb(NO_3)_2$ after 12^{th} and 48^{th} hour respectively.*

The ability of removing lead from sterile distilled water supplemented with Lead was checked by the addition of sodium alginate beads containing consortium and it was compared with the control set where no consortium was added. It was found that in control set the concentration of lead remained almost same for 3^{rd}, 6^{th}, 12^{th}, 24^{th} and 48^{th} hours in respect to the 0^{th} hour sample. The little variation of $Pb(NO_3)_2$ concentration found might be due to some precipitation of lead salts in time of incubation or instrumental error, which lies within a certain range. Whereas in the second set in which sodium alginate bead with consortium was added, 6.60% reduction was found within first 3 hours, which was negligible. But after that in next 3 hours (6^{th} hour's sample) the reduction was more than 50% (57.96%). At the end of 48^{th} hour 82.06% reduction of lead salts was observed (Fig. 1.a).

The next attempt was to check the efficiency of the consortium for removing lead from contaminated water body like Bheri. When Bheri water was supplemented with 2mM $Pb(NO_3)_2$ and kept at static condition for observation of the activity of indigenous microbes, only 5.04% reduction of lead was found after 6^{th} hr, then it reached to 20.62% after 12^{th} hour. Indigenous microbes were able to reduce 45.35% of lead from the solution after 48^{th} hour (Fig. 1.b). When Bheri water supplemented with lead was incubated with immobilized consortium 27.32% reduction of lead salts were observed within first 3 hours. After 6^{th}, 12^{th} and 24^{th} hours 35.19%, 42.56% and 72.77% lead reduction was observed (Fig. 2-5.b), which was higher than the reduction in the sterile water done by the consortium at particular time. This might be due to the synergistic effect of indigenous microbes and the immobilized consortium and as a result of their combined reduction efficiency; the percentage of reduction of the metal was increased as reflected in the result. But at the end of 48^{th} hour the efficiency of lead removal (81.52%) from Bheri water by immobilized consortium in presence of indigenous microbes was comparable with sterile water incubated with consortium (82.06%). From this we can conclude that immobilized consortium were efficiently able to reduce the metal concentration from sterile water as well

as natural water bodies contaminated with metal salts like lead. So this could be tried in ex-situ condition for bioremediation purpose as evident from the in-situ lab scale trial.

S.Das, S. Ray Chaudhuri, I. Mukherjee (WBUT); M.Sudarshan, A. Chakraborty and A.R. Thakur

2.2.15. Influence of Trace elements in immune functions in visceral leishmaniasis and postm kala-azar dermal leishmaniasis of India

Visceral leishmaniasis (VL) is an infection caused by *Leishmania* protozoa, which are usually transmitted by the bite of phlebotomine sand flies. It is endemic in 88 countries and India has about 50 per cent of the global burden of VL. To find out influence of trace element in different clinical forms of Indian leishmaniasis, blood samples of patients suffering from VL were collected from an endemic zone (Bihar) of India. The work aims to probe into the role of trace elements in the immune response towards the parasite which could help in developing strategies for therapy as well as immunoprophylactic measures against Indian forms of Leishmaniasis. For this different treatment regimes were considered using Amphotericin B, a common drug treatment for VL. Three groups of patients – Untreated (UT), Incomplete treatment(ICT) and complete treatment (CT) – were considered to compare with the healthy controls(HT).

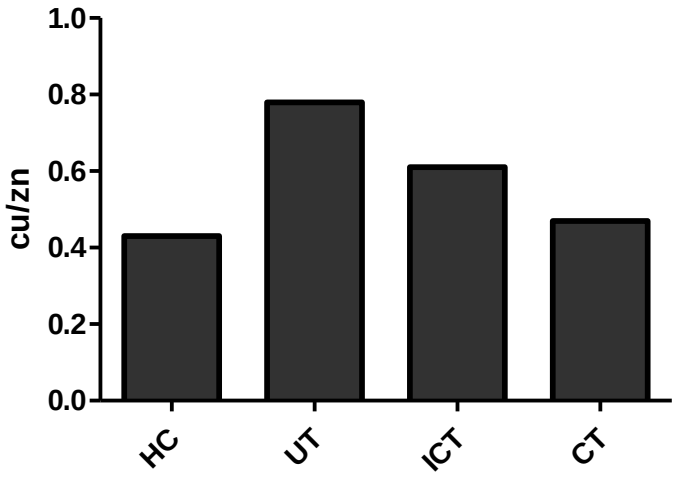

Elemental analysis was carried out by PIXE at IOP, Bhubaneswar. Results showed concentrations of Fe and Zn were significantly lower in VL patients than those of healthy control subjects, while that of Cu was much higher in the patients. Significant depletion of concentration of Br was also noticed. Cu/ Zn ratio, a useful pathophysiological marker for many diseases, was significantly higher in patients group and incomplete treatment groups than control and complete treatment groups respectively. During the course of treatment with Amphotericin B, elemental alterations were restored (as reflected by ICT group) and reached almost normalcy at the end of the treatment (as reflected by the CT group) of Cu/Zn in human blood samples of different study groups.

Concentration of Fe, Br, Cu and Zn measured by PIXE in human blood samples of different study groups ratio

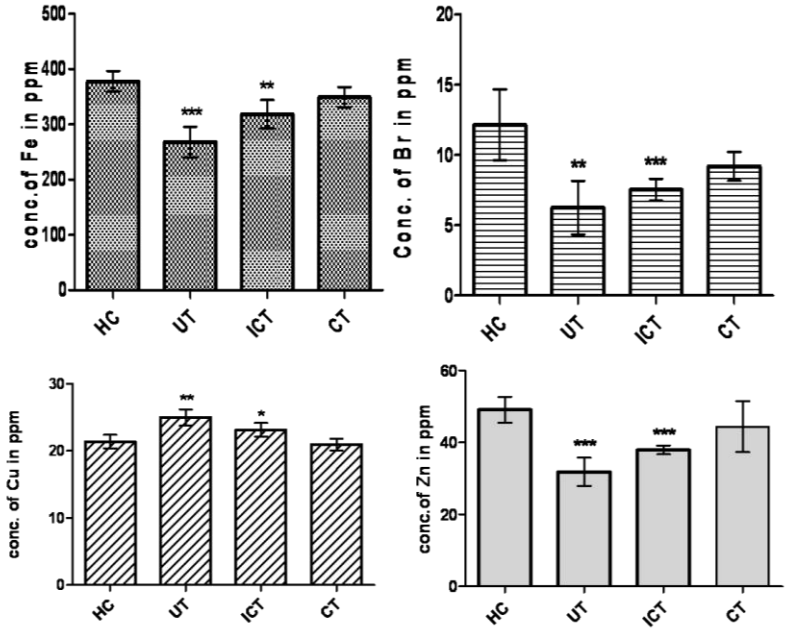

Sangita Lahiri (Barasat College); M. Manna, (Barasat College); M. Sudarshan and A. Chakraborty

2.2.16. Multielemental analysis of Soil Samples of tarai region in Uttarakhand

Soil minerals study is vital in terms of investigating the major soil forming compounds and to find out the fate of minor and trace elements, essential for the soil–plant interaction purpose. X-ray diffraction (XRD) has been a popular technique to search out the phases for different types of samples. For the soil samples, however, employing XRD is not so straight forward due to many practical problems. The soil samples were collected from an agricultural field of G.B. Pant University of Agriculture and Technology, Pantnagar, lying in the tarai region of Uttarakhand, India. The soil of this particular region of tarai area has been classified as Mollisols. In the current approach, principal component analysis(PCA) has been used to have an idea of the minerals present, in qualitative manner, in the soil under study. PCA was used on the elemental concentrations data of 17 elements, determined by the energy dispersive X-ray fluorescence (EDXRF) technique at UGC-DAE, Kolkata Centre. XRD analysis of soil samples has been done at Advanced Instrumentation Research Facility (JNU) to identify the minerals of major elements. Some prior treatments, like removal of silica by polytetrafluoroethylene(PTFE) slurry and grinding with alcohol, were given to samples to overcome the peak overlapping problems and to attain fine particle size which is important to minimize micro-absorption corrections, to give reproducible peak intensities and to minimize preferred orientation. A 2θ step of 0.051/min and a longer dwell time than normal were used to reduce interferences from background noise and to increase the counting statistics. Finally, the sequential extraction procedure for metal speciation study has been applied on soil samples. Atomic absorption spectroscopy (AAS) has been done at GBPUAT Pantnagar, was used to find the concentrations of metal fractions bound to various forms. Applying all the three probes, the minerals in the soils can be studied and identified, successfully.

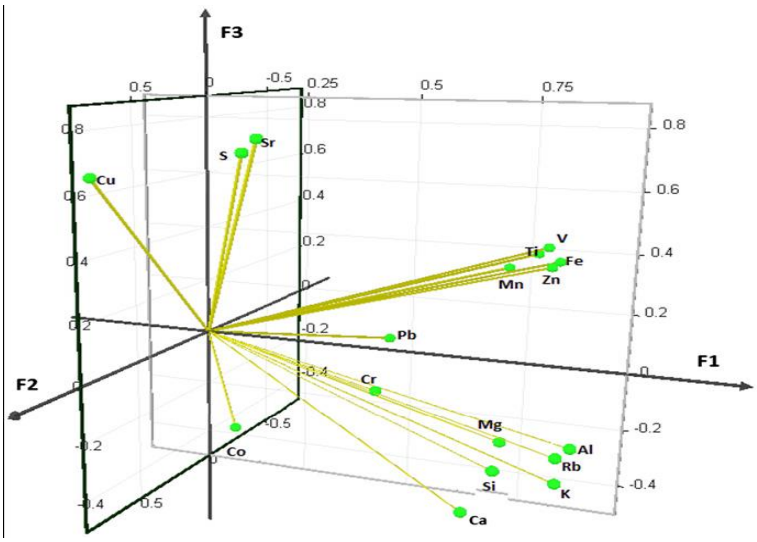

Fig. 1. 3-D loading plot among factor1, factor2 and factor3(orPC1,PC2andPC3) shows the grouping of elements. The elements nearer to each other in the plot have greate rhances to form complexes.

The first PC shows the high loadings of elements Mg, Al, Si, K, Ca, Ti, V, Fe, Mn, Zn and Rb. Clearly, the first PC alone is not able to predict the affinity between elements to form minerals but the study of PC1 with other PCs gives an idea.

H.M.Agarwal, Virendra Singh, G.Joshi (G.B.Pant Univerrsity); M.Sudarshan

2.2.17. Bioremediation of hexavalent chromium and associated heavy metals using heavy metalstress tolerant microbes isolated from chromite mine environment of Orissa

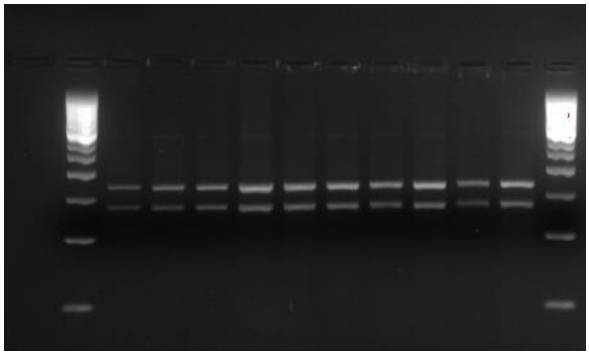

RFLP analysis of 10 *Bacillus* sp. Digested with ECORI

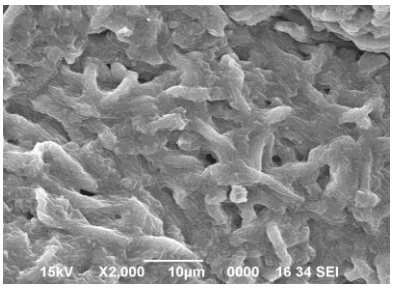

Cr(VI) bio-sorption by dead biomass

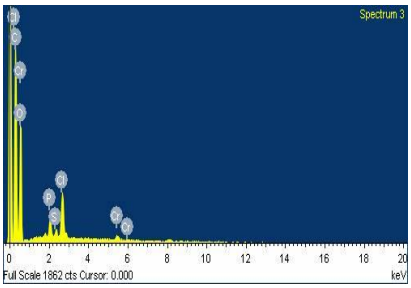

A. oryzae

Chromium being a very toxic metal, imposes various hazards in the environment so its remediation is extremely essential to keep the environment free of pollutant for safety of living beings. Since microbes are found to grow in metal contaminated sites, they are established to have higher tolerance towards such toxic heavy metals.

With this in the background, microbes growing in chromite mine of Sukinda were assessed with a view to find out possibility of using such microbes for Cr bioremediation. In this regard microbes isolated from heavy metal contaminated chromite mine environment of Sukinda were found to be highly Cr tolerant. To probe into the molecular mechanism of such tolerance, twenty highly chromium tolerant bacteria were characterized by means of biochemical, molecular techniques (16S rRNA gene sequence analysis) and their phylogenetic trees were constructed leading to their identification. The dead biomass of two isolated fungal strains viz., *P. citrinum* and *A. oryzae* were selected for Cr (VI) bioabsorption study. Different parameters such as, media, pH, temperature, shaking speed etc for efficient growth of fungi were optimized for use in bioabsoption study.

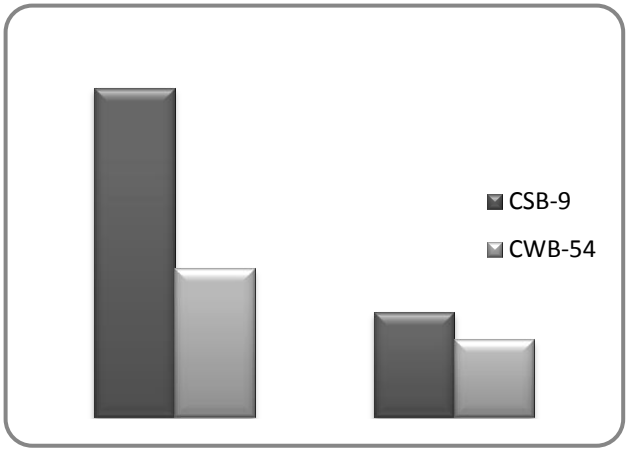

Protein Estimation of Extracellular and Intracellular enzyme

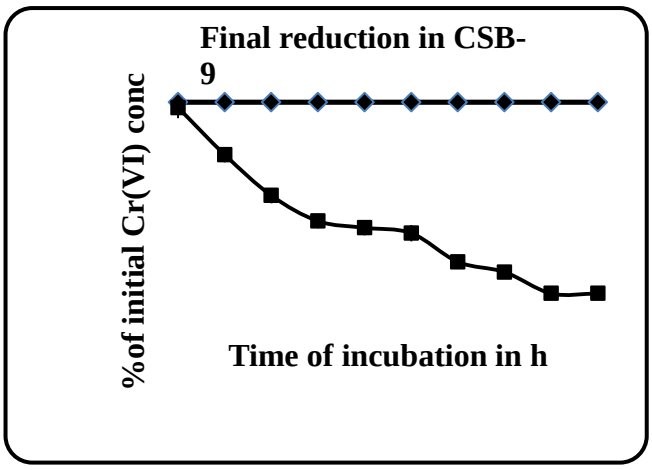

Final reduction in CSB-9

SEM-EDX analysis was carried out to study the accumulation of Cr(VI) by dead fungal biomass. Cr(VI) reduction by extracellular and cell-free extract of two bacteria viz., *Bacillus amyloliquifaciens (CSB-9)* and *Exiguobacterium mexicanum(CWB-54)* were undertaken along with optimisation of parameters for Cr(VI). Restriction Fragment Length Polymorphism (RFLP) of 10 *Bacillus* sp. isolated from chromite mine soil of Sukinda was conducted in order to study the genetic divergence of the bacteria.

Characterization and identification by 16S rRNA sequencing and phylogenetic analysis showed ten bacterial isolates to be *Bacillus* sp. The PCR-RFLP analysis of these ten *Bacillus* sp. showed the similar restriction patterns. The SEM-EDX study of two fungi isolated from chromite mine soil *P. Citrinum* and *A. oryzae* conform the bio-sorption of reduced chromium of the dead fungal mycelia surfaces. Cr(VI) reduction by CFE of CSB-9 and CWB-54 optimised for different parameters and final reduction conducted in optimised conditions showed CSB-9 and CWB-54 reduces 0.5 mM of Cr(VI) in 9 and 10 h respectively.

Sasmita Das, M.Sudarshan, A.Chakraborty, H.N.Thatoi

2.3. Photoelectron spectroscopy on INDUS-I, and other facilities of RRCAT

2.3.1. Study of Electronic Structure of TiCN films prepared by laser Irradiation

Nitriding and carburizing of metals are well known technique to improve the tribological properties like hardness and wear resistance of metal surface. From a fundamental point of view, our main aim is to correlate the electronic structure of $TiC_xN_{(1-x)}$ with its mechanical properties. We have investigated the bonding and electronic structure of $TiC_xN_{(1-x)}$ film prepared by laser irradiation under controlled atmosphere. Resonance photoemission electron spectroscopy (RPES) is a well established technique to study the electronic structure. In the present work, we have studied its detailed electronic structure using RPES in the incident photon energy range from 30 eV to 80 eV using Indus-1 synchrotron radiation source. Figure 1 shows the energy distribution curves in the photon energy range 30-60 eV of the specimen treated at 4J/cm^2 in the controlled atmosphere of 2 Bar pressure of CH_4 followed by 2 bar pressure of N_2 gas (purity > 99.999%) . Perusal of fig. 1 shows that an intensity maxima at 46 eV near to the Fermi level, the intensity enhancement is consistent with the resonance photoemission of Ti 3d states involved in the valence band of $TiC_xN_{(1-x)}$. It shows clearly the co-ordination between Ti, C and N. From the subsequent laser treatment in Ar-atmosphere changes the texture of the specimen, electronic structure of the film as a function of laser energy and a change in density of states have been observed near to the Fermi edge. These treatments induces the formation of Nitrogen rich TiCN to relatively Carbon rich TiCN compounds with a lower percentage. Detailed analysis of RPES studies on samples treated with different laser energy density is in progress.

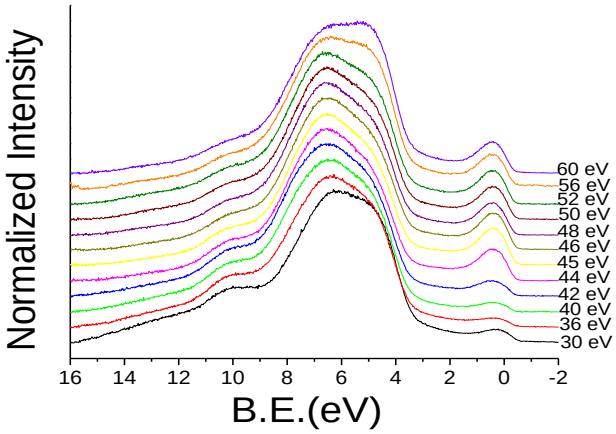

Fig. Valence band spectra at different photon energy of $TiC_xN_{(1-x)}$ film prepared by laser irradiation (4J/cm^2) under controlled atmosphere

Sheetal Soni, R.Gupta (DAVV, Indore); D.M. Phase

2.3.2. Electronic structure of buried Co-Cu interface studied with photoemission spectroscopy

Depth profiling type of measurement has been performed on the Co(100˚*A*)/Cu(50˚*A*) bilayer thin film. Valence band photoemission spectra were recorded at 50 eV photon energy as a function of sputtering time. The motivation of the present work is to understand the electronic structure of the buried Co/Cu interface and the nature of intermixing in the Co and Cu layers. X-ray reflectivity and transmission electron microscopy corroborate with the photoemission results and shows a very broad intermixed Co-Cu interface. The valence band of intermixed Co/Cu interface shows the Co and Cu 3*d* states which are considerably shifted towards higher and lower binding energy respectively as compared to the bulk elemental Co and Cu 3*d* states. The experimental observations are explained with the help of calculations based on projected augmented wave pseudo potential method using density functional theory. The origin and the shift of feature in the valence band of the Co-Cu interface are mainly due to the formation of two different Co and Co-Cu mixed nano-clusters.

Soma Banik, Sanjay Rai, S.K.Deb (RRCAT); D.M.Phase

2.3.3. Valence band study of Co doped ZnO thin films prepared by Sol-Gel technique

Here, we report the studies on the modifications in the electronic structure of Sol-gel grown polycrystalline Zn1-xCoxO (x = 0, 0.5 and 0.15) carried out using valence band spectroscopy (VBS) using Indus-1 synchrotron radiation source. X-ray diffraction measurements confirm the single phase nature having hexagonal wurtzite structure with space group P63mc. XPS measurements of Co 2p core level indicate that, Co ions are present in 2+ state in ZnO. Detailed investigations on the modifications in the electronic structure of ZnO due to Co doping have been carried out using valance band spectroscopy and Resonant photoemission spectroscopy. Data analysis is in progress

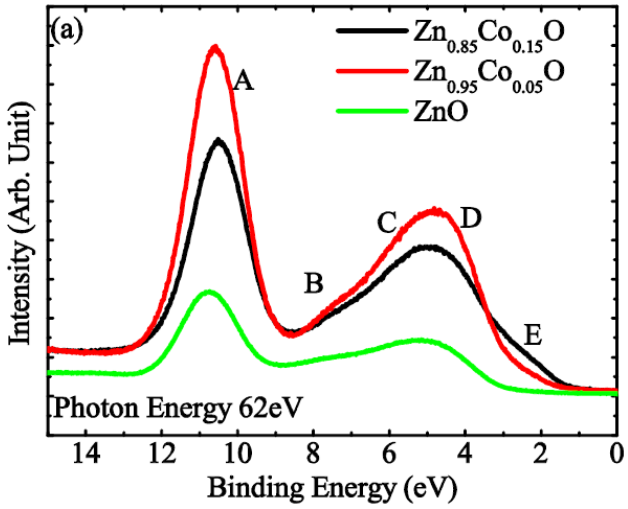

Fig. 1 Valence band spectra of ZnO and Co doped (0.05 and 0.15) ZnO recorded at 62 eV photon energy

D.G. Kuberkar and his group(Saurashtra Univ. Rajkot); D.M.Phase

2.3.4. Valence band structure of $YMnO_3$ and the spin orbit coupling

Electronic structure of pulsed laser deposited hexagonal-$YMnO_3$ film on Al_2O_3 (0001) substrate has been investigated by photoemission spectroscopy using variable energy photon sources. Resonance photoemission results reveal the charge transfer nature of h-$YMnO_3$ and variation in strength of hybridization between oxygen 2p and Mn 3d across the valence band region. The valence states sensitive to lattice distortion (inversion asymmetry) demonstrate the evolution of spin orbit interaction (SO). This SO along with its anisotropic behavior is well identified by the constant initial state plots.

Fig. Valence band spectra of h-YMnO3 thin film taken at different photon energies ranging 42-60 eV.

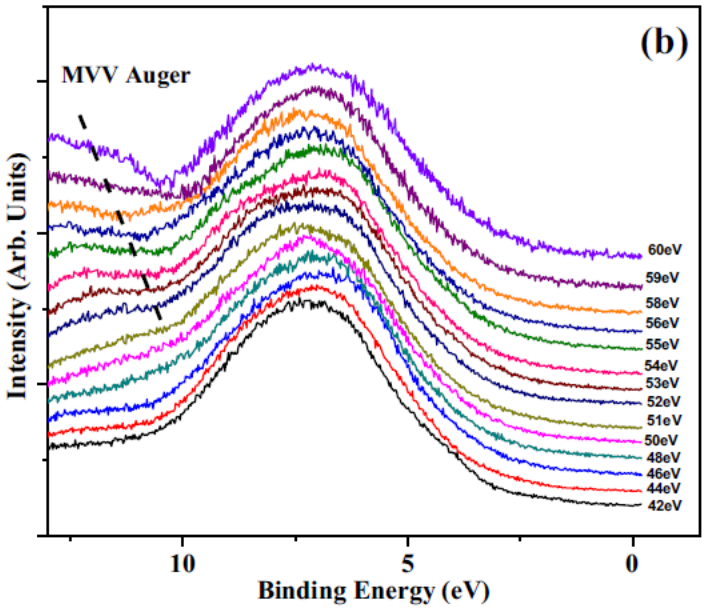

Manish Saharan, R.J.Choudhary and D.M.Phase

2.4. Collaborative Research using in-house facilities at Indore Centre

2.4.1. Bulk interface engineering for enhanced magnetization in multiferroic $BiFeO_3$ compounds

Composites of two antiferromagnetic perovskite oxides $BiFeO_3$ and $LaMnO_3$ was synthesized to study the change in bulk magnetic behavior. Composites with nominal compositions (1-x)$BiFeO_3$-x$LaMnO_3$ (x = 0, 5, 10, 20 wt. %) were synthesized by solid state reaction route. For all the samples, pure perovskite phase was obtained with no trace of impurities The structural analysis performed using X-ray diffraction and Raman spectroscopy indicated presence of phase separated compounds. The two entities retain their respective structure and phase in composite form. Significant enhancement in magnetic moment is observed in composite samples. The observed magnetization values are much higher than those expected from composition averaged Vegard's law. This is attributed to the uncompensated spins at the interface of two distinct antiferromagnetic phases.

Shreeja Pillai, Deepika Bhuwal, Vilas Shelke (Department of Physics, Barkatullah University, Bhopal); *A. Banerjee*

2.4.2. Influence of local structure on magnetic properties of layered cobaltites $PrBaCo_2O_{5+\delta}$, δ>0:5

The effect of local structure on the magnetic and transport properties of the layered perovskites has been investigated. The samples $PrBaCo_2O_{5+\delta}$, (δ = 0.8 and 0.67) crystallize in the same 112 type tetragonal structure but have different magnetic ground states. Extended x-ray absorption fine structure (EXAFS) spectroscopy has been employed to explain the changes in magnetic interactions based on the rotation and tilting of CoO polyhedra in these oxygen-rich double perovskites.

In the case of δ = 0.80 the inward rotation and tilting of the neighboring $Co^{3+}O$ and $Co^{4+}O$ polyhedra about the c-axis facilitates the DE mechanism between LS Co^{4+} and HS/IS Co^{3+} ions leading to FM order, while in the case of δ = 0:67 the tilting and outward rotation of the neighboring $Co^{3+}O$ polyhedra away from each other supports Co^{3+}–O–Co^{3+} superexchange mediated AFM ordering.

S. Ganorkar, K. R. Priolkar, P. R. Sarode (Goa University); S. Emura (Osaka University, Japan); R Rawat and A Banerjee

2.4.3. Oxygen vacancy induced phase formation and room temperature ferromagnetism in undoped and Co-doped TiO_2 thin films

TiO_2 and Co-doped TiO_2 (CTO) thin films are deposited at various oxygen partial pressures by pulsed laser deposition. The phase, stoichiometry and morphology of these films are examined by XRD, Raman, RBS and FESEM. All the films exhibit room temperature ferromagnetism (RTFM) independent of their phase. Films deposited at 0.1mTorr oxygen partial pressure show a complete rutile phase confirmed from glancing angle x-ray diffraction and Raman spectroscopy. At the highest oxygen partial pressure, i.e. 300mTorr, although the TiO_2 film shows a complete anatase phase, a small peak corresponding to the rutile phase along with the anatase phase is identified in the case of CTO film. An increase in O to Ti/(Ti+Co) ratio with increase in oxygen partial pressure is observed from Rutherford backscattering spectroscopy. It is revealed from x-ray photoelectron

spectroscopy (XPS) that oxygen vacancies are found to be higher in the CTO film than TiO_2, while the valency of cobalt remains in the +2 state. Therefore, the CTO film deposited at 300mTorr does not show a complete anatase phase unlike the TiO_2 film deposited at the same partial pressure. We conclude that RTFM in both films is not due to impurities/contaminants or due to any Co cluster in the film. This is confirmed from the XPS depth profiling and cross-sectional transmission electron microscopy (TEM) studies and is attributed to the oxygen vacancies. The magnitude of moment, however, depends not only on the phase of TiO_2, the crystallinity of the films plays an important role.

P. Mohanty, Chandana Rath (BHU); N. C. Mishra (Utkal University, Bhubaneswar);, S. Annapoorni (University of Delhi); R. J. Choudhary, N. P. Lalla, T. Shripathi and A. Banerjee

2.4.4. Thermally Stimulated Depolarization Current (TSDC) technique used to study various relaxation phenomenon of poly Caprolactone film

Poly Caprolactone (PCL) is a biodegradable polymer. The degradation of PCL is slower and produces less acidic degradation products; therefore the PCL seems a suitable polymer for the efficient tissue regrowth and a drug delivery vehicle for a sustain drug release mechanism. It has a low glass transition temperature Tg of 213K and a melting temperature Tm of 333K. TSDC technique is used to study the dipolar relaxation in PCL film of 0.2mm thickness. The dipolar behavior of the PCL film has been studied in 80K-300K temperature range at various poling fields EP while keeping the other parameters; such as poling temperature TP, poling time tP and heating rate constant. The presence of β and α peak in the given TSDC spectrum shows the exclusive dipolar relaxation of the PCL polymer while the presence of high temperature α' peak may come as a result of the relaxation of the free space charge. We have also studied the effect of different poling temperatures on the various relaxation mechanisms involved in the PCL. For that we have done the TSDC at various poling temperatures but kept the poling filed constant. Here we can see that how poling at lower temperature suppresses the higher temperature TSDC peaks. This work is a part of the DST project on "Electret State in Bio-degradable medicalpolymers"

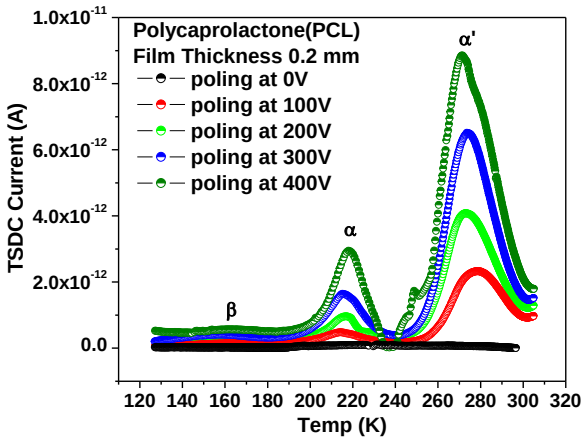

Figure:1 TSDC Spectrum of Poly Caprolactone film as a function of different poling fields

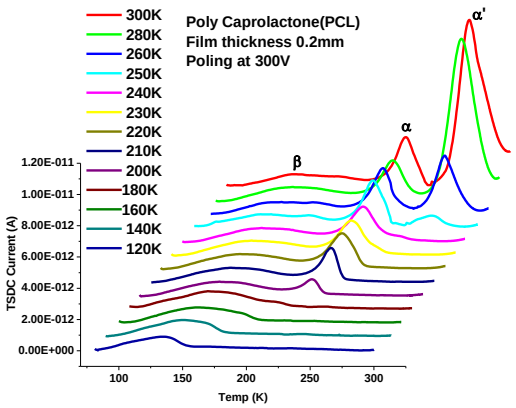

Fig:2 TSDC spectrum of Poly Caprolatone film at same poling field but at different poling temperatures

Manju Mishra Patidar, R. Nath and V. Ganesan

2.4.5. Bulk electronic structure of Al-Pd-Mn and Al-Cu-Fe quasicrystals

In this study, we have employed hard x-ray photoelectron spectroscopy (HAXPES) to study the bulk electronic structure of quasicrystals and thus disentangle it from the surface effects. We resolve a controversial issue regarding the mechanism for the formation of quasicrystalline solids, i.e., the existence of a pseudogap at the Fermi level. The near Fermi level HAXPES spectra of icosahedral fivefold Al-Pd-Mn and Al-Cu-Fe quasicrystals demonstrate the presence of a pseudogap, which is not observed earlier in surface sensitive low energy photoemission because the spectrum is affected by a metallic phase near the surface. In contrast to Al-Pd-Mn, in Al-Cu-Fe the pseudogap is fully formed; i.e., the density of states reaches zero at E_F indicating that it is close to the metal-insulator phase boundary. This work has been published in Phys. Rev. Lett., 109, 216403 (2012).

P. Rajput and J. Zegenhagen [ESRF, France]; A. Gloskovskii [PETRA, Germany]; D. L. Schlagel and T. A. Lograsso [Ames Lab., U.S.A.]; and K. Horn [FHI-MPG, Germany]; J. Nayak, M. Maniraj, A. Rai, S. Singh and S. R. Barman

2.4.6. Dielectric relaxation spectroscopy of phlogopite mica

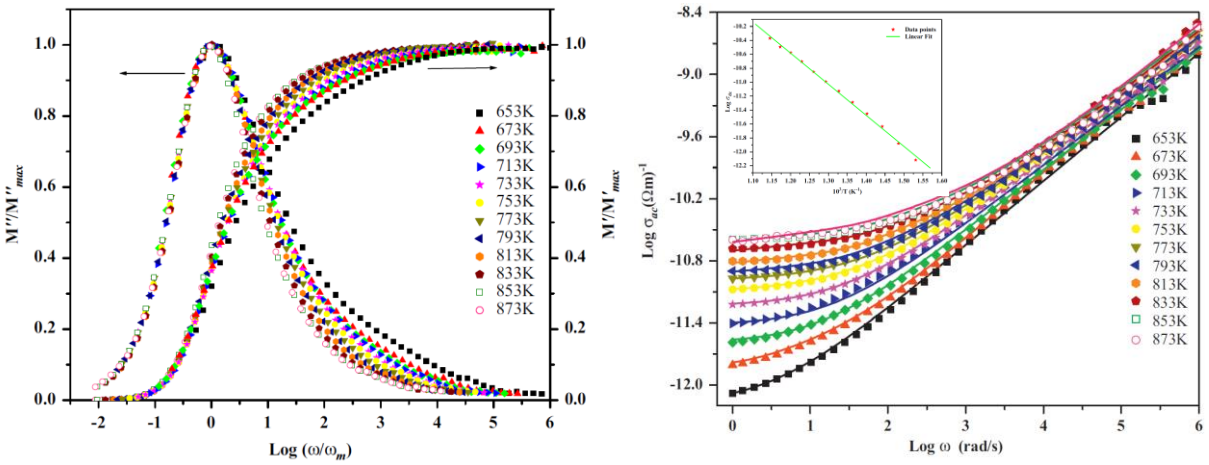

An in-depth investigation of the dielectric characteristics of annealed phlogopite mica has been conducted in the frequency range 0.1Hz–10MHz and over the temperature range 653–873K. The frequency dependence of the *M"* and dc-conductivity is found to obey an Arrhenius law and the activation energy of the phlogopite mica calculated from both spectra is similar. The electric modulus and conductivity data have been fitted with the Havriliak–Negami function. Scaling of *M'*, *M"*, and ac-conductivity has also been performed in order to obtain insight into the relaxation mechanisms. The scaling behaviour indicates that the relaxation describes the same mechanism at different temperatures. The study elaborates that the investigation of dielectric relaxation in the phlogopite mica will be helpful for various applications of this material in electrical engineering.

Navjeet Kaur, M Singh, A Singh, L Singh (GNDU); A.M. Awasthi

2.4.7. Magnetoresistance, powder neutron diffraction, and theoretical studies on Mn_2NiGa

We have observed spin-valve-like magnetoresistance behaviour in a magnetic shape memory alloy Mn_2NiGa crystal at room temperature. We establish from neutron diffraction and theoretical studies that Mn_2NiGa is a ferrimagnetic material with antiparallel alignment of the Mn spin moments. On the basis of neutron diffraction, magnetization behaviour and theoretical studies, the origin of the unexpected behaviour of magnetoresistance has been ascribed to the presence of antisite disorder where about 13% of the Ga sites are occupied by Mn atoms. We establish that these antisite defects for ferromagnetic nanoclusters with parallel alignment of Mn spin moments in a Mn2NiGa bulk lattice that has antiparallel Mn spin moments. The direction of the Mn moments in the soft ferromagnetic cluster reverses with the external magnetic field. This causes a rotation or tilt in the antiparallel Mn moments at the cluster-lattice interface resulting in the observed asymmetry in magnetoresistance.

S. Esakki Muthu and S. Arumugam (Bharathidasan University, Tiruchirappalli); E. Suard (ILL, Grenoble); A. Senyshyn (Technische Universitat Muenchen, Germany); P. Rajput (ESRF, Grenoble); R. Ranjan (IISc, Bangalore); D. L. Schlagel and T. A. Lograsso (Ames Lab., USA); A. Chakrabarti [RRCAT]; S. Singh, R. Rawat, S. W. D'Souza, S. Banik, S. Bhardwaj, A. M. Awasthi, S. R. Barman

2.4.8. Mixed alkali effect in physical and optical properties of $Li_2O–Na_2O–WO_3–B_2O_3$ glasses

Glasses with composition xLi_2O-$(30-x)Na_2O–10WO_3–60B_2O_3$ (where x=0, 5, 10, 15, 20, 25 and 30 mol%) have been prepared using the melt quenching technique. In the present work, the mixed alkali effect

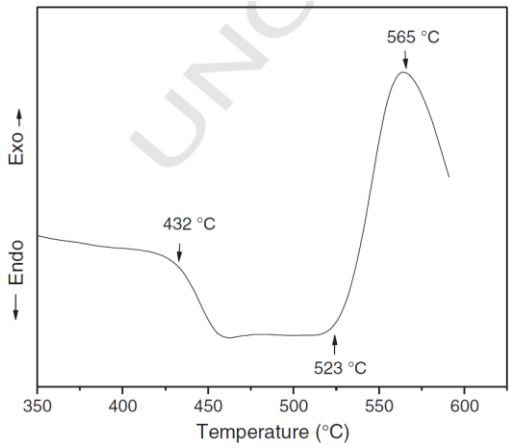

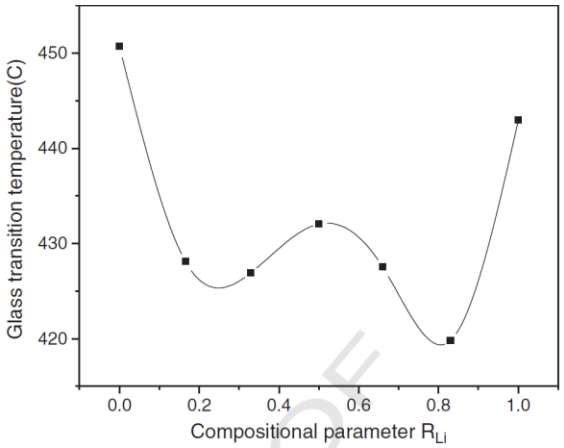

(MAE) has been investigated in the above glass system through density and modulated DSC studies. The density and glass transition temperature of the present gasses varies non-linearly, exhibiting the mixed alkali effect. From the optical absorption studies, the values of direct optical band gap, indirect optical band gap energy (E_o) and Urbach energy (ΔE) have been evaluated. The values of E_o and ΔE vary non-linearly with composition parameter, showing the mixed alkali effect. The electronic polarizability of oxide ions, optical basicity and the Yamashita–Kurosawa's interaction parameter have been examined to check the correlation among them and bond character. Based on good correlation among electronic polarizability of oxide ions, optical basicity and the Yamashita–Kurosawa's interaction parameter, the present glasses were classified as normal ionic (basic) oxides.

A. Edukondalu, M. Purnima, Ch. Srinivasy, Syed Rahman, K. Siva Kumar (Osmania University); T. Shripathi, A.M. Awasthi

2.4.9. Metal insulator transition in nano-crystalline $Pr_{0.67}Ca_{0.33}MnO_3$

In the phenomenological model of kinetic arrest of first order transition, the topology of devitrification curves obtained during CHUF protocol (cooling and heating unequal magnetic field) reveal a relation between kinetic arrest band and supercooling band. So far all the experimentally observed data indicated anti-correlation between the two i.e. regions with higher kinetic arrest temperature have lower supercooling temperature. Recently we observed first experimental evidence of correlated band in nano-crystalline $Pr_{0.67}Ca_{0.33}MnO_3$ (obtained from SINP, Kolkata) which is known to show a large variation in hysteresis width in H–T space. In this study we also explored the role of change in the relative width of the supercooling/superheating band and kinetic arrest band for a ferromagnetic metallic to antiferromagnetic insulating transition. It is shown that for a correlated kinetic arrest and supercooling bands, the topology of the devitrification curves (or transformation across the (H_K, T_K) band during warming) changes with the change in the relative width of these two bands. In addition to this, for a broader kinetic arrest band, the transformation temperature across the superheating band under constant H now depends on the arrested phase fraction. This is shown in following figure for nano-crystalline $Pr_{0.67}Ca_{0.33}MnO_3$ sample. Though the devitrification curve in figure (a) for cooling field around 5 Tesla looks similar to many other system, the curve in figure (b) show that metal insulator transition around 100 K in this case depends on the cooling field.

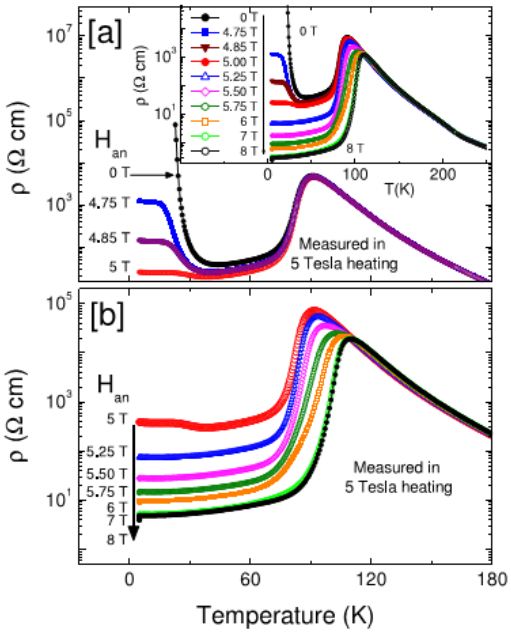

Figure 1: *Resistivity measured as function of temperature under 5 Tesla magnetic field during warming after cooling in labeled Magnetic field H_{an} for nano-crystalline $Pr_{0.67}Ca_{0.33}MnO_3$. Figure (a) shows the curve when sample is cooled in lower magnetic field than 5 Tesla showing a re-entrant metal to insulator to metal transition. Figure (b) shows the curve when cooling field is higher than 5 Tesla. These curve shows that metal insulator transition now depends on the cooling field or metallic phase fraction. Such behavior is expected for correlated kinetic arrest band (broader) and supercooling band.*

Kalipada Das, I Das (SINP, Kolkata); R Rawat, P Chaddah, Pallab Bag,

2.4.10. High figure-of-merit in Cu intercalated $TiSe_2$ thermoelectric material

The effect of Cu intercalation on thermoelectric properties of textured Cu_x-$TiSe_2$ (x= 0-0.15) alloy was

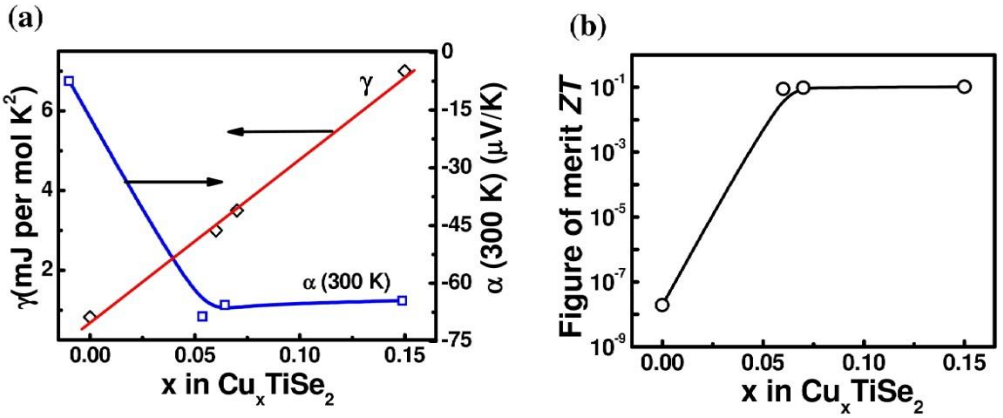

Fig. 1 (a) Electronic specific heat coefficient (γ) and Seebeck coefficient α (300 K)as a function of Cu concentration x in Cu_xTiSe_2. (b) Figure of merit ZT (at 300 K)as a function of x in Cu_xTiSe_2 (x = 0, 0.06, 0.07, 0.15).

studied. For x = 0.15, room temperature value of the figure-of-merit, defined as ZT ~$\alpha^2T/\rho k$, (where α, ρ and k are Seebeck coefficient, electrical resistivity and thermal conductivity, respectively), has been demonstrated to have improved by seven orders in magnitude from 1.93 x 10^{-8} to 0.104. Interestingly, all the three parameters α, ρ and k exhibited favorable adjust-ments on Cu intercalation. That is, there is increase in α and reductions in both ρ and k. The possible mechanisms of these changes have been discussed.

R. Bhatt, R. Basu, S. Bhattachraya, A. Singh, D. K. Aswal, S.K. Gupta (BARC, Mumbai); G. S. Okram, V. Ganesan

2.4.11. Structural, optical, electrical properties of degen-erate Cu_7Se_4 thin films

Formation of polycrystalline copper selenide thin films of composition Cu_7Se_4 was confirmed using XRD, which further provides lattice constant, particle size, dislocation density, number of crystallites per unit area and strain in the film. Hall data (300K) gives hole-type of conduction, carrier mobility and carrier concentration of nearly 10^{22} cm^{-3} that suggests degenerate semiconductors having optical band gap of 2.25eV.

Seebeck coefficient confirms hole-type of conduction. The data from the analyses of Hall measurements and thermoelectric power have been combined to evaluate important material parameters such as mean free path, relaxation time, Fermi energy and effective mass. Certain possible applications of the prepared film in various fields are also discussed.

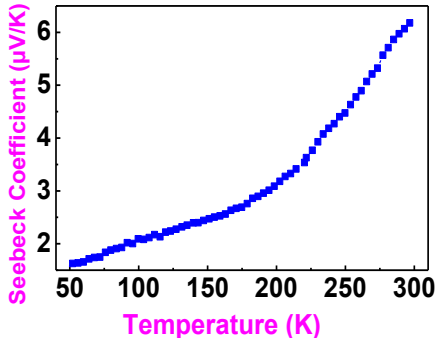

Fig. 1 Seebeck coefficient of Cu_7Se_4 thin film.

K.S. Urmila, A. T. Namitha and B. Pradeep (CUSAT, Kochi, Kerala); R. R. Philip (U. C. College, Aluva, Kerala); V. Ganesan, G.S. Okram

2.4.12. Optoelectronic and low temperature thermoelectric effects in the OVC n-$CuIn_3Se_5$ thin films

Optoelectronic properties and low temperature thermoelectric effects were studied on polycrystalline thin films of ternary chalcopyrite ordered vacancy compound n-$CuIn_3Se_5$. The three source vacuum co-evaporation method prepared thin films were characterized for their structure, morphology and composition using X-ray diffraction, atomic force microscopy and X-ray photoelectron spectroscopy, respectively. Optical and optoelectronic measurements were done to obtain the band gap, carrier con-centration, and photosensitivity of the materials. The thermopower exhibited a non-degenerate semiconducting nature, establishing Boltzmann statistics relation between carrier density and Fermi level in the films. While ionized impurity scattering has been detected near room temperature, an enhanced negative thermopower due to contribution from phonon drag has been noticed toward lower temperature. Thermopower tog-ether with Hall coefficient and conduc-tivity measurements permitted the correlation of density of states, carrier concentration, drift velocity, and the effective mass of the carriers with the conductivity of the films.

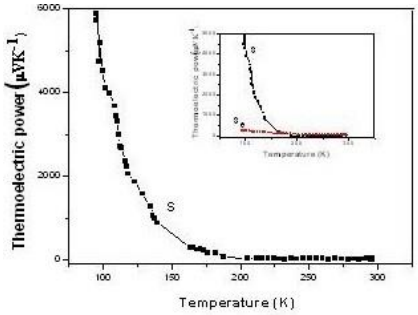

Fig. 1 Thermoelectric power in in-$CuIn_3Se_5$ Film. Inset shows the deviation of measured thermoelectric power (S) from the calculated electronic contribution to the thermoelectric power (Se)

R. Jacob, R. Geethu, R. R. Philip (UC College, Cochin, Kerala); B. Pradeep, K. S. Urmila (CUSAT, Cochin, Kerala); T. Shripathi, G. S. Okram, V. Ganesan

2.4.13. Effect of Chromium doping on the Resistivity Behavior of Gadolinium Manganite

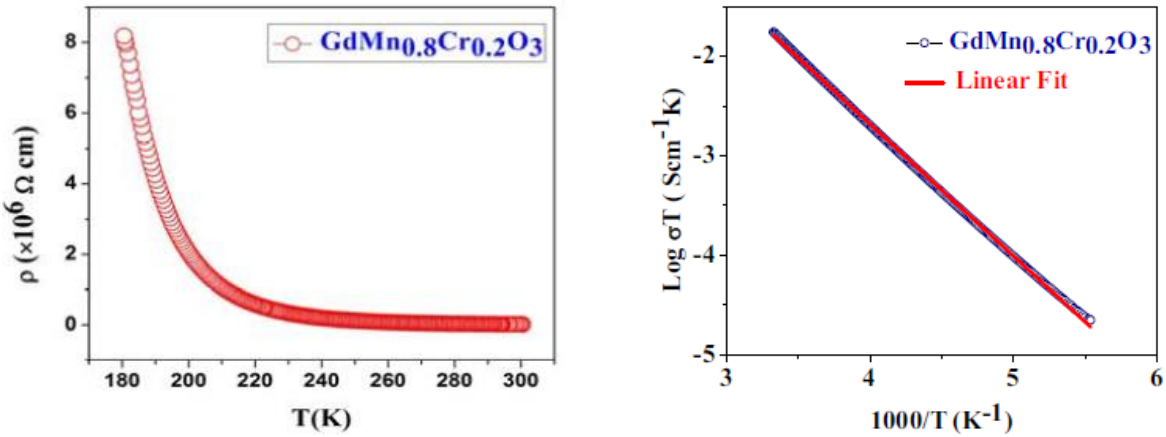

Fig. Left panel: Resistivity. Right panel: LogσT versus 1000/T (blue) and Arrhenius fit (red) using small polaron conductivity model.

Systematic investigation of structure and resistivity behaviour of $GdMnO_3$ with 20% Cr doping papered by conventional solid state reaction method has been undertaken. Upon Cr doping on the Mn site the lattice parameters and unit cell volume were reduced due to the smaller ionic radius of Cr^{3+} than Mn^{3+}. The Cr-doped manganites exhibit a large variation and semiconducting nature in resistivity values and the electronic transport can be explained by small polaron hopping model.

A. Modi, R. K. Thakur, R. Thakur, N.K.Gaur (Barkatullah University, Bhopal); G. S. Okram

2.4.14. Electrical Properties of Strontium Doped Yttrium Manganite Oxide

$Y_{1-x}Sr_xMnO_3$ (x= 0.1 and 0.2) perov-skites prepared by conventional solid state reaction method were carefully studied for their electrical properties after characterizing them. The XRD pattern showed the sharp peaks correspond to the hexagonal structure of the reported compounds with space group P63cm. The resistivity versus temperature plot infers a semiconducting like behavior in both reported compounds. The suppression in the resistivity has been witnessed with increasing concentration Sr^{2+} ions at yttrium site. The small polaron hopping conductivity model adequately describes the electrical conductivity behavior. The activation energy (E_a) was found to decrease as 'x' (Sr content) increases.

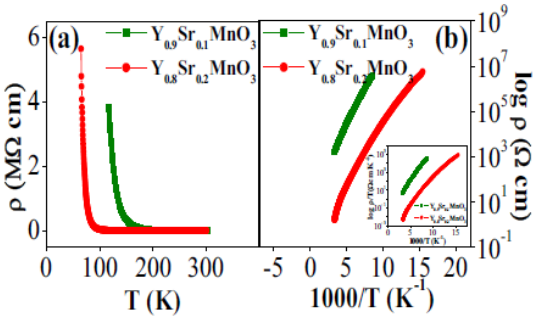

Fig. 1 (a) Resistivity of the two samples and (b) their logarithmic plot versus 1000/T; inset Logρ/T versus T.

R. K. Thakur, R. Thakur, N.K. Gaur (Barkatullah University, Bhopal); N. K. Kaurav (Holkar Sci. College, Indore); G. S. Okram

2.4.15. Structural, electrical and magnetic properties of Ce doped $La_{0.7}Ca_{0.3}MnO_3$ thin films

We have studied the structural, transport and magnetic properties of $La_{0.7}Ca_{0.3-x}Ce_xMnO_3$ (x = 0.0, 0,025, 0.05, 0.1 and 0.15) manganite thin films prepared by pulsed laser deposition technique on $LaAlO_3$ (001) substrate. The grown films are single phase and epitaxial in nature as reveal by X-ray diffraction and phi-scan. The temperature dependent resistivity measurements of these films reveal a metal–semiconductor transition at T_P and transition temperature are found to shifted lower temperature with Ce doping. Resistivity data at high temperature have been fitted with the variable range hopping model to estimate the density of states at Fermi level {N (E_F)}, while at low temperature electron–electron, electron–phonon and electron-magnon processes contributed in scattering of carriers. It was observed that N (E_F) decreases with Ce doping leads to a decrease in conductivity of the Ce doped samples. We observed maximum MR% value ~90 % near the T_P. Magnetization measurements reveal that long-range ferromagnetic ordering in all samples and the saturation magnetic moment increases as x increases.

Amit Khare, S. P. Sanyal (Barkhatullah University, Bhopal); R. J. Choudhary

2.4.16. Strain dependent stabilization of metallic paramagnetic state in epitaxial $NdNiO_3$ thin films

Epitaxial $NdNiO_3$ thin films have been deposited on $LaAlO_3$ and $SrTiO_3$ single crystals using pulsed laser deposition. Electrical transport and magnetic properties are controlled by substrate induced strain. Spectral changes at low temperature, for the film on $SrTiO_3$ substrate, indicate towards existence of charge ordering in antiferromagnetic insulating phase of $NdNiO_3$ thin film under tensile strain. Film deposited on $LaAlO_3$ substrate exhibits re-entrant metallic behaviour and paramagnetic character at low temperatures. Invariance of Raman spectra, with temperature, of film on this substrate reveals that the melting of charge ordering under compressive strain is responsible for stabilization of metallic phase at lower temperature.

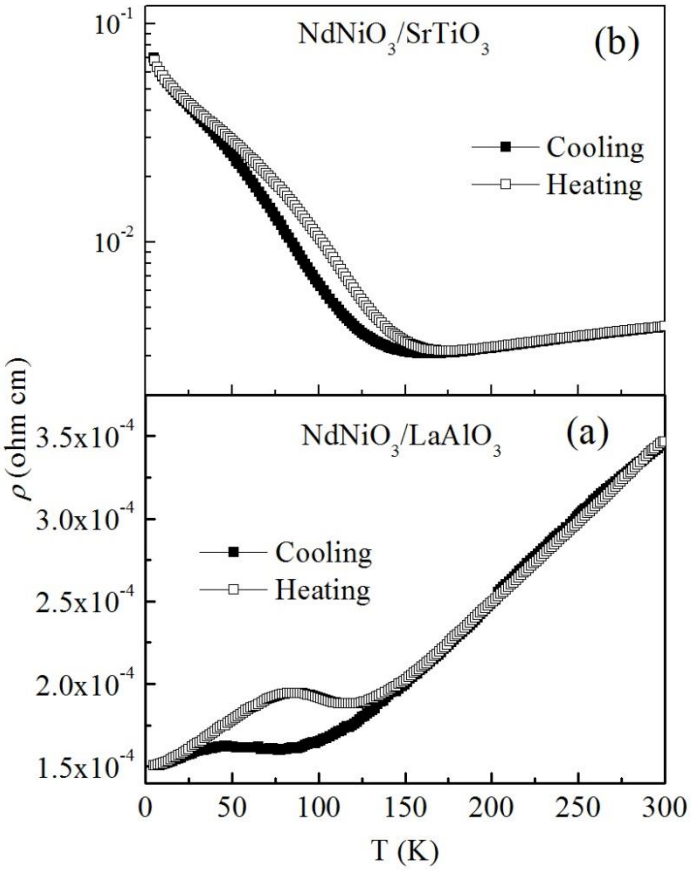

Fig.: Temperature dependence of electrical resistivity (ρ) in both cooling and heating cycles for $NdNiO_3$ thin films deposited on (a) $LaAlO_3$, and (b) $SrTiO_3$ substrates.

Yogesh Kumar (IUAC, N.Delhi); and Prof. Ravi Kumar (NIT Hamirpur); R. J. Choudhary

2.4.17 Study of the Glass transition temperature of Graphene-PVA composites using Temperature dependent FTIR spectroscopy

The composites of Polymer with graphene are one of the important hybrid materials in many technology sectors because the mechanical strength of polymer has been found to improve a lot after making their composites with graphene or like material. In this direction, we have carried out the experiments for making the composites of PVA (Poly vinyl alcohol) with graphene. In the present experiment, graphene is basically a reduced graphene oxide prepared using modified Hummer's method and then mix with PVA solution under continuous stirring followed by ultrasonic mixing. To determine the phase change behaviour of PVA after making composites with graphene temperature dependent FTIR measurement available at UGC-DAE CSR, Indore centre, India has been utilized.

We have recorded the FTIR spectra of PVA as a function of the temperature varying from 0^0C to 150^0C. The various IR bands observed were confirmed with the characteristics bands corresponding to the functional

groups of PVA with the available literature. With the increase in the temperature, change in intensity of various bands has been observed.

The following figure depicts the 2D contour plots to analyse the phase change behaviour and glass transition temperature of PVA. Such plots are acquired using MATLAB programme. This graph includes the variation in derivative of absorbance with respect to temperature, as a function of wavenumber and temperature. The adjacent figure depicts the dA/dT at each wavenumber.

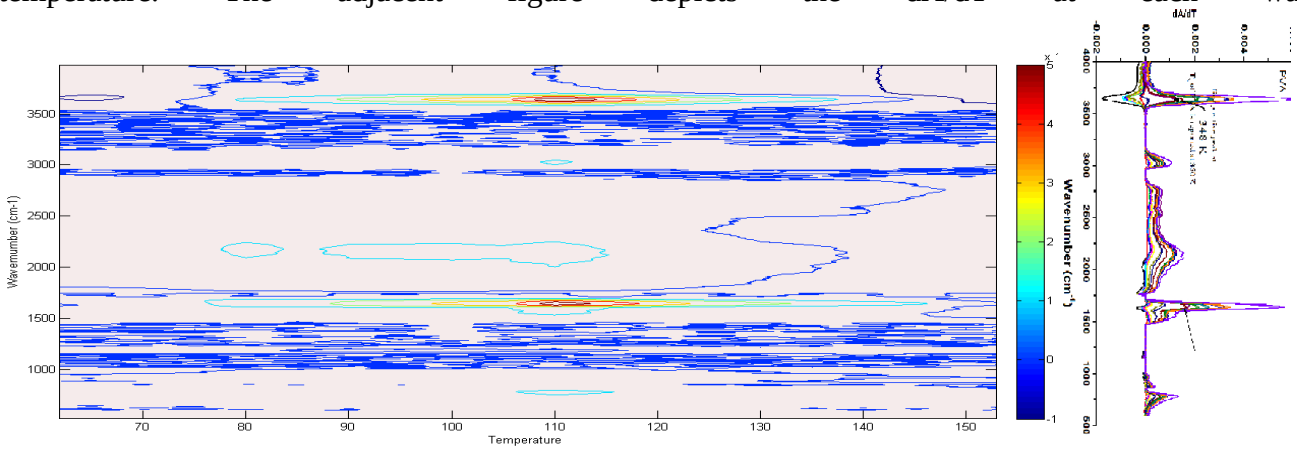

Increase in dA/dT of the IR bands after 75^0C, upto 110^0C can be observed. With further increase in temperature, dA/dT decreases. These regions are indicated by different colours in the contour plot, which occur during glass transition. It is clearly observed from the contour plot that the intensity of all bands starts changes pertains at 77^0C, clearly depicting the occurrence of change in structure of the PVA at this temperature, thus shows the occurrence of transformation in phase. The value of T_g obtained from the dA/dT vs $\bar{\nu}$ and the contour plots (77^0C) is consistent with that reported in literature. Abrupt change in dA/dT was observed in most of the bands, to different extent near the T_g, indicating structural changes in PVA, and phase transformation. Temperature dependent FTIR spectra of doped PVA composites is being analysed in similar manner.

Suman Mahendia, Neetu, Shyam Kumar (Kurukshetra University); U. P. Deshpande

2.4.18 Low temperature Fourier transform infrared transmission spectroscopy to study spin phonon coupling in $BiFeO_3$

Single phase $BiFeO_3$ (BFO) has widely recognizes as room temperature multiferroic. BFO comes under the class of perovskite type oxide, which display ferroelectric and ferromagnetic properties; interplay between these two orders would give rise to potential application in spintronic devices. In the present work, BFO is synthesized by microwave assisted-gel combustion route. The structure and phase purity of the sample was checked by X-ray powder diffraction (XRD) using Bruker AXS D8 Advance X-ray diffractometer equipped with copper target (λ_1,CuKα_1 = 1.5405 A^0). Magnetization measurements were performed with Vibrating Sample Magnetometer (Model 14T-VSM) at temperature (2- 350 K). Fourier Transform Infrared Spectroscopy (FT-IR) measurements were carried out on Fourier Transform Infrared spectrometer [Model: MAGNA 550 (USA), Range - 4000 cm^{-1} to 50 cm^{-1}].

The XRD pattern of BFO system is shown in Fig. 1. Rietveld refinement of the XRD pattern confirms that the sample is single phase rhombohedrally distorted perovskite structure with space group R3c.

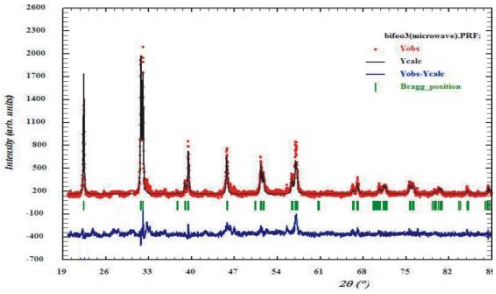

Fig.1 *Powder XRD patterns of BFO system*

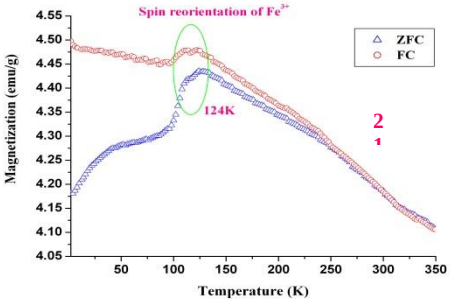

Fig.2 *Powder XRD patterns of BFO system*

Fig. 2 shows the temperature dependence of the ZFC and FC magnetizations under applied field H = 2 kOe while warming the sample from 2 to 350 K. The sample exhibit an irreversible thermomagnetization process below 213 K for 2 kOe field that is there exist an obvious difference between the ZFC curve and FC curve. The anomaly is observed near 124 K in the present work can be related to spin reorientation of Fe^{3+} ions.

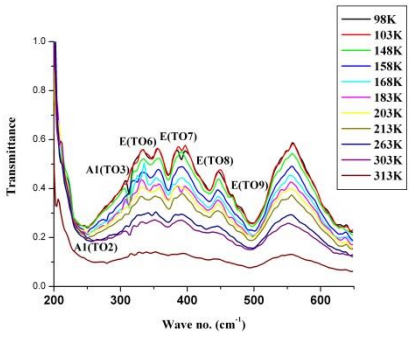

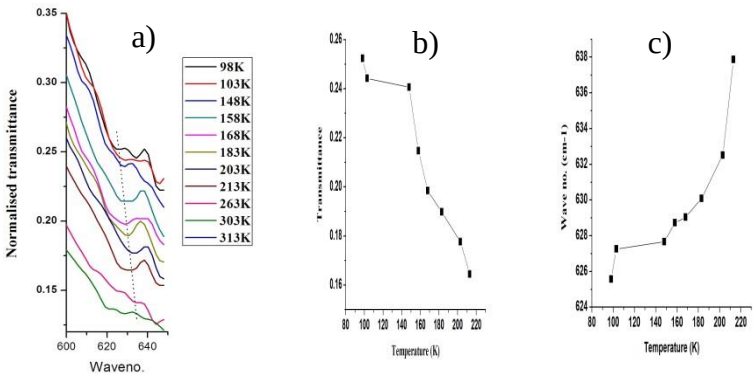

Fig.3 *The infrared transmission spectra measured at various temperatures for BFO system, plotted as transmittance versus the wave no. The arrow marks the additional phonon mode appears below ~213K*

Fig. 4 a) *Enlarged view of new additional phonon mode, dash line indicate the shifting of transmission peak towards higher energy side* ***b)*** *Temperature dependence of normalized transmission intensity of this phonon mode* ***c)*** *Temperature dependence of wave no. shift of this phonon mode*

Low temperature FTIR study exhibits additional phonon mode of vibration at 630cm^{-1} below 213K (Fig 4a) can be corresponding to new stretching vibration mode of FeO_6 octahedron, indicating that a local distortion of FeO_6 octahedron start occurring. This temperature is corresponding with the FC and ZFC bifurcation temperature in M versus T study. Commonly, the FC-ZFC bifurcation temperature is related to the onset of spin glass behaviour. The occurrence of this additional phonon mode at this particular temperature

suggests that there is strong spin-phonon coupling in BFO. This argument is further supported by the temperature dependence of this additional phonon peak. It can be seen that its peak position marginally shifts towards lower energy side with further decrease of temperature, hinting that the strength of the local lattice distortion get increased. On the other hand, the intensity of this phonon mode enhances upon cooling (fig 4b). Both these results clearly demonstrate the local distortion in FeO_6 octahedra. The curves (Fig 4b and c) shows anomaly around 124 K, which was also observed in M-T curve (fig 2) and related to spin reorientation of Fe^{3+} ions. It gives strong evidence for spin-phonon coupling in BFO system.

V.M.Gaikwad, S.A.Acharya (Nagpur University); U Deshpande

2.4.19 Structural, Optical And Electrical Properties Of Sb Doped And Undoped AgIn1-xGaxSe2 And Ag(InGa)5Se8 Thin Films

The Sb doped and undoped thin films of AgIn1-xGaxSe2 and Ag(InGa)5Se8 on optically flat soda lime glass substrates were prepared by a three stage co-evaporation process. Energy dispersive analysis of X rays and X-ray photo electron spectroscopy in conjunction with atomic force microscopic technique and scanning electron microscopic technique were used for compositional and surface morphological analysis respectively. The influence of both Sb doping and Ga% variation on the structural parameters of the films and on band gap tailoring was explored by estimating anion-cation bond lengths and optical band gaps. The temperature variation of the fundamental band gap of the doped and undoped films was further investigated by performing low temperature optical absorbance measurements in the temperature regime 90K to 301K. Rutherford scattering spectra quantified the thickness of the films used for conductivity (σ) measurements. The activation energies of these n-type films from ln (σ) versus temperature inverse graphs were used to elucidate defect levels in the films. Results obtained from UV-Vis transmission measurements at low temperature carried out at CSR Indore on Sb doped AIGS film are shown in Fig. 1.

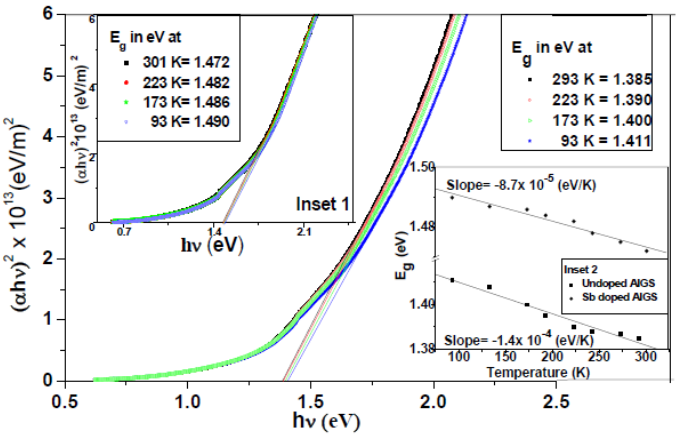

Fig. 1. $(\alpha h\nu)2$ vs. $h\nu$ plots showing the band gap Eg of a typical AIGS thin film at low temperatures. Inset 1: $(\alpha h\nu)2$ vs. $h\nu$ plots showing the band gap Eg of a typical Sb doped AIGS thin film at low temperatures. Inset 2: Eg vs. T plots for the determination of $(\Delta Eg/\Delta T)$.

Rajani Jacob, Rachel Reena Philip (Union Cristian College, Cochin) U.P.Deshpande, T. Shripathi, V.Ganesan

2.4.20 Solution grown Cu_2SnS_3 thin films for solar cells

In the second year of the project, electrical transport properties of the layer-by-layer solution deposited Cu_2SnS_3 films were investigated. Unlike controlled environments of vacuum deposition systems, solution

processing may yield films with unpredictable carrier transport due to inherent formation of gettering defects during processing. Thus understanding the nature of carrier transport in these films becomes crucial from basic and application points of view. Thermoelectric and Photothermolectric analysis has been employed to determine the carrier transport in Cu_2SnS_3 films in temperature 120 - 273 K. The effect of varying thickness and annealing temperatures on the electrical conduction are studied. The variation in conductivity is found to be thermally activated. The change in conductivity with thickness and annealing temperature is resolved into individual contributions of carrier concentration and mobility. Both carrier concentration and mobility change has been found to affect the conductivity under different conditions. The changes observed have been qualitatively correlated with incorporation of defects during layer by layer deposition of films. The change in concentration and distribution of these defects are suggested to alter observed changes in electrical transport of Cu_2SnS_3 films of different thickness and after annealing at different temperatures (Figure 1).

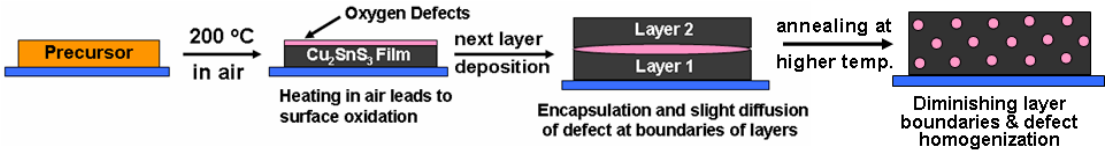

Figure 1: *Schematic representation of accumulation and change distribution of defects under deposition and post deposition processing of Cu_2SnS_3 films*

Thin Film Solar Cells (TFSC) with device architecture Graphite/ZnO/CTS/ITO/SLG were fabricated. The best cells yielded power conversion efficiency (PCE) of 2.10 % with open circuit voltage (V_{OC}), short circuit current density (J_{SC}) and fill factor (FF) of 0.816 V, 6.14 mA/cm^2 and 0.42 respectively under simulated AM 1.5 spectrum and power density of 100 mW/cm^2 (Figure 2). The series (R_s) and shunt (R_{sh}) resistances are, respectively, 80 and 10^3 ohms as determined from J-V characteristics. High shunt resistance indicates formation of crack or pore free, homogenous junction using a solution based technique. This together with high V_{oc} makes the solar cell favorable to be fabricated on large area for real time requirements.

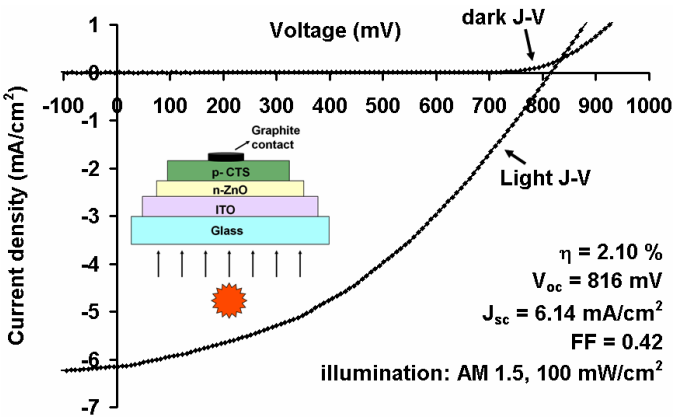

Figure 2: *J-V characteristics of n-ZnO/p-CTS solar cell under dark and illumination (AM 1.5, 100 mA/cm^2). Inset shows schematic of solar cell structure*

Devendra Tiwari, Tapas K. Chaudhuri (Charotar University, Changa)

2.4.21 X-ray reflectivity study of metal ion incorporated long chain fatty acid

Langmuir-Blodgett (LB) technique was used to deposit the 9 multilayers of cadmium arachidate (CdA_2) and cadmium stearate ($CdSt_2$) over the glass substrate. The detail of the deposition procedure is described in

literature [N. M. Das et. al., Physica B 407 (2012) 4777–4782]. The deposited films were characterize by the X-ray reflectivity (XRR) technique by High Resolution X-ray Diffraction system (Bruker D8 Discover Diffractometer using Cu-$K_{\alpha,}$ λ=1.543 Å wavelength,) at HRXRD laboratory in UGC-DAE CSR, Indore. The XRR patterns of 9 layers of both CdA_2 and $CdSt_2$ prepared by the LB thin film deposition technique are shown in Fig. 1. The fitting is done by using the parratt formation. From the fitting the layer by layer variation of the parameters such as thickness (d), electron density (ρ) and the roughness (σ) of the each sample is calculated. The layer by layer electron density profile (EDP) of both the films are shown in the inset of the respective graphs in Fig. 1. A few prominent Keissig fringes can be seen for XRR patterns of both the films and after that they overlap. Therefore it can be concluded that as the layer thickness increases, the small angle reflectivity decreases and the inter-mixing between the definite layer structures may cause the overlapping. Using the fitting, the total thickness of CdA_2 and $CdSt_2$ has been calculated to be 239.3Å and 214.9 Å respectively. This gives the average individual thickness as 26.6Å and 23.9 Å respectively for CdA_2 and $CdSt_2$. Using the relation $d/d_o = \cos(\theta)$, the tilt angle of the molecule with respect to the normal on the substrate is calculated to be 17.7° and 19° respectively.

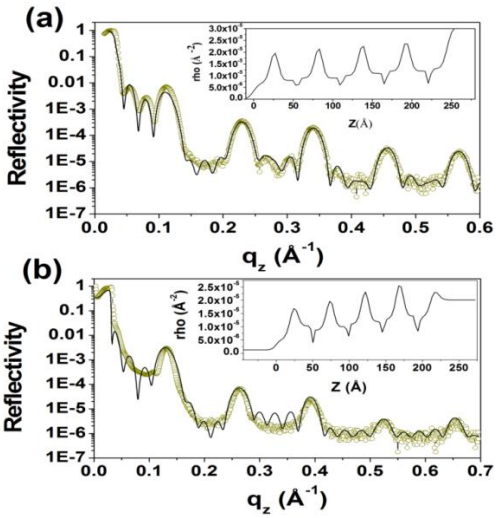

Fig. 1*: X-ray reflectivity of 9 layers of a) cadmium arachidate and (CdA_2) b) cadmium stearate ($CdSt_2$). In the inset the electron density profile of respected films are shown.*

It is seen that in 9 layers of CdA_2 (Fig. 1(a)) with the pure layer thickness an air gap of thickness ~3Å has been formed in between the tails of the long fatty acid chain. The electron density of the air gap was found to be around 4.2×10^{-6}(Å)$^{-2}$ which is very less in comparison to the individual layer electron density. The EDP of individual layer shown in the inset clearly depicts the formation of low dense air gaps as the dips and highly dense cadmium sites as the heights. Fitting also reveals that in case of CdA_2 there is an increase in the carbon chain length from 21.3Å to 23.6Å from substrate's near to outwards with decrease in electron density from 1.4×10^{-5} (Å)$^{-2}$ to 9.7×10^{-6} (Å)$^{-2}$. This shows a unique inverse relationship between the layer thickness and its electron density. The decrease in layer electron density along the outward direction with respect to the substrate may be due to the decrease in compactness of the layers and hence the tail-tail interactions loosen up and possibly as a result the interlayer air gap finds more room for its availability. In case of $CdSt_2$ also (Fig. 1(b)), the chain length and electron density of the individual monolayer found to be varying with respect to its adjacent layer. Comparing the layer properties from the fitting parameters CdA_2 is found to be deposited in more ordered fashion than that of $CdSt_2$. We may conclude that by increasing the number of carbon atoms in the fatty acid chain we can make better deposition of large number of layers, but then also amphiphilic character of the large fatty acid may limit the film deposition.

Nayan Mani Das, Dhrubojyoti Roy and P. S. Gupta (Department of Applied Physics, Indian School of Mines, Dhanbad); Mukul Gupta

2.4.22 Development of oxide based hybrid thin films for optoelectronic applications

Thin film of metal oxides has a great interest because of their application in different optoelectronics devices such as LED, sensor, photovoltaic, anti reflection coating for solar cell and photo anode materials for dye sensitized solar cell etc. Several deposition techniques such as chemical vapour, ion-assisted, pulsed laser, spin coating, rf-sputtering, sol-gel and LB are used to synthesize the metal oxide thin films. Among them pulsed laser deposition (PLD) is the simplest technique for preparation of thin films.

Thin films of TiO_2 - SiO_2 target were deposited at 750^oC substrate temperature in the presence of different oxygen gas pressure. The gas pressure was maintained by manual controller through wall and measured using a cold cathode gauge. The chamber was evacuated to a base pressure $1x10^{-6}$ Torr by turbo molecular pump. KrF excimer laser (λ= 248nm, 10Hz repetition rate) model LAMBDA PHYSIK,COMPEex was used for ablation of TiO_2 - SiO_2 composite target.Laser of 220 mJ energy was focused on the rotating target at 45^o incident angle. For cleaning, quartz substrates were rinsed first in acetone and then methanol for 15 min in ultrasonic bath before deposition. During the each deposition, target to substrate distance was kept at 4.5 cm. TiO_2 - SiO_2 thin films were deposited onto quartz substrate using 15,000 shots for 25 min at vacuum (ST-0) and different oxygen gas pressure 0.1, 1, 10, 50 mTorr (ST-1, ST-2, ST-3, ST-4). X-Ray diffraction studies were performed to get the information about structure of composite thin films. Above figure describes quite interesting features. The crystallinaty of the thin films decreases with oxygen gas pressure. Best crystallinity was obtained for 1 mTorr oxygen pressure. The XRD pattern of prepared thin films very well matches with the peak position of TiO_2 rutile crystal (JCPDS-78-1508). There is no signature of XRD peaks of SiO_2 crystal. The XRD pattern exhibits tetragonal structure with the space group $P4_2/mnm$ (136). The (h k l) values of most prominent peaks are shown in the XRD pattern. Raman Spectroscopy was carried out for the confirmation of prepared composite thin film and Atomic Force Microscopy (AFM) was carried out to study the surface morphology of prepared thin films.

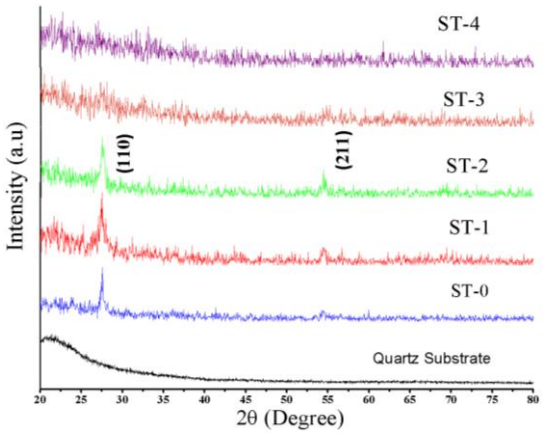

Fig.1 *XRD Pattern of thin films.*

A. K. Kunti, S.K. Sharma (I.S.M, Dhanbad), R.J. Choudhary and Mukul Gupta

2.4.23 Characterization of pulsed laser deposited SnO_2– Fe_2O_3 thin films

Transparent and electrically conducting oxide (TCO) films have found wide range of applications in solid state devices such as solar cells, display devices, gas sensors and electro-chromic devices. Among the TCO materials, SnO_2 is a popular choice for optoelectronic applications due to its low electrical resistivity and high optical transmittance along with good chemical stability. In a similar manner, Fe_2O_3 is a widely investigated material owing to its thermodynamic stability at high temperatures, non-toxicity and possesses a band gap (~2.2 eV) that lies in the visible range and has a relatively high refractive index.

Powder blends containing 50 wt% SnO_2 and 50 wt% Fe_2O_3 were properly weighed, mixed and thoroughly grounded in a mortar by mechanical means. These powder blends were subsequently used to produce 1 inch diameter pellet through pressing by applying 6 ton load followed by sintering at 1100°C for 4 hours. A KrF excimer laser source with laser energy 220 mJ (Lambda Physik COMPEX, λ =248 nm) was used to ablate the targets. The pulse repetition rate was set at 10 Hz. Deposition was carried out on quartz substrate at 750°C for growing composite films, while target to substrate distance was maintained at 4.5 cm. During deposition, oxygen partial pressure was maintained at $1x10^{-4}$ Torr.

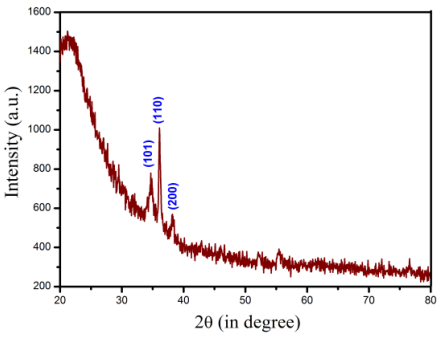

Fig.1 *XRD pattern*

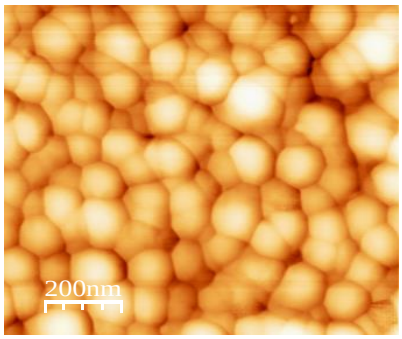

Fig.2 *AFM image*

X-ray diffraction (XRD) and atomic force microscopy (AFM) were used to investigate the morphology and structure of the films. Figure 1 shows the XRD spectrum of SnO_2–Fe_2O_3 composite thin films. The major peaks at the 2Θ values 34.05, 38.12 and 35.66° are indexed to the (101) and (200) of rutile SnO_2 (tetragonal) and (110) of Fe_2O_3 (hexagonal) respectively. Figure 2 shows the AFM studies of the prepared composite films which indicate that the surfaces are fairly smooth with rms roughness 2.59 nm and particle size 100-120 nm.

M. Chowdhury, S.K. Sharma (I.S.M Dhanbad); R.J. Choudhary and Mukul Gupta,

2.4.24 Effect of solvent system on the stability of fluorescent crown ether complexes of metal ions

Crown ethers containing fluorescent moieties can be developed as potential sensors for cations with concentrations as low as 10^{-5} M. In the present study we have prepared crystals of complexes of mono and dibenzo derivatives of crown ethers, 15-crown-5 and 12-crown-4 , with inorganic salts (fluoride, chloride, bromide, iodide and perchlorate salts of Na^+, K^+ and Li^+).

Proton (^1H) NMR, XRD, ESI, and IR have been used to elucidate the crystal structure and stoichiometry of these macrocyclic polyether complexes.UV spectroscopy was employed to monitor the binding event between the cation and crown ether. The complexes in solution were formed when the molar ratio of salt solution was ten folds greater than that of crown ether. Jobs plots were constructed to arrive at the stoichiometry of the complexes. 1:1stoichiometry was observed in all cases by UV spectroscopic titrations in acetonitrile solvent. ESI studies also confirmed the 1:1 stoichiometry of the complexes.

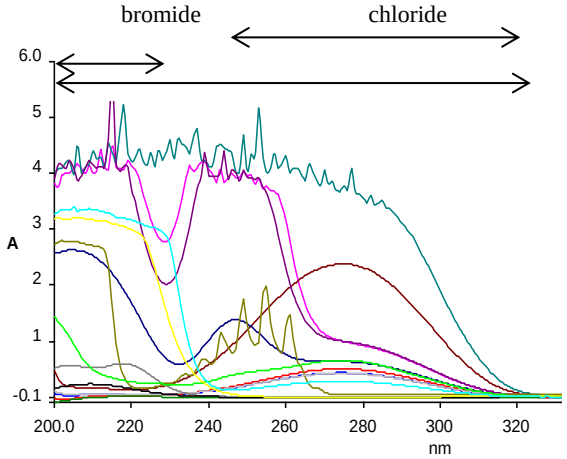

Fig.1. UV spectra; region of absorbtion of inorganic salts in acetonitrile at 10^{-3} M.

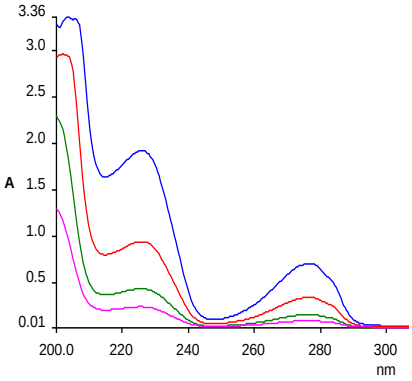

Fig.2. Absorbance of B15C5 at various concentrations.

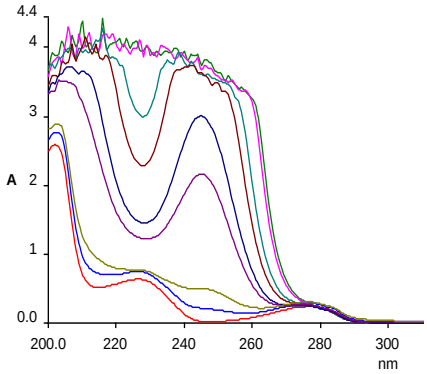

Fig. 3. Absorbance of B15C5 (0.26 x 10-3M) vs NaI (10-2M)

The complexes were further characterised by IR and ^{I}H NMR. The IR spectra show a shift in peak positions of Ar-O-CH_2 and CH_2-O-CH_2 protons when compared to that of free crown ethers(Table1.).

These shifts confirm ion-dipole interaction between the cation with the oxygen of ethereal oxygen atom (-O-CH_2-CH_2-) in formation of the complexes. The chloride and iodide salts absorb at the same wavelength as crown ether viz. 276 nm (Fig 1.and Fig 2.). The complexes do not show any new absorbtion peak. Therefore a method to determine the stability constants of these complexes after correction for absorbtion due to either species in various solvents like acetonitrile, chloroform, methanol, THF etc. is being developed. XRD intensities were collected on a Bruker D8 Advance X-ray difffractometer. Peak indexing is being carried out to assign crystal lattice to the complexes.

Table 1. Selected IR peaks of the free crown ethers and complexes

S.No.	Compound	Ar-O-R cm^{-}	R-O-R cm^{-1}
1	DB15C5	1230	1056
2	DB15C5.NaI	1205	1043
3	DB15C5.LiBr	1209	1047
4	B12C4	1259	1033
5	B12C4. LiBr	1245	1024
6	B12C4. LiClO4	1251	1041

Namrata Ghildiya, Geeta Joshinee Pant, M.S.M.. Rawat (Department of Chemistry, H.N. B. Garhwal University, Srinagar-Garhwal, Uttarakhand); Mukul Gupta

2.5 Collaborative Research using in-house facilities at Kolkata Centre

2.5.1. Room temperature ^{57}Fe Mossbauer spectroscopic investigation of Ni-Fe alloy

Mossbauer hyperfine parameters were measured for Ni-Fe alloy containing different proportion of nickel and iron . Ni concentration was varied from 0 to 75% in the samples. All the spectra were fitted with two discrete sextets. One sextet having hyperfine field ~ 330 kOe represents of α-Fe phase and the other sextet having lower hyperfine field was assigned to Ni_3Fe phase. It was seen that with increasing Ni concentration , the proportion of Ni3Fe phase increases. Low temperrature Mossbauer data will be recored to have more information .

G. Deo (IIT, Kanpur); S.P. Pati, D. Das

2.5.2. Mössbauer measurement of some chromite samples

Room temperature ^{57}Fe Mossbauer measuremenst were carried out on a few chromite samples procured from chromi-ferrous rocks of Andaman and Nocobar islands . All the spectra were fitted with three doublets corresponding to one ferrous (Fe2+) and two ferric(Fe^{3+}) site. Variation of ferrous/ferrous population was investigated to gather information on the prevailing atmosphere existed dorinf formation of these rocks.

T. Pal (GSI); S.P.Pati, D.Das

2.5.3. Room temperature Mossbauer studies of Fe_2O_3/ZnO nanocomposites

A series of samples, Fe_2O_3/ZnO nanocomposites milled for different durations (upto 30 hour) were studied by Mossbauer spectroscopy.. Calculated amount of powders (having 10 atomic wt% of Fe2O3) were milled under closed milling condition (vial is not opened during the milling process) without any additives (dry milling). The milling was carried out at 300 rpm for 30hrs keeping ball to powder mass ratio 10:1. Mossbauer spectra were obtained and fitted with a single sextet for all samples. However, the sample milled for 30 hours shows an additional doublet .All the hyperfine parameters of spectra represent the phase of Fe_2O_3. Magnetic and optical measurements will be carried out to have a definite conclusion.

Chandana Banerjee (Kalna College); S.P. Pati, D. Das

2.5.4. Hyperfine characterization of $CoFe_{2-x}Dy_xO_4$ (x=0.05, 0.1 and 0.15)

Mossbauer studies were carried out on dysprosium doped cobalt ferrites $CoFe_{2-x}Dy_xO_4$ (x=0.05, 0.1, 0.15).Each sample was sintered at two different temperatures (300 and 500^0C). For the samples annealed at 300°C, the Mössbauer spectra were fitted with two discrete sextets along with a doublet. The two individual sextets were assigned to the tetrahedral (A) and octahedral (B) sites of the ferrite and the doublet was assigned to the particles undergoing superparamagnetic relaxation. It was observed that with increasing dysprosium concentration (upto 0.1) the area ratio B to A site changes confirming the occupancy of Dy ions in the ferrite structure. Further increase in Dy concentration (x=0.15) caused a relaxation in the spectrum. For the samples

(x=0.05 and 0.1) annealed at 500°C the doublet disappeared. However, the doublet still persists for higher Dy concentration (x=0.15).

Hemant Kumar (Pantnagar University); A. Das, S.P. Pati, D. Das

2.5.5. Room temperature Mossbauer spectroscopic studies of $(Li_{0.5}Fe_{0.5})_{1-x}$ Zn_x Fe_2O_4

A systematic investigation on $(Li_{0.5}Fe_{0.5})_{1-x}$ Zn_x Fe_2O_4 (x varied from 0 to 1) was carried out by using room temperature ^{57}Fe Mössbauer spectroscopy. All the samples upto x=0.4 were fitted with two sextets assuming two different sites (tetrahedral and octahedral). However a presence of α-fe2O3 as an impurity phase was found in case of x=0.3 and 0.4. A relaxation occurs in the case of samples 0.5≤x≤0.7 and hence fitted with a distribution of hyperfine field along with a doublet. Finally, samples having 0.8≤x≤0.1 collapses to a single paramagnetic doublet.

S. Ram (IIT, Kharagpur); A. Das, S.P. Pati, D. Das

2.5.6. Positron annihilation studies on Sc doped AlZnMg alloys

Lifetime data was fitted with one life time value. With addition of Sc , the life time value was found to increase. At higher concentration of Sc (>0.6 wt%) , the sample is expected to have vacancies and interstitials. However additional lifetime due to presence of vacancy could not be fitted. This is most probably due to low concentration of defects in the sample.

M. Ghosh (BESU, Shibpur); A. Roychowdhury, D. Das

2.5.7. Positron annihilation lifetime study on TiO_2 with different metal (Sn, Ni, Mn) doping

Pristine and Sn, Ni and Mn doped TiO_2 nanoparticles were synthesized by the wet chemical route and characterized by positron annihilation lifetime technique. The recorded life time data was deconvoluted with three lifetimes.. Variation of defect sizes and their intensities were observed in samples with different doping elements.

A. Choudhury (Tezpur University); A. Roychowdhury, D. Das

2.5.8 Defect studies on alpha irradiated pristine and doped GaAs

Pristine and Sn , Te and Zn doped GaAs wafers were irradiated with 60 MeV alpha partricles . The irradiated GaAs samples were characterized by positron annihilation lifetime spectroscopy. Each Positron annihilation lifetime spectrum was fitted with two life times (τ_1 and τ_2). The lifetimes are assigned different type of defects present in the irradiated samples. Isochronal annealing studies are in progress to study the defect dynamics.

S. Pan, A.Sengupta (Visva Bharati University); A. Roychowdhury, D. Das

2.5.9. PAS study of ZnO nanoparticles synthesized by the co-precipitation technique

ZnO nanoparticles of different sizes are investigated by positron annihilation lifetime technique. The lifetime data was deconvoluted with three lifetime parameters. The shortest lifetime τ_1 and intermediate lifetime τ_2 both were found to decrease as the average particle increases. This indicates a decrease in Zn monovacancy concentration in the grain boundary regions and reduction of size of triple junctions at intersections of three or more grains with the increase of average particle size.

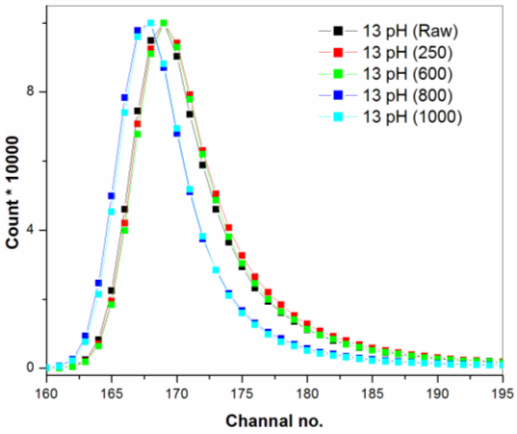

Fig. 1 Positron lifetime spectra of ZnO nanoparticles calcined at different temperature

Chandana Rath (Banaras Hindu University); A. Roychowdhury, D. Das

2.5.10. Magnetic and magneto-transport investigation of $Eu_{0.5}Sr_{0.5}Mn_{1-x}Co_xO_3$ perovskite

The perovskite manganite of nominal composition Eu0.5Sr0.5Mn1-xCoxO3 (x = 0, 0.02, 0.05, 0.1) has been investigated through transport and magneto-transport measurements. We observe field induced transition from antiferromagnetic insulating state to ferromagnetic metallic state below a certain temperature for x = 0, 0.02 and 0.05 samples on application of external magnetic field. Critical field required for insulator to metal transition depends strongly on the Co concentration. For x = 0.1 sample no transition is observed even for 150 kOe of applied magnetic field. Ground state of these samples at low temperature depends strongly on the previous history of applied magnetic field. We also observe large magnetoresistance (~ 99.9% for 150 kOe of applied magnetic field) below 100 K, which is connected to the field induced transition present in the sample.

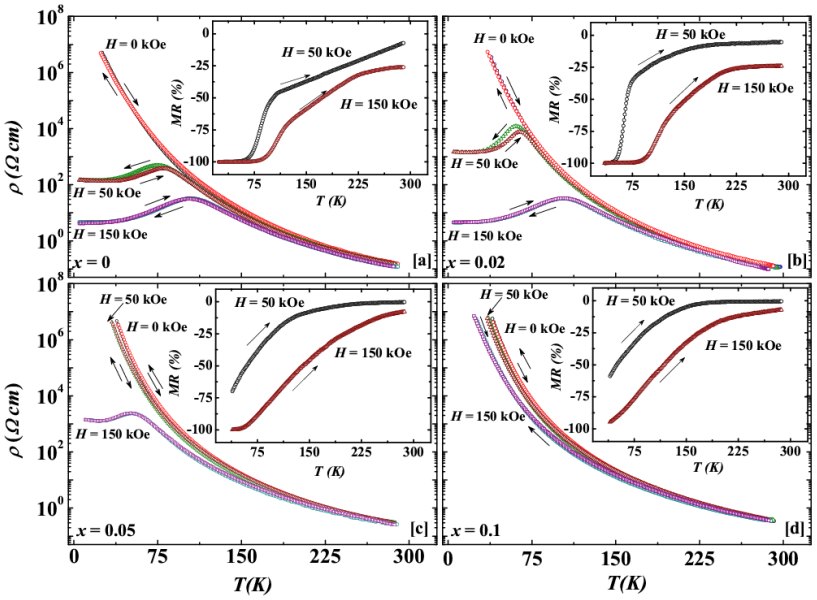

Fig.1 *Temperature variation of resistivity in presence of different applied magnetic field. Insets depict temperature variation of magneto resistance.*

S. Majumdar (IACS, Kolkata); P. Dutta, D. Das, S. Chatterjee

2.5.11 Metastability and inverse magnetocaloric effect in doped manganite $Nd_{0.25}Sm_{0.25}Sr_{0.5}MnO_3$

This compound shows a first order metallic ferromagnetic (FM) to insulating antiferromagnetic (AFM) phase transition on cooling. On application of external magnetic field (H), the AFM insulating state transforms to a metallic FM phase through metamagnetic transition. Considering, rich H and T induced phase transition, we carefully examined the metastability associated with the insulator-metal transition, and the role of two different kind of phase separation to the observed magneto-functional properties including colossal magnetoresistance. In order to understand the role of first order phase transition toward the observed anomalies, we have compared them with the corresponding data of a ferromagnetic shape memory alloy (FSMA) with nominal composition $Ni_2Mn_{1.36}Sn_{0.64}$ (NMS). We observe striking similarities between the transport and magnetic properties of two different materials (NSSMO and NMS), both showing field and temperature induced first-order magneto-structural transitions. Although such similarities are investigated only between two particular compositions, our observation can be generalized among vast compositions of manganites and FSMAs, where the temperature-driven first-order transition is sensitive to an applied magnetic field.

2.5.12 Metastability and inverse magnetocaloric effect in doped manganite $Nd_{0.25}Sm_{0.25}Sr_{0.5}MnO_3$

This compound shows a first order metallic ferromagnetic (FM) to insulating antiferromagnetic (AFM) phase transition on cooling. On application of external magnetic field (*H*), the AFM insulating state transforms to a metallic FM phase through metamagnetic transition. Considering, rich *H* and *T* induced phase transition, we carefully examined the metastability associated with the insulator-metal transition, and the role of two different kind of phase separation to the observed magneto-functional properties including colossal magnetoresistance. In order to understand the role of first order phase transition toward the observed anomalies, we have compared them with the corresponding data of a ferromagnetic shape memory alloy (FSMA) with nominal composition $Ni_2Mn_{1.36}Sn_{0.64}$ (NMS). We observe striking similarities between the transport and magnetic properties of two different materials (NSSMO and NMS), both showing field and temperature induced first-order magneto-structural transitions. Although such similarities are investigated only between two particular compositions, our observation can be generalized among vast compositions of manganites and FSMAs, where the temperature-driven first-order transition is sensitive to an applied magnetic field.

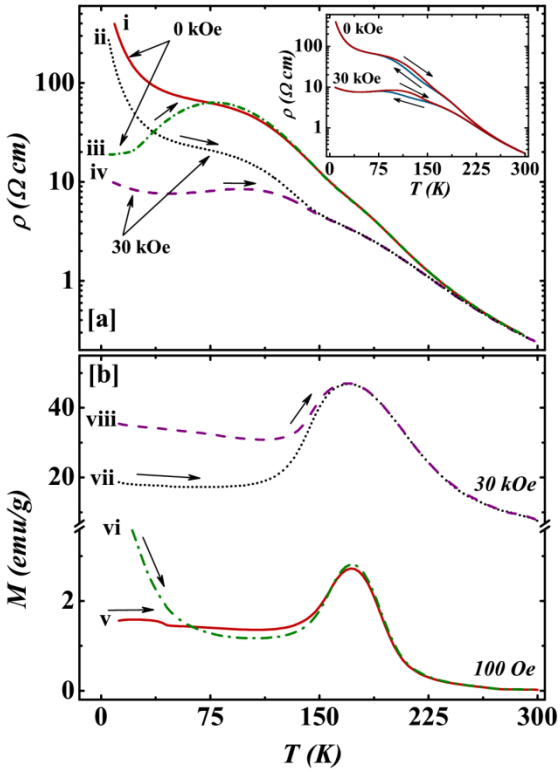

Fig.2 *Temperature variation of resistivity and magnetization recorded in different conditions.* [this fig is taken from J. Phys.: Condens. Matter. **24** (2012) 366001]

S. Giri, S. Majumdar (IACS, Kolkata); S. Chatterjee

2.5.13. Magnetic investigation of $Cu_{70.9}Al_{18.1}Mn_{11}$ shape memory alloy

The ferromagnetic shape memory alloy of nominal composition $Cu_{70.9}Al_{18.1}Mn_{11}$ has been studied through dc and ac magnetization measurements. Unlike other Cu containing shape memory alloys, Cu-Mn-Al systems of alloys show interesting magnetic behaviour. Ferromagnetism in Cu-Mn-Al alloys come from the Rudermann-Kittel-Kasuya-Yosida (RKKY) type ferromagnetic exchange interaction between Mn atoms. The studied alloy undergoes ferromagnetic to glassy transition below martensitic transition (MT). Clear frequency shift in ac susceptibility measurement is observed near the step like anomaly present in the zero field cooled dc magnetization data, which actually indicates the onset of spin glass freezing in the sample. The sample can be identified as a reentrant spin glass with both ferromagnetic and glassy phases coexisting together at low temperature. A strong magnetic memory effect is also observed at low temperature in this alloy. This work is going to be communicated shortly.

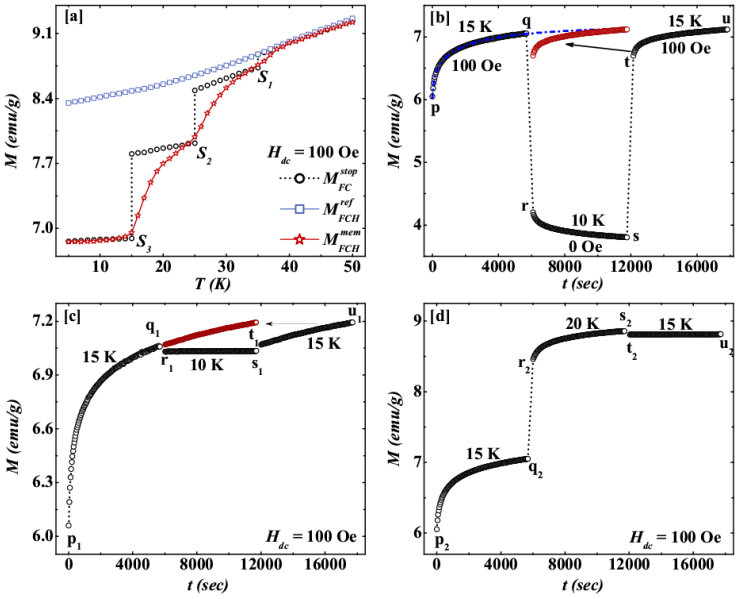

Fig.3 *Different magnetic memory measurements of* $Cu_{70.9}Al_{18.1}Mn_{11}$ *alloy*

S. Chattopadhyay, S. Giri, S. Majumdar (IACS, Kolkata); S. Chatterjee

2.5.14. Superconductivity in $Fe(Se_{0.4}Te_{0.6})_{0.8}$

Polycrystalline sample of $Fe(Se_{0.4}Te_{0.6})_{0.82}$ which is a member of Fe-Te-Se based superconducting materials, has been prepared following solid state reaction route in vacuum. This composition undergoes the superconducting transition around 12 K which is clearly visible in our magnetization as well as resistivity data. Temperature variation of heat capacity shows a weak anomaly near superconducting T_C whose nature differs from many other conventional superconductors. Both magnetization and heat capacity measurements reveal presence of multiple phase transitions above T_C. Interestingly, field dependence of magnetization shows ferromagnet like hysteric behaviour below the superconducting transition. Careful analysis based on X-ray diffraction and Mossbauer spectroscopy indicates

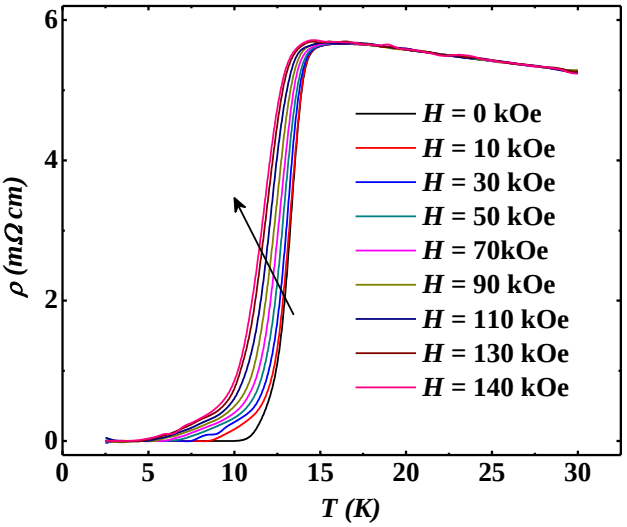

Fig.4 *Resistivity is plotted as a function temperature at different constant applied magnetic field.*

that this feature is intrinsic to the sample and therefore turns it to a potential candidate for magnetic superconductor. Thorough investigation is in progress to understand the possible correlation between magnetism and superconductivity in this exotic material.

S. Chattopadhyay, S. Giri, S. Majumdar (IACS, Kolkata); D. Venkateshwarlu, V. Ganesan; S. Chatterjee

2.5.15. Giant magnetoresistance and large exchange bias effect in $Ni_{46}Mn_{41}In_{13}$ shape memory alloy

The transport and magnetic properties of ferromagnetic shape memory alloy of nominal composition $Ni_{46}Mn_{41}In_{13}$isinvestigated. The alloy undergoes martensitic transition around 240 K. The region around this structural transition is found to highly metastable and susceptible to the applied magnetic field. Giant negative magnetoresistance (≈ - 64% at 70 kOe) is observed around the region of thermally driven martensitic transition. The sample also shows large exchange bias at low temperature. The Mn-Mn intersite antiferromagnetic correlation has an important role for the observation of these magneto-functional behaviours. This work is accepted for publication in *Journal of Alloys and Compounds*.

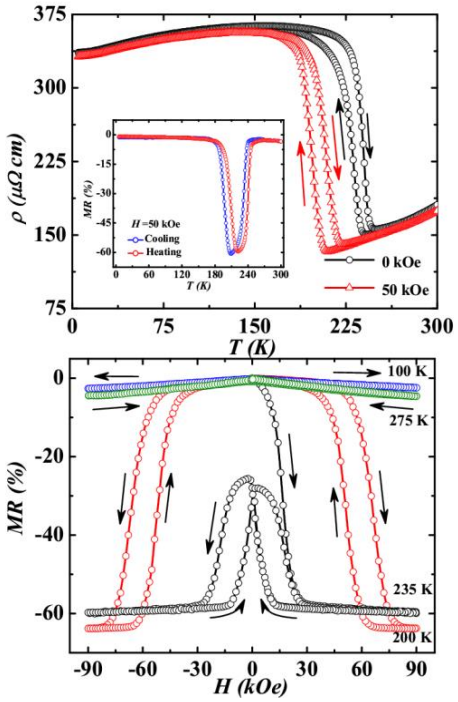

Fig.5: *Temperature and field variation of magnetoresistance*

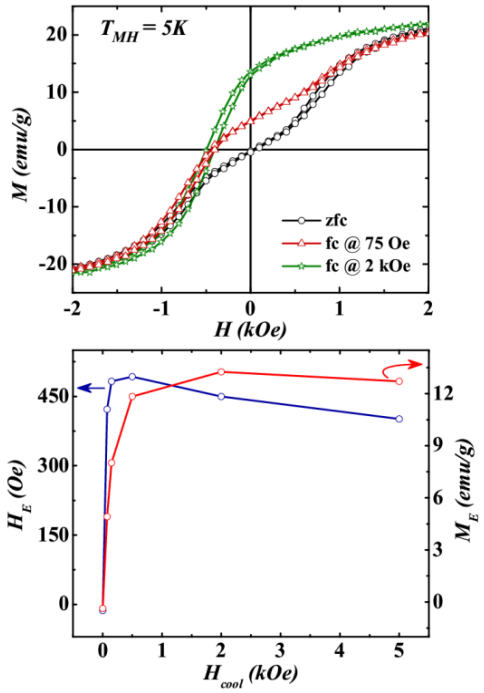

Fig.6: *Exchange bias measurement for $Ni_{46}Mn_{41}In_{13}$ alloy.*

S. Pramanick, S. Giri, S. Majumdar (IACS, Kolkata); V. V. Koledov, A. Mashirov (Kotelnikov Institute of Radioengineering and Electronics of RAS, Russia); A. M.Aliev, A. B. Batdalov (Amirkhanov Institute of Physics of Daghestan Scientific Center, Russia); B. Hernando, W.O. Rosa, L. Gonz´alez-Legarreta (Universidad de Oviedo, Spain); S. Chatterjee

2.5.16. Revival of martensitic instability in Ga doped Ni-Mn-In alloys

There is an important difference between Ni-Mn-Ga and Ni-Mn-Z (Z = In, Sn, Sb) alloys with respect to the occurrence of martensitic phase transition (MPT). The stoichiometric Heusler compound Ni_2MnGa as well as several neighbouring compositions undergo MPT, while no structural transition occurs in stoichiometric Ni_2MnZ compounds. One can induce MPT in Ni-Mn-Z alloys by doping excess Mn at the Z site, however, that is also restricted to a small window of doping concentration. It has been found that for Ni-Mn-In alloys, the

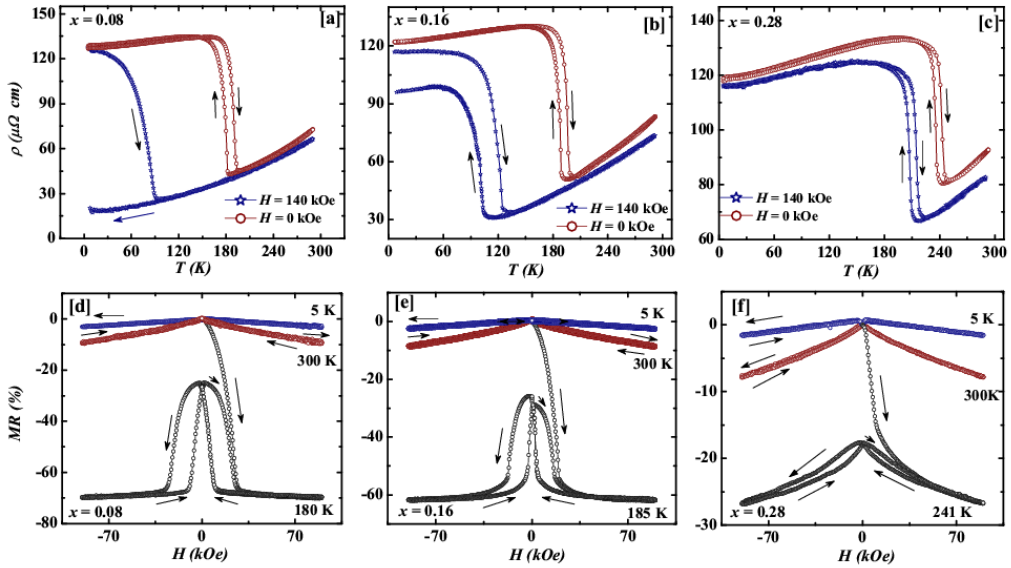

Fig.7 *Resistivity measured in heating and subsequent cooling protocols for x = (a) 0.08, (b) 0.16, and (c) 0.28 in zero field as well as in applied magnetic field. (d), (e) and (f) denote the isothermal magnetoresistance versus field data recorded at different temperatures for 0.08, 0.16and 0.28 samples respectively.*

compositions $Ni_2Mn_{1+p}In_{1-p}$ show MPT for $0.36 \leq p \leq 0.8$. Here p is the excess Mn atoms which have been added at the expense of In atoms. The martensitic start temperature (T_{MS}) for the end member p = 0.36 sample is reported to be 264 K. Interestingly, the MPT suddenly vanishes on slight reduction of p; for example, at p = 0.34, no signature of MPT is found down to 5 K. It appears that the MPT in Ni-Mn-In is less robust than the corresponding Ga alloys. In this work, we focused on some Ni-Mn-In alloys where In is partially replaced by Ga. We took p = 0.32 sample (*i.e.*, $Ni_2Mn_{1.32}In_{0.68}$) as the starting material, which does not show MPT. Our goal is to investigate whether MPT can be revived by suitable Ga doping at the In site, and for that purpose we studied $Ni_2Mn_{1.32}In_{0.68-x}Ga_x$ (x = 0, 0.04, 0.08, 0.16, 0.20, and 0.28) alloys. Interestingly, for small Ga substitution (x = 0.08), the MPT reappears in the sample, and on further Ga doping transition shifts to higher temperature. Samples showing thermally driven maretnsitic transition ($x \geq 0.08$) are also found to be susceptible to the applied magnetic field, and both magnetization and magnetoresistance indicate the signature of field-induced transition (see fig.7). Upon cooling under a magnetic field, we observe kinetically arrested state which is particularly prominent in low Ga containing samples (x = 0.08, 0.16) (see fig.7). It clearly

demonstrates that these Ga doped samples possess all the properties of metamagnetic shape memory alloys. This work is accepted for publication in *Intermetallics*.

S. Pramanick, S. K. De, S. Giri, S. Majumdar (IACS, Kolkata); D. Venkateshwarlu, V. Ganesan; S. Chatterjee

2.5.17. Magnetic and magneto transport investigation of $Mn_{11}Ge_8$ binary alloy

The transport and magnetic properties of the binary alloy of nominal composition $Mn_{11}Ge_8$ are reported here. The alloy undergoes paramagnetic to ferromagnetic transition around 275 K and ferromagnetic to antiferromagnetic transition around 160 K. Both the positive and negative magnetoresistance is observed depending upon the field strength. The sample shows positive magnetocaloric effect (about 3 J/kg-K) under 90 kOe of applied field. This work will be communicated shortly.

S. Pramanick, S. Giri, S. Majumdar (IACS, Kolkata); D. Venkateshwarlu, V. Ganesan, S. Chatterjee

2.5.18. Magneto-dielectric investigation of $CuCrS_2$

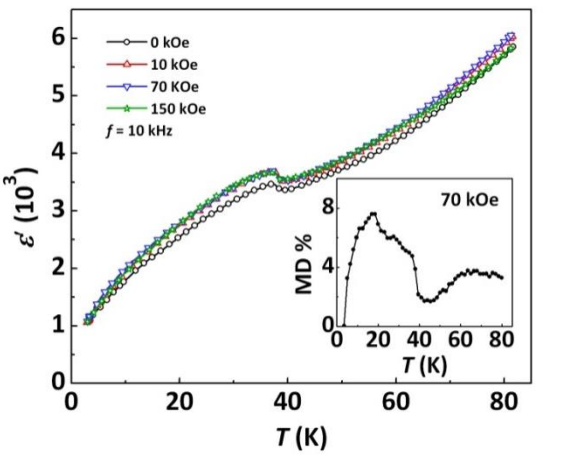

Fig.8: *Temperature dependence of dielectric constant at different magnetic fields measured at 10 kHz. Inset: Magnetodielectric percent in 70 kOe field calculated from the above data*

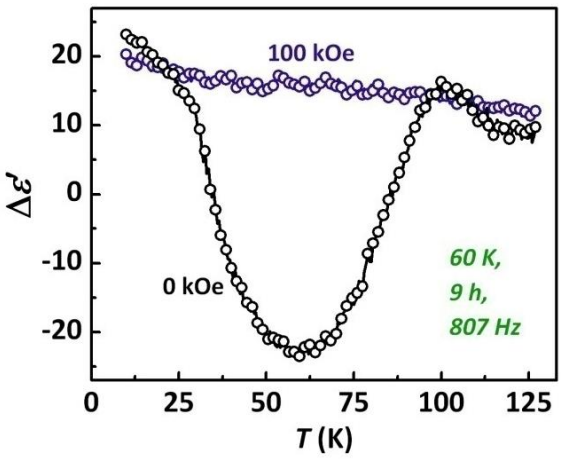

Fig.9: *Temperature dependence of difference in dielectric constants. One is measured without field and the other in 100 kOe field with waiting at 60 K for 9 h measured at an exciting field of 807 Hz*

A triangular lattice Heisenberg antiferromagnetic compound $CuCrS_2$ is investigated through magneto-dielectric measurements. Cr^{3+} spins are arranged at the corners of triangular lattice showing geometric frustration. $CuCrS_2$ is rhombohedral at room temperature and shows a structural transition to monoclinic structure at ~ 38 K, through which the frustration is released, while exhibiting different ordering below 38 K. Simultaneous antiferromagnetic (T_N) and dielectric transitions occur at the structural transition designating the compound to be a type II multiferroic compound. Neutron studies reveal a spiral spin order below T_N. Since such ordering often induces ferroelectricity, we intend to study the nature of the dielectric transition. We are also motivated to study any possible magnetoelectric coupling and magnetodielectric effect in the compound.

Magnetodielectric properties of the sample were studied in different protocols viz. temperature dependence with and without magnetic field, isothermal magnetic field dependence and time dependence with and without magnetic field. The data shows considerable magnetodielectric effect. Fig.8 shows $\varepsilon'(T)$ at different magnetic fields. The data measured in a magnetic field differs significantly from the zero field data. The magnetodielectric percent [defined as $\{\varepsilon(H)- \varepsilon(0) / \varepsilon'(0)\times100]$ in 70 kOe field is shown in the inset of fig.8. A strong response of magnetic field is also observed in the field dependence loops that increase with increasing magnetic field. Waiting or annealing at a fixed temperature of 60 K during the cooling cycle produced a distinct signature in the warming cycle under zero field. This is observable in the difference plot (between heating loops after waiting and without waiting) and is called as "dielectric memory". The memory was found to be erased on the application of magnetic field. The difference plot with and without magnetic field is shown in Fig.

A. Karmakar, K. Dey, S. Majumdar, S. Giri (IACS, Kolkata); S. Chatterjee

2.5.19. Optical and rheological study of gamma irradiated rare-earth nanoparticle based ferrofluids

The present work reports on the optical and rheological properties of unexposed and gamma irradiated rare-earth (RE) oxide nanoparticle-based ferrofluids (FF). The ferrofluids were prepared by dispersing surfactant coated gadolinium oxide (Gd2O3) nanoparticles in ethanol medium and later on subjected to energetic gamma irradiation (1.25 MeV) at select doses. As predicted from transmission electron microscopy and X-ray diffraction (XRD) studies, the synthesized nanoparticles are of <7 nm size which crystallize into cubic crystal structure. The photoluminescence response reveals creation of defect states on nanoparticle surfaces when FFs are subjected to gamma irradiation. Whereas, rheology measurements showed unusual shear thinning behavior of the ferrofluids. The flow behavior of all the samples can be correlated to the bi-exponential decay curve fitting which reveals that decay phenomenon is governed by two independent mechanism: fast and slow events. The variation of the decay parameter with irradiation dose is attributed to the creation of point defects and weakening of inter nanoparticle bonding.

N. Paul, D. Mohanta (Tezpur University); Abhijit Saha

2.5.20 Process Development of Radiation Resistant Optical Fiber

Ionizing radiations generate defects in silica glass which are responsible of optical darkening in UV-Vis region. The generation and elimination of defects are strongly guided by OH and other co-dopants. Hence, basic spectroscopic investigation is important to understand the radiation induced absorption behavior in silica glass prior to the fabrication of fiber. The absorption spectra of different optical fibre samples with varying OH content (in the range of 1900 ppm to <1 ppm) samples, ppm) of 2 mm were recorded before and after the exposure of gamma radiation. The variation of radiation induced absorption with OH concentration for different wavelength showed that the radiation-induced attenuation is high in the UV region and decrease gradually towards the visible range. FTIR spectroscopy was carried out to identify the OH concentration in the silica glass from the OH absorption at 3600 cm^{-1}.

Real time measurement of radiation induced attenuation in the optical fiber samples were carried out on online setup. The fiber with low OH concentration (1.16 ppm) shows an overall high RIA over the entire range

of 400-650 nm. In high OH fibers the initial increase of RIA immediately after radiation exposure has been attributed to the formation of E' centers and NBOHC with the concentration of NBOHC being more than the E' centers because of the presence of more Si-OH in high OH silica which are cleaved on radiation exposure to give NBOHC. Further optimization of the waveguide parameters of the fiber is in progress to expand the transmission range in the UV and IR.

A. Bhattacharjee, S. Pal, R. Sen, K. Dasgupta (CGCRI, Kolkata); G. Bhoumik (BARC); A. Datta, A. Saha

2.5.21. Optical characterization of nano-sized organic carbon particles emitted from a small gasoline engine

The nano-sized organic carbon (NOC) particles emitted from a small gasoline engine were characterized using various ex situ optical techniques to assess their hazardous impact. The exhaust gas was sampled iso-kinetically by a quartz probe and passed through de-ionized water to gather the hydrophilic carbonaceous particulates as hydrosol. The hydrodynamic diameter of the particles ranged between 1.7 and 3.6 nm at no load, with a mean diameter of 2.4 nm. The particle size in the engine exhaust was found to increase at higher loads, which is attributed to coagulation of the particles. The chemical structure of the particles was analyzed using UV–vis and infra-red spectroscopy. Both the band gap energy and oscillator strength data evaluated from the UV–vis absorbance showed that the NOC particles contained polyaromatic hydrocarbon structures with three to five aromatic rings. Infra-red spectroscopy analysis further confirmed the presence of aliphatic and carbonyl functionalities in the aromatic structures of the particles. The fine size of the particles, their high number concentration for the type of the engine under study and their structural features, make the particles extremely hazardous for environment and health.

B. Paul, A. Datta (Jadavapur University); A. Datta, A.Saha

2.6. Collaborative Research using in-house facilities at Mumbai Centre

2.6.1. Growth kinetics of gold nanoparticle clusters in presence of peptides: A DLS Study

The growth kinetics of nano-clusters from as-synthesized gold nanoparticles (AuNPs) in presence of peptide molecules, namely, deoxycytidine (dC) and deoxyadenosine (dA) in aqueous medium with neutral pH, was studied using the dynamic light scattering (DLS) technique in UGC-DAE CSR, Mumbai centre. It was observed that the formation of nano-cluster is favorable in presence of dC, whereas it was unfavorable in presence of dA. This observation was substantiated using UV-visible spectroscopy and transmission electron microscopy (TEM) techniques. The origin of the formation of gold nano-clusters was understood in terms of the inter-particle interaction potential which is controlled by the peptide molecules present around AuNPs. In Fig. 1, we have shown the time dependence of the growth of gold nano-clusters of size around 250 nm in presence of dC. Since the conformation of the peptide molecules depends on the solution ionic or pH condition, we have also studied the pH dependence of the size of the cluster and are shown in the inset of Fig. 2.1. In Fig. 2.2, we have shown the particle-particle interaction potential calculated using the DLVO formulation. From this figure it is clear that the particle-particle interaction potential was attractive in the as-synthesized AuNPs dispersion in presence of dC, and as the nano-cluster had grown to a stable size (~250 nm) the inter-particle interaction potential became repulsive. On the contrary, the inter-particle interaction potential in the as-synthesized AuNPs dispersion in presence of dA was repulsive (not shown), and therefore, could not form the nano-cluster. The surface charge of AuNPs in the as-synthesized dispersions in presence of both dC and dA was measured using the ζ-potential measurements. A manuscript has been communicated based on this work.

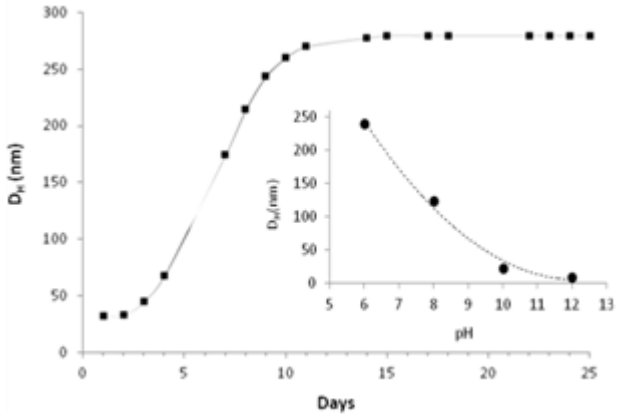

Fig.2. 1. *Growth of gold nano-clusters in presence of dC in water. Inset, pH dependence of the nano-cluster size*

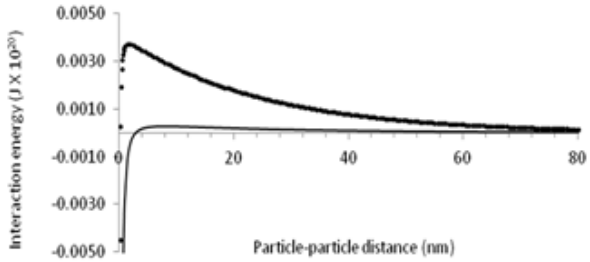

Fig. 2.2. *Inter-particles interaction energy plots using DLVO formulation for the as-synthesized Au-NPs dispersion in presence of dC (line curve) and for the dispersion in which gold nano-cluster has formed (circular dotted curve).*

A. Nimrodh Ananth, S. Umapathy, T. Ramprasath (Madurai Kamaraj University); M. A. Jothi Rajan (Arul Anandar College, Karumathur); G. Ghosh

2.7. Collaborative Research using in-house facilities at Kalpakkam Node

2.7.1. Carl Zeiss TEM Libra@200 HR

2.7.1.1. Study of particle size and morphology of IR Plasmon absorbing Silver nanoparticles

The particles were prepared by a deft manipulation of reagent ratio, pH and temperature, a wide-tunability of plasmon peaks from 400 to 1015 nm has been achieved. In contrast to previously reports, no strong reducing agent has been used in our work and anisotropic nanoparticles were synthesized in a single step at room temperature. TEM analysis revealed that the particles were having a pyramidal shape with a pentagonal base. The edge length of the penatagon was 20 nm and diagonal length of 40 nm. These nanostructures would be potentially useful in developing novel non-invasive diagnostic and therapeutic techniques.

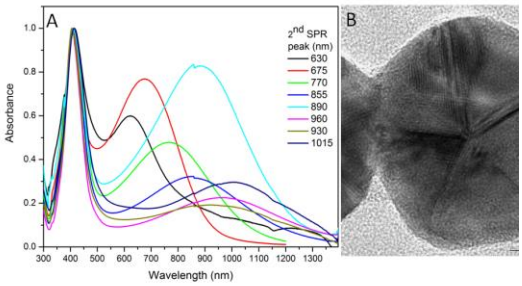

(A) UV-Vis absorption spectra of Ag nanoparticles (B) HR-TEM image of Ag NPs with 2nd Plasmon peak at 1015 nm

Amiya Priyam (BIT Mesra, Ranchi, Jharkhand.

2.7.1.2. Study on nanocrystalline hydroxyapatite (HAp- $Ca_{10}(PO_4)_6(OH)_2$) and magnesium incorporated Hap

The materials were synthesized by microwave method. The permittivity, ac conductivity, photoluminescence, wettability and *in vitro* bioactivity were enhanced for magnesium ion incorporated samples. TEM studies reveal that the incorporation of magnesium ions in HAp leads to reduction in the particle size of Mg1HAp and Mg3Hap, possibly due to the smaller ionic radii of magnesium ions to calcium ions. This material is a would be candidate for bone replacement application.

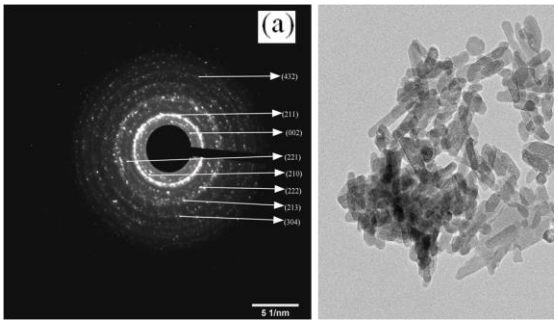

Diffraction pattern and TEM image of Mg doped HAp

K. Thanigaiarul (Anna University, Chennai)

2.7.2. FESEM with EDS facility

2.7.2.1. Studies on CdTe thin films

Polycrystalline films of CdTe were deposited by pulsed laser deposition technique. The films were studied for their microstructural and compositional properties. A typical micrograph alongwith the corresponding EDS spectra is shown alongside. From the EDAX measurements it was found that the deposited films are slightly tellurium rich. It was observed that CdTe films deposited here are polycrystalline in nature with compact grains. The grain size increased for films deposited at higher temperatures. Variations in the surface morphologies of the CdTe films deposited at different substrate temperatures are apparent from the micrographs. It was also inferred that the films became more compact when deposited at substrate temperatures greater than 573 K.

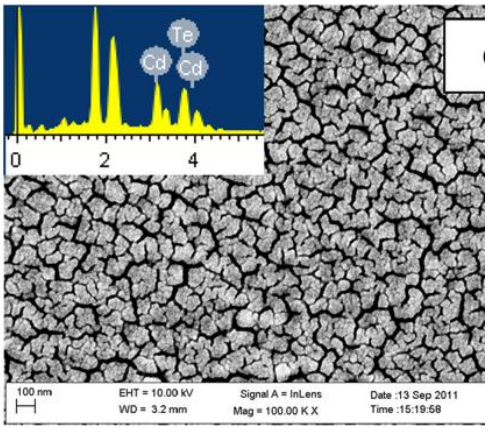

Fig. FESEM and EDS spectra of arepresentative CdTe film.

A. K. Pal (Jadavpur University, Kolkata)

2.7.2.2. Studies on Co-doped CuO flower/plates/particles-like nanostructures

A simple and rapid microwave-assisted combustion method was developed to synthesize Co-doped CuO flower/plates/particles-like nanostructures. The XRD confirmed the formation of single-phase monoclinic structure. The formations of various nanostructures were confirmed by HR-SEM. The results showed that the Co-doping has obvious effect on the morphology of the pure CuO. The optical properties were determined by DRS and PL spectra. The magnetic properties of various nanostructures were studied by VSM.

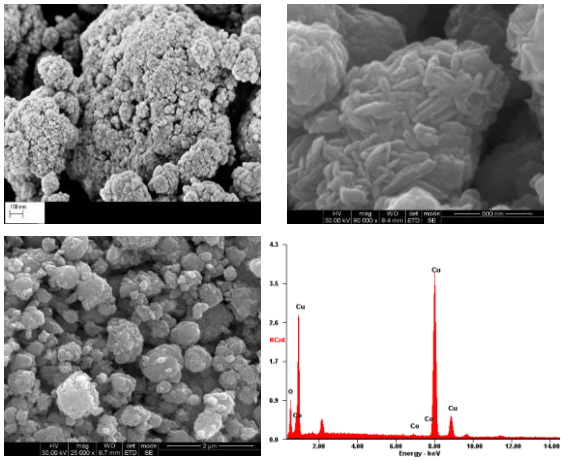

Fig. HR-SEM image of (a) pure CuO, (b) 0.5 wt% of Co-doped CuO, (c) 2.0 wt% of Co-doped CuO (d) EDS spectra of (a)

N. Mohamed Basith, J. Judith Vijaya, L. John Kennedy, M. Bououdina (Loyola College Chennai)

2.7.2.3. Studies on removal of cobalt from an alkaline waste using synthetic calcium Hydroxyapatite

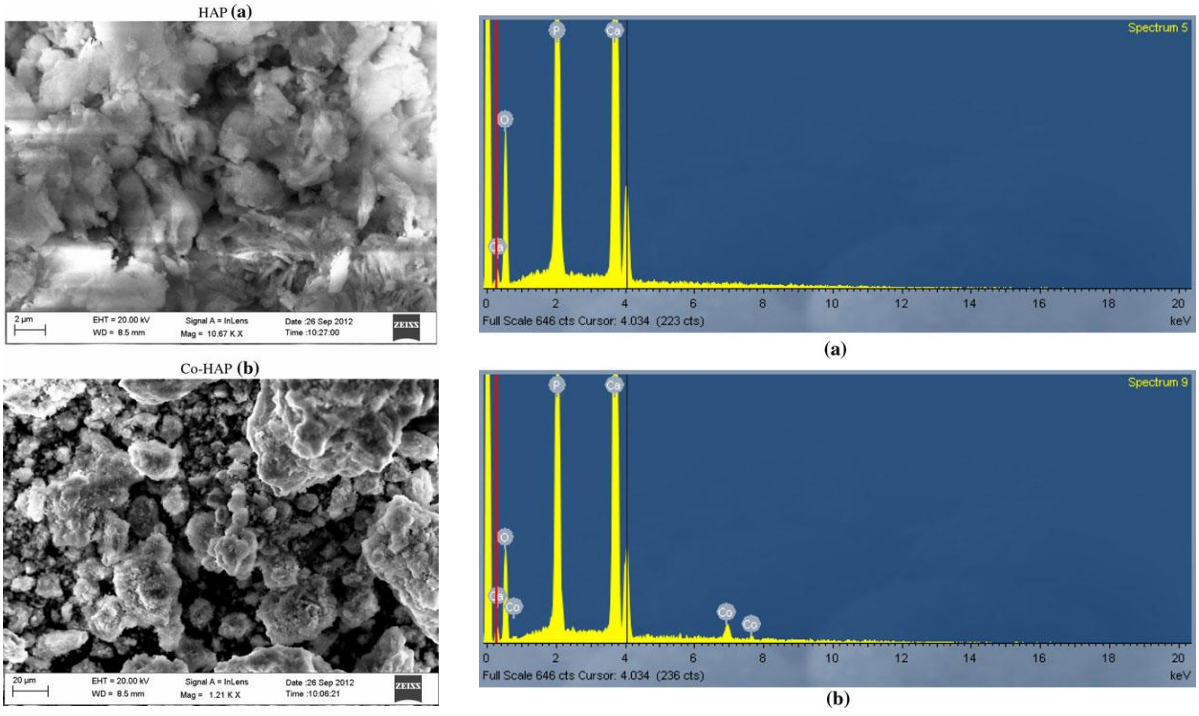

FESEM and corresponding EDS spectra of HAP and Co-HAP samples

The removal of cobalt from an alkaline waste solutions containing sodium was carried out using a radiotracer in a batch method using synthetic calcium hydroxyapatite (HAP). The influence of different parameters such as solution pH, contact time, cobalt concentration,and presence of other ions like sodium on cobalt removal was studied. The results indicated that the mechanism of cobalt removal by HAP was mainly due to chemisorption on a heterogeneous surface. According to SEM images , the surfaces of both HAP and cobalt doped HAP were found to be heterogeneous. The composition of the HAP powders prepared by the precipitation method was analyzed by energy dispersive X-ray spectroscopy (EDS).

The composition of cobalt doped HAP was also analyzed by the same technique and the results are shown above. The composition analysis by EDS shows that the Ca/P ratio in the original HAP samples is 1.60 instead of 1.67 characteristic for stoichiometric HAP. The slight calcium deficiency is common for the samples obtained by the wet methods.The EDS of cobalt doped HAP shows clearly the cobalt peak indicating that cobalt is being sorbed on HAP which is also supported by the physical appearance of the cobalt doped HAP, as because the HAP is colourless. But on contact with cobalt, it became violet in color.

Diganta Gogoi (KARP-BARC Facilities, Kalpakkam)

2.7.3. X-ray Photelctron Spectroscopy

2.7.3.1.Studies on the interfacial interactions of TiO_2 Nanoparticles with Bacterial Cells under light and dark conditions

The chemical states of titanium, after interaction with bacterial cells, were studied by X-ray Photoelectron Spectroscopy (XPS). Lyophilized, NP interacted bacterial cells (with NP concentration 1 µg/mL) and uninteracted cells were made into pellets (5mm × 1mm) and subjected to XPS analysisXPS analysis is a direct way for evaluating the surface reactivity of TiO_2 NPs where reduction of Ti (IV) to Ti (III) species can be confirmed. Figure shows the XPS spectrum of Ti 2p from the TiO_2 interacted bacterial cell surfaces under both light and dark conditions. The formation of Ti (III) species was confirmed from XPS analysis in both light and dark treated samples suggesting the possibility of redox reactions in the NP-cell interface. The interfacial reduction of TiO_2 NPs from Ti (IV) to Ti (III) species may lead to oxidative degradation of cell membrane, which is probably one of the major factors supporting cytotoxicity potential of these NPs (Biesinger et al 2010). Thus the generation of free radicals and Ti (III) species confirmed the occurrence of redox reactions at the cell–NP interface which indirectly proved oxidative disruption of cellular membrane. Hence this will facilitate the uptake/internalization of the NPs into the cells.

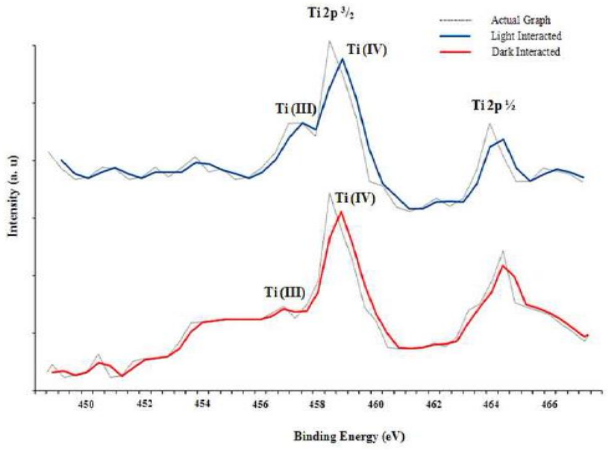

XPS spectra of TiO_2 nanoparticles under light and dark conditions

Amitava Mookherjee (VIT, Vellore)

2.7.3.2. Studies on GaSb films

GaSb films deposited by coevaporation technique were studies for their compositional analysis. The general survey XPS spectrum of a representative GaSb film deposited at 773 K., showed that the spectra is dominated by two pairs of strong peaks at ~534 eV and ~1121 eV for $Sb3d_{3/2}$ and $Ga2p_{3/2}$ core-level spectra, respectively There are a few lower intensity peaks for $Ga3d_{5/2}$ and $Ga3p_{1/2}$ at ~24 eV and 110 eV, respectively. The peak ~534 eV overlaps with that of O1s. Oxygen peak arises due to physisorbed oxygen at the surface. A very low intensity broad peak ~24.6eV of Ga3d peak is observed. Low intensity peaks of Sb4d around ~39 eV are also observed. These peaks are associated with the binding energies of Sb as Sb_2O_3 and Sb_2O_5. The low intensity of the oxide peaks of Ga and Sb signify the fact that very less amount of the oxides are present in the sample. Another low intensity peak~110eV corresponding to $Ga3p_{1/2}$ is also observed. The study confirmed the formation of GaSb bonds in the film.

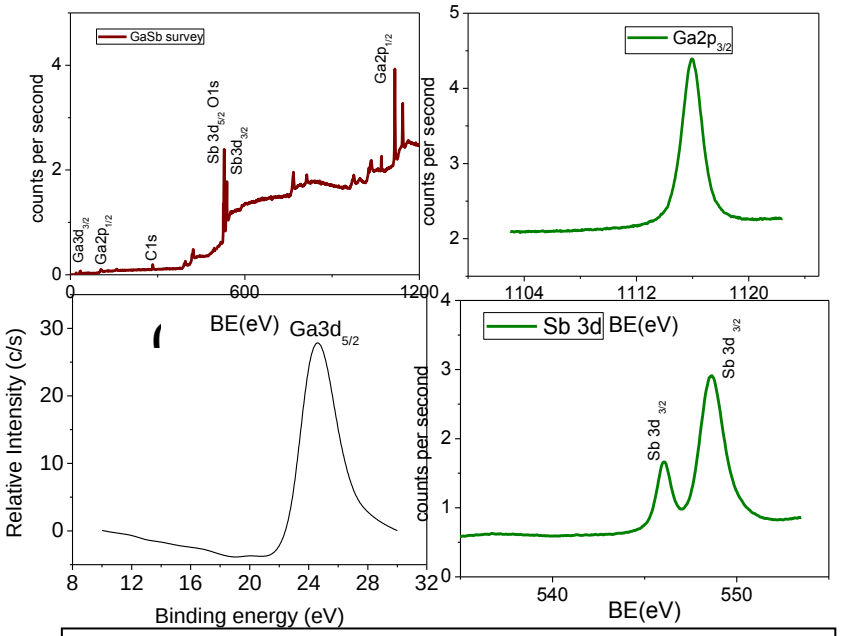

XPS spectra: a) survey, b) Ga2p , c) Ga 3d, d) Sb 3d

A K Pal (Jadavpur University, Kolkata)

3. In-house Research activities

3.1 Research activities at Indore Centre

3.1.1 Bulk magnetic Material and oxides

3.1.1.1 Study of magneto-electric properties of $BaTiO_3$ - $Ni_xZn_{1-x}Fe_2O_4$ composites

Magnetic, ferroelectric, and magneto-electric studies are studied on 0.9 $BaTiO_3$-0.1 $Ni_xZn_{1-x}Fe_2O_4$. The bi-phase nature of the prepared composites is confirmed by the x-ray diffraction measurements. The simultaneous presence of room temperature ferroelectric and magnetic orderings is confirmed by measuring the room temperature P-E and M-H loops of the prepared composites. The magneto-electric behavior is found maximum for the composite consisting of $Ni_{0:8}Zn_{0:2}Fe_2O_4$ as magnetic phase, which is explained on the basis of the magneto-strictive behavior of $Ni_xZn_{1-x}Fe_2O_4$phase

Sanjay Kumar Upadhyay, V.Raghavendra Reddy and Ajay Gupta

3.1.1.2 Effect of Co-doping on the resistivity and thermopower of $SmFe_{1-x}Co_xAsO$ ($0.0 \leq x \leq 0.3$)

Structural, electrical resistivity and thermopower of good-quality poly-crystalline $SmFe_{1-x}Co_xAsO$ samples for $0.0 \leq x \leq 0.3$ study showed that the spin-density wave observed at 130 K for $x = 0$ is suppressed when x = 0.05, above which superconductivity emerges due to injection of mobile electrons, supporting the substitution of Co^{3+} at Fe^{2+} site. However, super-conductivity disappears at $x = 0.3$.

The thermopower (S) data indicate that the majority of charge carriers is electron-like, there is noticeable deviations from the expected linear behavior in $S(T)$ at low temper-atures and S/T against temperature curves -at intermediate temperatures. These observations were interpreted on the basis of complex Fermi surface observed in this system.

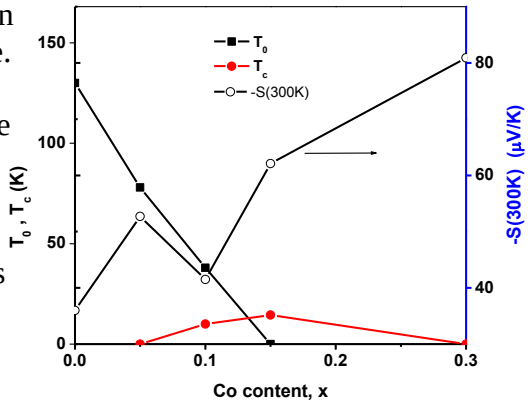

Fig.1 Doping dependence of T_c and electrical resistivity anomaly (T_0) (left axis). S(300) is also shown for comparison

G. S. Okram, A. Soni (CSR, Indore), N. Kaurav (Holkar Sci. College, Indore), A. Pal, V.P.S. Awana (NPL, New Delhi)

3.1.1.3 Magnetic glass in Shape Memory Alloy : $Ni_{45}Co_5Mn_{38}Sn_{12}$

Our studies on a Ni45Co5Mn38Sn12 ribbon sample demonstrated all the features crucial for unambiguously proving the system to be a “magnetic glass” by various thermomagnetization measurements, including CHUF measurements (figure 1). In this sample, the transition from Low magnetization martensite (LM-M) to Ferromagnetic austenite (FM-A) phases cannot be achieved at low temperature by the conventional protocol of

isothermal field variation of the zero field cooled state because of the limited range of experimentally accessible field. A magnetic field ~30T is required for this transition to occur at 5K in zero field cooled state whereas by following a novel protocol of field cooling and isothermally reducing the field (FC-MH) we have observed the transition between LM-M and FM-A phases within the accessible field range (14T) even at the lowest temperature (figure 2).

A qualitative phase diagram showing supercooling (SC), superheating (SH) and kinetic arrest (KA) bands from the variety of measurements has been constructed.

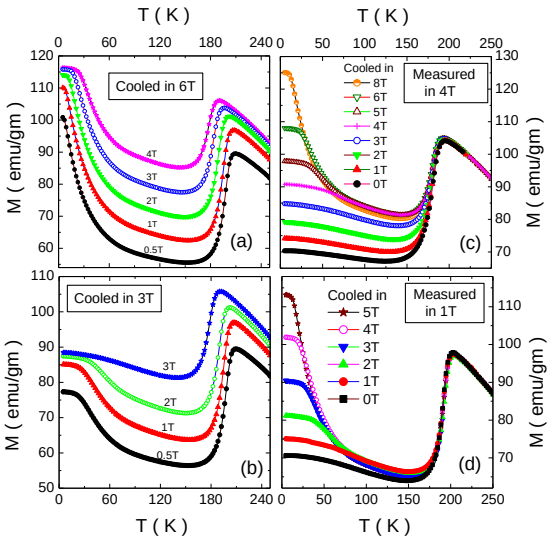

Figure 1. Magnetization as a function of temperature using the CHUF (cooling and heating in unequal field) protocol.

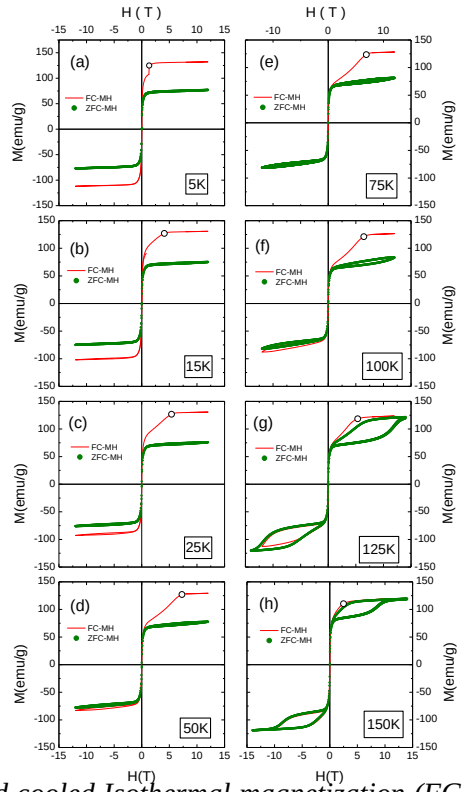

Figure 2.(a)–(h) Field cooled Isothermal magnetization (FC-MH) at various temperatures from 5 to 150 K are shown by solid red lines. Green symbols show zero field cooled M versus H curves (ZFC-MH)

Archana Lakhani, A. Banerjee, P. Chaddah

3.1.1.4 Low-temperature transmission electron microscopy and XRD studies on oxygen stoichiometric and off stoichiometric La_{1-x} Sr_x MnO_3 for x= 0.75 0.8 and 0.85

3D $La_{1-x}Sr_xMnO_{3-\delta}$ manganite has the widest 1-electron bandwidth and therefore charge-ordering (CO) is theoretically prohibited. But recent literature does report the occurrence of CO phase in this manganite. Oxygen stoichiometric and off-stoichiometric $La_{1-x}Sr_xMnO_{3-\delta}$ with x= 0.75, 0.80 & 0.85 have been synthesized to investigate the origin and the nature of CO reported in recent literature. The stoichiometry of the oxygen was determined using idiometric titration. LT-TEM and LT-XRD studies clearly reveal that stoichiometric cubic Pm3m LSMO with x=0.80 &0.85 directly transform to a $3d_{z2}$ ferro-orbitally ordered C-type anti-ferromagnetic

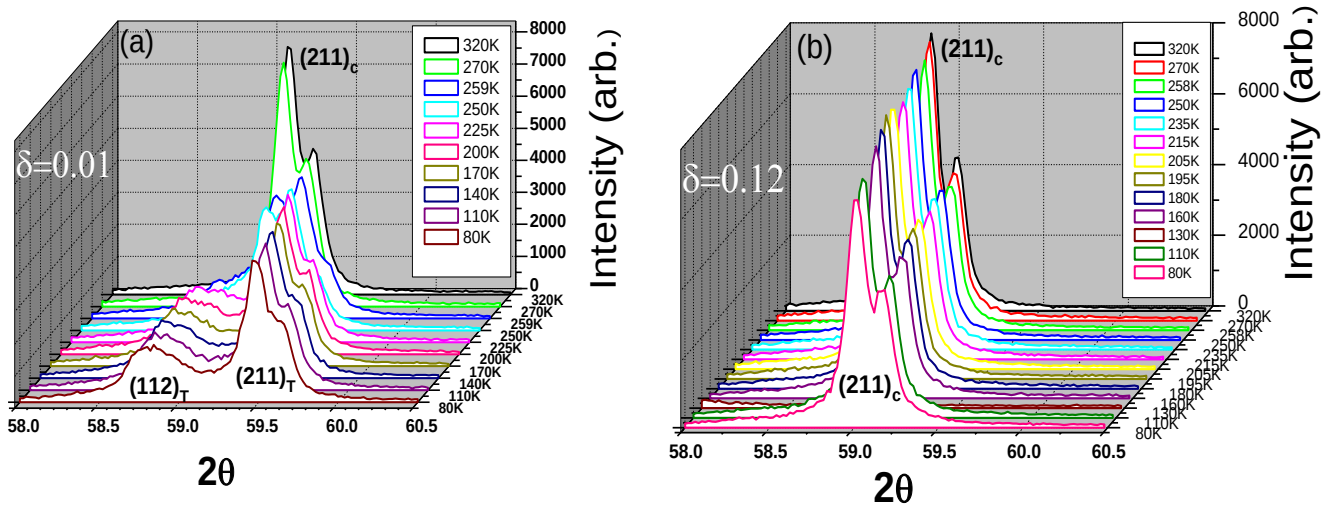

Temperature dependent 3D XRD graphs of (a) stoichiometric and (b) off- stoichiometric $La_{0.2}Sr_{0.8}MnO_{3-\delta}$ samples during cooling down to 80K.The splitting of (211) XRD peak is due to cubic-tetragonal (c/a=1.021) transition of the stoichiometric sample. But no such splitting is observed for the off- stoichiometric sample in (b).

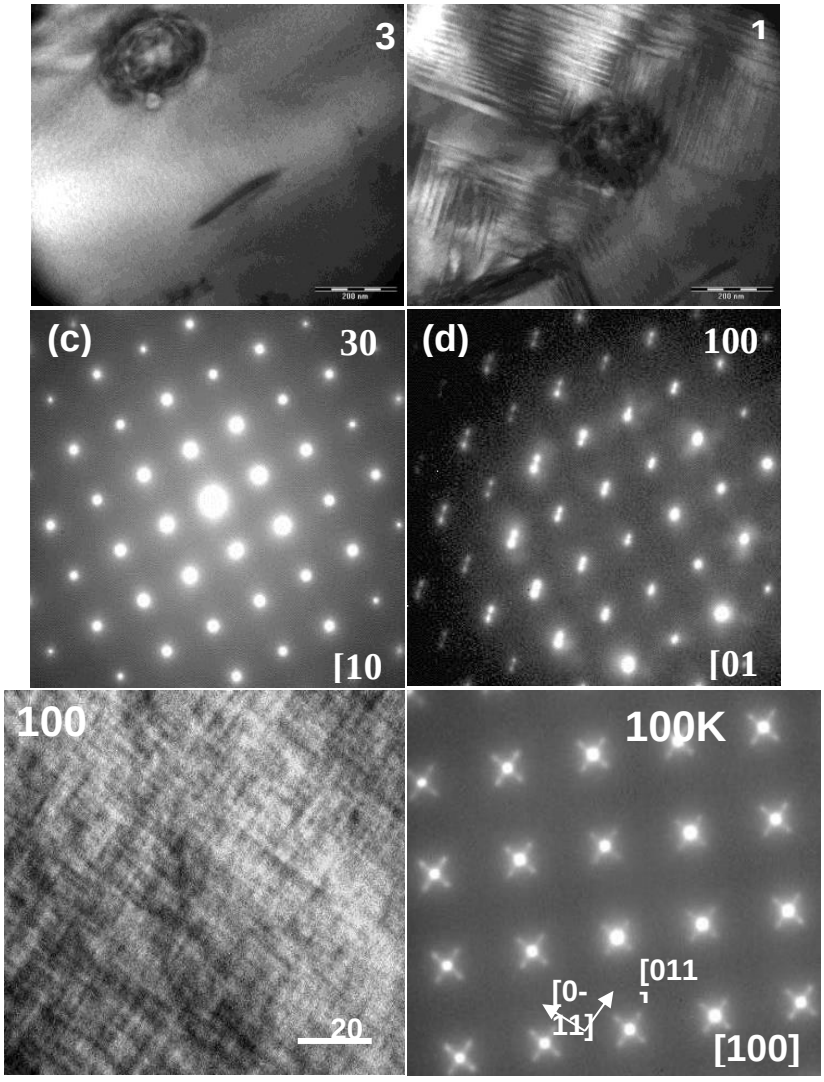

Electron micrographs of $La_{0.2}Sr_{0.8}MnO_{3-\delta}$ taken (a) at 300K and (b) at 100K. (b) shows nano-twined (10-20 nm) microstructure of the tetragonal phase appearing after the cubic to tetragonal transformation below 257K.(c)&(d) show SAD patterns from the same region taken corresponding to cubic and tetragonal states respectively. The splitting of the spots in (d) indicates a (011) mirror related twins.(e) High-resolution lattice-image of the charged-ordered (CO) phase observed for off-stoichiometric $La_{0.2}Sr_{0.8}MnO_{3-\delta}$ at 100K and (f) The corresponding SAD pattern of CO superlattice spots showing ~ 9x9 modulations along [011] and [0-11]. It can be noticed that the observed CO lattice fringes are not straight. It depicts that the $\mathbf{e_g}$-charge is not strongly pinned with the lattice due to lack of CJTD.

tetragonal phase with either I4/mcm or P4mm space-groups, see Fig.1a and Fig.2a-d. But the LSMO with lower (x) value i.e. x=0.75 under goes a phase competition. The basic perovskite lattice of the off-stoichiometric LSMO samples do not under go net tetragonal distortion, see Fig.1b but remain intact as undistorted cubic phase as confirmed by the Reitveld refinement of the temperature dependent XRD data. But the LT-TEM investigations done on oxygen off-stoichiometric LSMO with x=0.75 & 0.80 does show stabilization of CO phase down to 100K,see Fig.e,f.These observations directly imply that there exists a competition between CE-type charge-orbital ordering and ferro-orbital of $3d_{z2}$ orbitals, which is very sensitive to oxygen stoichiometry. In off-stoichiometric phase cooperative JT-distortion remains largely suppressed and the observed CO therefore is a direct consequence of long-range electron correlation effects. LT-TEM of stoichiometric LSMO with x=0.75 also exhibits nano-phase coexistence of $d_{x^2-y^2}$ type orbital ordering, giving rise to 2D CO phase in the matrix of an otherwise 1D CO phase of $3d_{z2}$ orbitals.

NP Lalla

3.1.1.5 Fractional power-law spectral response of $CaCu_3Ti_4O_{12}$ dielectric: Many-body effects

Spectral character of dielectric response in $CaCu_3Ti_4O_{12}$ across 0.5Hz–4MHz over 45–200K corresponding to neither the Debyean nor the KWW relaxation patterns rather indicates a random-walk like diffusive dynamics of moments. Non-linear relaxation here is due to the many body dipole-interactions, as confirmed by spectral-fits of our measured permittivity to the Dissado-Hill behaviour. Fractional power-laws observed in □*(□) macroscopically reflect the fractal microscopic configurations. Below ~100 K, the power-law exponent *m* (*n*) steeply decreases (increases), indicating finite length-scale collective response of moment-bearing entities. At higher temperatures, *m* gradually approaches 1 and *n* falls to low values, reflecting tendency towards the single-particle/Debyean relaxation.

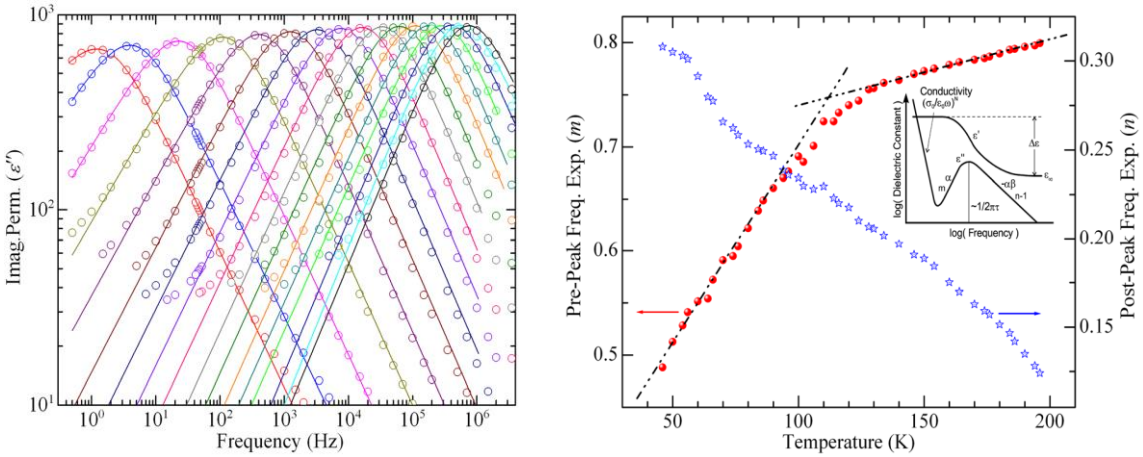

Jitender Kumar, A.M. Awasthi,

3.1.1.6 Investigation of charge states and multiferroicity in Fe-doped *h*-$YMnO_3$

Polycrystalline $YMn_{1-x}Fe_xO_3$ ($YMFO_x$) ($0 \leq x \leq 0.1$) compounds have been prepared in single phase and characterized by synchrotron X-ray diffraction, X-ray absorption near edge spectroscopy, magnetization, and dielectric measurements. Iron-substitution in hexagonal $YMnO_3$ causes intra-lattice changes exceeding those of the lattice cell. XANES provides mixed-valence Mn^{3+}/Mn^{4+} and Fe^{4+} charge states in these manganites, consistent with the observed decrease of the effective magnetic moment with Fe-doping. Magnetization $M(T)$ evidence antiferromagnetic ordering of the specimens with little weak ferromagnetism, and the metrices of exchange interaction suppress with Fe-doping, attributed to the lengthening of the Mn–O planar bond lengths. Dielectric □′(T) results showing highly doping-dependent anomaly at T_N indicate linear magneto-electric coupling.

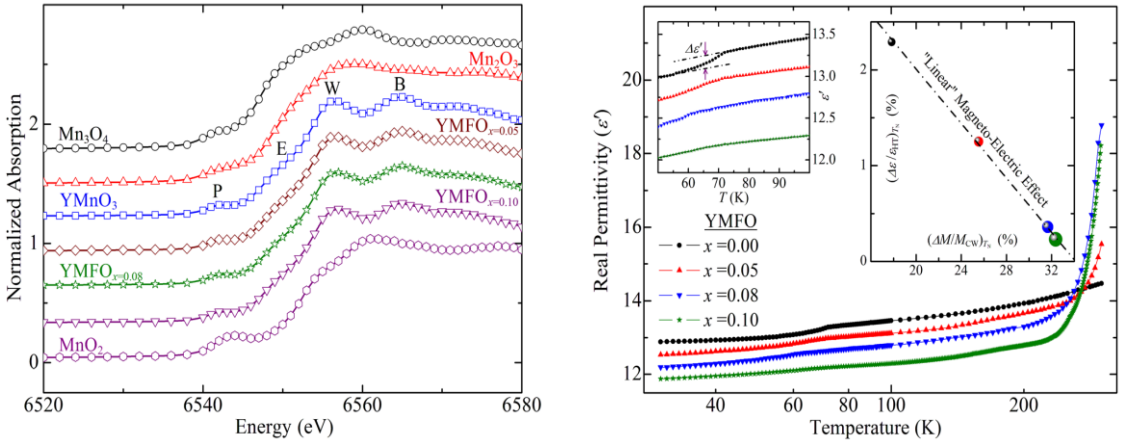

Sonu Namdeo, A.M. Awasthi, A.K. Sinha, M.N. Singh (RRCAT)

3.1.1.7 Superionic to insulator phase transition in $KTiOPO_4$ investigated with dc-bias field

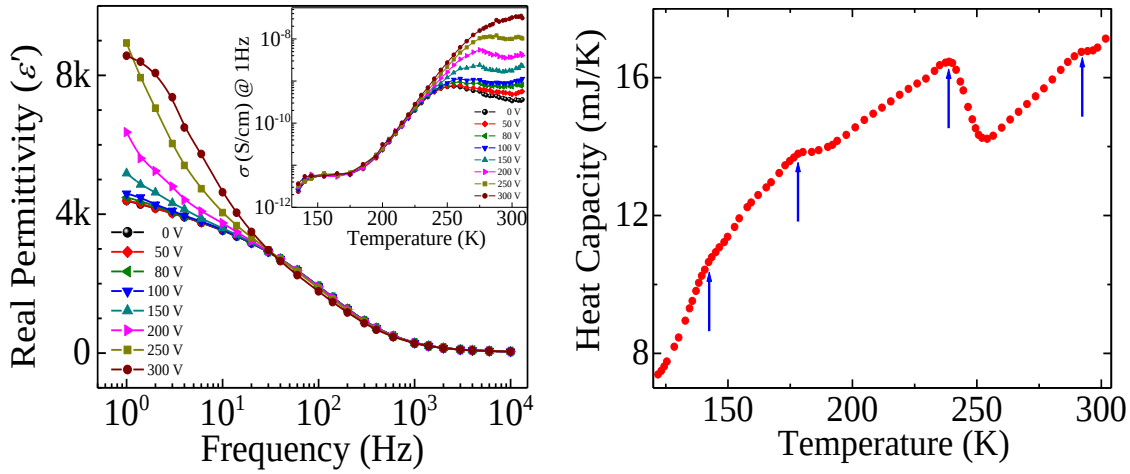

The dielectric and conducting properties of single crystal $KTiOPO_4$ (KTP) have been investigated in its superionic and insulating states at low temperatures under different dc-bias fields. The KTP undergoes a superionic to dielectric phase transition on lowering the temperature. In the superionic state, the conductivity is field-dependent while in dielectric state it is almost field insensitive. At room temperature and low frequencies, on applying dc-fields the dielectric constant of KTP increases whereas the conductivity shows almost two orders of magnitude increment.

Jitender Kumar, A.M. Awasthi

3.1.1.8 Glassy domain wall dynamics in KH_2PO_4 crystal: Effect of dc-bias *E*-field

We have investigated the effects of dc-bias electric field on the dielectric response in single crystal potassium dihydrogen phosphate (KH_2PO_4). The bias-field dependence (up to 500V) of permittivity precisely marks the glassy domain wall (DW) freezing temperature T_f (96K); changing its sign across the same, exactly where ε' is field-insensitive. Characteristic DW freezing time suggests segmental dynamics of the domain-walls; obeying Vogel-Fulcher divergence with a field-invariant Kauzmann temperature T_K, latter indicating no changes vs. dc-field in the structural configuration of DW's. A benchmark V_{dc} (150V) precisely splits the low- and high-field characters of the ferroelectric T_C, permittivity ε'_ω(123K), and the DW freezing activation energy E_a, which we attribute to a crossover from independent to interacting DW's. Over the temperature range hosting the DW response, field-cooled (poled) permittivity is higher than the zero-field-cooled (unpoled) case, being same elsewhere; neatly marking the dynamic regime of the domain-walls.

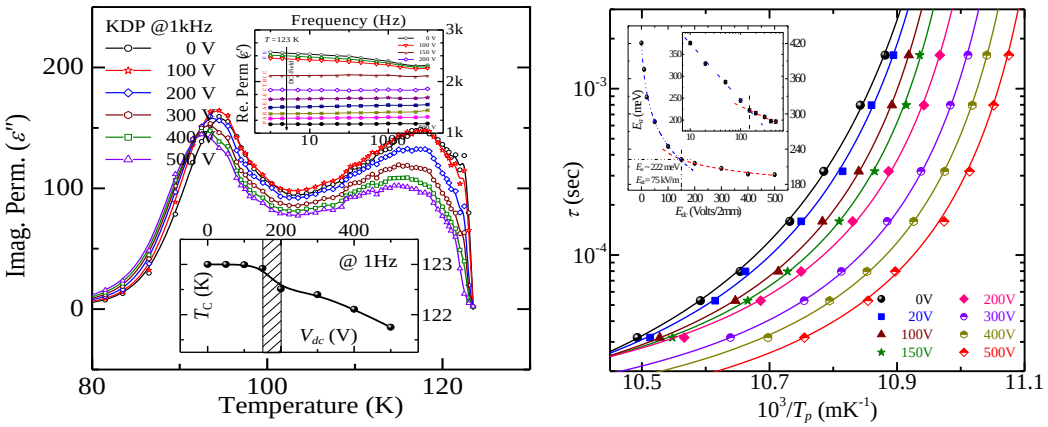

Jitender Kumar, A.M. Awasthi,

3.1.1.9 Evolution of structural phase coexistence in a half doped manganite $Pr_{0:5}Sr_{0:5}MnO_3$: An evidence for magneto-structural coupling and kinetic arrested structural phase

Temperature dependent x-ray diffraction measurements have been performed to understand the implications of magnetic phase coexistence on crystallographic structure in a half-doped manganite $Pr_{0:5}Sr_{0:5}MnO_3$. The compound shows a structural phase transition from high-temperature tetragonal-*I4/mcm* to low-temperature orthorhombic *Fmmm* symmetry around the ferromagnetic to antiferromagnetic transition (Fig.1).

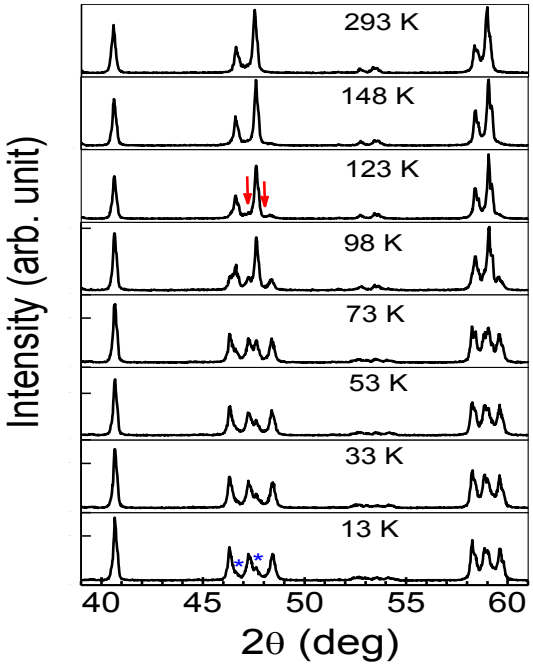

Fig. 1 Powder XRD patterns of $Pr_{0.5}Sr_{0.5}MnO_3$ collected during cooling run is presented at a few representative temperatures. A new reflection (marked by ↓), characteristic of the low-T phase, starts appearing below 148 K. The parent phase (marked by *) coexist with the new phase down to 13K.

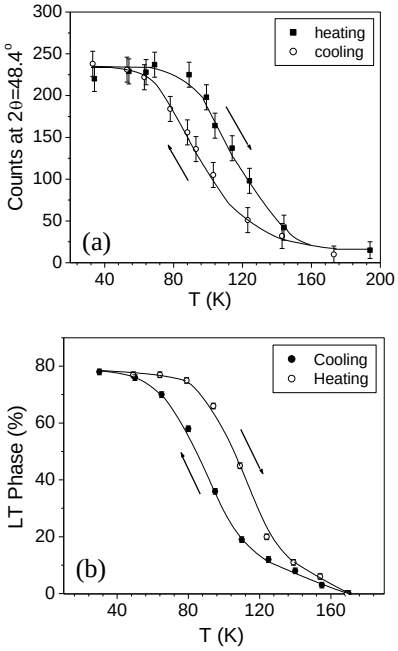

Fig. 2 Temperature variation of (a) total count at the peak related to the 400 refection of the low temperature (LT) phase and (b) molar fraction of LT AFM (Fmmm) phase obtained from the Rietveld refinement of XRD results collected during heating and cooling cycle. The arrows indicate the direction of temperature cycle.

Rietveld analysis shows the coexistence of these two structures emerges at high temperature within ferromagnetic state, and persists down to lowest temperature. Below around 40 K, however, this structural evolution stops, and a significant fraction (~ 22%) of untransformed high-temperature phase remains (Fig.2). This is a direct evidence of kinetically arrested broad first-order ferromagnetic to antiferromagnetic transition as found in the earlier magnetization study and thus establishing its magneto-structural coupling.

A. K. Pramanik, Rajeev Ranjan and A. Banerjee

3.1.1.10 Observation of different spin behavior with temperature variation and Cr substitution in a multiferroic compoundYMn_2O_5 -

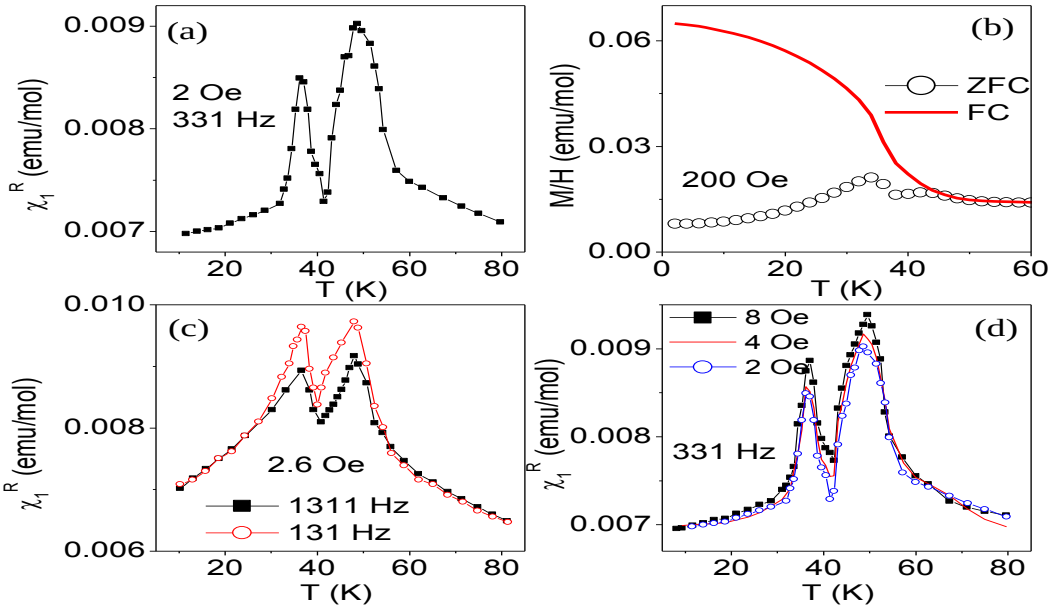

For the YMn_2O_5 compound (a) Temperature response of real part of ac susceptibility (χ_1^R). (b) Zero field cooled and Field cooled magnetization at 200 Oe static magnetic field. (c) and (d) Frequency and field dependence of χ_1^R respectively.

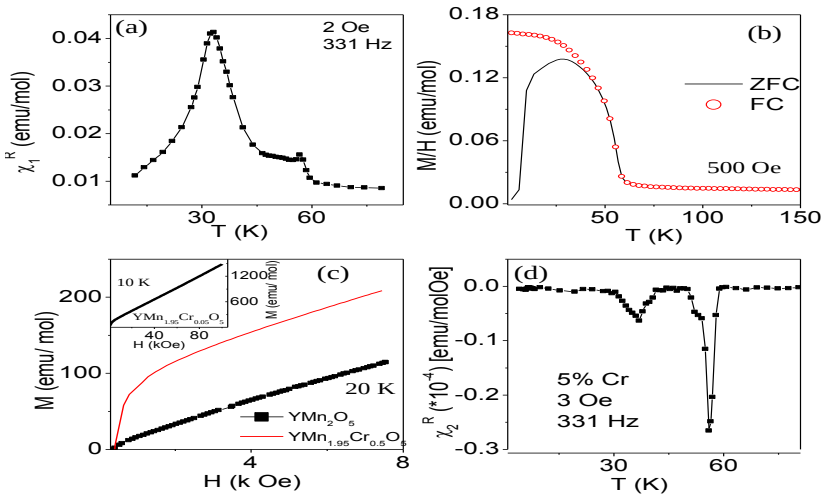

(a)Temperature response of real part of ac susceptibility (χ_1^R) for the compound $YMn_{1.95}Cr_{0.05}O_5$. (b) Zero field cooled and Field cooled magnetization for the same sample at 500 Oe. (c) Magnetization as a function of magnetic field at 10K for both compounds YMn_2O_5 and $YMn_{1.95}Cr_{0.05}O_5$. Inset: Magnetization as a function of magnetic field at 10K for $YMn_{1.95}Cr_{0.05}O_5$ upto 100 kOe. (d)Temperature response of real part of second order of ac susceptibility ((χ_2^R)) for the compositions $YMn_{1.95}Cr_{0.05}O_5$.

The collective response of the spins is explored through low field bulk magnetic measurement for the series $YMn_{2-x}Cr_xO_5$ (x = 0.0 and 0.05. Low field ac-susceptibility and dc-magnetization of YMn_2O_5 shows multiple transitions in analogy to those observed in electrical measurement of the compound (Fig.1).

Perturbing the parent compound with a small doping (2.5%Cr) causes a drastic change in the long range magnetic behavior. It is observed that, $YMn_{1.95}Cr_{0.05}O_5$ under goes a ferromagnetic ordering with an enhanced magnetic ordering temperature as compared to the parent, which undergoes an antiferromagnetic ordering. Appearance of spontaneous magnetization without any major change in the atomic structure is rather significant since the parent compound is an important multiferroic material (Fig.1).

In addition, magnetic memory effect is observed in the Cr substituted compound whereas it is absent in the parent compound.

K. Mukherjee, Kranti Kumar, and A. Banerjee

3.1.1.11 Tuning the phase transition dynamics by variation of cooling field and metastable phase fraction in Al doped $Pr_{0:5}Ca_{0:5}MnO_3$ -

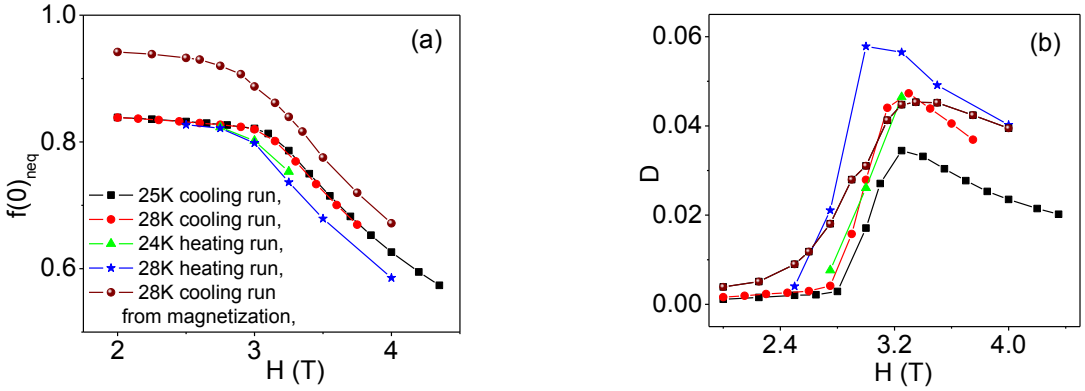

The non-equilibrium phase fraction at t=0 [$(f(0)_{neq}$] and (b) the decay rate (D) versus cooling fields at different temperatures and thermal cycle. The symbols in figure (a) and (b) are the same for a particular temperature and run.

Effect of field, temperature and thermal history on the time dependence in resistivity and magnetization in the phase separated state of Al doped $Pr_{0:5}Ca_{0:5}MnO_3$ is studied in detail. The rate of time dependence in resistivity is much higher than that of magnetization and it exhibits a different cooling field dependence due to percolation effects. Our analysis shows that the time dependence in physical properties depends on the phase transition dynamics, which can be effectively tuned by variation of temperature, cooling field and metastable phase fraction. The phase transition dynamics can be broadly divided into the arrested and un-arrested regimes, and in the arrested regime this dynamics is mainly determined by time taken in the growth of critical nuclei. An increase in cooling field and/or temperature shifts this dynamics from the arrested to un-arrested regime, and in this regime, this dynamics is determined by the thermodynamically allowed rate of formation of critical nuclei, which in turn depends on the cooling field and available metastable phase fraction. At a given temperature, a

decrease in metastable phase fraction shifts the crossover from arrested to un-arrested regimes towards lower cooling field.

It is rather significant that in spite of the metastable phase fraction calculated from resistivity being somewhat off that of magnetization, their cooling field dependence exhibits a striking similarity, which indicates that the dynamics in arrested and un-arrested regimes are so different that it comes out vividly provided that the measurements are performed around the percolation threshold.

Devendra Kumar, Kranti Kumar, A Banerjee and P Chaddah

3.1.1.12 Ta doped $HfFe_2$

Ta doped $HfFe_2$, which orders in $MgZn_2$ type hexagonal crystal structure, shows first order transition from ferromagnetic to antiferromagnetic state with increasing temperature. The transition temperature decreases with increasing Ta concentration and is known to vanish for 20 to 25 atomic percentage of Ta substitution at Hf site. Our study within this concentration range showed that the transition shifts to near zero K for about 23% Ta substitution. Magnetization measurements for nearby composition showed thermomagnetic irreversibilities at low temperature due to kinetic arrest of first order transition. These thermomagnetic irreversibilities include different magnetic state states before and after field cycling for temperatures less than 30 K, non-monotonic variation of upper critical field (field required for AFM to FM transition) and re-entrant transition for CHUF (cooling and heating in unequal magnetic field) measurement.

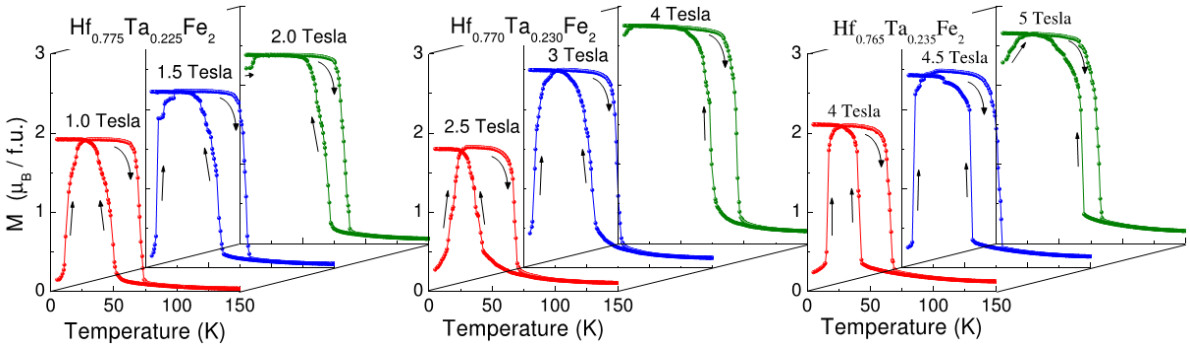

Figure1: M vs. T for Ta doped HfFe2 compositions showing re-entrant transition for zero field cooled curves.

Figure 1 shows the magnetization measurement during warming (ZFCW: measured after zero field cooling) and subsequent cooling (FCC) under labeled magnetic field for such three compositions. It shows difference between ZFCW and FCC which decreases with increase in applied magnetic field. The ZFCW curve for respective composition shows a re-entrant transition AFM to FM (devitrification) followed by FM-AFM with increase in temperature. Phase diagram based on detailed isothermal magnetization measurement showed non-monotonic variation of upper critical field and monotonic rise in H_K (critical field below which AFM state remains arrested) as x varies from 0.225 to 0.235. It shows that the formation of a magnetic glass becomes more favorable with increasing Ta content. Since the lattice parameters decreases monotonically as Ta content increases, it favor a direct exchange magnetic coupling, as the wave function overlap would rise exponentially, over a conduction electron mediated coupling (that would not vary much with interatomic spacing). Therefore,

these results could be relevant to the proposal of Chaddah and Banerjee [arXiv:1004.3116v3] that a magnetic glass is formed when the magnetic latent heat is weakly coupled (cf the sample specific heat) to the thermal conduction process.

R. Rawat, Pallab Bag, P D Babu, V Siruguri and P Chaddah

3.1.1.13 Ge and Cr doped Mn_2Sb

Ge and Cr doped Mn_2Sb samples are prepared to study the first order antiferromagnetic to ferrimagnetic transition. Our study on Ge doped system revealed that transition temperature variation with Ge doping is quite similar to that has been observed in Cr doped system. This was a surprising result as Ge is substitute for nonmagnetic Sb, whereas Cr has been substituted for Mn which is magnetic. For composition with transition at lower temperature, we observed thermomagnetic irreversibility associated with kinetic arrest of first order transition. Magnetization measurement showed that with increasing Ge content the jump in magnetization across AFM to FRI transition temperature first increase and then decreases. For composition with transition temperature near room temperature, the transition is accompanied with a small jump in magnetization and resistivity. Some of these preliminary results were presented at DAE SSPS-2012 held at BARC Mumbai.

Pallab Bag, Rohit Kumar, Pallavi Kushwaha and R Rawat

3.1.1.14 Gd_2In compound

Gd_2In compound shows paramagnetic to antiferromagnetic transition (~187 K) followed by first order antiferromagnetic to ferromagnetic transition (~100 K) with lowering temperature. We studied substitution effect at magnetic as well as at non-magnetic site in this compound. The Al-substitution at non-magnetic site results in a suppression of AFM-FM transition temperature. However MR and hysteresis width remained unaffected whereas Tb substitution results in larger hysteresis width and smaller MR associated with metamagnetic transition. The hysteresis width is shown to be dependent on substitution and remains almost invariant with temperature and magnetic fields. Some of these results are presented at DAE Symposium 2012 held at BARC, Mumbai

Vikram Singh, Pallab Bag and R Rawat

3.1.1.15 Precursor state of Skyrmions in MnSi: a heat capacity study

The Skyrmion lattice is classified as a typical topological excitation, and the precursor state of skyrmions is equally interesting. This exotic phase in MnSi through heat capacity is explored. We have used the option of varying magnetic fields under isothermal conditions in a precise fashion in addition to the usual routines and could establish the phase diagram. The magnetic phase diagram of MnSi based on the detailed magneto-heat capacity study is presented. It shows the A-phase, a precursor to the formation of stable skyrmion lattice, along with the intermediate, helical, conical, ferromagnetic and paramagnetic phases. The field isotherms of specific heat in and around the transition temperature reveal the different magnetic modulations. The local minima represent the relatively low entropy state due to the formation of A-phase as a precursor to the stable skyrmion lattice. The field-induced second-order phase transition is observed by melting the intermediate phase. The

region of existence of first-order phase transition is found to be, effectively, from helical to the intermediate phase.

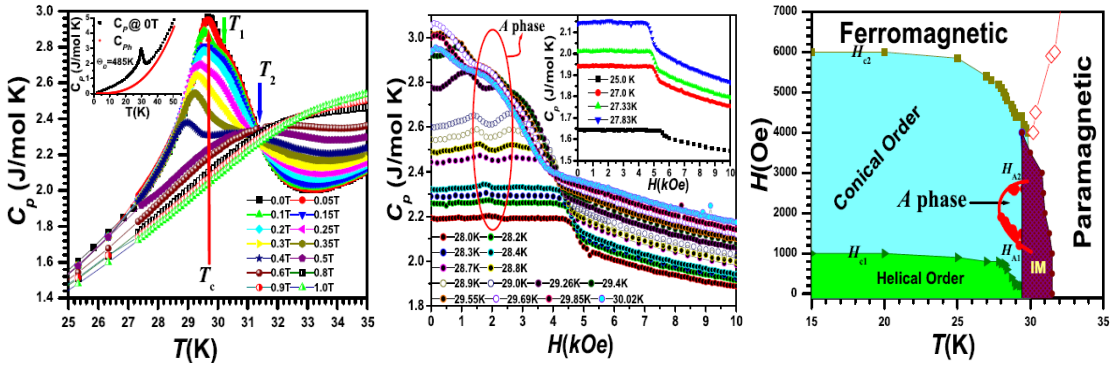

S. Shanmukharao Samatham and V. Ganesan

3.1.1.16 Electrical resistivity near critical concentration of (Ce1-xNdx)3Al

Cerium based intermetallic compound (Ce1-x Nd x)3Al shows many properties like heavy Fermion, structural phase transition, valence fluctuation and hybridization of conduction electron with the localized 4f electron of the cerium ion. There is a competition between RKKY and Kondo ordering in these compounds. For x = 0.0 i.e. Ce3Al shows structural phase transition from hexagonal to monoclinic as well as valence fluctuation below 110 K, antiferromagnetic ordering below 2.8 K, heavy fermion behavior and Kondo effect due to hybridization of conduction electron with 4f electrons of the cerium ion below 20K. When we dope the Nd on the site of Ce, up to 30% it shows kondo as well as structural transitions. For 40% doping of Nd, the system shows no transition like Kondo and structural and this may be due to the compensation of magnetic moments of Ce and Nd ions. Doping of Nd, for x ≥ 50%, shows ferromagnetism at low temperatures till Nd3Al. This region of doping shows marked deviation in resistivity with magnetic fields owing to its nearness to a possible QCP like state.

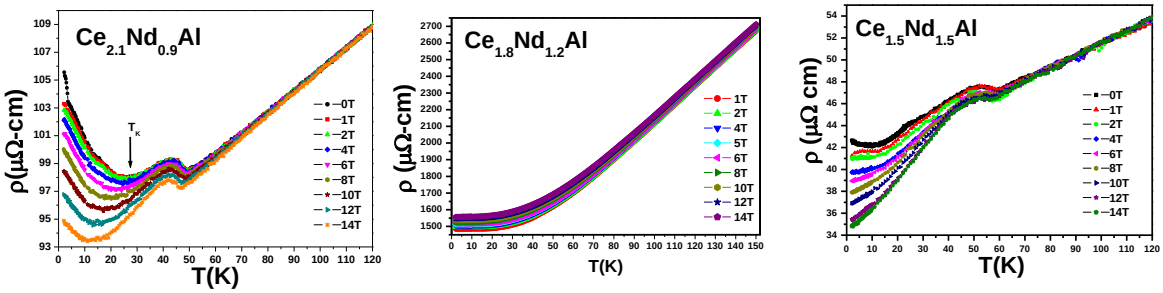

Durgesh Singh and V. Ganesan

3.1.1.17 Superconductivity in Si doped Niobium Oxy Nitrides

Superconductivity has been observed recently in a family of compounds known as Niobium Oxy Nitrides with a Tc of ~18K. They also show a remarkable hardness and hence there is a wide spread interest in understanding the material properties pertaining to this family. Studies on various dopants reveal that Si is good and also enhances the critical current density. Resistivity measurement of (Nb0.87Si0.09□0.04) (N0.87O0.13) is shown in Fig-1 and shows the zero field superconducting transition temperature as 17.4K. The variation of Hc with field is non-BCS and is quite linear. Field induced broadening at higher fields is not due to material inhomogeneity by is ascribed to thermodynamic fluctuations. A field of 14T is not sufficient to make the material normal. In order to understand TAFF plots have been invoked and are shown in Fig 2. The activation energy varies exponentially as a function of field as compared to the Kramer's formalism. Different scaling functions are being tried to understand including that of LLL schemes and the work is in progress.

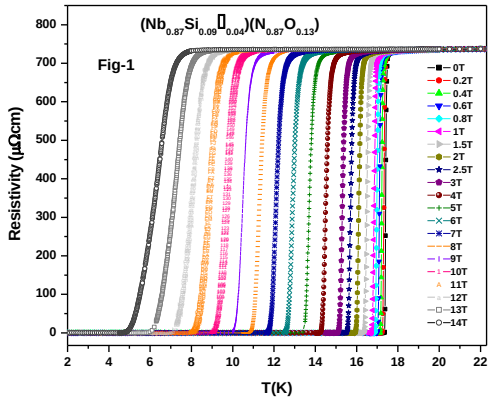

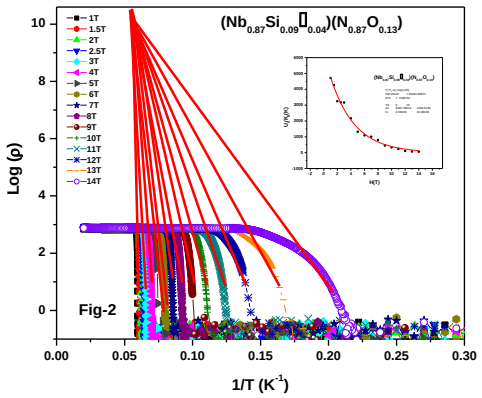

D. Venkateshwarlu, Y. Ohashi, S.Kikkawa, I.Felner, M.I.Tsindlekht, J.V.Yakhmi ,V.Ganesan

3.1.2 Thin films and Multilayers

3.1.2.1 Evolution of structural and magnetic properties of amorphous CoFeB film with thermal annealing

Evolution of structural and magnetic properties of amorphous $Co_{68}Fe_{14}B_{18}$ thin film with thermal annealing has been studied. Initially the film exhibits a structural relaxation as evidenced by annihilation of excess free volume and an increase in topological short range order. Annealing at 473 K results in precipitation of primary phase followed by formation of boride phase at a still higher temperature of 598 K. Iron preferentially precipitates out in the primary phase, resulting in the formation of bcc $Co_{58}Fe_{41}$. This suggests an affinity of Co towards B. Such affinity between Co and B is evidenced even in the as-deposited film, using HAXPES measurements. As-deposited film exhibits an in-plane uniaxial magnetic anisotropy which disappears at a temperature well beyond crystallization temperature, suggesting that the origin of anisotropy is mainly a chemical short range order in the system. Variation in the coercivity with thermal annealing can be understood in terms of random anisotropy model. Precise measurement of Fe self-diffusion using neutron reflectivity

shows that diffusion length associated with annihilation of excess free volume in the film is about 0.5 nm. This agrees with the length scale of structural fluctuations in amorphous alloys. SIMS measurements show that thermal annealing results in depletion of B in the region of the interface with the substrate, with associated faster Fe diffusion in this region. This faster diffusion of Fe may be a possible cause of preferential crystallization of the film in the interfacial region as seen in some earlier studies

Ranjeeta Gupta and Ajay Gupta

3.1.2.2 Effect of confinement on melting behaviour of cadmium arachidate Langmuir-Blodgett multilayer

The effect of confinement between two metallic layers on the melting behaviour of a 13 monolayer cadmium arachidate (CdA) Langmuir-Blodgett (LB) multilayer has been studied. Temperature dependent diffraction measurements provide information about structural changes occurring in the film plane as well as in the out-of-plane direction. X-ray standing waves have been used to achieve depth selectivity in diffraction measurements. It is found that, the difference in melting behaviour of the surface and the bulk, which is observed in the film with free surface, disappears in the case of confined films; while the free surface transforms to hexaticlike phase via an intermediate smectic phase, confinement results in disappearance of this phase, and the sequence of transformations in the bulk and the interfacial regions becomes identical. Some anisotropy between $(01 + 1\bar{1})$ and (10) directions remains, with coherence along (10) direction decreasing at a faster rate. The confinement between metallic layers also significantly reduces the tilting of the chains observed at higher temperature. Further, both in the case of film with free surface and confined films, melting at the surface/interface occur at a lower temperature as compared to the bulk

Pallavi Pandit, Ajay Gupta and Dileep Kumar

3.1.2.2 Ion beam sputtered FINEMET Film of $Fe_{73.9}Cu_{0.9}Nb_{3.1}Si_{13.2}B_{8.9}$ Alloy: *An in-situ MOKE investigation*

Ion beam sputtered thin films of amorphous $Fe_{73.9}Cu_{0.9}Nb_{3.1}Si_{13.2}B_{8.9}$ (FINEMET) alloy are studied with film growth (from fraction of nm to few nm). The influence of thermal treatment on the selected film thickness was also investigated.

An explicit hysteresis loop with coercive field of ~ 3.2 Oe is appeared upon depositing 2.0 nm thick film and the film exhibits significant increase in the coercive field up to 31.0 nm due to the thermodynamic dependence. Thickness dependent coercive field and Kerr signal suggest absence of magnetic dead layer at the SiO_2/Finemet film interface. The film with thickness of 41 nm possesses uniaxial magnetic anisotropy in the film plane. However upon annealing at 598 K, film becomes almost isotropic as revealed by in-situ thermal annealing treatment (in-set figure1). This behaviour could be attributed to relieving of the internal stresses which might have generated during the film deposition. Further in-situ thermal annealing treatment shows the optimum magnetic softest behaviour of the film with coercive field ~0.5±0.1 Oe upon annealing at the temperature of ~663 K. The Curie temperature of the 41 nm thick amorphous film is evaluated to be ~ 673 K, the onset nanocrystallisation temperature of the film was ~ 727K. Origin of magnetic anisotropy in amorphous magnetic film is not clear yet and is under study.

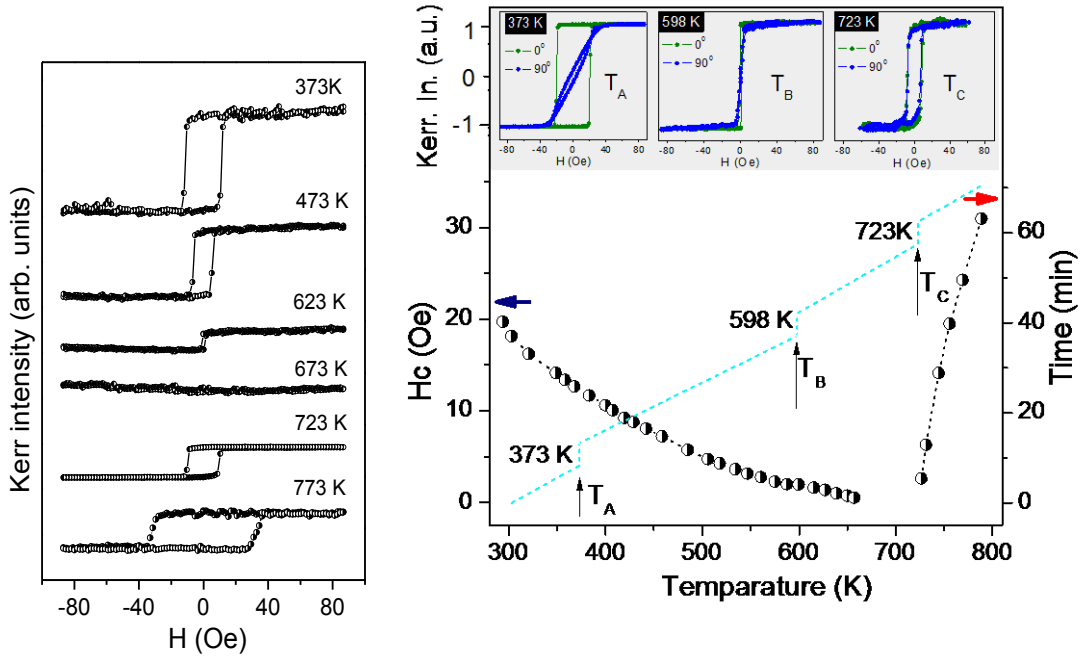

Representative data of a) Hysteresis loops at different temperature and b) Variation of coercivity (for loops taken in direction of easy axis of magnetization) as a function of temperature

Dileep Kumar, Pooja Gupta and Ajay Gupta

3.1.2.3 Presence of positive and negative exchange bias in single Co /CoO/Co (FM-AFM-FM) trilayer structure

Co/CoO/Co polycrystalline film was grown on Si (001) substrate and magnetic properties have been investigated using in-situ MOKE during growth of the sample. Magnetic anisotropy with easy axis perpendicular to the film surface has been observed in top Co layer, whereas bottom layer was found to be soft with in-plane magnetization without any influence of top layer. Ex-situ in-plane and out-of-plane diffraction measurements revealed that the growth of Co on oxidized interface takes place with preferential orientation of c-axis perpendicular to the film plane, which results in the observed perpendicular magnetic anisotropy. Texturing of the c-axis is expected to be a result of minimization of the interface energy due to hybridization between Co and oxygen at the interface. The detailed magnetic measurements using SQUID magnetometer were also done in order to investigate exchange bias effect in the present sample, where a single anti-ferromagnetic layer (CoO) of 2.6 nm thickness is coupled with two ferromagnetic (FM) Co film in different magnetic state. Actually, exchange biased effect results in a unidirectional shift of hysteresis loop when sample is cooled below the Neel temperature (T_N). Because of technological applications such as spin valves in magnetic reading heads and magnetic random access memories, this effect remains at the forefront of the research in thin film magnetism. In the present case, detailed zero fields cool (ZFC) and filed cool (FC) measurements revealed that this sample structure shows both negative and positive exchange bias effect in the single sample. Figure 1 clearly shows the two hysteresis loops, where one with low coercivity shifts 80 Oe in the positive field direction (positive exchange; H_{+eb}~ 80 Oe) and other with higher coercivity shifts ~0.8 kOe in

the negative field direction (Negative exchange; H_{-eb}~ 0.8 kOe). As shown in figure2, these magnetic measurements have also been supported by the filed cool transport measurements. Origin of such behavior may be attributed to the interface exchange coupling at the interfaces CoO-on-Co and Co-on-CoO (top and bottom interface) due to the different spin structure.

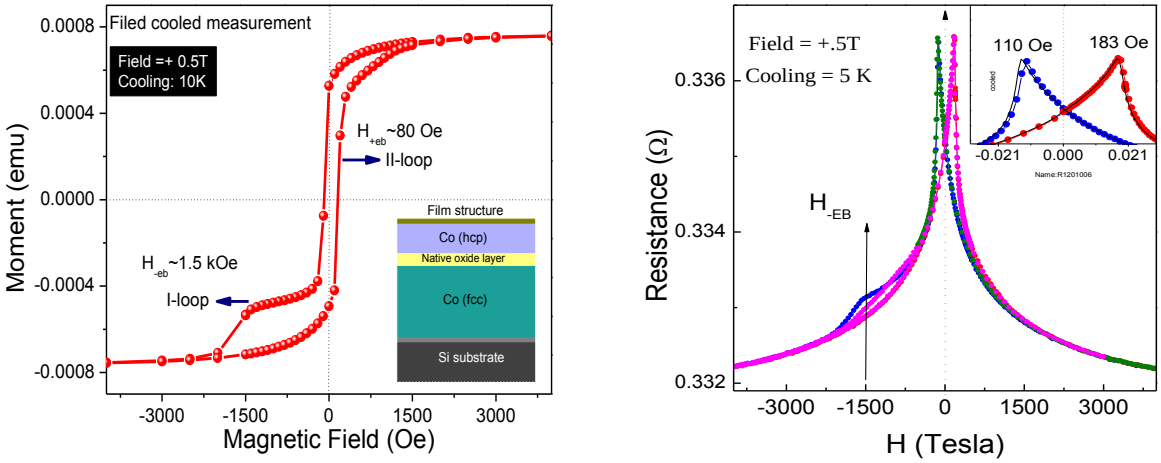

Figure1*: Hysteresis loop measured at 10 K after field cooling at 0.5 Tesla from 300K. The component with lower Hc and higher Ms may correspond to the bottom Co-CoO interface. Inset of the figure shows sample structure*
Figure2*: Magnetoresistance (MR) measured at 5K after field cooling at 0.5T*

Dileep Kumar, Pawan Patidar and Ajay Gupta

3.1.2.4 Migration of Ag trough Ni layer in Ag/Ni bilayer system

Fe/Ag, Ni/Ag and Co/Cu etc. are the magnetic multilayer systems which has a large positive heat of mixing both in solid as well as in liquid phases. (ΔH^{solid} = 30 to42 kJ/ mol ; ΔH^{liq} =15 to 28 kJ/ mol). Extensive studies have been done in literature to see possible intermixing and magnetic properties in these systems using technique like heavy ion irradiation and temperature annealing. It has been argued that total free energy of the system due to large contribution of the interface energy plays an important role to drive these systems in intermixed state.

In the present work, we have tried to see, if by further modifying the interfacial free energy by depositing Ni on Ag islands structure, whether it is possible to achieve intermixing in the system by thermal annealing. For this purpose Ag film with connecting islands has been deposited on Si substrate using ion beam sputtering method and further 40 nm Ni layer is deposited to make Ni/Ag bilayer. In-situ magnetic hysteresis loops were recorded using in-situ MOKE with sample temperature up to 300^0C. It was found that after 300^0C hysteresis loop was disappeared. In order to understand the magnetic behavior, ex-situ x-ray reflectivity, XRD, AFM, and secondary neutral mass spectrometry (SNMS) measurements were done and found that Ag material segregate on top through Ni layer. As shown in Figure 1 and 2, SNMS measurements on as-prepared bilayer and in annealed state (300C) confirm the segregation of Ag. At around 300C, disappearance of the magnetic

properties may be attributed to the formation of Ni nanoparticles due to segregation of the Ag through Ni. Magnetic measurements at low temperature and XRD in out of plane configuration are still in the process in order to understand the cause of the bulk segregation in this system.

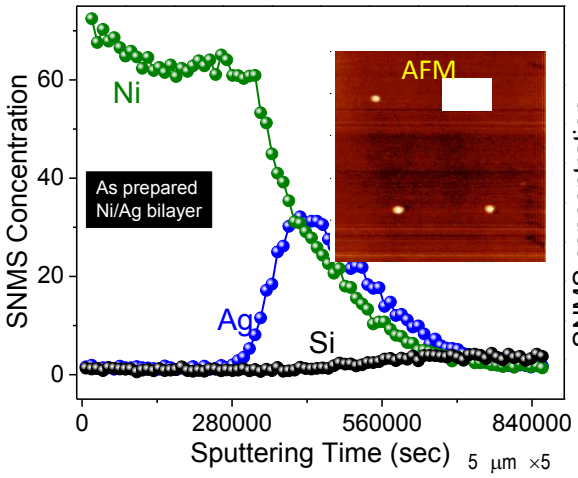

Figure 1

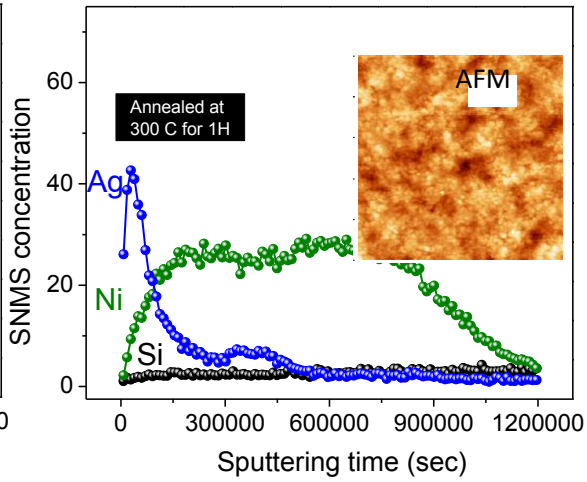

Figure 2

Figure1: *SNMS concentration-Vs-sputter time profile of as prepared Ni/Ag bilayer on Si substrate**.** Inset is AFM image*

Figure2: *SNMS concentration-Vs-sputter time profile of 300C annealed Ni/Ag bilayer on Si substrate**.** Inset is AFM image*

Dileep Kumar, Priyanka Yogi and Ajay Gupta

3.1.2.5 Study of epitaxial magneto-electric $GaFeO_3$ prepared by sol-gel route

Epitaxial thin films of $GaFeO_3$ (GFO) with different thicknesses (22 - 170 nm) are prepared on (001) oriented yttria-stabilized zirconia substrate using pulsed laser deposition. The M-H data measured below Curie temperature (T_C) mimics two phase composite magnetic system consisting of hard and soft magnetic phases. The results are explained in terms of Fe distribution among the available cation sites of GFO. Thermo-magnetic irreversibility and cusp in zero-field cooled magnetization is observed for all the films and are explained in terms of the magnetic anisotropy of the GFO

Kavita Sharma, V.Raghavendra Reddy and Ajay Gupta

3.1.2.6 Silicide Layer Formation in Evaporated and Sputtered Fe/Si Multilayers

In Fe/Si multilayers silicide layer is formed due to the spontaneous interdiffusion of Fe and Si atoms, its thickness at the interface plays a very important role in determining the physical properties of Fe/Si multilayers.

In this work, we quantify the composition and asymmetry of the silicide layer thickness in Fe/Si multilayers (with same nominal multilayer structure) deposited using e-beam evaporation and direct current-magnetron sputtering (dc-MS) method. Fig. 1 shows the polarized neutron reflectivity (PNR) pattern of the samples prepared using e-beam and dc-MS techniques. The separation of critical edges in the spin up (R^+) and down (R^-) reflectivity in PNR pattern is a measure of average magnetic moment as shown in the inset of Fig.1. Fitting of the PNR data reveals that iron silicide interlayer at the interface is non-magnetic and nuclear scattering length density (SLD) is about 6.4×10^{-6} Å^{-2} which is close to the SLD of iron silicide having CsCl (B2) structure. The SLD of silicide layer depend upon the number of Fe and Si atoms per unit volume and hence upon the structure of the silicide.

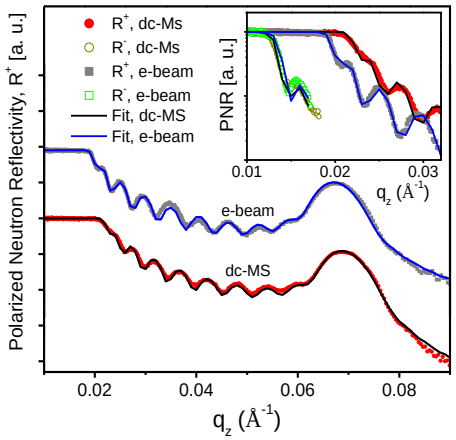

Fig.1 PNR pattern of Fe/Si multilayers deposited using e-beam evaporation and dc-MS techniques. Inset of the figure compares the critical edges.

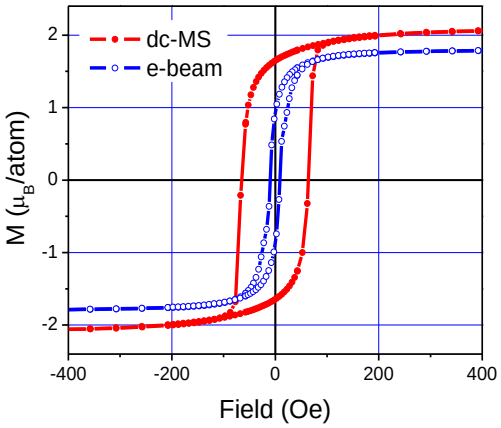

Fig.2 Hysteresis loop of Fe/Si multilayers deposited using e-beam evaporation and dc-MS techniques.

It was also found that silicide layer thickness at Fe/Si and Si/Fe interfaces are different, both in e-beam and dc-MS samples. More remarkably, the thickness of the silicide layers is significantly larger in e-beam sample as compared to dc-MS sample which can be understood in terms of the difference in adatom energies in evaporation and sputtering methods. The difference in the silicide layer thicknesses at the Fe/Si or Si/Fe interfaces can be understood in terms of difference in the surface free energy (γ) of Fe (γ=2.55 Jm^{-2}) and Si ((γ=1.1 Jm^{-2}). Fig.2 shows hysteresis loop of the samples deposited by dc-MS and e-beam methods. The observed values of average magnetic moment in SQUID-VSM are matching well with those obtained by fitting of the PNR data. Further, coercivity of samples deposited by dc-MS and e-beam are 62 Oe and 11 Oe, respectively. This difference can be understood in terms of the difference in grain size of the samples based on random anisotropy model. In summary, a quantitative analysis reveals that both interface roughness and the silicide layer thicknesses get reduced in dc-MS samples as compared to e-beam samples. Moreover, it is remarkable to observe that the overall thickness of silicide layer depends significantly on the deposition method.

S. M. Amir, Mukul Gupta and Ajay Gupta; Jochen Stahn (PSI, Switzerland)

3.1.2.7 Suppression of atomic diffusion of iron and nitrogen in presence of additives X=Al, Ti and Zr in iron nitride thin films

Iron nitrides are important materials for its vital applications in tribological coatings, magnetic memory devices, high frequency read write heads etc. However due to weak Fe-N bonding, thermal stability of this compound is rather poor. In view to this, it was proposed in the literature that the addition of small amount of third elements X=Al, Ti, Zr etc. which have high affinity for nitrogen and simultaneously having high X-N heat of formation will leads to improve the thermal stability of Fe-X-N compounds remarkably. The basic mechanism corresponding to such improvement in thermal stability of these compounds is the suppression of diffusion of Fe and N in presence of these additives. However there were no experimental studies to confirm this idea. In the present work, we have studied the Fe and N self-diffusion in Fe-X-N thin films, we have prepared the iron nitride thin films with 5 at.% of additives X=Al, Ti and Zr using magnetron sputtering, for better comparison, Fe-N film without any additives was also prepared, the films were deposited in multilayer structure form of type *[^{57}Fe-X-N(6 nm)|Fe-X-N(6 nm)]x10|substrate and [Fe-X-^{15}N(8nm)|Fe-X-N(8nm)]x25|substrate*, to measure the self -diffusion of Fe and N respectively. The structural and magnetic properties of the deposited films were investigated using x-ray diffraction (XRD) and superconducting quantum interference device (SQUID), the self-diffusion measurements have been carried out using neutron reflectivity (NR) at SINQ- PSI Switzerland, and nuclear resonance reflectivity (NRR) at Mössbauer resonance energy of 14.4keV for ^{57}Fe at P01-Beamline PETRA, Germany.

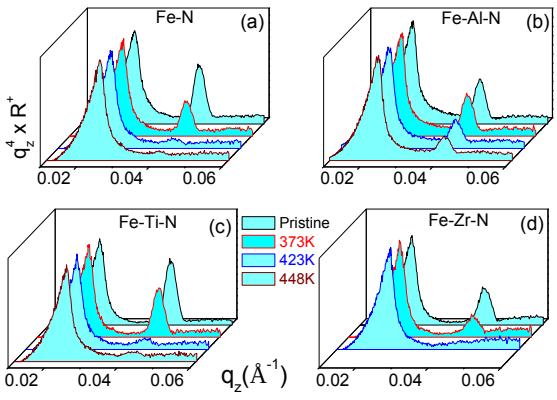

Fig. 1. NR patterns of Fe-N(a), Fe-Al-N(b), Fe-Ti-N(c), and Fe-Zr-N(d) thin films annealed at various annealing temperatures. Here Bragg's peak was observed due to scattering length contrast of ^{nat}N and ^{15}N.

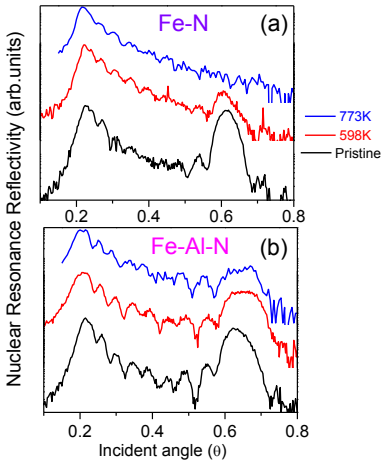

Fig.2. Nuclear Resonance Refelectivity patterns of Fe-N(a), Fe-Al-N(b) thin films taken at Mössbauer resonance energy 14.4 keV.

The thermal stability in this compound was studied by performing vacuum annealing of these samples and subsequently characterizations of the samples were performed with various techniques. From XRD and SQUID measurements (not shown) it was found that films are nanocrystalline with bcc-Fe structure, with annealing additional iron nitride phases starts appearing in the pure iron nitride sample, whereas with presence of additives no additional phases were observed. From SQUID measurement it was found that soft magnetic

properties improved significantly with presence of additives. Fe and N self-diffusion measurements were performed using NR and NRR, obtained results were shown in fig. 1 and 2 respectively. Fig. 1(a)-(d) shows the NR pattern of FeN(a), Fe-Al-N(b), Fe-Ti-N(c) and Fe-Zr-N(d) thin films of type *[Fe-X-^{15}N(8nm)|Fe-X-N(8nm)]x25|substrate*, Bragg's peak observed in the NR pattern was due to neutron scattering length density contrast for $^{natural}N$ and ^{15}N, with subsequent annealing due to diffusion of N across the interface decay of Bragg peak intensity can be observed. It can be clearly seen that with presence of additive Al there is substantial decrease in atomic diffusion of N as compared to pure Fe-N film. However with Ti and Zr addition no such suppression in atomic diffusion of N was seen. In account of these results, we have performed NRR measurements on two sets of samples, with and without addition of Al on multilayer of type *[^{57}Fe-X-N(6 nm)|Fe-X-N(6 nm)]x10|substrate* to study self diffusion of Fe, the obtained NRR patterns with annealing were shown in fig 2(a)-(b) for Fe-N and Fe-Al-N films respectively. It can be seen that in presence of Al the Fe diffusion is remarkably reduced, Bragg's peak can be observed even when sample was annealed at 773K, whereas in pure Fe-N sample it gets disappear up to this temperature. The obtained results can be understood in terms of heat of formation of Fe-N/X-N and the affinity for N to Fe and X. In addition the grain boundary precipitates in the form of X-N plays a significant role in improving the thermal stability of Fe-X-N films.

Akhil Tayal, Mukul Gupta and Ajay Gupta; Kai Schlage, H-C Wille (DESY, Germany) Jochen Stahn (PSI, Switzerland)

3.1.2.8 Enhancement of Ferromagnetic metallic phase fraction by extrinsic disorder in phase separated $La_{5/8-y}Pr_yCa_{3/8}MnO_3$ (y=0.45) thin film

Our study shows that extrinsic disorder plays decisive role in shaping inhomogeneities at large length scale in phase separated system. Epitaxial $La_{5/8-y}Pr_yCa_{3/8}MnO_3$ (y=0.45) thin films grown on $SrTiO_3$, $LaAlO_3$ and $NdGaO_3$ substrates exhibited comparable biaxial strain while markedly dissimilar extrinsic disorder. Compressively strained film on $LaAlO_3$ is found free from extrinsic disorder manifesting robust insulating phase with small phase separation while film grown on SrTiO3 depicted huge extrinsic disorder due to strain relaxation process which invokes phase separation at large length scale that is sufficient to cross percolation threshold and being the cause for occurrence of metal insulator transition

In the present report LPCMO thin films are grown on different substrates that provide very interesting physical situation. The strain value is found to be comparable in all the three films and extrinsic disorder (inhomogeneous strain field) has quantitatively significant difference. Extrinsic disorder is found to be strongly influencing phase separation in LPCMO thin films.

The morphology of the three films is probed using AFM and is shown in figure 1 (a-c) that showed very interesting differences. Left panel of figure shows island height variation of the films and right panel of figure shows surface morphology of the corresponding films. FLAO film revealed very smooth surface morphology with a root-mean-square (rms) roughness ~5 Å and negligible island height variation. Smooth surface and very small grain size as well as height distribution for this particular film indicate towards uniform growth of the film. Observation of Keissig fringes in the XRD pattern for this film certify defect free atomic level uniform film growth . FNGO film showed increased surface (rms) roughness of ~11 Å and non uniform island height indicating increase in surface disorder when compare with FLAO film. On the other hand FSTO film exhibited huge surface (rsm) roughness ~25 Å with large distribution in island height. In FSTO lattice misfit energy is large compared to its elastic strength and in order to minimize this large elastic energy a self strain relaxation

process is invoked during film growth that produces a variety of lattice defects and non-uniform distribution of strain by formation of nonuniform islands. ,30 Therefore, huge strain disorder emerges in this film that reflects in large peak width in XRD study. Schemetic view of this strain disorder is given in figure 1(d).

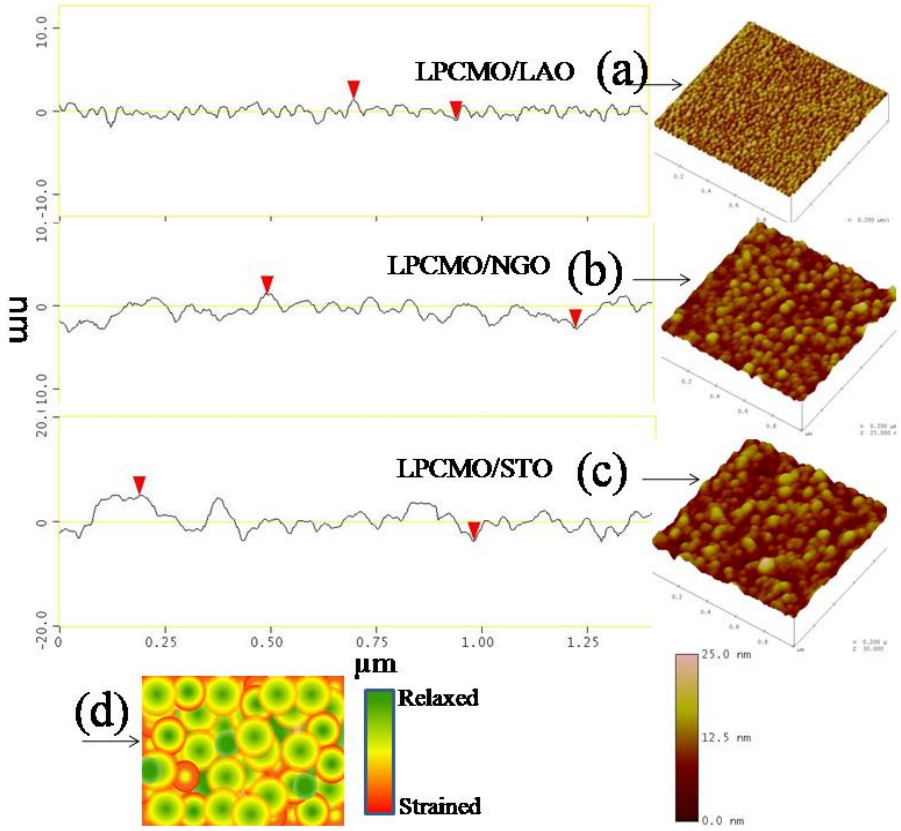

Figure (a,b,c) *(Right panel) AFM image (scan area 1µm × 1µm) showing surface morphologies of FLAO, FNGO and FSTO films respectively and (Left panel) shows island height variation (in nm) across the diagonal of scanned area.* ***(d)*** *shows schematic description of strain field inhomogeneities within FSTO film. Here relaxed phase is represented by green color and strained phase is represented by red color.*

Temperature dependent resistivity data in cooling and warming cycle of all films is shown in Figure 2 (a-c). FLAO film showed insulating behavior down to 115K and the magnitude of the resistance became beyond our measurement limit below this temperature. The behavior is typical of a robust COO-AFI phase because a 2T field is not able to make any significant change in the resistance. FNGO film also shows insulator behavior in zero Tesla magnetic field (H = 0T) cooling and resistance value became beyond measurement limit blow 100K, however, resistance curve measured in cooling and warming cycle bifurcates below 152 K. On the application of 2 T field, film showed a TMI at 103K in cooling cycle and at 113K in warming cycle with thermal hysteresis (TMI (peak) cooling - TMI (peak) warming) of 10K. Interestingly, FSTO film displayed TMI at 105K in cooling cycle and 134 K in warming cycle with thermal hysteresis of 29K even in the H = 0T. On the application of 2T field transition shifted towards higher temperature (~160K) with decrease in hysteresis width (~5K). Isothermal R-H measurement at 5K (after zero field cooling) also show that AFI state is robust in FLAO film. As shown in figure 3(d) resistivity for

FLAO become measureable above 7 Tesla and remains within this range with reducing magnetic field to zero. Whereas for FNGO and FSTO film the field induced sharp change in resistance is observed at lower field values i.e. ~5 Tesla and 2 Tesla, respectively {figure 2 (e-f)}. This is consistent with our resistivity results discussed above.

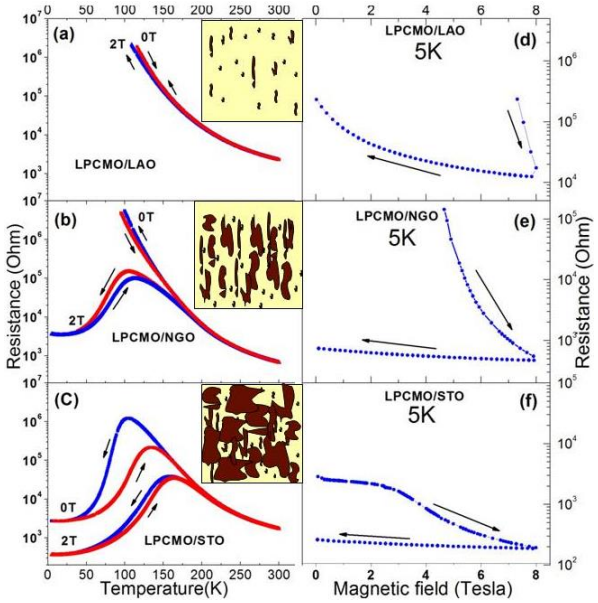

Figure 2: (a,b,c): *Temperature dependent resistivity data of FLAO, FNGO and FSTO films in zero Tesla and 2 Tesla magnetic fields.* ***(d,e,f):*** *R-H measurements of FLAO, FNGO and FSTO films at 5 K in field sweeping from 0 Tesla to 8 Tesla and 8 Tesla to 0 Tesla. Insets show schematic representation of phase separation in all the three Films. Here FMM phase is represented by brown color (dark) and COO-AFI phase is represented by yellow color (light).*

In summary, our study shows importance of extrinsic disorder on the phase separation in LPCMO thin films. This study demonstrates that extrinsic disorder in the form of strong strain field inhomogeneities are developed during strain relaxation mechanism that produce phase separation at larger length scales.

V.G. Sathe, Dileep K. Mishra, R. Rawat, V. Ganesan

3.1.2.9 Signature of Spin-Phonon Coupling in Sr_2CoO_4 Thin Film: A Raman Spectroscopic Study:

Thin films of Sr_2CoO_4 are grown on (100) MgO substrate using pulsed laser deposition. Magnetization measurement reveals ferromagnetic transition at temperature (T_C) 255 K. We have investigated its phonon spectra and its evolution with temperature using Raman spectroscopy. We observed mainly four Raman active modes centered at around 280, 410, 470 and 630 cm^{-1} for SCO, consistent with the group theoretical prediction for the space group I4/mmm. According to the group theoretical prediction, the low frequency modes at ~ 280 and 410 cm^{-1} assigned as $E_{1g}(2)$ and $A_{1g}(2)$ modes respectively involve only motion of Sr – atoms in ab-plane and out of plane direction respectively. Temperature dependent Raman spectra indicate that there is no change

in spectral signature across the paramagnetic-ferromagnetic transition which suggests that there is no structural phase transition in the investigated temperature range. However, we observe that the wavenumber and line-width of the prominent A_{1g} mode generally follows the anharmonic behavior apart from noticeable deviation in the vicinity of T_c {shown in Figs. 1(a) and 1 (b)}. In Fig. 2 we compare the experimental values of $\Delta\omega(T) = \omega_{anh}(T)-\omega(T)$ and $[M(T) / Ms]^2$. Close correlation between the frequency shift and magnetization is clearly evident in the temperature range of 215K to 255 K, which suggests that the anomaly in the vicinity of T_c is owing to spin-phonon coupling in the material.

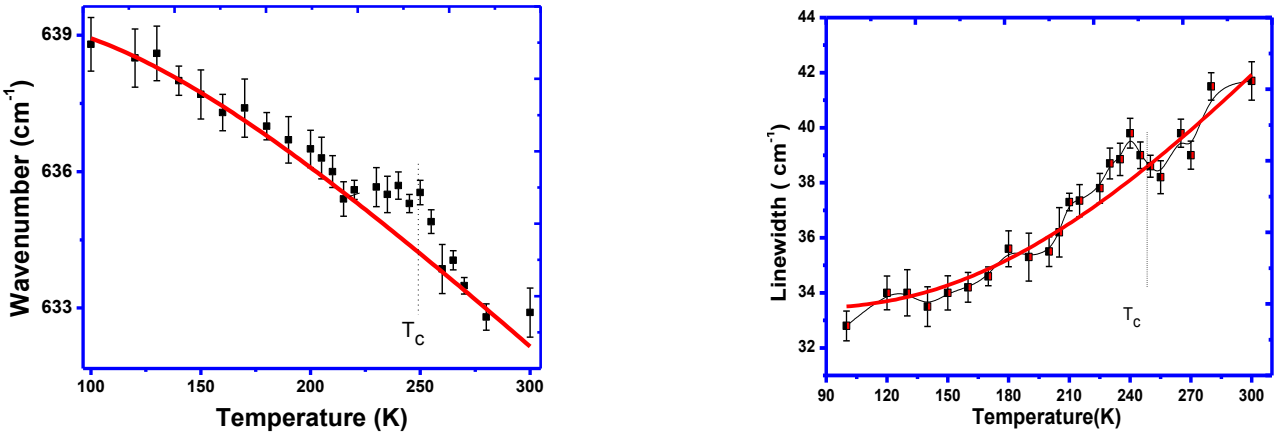

Temperature dependence of (a) wave number and (b) line-width of $A_g(1)$ mode, the solid red lines shows best fit to the anharmonic behaviour.

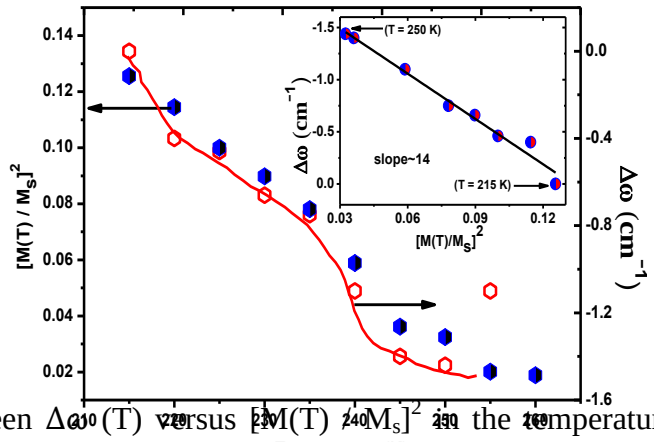

Plot of $\Delta\omega(T)$ and $[M(T)/M_s]^2$ with temperature for $A_{1g}(1)$ stretching mode. Solid line in inset shows the linear least square best fit to the data of $\Delta\omega(T)$ versus $[M(T)/M_s]^2$ in the temperature range of 215 K to 250 K.

Plot between $\Delta\omega(T)$ versus $[M(T) / M_s]^2$ in the temperature range 215 K - 250 K ; which can be used to estimate spin-phonon coupling strength (λ), is shown in the inset of Fig. 2. The estimated value of $\lambda \sim 3.5$ cm^{-1}.

Pankaj K Pandey, R. J. Choudhary, and D. M. Phase

3.1.2.10 $La_{5/8-y}Pr_yCa_{3/8}MnO_3$ (y=0.45) thin film

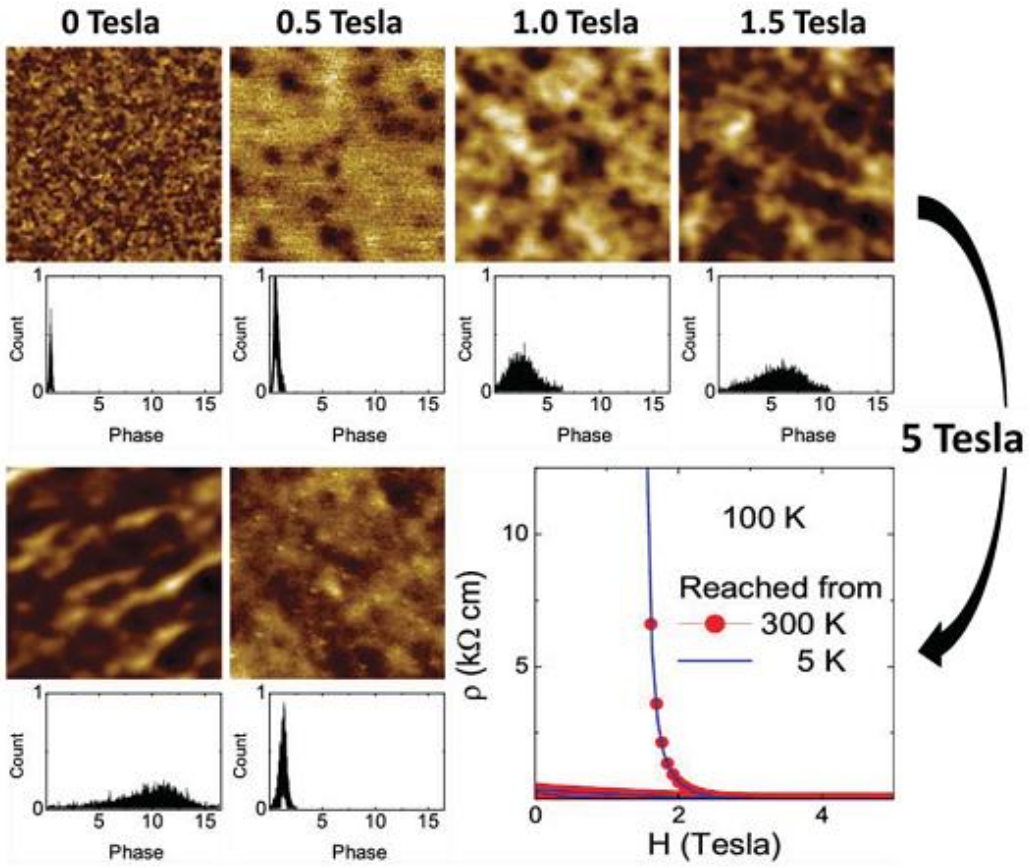

Figure 1: MFM images showing growth of ferromagnetic metallic (FMM) phase (dark color) with increasing magnetic field (top panel) and decreasing magnetic field (bottom panel) along with corresponding histograms at 102K. Measurement temperaure reached in zero field cooled condition and image represents 5μm x 5μm area of the sample. Contrast in 0 Tesla image after field cycling (bottom left image) is arising due to randomly oriented domain of FMM phase. Bottom right inset shows isothermal magnetoresistance curve at 100 K measured for two condition; when measurement temperature is reached (i) from 5 K in zero field and (ii) from 300 K in zero field. These curve shows open loop where resistivity is higher than our instrument's measurement range and after field cycling it remains in the metallic state at 0 Tesla.

First-order antiferromagnetic insulating (AFI)-ferromagnetic metallic (FMM) transition as a function of temperature and magnetic field is studied using magnetic force microscopy (MFM) in $La_{5/8-y}Pr_yCa_{3/8}MnO_3$ (y=0.45) thin film grown on $NdGaO_3$ substrate. We were able to scan same area over a wide temperature range (150-60 K) both during cooling as well warming to study the nucleation and growth of AFI and FMM regions in the presence of 1 Tesla applied magnetic field. During cooling FMM phase nucleates well above metal insulator transition temperature (T_{MI}) obtained from resistivity measurement. It showed that apparent variable

range hopping behavior in resistivity near T_{MI}, is a consequence of the changing AFM to FMM phase fraction rather than change in transport mechanism. During warming back transformation takes place within a narrow temperature window compared to that observed during cooling. A comparison of AFI to FMM transformation during in-field cooling with reverse transformation during warming of the same region, showed that it cannot be described solely in terms of the broad first-order transition due to quench disorder.

In addition to this, isothermal field cycling even around 100 K showed different magnetic state before and after the application of magnetic field (figure 2). Corresponding isothermal magnetoresistance curve showed an open loop consistent with MFM measurements. Since open loop is observed both during warming as well as cooling i.e. when 100 K is reached from 5 K and when 100 K is reached from 300 K, it is attributed to kinetic arrest of the first order transition.

Growth morphology of the FMM phase is observed to be path dependent as larger size FMM regions (but with smaller net fraction) are observed for isothermal field induced transition when compared to field cooling (figure 3). Difference in phase fraction could be explained as an interplay between supercooling (H*, T*) and kinetic arrest (H_K, T_K) band shown schematically in figure 3 (c). When system is cooled in zero field condition, AFM phase remains arrested as (H_K, T_K) band is crossed before crossing the (H*, T*) band. It results in smaller FMM phase compared to that observed for cooling in the presence of magnetic field.

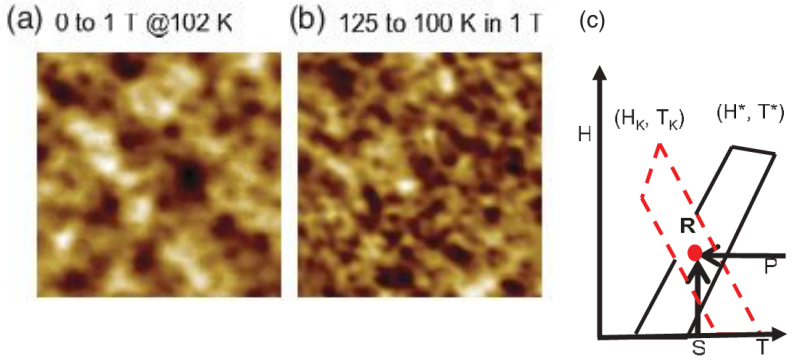

Figure 2: MFM images (5μm x 5μm) around 100 K and 1 Tesla measured for two paths in H-T space (a) isothermal application ofmagnetic field at 102 K after zero field cooling (path SR) and (b) cooled from 125 K to 100 K in the presence of applied magnetic field (path PR). These images shows smaller size FMM region but with larger net fraction for cooling in the presence of magnetic field. The difference in FMM phase fraction can be explained as an interplay of kinetic arrest (H_K, T_K) band and supercooling (H*, T*) band shown sechmetically in figure (c).

R. Rawat, Pallavi Kushwaha, Dileep K Mishra and V Sathe

3.1.2.12 Electrical, magnetic and magnetotransport properties of pulsed laser deposited epitaxial thin films of $La_{0.7}Ca_{0.3}Mn_{1-x}Al_xO_3$.

Thin films of $La_{0.7}Ca_{0.3}Mn_{1-X}Al_XO_3$ (X= 0, 0. 05, 0.15) are grown by PLD on LAO, STO and NGO substrates. X-ray diffraction measurements reveal the single phase orthorhombic structure of all the grown films. Further Phi scan measurements confirm their epitaxial nature. Through electrical measurements we

observe that the metal to insulator transition (MIT) temperature shifts to low temperatures with Al doping in LCMO. This shifting in MIT is also found to be dependent on the substrate used for deposition. A shifting in paramagnetic to ferromagnetic transition (PFT) temperature T_c is also realized in the magnetic measurements. Lowering of MIT and PFT temperature is associated with the disordered induced by the non magnetic Al ion in the Mn-O network. Magneto-transport results are consistent with the electrical and magnetic behavior of these samples. Spin glass behavior is also investigated in the highest Al dopes samples.

Manish Saharan, D.M.Phase and R.J.Choudhary

3.1.2.13 Band offset measurements and magneto-transport properties of epitaxial TiO2-x (x= 0.05)/La0.7Sr0.3MnO3 hetero-structure

We have studied the electronic transport behaviour and band offset properties of the epitaxial TiO_{2-x} (x=0.05)/$La_{0.7}Sr_{0.3}MnO_3$hetero-structure. The bilayer shows non-linear I-V characteristics at different temperatures as well as negative magneto-resistance with the application of magnetic field. Valence band offset (VBO) was measured using photoelectron spectroscopy and consequently the conduction band offset (CBO) was determined. It is found that type-I alignment takes place at the interface (shown in Fig.). The value for CBO (1.1eV) is much lower than VBO (2.3eV), suggesting that transport is mainly dominated by electrons.

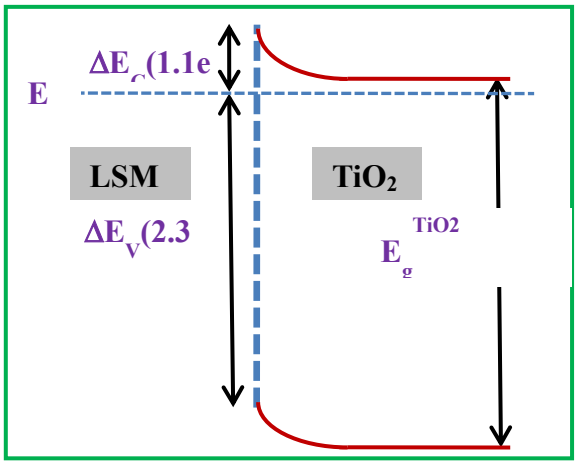

Representation of Type-I band alignment at the TiO_2/LSMO interface, measured using photoelectron spectroscopy.

R. J. Choudhary, Komal Bafna and D. M. Phase

3.1.2.14 Effect of silver addition on structural, electrical and magnetic properties of Fe3O4 thin films prepared by pulsed laser deposition

The structural, electrical and magnetic properties of Ag_x-$(Fe_3O_4)_{1-x}$(x= 0, 0.02, 0.10) composite films were investigated by X-ray diffraction (XRD), X-ray photoelectron spectroscopy (XPS), resistivity as well as magnetization (both temperature and field dependent) measurements. The samples used in present work were

prepared by pulsed laser deposition (PLD) technique on single crystal Si (111) substrate. XRD spectra reveal that Ag added samples show polycrystalline growth on Si substrate in distinction to oriented growth of Fe_3O_4 on similar substrate. XRD and XPS data confirm that silver is present in metallic form. Temperature dependent resistivity data corresponding to all the three samples show a well-known Verway transition around 121 K {shown in Fig. (a)}. The resistivity pattern corresponding to Ag_x (x=0.10) added sample shows the tunneling behavior below the Verway transition which is attributed to the accumulation of silver clusters across the boundary of Fe_3O_4 grains and thereby changing the transport behavior at low temperature.

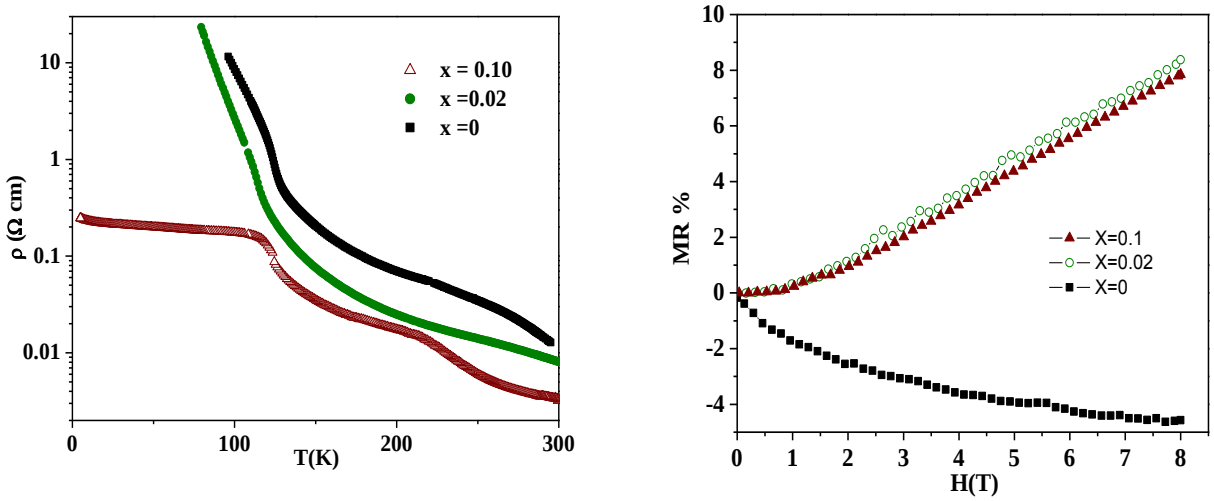

a) Resistivity vs temperature and (b) MR% vs magnetic field (H) behavior of Ag(x) - Fe_3O_4 composite thin films

Ag_x (x=0.02, 0.10) added Fe_3O_4 films show positive magnetoresistance which is in contrast to negative magnetoresistance observed in pure Fe_3O_4 (Fig. (b). Magnetization measurements reveal that Ag granules reduce the saturation magnetization of Fe_3O_4.

Ridhi Master, R. J. Choudhary, and D. M. Phase

3.1.2.15 Effects of Sintering Temperature Variation on Microstructure and Magnetic nature of Al Diluted $La_{0.7}Ca_{0.3}MnO_3$

The samples of $La_{0.7}Ca_{0.3}Mn_{1-X}Al_XO_3$ (X= 0,0.05,0.15) are synthesized at two different sintering temperature 1200^{o}C and 1400^{o}C. The phase purity of the samples is analyzed using x-ray diffraction measurements. The microstructural evolution for different sintering temperatures is carefully tracked using scanning electron microscope (SEM). Increase in grain size with increasing sintering temperature is well identified in SEM images. Variation in the magnetic nature of the samples sintered at different temperature is seen in temperature dependent magnetization M(T) measurements. Further M(T) results reveal that Al doped samples show strong dependence of their magnetic behavior on sintering temperature as compared to undoped $La_{0.7}Ca_{0.3}MnO_3$.

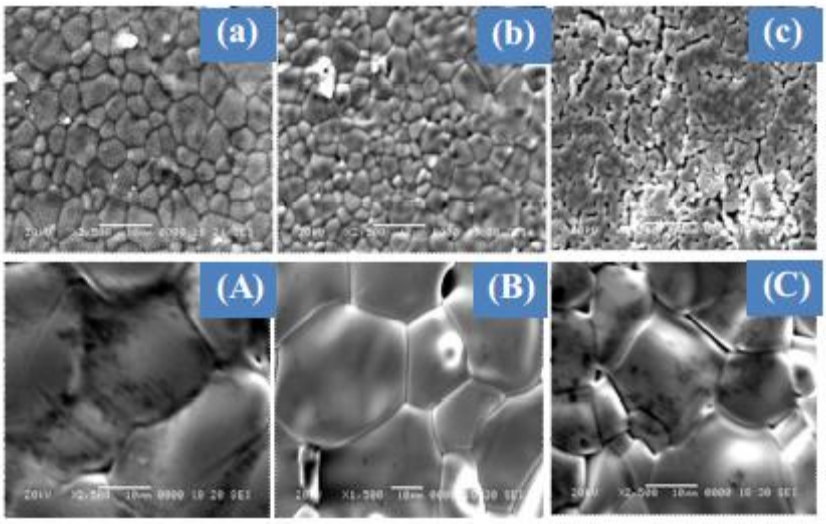

SEM micrographs of undoped (a, A) and 5% (b, B), 15% (c, C) Al doped LCMO samples sintered at 1200^{o}C (a,b,c) and 1400^{o}C (A,B,C)

Manish Saharan, R.J.Choudhary and D.M.Phase

3.1.3 Nanomaterials

3.1.3.1 Low temperature UV-Vis spectra of nanosheets and bulk powder of α-Fe_2O_3

UV-Vis diffuse reflectance spectra were recorded on nanosheets and bulk powder of α-Fe_2O_3 below room temperature. The results are shown in Fig. 1. It can be seen from Fig. 1a that width of absorption bands decreases with decreasing temperature. As a result the position adjacent overlapping band can be observed with better accuracy, which is an advantage of recording the spectra at low temperature. In case of nanosheets, the position and relative intensity of absorption bands (Fig. 1b) are remarkably different than in bulk sample. The bands b, d are blue-shifted by ~40 nm. The absorption band b arises from electronic transition across the bandgap. The sheets are very thin (~20 nm) along c-axis. Blue-shift of this band is attributed to quantum confinement effect arising from reduced dimension of the sheets along the c-axis. The band c is red-shifted, whereas the band d is blue-shifted. Both the bands are broadened. Also, absorption bands in the range 1000-1300 nm are observed only in nanosheets sample. The broadening and shifting of bands, additional bands, all are attributed to stress effects. Raman and XRD measurements revealed that there is high residual compressive stress (1.4–2.1 $GNcm^{-2}$) along c-axis and tensile stress of 0.4–0.8 GNm^2 normal to c-axis. The influence of such anisotropic stress on the ligand-field transitions requires further investigation. It has been established that stress can bring about change in electronic structure, which in turn affects the electronic absorption spectra in the UV-Vis measurements.

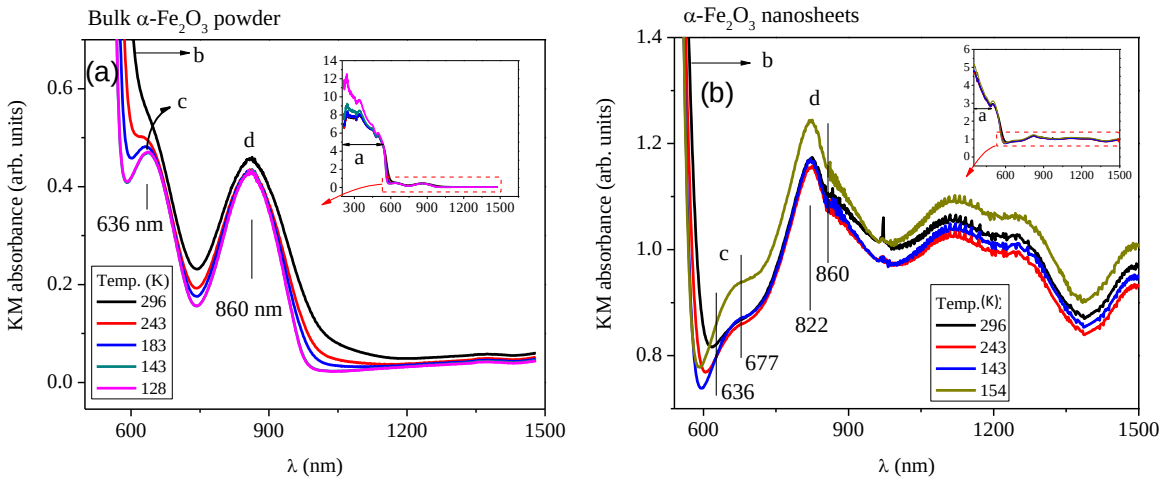

Fig. 1. Kubelka-Munk absorbance calculated from diffuse UV-Vis reflectance spectra recored at different temperatures is shown for (a) bulk α-Fe_2O_3 powder, and (b) α-Fe_2O_3 nanosheets. The absorption bands arising from different mechanism are indicated as b: pair excitation process and transition across the bandgap; c and d: two different ligand-field (d-d) transitions of Fe^{3+} ion. The absorption spectra of nanosheets are remarkably different than those of bulk.

U.P. Deshpande, T. Shripathi, A.V. Narlikar

3.1.4 Other studies

3.1.4.1 Bulk electronic structure of Al-Pd-Mn and Al-Cu-Fe quasicrystals

In this study, we have employed hard x-ray photoelectron spectroscopy (HAXPES) to study the bulk electronic structure of quasicrystals and thus disentangle it from the surface effects. We resolve a controversial issue regarding the mechanism for the formation of quasicrystalline solids, i.e., the existence of a pseudogap at the Fermi level. The near Fermi level HAXPES spectra of icosahedral fivefold Al-Pd-Mn and Al-Cu-Fe quasicrystals demonstrate the presence of a pseudogap, which is not observed earlier in surface sensitive low energy photoemission because the spectrum is affected by a metallic phase near the surface. In contrast to Al-Pd-Mn, in Al-Cu-Fe the pseudogap is fully formed; i.e., the density of states reaches zero at E_F indicating that it is close to the metal-insulator phase boundary. This work has been published in Phys. Rev. Lett., 109, 216403 (2012).

J. Nayak, M. Maniraj, A. Rai, S. Singh [UGC-DAE CSR, Indore]; P. Rajput and J. Zegenhagen [ESRF, France], A. Gloskovskii [PETRA, Germany] ; D. L. Schlagel and T. A. Lograsso [Ames Lab., U.S.A.] and K. Horn [FHI-MPG, Germany]

3.1.4.2 Magnetoresistance, powder neutron diffraction, and theoretical studies on Mn_2NiGa

We have observed spin-valve-like magnetoresistance behaviour in a magnetic shape memory alloy Mn_2NiGa crystal at room temperature. We establish from neutron diffraction and theoretical studies that Mn_2NiGa is a ferrimagnetic material with antiparallel alignment of the Mn spin moments. On the basis of neutron diffraction, magnetization behaviour and theoretical studies, the origin of the unexpected behaviour of magnetoresistance has been ascribed to the presence of antisite disorder where about 13% of the Ga sites are occupied by Mn atoms. We establish that these antisite defects for ferromagnetic nanoclusters with parallel alignment of Mn spin moments in a Mn2NiGa bulk lattice that has antiparallel Mn spin moments. The direction of the Mn moments in the soft ferromagnetic cluster reverses with the external magnetic field. This causes a rotation or tilt in the antiparallel Mn moments at the cluster-lattice interface resulting in the observed asymmetry in magnetoresistance. This work has been published in Phys. Rev. Lett., 109, 246601 (2012).

S. Singh, R. Rawat, S. W. D'Souza, S. Banik, S. Bhardwaj, A. M. Awasthi [UGC-DAE CSR, Indore]; S. Esakki Muthu and S. Arumugam [Bharathidasan University, Tiruchirappalli]; E. Suard [ILL, Grenoble]; A. Senyshyn [Technische Universitat Muenchen, Germany]; P. Rajput [ESRF, Grenoble]; R. Ranjan [IISc, Bangalore]; D. L. Schlagel and T. A. Lograsso [Ames Lab., USA]; A. Chakrabarti [RRCAT]

3.1.4.3 Thermally Stimulated Depolarization Current (TSDC) technique used to study various relaxation phenomenon of poly Caprolactone film.

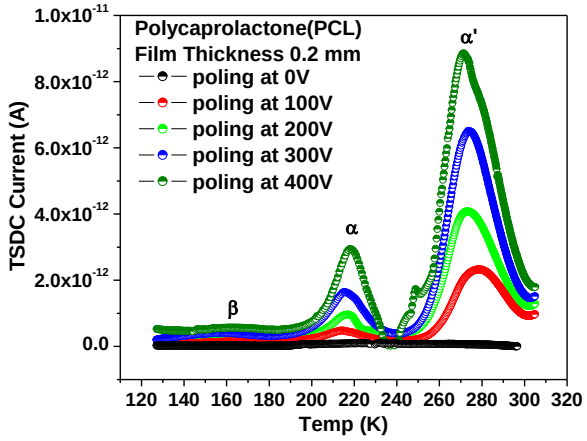

Figure:1 TSDC Spectrum of Poly Caprolactone film as a function of different poling fields

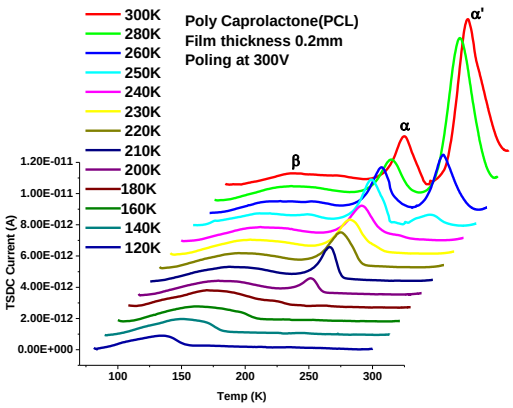

Figure: 2 TSDC spectrum of Poly Caprolatone film at same poling field but at different poling temperatures

Poly Caprolactone (PCL) is a biodegradable polymer. The degradation of PCL is slower and produces less acidic degradation products; therefore the PCL seems a suitable polymer for the efficient tissue regrowth and a drug delivery vehicle for a sustain drug release mechanism. It has a low glass transition temperature Tg of 213K and a melting temperature Tm of 333K. TSDC technique is used to study the dipolar relaxation in PCL film of 0.2mm thickness. The dipolar behavior of the PCL film has been studied in 80K-300K temperature

range at various poling fields EP while keeping the other parameters; such as poling temperature TP, poling time tP and heating rate constant. The presence of β and α peak in the given TSDC spectrum shows the exclusive dipolar relaxation of the PCL polymer, while the presence of high temperature α' peak may come as a result of the relaxation of the free space charge. We have also studied the effect of different poling temperatures on the various relaxation mechanisms involved in the PCL. For that we have done the TSDC at various poling temperatures but kept the poling filed constant. Here we can see that how poling at lower temperature suppresses the higher temperature TSDC peaks. This work is a part of the DST project on "Electret State in Bio-degradable medicalpolymers"

Manju Mishra Patidar, R. Nath and V. Ganesan

3.1.4.4 Phase contrast imaging of fenugreek leaf

Phase contrast imaging techniques can successfully be employed to the study of plant growth, interplay between plant and the soil and for studying the growth of leaves under certain conditions. In this work, we have studied the growth of plant leaf under the UV light filters. The samples chosen were Trigonella (fenugeek) leaf samples. The plants were grown under either the normal sunlight (group A) or inside the UV light filtered (280-315 nm wavelength range excluded using special polythene cages) (group B). After sufficient growth of plants has taken place, the leaves were cut and dried. With the plant physiological techniques, initial characterization was performed, which revealed that under UV-B exclusion, the overall growth of the plant is enhanced. Expansion of the leaf (3-4 times as compared to the normal fenugreek leaf) takes place in all directions, making it larger than normal leaf. However, the thickness of the leaf is reduced.

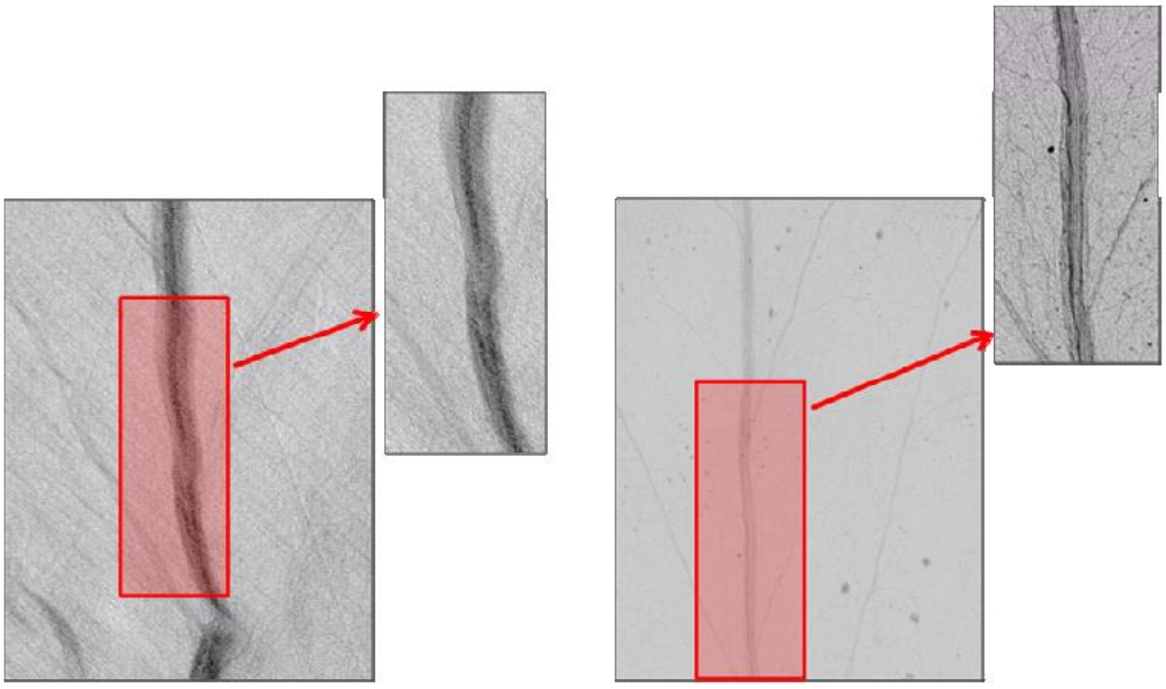

Figure: Trigonella (fenugreek) leaves grown under (a) normal sunlight and (b) UV-B excluded light. Figures are not to scale.

These features are also observed from the phase contrast imaging performed using polychromatic Bremsstrahlung x-ray radiation. The instrument consists of an x-ray microfocus source (160.5 kV 1 mA, 5 µm focal spot size, tungsten target), sample manipulator and CCD detector. The images were recorded in the phase propagation geometry. From these images, it is clearly observed that there are changes in the midrib (xylem, which is known as middle water conducting tissue of the leaf). It becomes thinner, less absorbing (appearing lighter in the image) and fibrous as a result of reduction in lignin (an integral part of the secondary cell walls of plants) deposition in the UV-B treated samples. The most common function of the lignin is the support through strengthening of xylem cells in plants. Also, due to less thickness of the leaf, cell structure is also visible, which was not seen in case of normal leaf where more absorption takes place due to higher thickness (cells are stacked). These are initial experiments and advanced experiments are being planned.

S. Tripathi, A. Fatima and T. Shripathi; K. N. Guruprasad, Juhi Joshi, Life Sciences, DAVV, Indore), Y. Kashyap, A. K. Agrawal, P. S. Sarkar, A. Sinha (BARC, Mumbai)

3.2 Research activities at Kolkata Centre

3.2.1 Trace element studies

3.2.1.1 Physico-chemical characterization of street dust and re-suspended dust from vegetation canopies in an Indian metropolis Kolkata

Air-pollution has become a global threat to both living and non-living entities. As far as the human health is concerned, air-pollutants of major concern are the atmospheric dust of various sizes (0.1 to 10 µm in diameter), which comprises airborne materials from various sources such as industries, vehicular exhausts, human activities etc. Characterization of such dust particulates is necessary for designing an effective pollution management strategy. With the above mentioned facts as our background information, present study was undertaken to analyze the size distribution and investigate the elemental (by SEM-EDX) and mineralogical components (by XRD) of the street dusts and the dusts deposited on the leaves of roadside trees. Samples were collected from representative areas of megacity Kolkata namely Behala Chaurasta-BC, Ultadanga-UD, Karunamoyee-KM and a site away from urban areas Baruipur-BP. Variations in size, mineral and elemental composition were observed. Size distribution of dust particles from street and plant canopies has shown variations in micron range. Particles were present in a wide range of diameters up to 50 micron, however the analysis also showed that there are particles of diameter less than 2 micron (fine particles) mainly originating from anthropogenic activities. Dust from the tree canopies composed of bit finer particles where as dust from streets are composed of mixture different sized particles dominated with coarser particles. Two main categories of particles were observed. Category-1 includes suspended soil dust (primarily soil mineral/lithogenic) such as the angular-shaped material. This category also has particles from natural sources including materials of organic origin (pollen, bacteria, fungal spores etc.). Categoty-2 particles are mainly from anthropogenic sources mostly emitted from high temperature combustion processes are characterized by their spherical shapes. This type of particles occurs as individual particles but also in aggregate form as agglomerates of similar-sized particles and individual large particles caring several smaller attached particles. Both street dust and dust from canopies comprises of organic and inorganic components. Inorganic components represent various elements and mineral compound. Elemental profiling by SEM-EDX have shown the the chemical signatures of Si, V, Cr,

Mn, Fe, Cu, Zn and Pb on the dust particles collected from leaf surfaces. Larger particles are mainly Si rich indicating geological origin whereas smaller particles have shown association of various trace elements. It has been reported by that heavy metals are associated with small size particulates. Elements detected in the present study have been revealed by several studies in different parts of the world. These elements in the dust have

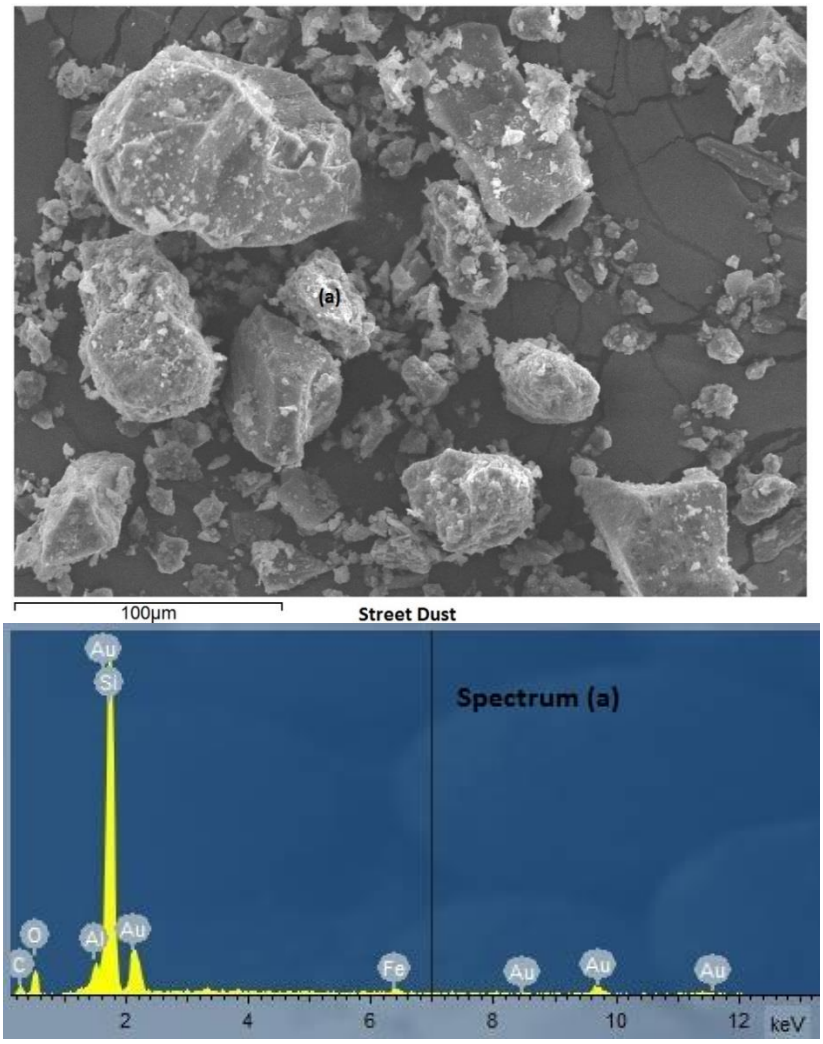

Figure1a. Scanning Electron Micrograph and X-ray spectrum of Street Dust

multiple origins that include re-suspended dust, vehicular exhaust, materials from construction and or demolition, and various anthropogenic activities. The major mineral components identified in street dust were quartz and potential clay forming minerals such as albite, microcline, chlorite and muscovite. Minerals identified in dusts from leaf surfaces were similar to those found in street dust samples except the fact that the intensities were less in comparison to that of street dust. This clearly confirmed that there are inputs from road to leaf surfaces. Detected minerals are quartz (abundant) along with clay forming minerals such as calcite, gypsum, albite, microcline, chlorite, muscovite and oxides of iron (magnetite and hematite) and titanium, in both street dust and dust from leaf surfaces. Abundance of quartz is more in street dust than the dust deposited on canopies. This observation is parallel to the elemental profiling SEM-EDX that is, street dust contain coarse

particle rich with Si. Presence of Iron oxides in the atmospheric dust may be attributed to anthropogenic inputs of magnetic minerals. Variation in elemental and mineral composition with respect to size distribution as observed in our present study has been reported by several researchers. From the study it is evident that the information on mineralogical and elemental composition of street dusts and dusts deposited on the leave surfaces of roadside trees can act as indicator of air-pollution.

This work was carried out under UK-Commonwealth Scholarship program at Department of Material Science and Metallurgy, University of Cambridge, UK.

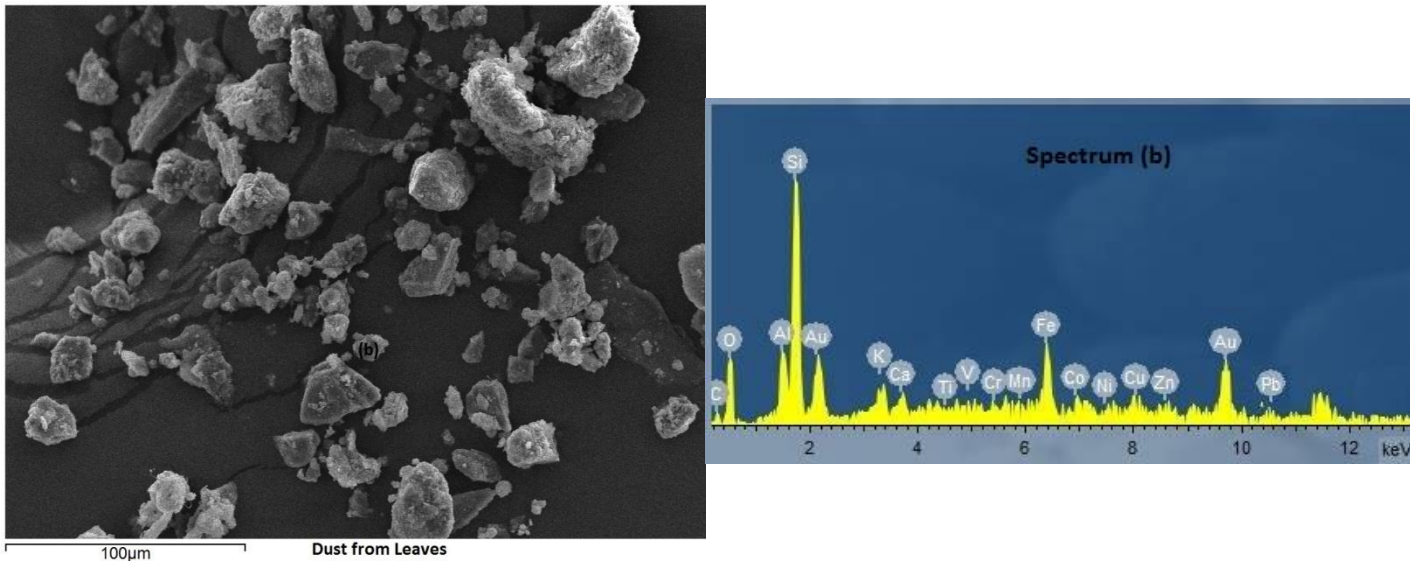

Figure1b. Scanning Electron Micrograph and X-ray spectrum of Dust collected from leaves

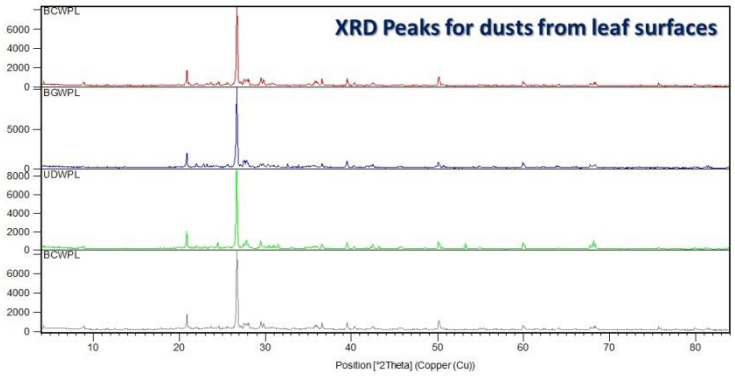

Figure2. XRD Spectrum of dust collected from leaves

S.S.Ram,(UGC-DAE CSR KC) R.V.Kumar, (University of Cambridge, UK) P. Chaudhuri (University of Calcutta) S. Chanda, (Allergy & Asthma Research Centre, Kolkata) S.C.Santra, (University of Kalyani) M. Sudarshan and A. Chakraborty

3.2.2 Condensed matter studies

3.2.2.1. Interface magnetism in mechanically milled Fe/CoO nanocomposites

Nanocomposites comprising ferromagnetic α-Fe and antiferromagnetic CoO are prepared successfully by the high energy ball-milling method. XRD and TEM measurements confirm the pure phase polycrystalline nature of the nanocomposites having average particle size 15 nm for 30 hour milled sample. Reduction of crystallite size and increase of microstrain are observed with increasing milling duration. Mössbauer measurements show the presence of superparamagnetic doublet in higher hour milled samples, which represents the presence of a broad distribution in particles sizes. Positron annihilation lifetime spectra confirm the existence of interfacial defects in the nanocomposites. A significant horizontal shift in the hysteresis loop was observed along the field axis when the sample is cooled in FC condition which confirms the presence of exchange bias in the system. High-field bifurcation in temperature dependent ZFC-FC magnetization indicates the presence of spin-glass like (SGL) phase. Observed temperature dependent field cooled memory effect is also an indication of SGL phase. But memory effect is absent in the time dependent relaxation measurements. Hence an ambiguity exists in understanding the possible reasons of the observed SGL phase. Polydispersity and defects are argued to be possible causes of the observed SGL behavior.

S.P. Pati, S. Kumar (Jadavpur University) and D.Das

3.2.2.2 Structural, hyperfine and magnetic characterization of Fe/MnO nanocomposites.

Fe/MnO nanocomposites have been prepared by the high energy ball milling method. Decrease in crystallite size and increase in microstrain with milling duration are observed from the Rietveld refinement of XRD data. TEM picture showed that the Fe nanoparticles are dispersed in the MnO matrix. Mössbauer spectra of nanocomposites ball milled up to 20hr showed a single sextet with gradual increase in line width. However, the sample milled for 30hr showed an additional doublet which is assigned to the Fe atoms undergoing superparamagnetic relaxation. Temperature dependent dc and ac magnetization measurements indicated the presence of relaxation in the sample. The relaxation may be caused by both SGL and superparamagnetic phases if present in the sample. FC memory effect indicates the presence of SGL phase in the sample. The effect of temperature cycling on ZFC magnetization supports this assumption.

S.P. Pati, S. Kumar (Jadavpur University) and D.Das

3.2.2.4 Positron annihilation lifetime studies on Fe_3O_4/CdS nanocomposites

A detailed study of the microstructural defects in Fe_3O_4/CdS nanocomposites were carried out by positron annihilation lifetime (PAL) measurements. The typical positron lifetime spectra obtained for the samples were fitted with three lifetime component τ_1, τ_2, τ_3 with relative intensities I_1, I_2 and I_3 respectively. The variation of positron lifetimes and their relative intensities with concentration of magnetite in the nanocomposites are studied.

A Roychowdhury, A. K. Mishra, S. P. Pati and D. Das

3.2.2.3 Magnetic and magneto-transport investigation of $Eu_{0.5}Sr_{0.5}Mn_{1-x}Co_xO_3$ perovskite

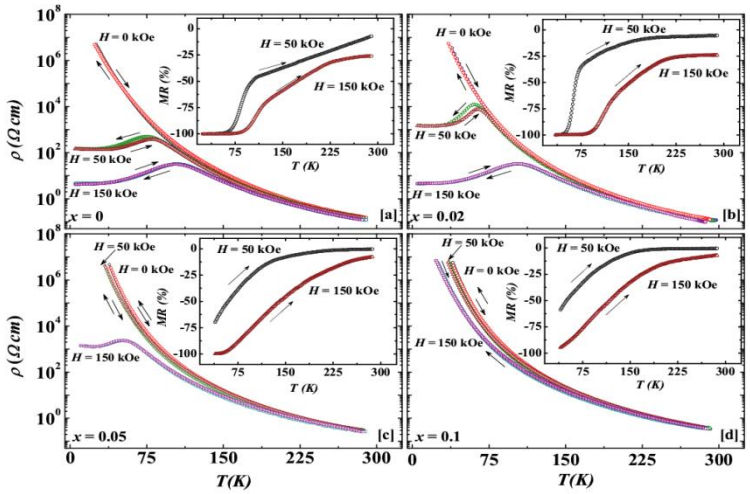

Fig.1 Temperature variation of resistivity in presence of different applied magnetic field. Insets depict temperature variation of magneto resistance.

The perovskite manganite of nominal composition $Eu_{0.5}Sr_{0.5}Mn_{1-x}Co_xO_3$ (x = 0, 0.02, 0.05, 0.1) has been investigated through transport and magneto-transport measurements. We observe field induced transition from antiferromagnetic insulating state to ferromagnetic metallic state below a certain temperature for x = 0, 0.02 and 0.05 samples on application of external magnetic field. Critical field required for insulator to metal transition depends strongly on the Co concentration. For x = 0.1 sample no transition is observed even for 150 kOe of applied magnetic field. Ground state of these samples at low temperature depends strongly on the previous history of applied magnetic field. We also observe large magnetoresistance (~ 99.9% for 150 kOe of applied magnetic field) below 100 K, which is connected to the field induced transition present in the sample.

P. Dutta, D. Das, S. Chatterjee (UGC-DAE CSR, Kolkata Centre), S. Majumdar (IACS, Kolkata)

3.2.3 Chemical sciences & radiochemistry

3.2.3.1 Evolution of biofunctional semiconductor nanocrystals: A calorimetric investigation

Semiconductor nanomaterials have found numerous applications in optoelectronic device fabrication and in platforms for drug delivery, hyperthermia cancer treatment, and in various other biomedical fields because of high photochemical stability and size-tunable photoluminescence (PL). However, little attention has been paid in exploring the energetics of formation of these semiconductor nanoparticles. We demonstrate that formation of nanocrystal with biofunctionalization supported by widely used groups, BSA and cysteine is an exothermic spontaneous process driven by enthalpy. The whole energetics of the reaction shows that formation of smaller particle is favored with lower synthesis temperature. Further, it is shown that thermodynamics of nanoparticle formation is strongly influenced by the conformation of the protein matrix. We also demonstrate that protein supported formation of nanocrystal is thermodynamically more favorable compared to that formed with smaller

organic thiol groups. The favorable enthalpy of formation compensates unfavorable entropy, resulting in favorable Gibbs free energy. Thus, this study can open up new avenues for establishing a thermodynamic basis for the design of nanosystems with new and tunable properties.

D. Ghosh, S. Mondal, C. N. Roy and A. Saha

3.2.3.2 Microcalorimetric investigation in the formation of dendrimer-quantum dot hybrid materials: Implications in size and size distribution of nanocrystals

Synthesis of inorganic-organic hybrid nanomaterials has attracted considerable interest in recent years because of its multifaceted applications, such as optoelctronics, cellular imaging, drug delivery, etc. Maneuvering the controlling parameters is a key to the successful fabrication of good quality materials. However, the fundamental aspect pertaining to thermodynamics of growth of such nano hybrid materials has so far not been unraveled. Here, we have investigated the energetics behind the formation of semiconductor-dendrimer hybrid materials using isothermal calorimetry. It is observed that heat change saturates faster with increase in starting materials or monomer concentrations, which is similar to metal nanoparticles. Interestingly, unlike metal nanoparticles, the heat change increases with the growth of the semiconductor nanoparticles. We have also shown the variation of thermodynamic parameters with change in synthesis conditions, such as temperature, dendrimer generation and dendrimer core or surface groups. We demonstrate that the formation of quantum dot-dendrimer hybrid materials is an exothermic, spontaneous and enthalpy driven process. Further, lower temperature thermodynamically favors the formation of smaller particles with greater size focusing. The observed results suggest that the greater binding constant leads to the formation of particles of smaller dimensions. The dependence of ratio of concentrations of reacting metal ions (Cd or Zn) to sulfide ions show a differential size pattern for CdS and ZnS nanoparticles, which has been interpreted in terms of binding constants determined calorimetrically. It is shown that enthalpy-entropy compensation takes place in the synthesis process affording favorable free energy. Such investigation can provide a useful guideline for synthesis of better quality semiconductor-dendrimer hybrid nanomaterials.

S. Mondal, D. Ghosh, C. N. Roy and A. Saha

3.2.3.3 A Comprehensive Comparative Evaluation of Synthesis Methodologies of Silver Nanoparticles and its Implications in SERS Activity

The preparation and characterization of silver nanoparticles with different shapes and sizes has established the significance of each of these parameters to tailor the resulting plasmonic characteristics of the material [1]. Many synthetic procedures have been developed so far which indicates the importance of the system. But comparative assessment of such processes regarding sizes, distributions etc were not much available in literatures till now. By choice of suitable experimental conditions, capping agents and reducing agents during the synthesis by chemical bottom up approach, we can have control over the shapes and sizes of the produced nanoparticles [2]. This has prompted us to make a critical assessment of various aqueous synthetic procedures with particular reference to the glucose mediated synthesis [3] due to its facile applicability towards biocompatible systems. In this context we have studied temperature variation, concentration variation and time variation during the particular synthesis process. We have also characterized different physicochemical

properties of synthesized silver nanoparticles using absorption spectroscopy, DLS, TEM and Raman spectroscopy. These provide us an idea in detail about the applicability of the particular species in different fields. Silver nanoparticles are widely used as SERS active materials. Here we have investigated the SERS activity of all the synthesized silver nanoparticles in detail employing crystal violet as a model Raman active dye molecule that helps us to optimise the conditions for better Raman activity. Herein, we have tried to analyze the effects of different physicochemical aspects of Ag nanoparticles on SERS enhancement [4]. These findings help us understand the mechanism of interaction between silver nanoparticles and dye molecule during SERS.

C. N. Roy, D. Ghosh, S. Mondal and A. Saha

3.2.3.4 One-Pot Aqueous Synthesis of CdS_xSe_{1-x} Alloyed Quantum Dots

Semiconductor nanocrystals exhibit quantum confinement effects such as size-dependent optical and electronic properties for applications in photovoltaics, light-emitting diodes, photocatalysis, bioassays and electronics. Specific applications require multiple characteristics in a single system. Solution to the problem of dual requirements is to employ alloy nanocrystals. By varying composition, we can alter the physical and optical properties. In this work, we report the synthesis of homogeneous CdS_xSe_{1-x} quantum dots over the range x = 0-1 in a simple aqueous method. The nanocrystals are characterized with respect to size by UV-Vis spectroscopy, PL spectroscopy, Dynamic light Scattering, XRD, lifetime measurements and finally by Transmission Electron Microscopy (TEM). We have synthesized the cysteine capped alloyed CdSSe nanocrystals by adding S^{2-} and Se^{2-} simultaneously to the Cd-cys complex at pH 11.8 and finally heating at 100^0C with continuous stirring. The Se^{2-} was prepared by reducing Se powder with $NaBH_4$. UV-vis absorption and PL spectra for the alloy nanocrystals appears in between the spectra of CdS and CdSe quantum dots. A significant peak shift was observed. At the same reaction condition, CdS shows absorption at 370 nm, CdSe at 440 nm, whereas alloyed CdSSe QDs show absortion at 398 nm. Similarly, alloyed QDs show PL wavelength maximum at 515 nm, whereas CdS QDs and CdSe QDs show maxima at 500 nm and 544 nm, respectively. Typical TEM image confirms the formation of alloyed QDs. TEM images confirm well distribution of QDs and size of about 10 nm. DLS data match well with the size. The QDs were also characterized by XRD and lifetime measurements. Typical TEM images are shown in the figures. Thus we report a simple aqueous route to synthesize alloyed CdSSe QDs, which may have application in in-vivo imaging, photo voltaics etc.

S. Mondal, D. Ghosh, S. C. Bhattacharya (Jadavpur University) and A. Saha

3.2.3.5. Facile synthesis of size tunable Ag-TiO_2 hybrid nanocomposites

The efficiency of photo-catalytic activity of nano TiO_2 can be enhanced by reducing the recombination of holes and electrons. In view of this attempt has been made to synthesize Ag-TiO_2 hybrid nano-composites. Hybrid Ag-TiO_2 was prepared by controlled hydrolysis of Ti–tetra isopropoxide in a medium containing the biocompatible Ag nanoparticles core pre-synthesized by γ-radiolysis method. From UV–VIS spectra, two different characteristic peaks were obtained corresponding to surface-plasmon peak of Ag NPs at ~405 nm and TiO_2 NPs at ~290 nm. The results show that there is a red shift in the Ag peak and a blue shift in case of TiO_2 along with suppression in the intensity of the Ag SPR peak when compared to their pure counterparts. This indicates the formation of the hybrid Ag-TiO_2 nanocomposites. Transmission electron microscopy on the synthesized materials shows formation of the composite structure with Ag in the core. We have also prepared

two different sizes of Ag-nanoparticles (15 nm and 5 nm) as the core and tried to see the effect on TiO_2 shell. The shell-thickness varied from 25 nm to 10 nm as measured by the DLS technique. However, with increasing the amount of Ti-isopropoxide, precursor of TiO_2 NPs, a red-shift in peak at 290 nm was observed. It is well known fact that the introduction of TiO_2 shell would reduce the surface charge density on the Ag core. So it is expected that with increasing the amount of Ti-isopropoxide, the intensity of the Plasmon peak at 405nm would decrease. We observed the similar trend but up to a critical amount of Ti- isopropoxide.

Y. N. Rao, A. Datta, and A. Saha; . D. Banerjee, S. K. Das (VECC)

3.2.3.6. Gamma irradiation route to photoluminescent selenium-based QDs under ambient conditions and its function as a copper ion fluorescence sensor

Among the semiconductor nanoparticles (NPs), ZnSe is of great promise in diverse biological applications because these direct band gap group II-VI materials are highly luminescent suitable for in-vivo imaging, bio-sensing, etc. and both Zn and Se are biologically acceptable constituents for being available in cellular mileau. However, synthesis of ZnSe NPs in aqueous media through conventional soft chemical method has not been very successful so far. The proposed irradiation assisted strategy demonstrates aqueous synthesis of stable, monodisperse and luminescent ZnSe NPs capped with chelating ethylene diamine under ambient conditions and at room temperature. In the present work, radiation chemical method has helped in slow and *in-situ* release of selenium ion from sodium selenosulphate. The concentrations of pre-additives such as zinc salt, selenium source and ethylene diamine were optimized for obtaining good quality particles. The dose effect was studied by varying the dose from 7 kGy to 90 kGy. Selective quenching of luminescence of as-synthesized quantum dots (QDs) by Cu^{2+} ions vis-à-vis other physiologically relevant cations has been observed. The linear portion of the quenching plot due to Cu^{2+} ion on ZnSe nanoparticles can be used for determination of Cu^{2+} ions with detection limit in micro-molar range. The observed reduction confirms that the electron transfer takes place from nanoparticles rather than from associated liagnd.

Y. N. Rao, A. Datta, A. Saha; S. K. Das (VECC)

3.2.4 Nuclear structure

3.2.4.1 Novel methods for lifetime measurements using ultra low density backing

The Doppler effect is employed in several techniques for determining lifetimes of excited nuclear states. In most of these techniques the excited state of the nucleus is created in a nuclear reaction employing a unidirectional beam of at least several MeV and consequently the Doppler effect (depending on the lifetime of the level which is being de-excited by the gamma transition), will cause either a shift or shape of the emitted □-ray. Depending on the lifetimes of the states of interest, the aforesaid Doppler effect is implemented in Recoil Distance Method (RDM, for lifetimes ~ tens of picoseconds) or Doppler Shift Attenuation Method (DSAM, for lifetimes ~ hundreds of femtoseconds – one ps). States with lifetimes in the range ~ 1 to 10 picoseconds, thus, are at the limits of the conventional Doppler shift techniques.

A novel proposition of the nuclear physics group at Kolkata Centre was to use ultra-low density material as backing for the DSAM technique, thus increasing it's sensitivity to lifetimes in the range of 1 to 10 ps. This was hitherto impossible with heavy element (gold, lead, tantalum) backing typically used in conventional DSAM

experiments. Aerogel was chosen as the backing material for it's ultra-low density (~ 0.095 g/cm3) and commercial availability (procured from Aerogel Technologies, USA). The technique was applied for the first time in an experiment aimed at quest for tetrahedral band in ^{156}Dy, carried out at the Indian National Gamma Array (INGA), stationed at TIFR, Mumbai. Search for higher-order symmetries (tetrahedral, octahedral) is being zealously pursued in many of the contemporary nuclear structure endeavours, across the globe. In a recent experiment at GAMMASPHERE (ANL, USA), one of the bands in ^{156}Dy was observed to indicate the signatures of a tetrahedral band but required lifetime measurements, in the range of ~ tens of picoseconds, for confirmation of the same. These lifetimes, at the limits of the conventional RDM and DSAM practices, required the novel technique with aerogel backed target.

The ^{156}Dy nucleus was populated using the reaction ^{148}Nd(^{12}C,4*n*)^{156}Dy at $E_{lab.}$ = 60 MeV. The target was Nd_2O_3, enriched in ^{148}Nd, on Aerogel backing. This novel target was prepared by Kolkata Centre in collaboration with the target laboratory of IUAC, New Delhi at IUAC. Owing to the fragile nature of the aerogel material, particularly under pressure, it was housed in a protective perspex casing. The fabrication of the target using evaporation technique was then carried out with the aerogel in the housing, as illustrated in the adjacent figures. Further, the target was used in the in-beam experiment with the same housing arrangement preserved.

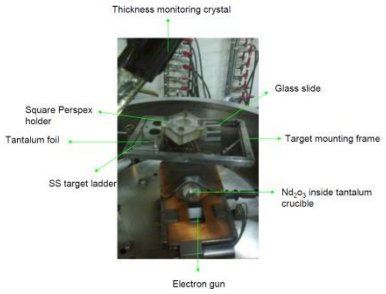

Mouting arrangements in the E-beam deposition unit at IUAC

Aerogel with the sample holder

Data analysis procedures are in progress to evaluate the results of implementing this novel target system. Apart from the reactions of the ^{12}C beam on ^{148}Nd target, the beam also reacted with the Si and oxygen components of the aerogel backing, thus populating a range of nuclei in the A ~ 20-40 region. Many of these nuclei have been extensively studied in the past and thus provided effective insight to validate this technique. For instance, the ^{38}Ar nucleus that was populated in the current experiment by reaction of ^{12}C beam on ^{28}Si component of aerogel backing. The same nucleus was also populated in one of the previous experiments of the Kolkata Centre at IUAC, New Delhi, with the reaction of ^{16}O beam on ^{27}Al target on ^{27}Al backing. The level structure of the nucleus has a 1 ps level de-exciting by 1823 keV transition. While with the Al backing in the previous (IUAC) experiment, the 1823 keV peak merely showed Doppler shapes in the angular spectra, with the aerogel medium used in the present experiment, the same peak was observed to exhibit complete Doppler shifts, indicating the sensitivity of the technique to lifetimes in this range. The corresponding spectra from two different experiments are shown in the adjacent figure.

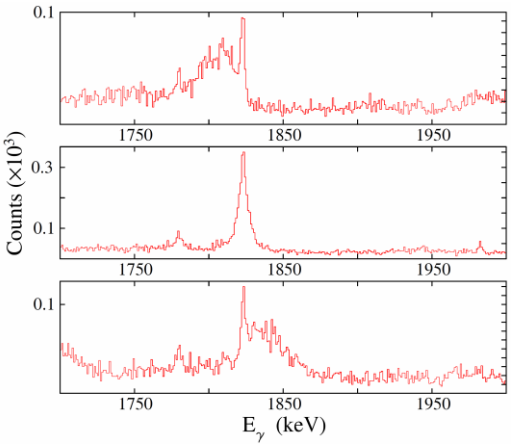

The 1823 keV peak from ^{38}Ar nucleus at backward angle (upper panel), 90^o (middle panel) and forward angle (lower panel), as observed in the experiment at IUAC, New Delhi.

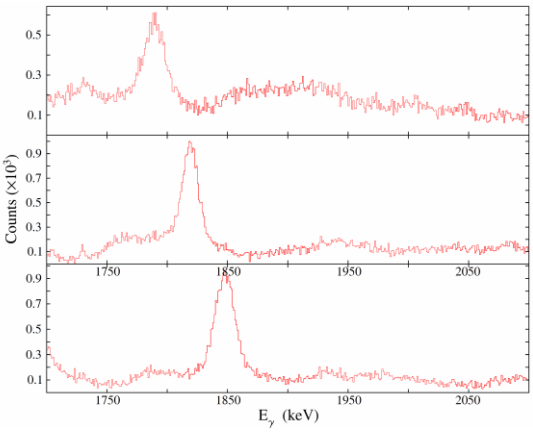

The 1823 keV peak from ^{38}Ar nucleus at backward angle (upper panel), 90^o (middle panel) and forward angle (lower panel), as observed in the experiment at TIFR, Mumbai.

The analysis is in progress to obtain quantitative estimates for the level lifetimes.

UGC-DAE CSR -KC, Guru Ghasidas Vishwavidalaya, Andhra University, University of Manchester, IUAC, BARC, TIFR

3.2.4.2 Spectroscopy of N ~ Z *sd-pf* Nuclei

Nuclei which belong to the interface of the *sd-pf* shells especially the *N* ~ *Z* nuclei are of contemporary interest as these nuclei nuclei belong to the transient region where the nuclear deformation is not well. The structure of these nuclei could be investigated within the framework of large basis shell model calculations involving the *fp* shells, whose occupation would favour deformed structures.

From this view-point it would be of interest to investigate the level structure of ^{26}Mg, ^{29}Si, ^{41}Ca *sd-pf* nuclei. Till date heavy-ion induced high resolution gamma spectroscopy measurements have not been attempted in these nuclei. The ^{13}C,^{16}O + ^{18}O,^{27}Al reactions at an incident energy of around 34 MeV were used to populate the high spin structures in these nuclei. The de-exciting gamma transitions were detected using the INGA. The use of INGA is optimized for such investigation primarily due to (i) the enhanced detection efficiency for E_γ > 1 MeV, and we expect the level structure of these nuclei to be dominated by such high energy gamma transitions; (ii) the detectors were placed at 148^o, 123^o, 90^o, 57^o and 32^o *w.r.t* the beam axis. This not only allowed us to obtain the lifetime of the levels using the conventional DSAM, but allowed us to identify fully shifted transitions in a consistent and conclusive manner; (iii) the use of clovers facilitated polarization measurements which are crucial to uniquely assign the electromagnetic nature of the transitions.

The data was sorted using the IUCSORT and RADWARE software, using the conventional angle dependent E_γ-E_γ matrices. Since the level lifetime of most of the levels of interest is less than the stopping time in the Ta backing, stopped component of the corresponding transition peaks were not observed. The angle dependent matrices were used to identify the fully shifted transitions. The situation for the 3157 keV , $^{11}/_{2}^{-} \rightarrow {}^{7}/_{2}^{-}$ transition belonging to ^{29}Si is depicted below :

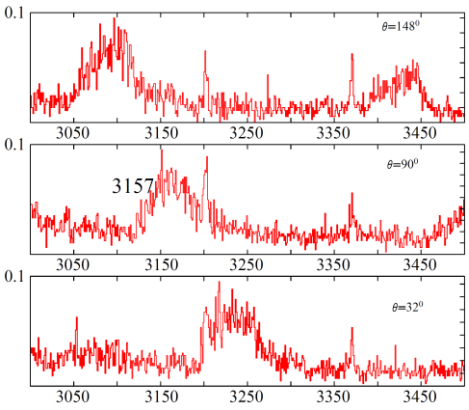

Representative angle dependent gated spectra illustrating the observed Doppler shifts in fast transitions.

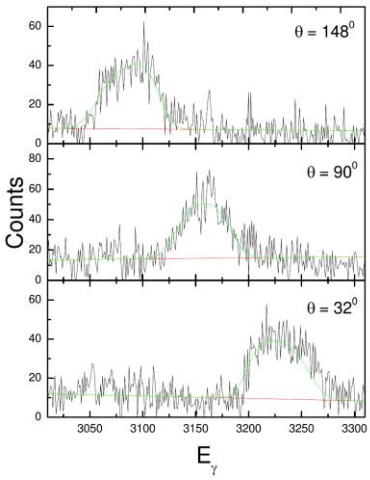

The spectra illustrates the γ-ray Doppler pattern for the 3157. The smooth line represents the calculated lineshape

The detailed analysis of these Doppler shifts/ shapes allow us to extract the level lifetime. A representative analysis of the observed Doppler pattern for the above transitions using the conventional code LINESHAPE is presented in the figure below.

The Clover detectors placed at 90^o w.r.t the beam-axis allow us to perform linear polarization measurements. The emission plane is defined by the beam-axis and the direction of initial γ-ray. If the incident γ-rays undergoes a Compton scettering, then it can be detected in the adjacent crystals of the same clover. These events are analyzed to compute the parallel and perpendicular (w.r.t the emission plane) scattered events, which is a signature of the electro-magentic nature of the transition, and we obtain the Polarization Asymmetry (Δ), which is defined as

$$\Delta = \frac{[a(E_\gamma)N_\perp] - N_\parallel}{[a(E_\gamma)N_\perp] - N_\parallel}$$

Where, $a(E_\gamma)$, is the normalization factor corresponding to the asymmetry of the array (INGA@TIFR), and is obtained from the radioactive sources.

The figure below depicts the energy dependence of this factor for the present INGA configuration (at TIFR).

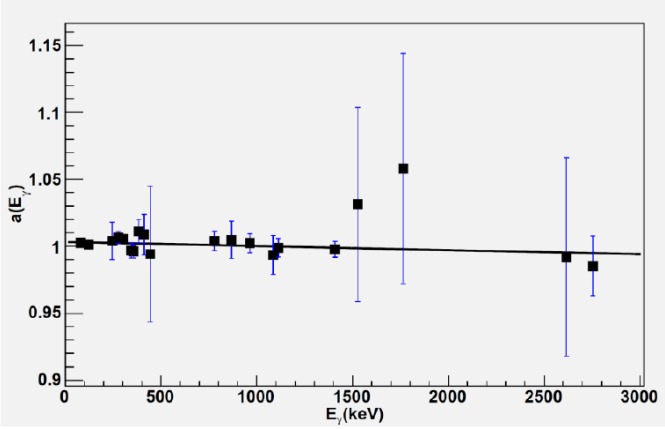

The normalization factor $a(E_\gamma)$ ploted as function of the γ-ray energy E_γ for INGA @ TIFR

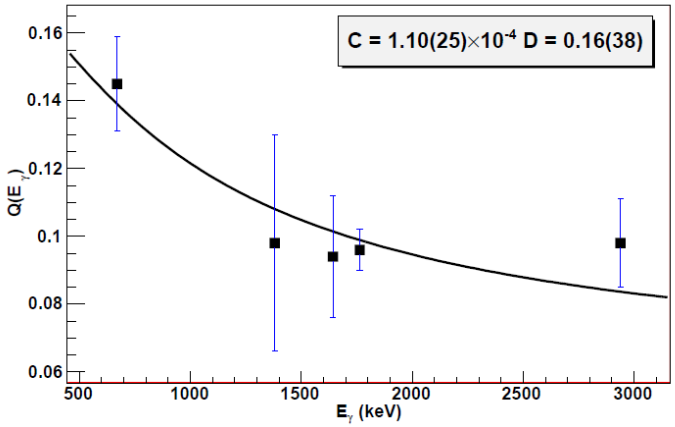

The Polarization sensitivity $(Q)$for the INGA @ TIFR. The solid line represents the fit to the present data

To polarization asymmetry is related to the polarization (P) and the polarization sensitivity (Q)as

$$P = \frac{\Delta}{Q}$$

The polarization sensitivity of the INGA @ TIFR is shown in the figure (b) above and has been determined up to Eγ ~ 3 MeV.

The polarization asymmetry is negative for pure magnetic transitions whereas a positive value indicates electric nature, whereas mixed transitions would have a near zero value of the polarization asymmetry. Hence, these measurements combined with the conventional coincidence intensity anisotropy allow us to unambiguously assign the multipolarity of the γ-transitions.

The level schemes of ^{26}Mg, ^{29}Si & ^{41}Ca have been developed and attempts are in progress to understand the observed structure within the framework of the theoretical nuclear models.

UGC-DAE CSR -KC, Guru Ghasidas Vishwavidalaya, Kota University, University of Notre Dame, IUAC, BARC, TIFR

3.2.4.3 Digital Pulse Processing Simulations in MATLAB® & OCTAVE for Nuclear Spectroscopy

Conventionally the output pulse from a radiation detector is processed by the front-end NIM based analog shaping & timing amplifiers followed by ADC and subsequent interfacing & storage protocols / systems. The interfacing protocol is an heabily dependent on the architecture of the data acquisition system. Recently novel systems based on the Digital Signal Processing concepts are been extensively used in in-beam experiments. These systems provide a compact and self-contained pulse-processing and histograming components. In DSP based systems, the pre-amplifier signal from the detector is directly digitized by a fast

flash ADC and is then processed completely in the digital domain. Thus allowing for a compete numerical analysis of the detector pulse signals & the numerical algorithms replace conventional pulse circuitry.

The current work investigates the different used for pulse shaping in DSP systems. A digital pulse processor computes the pulse height from the detector data sampled by a fast & high-resolution ADC. The post-processing setup involves streaming of the sampled ADC data into real-time processors usually implemented in FPGAs. The pulse is then processed by recursive algorithms which shape the pulse for an optimum S/N ratio.

Recursive algorithms (for Trapezoidal, Triangular, Gausain shaping) have been developed using the MATLAB® and OCTAVE as the numerical computing environment under the Windows and LINUX operating systems and have been tested on simulated pre-amplifier pulses. It has been established that the Trapezoidal shaping has an advantage that it circumvents the loss in resolution due to ballistic deficits, provided the time duration of the flat top must be long enough to accommodate the rise time variations, the results of the present simulations are depicted in the figure below

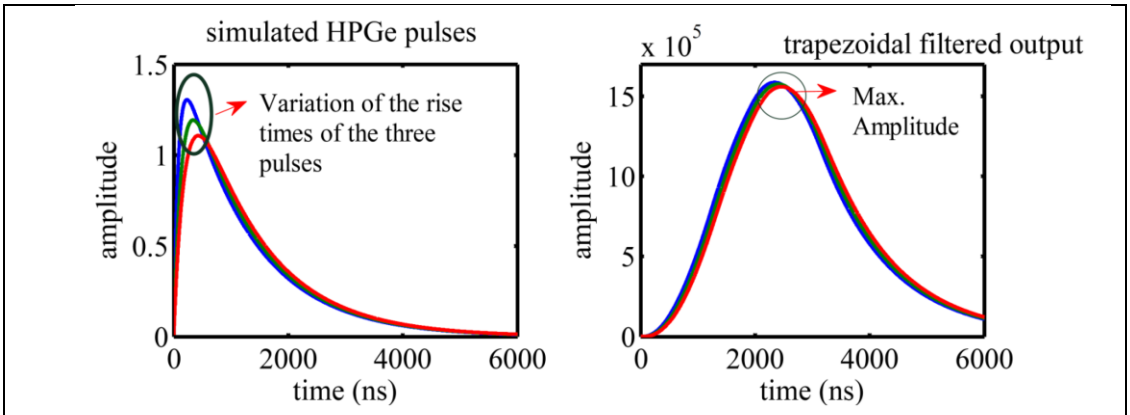

Trapezoidal shaping for removal of ballistic deficit

The simulations then were modified to (i) include the effect of noise in the pre-amplifier pulse (ii) the influence of the sampling frequency on the preservation of the pluse characteristics. Efforts are in progress to extend the simulations for obtaining the time information from these pulses *i.e* development of digital CFD algorithms are in progress.

UGC-DAE CSR, KC, Jadavpur University

3.2.5 Radiation biology

3.2.5.1 Study on high fat diet induced stress

To evaluate the High fat diet induced oxidative stress and protection by different compounds. Chiefly Mitochondrial Membrane Potential change in metabolic condition was evaluated.

Anindita Chakraborty; Sanjit Dey (Univeristy of Calcutta)

3.2.5.2 Study on radioprotective efficacy of various compounds

To evaluate the radioprotective efficacy of quercetin, ferulic acid, naringin, coconut water concentrates. The Red blood cells were used for differential change of fluorescence pattern after radiation and treatment of quercetin.

Effect of quercetin on the gamma radiation mediated intracellular ROS level. 10µl of erythrocytes (5×106) were incubated with PBS with saturating concentration of DCFDA (1 µg/ml) in the dark for 30 minutes at room temperature. The DCFDA fluorescence signal was detected using 480 nm excitation and 530 nm emission light. For each sample, auto fluorescence signal of unstained erythrocytes were measured and used to adjust the fluorescence intensity of DCFDA stained erythrocytes. Data were analyzed using FlowJO software (version7.6.5). Analysis of FL-1fluorescence was performed with gating on the total unstained RBC population to identify the live RBC population (46.6%). Same gate was used for all the samples to measure the FL-1 fluorescence intensity. A. Represents the Side scatter versus Forward scatter plot of the total population. B. Represents the level of fluorescence of individual group. C. It represents the statistical comparison of four different group for three individual experiments (Error bars are SEM and n=3)

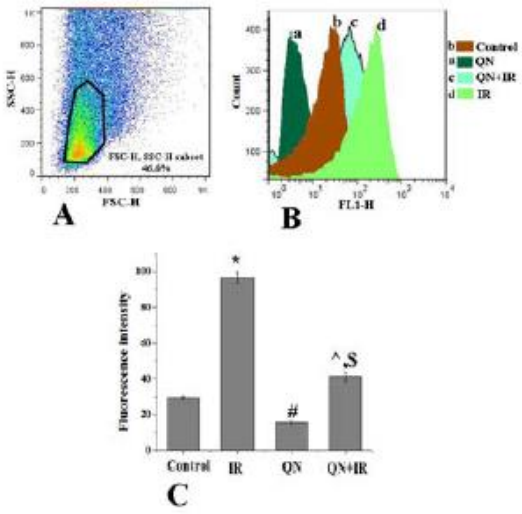

Dipanwita Mukherjee, Anindita Chakraborty; Dipesh K. Das, Anirban Chakraborty, Mahuya Sinha, Krishnendu Manna, Sekhar Bhattacharjee, Sanjit Dey (Calcutta University)

3.2.5.3 *Effect of environmental carcinogens on some aspects of cytoskeletal integrity*

Hepatocellular carcinoma (HCC) is an intractable disease with an extremely high mortality rate. Recurrence and metastasis are commonly associated with poor prognosis of hepatocellular carcinoma. Unfortunately, no promising curative therapy for HCC metastasis is available as yet; therefore, treatment for advanced HCC still remains a formidable challenge. As such, there is a need to make deeper understanding of the process of development of hepatocellular carcinoma, so as to elucidate biomarkers for its early detection. Although large body of evidence has demonstrated importance of RhoGTPases/Rho-effector pathway in metastasis development via orchestrating the cell cytoskeletal reorganization, role of RhoA in early tumorigenesis has not yet been unraveled. The objective of the present work is to study whether cytoskeleton experiences any detectable transformation at a very early phase of chemically induced hepatocellular carcinoma. Swiss Albino mice (age - 3-4 weeks) were chosen as the animal models. These mice were exposed to chemical carcinogens *p*-DAB (0.06%, administered orally, 165mg/kg bw/mouse/day) and DENA (injected intraperitoneally, single dose, 200mg/kg). Animals sacrificed at the initiation stage 5-6 weeks after onset of the carcinogen exposure were taken up to study cytoskeletal integrities.

Whole cell extract of liver tissue was prepared with the help of radioimmunoprecipitation assay (RIPA) buffer (0.1% sodium dodecyl sulfate, 0.5% deoxycholic acid, 1% Igepal, 150 mM NaCl and 50 mM Tris-HCl). To prepare the cytosolic fraction, liver was sonicated (Sonicator- Omni-Ruptor 4000) using tissue homogenization buffer (50mM Tris-HCl [pH 8], 10 mM KCl, 1 mM EDTA disodium salt, 0.2% nonyl phenoxylpolyethoxylethanol, 10% glycerol, and 1 µg/mL each of leupeptin and aprotinin in distilled water) and centrifuged using cold centrifuge (SORVALL RC6 PLUS) to separate cytosolic fraction. Protein concentration was determined by the method of Lowry *et al*., (1951). Equal amounts of protein (50 µg) in each lane were subjected to 10% sodium dodecyl sulfate-polyacrylamide gel electrophoresis and transferred to a nitrocellulose membrane. The membrane was blocked with 3% bovine serum albumin solution and kept overnight at 4ºC. Immunoblotting was done using monoclonal antibody to mouse NF-κB (p65), RhoA, and Cdc42. β-Actin was used as loading control for cytosolic extracts. Immunoblots were imaged by Gel Doc (G: BOX, Syngene) and the images were analyzed using Quantity One software (Bio-Rad Laboratories, Hercules, CA, USA).

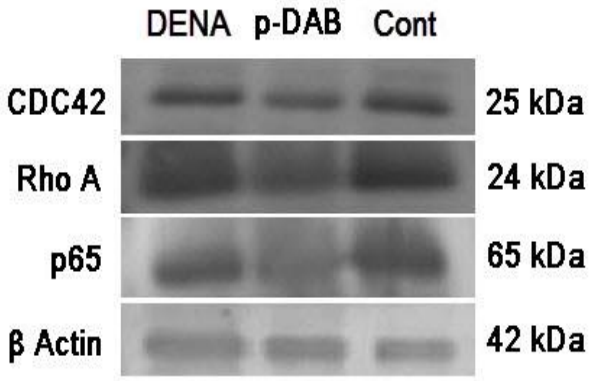

Fig. 1 Expression pattern of cytoskeletal regulatory proteins by westernblotting

Fig. 1 highlights down-regulation of cdc42, RhoA, and p65 expression in both the carcinogen treated groups when compared to their normal counterparts. Considerable negative induction is noted in p65 expression of *p*-DAB treated groups with respect to that of the control. Expression patterns of cdc42, RhoA in *p*-DAB treated groups also exhibit similar trend showing appreciable down regulation of these two marker proteins with respect to the normal counterparts. In DENA treated groups although significant down regulation of p65 expression is evident with respect to that of the control, there is no significant change of expression of cdc42 and RhoA with respect to the expression of these proteins found in the control group.

Present data reflect distortion of the cytoskeleton commences at the very early initiation phase of hepatic cancer. Our findings reflect involvement of cytoskeleton transformation is initiated from a very early stage of carcinogenic development rather than only at a later stage of metastasis.

Dipanwita Mukherjee, Anindita Chakraborty

3.3 In-house research activities at Mumbai centre

3.3.1 Neutron scattering studies

3.3.1.1 Structure-Property Correlation for the Intermediate Anti-Ferroelectric Ordering in $Na_{0.5}Bi_{0.5}TiO_3$ system – Support from Neutron Diffraction Study

$Na_{0.5}Bi_{0.5}TiO_3$ (NBT) is one among the promising lead-free ferro/piezo-electric material, which is being exploited more in the recent years for suitable device applications. Interestingly, NBT has several high temperature phase transitions with one among them, is the intermediate anti-ferroelectric (AFE) transition around 200°C. At room temperature it stabilizes in *R*3*c* symmetry with anti-phase ($a^-a^-a^-$) tilted TiO_6 octahedra. However, for strong application point of view long range ferroelectric (FE) ordering over a wide range of temperature is more favorable. In this context, the aim of this present study is to understand the nature of AFE ordering in NBT system. In view of this scenario, we have synthesized NBT through conventional solid state reaction technique.

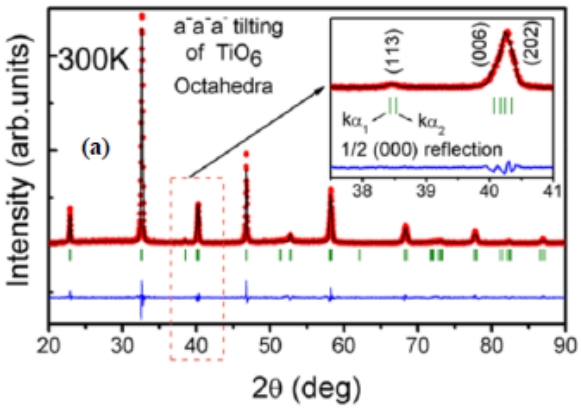

Room temperature x-ray diffraction pattern.

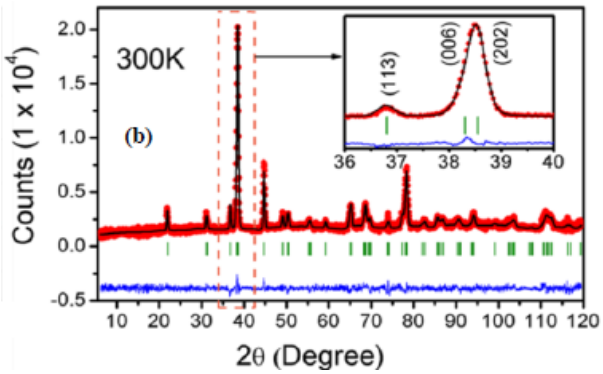

Room temperature neutron diffraction pattern measured on PD-III (FCD) at Dhruva using a wavelength of 1.48Å.

X-ray diffraction analysis reveals single phase characteristics with weak Bragg reflection around $2\theta \cong 38.5^o$ indicates the ½(000) [i.e., (113)] super-lattice (SL) reflection corresponding to a-a-a- tilting of TiO6 octahedra (see inset of Fig.(a)). In order to exactly determine the octahedral tilt angle and verify the SL reflection, Neutron diffraction (ND) experiment was performed at Dhruva Centre. ND experiment also confirmed the single phase characteristics of NBT and existence of SL reflection (see inset of Fig. (b)). Further, the octahedral tilt angle ($\omega° = 8.38$) determined from ND is found very close to that from X-ray diffraction measurements (i.e., $\omega° = 7.39$). This paved us to perform the high temperature (HT)-XRD measurements to estimate the variation of ω° angle with temperature and correlated them with HT-Raman, Impedance results and also along with the observed AFE ordering from HT- P vs. E measurements.

S. Rayaprol and V. Siruguri; T. Karthik, Saket Asthana (IIT-Hyderabad),

3.3.1.2 Neutron Diffraction Evidence for Reentrant Transition in a Magnetic Shape Memory Alloy using CHUF Protocol

Neutron diffraction in presence of an external magnetic field is employed to illustrate structural evidence for the kinetic arrest of the first-order phase transition from the high temperature austenite phase to the low temperature martensite phase in the magnetic shape memory alloy $Ni_{37}Co_{11}Mn_{42.5}Sn_{9.5}$ and the formation of a glass-like arrested state (GLAS). The CHUF (cooling and heating under unequal fields) protocol has been used to establish phase coexistence of metastable and equilibrium states of GLAS in the neutron diffraction patterns.

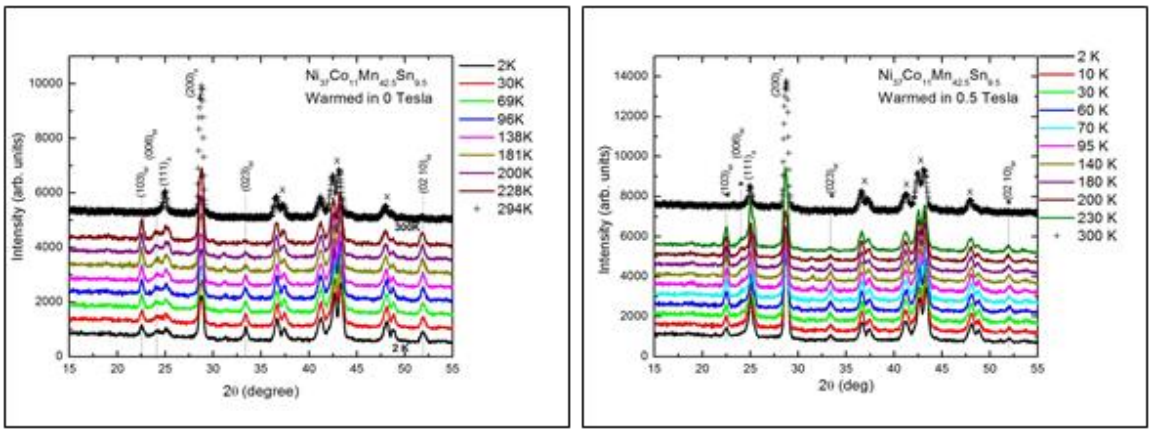

(left) Neutron diffraction patterns as a function of temperature. Indices with subscript 'A' belong to the austenite phase while those with subscript 'M' belong to the 10M martensite phase. Peaks in the regions marked as 'X' are contributions from the magnet shroud. Patterns have been offset for clarity. (right) Neutron diffraction patterns obtained using the CHUF protocol. The sample was cooled from 300 K to 2 K in a field of 7 Tesla which is isothermally reduced to 0.5 T. Data were taken in the warming cycle.

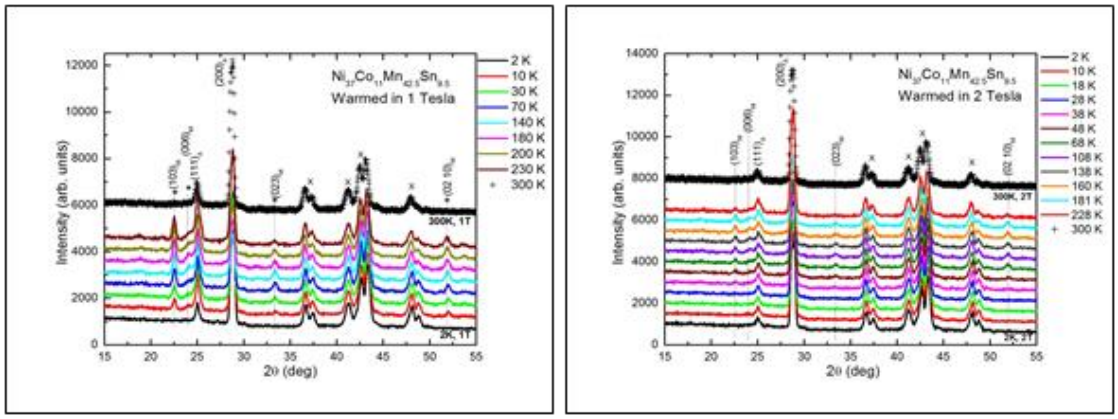

Neutron diffraction patterns obtained using the CHUF protocol. The sample was cooled from 300 K to 2 K in a field of 7 Tesla which is isothermally reduced to 1T (left figure) 2.0 T (right figure). Data were taken in the warming cycle.

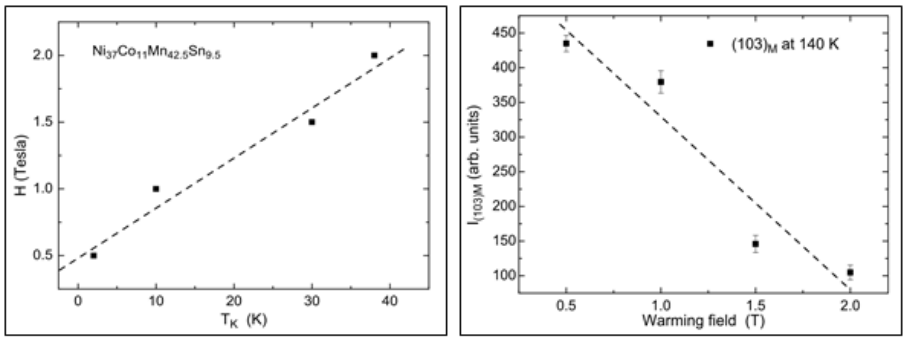

H-T diagram showing the kinetic arrest line across which there would be a devitrification from the arrested metastable austenite phase to the equilibrium martensite phase during warming cycle. Integrated intensity of the (103) reflection of the 10M martensite phase as a function of the warming field at 140 K.

V. Siruguri, S. D. Kaushik, P. D. Babu, P. Chaddah, Aniruddha Biswas, S. K. Sarkar, Madangopal Krishnan (BARC)

3.3.1.3 Structure and Magnetism of Bixbyite $FeMnO_3$ Prepared by Mechanochemical Synthesis Method

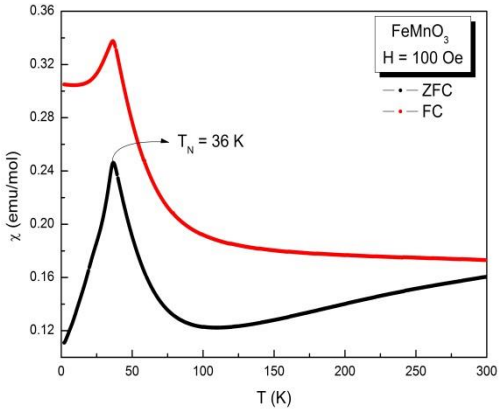

Low field magnetic susceptibility plot for $FeMnO_3$. The ZFC-FC bifurcation in the entire temperature range of measurement, indicate strong magnetic anisotropy in this compound.

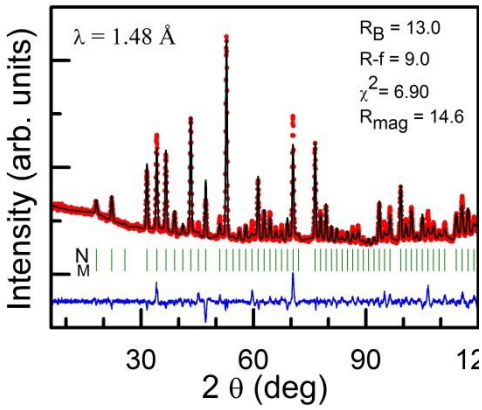

Rietveld refinement of neutron diffraction data taken at T = 300K. The two rows of vertical tick marks indicate nuclear and magnetic Bragg peak positions.

The compound $FeMnO_3$ has been prepared by mechanochemical synthesis using a high energy ball mill. The structure and magnetism have been studied using powder neutron diffraction and magnetization measurements. The compound crystallizes in the mineral bixbyite structure. The structure comprises of two Wyckoff sites, 8*b* and 24*d*, which are populated by both Fe and Mn in equal proportions. Oxygen ions are found at 48*e* site. Magnetization measurements exhibits ferrimagnetism at 300 K and antiferromagnetic (T_N) ordering around 36 K. Magnetic structure has been determined from the Rietveld analysis of the neutron

diffraction pattern recorded at 300 K. Interaction between Fe and Mn atoms is antiferromagnetic. The ferrimagnetism is believed to arise from the anti-parallel alignment of unequal moments of Fe and Mn ions at both 8*b* and 24*d* sites respectively.

The magnetic structure of $FeMnO_3$ was refined assuming 16 pairs of Fe-Mn depending upon the symmetry positions. The structure was refined using a propagation vector, k = [0 0 0]. The Fe and Mn site moments (in μ_B) obtained from the refinement are 2.48 (-1.0) per Fe(Mn) at 8*b* and 3.97 (-3.01) per Fe(Mn) at 24*d* sites, respectively. The negative sign on Mn moments indicates that Fe and Mn moments are coupled antiferromagnetically. Detailed low temperature neutron diffraction and other physical property studies on this novel compound are currently underway.

S. Rayaprol, S. D. Kaushik, P. D. Babu, and V. Siruguri

3.3.1.4 emperature Dependent Neutron Diffraction of Magneto-Dielectric $GaFeO_3$.

Temperature dependent neutron diffraction (2–290 K) measurement are carried out on polycrystalline magnetoelectric $GaFeO_3$. From the neutron diffraction data, evidence for the magnetostriction and increased disorder at Fe sites close to the ferrimagnetic Curie transition temperature (T_C) is observed. In addition to it from Mossbauer data, it is observed that the Lamb–Mossbauer factor as a function of temperature, which is related to the integral over the first Brillouin zone of the phonon spectrum, shows an unequivocal variation at the T_C. The observations are discussed in terms of spin–phonon coupling.

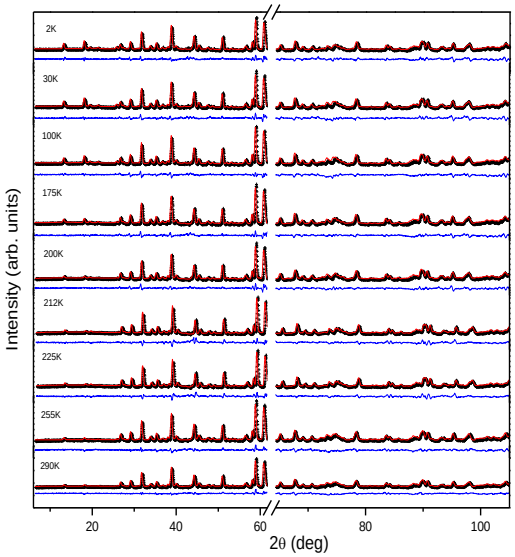

Recorded low-temperature (2–290 K) ND patterns are shown. As the temperature is reduced ($T < T_C$) and ferromagnetic ordering sets in the sample, enhancement in the intensity of (110), (020), (101) and (111) peaks at 2 positions of 13.2^0, 18.1^0, 19.4^0 and 21.3^0 respectively are observed. The diffraction patterns are fitted with Rietveld refinement, considering the orthorhombic structure with space group $Pc2_1n$ for the estimation of various parameters

K. Sharma, V. R. Reddy, A. Gupta, S. D. Kaushik, and V. Siruguri

3.3.1.5 Low temperature Neutron Diffraction Studies on Nanocrystalline $CoCr_2O_4$

Neutron diffraction studies were carried out on nanocrystalline $CoCr_2O_4$ at various temperatures across its magnetic ordering temperature. In Fig. 3.15 neutron diffraction patterns of CoCr2O4 measured at lowest (T = 2.7 K) and highest (room temperature) temperatures are shown. At the lowest temperature, magnetic structure has also been refined. Detailed analysis of the neutron diffraction data is currently under progress.

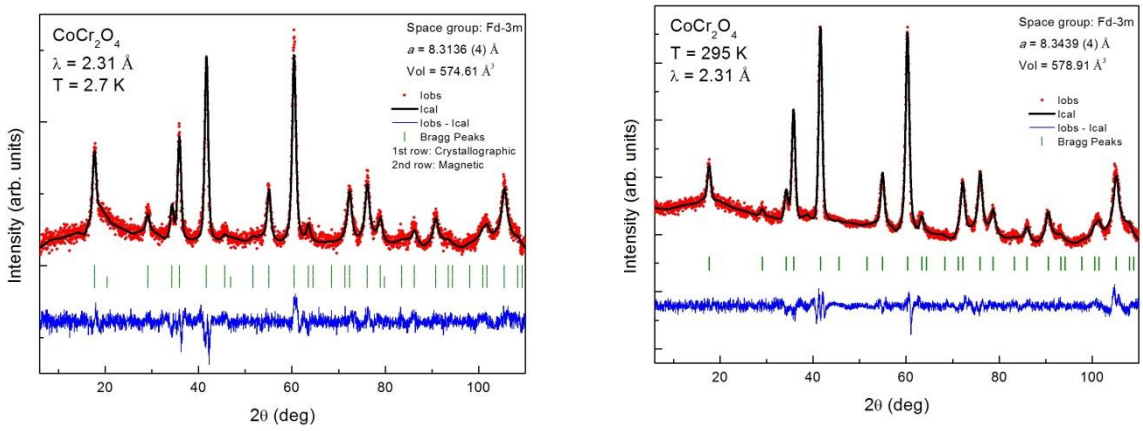

Neutron diffraction pattern for nanocrystalline $CoCr_2O_4$ measured at (a) T = 2.7 K and (b) T = 295 K.

S. Rayaprol, V. Siruguri;C. Rath (IT-BHU),

3.3.1.6 Neutron Diffraction Studies on $Ho_{1-x}Y_xMnO_3$ ($0 \leq x \leq 0.75$)

Hexagonal $HoMnO_3$ is one of the intensively researched multiferroic compounds among the *R*MnO_3 family due to intriguing physics lying behind the complex magnetic phase diagram. $HoMnO_3$ exhibits multiple orderings at around 70, 45 and 25 K due to magnetic ordering of Mn sub-lattice, Mn spin reorientation and coupling between Ho and Mn spins, respectively. The interaction between Ho and Mn is more pronounced at ~ 5 K due to ordering of Ho spins also. These complex magnetic orderings affect the evolution of ferroelectricity, which broadly originates from the buckling of Ho layer and tilting of the MnO_5 polyhedra, similar to that in observed in hexagonal $YMnO_3$.

We have undertaken a systematic study to understand the role of magnetic Ho layer in inducing ferroelectric property in $HoMnO_3$. Recent low temperature magneto-dielectric, magnetization and specific heat study shows that the frustration in $HoMnO_3$ is released by substituting Y at Ho site. To this effect, a series of compounds have been prepared by partially replacing magnetic Ho^{3+} by non-magnetic Y^{3+} ion in the stoichiometric form, $Ho_{1-x}Y_xMnO_3$. In the present work, we present and discuss results of neutron diffraction experiments carried out at low temperatures. The following figure show the neutron diffraction patterns recorded at T = 15 K. It is known from the literature that at this temperature Ho is not completely ordered, but there is coupling between Ho and Mn ions. From the Rietveld analysis of the ND data we observed that with increasing Y substitution, Mn moment decreases consistently, which can be attributed to the decrease in the coupling of Mn with Ho ion due to partial replacement of Ho by Y.

The variation observed in bond angles and bond lengths can be understood in terms of modification in the tilting angle of MnO_5 polyhedra. Since the tilting of MnO_5 polyhedra is known to affect the ferroelectric properties, the present study provides an insight in to the ferroelectric properties in $HoMnO_3$.

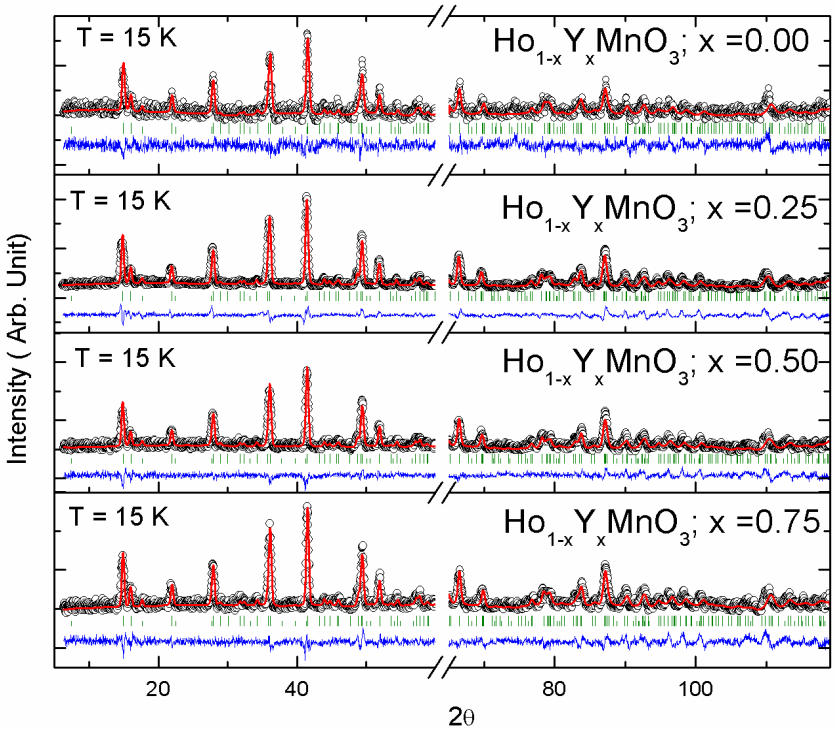

Rietveld refined neutron diffraction patterns of $Ho_{1-x}Y_xMnO_3$ (x = 0 - 0.75) at 15 K. The break in the pattern at 2□ ~ 60-65 is due to background from cryogen free magnet

S. D. Kaushik, S. Rayaprol and V. Siruguri

3.3.1.7 Low Temperature Neutron Diffraction Studies on $YMn_{1-x}Fe_xO_3$ (x = 0.0, 0.05, 0.10)

In multiferroic hexagonal YMnO3, Mn plays significant role as buckling in the MnO5 polyhedra pave the way of geometrical frustration which give rise to ferroelectricity in the compound. In order to see the effect diversifying the magnetic ion on multiferroic properties, hexagonal YMnO3 samples with 0, 5 and 10% Fe doping at Mn site were prepared. Low temperature Neutron diffraction experiments were carried out on YMn1-xFexO3 (x = 0, 0.05, 0.10). Observed pattern is fitted with single phase in Rietveld refinement which indicates the phase purity of the sample. It also signifies the solubility of the 10% Fe in $YMnO_3$. Magnetic structure was analyzed as secondary phase.

On carefully analyzing the low temperature ND pattern, it is observed that weightage of prominent magnetic peak (010, 100) at ~ 16.04 in pure $YMnO_3$ gets systematically transferred to (011, 101) at ~17.67 degree with respect to Fe doping at Mn site. This indicates about the modification in the spin structure. We are in process of analyzing the data to ascertain this fact, and also want to evaluate that how this modified spin structure affects the magnetic properties of this compound.

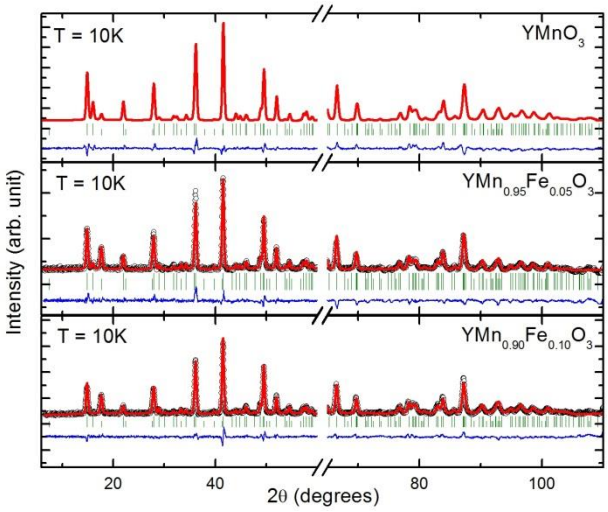

Rietveld refined neutron diffractio patterns of $Ho_{1-x}Y_xMnO_3$ (x = 0 0.75) at 15 K. The break in th pattern at 2θ ~ 60-65 is due t background from cryogen fre magnet

S. Namdeo, A. M. Awasthi, S. D. Kaushik, and V. Siruguri

3.3.1.8 Study of Influence of Doping on the Physical Properties of $CoCr_2O_4$ Bulk Samples

A series of polycrystalline sample with partial substitution of Cr by Fe has been prepared and studied for its structural properties by neutron diffraction using a wavelength of 2.31Å. Our primary objective is to study the influence of iron substitution for chromium on the magnetism and magneto-dielectric properties of $CoCr_2O_4$. In the following Fig. 3.23, room temperature neutron diffraction pattern for Fe doped samples is shown. We plan to carry out detailed low temperature neutron diffraction experiments on these samples. We also plan to carry out other physical property measurements which will be complimentary to neutron diffraction studies.

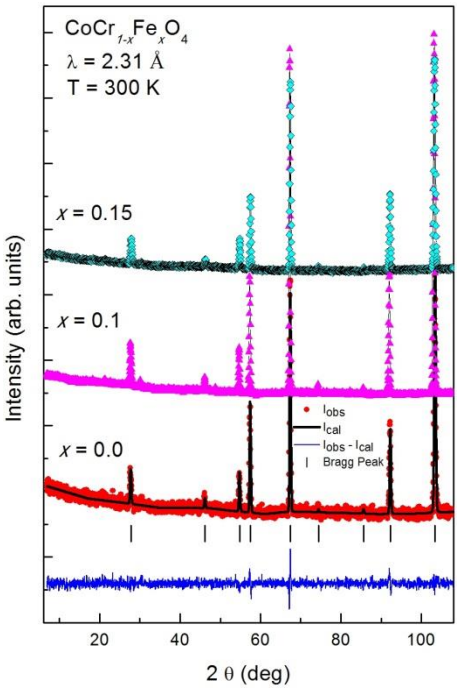

Fig. *Rietveld refinement of undoped polycrystalline sample of $CoCr_2O_4$ is shown. The raw data of Fe doped (x = 0.1 and 0.15) samples are also plotted*

S. Rayaprol,V. Siruguri; Dilip Pal, P. Rajender (IIT-Guwahati),

3.3.1.9 Low Temperature Neutron Diffraction Study of $Nd_{1-x}Sr_xCrO_3$ ($0.05 \leq x \leq 0.15$)

Low temperature magnetic structure of Sr substituted $NdCrO_3$ has been investigated using neutron diffraction in the temperature range of 2 K to 300 K. Rietveld analysis of neutron diffraction patterns led us to conclude that the Cr moments have a G_y type of alignment of spins while the Nd moments align in a $-C_z$ type fashion for all three samples. The weighted average $Cr^{3+/4+}$ ions moments were 3.19(7), 2.77(3)and 2.57(7) μ_B close to its theoretical Cr^{3+} moment value namely $3\mu_B$ at 2 K for the x = 0.05, 0.1 and 0.15 samples respectively. While the Nd^{3+}moments for the three samples at 2K were 3.0(1), 2.39(8) and 2.2(2), respectively.

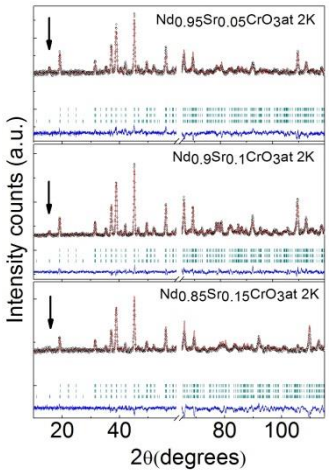

Rietveld fitted Neutron diffraction patterns, for the x = 0.05, 0.1 and 0.15 sample at 2 K

Keka R. Chakraborty (SSPD, BARC), S. Mukherjee, A. K. Tyagi (Chemistry Division, BARC), C. L. Prajapat, M. R. Singh (TPD, BARC), S. D. Kaushik, S. Rayaprol and V. Siruguri

3.3.1.10 Magnetic Structure of the exotic intermetallic compound, Nd_7Rh_3

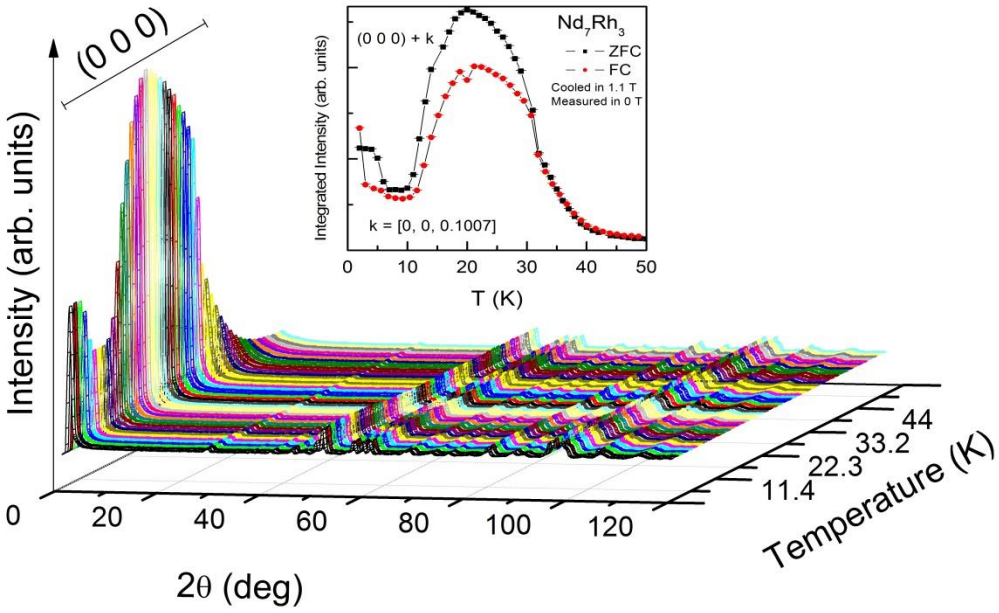

Fig. *Neutron diffraction patterns of Nd_7Rh_3 measured at various temperatures across its magnetic ordering temperatures (T_{N1} = 32 K, T_{N2} = 16K). At lower angles (~ $2\theta = 2.3^o$) the evolution of magnetic peak across T_N can be clearly seen. The inset exhibits the variation of the integrated intensity of the first magnetic peak at Q = 0.1$Å^{-1}$.*

Following our previous experiments at FCD-Dhruva and HZB-Berlin, we extended our studies on Nd_7Rh_3 to explore the magnetic structure of Nd_7Rh_3 by accessing low-Q range using D1B at ILL, Grenoble. The strong antiferromagnetic peak could be observed at Q value of 0.1$Å^{-1}$. Magnetic structure of Nd_7Rh_3 has been derived by refining the magnetic part of the neutron diffraction profile. In Fig. 3.21, the thermal evolution of the antiferromagnetic peak is shown. Detailed analysis of the neutron diffraction obtained at ILL are currently under progress.

S. Rayaprol, V. Siruguri; E. V. Sampathkumaran (TIFR, Mumbai), Andreas Hoser (HZB, Berlin), C. Ritter (ILL, Grenoble)

3.3.2 X-ray diffraction

3.3.2.1Exchange Bias in Ball Milled $LaFeO_3$

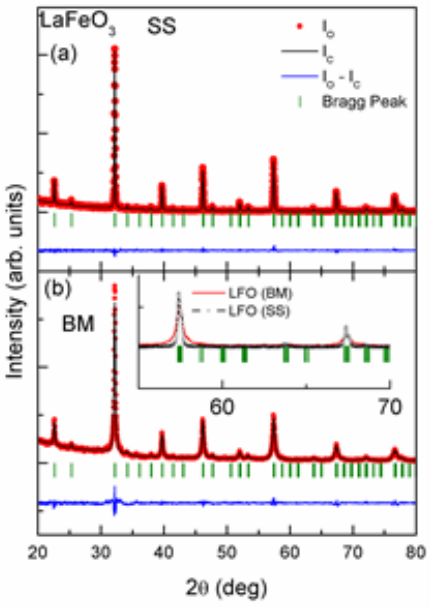

Rietveld fitted XRD pattern for bulk and ball milled samples. The refinement shows that sample crystallize in an orthorhombic structure, space group Pbnm. The unit cell parameter were found to be a = 5.5551 Å (5.5559 Å), b = 5.5622 Å (5.5626 Å), c = 7.8519 Å (7.8535 Å) for bulk and (Ball milled) sample, thus implying that ball-milling does not change cell dimensions. However, the XRD reflections for Ball milled sample are broadened thus indicating the reduced grain size in Ball milled sample which is turns out to be 34 nm.

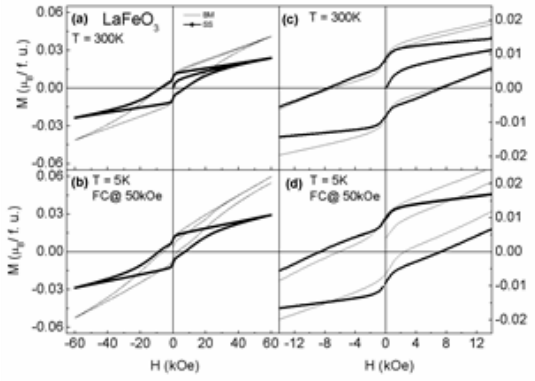

M-H loops of LaFeO3 (bulk and ball milled sample) at (a) 300K, (b) 5K after FC in 50kOe and (c) and (d) shows the enlarged part of M-H XRD patterns for (a) bulk and (b) Ball milled sample.

$LaFeO_3$ has an orthorhombic distorted perovskite structure which orders antiferromagnetically in G type canted magnetic structure (T_N = 750K). In the structure, Fe^{3+} ion is surrounded by six O^{2-} ions thus forming a FeO_6 octahedron while La^{3+} ions are inserted between these octahedra. Non-stoichiometry of oxygen in $LaFeO_3$ results in the mixed valence iron such as Fe^{2+}/Fe^{3+}. Oxygen non-stoichiometry strongly influences the physical properties. Therefore, the structure, properties and potential applications are strongly dependent on the sample preparation method. In some recent reports, *exchange bias* was observed in $LaFeO_3$ nano particles which gives another dimension to technological applicability of $LaFeO_3$ and offers understanding of the fascinating physics behind the existence of this phenomenon. We synthesized bulk polycrystalline (bulk) sample of $LaFeO_3$ from solid state reaction and nanocrystalline sample by high energy ball milling. Room temperature structural properties of both the samples were studied by using X-ray diffraction (XRD). Magnetic measurements were carried out using Quantum Design make physical property measurement system based vibrating sample magnetometer.

Magnetization measurements were carried out using powders of both samples. The magnetic susceptibility curves for both bulk and Ball milled samples in the range 2-350 K are qualitatively similar to the reported ones. Fig. 3.19 shows the magnetic hysteresis loops measured at 300K and at 5K after cooling the samples in a field of 50 kOe. For more clarity, the adjacent figure shows the enlarged view of central part of the loops. Magnetization does not saturate up to 60 kOe in all cases, however the hysteresis loop at 300 K in Ball milled sample closes at a field higher than compared to the one observed in bulk sample. At T = 5K, in the case of bulk sample, the loop does not merge up to 60 kOe. On careful observation of Fig. 3.20 (d), which shows the field cooled hysteresis loop for ball milled sample, we see a shift in origin of the loop by ~1850 Oe at 5K. The shift is calculated from coercive field values. This shift of origin of M-H loops is indicative of exchange bias in ball milled sample. The value of exchange bias obtained is more than the reported value of 1550 Oe for 40-45 nm particle size of LaFeO3 sample prepared by sol-gel method.

S. D. Kaushik, S. Rayaprol, P. D. Babu and V. Siruguri

3.3.3 Dielectric studies

3.3.3.1 Size-dependent dielectric properties of nanocrystalline $CoFe_2O_4$

The dielectric properties of nanocrystalline $CoFe_2O_4$ compound synthesized by gel-combustion with two different crystallite sizes - 6nm and 50nm- were studied over 130K to 293K. At 100Hz, the observed relative permittivity for the 50 nm sample was found to increase from 20 at 163K to about 300 at 293K, while for the of 6 nm sample, it was found to increase to about 6000 at 293K. The *dc* conductivity, extracted from the experimentally observed ac conductivity data, was also larger in the 6nm sample by an order of magnitude. Conduction was fond to be due to polarons obeying the Mott variable-range hopping (VRH) behavior. The presence of Co^{2+} and Fe^{3+} in the octahedral sites in $CoFe_2O_4$ may lead to the formation of the polarons. The larger dc conductivity in 6 mm sample across all temperatures studied, suggests that polaron creation may be much easier in the nanocrystalline phase. It appears that the dielectric properties and dc conductivity have a significant dependence on crystallite size in this material.

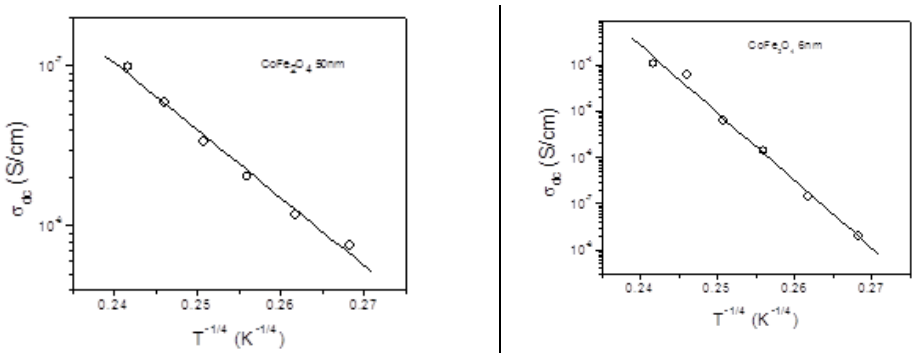

Temperature-dependent dc conductivity of (a) 50nm and (b) 6nm $CoFe_2O_4$ samples. Solid lines are fit to the data according to the Mott VRH relationship.

S. K. Deshpande; S. N. Achary (Chemistry Division, BARC)

3.3.3.2 Dielectric relaxation study of 2-D confined water in saponite clay

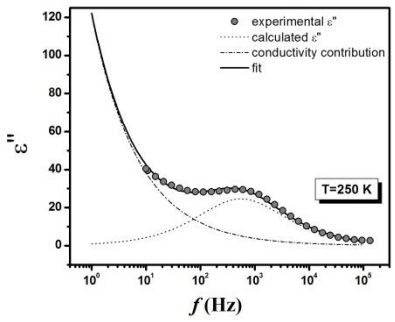

Dielectric response (ε'' (f)) vs. f) for hydrated clay at 250 K. The solid line represents the fit to the response using sum of power law and HN function; dotted and dash-dot curves represent the main relaxation process and conductivity contribution, respectively.

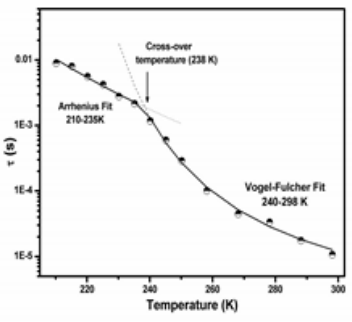

Temperature dependence of relaxation time (τ) for the main relaxation process in hydrated saponite clay, fitted to Arrhenius (210-235 K) and Vogel-Fulcher (240-300 K) functions.

Dielectric studies on saponite clay powder samples, containing water confined between the aluminosilicate layers in the clay structure, were carried out over 10 Hz to 1 MHz at several temperatures between 190-298 K. Analysis of the dielectric relaxation peak, attributed to interfacial polarization involving the confined water molecules, reveals a strong temperature dependence of the relaxation time. The dynamics of the confined water molecules show a cross-over from non-Arrhenius to Arrhenius behavior near 240K, indicating a transition. Our results suggest that substantial amount of liquid water exists above 240K, and the cross-over is related to the partial freezing of confined water.

S. K. Deshpande; P. K. Pujari (RCD, BARC)

3.3.3.3 Dielectric response of Fe-doped $BaTiO_3$

Dielectric measurements were carried out on $BaTiO_3$ samples with 5%, 8% and 20% Fe doping at the Ti site. The measurements were done over a frequency range of 100 Hz to 5 MHz at several temperatures while heating from room temperature to 300C (573K). While normal ferroelectric behavior was found to be retained even at 5% Fe doping, a relaxor-like response with large permittivity was seen in the 20% Fe-doped sample, with Vogel-Fulcher behavior of the relaxation frequency.

S. K. Deshpande; A. K. Tyagi (Chemistry Division BARC)

In addition to these studies, dielectric measurements were carried out on $BaFe_{12-x}Cu_xTi_xO_{19}$ (x = 1, 1.5, 2) ferrites (*V. V. Soman, Priyadarshini College of Engineering, Nagpur);* $La_{1-x}Bi_xMnO_3$ (x = 0, 0.1, 0.2, 0.3, 0.4, 0.5, 0.6) (*V. Dayal, Maharaja Institute of Technology, Mysore);* $Pb(Fe_{0.67}W_{0.33})O_3$+$Pb(Fe_{0.5}Nb_{0.5})O_3$ solid solutions (*B. Angadi,(Bangalore University, Bangalore);* Multiferroic $CaMn_7O_{12}$ (*S. N. Achary, Chemistry Division, BARC); and S. K. Deshpande.*

3.3.4 Other studies

3.3.4.1 Counterions binding with amino acid residues in protein-nanoparticles interaction

The protein-nanoparticles electrostatic interaction is an important aspect in biomedical applications of nanoparticles. It is also to be noted that different ions have remedial functions for different diseases in our body. Recently, we have published a paper [G. Ghosh et al., *Colloids Surf. B: Biointerfaces*, 103 (2013) 267] showing how a particular protein, e.g., net positively charged hen egg white lysozyme (HEWL with pH < pI), can be bound on nanoparticles, e.g., negatively charged iron oxide nanoparticles (IONPs), via electrostatic attraction and, as a consequence, counterions, e.g., sodium counterions (Na^+), associated with the nanoparticles can be delivered and attached with amino acid residues to unfolded the protein secondary structure. Based on these

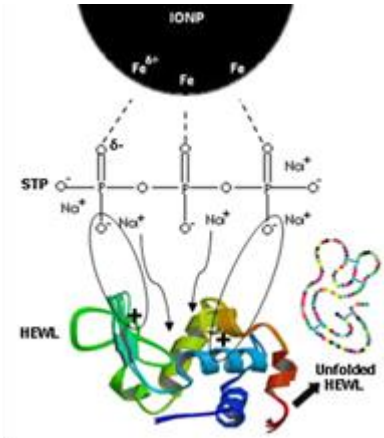

Binding of HEWL on STP-IONPs through electrostatic attraction and diffusion of Na+ ions causing unfolding of HEWL

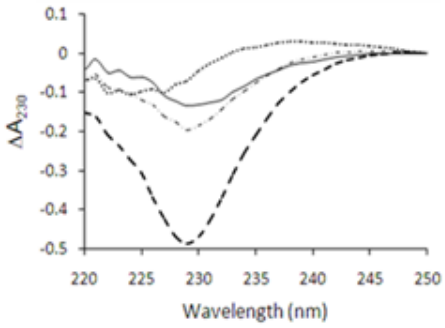

UV absorption difference (ΔA_{230}) at 230 nm between HEWL solutions after incubation with ligand-IONPs and the native HEWL solution.

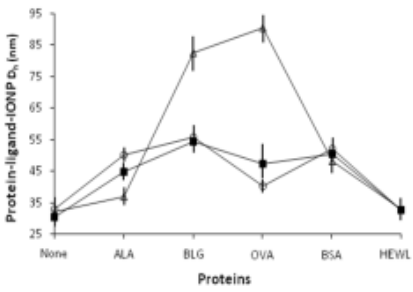

Hydrodynamic diameter (Dh) of ligand-IONPs before (None) and after incubation with ALA, BLG, OVA, BSA and HEWL.

observation we have proposed a model on the protein-nanoparticles electrostatic interaction which recommends two situations, namely, (i) a charged protein in a liquid medium will bind only on the oppositely charged nanoparticle surface, and (ii) counterions associated with the functionalized nanoparticles (due to surface ligands) will diffuse, bind with the amino acid residues and modify the secondary structure of the protein. This model is pictorially depicted in Fig. 3 where the surface ligand is sodium tri-phosphate (STP).

We have further studied the effect of the size and the charge of counterions on binding and unfolding of protein secondary structure in the protein-nanoparticles electrostatic interaction. For this purpose, we have functionalized IONPs with four different citrate molecules, namely, tri-lithium citrate (TLC), tri-sodium citrate (TSC), tri-potassium citrate (TKC) and tri-magnesium citrate (TMC) having Li^+, Na^+, K^+ and Mg^{2+} counterions, respectively. In all dispersions the ligand-IONPs size was measured to be between 20 – 30 nm using the DLS technique. HEWL (pH < pI) was incubated in these dispersions for 48 hrs. and the ζ-potential measurement has confirmed the binding of proteins on the ligand-IONPs. Circular Dichroism (CD) and uv-visible measurements have shown that the unfolding of the HEWL secondary structure has followed the order of counterions as $Li^+ > Na^+ > K^+ \geq Mg^{2+}$. Using DLS, we have found that all dispersions became unstable due to formation of aggregates of protein-ligand-nanoparticles conjugates of size between 500 – 1000 nm, after incubation with HEWL. From the ultraviolet light absorption difference at 230 nm (ΔA_{230} in Fig. 4) between the solutions of HEWL after incubation with ligand-IONPs and that of native HEWL solution, it was clear that the unfolding was taken place due to the change in hydrophobic environments around the tyrosine and tryptophan residues of the protein side chains. From FTIR spectra also we have observed the unfolding of the secondary structure of HEWL due to transformation from α-helix to β-sheet conformations. This investigation has supported our proposed protein-nanoparticles electrostatic interaction model. A manuscript is under preparation based on the above study.

We have also investigated the applicability of our proposed model in the case of proteins, like, α-lactalbumin (ALA), β-lactaglobulin (BLG), ovalbumin (OVA), and bovin serum albumin (BSA), with iso-electric point (pI) less than solution pH, i.e., pH > pI. These proteins are, therefore, net negatively charged in neutral aqueous medium. For this investigation, we have functionalized IONPs with cationic surfactants, like, cetyl pyridinium chloride (CPC), cetyl ammonium bromide (CTAB) and cetyl pyridinium Iodide (CPI) have counterions Cl^-, Br^- and I^-, respectively. We have indeed observed that the negatively charged proteins did bind, but HEWL did not bind, on the positively charged IONPs as confirmed by the ζ-potential measurements. We have also observed that the binding of counterions with amino acid residues of bound protein side chains has followed the recommendation of Hoffmeister series, i.e., number of counterions binding has followed the order as $Cl^- > Br^- > I^-$. Surprisingly, the counterions binding with amino acid residues has caused unfolding to only β-structured proteins, e.g., BLG and OVA; but α-structured proteins, e.g., ALA and BSA, were unaffected. The unfolding of proteins has caused the formation of aggregations of protein-ligand-IONPs conjugates, as observed by the DLS technique (see Fig. 5). A manuscript has been submitted recently based on the above study.

G. Ghosh and L. Panicker, K. C. Barick (B.A.R.C.)

3.3.4.2 Magnetization study of Ni doped ZnO Nanoparticle

Metal oxide of zinc, generally referred as II-VI wide band semiconducting material, is a very intensively characterized material due to its technological vitality. ZnO in bulk phase is diamagnetic in nature, however there are certain reports that in the nanophase of ZnO demonstrate super-paramagnetic/ferromagnetic behavior.

Furthermore, doping of transition metal at Zn site is expected to significantly alter the magnetic properties of these nanostructures, as also reported recently in literature, though the exact cause of origin of the magnetism is highly controversial due to numerous reasons such as secondary phase, defects and magnetism connection, oxygen vacancy etc.

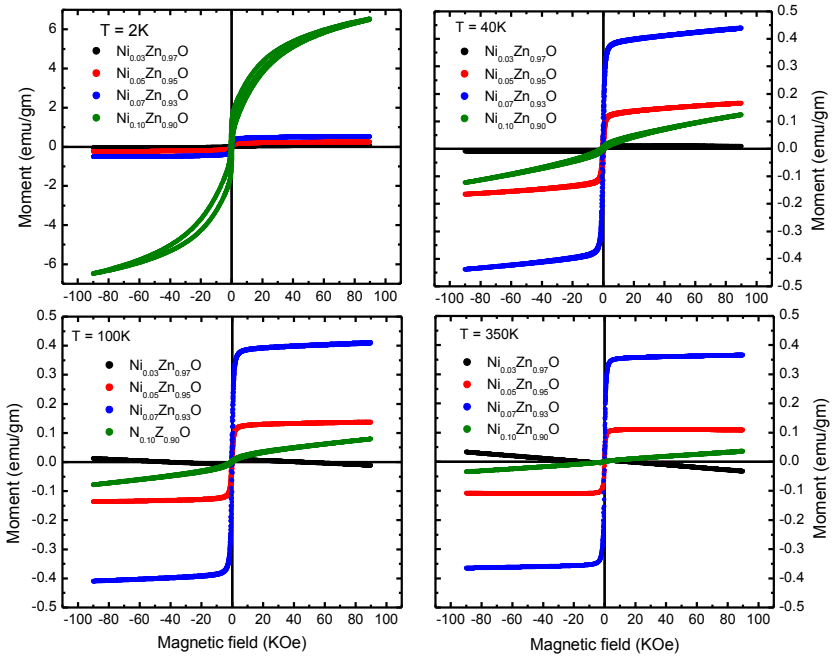

Magnetization study of Ni doped ZnO nanoparticle

We have initiated a study on Ni doped ZnO nanoparticle, series of Ni doped ZnO samples are prepared in nanostructures (~20 nm) form by employing 'electro-explosion of wire (EEW)' technique which is capable of producing large amount of magnetic-semiconductor nanostructures without any extraneous impurity. The magnetization of these $Ni_xZn_{1-x}O$ (x = 0.03, 0.05, 0.07, 0.10) are studied using PPMS-vibrating sample magnetometer at Mumbai Centre. Fig 3.22, shows M-H curve taken at various temperature for these samples. It is evident from the figure that, 3% Ni doped ZnO shows diamagnetic behavior down to 2K from 350K, on increasing the level of Ni concentration ferromagnetic like behavior sets in. At 10% Ni doping clear ferromagnetic behavior at 350 K is observed but saturation moment is not achieved fully even at 90 kOe. Saturation magnetization is less than the lower Ni concentration sample up to 40K, but at 2K, saturation magnetization sharply increases (~ $6\mu_B$/gm), origin of such high magnetization may lie in the existence of finite percentage of NiO present in 10% doped sample, which may have not been detected in the XRD pattern.

We further plan to carry out the systematic neutron diffraction study to clearly identify the location of Ni in the ZnO structure; it will also help in understanding about the formation of separate NiO phase if any.

A. Sahai, N. Goswami (J. I. I. T, Noida) and S. D. Kaushik

3.3.4.3 Effect of La, Gd co-doping on the magnetic properties of $BiFeO_3$

$BiFeO_3$ is well known multiferroic material with G type antiferromagnetic ordering and superposed on it is 62 cycloidal magnetic structures with a periodicity of 62 nm. In this study the effect of co-doping on the magnetic properties of $BiFeO_3$, La and Gd were simultaneously doped in place of Bi and magnetic measurements were carried out to using the PPMS-VSM facility at Mumbai Centre. The M–H hysteresis loops of the (La,Gd)$BiFeO_3$ [LGBFO] samples at different temperatures show a non-zero remnant magnetization (M_r) and coercive field (H_C) for all samples. The magnetization curves do not saturate even in fields up to 9T and show presence of the long range antiferromagnetic (AFM) order in these samples. As reported in previous studies, the doping of La and Gd independently in $BiFeO_3$ known to effectively modify its space modulated spin structure and liberate the magnetization locked within the cycloid which results in a remarkable enhancement in H_C and M_r. In these co-doped samples, the dilution of the spin cycloidcity and the decrease in the bond lengths (Bi-O), bond angle (Fe–O–Fe) which is a result of distortion created by the La^{3+} and Gd^{3+} doping may be possible reasons for the enhancement observed in magnetization, as these changes in oxide systems generally influence the magnetic properties, having indirect exchange interactions. Moreover, Gd doping can bring new magnetic interactions into the system as Gd^{3+} is a magnetic ion with magnetic moment 7.8 μ_B. Hence as the concentration of Gd (y) increases, a noticeable and systematic increase is observed in the remnant magnetization (M_r) and high field magnetization (M_{9T}) exhibiting the maximum values for the highest Gd doping composition of $y = 0.15$ in the entire temperature region. This is due to the high coercivity exhibited by the La doped BFO than Gd doped BFO. That means Lanthanum is in control for the H_C while Gd is responsible for the enhancement in M_r and M_{9T} but further, thorough studies are highly essential to differentiate each contribution.

P. D. Babu; P. Suresh, S. Srinath (University of Hyderabad)

3.4 Research activities at Kalpakkam NODE

3.4.1 Study of particle size and morphology of IR Plasmon absorbing Silver nanoparticles

The particles were prepared by a deft manipulation of reagent ratio, pH and temperature; a wide-tunability of plasmon peaks from 400 to 1015 nm has been achieved. In contrast to previously reports, no strong reducing agent has been used in our work and anisotropic nanoparticles were synthesized in a single step at room temperature. TEM analysis revealed that the particles were having a pyramidal shape with a pentagonal base. The edge length of the penatagon was 20 nm and diagonal length of 40 nm. These nanostructures would be potentially useful in developing novel non-invasive diagnostic and therapeutic techniques

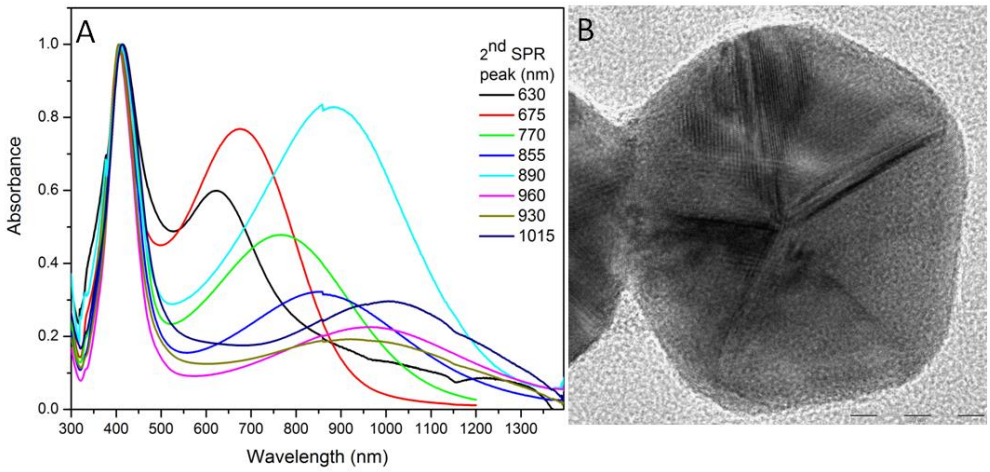

(A) UV-Vis absorption spectra of Ag nanoparticles (B) HR-TEM image of Ag NPs with 2nd Plasmon peak at 1015 nm

with Dr. Amiya Priyam, BIT Mesra, Ranchi, Jharkhand

3.4.2 Study on nanocrystalline hydroxyapatite (HAp- $Ca_{10}(PO_4)_6(OH)_2$) and magnesium incorporated Hap

The materials were synthesized by microwave method. The permittivity, ac conductivity, photoluminescence, wettability and *in vitro* bioactivity were enhanced for magnesium ion incorporated samples. TEM studies reveal that the incorporation of magnesium ions in HAp leads to reduction in the particle size of Mg1HAp and Mg3Hap, possibly due to the smaller ionic radii of magnesium ions to calcium ions. This material is a would be candidate for bone replacement application.

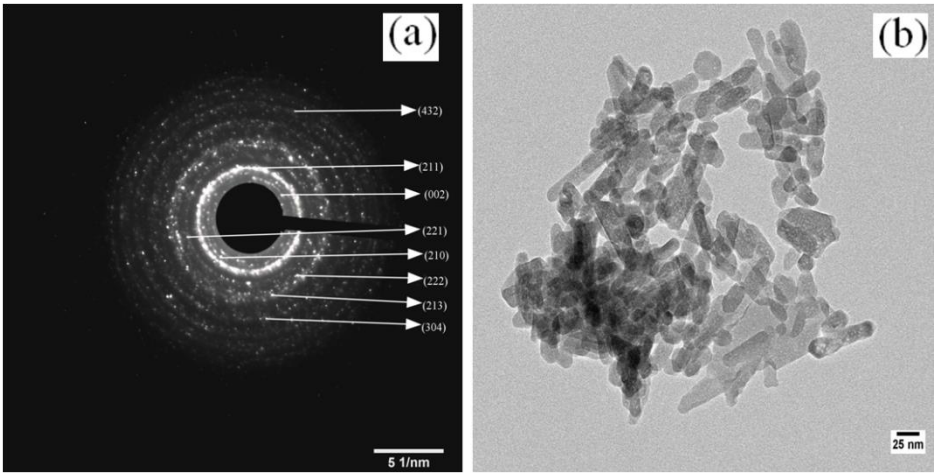

Diffraction pattern and TEM image of Mg doped HAp

with K. Thanigaiarul, Anna University, Chennai

3.4.3 Studies on CdTe thin films

Polycrystalline films of CdTe were deposited by pulsed laser deposition technique. The films were studied for their microstructural and compositional properties. A typical micrograph alongwith the corresponding EDS spectra is shown alongside. From the EDAX measurements it was found that the deposited films are slightly tellurium rich. It was observed that CdTe films deposited here are polycrystalline in nature with compact grains. The grain size increased for films deposited at higher temperatures. Variations in the surface morphologies of the CdTe films deposited at different substrate temperatures are apparent from the micrographs. It was also inferred that the films became more compact when deposited at substrate temperatures greater than 573 K

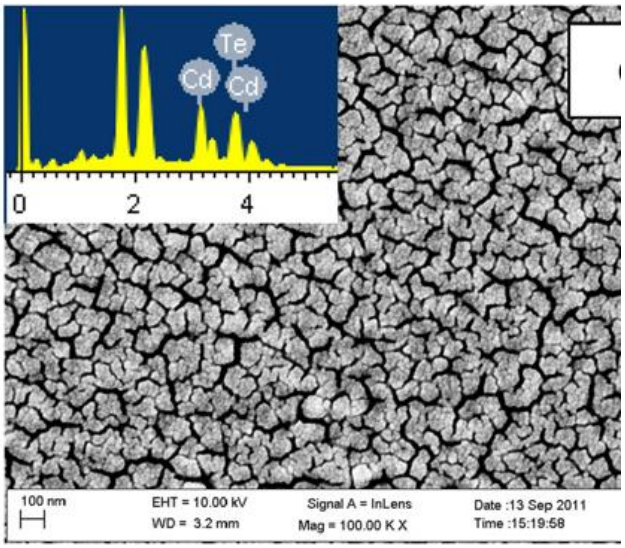

FESEM and EDS spectra of arepresentative CdTe film.

Work carried out in collaboration with Prof. A. K. Pal, Jadavpur University, Kolkata.)

3.4.5 Studies on Co-doped CuO flower/plates/particles-like nanostructures

A simple and rapid microwave-assisted combustion method was developed to synthesize Co-doped CuO flower/plates/particles-like nanostructures. The XRD confirmed the formation of single-phase monoclinic structure. The formations of various nanostructures were confirmed by HR-SEM. The results showed that the Co-doping has obvious effect on the morphology of the pure CuO. The optical properties were determined by DRS and PL spectra. The magnetic properties of various nanostructures were studied by VSM.

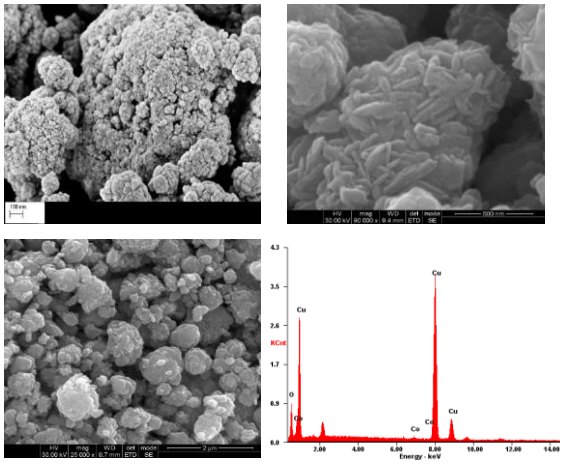

HR-SEM image of (a) pure CuO, (b) 0.5 wt% of Co-doped CuO, (c) 2.0 wt% of Co-doped CuO (d) EDS spectra of (a)

Work carried out with N. Mohamed Basith, J. Judith Vijaya, L. John Kennedy, M. Bououdina, Loyola College Chennai

3.4.6 Studies on removal of cobalt from an alkaline waste using synthetic calcium hydroxyapatite

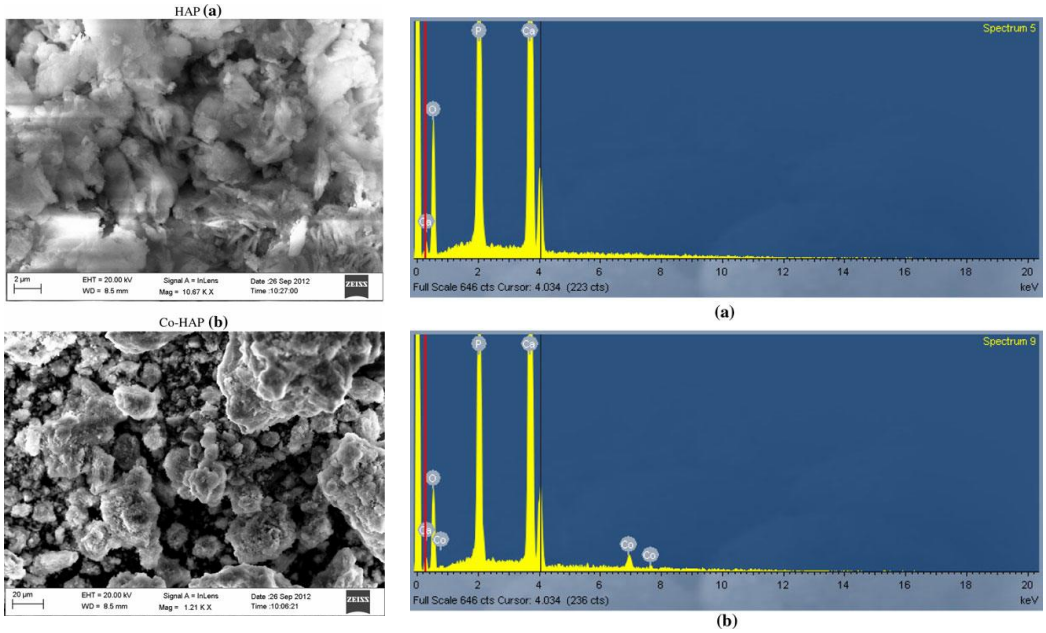

FESEM and corresponding EDS spectra of HAP and Co-HAP samples

The removal of cobalt from an alkaline waste solutions containing sodium was carried out using a radiotracer in a batch method using synthetic calcium hydroxyapatite (HAP). The influence of different parameters such as solution pH, contact time, cobalt concentration,and presence of other ions like sodium on

cobalt removal was studied. The results indicated that the mechanism of cobalt removal by HAP was mainly due to chemisorption on a heterogeneous surface. According to SEM images , the surfaces of both HAP and cobalt doped HAP were found to be heterogeneous. The composition of the HAP powders prepared by the precipitation method was analyzed by energy dispersive X-ray spectroscopy (EDS).

The composition of cobalt doped HAP was also analyzed by the same technique and the results are shown above. The composition analysis by EDS shows that the Ca/P ratio in the original HAP samples is 1.60 instead of 1.67 characteristic for stoichiometric HAP. The slight calcium deficiency is common for the samples obtained by the wet methods.The EDS of cobalt doped HAP shows clearly the cobalt peak indicating that cobalt is being sorbed on HAP which is also supported by the physical appearance of the cobalt doped HAP, as because the HAP is colourless. But on contact with cobalt, it became violet in color.

Work carried out with Diganta Gogoi, KARP-BARC Facilities, Kalpakkam

3.4.7 Studies on the interfacial interactions of TiO2 Nanoparticles with Bacterial Cells under light and dark conditions

The chemical states of titanium, after interaction with bacterial cells, were studied by X-ray Photoelectron Spectroscopy (XPS). Lyophilized, NP interacted bacterial cells (with NP concentration 1 µg/mL) and uninteracted cells were made into pellets (5mm × 1mm) and subjected to XPS analysisXPS analysis is a direct way for evaluating the surface reactivity of TiO2 NPs where reduction of Ti (IV) to Ti (III) species can be confirmed. Figure shows the XPS spectrum of Ti 2p from the TiO2 interacted bacterial cell surfaces under both light and dark conditions. The formation of Ti (III) species was confirmed from XPS analysis in both light and dark treated samples suggesting the possibility of redox reactions in the NP-cell interface. The interfacial reduction of TiO2 NPs from Ti (IV) to Ti (III) species may lead to oxidative degradation of cell membrane, which is probably one of the major factors supporting cytotoxicity potential of these NPs (Biesinger et al 2010). Thus the generation of free radicals and Ti (III) species confirmed the occurrence of redox reactions at the cell–NP interface which indirectly proved oxidative disruption of cellular membrane. Hence this will facilitate the uptake/internalization of the NPs into the cells.

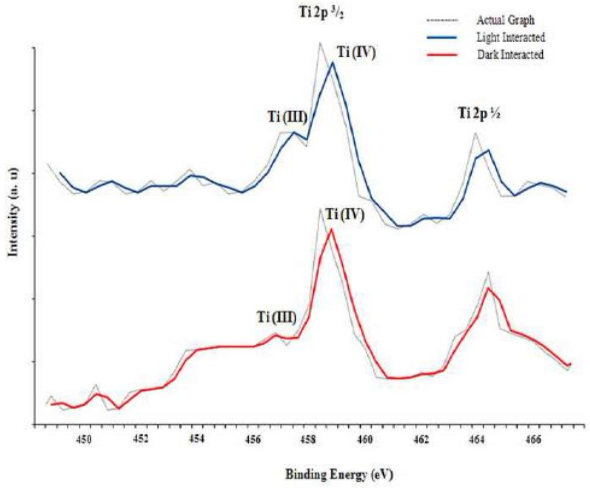

XPS spectra of TiO_2 nanoparticles under light and dark conditions

Work carried out with Prof Amitava Mookherjee, VIT, Vellore

3.4.3.2 Studies on GaSb films

GaSb films deposited by coevaporation technique were studies for their compositional analysis. The general survey XPS spectrum of a representative GaSb film deposited at 773 K., showed that the spectra is dominated by two pairs of strong peaks at ~534 eV and ~1121 eV for $Sb3d_{3/2}$ and $Ga2p_{3/2}$ core-level spectra,

respectively There are a few lower intensity peaks for $Ga3d_{5/2}$ and $Ga3p_{1/2}$ at ~24 eV and 110 eV, respectively. The peak ~534 eV overlaps with that of O1s. Oxygen peak arises due to physisorbed oxygen at the surface. A very low intensity broad peak ~24.6eV of Ga3d peak is observed. Low intensity peaks of Sb4d around ~39 eV are also observed. These peaks are associated with the binding energies of Sb as Sb_2O_3 and Sb_2O_5. The low intensity of the oxide peaks of Ga and Sb signify the fact that very less amount of the oxides are present in the sample. Another low intensity peak~110eV corresponding to $Ga3p_{1/2}$ is also observed. The study confirmed the formation of GaSb bonds in the film

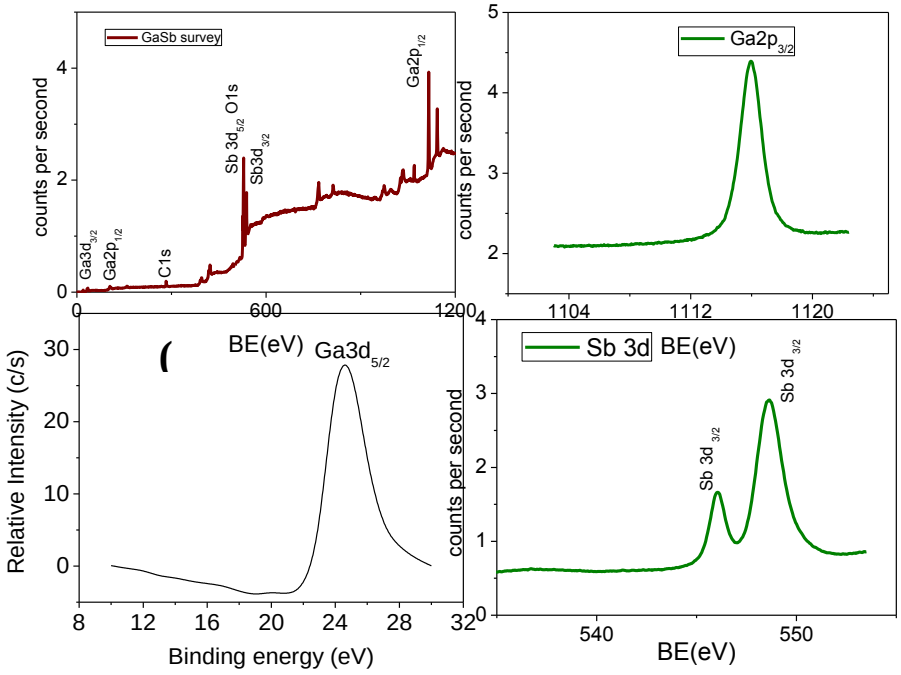

XPS spectra: a) survey, b) Ga2p , c) Ga 3d, d) Sb 3d

.Work carried out with Prof A K Pal, Jadavpur University, Kolkata

4. New Facilities Acquired/Developed

4.1 At Indore Centre

4.1.1Low-Temperature/High Magnetic-Field Dielectric-Characterization (LTHMDC) Facility

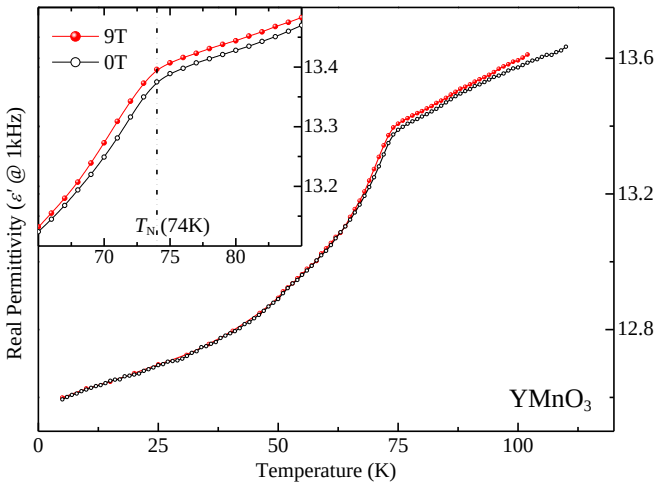

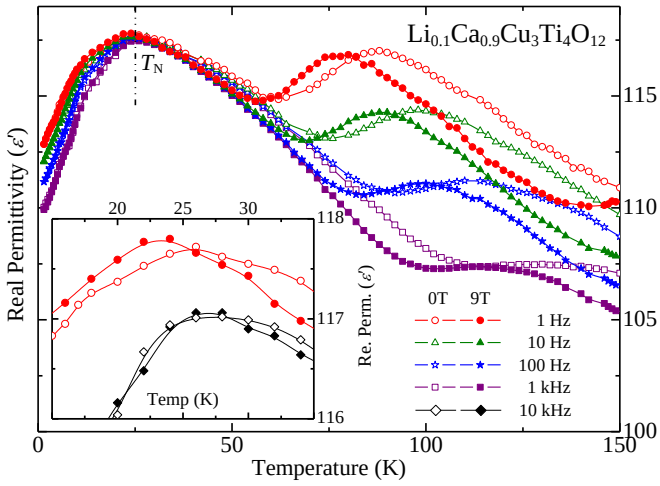

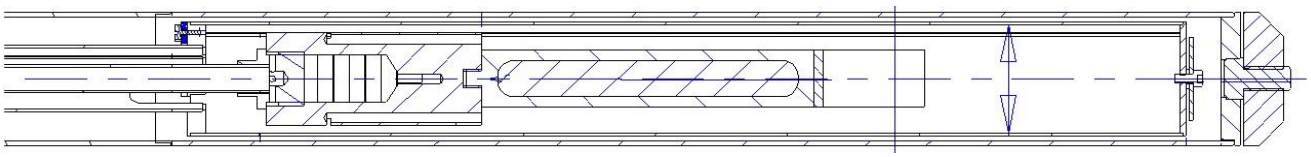

The compact VTI (variable temperature insert) of the LTHM system (Oxford Instruments Nano Science, installed at Indore centre during last quarter/2012) accommodates custom-built modular sample-holders for thermal and dielectric measurements down to 1.5K (10mK stability) & up to 9T field (1T/min max. ramp rate). Special cryocoax cables are incorporated for accurate dielectric characterization, with or without high dc-bias

(±500V) E_{dc}-field. A modulation field B_{ac} (±100 Oe @ 50-10^4 Hz) is also available, independent of the persistent mode B_{dc} operation. The set up precisely measures dielectric constant as small as ~O(10) over mHz-MHz/1.5-300K range, provided the pellet-specimen's resistance exceeds some ~100kOhms.

Preliminary data taken on $YMnO_3$ showed that the sharp anomaly in permittivity (ε') at the AFM-ordering (T_N ~ 74K) remains unaffected up to 9T magnetic field, with highly matched tracking of without and with-field data for T < 50K. Small (≤ 0.2%) but very clear positive magneto-capacitance was measured near T_N, with 9T field. Complex permittivity (ε^*) of Li-doped $CaCu_3Ti_4O_{12}$ measured under 9T field shows prominent magneto-capacitance effects on the polaron-like relaxation across ~100K. Weakly-dispersive magneto-electric anomaly near T_N (25K) revealed only minute effects (at the lowest ω's), in the otherwise quantum paraelectric LCCTO.

A.M. Awasthi (amawasthi@csr.res.in)

4.1.2.Polarised light beamline on Indus-2

Design of the proposed polarized light beamline was worked out in the year 2002 and the same was also published in International journal viz., Nuclear Instruments and Methods in Physics Research, (2003) Vol.199, page 520. After finalizing the technical details tender enquiry was floated for the different parts of the beamline. Most of the parts are now received from respective suppliers (M/S Horiba Jobin Yvon, France, Vacuum Generators, UK, Varian, USA). After receipt of different components we started installing the individual component at their respective position. Assembly work of different sections of beamline is completed and its vacuum testing is under progress. Work of windowless front end testing is also completed in collaboration with RRCAT engineers. Radiation hutch design and development is also completed and complete hutch is erected at the beamline site in Indus-2 experimental hall.

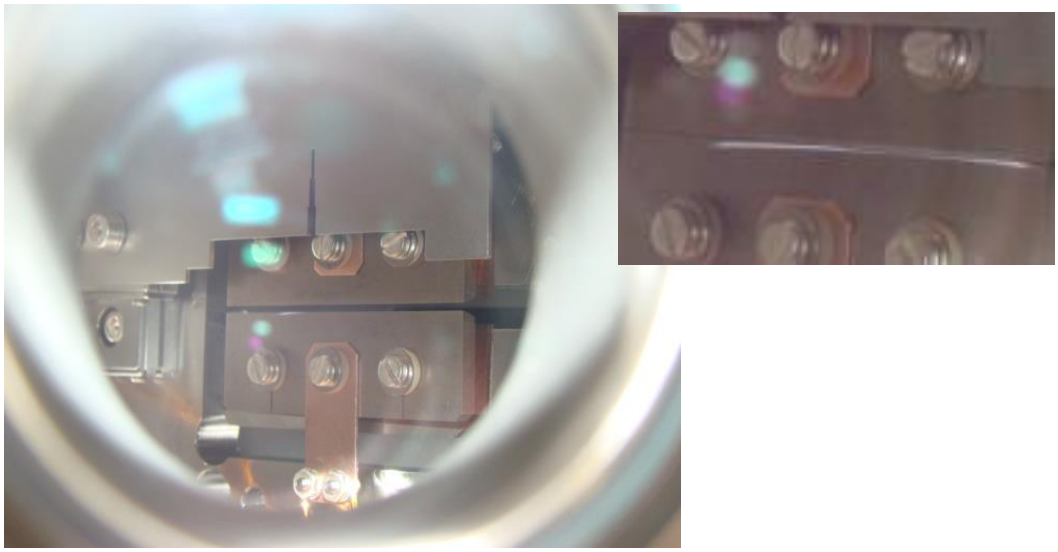

Fig. 1: Photograph of the optical component of the beam taken at the entrance slit of BL-1 at Indus -2 beam current of 90 mA and 2.5 GeV. With an opening of 1000 µm beam is passing through the slits. Inset shows the positioning of the beam with an opening of 10 µm

Commissioning of Polarized Light Beamline (PLB) installed at the BL-1 port of Indus-2 has been done recently. Prior to commissioning of the beamline, its major components e.g. Polarization selection aperture (PSA) chamber, Pre-mirror chamber, entrance slit chamber, monochromator chamber, exit slit chamber and post mirror chamber were placed at their respective positions and aligned mechanically. Thereafter connecting pipes, bellows, crosses, gate valves etc were connected and beamline was evacuated to achieve a pressure in the range of 2×10^{-10} mbar. Thereafter, the beamline was vented again and optical components e.g. pre-mirror, grating monochromator, and post mirror were installed. Then beamline was evacuated again to achieve UHV conditions and commissioning of the beamline started. Starting from a low current of 10 mA of Indus-2, beam current up to 100 mA was introduced in about five steps with exposure time of at least 12-15 hours at each step. A photograph of the optical component of the beam at the entrance slit is shown in figure 1.

After commissioning of the beamline, beam can be taken at our beamline routinely. Efforts are now being to do the finer alignment of monochromator, exit slit and post mirror with the SR beam. The zero order beam reflected from the monochromator has already been observed at the sample position.

D.M.Phase, Mukul Gupta and Ajay Gupta (dmphase@csr.res.in)

4.2 Mumbai Centre

4.2.1 New Sample Environment at CSR beam line at Dhruva

Actual photograph of the CCR mounted on the sample table on neutron diffraction (FCD-PD-3) beam line at Dhruva reactor.

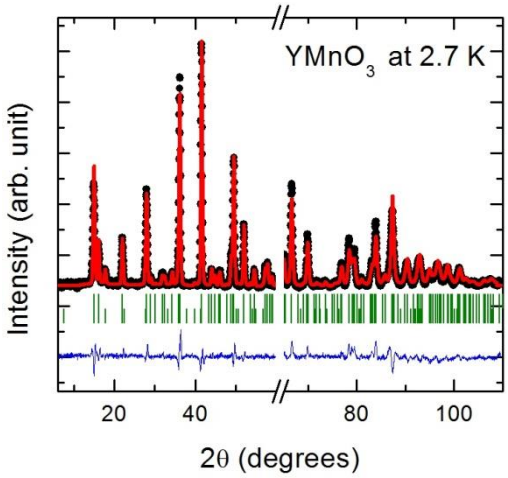

The figure shows neutron diffraction pattern at 2.7 K for $YMnO_3$

(Sample courtesy: Dr. A. M. Awasthi, UGC-DAE CSR Indore Centre).

In order to carry out solely zero field temperature dependent neutron diffraction study at CSR beam line at Dhruva, M/s A. S. Scientific, UK made, Close Cycle Refrigerator (CCR) based sample environment was recently installed. The cool down time for the CCR is close to 3 hr. from room temperature. A variable

temperature insert (VTI) is latched to the second stage of the CCR. The minimum temperature at sample can be achieved is ~ 2.7K by using the helium exchange gas in the sample space. Added advantage for VTI is that the sample can be changed at any temperature.

V.Siruguri (siruguri@csr.res.in

4.3 Kolkata Centre

4.2.1 D8 Advance X-ray Diffractometer

The D8 Advance X-ray Diffractometer from Bruker AXS installed in the Material Science lab of Kolkata Centre is equipped with three X-ray sources of Cu, Fe, and Co. Scintillation and fast Lynx eye Solid State Strip detectors are used for obtaining the diffractogram. The sample stage is fixed. The system can be configured in Brag –Brentano Geometry for powder samples as well as in the parallel beam geometry for thin film samples.

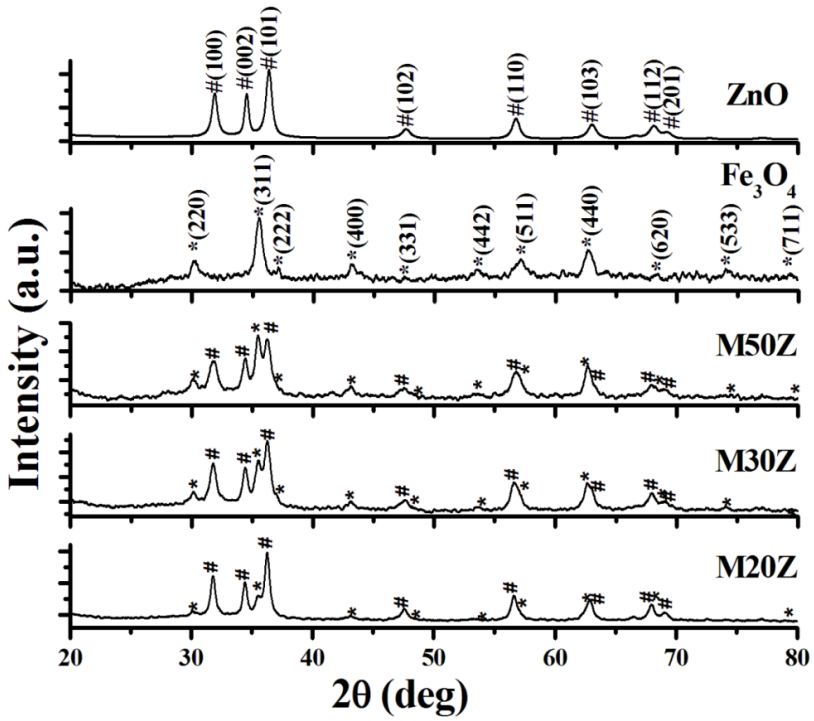

For doing XRD of thin films at very low angles Goebel mirror is available. Currently the Goebel mirror is only available for Cu X-ray source. All the measurements are done at room temperature under normal atmospheric conditions. The system is totally automated and qualitative and quantitative phase identification, crystal structure solution from powder samples, crystallite size determination, micro strain analysis, residual stress analysis, and preferred orientation of the samples can be done using the software supplied by the manufacturer.

AK Sinha (aks@delta.iuc.res.in)

4.4 Kalpakkam Node

4.4.1 Hot Isostatic Press (HIP):

The HIP (from M/S American Isostatic Press, USA), installed at Kalpakkam Node, finds its applications in a wide spectrum of metallurgy, material science synthesis and casting. Due to its feature to generate and retain extreme condition of temperature and pressure in inert environment, materials can be prepared with high density and reduced micro-porosity through the mechanism of plastic deformation and diffusion bonding. Following are its features:

- Capable of 30,000 psi and 2200°C
- Fully automated and has Kanthal and Platinum furnaces
- Load capacity is 3" diameter x 5" long
- Simple and economical HIP

4.4.2 Helios-Nano 600i from M/s FEI Qunta, Switzerland

This state of the art machine (from M/s FEI Qunta, Switzerland),), installed at Kalpakkam Node, is capable of preparing electron transparent thin lamellae from bulk specimens for high quality TEM characterization. For selection of precise regions of required chemistry and crystallographic orientation, it is equipped with several features which can also be used for material characterizations. These are:

- Dual beam SEM with EDX, EBSD and FIB technology
- Loadlock facility for quick loading of samples
- Omniprobe facility

4.4.3 Materials Studio code:

Computer simulation code "materials studio" (from M/s Accelrys, USA),), installed at Kalpakkam Node, is very useful for many ab-initio calculations in physical, engineering and chemical sciences, has been installed. This code provides a complete range of simulation capabilities from quantum, atomistic, mesoscale, statistical, analytical and crystallization tools. The features of the computational system are:

- Two nos of 4- socket multicore Intel Xeon server E7-4870 (HP Proliant DL580 Gen 7 model) with 6.4 GT/s Intel QPI bus speed
- Two nos of 2 x Intel Xeon 5687 , 4 core (HP Z800 workstation) with 6.4 GT/s Intel QPI bus speed

- HP LTO-5 backup device
- Ten nos of client workstations (HP Compaq 8200 elite model)

4.4.4 X-ray Photoelectron spectroscopy (XPS) (M/s Specs, Germany)

This instrument is recently installed at Kalpakkam Node. The power of this surface characterization tool is enhanced by a quasi in-situ high-temperature high-pressure reaction cell attached to the main analysis chamber, where surface reactions can be performed in a controlled reactive environment and immediately transferred to the analysis chamber in UHV, without exposing to environment.

- Useful for determining the oxidation states of the component elements
- Pellets and thin films can be studied
- HPC can study in-situ reactions upto 800°C

4.4.5 FIB-SEM AURIGA from M/S Carl Zeiss,Germany:

The new CrossBeam Workstation (FIB-SEM) from M/S Carl Zeiss uses the best-in-class FIB column and the proprietary GEMINI e-Beam column together with a completely new designed vacuum chamber for advanced surface characterization has been installed at the Kalpakkam Node of UGC-DAE CSR, in June 2012. Some of the important features are :

- Innovative FIB technology with best-in-class resolution (< 2.5 nm)
- High resolution live FE-SEM monitoring of the entire preparation process
- Advanced gas processing technology for ion and e-beam assisted etching and deposition

4.4.5 4. 15T Magnetoresistance system

This system will allow measurement of resistance at magnetic fields upto 15T. The system has just arrived.

For further information regarding Kalpakkam Node please contact Dr. G Amarendra (ga@csr.res.in)

5. Publications in Journals

Names of authors from Universities and colleges are shown in bold face, names of authors from UGC-DAE CSR are underlined and those from DAE marked by #

5.1Publications from Collaborative research:

1. Interplay of superconductivity and charge density wave ordering in pseudoternary alloy compounds: $Lu_2Ir_3(Si_{1-x}Ge_x)_5$, $Lu_2(Ir_{1-x}Rh_x)_3Si_5$, and $(Lu_{1-x}Sc_x)_2Ir_3Si_5$.N.S. Sangeetha, A. Thamizhavel[#], C.V. Tomy[#], Saurabh Basu[#], A.M. Awasthi, S. Ramakrishnan[#], and D. Pal, Phys. Rev. B. **86**, 024524 (2012).

2. Enhancement in the magnetic moment with Cr3+ doping and its effect on the magneto-structural properties of Ce0.1Y2.9Fe5O12, S. R. Naik and A. V. Salker, Phys. Chem. Chem. Phys., 2012, 14, 10032–10040

3. Synthesis and effect of post-deposition thermal annealing on morphological and optical properties of ZnO thin film, Ajaya Kumar Singh, Gautam Sheel Thool, Soumya R. Deo, R. S. Singh, Ashish Gupta, Res Chem Intermed DOI 10.1007/s11164-012-0524-y

4. Mixed alkali effect in physical and optical properties of $Li_2O–Na_2O–WO_3–B_2O_3$ glasses, **A. Edukondalu**, **M. Purnima**, **Ch. Srinivasy**, T. Shripathi, A.M. Awasthi, **Syed Rahman**, **K. Siva Kumar**, J. Non-Cryst. Solids **358**, 2581 (2012).

5. Dielectric relaxation spectroscopy of phlogopite mica, **Navjeet Kaur**, **Mohan Singh**, **Anupinder Singh**, A.M. Awasthi, **Lakhwant Singh**, Physica B: Condensed Matter 407, 4489 (2012).

6. Structural Studies and Valence Band Splitting Parameters in Ordered Vacancy Compound $AgGa_7Se_{12}$.**Rajani Jacob, R. Geethu**, T. Shripathi, V. Ganesan, U. P. Deshpande, Shilpa Tripathi, **B. Pradeep, Rachel Reena Philip**, J. Inorg. Organomet. Polym., 22, 1229 (2012)

7. Investigation of surface properties of Ar-plasma treated polyethylene terephthalate (PET) films.**S.M. Pelagade, N.L. Singh, A. Qureshi, R.S. Rane, S. Mukherjee**, U.P. Deshpande, V. Ganesan, T. Shripathi, Nucl. Instru. Meth., 289, 34 (2012)

8. Intensity-dependent transient photodarkening in visible and far infrared absorption spectra of $As_{50}Se_{50}$ thin film. A.R. Barik, Mukund Bapna, Ramakanta Naik, U.P. Deshpande, T. Shripathi, K.V. Adarsh Mat. Chem. Phys., published online in Dec. 2012.

9. Non-toxic, earth-abundant 2% efficient Cu_2SnS_3 solar cell based on tetragonal films direct-coated from single metal-organic precursor solution. **Devendra Tiwari, Tapas K. Chaudhuri**, T. Shripathi, U.P. Deshpande, R. Rawat, Solar Energy Materials & Solar Cells, 113, 165 (2013).

10. Cu_2SnS_3 as a potential absorber for thin film solar cells, **D. Tiwari, T. K. Chaudhuri**, T. Shripathi and U. Deshpande, Solid State Physics: AIP Conference Proceedings 1447 (2012) 1039 – 1040

11. Degradation study on structural and optical properties of annealed Rhodamine B doped poly(vinyl) alcohol films, **J. Tripathi,** S. Tripathi, **J.M. Keller, K. Das**, T. Shripathi, Polymer Degradation and Stability **98** (2013) 12-21

12. Ultra Low-k Property of Hydrogenated Carbon Nitride: Chemical evaluation, Abhijit Majumdar; Sadhan C Das; Thoudinja Shripathi; Rainer Hippler, Chemical Physics Letters, **524** (2012), 62-67.

13. Shake up satellites and fluorescence property of carbon nitride and hydrogenated carbon nitride: Annealing effect, Abhijit Majumdar, Sadhan Chandra Das, T. Shripathi, Joachim Heinickec,Rainer Hipplera, Surface Science, **609** (2013) 53-61, doi.org/10.1016/j.susc.2012.11.003

14. Influence of Rhodamine (B) doping on vibrational, morphological and absorption properties of poly(vinyl) alcohol **Tripathi, J.; Keller, J. M.; Das, K.**; Tripathi, S.; Shripathi, T.; Journal of Physics and Chemistry of Solids, Volume 73, Issue 8, p. 1026-1033.F 1.499.DOI: 10.1016/j.jpcs.2012.03.011.

15. Role of ultra thin pseudomorphic InP layer to improve the high-k dielectric/GaAs interface in realizing metal-oxide-semiconductor capacitor Souvik Kundu, Nripendra N. Halder, D. Biswas, P. Banerji, T. Shripathi and S. Chakraborty. J. Appl. Phys. 112, 034514 (2012); doi: 10.1063/1.4745896

16. tructural, optical and chemical characterization of Rhodamine (B) doped poly (vinyl) alcohol films**, J. Tripathi, J.M. Keller, K. Das**, S. Tripathi, A. Fatima, T. Shripathi, Applied Surface Science, 261 (2012) 481–487.

17. Nanoparticle Induced Piezoelectric, Super Toughened, Radiation Resistant, Multi-functional Nanohybrids, Vimal K. Tiwari , T. Shripathi, N. P. Lalla, and Pralay Maiti, Nanoscale 4, 167 (2012) (IF 4.109)

18. Electron irradiation effects on TGA-capped CdTe quantum dots. Chethan Pai, M.P. Joshi#, S. Raj Mohan#, U.P. Deshpande, T.S. Dhami#, Jayakrishna Khatei, K.S. Koteshwar Rao, and Ganesh Sanjeev, J. Phys. D: Appl. Phys. 46, 175304 (2013).

19. Growth of Pd4S, PdS, and PdS2 films by controlled sulfurization of sputtered Pd on native oxide of Si. R. Bhatt, S. Bhattacharya, A. Singh, U.P. Deshpande, C. Surger, S. Basu, D.K. Aswal, S.K. Gupta, Thin Solid Films 539, 41 (2013) .

20. Dielectric properties of sol-gel synthesized $SrTiO_3/Ba_{0.7}Sr_{0.3}TiO_3$ and $SrTiO_3$ / $Ba(Zr_{0.3}Ti_{0.7})O_3$ thin film hetrostructures.A.N.Tarale, M.M.Sutar, D.J. Salunkhe, P.B.Joshi, S.B.Kulkarni, R.C.Pawar, C.S.Lee, D.M.Phase, M.Gupta, R.J.Choudhary, Journal of Materials Science 24(4) 1308 (2013).

21. Studies on highly resistive ZnO thin films grown by DC discharge assisted pulsed laser deposition.A.K.Das#, P.Misra#, R.Kumar#, T.Ganguli#, M.K.Singh#, D.M.Phase , L.M.Kukreja#, Applied Physics A March (2013).

22. Room temperature positive magnetoresistance and field effect studies of mangnite- based heterostructure. **Uma Khachar, P.S. Solanki**, R. J. Choudhary, D. M. Phase, V. Ganesan, **D.G. Kuberkar,**Appl.Phys.A 108(3), 733 (2012).

23. Electron electron interactions based metal-insulator transition in Ga doped ZnO thin films. **R.V.M.Naidu, A.Subrahmanyam, A.Verger, M.K.Jain**, S.V.N.Bhaskar Rao#, S.N.Jha# and D.M.Phase,Electronic Materials Letters 8(4) 457 (2012).

24. Synthesis and characterisation of Ba0.7Sr0.3TiO3, BaZr0.3Ti0.7O3 thin film hetrostructures. **A.N.Tarale, S.R.Jigajeni, D.J.Salunkhe, P.B.Joshi, S.B.Kulkarni**, D.M.Phase, R.J.Choudhary, S.K.Deshpande, Journal of Materials Science 23, 557 (2012).

25. Effect of defect dipoles on the dielectric and electrical properties of Mn: $K_2Ti_6O_{13}$ lead free ceramics : EPR spectroscopy cum dielectric spectroscopy. **S.V.Vikram, D.Maurya,** D.M.Phase, **V.S.Chandel,**Jounal of Materials Science 23 (3), 718 (2012).

26. Electronic structure of buried Co-Cu interface studied with photoemission spectroscopy. S.Banik#, S.Barman#, S.K.Rai#, D.M. Phase, A.K.Srivastav#, G.P.Das# and S.K.Deb# J. Appl. Phys. 112, 103702 (2012).

27. The Effect of Mn Substitution on Properties of $Bi_{1.6}Pb_{0.4}Sr_2Ca_{2-x}$ Mn $_x$ Cu_3O_y Superconductors, **Indu Verma**, R. Rawat, V. Ganesan, D. M. Phase, and **B. Das,** Journal of Superconductivity and Novel Magnetism 25, 85 (2012).

28. Band alignment and interfacial structure of ZnO/Ge heterojunction investigated by photoelectron spectroscopy. Shreyashkar D.S.#, R. S. Ajimsha# , V. Sahu#, Ravi Kumar# , P. Misra#, D.M.Phase, S.M.Oak#, L.M. Kukreja# , T. Ganguli#, S.K.Deb#,Appl. Phys. Lett. 101, 212109 (2012).

29. Magnetic and transport properties in thin film of Fe_2CrAl. **Snehal Jani, Jagdish Nehra, Vishal Jain, N. Lakshmi**, R. J. Choudhary, **P. L. Paulose**, D. M. Phase, **K. Venugopalan**, V. R. Reddy and Ajay Gupta. J. Expt. Nanoscience, (2012). DOI: 10.1080/17458080.2012.692488.

30. 200 MeV Ag15+ ion induced surface modification and transport behaviour in manganite based thin film devices, **Ashish Ravalia, Megha Vagadia, P.S. Vachhani** , R.J. Choudhary, D.M. Phase, **K. Asokan, D.G. Kuberkar**, Applied Surface Science 258 4203– 4206 (2012).

31. Effect of oxygen partial pressure and Fe doping on growth and properties of metallic and insulating molybdenum oxide thin films. **Shailja Tiwari**, Ridhi Master, R. J. Choudhary, D. M. Phase and **B. L. Ahuja**, J. Appl. Phys. **111**, 083905 (2012).

32. Improved crystallinity, spatial arrangement and monodispersity of submicronLa0.7Ba0.3MnO3 powders: A citratechelation approach, **Ch. N.Rao** , S.S. Samatham , V.Ganesanb, V.G.Sathe , D.M.Phase , **S.N.Kale,** Journal of Magnetism and Magnetic Materials **324** (2012) 3766–3772.

33. Growth and characterization of nano-structured Sn doped ZnO. A.D. Acharya , **Shweta Moghe , Richa Panda , S.B. Shrivastava**, Mohan Gangrade , T. Shripathi , D.M. Phase, V. Ganesan , Journal of Molecular Structure 1022 (2012) 8–15

34. Gas phase condensation of few-layer graphene with rotational stacking faults in an electric-arc Soumen Karmakar , Ashok B. Nawale , Niranjan P. Lalla , Vasant G. Sathe ,Sadhu K. Kolekar , Vikas L. Mathe , Asoka K. Das , Sudha V. Bhoraskar , Carbon,**55** (2013) 209-220

35. Feasibility of magnetic Compton scattering in measurement of small spin moments: A study on $LaFe_{1-x}Ni_xO_3$ (x=0.4 and 0.5). **Alpa Dashora, Jagrati Sahariya,** R.J. Choudhary, D.M. Phase, M. Itou, Y. Sakurai, and **B.L. Ahuja**, Appl. Phys. Lett. 102, 142403 (2013).

36. Strain dependent stabilization of metallic paramagnetic state in epitaxial NdNiO3 thin films. Yogesh Kumar, R. J. Choudhary, S K Sharma**,** M Knobel, and Ravi Kumar, Appl. Phys. Lett. 101, 132101 (2012).

37. Irradiation induced modification in transport properties of LaNiO3 thin films: An x-ray absorption study. Yogesh Kumar, A. P. Singh, S K Sharma**,** R. J. Choudhary, P. Thakur, M Knobel, N. B. Brookes and Ravi Kumar, Appl. Phys. Lett. 101**,** 112103 (2012).

38. Structural, electrical and magnetic properties of Ce doped $La_{0.7}Ca_{0.3}MnO_3$ thin films. **Amit Khare**, R. J. Choudhary and **S. P. Sanyal**, J. Appl. Phys. 112, 023714 **(2012).**

39. Strain controlled systematic variation of metal-insulator transition in epitaxial $NdNiO_3$ thin films. Yogesh Kumar, R. J. Choudhary, and Ravi Kumar, J. Appl. Phys**.** 112, 073718 (2012).

40. Oxygen vacancy induced phase formation and room temperature ferromagnetism in undoped and Co doped TiO_2 thin films. **P Mohanty, N C Mishra,** R J Choudhary, A Banerjee, T Shripathi, and **Chandana Rath**, J. Phys. D Appl. Phys. 45 325301 (2012).

41. Green luminescence and room temperature ferromagnetism in Cu doped ZnO, Z. A. Khan[#], A. Rai, S. R. Barman, and S. Ghosh[#], Appl. Phys. Lett. 102, 022105 (2013).

42. Synthesis of nanosize and sintered $Mn_{0.3}Ni_{0.3}Zn_{0.4}Fe_2O_4$ ferrite and their structural and dielectric studies, U.B. Gawas[#], V.M.S. Verenkar[#], S.R. Barman, S.S. Meena, P. Bhatt,J. Alloys Comp. 555, 225 (2013).

43. Effect of growth temperature on structural, electrical and optical properties of dual ion beam sputtered ZnO thin films, S. K. Pandey, C. Mukherjee, P. Mishra, M. Gupta, S. R. Barman, S. W. D'Souza, S. Mukherjee, J. Mater. Sci.: Mater. Electron,doi: 10.1007/s10854-013-1130-5 (2013).

44. Electronic structure of Fe_2CrSn, A.Chakrabarti[#], S. W. D'Souza, and S. R. Barman.Physica B 407, 3547 (2012).

45. Optimization of smart Heusler alloys from first principles, P. Entel, M. Siewert, M. E. Gruner, Chakrabarti[#], S. R. Barman, V. V. Sokolovskiy, V. D. Buchelnikov. J. Alloys Compd. doi:10.1016/j.jallcom.2012.03.005

46. Synthesis and signature of M-E coupling in novel self-assembled $CaCu_3Ti_4O_{12}$-$NiFe_2O_4$ nanocomposite structure. Anju Ahlawat, V. G. Sathe, V. Ganesan, D. M. Phase, and S. Satapathy[#],J. Appl. Phys. 111, 074302 (2012).

47. Improved crystallinity, spatial arrangement and monodispersity of submicron $La_{0.7}Ba_{0.3}MnO_3$ powders: A citrate chelation approach. **N. Rao,** S. Shanmukharao Samatham, V. Ganesan, V.G. Sathe, D.M. Phase, **S.N. Kale,** Journal of Mag. Mag. Mater. **324**, (2012) 3766.

48. Effects of chemical analytes on zinc tetraphenylporphine thin films studied by vibrational spectroscopy and density functional theory. **G.S.S. Saini, Sukh Dev Dogra, Gurpreet Singh, S.K. Tripathi, Sarvpreet Kaur,** Vasant Sathe, **B.C. Choudhary,**Vibrational Spectroscopy **61**, (2012) 188

49. Highly Conducting Phosphorous Doped nc-Si:H Thin Films Deposited at High Deposition Rate by Hot-Wire Chemical Vapor Deposition Method. **V. S. Waman, M. M. Kamble, S. S. Ghosh, Azam Mayabadi,** V. G. Sathe, **D. P. Amalnekar, H. M. Pathan, and S. R. Jadkar,** Journal of Nanoscience and Nanotechnology **12**, (2012) 1–8,

50. Influence of helium dilution of silane on microstructure and opto-electrical properties of hydrogenated nanocrystalline silicon (nc-Si:H) thin films deposited by HW-CVD,**V.S. Waman, M.M. Kamble, S.S. Ghosh, R.R. Hawaldar, D.P. Amalnerkar,** V.G. Sathe**, S.W. Gosavi, S.R. Jadkar,** Materials Research Bulletin **47**, (2012), 3445

51. Blue shift of optical band-gap in LiNbO3 thin films deposited by sol–gel technique,S. Satapathy[#], Chandrachur Mukherjee[#], Taruna Shaktawat[#], P.K. Gupta[#], V.G. Sathe, Thin Solid Films **520**, (2012), 6510

52. Fine-Tuning of Relative Fraction of Amorphous and Crystalline Phases in Hydrogenated Silicon Prepared by PE-CVD Method. **A.M. Funde, V.S. Waman, M.M. Kamble, M.R. Pramod, S.P. Gore, G.R. Roze,** V.G. Sathe**, S.W. Gosavi, S.R. Jadkar,** Energy Procedia **15**, (2012) 229–239

53. Optical, thermal, and structural properties of Nb_2O_5–TeO_2 and WO_3–TeO_2 glasses**Arshpreet Kaur, Atul Khanna,** Vasant G. Sathe,Phase Transitions 1-22 (2012) DOI:10.1080/01411594.2012.727998

54. Spectroscopic studies of tantalum doped borate glasses, **M. Sharada, D. Suresh Babu,** Physica B: Condensed Matter **407**, (2012), 3945–3955

55. Enhancement in the magnetic moment with Cr^{3+} doping and its effect on the magneto-structural properties of $Ce_{0.1}Y_{2.9}Fe_5O_{12}$, **S. R. Naik and A. V. Salker,** Phys. Chem. Chem. Phys., **14**, (2012)10032–10040

56. Change in the magnetostructural properties of rare earth doped cobalt ferrites relative to the magnetic anisotropy, **S. R. Naik and A. V. Salker,** J. Mater. Chem., **22**, (2012) 2740

57. Amorphization and disorder of PrFeO3 thin films after heavy ion irradiation**Feroz Ahmad Mir, M. Ikram, Ravi Kumar,** Applied Radiation and Isotopes **70** (2012) 2409–2415

58. Comparative studies on conventional solution and Sankaranarayanan–Ramasamy (SR) methods grown potassium sodium tartrate tetrahydrate single crystals, **T. S. Shyju, S. Anandhi and R. Gopalakrishnan,** CrystEngComm, **14**, (2012) 1387

59. Structural, transport and spectroscopic properties of Ti4+ substituted magnetite: $Fe_{3-x}Ti_xO_4$ Dinesh Varshney, Arvind Yogi, Materials Chemistry and Physics **133** (2012) 103

60. Crystal structure refinement of $Bi_{1-x}Nd_xFeO_3$ multiferroic by the Rietveld method **Ashwini Kumar, Dinesh Varshney,** Ceramics International **38** (2012) 3935

61. Structural and Mössbauer investigation of nanocrystalline $SrFe_{1-x}Ti_xO_{3-\delta}$., **A.Sendilkumar**, P.D.Babu, M.Manivelraja, V.R.Reddy , A.Gupta and **S.Srinath**., JACS (Accepted)

62. Investigation of structural and magnetic properties of $Ni_{0.5}Zn_{0.5}Fe_2O_4$ nano powders prepared by self-combustion method., **V.D.Sudheesh, J.Nehra, A.Vinesha, V.Sebastianb, N.Lakshmi, Dimple P. Dutta**, V.R. Reddy**, K.Venugopalan**, Ajay Gupta., *Materials Research Bulletin 48 (2013) 698–704*

63. Structural, microstructural, magnetic and hyperfine characterization of nanosized $Ni_{0.5}Zn_{0.5}Fe_2O_4$ synthesized by high energy ball-milling method, **S.Dey, S.K.Dey, B.Ghosh**, V.R.Reddy **and S.Kumar**., Materials Chemistry and Physics 138 (2013) 833

64. Effect of silver incorporation in phase formation and band gap tuning of tungsten oxide thin films **R. Jolly Bose, R. Vinod Kumar, S. K. Sudheer,** V. R. Reddy**,** V. Ganesan**, V.K.M.Pillai**., J. Appl. Phys. 112 (2012) 114311

65. Influence of local structure on magnetic properties of layered cobaltites $PrBaCo_2O_{5+\delta}$, $\delta > 0.5$ **S Ganorkar, Kaustubh R Priolkar, Prabhaker R Sarode**, Alok Banerjee, Rajeev Rawat and S Emura, J. Phys.: Condens. Matter 24 (2012) 476003.

66. Effect of Sb and Si doping on the superconducting properties of $FeSe_{0.9}$,Sudesh, S. Rani, G.D. Varma, Physica C 485 (2013) 137

67. Investigation into the superconducting threshold of $Bi_{1.6}Pb_{0.4}Sr_2Ca_{n-1}Cu_nO_{2n+4+\delta}$, n=2, 2.5, 4 perovskites synthesized by glassy precursor route with Thermal and Raman spectroscopic techniques, **T. Kannan, P. Predeep**, J Therm Anal Calorim, DOI 10.1007/s10973-012-2845-x

68. Investigation of electrical resistivity and magnetotransport properties of the $La_{0.67}Ca_{0.33}Mn_{0.99}Fe_{0.01}O_3$ perovskite oxide, **Vijaylakshmi Dayal, Punit V Kumar**, Solid State Communications 158 (2013) 70

69. Adiabatic to non adiabatic change in conduction mechanism of Zn doped $La_{0.67}Sr_{0.33}MnO_3$ perovskite. **Hilal Ahmed, Shakeel Khan, Wasi Khan, Razia Nongjai, Imran Khan**, Journal of Alloys and Compounds 563 (2013) 12.

70. The extrinsic origin of magnetodielectric effect in La_2NiMnO_6 double pervoskite, **Devi Chandrasekhar, A. K. Das, A. Venimadhav**, J. Phys.: Condens. Matter 24 (2012), 495901.

71. Structural, transport and magnetotransport in nonmagnetic Al^{3+} doped mixed valent $La_{0.7}Ca_{0.3}Mn_{1-x}Al_xO_3$ manganites, **Jalshikhaba S. Rathod, Uma Khachar, R. R. Doshi, P. S. Solanki and D. G. Kuberkar**, International Journal of Modern Physics B, 26 (2012) 1250136.

72. Transport and Magneto-Transport Properties of Ru Doped $Ln_{0.67}Sr_{0.33}MnO_3$ (Ln = La, Pr, and Nd), Deepshikha Bhargava, Tejas M. Tank, Ashish Bodhaye and Sankar P. Sanyal, Trans Indian Inst Met (2012); DOI 10.1007/s12666-012-0155-4

73. Effect of Sintering Temperature on the Glassy Precursor Synthesis of Superconducting $Bi_{1.6}Pb_{0.4}Sr_2Cu_4Ca_3O_{12+\delta,}$ **T. Kannan** and **P. Pradeep**, J Supercond Nov Magn. 25 (2012) xxxxx.DOI 10.1007/s10948-012-1703-1

74. Effect of "dipolar-biasing" on the tunability of tunneling magnetoresistance in transition metal oxide systems, **P. Anil Kumar** and **D. D. Sarma**, Appl. Phys. Letters 100 (2012) 262407.

75. Correlation Between Charge, Spin and Lattice in La–Eu–Sr Manganites, **K. Raju, S. Manjunathrao** and **P. Venugopal Reddy**, J. Low Temp Phys. 168 (2012) 334; DOI 10.1007/s10909-012-0630-7.

76. Wide Range Magnetoresistance in Rare Earth Manganite Through Substitution of Magnetic Impurity, Reena Singh, Deepika Bhuwal, Rashmi Yadav, Subhash Khatarkar, and **Vilas Shelke**, IEEE Transactions on Magnetics 48 (2012) 1155.

77. Band offset measurements and magneto-transport properties of epitaxial TiO_{2-x} (x = 0.05)/$La_{0.7}Sr_{0.3}MnO_3$ heterostructure, R. J. Choudhary, Komal Bapna, and D. M. Phase, Appl. Phys. Lett. 102 (2013) 142408.

78. Low temperature thermoelectric properties of Cu intercalated TiSe2: a charge density wave material, Ranu Bhat#, Ranita Basu#, S. Bhattacharya, A.Singh, D.K.Aswal, S.K.Gupta, G.S.Okram, V.Ganesan, D.Venkateshwarlu, C. Surgers, M. Navaneethan, Y.Hayakawa, Applied Physics A (Accepted)

79. Role of strain and microstructure in chemical solution deposited La0.7Pb0.3MnO3 manganite films: Thickness dependent swift heavy ions irradiation studies, **Bharat Kataria, P.S. Solanki, Uma Khachar, Megh Vagadia, Ashish Ravalia, M.J. Keshvani**, **Priyanka Trivedi**, D. Venkateshwarlu, V. Ganesan, **K. Asokan, N.A. Shah, D.G. Kuberkar**, Radiation Physics and Chemistry (2013) In Press

80. Attenuating Large Magneto-Entropy, Heat-Capacity And Adiabatic Temperature,Change in Heusler Ni41-XMn50Sn9+X(X=1.5) Alloys, **A. A. Prasanna, S. Ram**, V. Ganesan and S. Shanmukharao Samantham, Journal of Emerging Trends in Engineering and Applied Sciences (JETEAS) 3 (4), (2012) 601

81. Investigation of Surface Free Energy for PTFE Polymer by Bipolar Argon Plasma Treatment",**S. M. Pelagade, N. L. Singh, R. S. Rane, S. Mukherjee,** U. P. Deshpande, V. Ganesan, T. Shripathi, Journal of Surface Engineered Materials and Advanced Technology 2 (2012) 132

82. Bulk-heterojunction morphology control during spin coating: Modelling diffusion assisted phase separation, **Ghosh, S.S., Lonkar, G.S., Mahajan, M.S., Jadkar, S.R., Waman, V.S., Kamble, M.M**., Ganesan, V**., Sali**, **J.V**.,Applied Physics Letters, 101 (17), art. no. 173305, . (2012)

83. Optoelectronic and low temperature thermoelectric effects in the OVC n-CuIn3Se5 thin films, **Jacob, R., Geethu, R**., Shripathi, T., Okram, G.S., Ganesan, V., **Pradeep, B., Urmila, K.S., Philip, R.R**., Physica Status Solidi (A) Applications and Materials Science, 209 (11), pp. 2195-2200. (2012)

84. Dielectric, magnetic, and thermodynamic properties of Y 1-xSrxMnO3 (x = 0.1 and 0.2), **Thakur, R.K., Thakur, R**., Shanmukharao Samatham, S**., Kaurav, N**., Ganesan, V., **Gaur, N.**K., Okram, G.S., Journal of Applied Physics, 112 (10), art. no. 104115, . (2012)

85. Effect of silver incorporation in phase formation and band gap tuning of tungsten oxide thin films,Jolly Bose,R.,Vinod Kumar,R., Sudheer,S.K., Reddy,V.R., Ganesan,V.,Mahadevan Pillai, V.P. Journal of Applied Physics, 112 (11), art. no. 114311,(2012)

86. Thermal and magnetic response of divalent Sr doped hexagonal YMnO3, **Thakur, R.K., Thakur, R**., Bharathi#, A., Ganesan, V., Gaur, N.K.,Modern Physics Letters B, 26 (30), art. no. 1250201 (2012)

87. Improved crystallinity, spatial arrangement and monodispersity of submicron La 0.7Ba 0.3MnO3 powders: A citrate chelation approach,Rao, C.N#., Samatham, S.S., Ganesan, V., Sathe, V.G., Phase, D.M., Kale, S.N#.Journal of Magnetism and Magnetic Materials, 324, 3766 (2012)

88. Anomalous thermal expansion of Sb 2Te 3 topological insulator, Dutta#, P., Bhoi#, D., Midya, A#., Khan, N#., Mandal, P#., Shanmukharao Samatham, S., Ganesan, V.,Applied Physics Letters, 100, 251912 (2012)

89. Transparent conducting indium molybdenum oxide films by pulsed laser ablation,**Beena, D., Vinodkumar, R., Navas, I**., Ganesan, V., **Yamuna, A., Mahadevan Pillai, V.P**, Journal of Alloys and Compounds, 539, 63 (2012)

90. Grain morphology and size disorder effect on the transport and magnetotransport in Sol-Gel grown nanostructured manganites, **Kuberkar, D.G., Doshi, R.R., Solanki, P.S., Khachar, U., Vagadia, M., Ravalia**, A., Ganesan, V. Applied Surface Science, 258, 9041 (2012)

91. Effect of Co substitution on the magnetic properties of BiFeO 3, **Ray, J., Biswal, A.K., Acharya, S**., Ganesan, V., **Pradhan, D.K., Vishwakarma, P.N**. Journal of Magnetism and Magnetic Materials, (Article in Press) (2012)

92. Large Adiabatic Temperature Change in Magnetoelastic Transitioin in Nanocrystallites of Heusler Ni50Mn32Sn18 Alloys. **A.A.Prasanna, S.Ram**, V. Ganesan and S.S.Rao, A book chapter in Functional Materials published by McMillan Publishers India Ltd, New Delhi (2012)

93. Bulk interface engineering for enhanced magnetization in multiferroic BiFeO3 compounds. S**hreeja Pillai, Deepika Bhuwal**, Alok Banerjee, and **Vilas Shelke**. Appl. Phys. Lett**.** 102, 072907 (2013).

94. Structural, Optical and Magnetic Properties of Multiferroic $GdMnO_3$ Nanoparticles.**P. Negi, G. Dixit, H. M. Agrawal, and R. C. Srivastava**.J. Supercond. Nov. Magn**.**, 26, 1611 (2013).

95. Functionalization of $La_{0.7}Sr_{0.3}MnO_3$ nanoparticles with polymer: Studies on enhanced yperthermia and biocompatibility properties for biomedical applications.**N. D. Thorat, V. M. Khot, A. B.Salunkhe**, R. S. Ningthoujam[#], **S. H. Pawar**.Colloids and Surfaces B: Biointerfaces**,** 104, 40 (2013).

96. Surface functionalized LSMO nanoparticles with improved colloidal stability for hyperthermia applications.**N. D. Thorat, V. M. Khot, A. B. Salunkhe**, **A. I. Prasad**, R. S. Ningthoujam[#] and **S. H. Pawar**.J. Phys. D: Appl. Phys., 46, 105003 (2013).

97. Low temperature magnetic ground state in bulk $Co_{0.3}Zn_{0.7}Fe_2O_4$ spinel ferrite system: Neutron diffraction, magnetization and ac-susceptibility studies. **Harshida Parmar, Prashant Acharya, R.V.Upadhyay**, V. Siruguri, Sudhindra Rayaprol.Solid State Sciences, 153, 60 (2013).

98. Effect of Co substitution on the magnetic properties of $BiFeO_3$. **J. Ray, A. K. Biswal, S. Acharya**, V.Ganesan, **D. K. Pradhan, P. N.Vishwakarma**. J. Magn. Magn. Mater**.**, 324, 4084 (2012).

99. Enhancement in the magnetic moment with Cr^{3+} doping and its effect on the magneto structural properties of $Ce_{0.1}Y_{2.9}Fe_5O_{12,}$ **S. R. Naik and A. V. Salker**.Phys. Chem. Chem. Phys**.**, 14, 10032 (2012).

100. Proton radioactivity half-lives with Skyrme interactions, **T. R. Routray, A. Mishra, S. K. Tripathy, B. Behera** and D. N. Basu[#], European Physical Journal A 48 (2012) 12077.

101. Optical potential obtained from relativistic-mean-field theory-based microscopic nucleon–nucleon interaction: applied to cluster radioactive decays, B**. Singh, M. Bhuyan,** S. K. Patra[#] and **Raj K. Gupta**, **J. Phys. G: Nucl. Part. Phys. 39 (2012) 025101.**

102. Optical characterization of nano-sized organic carbon particles emitted from a small gasoline engine, **B. Paul**, **A. Datta**, A. Datta and A. Saha, Particulog*y* (2013), In press.

103. A comparison of chemical structures of soot precursor nanoparticles from liquid fuel combustion in flames and engine", **B. Paul**, **A. Datta**, A. Datta and A. Saha Journal of Nanoparticle Research (2013), In press.

104. Biophysical studies of mutated K562 DNA (Erythroleukemic cells) binding to Adriamycin and Daunomycin reveal that mutations induce structural changes influencing binding behaviour, **D. Ghosh**, **C. Saha**, M. Hossain, **S. K. Dey**, G. Suresh Kumar, Journal of Biomolecular Structure and Dynamics (2012), In press,

105. Black tea extract: A supplementary antioxidant in radiation induced damage to DNA and normal lymphocytes, **D. Ghosh**, **S. Pal**, **C. Saha**, **A. K. Chakrabarti**, **S. C. Dutta**, **S. K. Dey**, Journal of Environmental Pathology, Toxicology and Oncology 31, 155 (2012)

106. Studies on black tea (Camellia sinensis) extract as a potential antioxidant and a probable radioprotector' **S. Pal**, **C. Saha**, **S. K. Dey**, Radiation and Environmental Biophysics (2013), In Press.

107. Influence of galloyl moiety in interaction of epicatechin with bovine serum albumin: A spectroscopic and thermodynamic characterization, **S. Pal**, **C. Saha**, M. Hossain, **S.K. Dey**, G. Suresh Kumar. PLosOne, 7, e43321 (2012).

108. Fabrication of polypyrrole/graphene oxide nanocomposites by liquid/liquid interfacial polymerization and evaluation of their optical, electrical and electrochemical properties, **C. Bora**, **S.K. Dolui**. Polymer **53**, 932 (2012).

109. Structural and magnetic properties of geometrically frustrated multiferroic $ErMnO_3$ nanoparticles. **B. Raneesh**, A. Saha, D. Das, **N. Kalarikkal**, *Journal of Alloys and Compounds* 551, 654 (2013).

110. Effect of gamma radiation on the structural, dielectric and magnetoelectric properties of nanostructured hexagonal $YMnO_3$, **B. Raneesh**, A. Saha and **N. Kalarikkal**, Radiation Physics and Chemistry (2013), In Press.

111. Spectroscopic properties of γ-irradiated rare earth oxide based ferrofluids, **M. Devi**, **N. Paul, D. Mohanta** and A. Saha, Journal of Experimental Nanoscience, 7, 586 (2012).

112. Optical and rheological study of gamma irradiated rare-earth nanoparticle based Ferrofluids, **N. Paul, D. Mohanta** and A. Saha, Nuclear Instruments and Methods in Physics Research *B* 292, 45 (2012).

113. Synthesis, structure, DNA binding, and nuclease activity of a 3d–4f mixed metal nitrosyl complex$[Pr(phen)_2(MeOH)(H_2O)_2][Fe(CN)_5(NO)](Phen)(DMF)(MeOH)$, **S. R. Chowdhury**, **M. Selim**, **S. Chatterjee**, S. Igarashi, Y. Yukawa and **K. K. Mukherjea,** Journal of Coorination Chemistry, 65, 3469 (2012**).**

114. Self assembled site for luminescence generation: Polyethylene Glycol Vesicles, S. **P. Paik**, **S. K. Ghatak**, D. Dey and **K. Sen,** Analytical Chemistry *84*, 7555 **(**2012**).**

115. Oxidative Degradation of Fensulfothion by Hydroxyl Radical in Aqueous Medium, **M. M. Sunil Paul, U. K. Aravind**, G. Pramod and **C. T. Aravindakumar**, Chemosphere (2013) (in press).

116. Facile room temperature synthesis of Lanthanum Oxalate nanorods and their interaction with antioxidative Naphthalimide derivative, **S. Chall**, **S. Pramanik**, **S. Dhar**, A. Saha and **S. C. Bhattacharya**, Journal of Nanoscience and Nanotechnology, 12, 2229 (2012).

117. Single step aqueous synthesis of pure rare earth nanoparticles in biocompatible polymer matrices, **S. Chall**, A. Saha, S. K. Biswas, A. Datta and **S. C. Bhattacharya**, Journal of Materials Chemistry 22, 12538 (2012).

118. Sodium titaniumsilicate as ion exchanger: synthesis, characterization and application in separation of ^{90}Y from ^{90}Sr, **R. Chakraborty** and **P. Chattopadhyay**, J. Radioanal. Nucl. Chem. (accepted).

119. Polymerized linseed oil coated quartz crystal microbalance for the detection of volatile organic vapours, **R. Das**, S. Biswas, **R. Bandyopadhyay**, **P. Pramanik**, Sensor and Actuator B: Chemical (2013), In press.

120. Sodium titaniumsilicate as ion exchanger: synthesis, characterization and application in separation of ^{90}Y from ^{90}Sr; **R. Chakraborty** and ***P. Chattopadhyay***; Journal of Radioanalytical and Nucear. Chemistry, 294, 31 (2012).

121. One-dimensional Ti–O based nanotubes as ion exchanger: synthesis, characterization and application in radiochemical separation of carrier-free ^{137m}Ba from ^{137}Cs; **R. Chakraborty**, B. Sen, S. Chatterjee and **P. Chattopadhyay**; *Radiochimica Acta*, 101, 33 (2013).

122. Study of photoinduced interaction between calf thymus-DNA and bovine serum albumin protein with $H_2Ti_3O_7$ nanotubes; **R. Chakraborty**, S. Chatterjee, S. Sarkar and **P. Chattopadhyay**, Journal of Biomaterial Nanobiotechnology, 3**,** 462 (2012).

123. Study of trace metals in Indian major carp species from wastewater-fed fishponds of East Calcutta Wetlands, **Anulipi Aich**, Anindita Chakraborty, Mathumal Sudarshan, **Buddhadeb Chattopadhyay** and **Subhra Kumar Mukhopadhyay**. Aquaculture Research 43 (1), 53-65 (2012)

124. Radio-attenuated leishmanial parasites as immunoprophylactic agent against experimental murine visceral leishmaniasis, **Sanchita Datta, Rupchand Adak, Priyanka Chakraborty, Arun Kumar Haldar, Surajit Bhattacharjee**, Anindita Chakraborty, Syamal Roy, **Madhumita Manna**. Experimental Parasitology 130, 39–47 (2012)

125. Therapeutic immunization with radio-attenuated Leishmania parasites through i.m.route revealed protection against the experiment murine visceral leishmaniasis, Sanchita Datta, **Madhumita Manna**, **Supriya Khanra, Moumita Ghosh Radhaballav Bhar**, Anindita Chakraborty, Syamal Roy. Parasitology Research 111, 361-369 (2012)

126. Physiological and chemical response of epiphytic lichen, Flavoparmelia caperata (L.) Hale, to the urban environment of Kolkata, India. S. Majumder, D. Mishra, S. S. Ram, **N. K. Jana**, **S. Santra**, M. Sudarshan, A. Chakraborty, Environmental Science and Pollution Research. DOI: 10.1007/s11356-012-1224-2. (2012)

127. A study on soil physico-chemical, microbial and metal content in Sukinda chromite mine of Odisha, India., **S. Das**, S. S. Ram, **H. K. Sahu**, **D. S. Rao**, A. Chakraborty, M. Sudarshan, **H. N. Thatoi**. Environmental Earth Sciences. DOI 10.1007/s12665-012-2074-4 (2012)

128. Heavy metal contamination, physico-chemical and microbial evaluation of water samples collected from chromite mine environment of Sukinda, India., **S.Das, S.C. Patnaik, H.K.Sahoo**, A.Chakraborty, M.Sudarshan, **H.N.Thatoi**. Transactions of Non-ferrous metal society of China, 23(2), 484-493 (2013)

129. Morphological and protein profile alterations in *Withania somnifera* L.with response to iron stress.**Rout J. R, Sahoo S.L** . Indian Journal of Life sciences 2(1): 21-25. (2012).

130. Copper stress induced alterations in protein profile and antioxidant enzyme activities in the in vitro grown *Withania somnifera* L, **Jyoti R Rout** , Shidharth S Ram , **Ritarani das**, Anindita. Chakrabortyy, Mathummal. Sudarshan, **Santilata Sahoo.** Physiology and Molecular Biology of Plants doi 10.1007/s12298-013-167-5 (2013)

131. Antioxidant enzyme gene expression in response to copper stress in *Withania somnifera* L. Plant Growth Regulation **Rout J. R, Sahoo S.L**(On line-DOI: 10.1007/s10725-013-9806-7), 2013

132. Anthracene appended coumarin derivative as a Cr(III) selective turn-on fluorescent probe for living cell imaging: A green approach towards speciation studies, **SubarnaGuha, SisirLohar, Arnab Banerjee, Animesh Sahana**,Jesús Sanmartín Matalobos, **Debasis Das**,Anal Methods, 4 (2012) 3163.

133. Thiophene anchored coumarin derivative as a turn-on fluorescent probe for Cr^{3+}: Cell imaging and speciation studies, **SubarnaGuha, SisirLohar,AnimeshSahana, Arnab Banerjee, Debasis Das**,Talanta 91 (2012) 18.

134. Thiophene anchored naphthalene derivative: Cr^{3+} selective turn-on fluorescent probe for living cell imaging, Analytical methods,**Sudipta Das, AnimeshSahana, Arnab Banerjee, SisirLohar, SubarnaGuha**, JesúsSanmartínMatalobos, **Debasis Das**,Anal Method, 4 (2012) 225**4**.

135. Ni(II) induced excimer formation of a naphthalene based fluorescent probe for living cell imaging,**Arnab Banerjee, AnimeshSahana, SubarnaGuha, SisirLohar**, IpsitHauli, **SubhraKantiMukhopadhyay**,JesúsSanmartínMatalobos,**Debasis Das**, Inorg. Chem. 51 (2012) 5699.

136. Cd(II) triggered excimer-monomer conversion of a pyrene derivative: Time dependent red-shift of monomer emission with cell staining application,**AnimeshSahana, Arnab Banerjee, SisirLohar, SubarnaGuha, Sudipta Das, SubhraKantiMukhopadhyay, Debasis Das**,Analyst, 137 (2012) 3910.

137. Highly selective organic fluorescent probe for azide ion: Formation of a "Molecular Ring",AnimeshSahana, **Arnab Banerjee, SubarnaGuha, SisirLohar, AmarnathChattopadhyay, SubhraKantiMukhopadhyay, Debasis Das,** Analyst, 137 (2012) 1544.

138. Crystal structure and interaction of 6-amino coumarin with nitrite ion for its selective fluorescence detection, **SubarnaGuha, SisirLohar**, Michael Bolte, Damir A. Safin, **Debasis Das**, Spec. Lett.45 (2012) 225.

139. A naphthalene exciplex based Al^{3+} selective on-type fluorescent probe for living cell at physiological pH range: Experimental and computational studies,**Arnab Banerjee, AnimeshSahana, Sudipta Das, SisirLohar, SubarnaGuha, BidishaSarkar, SubhraKantiMukhopadhyay, Asok K Mukherjee, Debasis Das**, Analyst, 137 (2012) 2166.

140. Al^{3+} induced green luminescent fluorescent probe for cell imaging and naked eye detection, **DebasisKarak, SisirLohar, AnimeshSahana, SubarnaGuha, Arnab Banerjee, Debasis Das**, Anal Methods, 4 (2012) 1906.

141. Spectroscopic studies of a new multi-element sensitive fluorescent probe derived from 2-(2-pyridyl)benzimidazole: Selective discrimination of Zn^{2+} from its congeners,**SisirLohar**, DebasisKarak**,SubarnaGuha, Arnab Banerjee, AnimeshSahana, Debasis Das**, Spec. Lett.DOI: accepted, 2012.

142. Bacterial isolatesof marine coast as commercial producer of proteas **S.Das, I.Mukherjee**, M.Sudarshan, T.P.Sinha, **A.R.Thakur** and **Shaon Raychoudhury** , Online Journal of Biological Sciences, 12, (3) 96-107, 2012

143. Isolation of nitrate and phosphate removing bacteria from various environmental sites, Debroy S, S.Das, S.Ghosh, S.Banerjee, D.Chatterjee, A.Bhattachatya, I.Mukherjee and Shaon Raychaudhuri, Online journal of Biological Sciences, 12 (2) 62-71, 2012

144. Degumming of Raw Silk Fabric With the help of marine extracellular proteas, **Das Shumana**, Mathummal Sudarshan, **Ashoke Ranjan Thakur** and **Shaon Raychaudhuri**, American Journal of Biochemistry and Biotechnology9 (1) 12-18, 2013

145. Peptide assisted synthesis and functionalization of gold nanoparticles and their adsorption by chitosan particles in aqueous dispersion, **A. Nimrodh Ananth**, **S. Umapathy**, G. Ghosh, **T. Ramprasath**, **M. A. Jothi Rajan**, Adv. Nat. Sci: Nanosci. Nanotechnol. **3** (2012) 045010.

146. Counterion induced irreversible denaturation of hen egg white lysozyme upon electrostatic interaction with iron oxide nanoparticles: A predicted model, G. Ghosh, L. Panicker#, R.S. Ningthoujam#, K.C. Barick#, R. Tewari#, Colloid Surf. B: Biointerface **103** (2013) 267.

147. Spectroscopic Approach of the Interaction Study of Amphiphilic Drugs with the Serum Albumins – **A.B. Khan, J.M. Khan, M.S. Ali, R.H. Khan** and **Kabir-ud-Din:** Colloids Surf. B, **87**(2011) 447-453.

148. Interaction of Amphiphilic Drugs with Human and Bovine Serum Albumins by Various Spectroscopic Techniques – **A.B. Khan, J.M. Khan, M.S. Ali, R.H. Khan** and **Kabir-ud-Din**: Spectrochim. Acta, Part A **97**(2012)119-124.

149. Synthesis of stimuli responsive PEG47–b-PAA126–b-PSt_{32} triblock copolymer and its self-assembly in aqueous solutions - **S. Chavda, S. Yusa, M. Inoue, L. Abezgauz, E. Kesselman, D. Danino, P. Bahadur,** European Polymer Journal **49** (2013) 209–21.

150. Thermodynamic Energetics of Charged Micellar Solutions with and without Salts at the Cloud Point- **Sanjeev Kumar** and **Arti Bhadoria**, J. Chem. Eng. Data **57** (2012) 521-525.

151. Morphologies near Cloud Point in Aqueous Ionic Surfactant: Scattering and NMR Studies- **Sanjeev Kumar, Arti Bhadoria, Harsha Patel** and V.K.Aswal#, J. Phys Chem.B **116** (2012) 3699-3703.

152. Single phase synthesis and room temperature neutron diffraction studies on multiferroic $PbFe_{0.5}Nb_{0.5}O_3$ – **S. Matteppanavar**, **B. Angadi** and S. Rayaprol, AIP Conf. Proc. **1512** (2013) 1232.

153. Low temperature magnetic ground state in bulk $Co_{0.3}Zn_{0.7}Fe_2O_4$ spinel ferrite system: Neutron diffraction, magnetization and ac-susceptibility studies, **Harshida Parmar**, **Prashant Acharya**, **R. V. Upadhyay**, V. Siruguri and S. Rayaprol, Solid State Commun. **153** (2013) 60 – 65.

154. Ionic liquid induced sphere-to-ribbon transition in the block copolymer mediated synthesis of silver nanoparticles- **Saurabh S. Soni, Rohit L. Vekariya,** and V. K. Aswal#, RSC Adv. (2013) Advance Article (DOI: 10.1039/C3RA41138A).

155. Investigation of atomic anti-site disorder and ferrimagnetic order in the half-metallic Heusler alloy Mn_2VGa; **K. Ramesh Kumar**, **N. Harish Kumar**, P D Babu, **S. Ventakesh** and S Ramakrishnan; J. Phys. Condes. Matter: **24**, 336007 (2012)

156. Concentration dependence in kinetic arrest of first order magnetic transition in Ta doped $HfFe_2$; R. Rawat, P. Chaddah, Pallab Bag, P. D. Babu and V. Siruguri, J. Phys. Condens. Matter: **25** 066011 (2013)

157. Positive Temperature coefficient of resistance of tetragonal Ti^{4+} doped nano $SrFeO_{3-\delta}$; **A. Sendilkumar**, **K. C. James Raju**, P.D. Babu and **S. Srinath**; J. Alloys and Compounds **561**, 714 (2013)

158. Structural and Mössbauer investigation of nanocrystalline $SrFe_{1-x}Ti_xO_{3-\delta}$; **A. Sendilkumar**, P. D. Babu, **M. Manivelraja**, V. R. Reddy, A. Gupta, and **S. Srinath**; J. Am. Ceram. Soc. (2013, in press)

159. Size dependent magnetic and dielectric properties of nano $CoFe_2O_4$ prepared by a salt assisted gel-combustion method; K. Vasundhara#, S. N. Achary#, S. K Deshpande, P. D. Babu, S. S. Meena# and A. K. Tyagi#; J. Appl. Phys.113,194101 (2013)

160. Investigation of Structural and magnetic phases of $Y_{0.5}Ca_{0.5}MnO_3$ nano crystallites - **Putul Malla Chowdhury**, **Barnali Ghosh**, **A. K. Raychaudhuri**, S. D. Kaushik and V. Siruguri, J. Nano Part. Res. **15** (2013) 1585.

161. Mössbauer Effect in Tetragonal $SrFeO_{3-\delta}$, **A. Sendilkumar**, V.R.Reddy , **M. Manivel Raja**,P.D. Babu, A. Gupta, **S. Srinath**, AIP Conf. Proc. **1447**, 1241 (2012)

162. Size effect on the structural, magnetic and magnetotransport properties of electron doped manganite La0.15Ca0.85MnO3, **Rini Thomas, Gangadhar Das, Rajib Mondal, R. Pradheesh, R. N. Mahato,** T. Geetha Kumary#**,** R. Nirmala, A. V. Morozkin, J. Lamsal, W. B. Yelon, A. K. Nigam and S. K. Malik**,** Journal of Applied Physics **111** (2012) 07D729

163. Structural phase analysis of nanocrystalline Mg:ZrO2 ,**S. Senthilkumaran, A. Ahamed Fazil, S. Kannan, P. Thangadurai ,** AIP Conf. Proc. 1512, 376 (2013

164. Epicatechin ameliorates ionising radiation-induced oxidative stress in mice liver, Mahuya Sinha, Dipesh K. R. Das, Krishnendu Manna, Sanjukta Datta, Tanusree Ray, Alok Kumar Sil& Sanjit Dey. Free Radical Research, 46(7), 842-849, (2012)

165. Radiation Protection by Major Tea Polyphenol, Epicatechin, Dipesh Kr Das, Mahuya Sinha, Amitava Khan, Kankana Das, Krishnendu Manna and Sanjit Dey. Int J Hum Genet, 13(1), 59-64, (2013)

166. Amelioration of ionizing radiation induced lipid peroxidation in mouse liver by Moringa oleifera Lam. Leaf extract, Mahuya Sinha, Dipesh Kr Das, Sanjukta Datta, Santinath Ghosh and Sanjit Dey. Indian Journal of Experimental Biology, 50: 209-215 (2012)

167. Alterations in transcriptome and proteome in metallothioneins following oxidative stress induced by sub-lethal doses of cadmium and gamma rays in Plantago ovata Forsk, Nirmalya Ghosal, Shonima Talpatra, Amitava moulick, Anindita Chakraborty and Sarmistha Sen Ray Chaudhuri. International Journal of Radiation Biology Vol 89(7), 571-582 (2013) (doi:10.3109/09553002.2013.782109).

168. Molecular cloning, modeling and characterization of type 2 metallothionein from *Plantago ovata* Forsk, Amitava Moulick, Debasis Mukhopadyay, Shonima Talpatra, Nirmalya Ghoshal and Sarmistha Sen Ray Chaudhuri. Accepted in "Sequencing" on 11th Feb 2013.

169. Plantago ovata metallothionein type 1 (mt 1) gene, partial cds, Nirmalya ghoshal and Sarmistha Ray Chaudhuri. GenBank Accession: JN798189.1 GI:363498963

170. Plantago ovata metallothionein type 3 (mt 3) gene, partial cds, Nirmalya ghoshal and Sarmistha Ray Chaudhuri. GenBank Accession: JX560797.1 GI:410031850

171. Gamma irradiation in modulating cadmium bioremediation potential of Aspergillus sp, Dipanwita Das, A. Chakraborty, S.Bhar, M.Sudarshan, S.C.Santra. IOSR journal of Environmental Sc.,Toxicology and Food Technology,3(6), 51-55 (2013)

172. Exposure to ionizing radiation –a possibility for lignocellulosic metal stressed waste degradation by microbes?' Dipanwita Das, A. Chakraborty, S.C.Santra. Indian Biologist 45(1), 105-112 (2013)

173. Study of physical properties of nanocrystalline nickel, Satish, G.S. Okram and N. Gupta, Intern. J. Eng. Res. Dev. 3, 41-46 (2012).

174. Raman Spectroscopy: Basics and Applications (Book Chapter) PJ McNally, VG Sathe, Nanomaterials: Processing and Characterization with Lasers, 495-534 Wiley-VCH Verlag GmbH & Co. KGaA

175. Structure–property correlations in lead silicate glasses and crystalline phases**Arshpreet Kaur, Atul Khanna, Sapna Singla, Anupam Dixit, G.P. Kothiyal, K. Krishnan, Suresh K. Aggarwal,** V. Sathe**, Fernando González & Marina González-Barriuso,** Phase Transitions 1-19 (2012) DOI:10.1080/01411594.2012.707655

176. Highly conducting phosphorous doped n-type nc-Si:H films by HW-CVD for c-Si heterojunction solar cells. **Vaishali S. Waman, Mahesh M. Kamble, Sanjay S. Ghosh, Azam Mayabadi,** Vasant. G. Sathe**, Habib M. Pathan, Shashikant D. Shinde, Kiran P. Adhi and Sandesh R. Jadkar,** RSC Adv., **2**, (2012),9873-9880,DOI:10.1039/C2RA21618C

177. Effect of Cd dopant on electrical and optical properties of ZnO thin films prepared by spray pyrolysis route, **Acharya, A.D.**, **Moghe, S., Panda, R**., **Shrivastava, S.B**., Gangrade, M., Shripathi, T., Phase, D.M., Ganesan, V., Thin Solid Films, 525, pp. 49-55. (2012)

178. Growth and characterization of nano-structured Sn doped ZnO, **Acharya, A.D., Moghe, S., Panda, R., Shrivastava, S.B**., Gangrade, M., Shripathi, T., Phase.D.M., Ganesan, V.Journal of Molecular Structure, 1022, 8 (2012)

179. Pygmy dipole strength in ^{86}Kr and systematics of N=50 isotones.R. Schwengner, R. Massarczyk, G. Rusev, N. Tsoneva, D. Bemmerer, R. Beyer,R. Hannaske, A. R. Junghans, J. H. Kelley, E. Kwan, H. Lenske, M. Marta, R. Raut, K. D. Schilling, A. Tonchev, W. Tornow, and A. Wagner.Phys. Rev. C 87, 024306(2013).

180. Electromagnetic dipole strength of 136Ba below the neutron separationenergy, R. Massarczyk, R. Schwengner, F. Dönau, E. Litvinova, G. Rusev, R. Beyer, R. Hannaske, A. R. Junghans, M. Kempe, J. H. Kelley, T. Kögler, K. Kosev, E. Kwan, M.

Marta, A. Matic, C. Nair, R. Raut, K. D. Schilling, G.Schramm, D. Stach, A. P. Tonchev, W. Tornow, E. Trompler, A. Wagner, andD. Yakorev, Phys. Rev. C 86, 014319(2012)

181. Onset of deformation at N=112 in Bi nuclei H. Pai#, G. Mukherjee#, R. Raut, S. K. Basu#, A. Goswami#, S. Chanda, T.Bhattacharjee#, S. Bhattacharyya#, C. Bhattacharya#, S. Bhattacharya#, S. R.Banerjee#, S. Kundu#, K. Banerjee#, A. Dey#, T. K. Rana#, J. K. Meena#, D.Gupta, S. Mukhopadhyay#, Srijit Bhattacharya#, Sudeb Bhattacharya#, **S.Ganguly,** R. Kshetri#, and **M. K. Pradhan**, Phys. Rev. C 85, 064317(2012)

182. Photodisintegration cross section of the reaction $^{4}He(\gamma,\nu)^{3}He$ at thegiant dipole resonance peak, W. Tornow, J. H. Kelley, R. Raut, G. Rusev, A. P. Tonchev, M. W. Ahmed, A. S. Crowell, and S. C. Stave, Phys. Rev. C 85, 061001(2012)

183. First determination of an astrophysical cross section with a bubblechamber the $^{15}N(\alpha,\gamma)^{19}F$ reaction, C. Ugalde, B. DiGiovine, D. Henderson, R.J. Holt, K.E. Rehm, A. Sonnenschein, A. Robinson, R. Raut, G. Rusev, A.P. Tonchev, Physics Letters B719, 74(2013)

184. Evidence for Multiple Chiral Doublet Bands in ^{133}Ce, A. D. Ayangeakaa, U. Garg, M. D. Anthony, S. Frauendorf, J. T. Matta, B. K. Nayak, D. Patel, Q. B. Chen, S. Q. Zhang, P. W. Zhao, B. Qi, J. Meng, R. V. F. Janssens, M. P. Carpenter, C. J. Chiara, F. G. Kondev, T. Lauritsen, D. Seweryniak, S. Zhu, S. S. Ghugre, and R. Palit, Phys. Rev. Lett. **110**, 172504

185. Tidal Waves in ^{102}Pd: A Rotating Condensate of Multiple *d* Bosons A. D. Ayangeakaa, U. Garg, M. A. Caprio, M. P. Carpenter, S. S. Ghugre, R. V. F. Janssens, F. G. Kondev, J. T. Matta, S. Mukhopadhyay, D. Patel, D. Seweryniak, J. Sun, S. Zhu, and S. Frauendorf, Phys. Rev. Lett. 110, 102501

186. Evolution of structural phase coexistence in a half doped manganite $Pr_{0.5}Sr_{0.5}MnO_3$: An evidence for magneto-structural coupling.**A. K. Pramanik**, **Rajeev Ranjan**, A. Banerjee.J. Magn. Magn. Mater., 325, 29 (2013).

187. Complex $GdSc_{1-x}In_xO_3$ oxides: synthesis and structure driven tunable electrical properties, V. Grover[#], R. Shukla[#], D. Jain[#], S. K. Deshpande, A. Arya[#], C. G. S. Pillai[#] and A. K. Tyagi[#], Chem. Mater. **24**, (2012) 2186.

188. Modulatory role of quercetin against gamma radiation mediated biochemical and morphological alterations of red blood cells. **Dipesh K. Das, Anirban Chakraborty, Mahuya Sinha, Krishnendu Manna, Dipanwita Mukherjee**, Anindita Chakraborty, **Sekhar Bhattacharjee** and **Sanjit Dey**. *International Journal of Radiation Biology*, 2013; Early Online: 1–11 (2013).

189. Structural transport properties of Dy substituted $YBaCo_4O_7$ – **Bharat Singh, Naresh Kumar**, S. Rayaprol and **N. K. Gaur**, AIP Conf. Proc. **1512** (2013) 956.

190. Structure-transport correlations in mono-valent Na+ doped $La_{1-x}Na_xMnO_3$, **S. Kansara**, **D. D. Pandya**, **B. Nimavat**, **C. M. Thaker**, **P. S. Solanki**, S. Rayaprol, M. R. Gonal#, **N. A. Shah**, and **D. G. Kuberkar**, Adv. Mater. Res. **665** (2013) 1.

191. Metal flux crystal growth technique in the determination of ordered superstructure in EuInGe, **U. Subbarao**, **A. Sebastian**, S. Rayaprol, **C. S. Yadav**, **A. Svane**, **G. Vaitheeswaran**, and **Sebastian C. Peter**, Cryst. Growth Des. **13** (2013) 352 – 359.

192. Magnetism driven ferroelectricity above liquid nitrogen temperature in Y_2CoMnO_6, **G. Sharma**, **J. Saha**, S. D. Kaushik, V. Siruguri and **S. Patnaik** (under review in Applied Physics Letters).

193. Magnetization and neutron diffraction study of $Tb_{0.9}Y_{0.1}MnO_3$ - Keka R. Chakraborty#, R. Shukla#, M. D. Mukadam#, S. D. Kaushik, A. K. Tyagi#, V. Siruguri and S. M. Yusuf# AIP Conf. Proc. **1512** (2013) 1094.

194. Enhancement of Photoluminescence in ZnS/ZnO Quantum Dots Interfacial Heterostructures. M. Rajalakshmi#, **S. Sohila**, **R. Ramesh**, and G.M. Bhalerao, Mater. Res. Bull. **47** (2012) 2668-72

195. Optical redshift in the Raman scattering spectra of Fe-doped multiwalled carbon nanotubes: Experiment and theory. G. M. Bhalerao, M. K. Singh#, A. K. Sinha#, and Haranath Ghosh#, Phys. Rev. B **86** (2012) 125419

196. Dynamic disorder and the α-β phase transition in quartz-type $FePO_4$ at high temperature investigated by total neurton scattering, Raman spectroscopy, and density functional theory. G. M. Bhalerao, P. Hermet, J. Haines, O. Cambon, D. A. Keen, M. G. Tucker, E. Buixaderas, and P. Simon, Phys. Rev. B **86** (2012) 134104.

197. Characterizing Microstructural Changes in Ferritic Steels by Positron Annihilation Spectroscopy: Studies on Modified 9Cr-1Mo steel, **S. Hari Babu**, K. V. Rajkumar#, S. Hussain, G. Amarendra#, C. S. Sundar# and T. Jayakumar# Journal of Nuclear Materials, 432 (2013) 266,

198. Growth of ZnTe films by pulsed laser deposition technique, **B. Ghosh, D. Ghosh**, S. Hussain, **R. Bhar, A.K. Pal**, Journal of Alloys and Compounds, **541 (** 2012) 104

199. Studies on CdTe films deposited by pulsed laser deposition technique, **B. Ghosh,** S. Hussain, **D. Ghosh, R. Bhar, A. K. Pal**. Physica B: Physics of Condensed Matter, **407** (2012) 4214

200. Electronic structure of Co2MnSn Heusler alloy, Madhusmita Baral#, Soma Banik#, Tapas Ganguli#, Aparna Chakrabarti#, A. Thamizhavel, D. M. Phase, A. K. Sinha#, and S. K. Deb#, AIP Conf. Proc. 1512, 842 (2013).

201. Two-source coevaporation technique for synthesis of indium phosphide films with controlled composition, **R.N. Gayen**, S. Hussain, **D. Ghosh, R. Bhar, A.K. Pal**, Journal of Alloys and Compounds, **531** (2012) 34

202. Studies on removal of cobalt from an alkaline waste using synthetic calcium hydroxyapatite, Diganta Gogoi#, A. G. Shanmugamani#, S. V. S. Rao#, T. Kumar# & P. K. Sinha#, Journal of Radioanalytical and Nuclear Chemistry,ISSN 0236-5731 J. Radioanal. Nucl. Chem. DOI 10.1007/s10967-012-2378-6

203. Low temperature dielectric properties of $YMn_{0.95}Ru_{0.05}O_3$, R. K. Thakur, R. Thakur, G. S. Okram, N. Kaurav, and N. K. Gaur, AIP Conf. Proc. 1512, 1238-1239 (2013).

204. Electrical properties of strontium doped yttrium manganite oxide, R. K. Thakur, R. Thakur, N. Kaurav, G. S. Okram, and N. K. Gaur, AIP Conf. Proc. 1512, 948-949 (2013).

205. Effect of chromium doping on the resistivity behavior of gadolinium manganite, A. Modi, R. K. Thakur, R. Thakur, G. S. Okram, and N. K. Gaur, AIP Conf. Proc. 1512, 1294 (2013).

206. Reduction of anatase TiO on Si (111) by ion beam sputtering, **VRR Medicherla, RR Mohanta, KL Mohanta**, Nimai C Nayak#, S Choudhary#, S Majumder#, V Solanki#, Shikha Varma#, D.M Phase, V Sathe, AIP Conf. Proc. **1461**, pp. 403-407 (2012)

207. Crystallographic phase control of TiO in thin films deposited by asymmetric bipolar pulsed DC sputtering **PR Sagdeo**, Sekh Maidul#, DD Shinde#, JS Misal#, S Thakur#, NK Sahoo#, A Sagdeo#, S Rai#, C Mukherjee#, K Rajiv#, VG Sathe, M Gupta, *AIP Conf. Proc.* **1451***, 121 (2012);*

208. Transport, magneto transport and magnetic properties of Ru substituted NdMnO3,Deepshikha Bhargava, Tejas M. Tank, Rajeev Rawat, and Sankar P. Sanyal, AIP Conf. Proc. 1536 (2013) 865

209. Core level spectra of disordered Cu-Ni alloys, V. R. R. Medicherla, S. K. Parida, Pallab Bag, Rajeev Rawat, T. Shripathi et al., AIP Conf. Proc. 1461 (2012) 275

210. "Enhanced ferroelectric, magnetoelectric and magnetic properties in Pr and Cr co-doped $BiFeO_3$ nanotubes fabricated by template assisted route", Rajasree Das, Gobinda Gopal Khan and Kalyan Mandal , J. Appl. Phys. **111**, 104115 (2012).

211. Phase –segregation limit in ZnCdO thin films deposited by sol-gel method : Astudy of structural, optical and electrical properties. **Amanpal Singh, Dinesh Kumar**, P.K.Khanna,**Mukesh Kumar** and **B. Prasad**, ECS Journal of Solid State Science and Technology . 2(9),Q136-Q141 (2013)

212. Magnetic properties of sol-gel derived Gd2O3 nanoparticles, **R. Ray**, **Sumita Biswas, S. Das,** and **M. Patra**, AIP Conf. Proc. 1447, 319 (2012).

213. Promising role of ferulic acid, atorvastatin and their combination in ameliorating high fat diet-induced stress in mice, **Swaraj Bandhu Kesh, Kunal Sikder, Krishnendu Manna, Dipesh Kr. Das, Amitava Khan, Nilanjan Das, Sanjit Dey**. Life Sciences, 92, 938–949 (2013)

214. Dielectric relaxation behavior of AxCo1−xFe2O4 (A = Zn, Mg) mixed ferrites **Kavita Verma, Ashwini Kumar, Dinesh Varshney,** Journal of Alloys and Compounds **526**, 91-97

215. Polycaprolactone composites with TiO2 for potential nanobiomaterials: tunable properties using different phases, **Kamal K. Gupta, Akshay Kundan, Pradeep K. Mishra, Pradeep Srivastava, Sujata Mohanty, Narendra K. Singh, Abhinay Mishrad and Pralay Maiti,** Phys. Chem. Chem. Phys.**14**, 12844-12853

216. Thermoluminescence Study of UV and Gamma Irradiated Limestone, **Jagjeet Kaur, Vikas Dubey, Suryanarayana N.S., Sadhana Agrawal and S.J. Dhoble,** International Journal of Nanotechnology and Applications **6**, 97-104 (2012) ISSN 0973-631X.

217. Structural, photoluminescence and optical propertiesof chemically deposited (Cd12xBix)S thin films as a function of dopant concentration, **R. Das, Rajesh Kumar, ,** Springer Science+Business Media, LLC 2012

218. Synthesis, Characterization and Electrical Conductivity Measurements, of Polypyrrole/ Montmorillonite Nanocomposites , **Priyanka Parmar, Pragyesh Agrawal and Rakesh Bajpai,** Advanced Materials Research **585**, 228-232 (2012).

219. Solubility limits and microwave dielectric properties of Ca(ZrxTi1x)O3 solid solution, **S. Parida, S.K. Rout, N. Gupta , V.R. Gupta ,** Journal of Alloys and Compounds **546**, 216–223 (2013).

220. Magnetic and electrical properties of In doped cobalt ferrite nanoparticles, **Razia Nongjai, Shakeel Khan, K. Asokan, Hilal Ahmed, and Imran Khan,** Journal of Applied Physics 112, 084321 (2012).

221. Structural and Optical Properties of Pure and Copper Doped NiS Nanoparticles, **Banerjee M. , Chongad L., and Sharma A. ,** Manuscript No: ISCA-ISC-2012-15PhyS-34.

222. Self-assembled monolayer coated gold-nanoparticle catalyzed aerobic oxidation of a-hydroxy ketones in water: an efficient one-pot synthesis of quinoxaline derivatives, **Tamalika Bhattacharya, Tridib K. Sarma and Sampak Samanta,** Catal. Sci. Technol. **2**, 2216–2220 (2012).

223. Optical and kinetic studies of CdS:Cu nanoparticles, **Raunak Kumar Tamrakar, D. P. Bisen,** Res Chem Intermed (Nov. 2012) DOI 10.1007/s11164-012-0816-2,

224. Synthesis and photoluminescence of CdSe/PVA nanocomposites, **Kamal Kushwah, Nitendra Gauta, P Sing, Meera Ramrakhain,** Journal of Physics: Conference Series 365, 012014 (2012).

225. Modification in Properties of Fly Ash through Mechanical and Chemical Activation, **A. Sharma, K. Srivastava, V. Devra and A. Rani,** American Chemical Science Journal 2, 177-187

226. Hydrothermal in situ preparation of TiO2 particles onto poly(lactic acid) electrospun nanofibres, **Kamal K. Gupta, Pradeep K. Mishra, Pradeep Srivastava, Mayank Gangwar, Gopal Nath, Pralay Maiti,** Applied Surface Science **264**, 375–382(2013).

227. Microwave green synthesis of PVP-stabilised gold nanoparticles and their adsorption behaviour for methyl orange , **Jolly Pal and Manas Kanti Deb,** Journal of Experimental Nanoscience (Jul 2012); DOI.org/10.1080/17458080.2012.667160

228. Microwave-assisted synthesis of platinum nanoparticles and their catalytic degradation of methyl violet in aqueous solution, **Jolly Pal, Manas Kanti Deb, Dhananjay Kumar Deshmukh, Bhupendra Kumar Sen ,** Applied Nanoscience (Oct. 2012); DOI 10.1007/s13204-012-0170-0

229. Removal of methyl orange by activated carbon modified by silver nanoparticles, **Jolly Pal, Manas Kanti Deb, Dhananjay Kumar Deshmukh, Devsharan Verma,** Applied Water Science (2013); DOI 10.1007/s13201-013-0087-0.

230. Structural and Dielectric studies of Eu3+/Ag nanocrystallites: SiO2-TiO2 Matrices, **Arun Kumar K V, Sunil Thomas, Manju Gopinath, Biju P R, Unnikrishnan N V,** Journal of material Science-Materials in electronics **24**, 1727.

231. Synthesis, spectroscopic, thermal and antimicrobial studies of toluene - 3,4-dithiolatoarsenic(III) derivatives with some oxygen and sulphur donor ligands, **H. P. S. Chauhan and Sumit Bhatiya,** Spectrochimica Acta Part A: Molecular and Biomolecular Spectroscopy 97, 1133-1139(2012).

232. Microstructure and Magnetic Properties of (Fe100-xCox)84.5Nb5B8.5P2 Alloys, **S. N. Kane, S. Tripathi, M. Coisson, E.S. Olivetti, P. Tiberto, F. Vinai, M. Baricco, G. Fiore**, **A. Apolinário, C.T. Sousa, J. P. Araujo, L. K. Varga,** J. Alloys and Compounds **536** S337 (2012).

233. On the optimization of soft magnetic properties of high Bs Fe83.7B14.8Cu1.5 nanocrystalline alloy, **S. N. Kane, Kalpana Singh, Nandkishor Ghodke, L. K. Varga** and A. Gupta, Journal of Physics: Conference Series **365** (2012) 012015

234. Growth and characterization of ferrite film prepared by pulsed laser deposition, **S. N. Kane, M. Satalkar**, D. M. Phase, R. J. Chaudhary, **A. Pasko, M. LoBue, and F. Mazaleyra,** Journal of Physics: Conference Series **365** (2012) 012023.

235. Structural relaxation induced changes in properties and crystallization behaviour of Co80Zr10V10 alloys, **S. N. Kane, S. Panchal, E. Fleury,** Journal of Physics: Conference Series **365** (2012) 012035

236. Growth and characterization of ferrite film prepared by pulsed laser deposition, **S. N. Kane, M. Satalkar,** D. M. Phase, R. J. Chaudhary, **A. Pasko, M. LoBue, and F. Mazaleyrat,** Journal of Physics: Conference Series 365 (2012) 012023

237. Soft Magnetic properties of Mg0.7-xNi0.3ZnxFe2O4 ferrites synthesized by sol-gel auto-combustion technique without post-preparation thermal treatment, **A. Ghosh, M. Satalkar, S. Rathod. S. P. Nag, P. Vyas, S. N. Kane,** N. Ghodke, R. Prasad, R. Dwivedi, International Journal of Modern Physics: Conference Series (In-Press)

238. Influence of Mn Addition On Magnetic And Structural Properties of Barium Hexaferrite, **A. Ghosh, A. Pasko, S. N. Kane, M. Satalkar, R. Prasad, R. Diwedi,S. Ladole, A. S. Aswar**, G. N. P. Oliveira, A. Apolinário, C. T. Sousa, J. P. Araujo and F. Mazaleyrat, American Institute of Physics Conference Proceedings (In-Press)

239. Photoluminescence Investigation of CdWO4:Ce,Er doped nano Phosphors, **Dhaval Modi , M. S. D.Tawde, S. Garg, V. Vishwnath,D. Khatri,N. Patel, K. V. R. Murthy,** International Journal of Luminescence and its applications **2**, 27 (Aug. 2012); ISSN 2277 – 6362.

240. Effect of Reaction Parameters on Structural and Photoluminescence properties of Cerium doped PbWO4 Nano Phosphor, **D.Tawde, M.Srinivas, D. Modi, N. Patel, Verma Vishwanath and K.V.R.Murthy,** International Journal of Luminescence and its applications **3**, 79 (Jan 2013); ISSN 2277 – 6362.

241. Structural and surface morphological studies of long chain fatty acid thin films deposited by Langmuir Blodgett technique, **N. M. Das, D. Roy**, Mukul Gupta, **P. S. Gupta,** Physica B 407, 47774782 (2012).

242. Atomic Force Microscopy Analysis Of Effect Of RF/DC Power Ratio On The Properties Of Co-Sputtered Tixal1-Xn Thin Films, **Ashwini Kumar Singh, Neelam Kumari, S. K. Mukherjee & P.K. Barhai,** IJRRAS 14 (3) March 2013; www.arpapress.com/Volumes/Vol14Issue3/IJRRAS_14_3_15.pdf

243. Effect of annealing on structure and magneto-transport properties of Fe/Au multilayer, S. Singh#, S. Basu#, C. L. Prajapat#, and Mukul Gupta, AIP Conf. Proc. 1512, pp. 730-731; doi:http://dx.doi.org/10.1063/1.4791245.

244. Thermal diffusion in Ni/Al multilayer, M. Swain#, D. Bhattacharya#, S. Singh#, Mukul Gupta, and S. Basu#, AIP Conf. Proc. 1512, pp. 678-679; doi:http://dx.doi.org/10.1063/1.4791219

5.2 Publications from in-house research

245. Metal insulator transition in nanocrystalline $Pr_{0.67}Ca_{0.33}MnO_3$: correlation between supercooling and kinetic arrest, R Rawat, P Chaddah, Pallab Bag, Kalipada Das# and I. Das#, J. Phys.: Condens. Matter 24 (2012) 416001.

246. Investigation of charge states and multiferroicity in Fe-doped h-$YMnO_3$, Sonu Namdeo, A.K. Sinha[#], M.N. Singh[#], and A.M. Awasthi, J. Appl. Phys. **113**, 104101 (2013).

247. Fractional power-law spectral response of $CaCu_3Ti_4O_{12}$ dielectric: many-body effects, Jitender Kumar and A.M. Awasthi, Appl. Phys. Lett. **101**, 062908 (2012).

248. Discovery of strange kinetics in bulk material: correlated dipoles in $CaCu_3Ti_4O_{12}$, A.M. Awasthi *and Jitender Kumar*, J. Appl. Phys. **112**, 054108 (2012).

249. Note: Development of fast heating inert gas annealing apparatus operated at atmospheric pressure, S. C. Das,, A. Majumdar, T. Shripathi, and R. Hippler Rev. Sci. Instrum. 83, 046109 (2012); doi.org/10.1063/1.4704836.

250. Energy and Angle dependent Photoemission study on Si/GeMultilayers using Synchrotron Radiation, S. Tripathi, **A. Sharma** and T. Shripathi, Vaccum (2012) (accepted).

251. Magnetic glass in Shape Memory Alloy : $Ni_{45}Co_5Mn_{38}Sn_{12}$ Archana Lakhani, A. Banerjee, P. Chaddah**,** X. Chen, R. V. Ramanujan. J. Phys.: Condens. Matter **24** 386004(2012).

252. Study of ultrathin magnetic cobalt films on MgO (001).Gagan Sharma, U. P. Deshpande, Dileep Kumar, and Ajay Gupta, J. Appl. Phys. 112, 023910 (2012)

253. Spin-valve-like magnetoresistance in Mn_2NiGa at room temperature, Sanjay Singh, R. Rawat, **S.E. Muthu**, S.W. D'Souza, E. Suard*, A. Senyshyn*, S. Banik[#], P. Rajput*, S. Bhardwaj, A.M. Awasthi, R. Ranjan*, **S. Arumugam**, D.L. Schlagel*, T.A. Lograsso*, Aparna Chakrabarti[#], and S.R. Barman, Phys. Rev. Lett. **109**, 246601 (2012).

254. Modulated structure in the martensite phase of $Ni_{1.8}Pt_{0.2}MnGa$: a neutron diffraction study, Sanjay Singh, K.R.A. Ziebeck*, E. Suard*, P. Rajput*, S. Bhardwaj, A.M. Awasthi, and S.R. Barman, Appl. Phys. Lett. **101**, 171904 (2012).

255. Effect ofconfinement on melting behaviour of cadmium arachidate Langmuir Blodgett multilayer",Pallavi Pandit, Ajay Gupta, Dileep Kumar, **M. Banerjee** and Sigrid Bernstorff *Langmuir* 29 (3950) 2013 DOI: 10.1021/la304463q

256. Effect of silver addition on structural, electrical and magnetic properties of Fe_3O_4 thin films prepared by pulsed laser deposition. Ridhi Master, R. J. Choudhary, and D. M. Phase, J. Appl. Phys 111, 073907 (2012)**.**

257. Resonant photoemission study of epitaxial $La_{0.7}Sr_{0.3}MnO_3$ thin film across Curie temperature.Komal Bapna, R. J. Choudhary, and D. M. Phase, Appl. Phys. Lett. 101, 242402 (2012).

258. Evolution of different structural phases of TiO_2 films with oxygen partial pressure and Fe doping and their electrical properties. Komal Bapna, R. J. Choudhary, and D. M. Phase, Mat. Res. Bull. 47 2001–2007 (2012).

259. Synthesis and signature of M-E coupling in novel self-assembled $CaCu_3Ti_4O_{12}$-$NiFe_2O_4$ nanocomposite structure, Anju Ahlawat, V. G. Sathe, V. Ganesan, D. M. Phase and S. Satapathy#, J. Appl. Phys **111**, 074302 (2012).

260. Effect of Co-doping on the resistivity and thermopower of $SmFe_{1-x}Co_xAsO$ ($0.0 \leq x \leq 0.3$), G. S. Okram, N. Kaurav, A. Soni, A. Pal and V.P.S. Awana, AIP Advances 2, 042137(1-7) (2012).

261. Thermopower of vanadium group of metals: A revisit, G. S. Okram, Ind. J. Cryogenics 38, 34-38 (2013).

262. Signature of Spin-Phonon Coupling in Sr_2CoO_4 Thin Film: A Raman Spectroscopic Study. Pankaj K. Pandey, R. J. Choudhary, Dileep K. Mishra, V. G. Sathe, and D. M. Phase, Appl. Phys. Lett. 102, 142401 (2013).

263. Bulk electronic structure of quasicrystals,J. Nayak, M. Maniraj, A. Rai, S. Singh, Parasmani Rajput, A. Gloskovskii, J. Zegenhagen, D. L. Schlagel, T. A. Lograsso, K. Horn, and S. R. Barman, Phys. Rev. Lett. 109, 216403 (2012).

264. Modulated structure in the martensite phase of $Ni_{1.8}Pt_{0.2}MnGa$: a neutron diffraction study, S. Singh, K. R. A. Ziebeck, E. Suard, P. Rajput, S. Bhardwaj, A. M. Awasthi, and S. R.Barman, Appl. Phys. Lett. 101, 171904 (2012).

265. (3+1)D superspace description of the incommensurate modulation inthe premartensite phase of Ni_2MnGa: a high resolution synchrotron x-ray powder diffraction study, S. Singh, J. Nayak, A. Rai, P. Rajput, A. H. Hill, S. R. Barman, and D. Pandey[#], J. Phys. Condens. Matter FT 25, 212203 (2013).

266. An x-ray absorption spectroscopy study of Ni-Mn-Ga ferromagnetic shape memory alloys, V. G. Sathe, A. Dubey#, S. Banik#, S. R. Barman, L. Olivi, J. Phys. Condens. Matter 25, 046001 (2013).

267. Evidence of Fano resonance in temperature dependent Raman study of CaCu3Ti4O12 and SrCu3Ti4O12 , Dileep K Mishra and V G Sathe, J. Phys.: Condens. Matter FTC 24 (2012) 252202 (IOP SELECT).

268. Study of 0.9 BaTiO3-0.1 NixZn1-xFe2O4 magneto-electric composite ceramics"., Sanjay Kumar Upadhyay and V. Raghavendra Reddy., J. Appl. Phys., 113 (2013) 114107.

269. Study of Aging & De-Aging Behaviour in Un-Doped Polycrystalline Ferroelectric BaTiO3.Sanjay Kumar Upadhyay, V. Raghavendra Reddy, Kavita Sharma, Anil Gome & Ajay Gupta., Ferroelectrics 437 (2012) 171

270. Magnetic and ^{57}Fe Mössbauer study of magneto-electric $GaFeO_3$ prepared by sol-gel route" Kavita Sharma, V. Raghavendra Reddy, Ajay Gupta, A.Banerjee and A.M.Awasthi *J. Phys.: Condens. Matter., 25 (2013) 076002*

271. Low Temperature irreversible field induced magnetic transition in Gd_5Ge_3,Pallavi Kushwaha and R. Rawat, Solid State Communications 152 (2012) 1824.

272. Direct visualization of the first order magnetic transition in $La_{5/8-y}Pr_yCa_{3/8}MnO_3$ (y=0.45) thin film, R. Rawat, Pallavi Kushwaha, Dileep K. Mishra and V.G. Sathe, Phys. Rev. B 87 (2013) 064412.

273. Enhancement of the ferromagnetic metallic phase fraction by extrinsic disorder in phase separated $La_{5/8-y}Pr_yCa_{3/8}MnO_3$ (y = 0.45) thin film, Dileep K Mishra, V G Sathe, R Rawat and V Ganesan, J. Phys.: Condens. Matter 25 (2013) 175003.

274. Raman tensor and domain structure study of single-crystal-like epitaxial films of $CaCu_3Ti_4O_{12}$ grown by pulsed laser deposition. Anju Ahlawat, Dileep K Mishra, VG Sathe, Ravi Kumar[#], TK Sharma[#], J. Phys.: Condens. Matter **25** (2013) 025902

275. Precursor state of Skyrmions in MnSi : a heat capacity study,S. Shanmukharao Samatham and V. Ganesan, Phys. Status Solidi RRL, 7(3), 184 (2013)

276. Competing localization and quantum interference effects in Fe0.9Co0.1Si, S. Shanmukharao Samatham, Venkateshwarlu D, Mohan Gangrade and V. Ganesan, Physica Status Solidi B, 249(11), 2258 (2012)

277. Azimuthal angle dependence of nanoripple formation on Si (100) by low energy ion erosion,Sarathlal K. V., Satish Potdar, Mohan Gangrade, V. Ganesan, Ajay Gupta, Adv. Mat. Lett. 2013, 4(6), 398-401

278. Coexistence of interacting ferromagnetic clusters and small antiferromagnetic clusters in La0.5Ba0.5CoO3",Devendra Kumar and A Banerjee, J. Phys.: Condens. Matter 25, 216005 (2013)

279. On the correlation between supercooling, superheating and kinetic arrest in a magnetic glass $Pr_{0.5}Ca_{0.5}Mn_{0.975}Al_{0.025}O_3$. Kaustav Mukherjee, Kranti Kumar, Alok Banerjee, and Praveen Chaddah. Euro. Phys. J. B., 86, 21 (2013).

280. Magnetic and ^{57}Fe Mössbauer study of magneto-electric $GaFeO_3$ prepared by the sol–gel route. Kavita Sharma, V. Raghavendra Reddy, Ajay Gupta, A. Banerjee and A. M. Awasthi.J. Phys.: Condens. Mater 25, 076002 (2013).

281. Observation of different spin behavior with temperature variation and Cr substitution in a multiferroic compound YMn_2O_5. K. Mukherjee, Kranti Kumar and A. Banerjee. Solid State Commun., 153, 66 (2013).

282. Tuning the phase transition dynamics by variation of cooling field and metastable phase fraction in Al doped $Pr_{0:5}Ca_{0:5}MnO_3$,Devendra Kumar, Kranti Kumar, A. Banerjee and P. Chaddah,J. Phys.: Condens. Mater 24, 386001 (2012).

283. Memory effects in exchange coupled Fe/Co_3O_4 nanocomposites, S. P. Pati, **S. Kumar** and D. Das, *Mater. Chem. Phys.* 137 (2012) 303-309.

284. Signature of exchange bias and spin-glass like phenomena in Fe/CoO nanocomposite, S. P. Pati, A. Roychowdhury, **S. Kumar** and D.Das. *J. Appl. Phys.* 113, 17D708 (2013).

285. Magnetically addressable fluorescent Fe_3O_4/ZnO nanocomposites: structural, optical and magnetic studies, A. Roychowdhury, S.P. Pati, A.K. Mishra, **S.Kumar** and D.Das *J Phys Chem solids* 74, (2013) 811.

286. Metastability and inverse magnetocaloric effect in doped manganite ($Nd_{0.25}Sm_{0.25}Sr_{0.5}MnO_3$) and ferromagnetic shape memory alloy ($Ni_2Mn_{1.36}Sn_{0.64}$): A comparison S. Chatterjee, S. Giri, S. Majumdar, *J. Phys.: Condens. Matter* **24** (2012) 366001.

287. Physico-ChemicalAspects of QuantumDot−VasodialatorInteraction: Implications in Nanodiagnostics, S. Mondal, S. Ghosh, D. Ghosh, and A. Saha, *Journal of Physical Chemistry C* 116, 9774 (2012).

288. Radiation Chemical Route for Synthesis of Semiconductor Nanomaterials. In *Radiation Synthesis of Compounds and Materials*. A. Saha**,** 2013, pp 503, Ed. B. Kharisov, *CRC Press USA (Taylor & Francis).*

289. SEMEDS: An important tool for air pollution biomonitoring, S. S. Ram, **S. Majumdar**, **P. Chaudhuri**, **S. C. Santra, P.K.Maiti**, M.Sudarshan, A. Chakraborty. Micron, 43 (2-3): 490-493 (2012)

290. Plant canopies as trap for re-suspended dust particulates contaminated with heavy metals. S.S. Ram, **S.Majumdar, P.Chaudhuri, S.C. Santra, P.K. Maiti,** M. Sudarshan, A. Chakraborty, Mitigation and Adaptation Strategies for Global Change. DOI: 10.1007/s11027-012-9445-8 (2012)

291. Structure and Magnetism of $FeMnO_3$, S. Rayaprol, S. D. Kaushik, P. D. Babu and V. Siruguri, AIP Conf. Proc. **1512** (2013) 1132.

292. Exchange bias in ball-milled $LaFeO_3$, S. D. Kaushik, S. Rayaprol, P. D. Babu and V. Siruguri, AIP Conf. Proc. **1512** (2013) 1164.

293. Temperature dependent 57Fe Mossbauer and neutron diffraction study of magneto-electric $GaFeO_3$- V. Raghavendra Reddy, Kavita Sharma, Ajay Gupta, S. D. Kaushik, V. Siruguri J. Phys.: Conden. Matter, **24** (2012) 376001.

294. Neutron diffraction evidence for kinetic arrest of the first-order austenite to martensite transition in $Ni_{37}Co_{11}Mn_{42.5}Sn_{9.5}$ - V. Siruguri, S. D. Kaushik, P. D. Babu, Aniruddha Biswas#, S. K. Sarkar#, Madangopal Krishnan#, P. Chaddah, arXiv: **1211.0238** (2012).

295. Synthesis of carbon nano-fibers on p-Si having improved temperature sensing capability, S.Hussain, **D. Ghosh, B. Ghosh, Subhajyoti Chaudhuri, R. Bhar, A.K. Pal**, Materials Science and Engineering: B **178**(2013) 83

296. Surface modification of GaAs induced by argon ion implantation, S Hussain, **R N Gayen, M B Dut, A K Pal,** Indian Journal of Pure & Applied Physics, **50** (2012) 650

297. Growth and electrical transport study in pulsed laser deposited Sr2CoO4 thin film on (001) MgO substrate. Pankaj K. Pandey, R. J. Choudhary, and D. M. Phase, AIP Conf. Proc. 1512, 634 (2013).

298. Effects of sintering temperature variation on microstructure and magnetic nature of Al diluted La0.7Ca0.3MnO3, Manish Kumar, R. J. Choudhary and D. M. Phase, AIP Conf. Proc. 1512, 1190 (2013).

299. Fourier transform infrared study of pulsed laser deposited Fe3O4 thin films grown on different substrates, Ridhi Master, D. M. Phase, R. J. Choudhary, U. P. Deshpande, and T. Shripathi AIP Conf. Proc. 1512, 724 (2013).

300. Study of GaFeO3 thin films prepared by PLD, Kavita Sharma, V. Raghavendra Reddy, Ajay Gupta, R. J. Choudhary, D. M. Phase, A. Banerjee, and V. Ganesan, AIP Conf. Proc. 1512, 720 (2013).

301. Temperature dependent structural studies of multiferroic $La_{0.7}Bi_{0.3}CrO_3$ perovskites, Aga Shahee and N. P. Lalla SOLID STATE PHYSICS: PROCEEDINGS OF THE 57TH DAE SOLID STATE PHYSICS SYMPOSIUM 2012, 3–7 December 2012 held in Indian Institute of Technology, Bombay, Mumbai, India, appeared in AIP Conf. Proc. 1512, pp. 60-61

302. Synthesis, Characterization and Magnetic Properties of Nanocrystalline Nickel, S. Das, N. P. Lalla and G. S. Okram, AIP Conf. Proc. 1512, 296 (2013).Kinetic arrest of the first-order to Pbnmphase transition in supercooled $LaxMnO_{3+\delta}$ (x = 1 and 0.9), Aga Shahee, Dhirendra Kumar, Chandra Shekhar# and N P Lalla, J. Phys.: Condens. Matter 24 (2012) 225405

303. Structural and transport properties of LaPrCaMnO3 (y= 0.45) thin films DK Mishra, R Rawat, VG Sathe – *AIP Conf. Proc.* ***1447****, 705 (2012)*

304. Competing Kondo and e-e interaction in Ce2.1Nd0.9Al, Durgesh Singh, S. Shanmukharao Samatham, Venkateshwarlu D, Mohan Gangrade and V. Ganesan, AIP Conf. Proc. 1512, 972-973 (2013)

305. Growth of Fluorine Doped SnO2 Nanostructures by Spin Coating of Ultrasonically Prepared Gel Precursor,Y C Goswami, Vijay Kumar, V Ganesan and P Rajaram, AIP Conf. Proc. 1512, 1290-1291 (2013)

306. Effect of Sn Substitution on Structural and Transport Properties of (La0.67Sr0.33)MnO3,Tejas M. Tank, V. Sridharan, S. Shanmukharao Samatham, V. Ganesan, and S. P. Sanyal, Proceeding of International Conference on Research Trends in Applied Physics and Material Science, AIP Conf. Proc. 1536, 573 (2013)

307. Magnetic-fluorescent nanocomposite: A case study on Fe3O4/ZnS, A. Roychowdhury, S. P. Pati, S. Kumar, and D. Das, AIP Conf. Proc. 1512, 246 (2013)

308. Magnetically addressable fluorescent Fe_3O_4/ZnO nanocomposites:Structural, optical and magnetization studies. A.Roychowdhury, S.P.Pati, A.K.Mishra , **S.Kumar** , D.Das, J.Phys.Chem.Solids74, 811 (2013)

309. Role of additives (X = Ti, Zr) in phase formation and thermal stability of FeXN thin films Akhil Tayal, Mukul Gupta, A. Gupta, M. Horisberger, J. Stahn, Thin Solid Films 536, 39–49 (2013).

310. Surfactant controlled interface roughness and spin-dependent scattering in Cu/Co multilayers, S. M. Amir, Mukul Gupta, A. Gupta, J. Stahn and M. Horisberger, Applied Physics A (Jan 2013), DOI 10.1007/s00339-012-7527-9; http://dx.doi.org/10.1016/j.tsf.2013.03.026

6. Presentations in Conferences/Symposia

1. Ink-based direct coating of new earth-abundant sulphides for thin film solar cells, **T. K. Chaudhuri, Devendra Tiwari and Anjana Kothari,** International Conference on Solar Energy Photovoltaic (ICSEP-2012),19-21 December 2012, KIIT University, Bhubaneswar, Odisha
2. Solution–processed, earth-abundant and non-toxic Cu_2ZnSnS_4 and Cu_2SnS_3 films for solar cells, **Tapas Chaudhuri and Devendra Tiwari**, 22nd International Photovoltaic Science and Engineering Conference (PVSEC-22), 5-9 November 2012, Hangzhou, China
3. Multiferroicity-alteration by Y- and Mn-site doping in $YMnO_3$, Sonu Namdeo, Suchita Pandey, and A.M. Awasthi, DAE-SSPS 2012.
4. Single step synthesis of ZnO nanostructure thick films and its application as CO gas sensor,**PB Orpe, AD Shinde, SW Gosavi, RC Aiyer,** V Sathe, Physics and Technology of Sensors (ISPTS), 1st international Conference Page 361 (2012)
5. Boron Doped nc-Si: H Window Layer Prepared by Hw-Cvd for Solar Cell Applications, **MR Pramod, MM Kamble, VS Waman, SP Gore, AM Funde,** VG Sathe, **KR Patil, SW Gosavi, SR Jadkar.** International Journal of Modern Physics: Conference Series **6** Pages 521-526 (2012)
6. Influence of Tb Substitution on Magnetic Transitions in Gd_2In , Vikram Singh, Pallab Bag and R Rawat, presented at DAE SSPS-2012 held at BARC, Mumbai.
7. Thermomagnetic Irreversibilities in Cr and Ge doped Mn_2Sb, Pallab Bag, Rohit Kumar, Pallavi Kushwaha and R. Rawat, presented at DAE SSPS-2012 held at BARC, Mumbai
8. Photoconductive Properties of Nano-Dots of CdS,Saniya Ayaz, Shakti Sanago, P. S. Khare, Richa Panda, D. Venkateshwarlu, A.D.Acharya, S. Shanmukharao Samatham, Mohan Gangrade and V. Ganesan, International Journal of Environmental Engineering and Management, 3(1), 431, (2012)
9. AFM, XRD and Resistivity of ZnO Nano-Doughnuts,Shakti Sanago, Saniya Ayaz, P. S. Khare, Richa Panda, D. Venkateshwarlu, A.D.Acharya, S. Shanmukharao Samatham, Mohan Gangrade and V. Ganesan, International Journal of Environmental Engineering and Management, 3(1), 435, (2012)
10. Studies on Structural, Infrared, Morphological, Electrical, and Magnetotransport Properties of Ba doped in NdMnO3 Nanocrystalline Compositions,Jessica R. Chocha, Pooja A. Chhelavda, D. Venkateshwarlu, S. Shanmukharao Samatham, V. Ganesan and J. A. Bhalodia, International Journal of Physics and Applications, 4(1), 13, (2012)
11. The nucleon-nucleon potential from relativistics mean field theory **B. B. Sahu**, **M. Bhuyan**, S. K. Singh[#] & S. K. Patra[#], Proc of DAE Symposium on Nuclear Physics 57 (2012) 198.
12. Nuclear matter and finite nuclei properties using simple effective interaction", **M, Bhuyan**, S. K. Singh[#], **S. K. Tripathy, T. R Routray, B. Behra,** B. K. Sharma, X Vinas, and S. K. Patra[#] , Proc of DAE Symposium on Nuclear Physics 57 (2012) 200.
13. The role of isoscalar-isovector coupling in symmetric energy of Infinite nuclear matter, ", **M, Bhuyan**, S. K. Singh[#], S. K. Patra[#] and P. K. Panda, Proc of DAE Symposium on Nuclear Physics 57 (2012) 608.
14. Proto-neutron Star with trapped Neutrinos, S. K. Tripathy, T. R. Routray and **B. Behera**, Proc of DAE Symposium on Nuclear Physics 57 (2012) 638.
15. Study of level scheme of ^{87}Zr, P. Banerjee[#], **S. Ganguly, H.P. Sharma**, M. Pradhan[#], **S. Chakraborty**, R Palit[#], V. Nanal[#], R.G. Pillay[#], S. Saha[#], J. Sethi[#] and S. Chatterjee[#], Proc of DAE Symposium on Nuclear Physics 57 (2012) 216.
16. Competing collectivity and multiplet structure in ^{154}Ho, **Dibyadyuti Pramanik,** Abhijit Bisoi[#], Subhendu Rajbanshi[#], S. Bhattacharya, Sudatta Ray[#], S.S.Ghugre, A.K. Sinha, S. Saha[#], J. Sethi[#], B. S. Naidu[#], R. Donthi[#], V. Nanal[#], R. Palit[#], M. Saha Sarkar[#], and **S. Sarkar**, Proc of DAE Symposium on Nuclear Physics 57 (2012) 212.
17. Study of deformed structures in N ~ Z nuclei, R. Bhattacherjee, R. Chakrabarti, S. S . Bhattacharjee, R. Raut, S. S Ghugre, **L. Chaturvedi**, **M. Kumar Raju, A. Dhal**, N . Madhavan, R. P. Singh, S. Muralithar, **B. K. Yogi**, U. Garg and A. K. Sinha, Proc of DAE Symposium on Nuclear Physics 57 (2012) 336.

18. Novel Method of Lifetime Measurements in ^{156}Dy with Aerogel Backing, A. K. Sinha, S.S. Bhattacharjee, R. Bhattacharjee, R. Raut, S. S Ghugre, R.P. Singh, N. Madhavan, S. Muralithar, **P.V. Madhusoodan Rao**, **M Kumar Raju, Krishichayan, L. Chaturvedi,** S. Saha[#], J. Sethi[#], R. Palit[#], S. Mukhopadhyay[#], G. Smith, and R. V. F. Janssens, Proc of DAE Symposium on Nuclear Physics 57 (2012) 338.

19. Digital Pulse Processing Simulations in MATLAB®& OCTAVEfor Nuclear Spectroscopy, **A. K. Tiwari**, R. Raut, K. Basu, S. S. Ghugre, **A. Gupta** and A. K. Sinha, Proc of DAE Symposium on Nuclear Physics 57 (2012) 944.

20. Enriched ^{148}Nd Target on Ultra Low-Density Backing, K. Basu, S. S. Bhattacharjee, R. Raut, S. S. Ghugre, Abhilash S R. ,D Kabiraj , Indu Bala, R.P. Singh, S. Muralithar, and A. K Sinha, Proc of DAE Symposium on Nuclear Physics 57 (2012) 946.

21. ER excitation function for ^{31}P + ^{170}Er, G. Mohanto, N. Madhavan, S. Nath, J. Gehlot, I. Mazumdar[#], A. Jhingan, Ish Mukul, **Maninder Kaur, Varinderjit Singh,** J. Sadhukhan[#], T. Varughese, D. A. Gothe[#], P. B. Chavan[#], A. K. Sinha, **R. K. Bhowmik,** S. Pal[#], V. S. Ramamurthy and A. Roy, Proc of DAE Symposium on Nuclear Physics 57 (2012) 460.

22. An effective Nuclear Model: from Nuclear Matter to Finite Nuclei, **T. R. Routray**, X. Vinas, **S. K. Tripathy, M. Bhuyan**, S. K. Patra[#], **B. Behera**, Proceedings of the 11th International Conference on Nucleus-Nucleus Collisions (NN2012), May 27-June 1, 2012, San Antonio, Texas, USA.

23. Signature of exchange bias and spin-glass like phenomena in Fe/CoO nanocomposite, S. P. Pati, A. Roychowdhury, **S. Kumar** and D. Das 12th Joint MMM/Intermag Conference held at Hyatt Regency, Chicago, Illinois, USA during January 14-18, 2013.

24. Milling Duration Induced Structural and Magnetic Properties of Fe/MnO Nanocomposites, S. P. Pati, A. Roychowdhury, **S. Kumar** and D. Das**,** International Conference on Recent Trends in Applied Physics and Material Science (RAM 2013) held at Govt. College of Engg. And Tech., Bikaner during February 01-02, 2013.

25. Magnetic Properties of $Cu_{70.9}Al_{18.1}Mn_{11}$ Alloy S. Chatterjee, and S. Majumdar, **AIP Conf. Proc. 1512 (2013) 1086.**

26. "Magnetic investigation of $Ni_{50}Mn_{33}In_{12}Ga_5$ alloy"S. Pramanick, S. Chatterjee, and S. Majumdar, **AIP Conf. Proc. 1512 (2013) 1088**

27. Evolution of biofunctional semiconductor nanocrystals: A calorimetric investigation, Debasmita Ghosh, Somrita Mondal, Chandra Nath Roy and Abhijit Saha, National Symposium on Radiation and Photochemistry (NSRP-2013), March 20-22, 2013, NEHU, Shilong, India.

28. Thermodynamic Insight into the Formation of Dendrimer-Semiconductor Hybrid Nanomaterials, Somrita Mondal, Debasmita Ghosh, Chandra Nath Roy and Abhijit Saha, National Symposium on Radiation and Photochemistry (NSRP-2013), March 20-22, 2013, NEHU, Shilong, India.

29. A Critical Evaluation of Aqueous Synthesis Methods of Silver Nanoparticles as SERS Active Materials, Chandra Nath Roy, Debasmita Ghosh, Somrita Mondal and Abhijit Saha, National Symposium on Radiation and Photochemistry (NSRP-2013), March 20-22, 2013, NEHU, Shilong, India.

30. Distribution of trace elements on leaves of roadside trees exposed to traffic generated dust pollution in and around Kolkata, India. S.S.Ram, **P. Chaudhuri**, S. Chanda, S.C.Santra, P.K.Maiti, R.V. Kumar, M. Sudarshan and A. Chakraborty. European Conference on X-ray Spectrometry,Vienna, Austria,18-22 June 2012.

31. Characterization of street dust and dusts absorbed on leaves collected in a metro-city: with special reference to size, mineralogy and elemental distribution. S.S.Ram, **P. Chaudhuri**, S. Chanda, S.C.Santra, R.V. Kumar, M. Sudarshan and A. Chakraborty. Urban Environmental Pollution, Amsterdam, The Netherlands, 17-20 June 2012.

32. Modulation of cadmium tolerance of *Aspergillus terreus* by Ionising radiation, D.Das, A.Chakraborty, **S.C.Santra**. 3rd World Congress on Biotechnology. Omics groups, Hyderabad, India, 13-15th September, 2012.

33. Profiling Cytoskeleton and Its Associated Proteins in Early Initiation Phase of Chemically Induced Carcinogenesis In Murine Model. D. Mukherjee, A. Chakraborty, A. Mukhopadhyay. 2012 World Cancer Congress. UICC Track 1 - Prevention and early detection (including tobacco control) Screening and early detection: technological advances.,Montreal,Canada, August 27th -30th, 2012

34. Potential of ionising radiation for modulating amylase and cellulase activity of *Aspergillus niger* under lead and zinc stress, D.Das, A. Chakraborty and **S.C.Santra**. International conference on "Environment and human health", National Environmental Science Academy (NESA), NewDelhi. 28-29th November, 2012

35. Insight to probe cytoskeleton and its associated proteins in early initiation phase of chemically induced carcinogenesis in murine model, D.mukherjee, A. Mukhopadhyay, and A. Chakraborty. Proceedings of International conference on "Environment and human health", pp-84, National Environmental Science Academy (NESA), NewDelhi. November 28th and 29th, 2012.

36. Iron toxicity induced antioxidant enzymes and its gene expression in Withania somnifera *L* Rout J.R, Sahoo S.L., Chakraborty A. and Sudarshan M... International Conference and 3rd World Congress on Biotechnology, Hyderabad, Andhra Pradesh, India. (2012)

37. Alterations of active oxygen scavenging enzymes in Withania somnifera L. subjected to zinc stress Rout J.R., Sardar S.S. and Sahoo S.L. International Conference on "Biotechnology Advances: Omics Approaches and Way Forward". Organized by Centre of Biotechnology, Siksha O Anusandhan University, Bhubaneswar, Odisha, India. pp. 74. (2012).

38. Antioxidant enzymes of Abutilon indicum L. under excess copper. Rout J.R, Sahoo S.L Das R., Ram S.S., Chakraborty A. and Sudarshan M. International Conference on Environment and Human Health". Organized by National Environmental Science Academy (NESA) and Jamia Hamdard, New Delhi, India. pp. 21. (2012).

39. Effect of antioxidant enzymes and metal distribution of Abutilon indicum L. under excess copper Rout J.R, Sahoo S.L., Chakraborty A. and Sudarshan M 37th Annual meet and P. Parija Memorial National Conference on "Recent Advances in Plant Biotechnology". Organized by Ravenshaw University, Cuttack, Odisha, India. pp. 71. (2012).

40. Withania somnifera L. Dunal: A review Rout J.R. and Sahoo S.L. (National Seminar on 'New Frontiers in Plant Science Research for Sustainable Development'. Organized by Prananath Autonomous College, Khordha, Odisha, India. pp. 77. 2012).

41. Interactions between Cationic Amphiphilic Drugs and Human Serum Albumin: A Small Angle Neutron Scattering Study – **Z. Yaseen**, V.K. Aswal# and **Kabir-ud-Din**, Recent Trends on Material Science Research (RTMSR- 2012), National Institute of Technology, Srinagar, Kashmir, Sept. 3-5, 2012.

42. Binding Studies of Amphiphilic Drugs Imipramine Hydrochloride and Promethazine Hydrochloride to Human Serum Albumin – **Z. Yaseen**, V. K. Aswal# and **Kabir-ud-Din**, 2nd International Symposium on Neutron Scattering, Bhabha Atomic Research Centre, Mumbai, Jan. 14 - 17, 2013, p. 90.

43. Clouding Behavior of Anionic Surfactant Solutions: A SANS Study- **Arti Bhadoria**, V. K. Aswal# and **Sanjeev Kumar**, 1st Asia-Oceania Conference on Neutron Scattering, held at Tsukuba, Japan, Nov 20-24, 2011.

44. Temperature Induced Solution Behavior of Surfactants: A SANS Study- **Arti Bhadoria**, Sugam Kumar#, V.K. Aswal# and **Sanjeev Kumar**, 15th International Conference on Small Angle Scattering, held at Sydney Convention & Exhibition Centre, Sydney, Australia, Nov 18-23, 2012.

45. Anomalous Heating Induced Micellar Growth in aqueous Anionic Surfactant: A SANS Study- **Sanjeev Kumar, Arti Bhadoria**, Sugam Kumar# and V. K. Aswal#, International Symposium on Neutron Scattering, held at held at Bhabha Atomic Research Centre, Mumbai, India, Jan 14-17, 2013.

46. Structure property correlation for high temperature Anti-ferroelectric ordering in $Na_{0.5}Bi_{0.5}TiO_3$ relaxor ferroelectric- **T. Karthik**, S. Rayaprol, P. U. Sastry#, V. Siruguri and **Saket Asthana**, 13th European Powder Diffraction Conference (EPDIC-13), 28th -31st Oct 2012, Minatec Centre, Grenoble, France.

47. Structure and magnetism of $FeMnO_3$ – S. Rayaprol, S. D. Kaushik, P. D. Babu and V. Siruguri, 57th DAE-Solid State Physics Symposium held at IIT-Bombay, Mumbai, Dec 3 – 7, 2012.

48. Exchange Bias in Ball-Milled $LaFeO_3$ – S. D. Kaushik, S. Rayaprol, P. D. Babu and V. Siruguri, 57th DAE-Solid State Physics Symposium held at IIT-Bombay, Mumbai, Dec 3 – 7, 2012.

49. Single phase synthesis and room temperature neutron diffraction studies on multiferroic $PbFe_{0.5}Nb_{0.5}O_3$ - **S. Matteppanavar**, **B. Angadi** and S. Rayaprol, 57th DAE-Solid State Physics Symposium held at IIT-Bombay, Mumbai, Dec 3 – 7, 2012.

50. Neutron diffraction study on $Pr_{0.7}Ca_{0.3-x}Sr_xMnO_3$: Effect of magnetic field, temperature and chemical pressure - S. Rayaprol, **A. Dogra**, S. D. Kaushik, P. D. Babu and V. Siruguri, International Symposium on Neutron Scattering, held at held at Bhabha Atomic Research Centre, Mumbai, India, Jan 14-17, 2013. (Oral presentation)

51. Neutron diffraction studies on $Ho_{1-x}Y_xMnO_3$ ($0 \leq x \leq 0.75$) - S. D. Kaushik, S. Rayaprol and V. Siruguri, International Symposium on Neutron Scattering, held at held at Bhabha Atomic Research Centre, Mumbai, India, Jan 14-17, 2013.

52. Single-step synthesis and low sintering temperature effects on the structure of $PbFe_{0.5}Nb_{0.5}O_3$ at 290 K: Neutron diffraction study - **S. Matteppanavar**, **B. Angadi** and S. Rayaprol, International Symposium on Neutron Scattering, held at held at Bhabha Atomic Research Centre, Mumbai, India, Jan 14-17, 2013.

53. Structural transport properties of Dy substituted $YBaCo_4O_7$ – **Bharat Singh, Naresh Kumar**, S. Rayaprol and **N. K. Gaur**, 57th DAE-Solid State Physics Symposium held at IIT-Bombay, Mumbai, Dec 3 – 7, 2012.

54. Magnetic properties of the rare-earth intermetallic compound Dy_5Si_4: Magnetization and Neutron Diffraction Studies – **R. Nirmala**, **A. V. Morozkin**, S. Rayaprol, S. D. Kaushik, V. Siruguri, **A. K. Nigam**, and **S. K. Malik**, International Symposium on Neutron Scattering, held at held at Bhabha Atomic Research Centre, Mumbai, India, Jan 14-17, 2013.

55. Influence of different ions (Me = Co, Ni, Mg) substitution on the ground state of $Me_{0.3}Zn_{0.7}Fe_2O_4$ spinel system – **Harshida Parmar**, **R. V. Upadhyay**, V. Siruguri and S. Rayaprol, International Conference on Magnetic Fluids (ICMF-2013) held at National Physical Laboratory, New Delhi in January 2013.

56. Low temperature neutron diffraction study of $Nd_{0.95}Sr_{0.05}CrO_3$ – Keka R. Chakraborty#, S. Mukherjee#, S. D. Kaushik, S. Rayaprol, V. Siruguri, A. K. Tyagi# and S. M. Yusuf#, International Symposium on Neutron Scattering, held at held at Bhabha Atomic Research Centre, Mumbai, India, Jan 14-17, 2013.

57. Magnetization and neutron diffraction study of $Tb_{0.9}Y_{0.1}MnO_3$ – Keka R. Chakraborty#, R. Shukla#, M. D. Mukadam#, S. D. Kaushik, A. K. Tyagi#, V. Siruguri and S. M. Yusuf#, 57th DAE-Solid State Physics Symposium held at IIT-Bombay, Mumbai, Dec 3 – 7, 2012.

58. Effect of Magnetic Field and Temperature on the Magnetic Structure of Rare-Earth rich intermetallic compounds; P. D. Babu, presented at International Symposium on Neutron Scattering, held at held at Bhabha Atomic Research Centre, Mumbai, India, Jan 14-17, 2013 (Oral Presentation).

59. Effect of lattice strain on the rotational tunneling states of NH_4^+ ions and non-Debye specific heat of $(NH_4)_xRb_{1-x}Br$; **P.S. Goyal**, P. D. Babu and **F. Jurany**; presented at International Symposium on Neutron Scattering, held at held at Bhabha Atomic Research Centre, Mumbai, India, Jan 14-17, 2013.

60. Rotational Tunneling States of NH 4+ ions and Specific Heat of $(NH_4)_xRb_{1-x}Br$; P. D. Babu, **P. S. Goyal** , presented at DAE Solid State Physics Symposium held at IIT Bombay during Dec 3- 7, 2012 (Oral presentation).

61. Neutron Diffraction Studies on Cobalt Substituted $BiFeO_3$, **Jashashree Ray**, **Achyuta Kumar Biswal**, **Sanghamitra Acharya**, P.D. Babu, V. Siruguri and P.N. Vishwakarma; presented at DAE Solid State Physics Symposium held at IIT Bombay during Dec 3- 7, 2012.

62. Synthesis and characterization of Pure and Doped ZnO Nano Particles by Solution Combustion Method, **Srinatha N, Basavaraj Angadi**, K.G.M.Nair#, International Conference on Recent Advances in Materials Science (RAMS 2012), Organised by Karnataka State higher Education Council (KSHEC) held at Atria hotel Bangalore during 6–8 November 2012.

63. Synthesis of Nano Crystalline, Cobalt Substituted ZnO by Gel-Combustion Method, **Srinatha N, Basavaraj Angadi**, K.G.M.Nair#, National Conference on Condensed Matter Physics and Applications (CMPA-2012) held at MIT, Manipal during 27-28 December 2012.

64. Magnetic properties of nanocrystalline electron-doped manganite Gd0.15Ca0.85MnO3, **Chhatarpal, Rajib Mondal, R. Nirmala,** T. Geetha Kumary **#, A.K. Nigam**, 4th international conference on Advanced Nano Materials(ANM 2012) held at Indian Institute of Technology Madras, Oct. 17-19, 2012.

65. Synthesis and magnetic property studies of nanocrystalline manganite Gd0.15Ca0.85MnO3, **Chhatarpal, Rajib Mondal, A. Muthukumaran**, T. Geetha Kumary#, **R. Nirmala**, National Conference on Magnetic Materials and Applications (MagMA-2012) held in IITMadras , 12 – 13 March 2012.

66. Size effect on the structural, magnetic and magnetotransport properties of electron doped manganite La0.15Ca0.85MnO3**, Rini Thomas, Gangadhar Das, Rajib Mondal, R. Pradheesh, R. N. Mahato, R. Nirmala, A. V. Morozkin, J. Lamsal, W. B. Yelon, A. K. Nigam and S. K. Malik,** 56th International Conference on Magnetism and Magnetic Materials (MMM 2011), 30 Oct - 3 Nov 2011 at Arizona, USA.

67. Mn doped Tin Oxide Nanoparticles – A Structural Study ,**B. Venu Gopal, Brajesh Nandan,** S. Amirthapandian#, B. K. Panigrahi**#, P. Thangadurai ,**Proceedings of the Proceedings of the 27th PSSI NATIONAL SYMPOSIUM On plasma and Technology (PLASMA-2012), ondicherry University, Dec. 10-13, 2012.

68. Doped ZnO anode material for organic light emitting diodes ,**R. Sudha, P. Thangadurai,** Proceedings of the Proceedings of the 27th PSSI NATIONAL SYMPOSIUM On plasma and Technology (PLASMA-2012), Pondicherry University, Dec. 10-13, 2012.

69. Structure and Microstructure analysis of Mn-doped SnO2 nanoparticles ,**B. Venugopal,** S**.** Amirthapandian#, B. K. Panigrahi#**, P. Thangadurai,** Conference Proceedings, 24th Annual General Meeting (AGM) of the Materials Research Society of India (MRSI), IGCAR, Kalpakkam, Feb. 11-13, 2013.

70. Utilization of residual $CdCl_2$ in CBD-CdS to realize grain growth in CdTe: A novel route, **B. Ghosh, D. Ghosh,** S.Hussain, G. Amarendra#**, B. R. Chakraborty, M. K. Dalai, G. Sehgal, R. Bhar and A. K. Pal**, Proceedings of MRSI –AGM 2013(Feb 11-13,2013)

71. Polymer latex nanocomposites: recent advances, **Deepalekshmi Ponnamma**, **Sabu Thomas** (Published in Conference Proceedings, Latex and Synthetic Polymer Dispersions 2012, Kuala Lumpur, Malaysia13-14 March 2012.

72. Interrelated Shape Memory and Payne Effect in Polyurethane/Graphene Oxide Nanocomposites, **Deepalekshmi Ponnamma, Kishor Kumar Sadasivuni, Michael Strankowsky, Paula Moldenaers, Sabu Thomas, Yves Grohens** (Accepted, RSC Advances)

73. Evolution from Graphite to Graphene Elastomer Composites: A Review, **Kishor Kumar Sadasivuni, Deepalekshmi Ponnamma, Sabu Thomas, Yves Grohens.** Accepted, Progress in Polymer Science)

74. Doped Cerium Oxide Nanostructures as Thin film Electrolyte for ITSOFC, **P.Arunkumar, K.Suresh Babu**, R.Ramaseshan#, and S. Dash#, 27th PSSI National Symposium (PLASMA - 2012), December 10-13, 2012 on Challenges on Power Generation & Lighting, Pondicherry University,Puducherry, India

75. Influence of annealing on texture properties of cerium oxide thin films, **P.Arunkumar, K.Suresh Babu,** R.Ramaseshan#, and S. Dash #, 24th AGM MRSI, Advanced Material for Energy Application, February 10-13, 2012, IGCAR, Kalpakkam, India.

76. Growth of ZnTe films by pulsed laser deposition technique, **B. Ghosh, D. Ghosh, Subhajyoti Chaudhuri,** S.Hussain**, R. Bhar, A.K. Pal,** National Conference on Sustainable Development through Innovative Research in Science and Technology, 28-29th September, 2012, Jadavpur University, Kolkata

77. Growth of CdTe films by pulsed laser deposition technique, **B. Ghosh,** S. Hussain**, D. Ghosh, D. Chakraborty, R. Bhar and A. K. Pa**l, National Conference on Sustainable Development through Innovative Research in Science and Technology, 28-29th September, 2012, Jadavpur University, Kolkata

78. The Ferromagnetism of diluted Zn1-xGdxO (x = 0.005, 0.01 and 0.5) thin films**, I. S. Roqan, S. Venkatesh,** S. Hussain**, I. Bantounas, U. Schwingenschlogl, M. Yousefi, J.B Franklin, M.P. Ryan, MA McLachlan,Neil M. Alford,** EMRS, Strasbourg, 27 Nov 2012

79. Single step synthesis of near-IR plasmonic silver nano-pyramids. **Abhishek Swarnkar**, **Satarupa Pattanayak**, **Amiya Priyam**, and G.M.Bhalerao, DAE-BRNS 4th Interdisciplinary Symposium on Materials Chemistry ISMC-2012 (11-15 Dec 2012), BARC Mumbai. **(Conference proceedings)**

80. Two-source coevaporation technique for synthesis of indium phosphide films with controlled composition, **D. Ghosh, R. N. Gayen,** S.Hussain**, R. Bhar and A. K. Pal**, Proceedings of MRSI –AGM 2013(Feb 11-13,2013)

81. Utilization of residual $CdCl_2$ in CBD-CdS to realize grain growth in CdTe: A novel route, **B. Ghosh, D. Ghosh,** S.Hussain, G. Amarendra#**, B. R. Chakraborty, M. K. Dalai, G. Sehgal, R. Bhar and A. K. Pal**, Proceedings of MRSI –AGM 2013(Feb 11-13,2013)

82. Novel BN/Pd composite films for stable Liquid Petroleum Gas sensor, **D. Ghosh, B. Ghosh,** S.Hussain, **Subhajyoti Chaudhuri, R. Bhar and A.K. Pal**, Proceedings of IWNST 2013 (Feb 28-Mar 1, 2013)

83. Synthesis of carbon nano-fibers on p-Si for improved temperature sensing capability, S. Hussain**, D. Ghosh, B. Ghosh, Subhajyoti Chaudhuri, R. Bhar and A.K. Pal**, Proceedings of IWNST 2013 (Feb 28-Mar 1, 2013)

7. Workshops and Seminars organized by UGC-DAE CSR

7.1 National Workshop on Experimental Proposals and Possibilities for the NUCLEAR STUDIES WITH INGA AT VECC

The current campaign of the Indian National Gamma Array (a multi clover array set up as a National Collaboration between the Universities & the Institutes) at TIFR is likely to be completed around this year end. The next campaign of INGA, in part, is being considered to be at VECC for experiments using the light ion beams. Routinely protons (~ 7–20 MeV) and alpha (~ 28 - 65 MeV) beams are available from the recently upgraded room temperature K130 Cyclotron at VECC.

A thematic user workshop National Workshop on Experimental Proposals and Possibilities for the Nuclear Studies with INGA at VECC was organized at VECC, during May 22-23, 2012 to deliberate on the possible experiments for the VECC campaign. The envisaged configuration of INGA at VECC would have about 12-14 Clover detectors with the possibility of replacing a few clovers with LEPS detectors. The workshop commenced with a brief introduction to the various elements of the array when housed at VECC, by Dr. S. R. Banerjee, the User Co-ordinator, VECC and Prof. A. Goswami, Dr S. S. Ghugre and Dr Sarmistha Bhattacharya, members of the local PICC for INGA at VECC.

This was followed by two days of intense discussion on the various facets of nuclear structure physics using light ions planned to be pursued in the aforesaid INGA campaign. There were around 29 presentations of which 15 were from the Universities (including IIT) and the rest were from the Institutes.

A few of the presentations highlighted the unique possibility of accessing the exotic nuclear shapes of contemporary interest such as tetrahedral symmetry using light ions. A few presentations emphasized the interesting physics in the Rare earth region such as the possibility of condensation of octupole phonons in ^{150}Sm, or the observation of octupole excitations around ^{146}Gd, hitherto inaccessible using the heavy-ion accelerator facilities available in the country. Some of the presentations also brought out the possibilities for pursuing experiments with cross-disciplinary impacts, one of them being spectroscopy of ^{136}Cs that has implications on neutrino less double beta decay. One presentation highlighted the use of standard gamma ray spectroscopy in Perturbed Angular Correlation measurements which is of relevance in disciples such as Material Science, Chemistry.

A salient feature of this workshop was that a majority of the presentations were from young faculties from the Universities, most of whom had used the INGA facility as research scholars for their respective Doctoral thesis.

7.2 Awareness Workshop – GITAM Institute of Science, GITAM University, Visakhapatnam June 26 – 27, 2012

A two day awareness workshop of UGC-DAE CSR was organized by the Mumbai Centre of the Consortium in association with GITAM Institute of Science, GITAM University, Visakhapatnam during 26 – 27 June, 2012. The main objective of the workshop was to create awareness among researchers from various universities, colleges and other academic institutions in the region on the kind of research that can be carried out using the highly sophisticated research facilities available at the different Centres of the Consortium with special emphasis on neutron scattering facilities at the Dhruva reactor, BARC available through the Mumbai Centre. About 50 participants registered for the workshop. There were about 27 faculty members and 23 students including those from GITAM University. The speakers for the workshop were drawn from the faculty of all three Centres of the Consortium and DAE Institutions; BARC and RRCAT, and GITAM University. The workshop was formally inaugurated Prof. D. Harinarayana, Pro-Vice Chancelor of GITAM University. Dr. V. Siruguri, Centre Director, Mumbai Centre of the Consortium explained briefly the mandate of UGC-DAE CSR and, in particular, that of Mumbai Centre. Dr. P. D. Babu, one of conveners, explained the purpose of the workshop. Prof. N. Lakshmana Das gave a vote of thanks.

The workshop consisted of 12 lectures spread over two days. The first lecture was given by Dr R. Mukhopadhyay, BARC, who gave an overview of National Facility for Neutron Beam Research (NFNBR) and described various neutron scattering facilities at BARC. Following this, Dr. Siruguri gave a lecture on basics of neutron scattering, where he explained the various scattering processes and the interaction mechanisms of neutron with condensed matter. Prof. Ajay Gupta, Centre Director, CSR Indore, gave an overview of thin film and multilayer research activity at Indore. He described with several examples how x-ray reflectivity could be used to study various thin films and multilayers. Dr. V.K. Aswal, BARC, delivered a lecture on small angle neutron scattering and its applications, especially in soft mater and biological systems. This was followed by an energetic talk on overview of Indus synchrotron facilities by Dr. Tapas Ganguly, RRCAT along with the results obtained using these facilities. He also gave details of various instruments that are already operational and those which would be available soon. The last session on day one was on neutron activation analysis (NAA). While Dr. R. Acharya, BARC talked about the basic principles and methodology of neutron activation analysis, Prof. Lakshmana Das dwelt on the applications of NAA to archeological studies, mainly related to earthenware samples excavated from Buddhist sites around Visakhapatnam and other parts of Andhra Pradesh.

The second day of the workshop began with the lecture by Dr. S.K. Deshpande, CSR Mumbai on broadband dielectric spectroscopy facility at Mumbai Centre. He gave details of various features of the facility and described results using several examples. This was followed by a lecture by Dr. P.D. Babu on the neutron powder diffractometer built and installed by the Mumbai Centre. He explained various aspects of the diffractometer and unique sample environment of low temperature and high magnetic fields with several results obtained using this facility. He also described the newly installed 9 Tesla PPMS based vibrating sample magnetometer with resistivity option. The next talk was given by Dr. S. Rayaprol, CSR Mumbai Centre on the Reitveld refinement method. He described the Rietveld method and demonstrated with number of examples how it can be effectively used to extract information from x-ray or neutron powder diffraction data. Dr. V. R. Reddy, CSR Indore, described various low temperature facilities that available at Indore Centre giving brief description of each facility with examples. The last talk of the workshop was given by Dr. J.B.M. Krishna, who described the radiation based research activity at CSR Kolkata Centre.

The workshop ended with a feedback and concluding session where participants gave their feedback and certificates of participation were distributed. This session was preceded by presentations by three participants, who described their research activity. Participants felt that the workshop was very useful and many of them were made aware of the facilities that are available at CSR centres.

7.3 Student awareness programme: Summer Training in Physics and Chemistry (STIPAC-2012)

A visit to the UGC-DAE CSR, Kalpakkam Node facilities was arranged for the students from different institutes undergoing summer training projects at IGCAR, Kalpakkam on 30th of June, 2012. The visiting students were graduates and undergraduates from both physics and chemistry background and from different institutes and colleges from across the country. A talk on the introduction to a career in scientific research was delivered by Dr. G.Amarendra. He also elaborated on the various opportunities available to pursue a career in science. Subsequently, the students were shown around the laboratories and introduced to the various existing instruments. They were also briefed about the various applications of the various instruments.

Students of STIPAC-2012

7.4 ONE DAY DISCUSSION MEETING ON LEISHMANIASIS: VACCINES AND IMMUNO-MODULATION

A one –day discussion meeting on *Leishmaniasis: Vaccines and Immunomodulation* was organized by the Centre on 28th December 2012 at UGC-DAE CSR Kolkata Centre Lecture hall.

Leishmaniasis, a disease prevalent in various parts of the world, being endemic in several countries including India, has become an issue of global concern. In India after an apparent dormancy for three decades the disease reemerged and presently its incidence in the country is among the highest in the world. The meeting was organized based on the understanding that till date there is no prophylaxis of the disease and the present scenario has become more complicated for the emergence of drug unresponsive parasites as well as for the co-infection with HIV. As it has been experienced that recovery from leishmaniasis, whether natural or drug induced, is usually accompanied by immunity against re-infection, development of a safe, effective and affordable vaccine seems to offer solution for controlling this fatal disease.

Eminent scientists and experts from the field were invited to deliver talks. The lectures highlighted present status of the disease, especially with respect to its immunomodulation and vaccine development through various routes.

Dr. A. K. Sinha, Center-Director, welcomed the guests and speakers followed by the perspective of the meeting by Dr Anindta Chakraborty. Dr Syamal Roy Chief Scientist, Indian Institute of Chemical Biology, Kolkata, introduced the audience to the world of vaccine and narrated the evolution of the vaccine finally pinpointing the culminating point i.e. the possibility of DNA vaccine for Leishmaniasis. Dr Bhaskar Saha from National Centre for Cell Science, Pune, highlighted the role of toll like receptors (TLR) and CD40 a molecule critical for many T and B cell responses in relation to leishmaniasis. Dr. (Ms) Nahid Ali, from IICB presented her findings on adjuvanted liposome-based antigen delivery system for long-term protection against experimental visceral Leishmaniasis, Prof. Subrata Majumdar, Bose institute, Kolkata, talked about a promising immunotherapeutic phytocompound against visceral leishmaniasis and Prof. (Ms) Mitali Chatterjee, Institute of Post Graduate medical Education and Research, Kolkata, detailed about the targets for immunochemotherapy in Leishmaniasis. The last lecture delivered by Dr. Madhumita Manna of Bethune College, Kolkata highlighted the findings of collaborative research program between the centre and the college where potential of radio attenuated Leishmania parasites as therapeutic and prophylactic agent against experimental murine visceral leishmaniasis was presented.

Each talk was followed with an interactive session with several queries, which were aptly answered by the speakers. Following the deliberations there was intense meeting between the speakers and scientists from our center to explore possibilities of collaboration with the different resource groups for a joint venture in this direction. It was proposed to prepare a project proposal to be submitted to funding agencies like Dept. of Biotechnology etc.

7.5 School on Neutrons as Probes of Condensed Matter (XV-NPCM-2013)

UGC-DAE Consortium for Scientific Research (CSR), Mumbai centre in association with Solid State Physics Division (SSPD) BARC organized a five day school on Neutrons as Probes of Condensed Matter (NPCM) from January 8 – 12, 2013 at BARC, Mumbai, which was fifteenth in this series of schools / workshops organized by CSR in association with BARC in highlighting the use of neutrons in condensed matter physics. This edition of the school was organized as a satellite workshop to the second International Symposium on Neutron Scattering (ISNS-2013) organized by DAE and BRNS during Jan 14 – 17, 2013. The XV-School on Neutrons as Probes of Condensed Matter (NPCM) was coordinated by Dr. Sudhindra Rayaprol (UGC-DAE CSR, Mumbai Centre) and Dr. Surendra Singh (SSPD, BARC). The school had about 60 participants of which 20 were faculty members and 40 were research students from Indian universities and research institutions. The participants were from almost all parts of India, farthest being Tezpur in the East, Chennai in South, Hamirpur in the north and Rajkot in the west.

The school comprised three days of lectures/tutorials and two days of experiments at Dhruva reactor, BARC. Eleven lectures covering various aspects of neutron scattering were delivered by invited speakers on the first two days of the school. All participants were taken inside BARC during the next two days for experimental sessions at Dhruva reactor. Participants were divided into 10 groups, and each group participated in two experiments over these two days. All the neutron scattering instruments available under the National Facility for Neutron Beam Research (NFNBR) were utilized for the experimental sessions. On the last day of the school, tutorials on neutron diffraction data analysis and small angle neutron scattering (SANS) data analysis were conducted.

The school started with the welcome remarks by Dr. Vasudeva Siruguri (Centre Director, UGC-DAE CSR Mumbai Centre), who welcomed the participants and briefed them about the mandate and activities of UGC-DAE CSR, especially Mumbai Centre. Dr. S.L. Chaplot (Head, SSPD, BARC) also welcomed the participants and elucidated the role of NFNBR in promoting research based on neutron scattering in India. The sessions of the school consisted of the following lectures: ***Basics of Neutron Scattering*** (Anil Jain, SSPD, BARC), ***General Overview of NFNBR*** (R. Mukhopadhyay, SSPD, BARC), ***Neutron diffraction - Chemical Structures*** (Amitabh Das, SSPD, BARC), ***Small Angle Neutron Scattering - I: Basics, Theory and Applications*** (V. K. Aswal, SSPD, BARC), ***Small Angle Neutron Scattering - II*** (Debasis Sen, SSPD, BARC), ***Polarized Neutron Reflectometry*** (Surendra Singh, SSPD, BARC), ***Neutron Diffraction - Magnetic Structures*** (P.D. Babu, UGC-DAE CSR, Mumbai Centre), ***Liquids and Amorphous Systems*** (P.S.R. Krishna, SSPD, BARC), ***Single Crystal Diffraction*** (R. Chitra, SSPD, BARC), ***Inelastic Neutron Scattering*** (Mala N. Rao, SSPD, BARC) and ***Quasi-Elastic Neutron Scattering*** (V.K. Sharma, SSPD, BARC). The following tutorials sessions were conducted: ***Rietveld Refinement Method using Fullprof Suite*** (S. Rayaprol, UGC-DAE CSR, Mumbai Centre), ***Rietveld Refinement Method for Magnetic Scattering*** (Amit Kumar, SSPD, BARC), and ***SANS Data Analysis*** (Sugam Kumar, SSPD, BARC). After the tutorial sessions, a few participants presented their research work and also mentioned how they plan to use neutron scattering in their research activities. The school also had an interactive session on the second day, chaired by Dr. S. Kailas (Director Physics Group, BARC). The session was

conducted by Dr. V. Siruguri. Dr. Kailas expressed his happiness on wide spectrum of participants in this school. He also enlightened the participants with the activities of the Department of Atomic Energy (DAE) in promoting basic sciences in the country. He emphasized that reactor, synchrotron, or accelerator based research can be taken up in the country using the large scale national facilities set up by DAE. He pointed out that UGC-DAE CSR could play an active role in bringing the accelerator based research facilities available at BARC under its ambit of promoting research through collaborative research schemes (CRS). He also highlighted the need of user-institute interaction for wider dissemination of information and to have a larger user base that can actually benefit from carrying out upfront research work.

In the concluding session on the last day, Dr. Siruguri briefly summarized the proceedings of the school and encouraged students and faculty members to come up with interesting problems which would involve the use of neutron scattering and related activities for the benefit of their own research work. Dr. S. Rayaprol proposed a vote of thanks. Certificates of participation were given to all participants. Participants were invited to give their feedback about the school. The school was well received by all participants, many of them being first-timers to neutron scattering, and they expressed their happiness in participating in this school.

7.6 Awareness workshop for University Users for Collaborative Research in Basic & Aplied Sciences

An Awareness workshop entitled Awareness workshop for University Users for Collaborative Research in Basic & Aplied Sciences was held at Patna Womens College, Patna on 9-10 January 2013. Jointly organized by the Department of Physics, Patna Womens College and UGC DAE CSR Kolkata Centre, this was first such workshop held in Bihar by the Centre.

The main thrust of the workshop was to wasm to familiarze the scientific community in The main thrust of the workshop was to familiarize the scientific community about the various types of available research facilities in the Consortium Centres and the DAE institutes at VECC-Kolkata, IOP-Bhubaneswar, RRCAT-Indore, BARC-Mumbai and IGCAR-Kalpakkam, specially in this part of the country. This, it was hoped , would develop interest in basic and inter-disciplinary research and also encourage potential collaborations with the Consortium in common fields of interest. The workshop consisted of invited talks from Scientists from VECC, Kolkata, UGC-DAE CSR Indore, Mumbai and Kolkata Centres and was attended by around 125 participants

The workshop was inaugurated by Prof. Ashok De, Director National Institute of Technology(NIT) Patna, who in his inaugural address said that such a workshop would go a long way to promoted basic and applied research in Bihar and also expressed his desire to support the Patna Womens college for further collaborations. Sri Amarjeet Sinha, IAS Principal Secretary, Dept. of Education, Govt. of Bihar, Patna the Guest of honour, gave an illuminating talk. Dr. Sister Marie Jessie A C, Principal, Patna Women's College, in her welcome address thanked the consortium for taking the initiative in holding such a workshop for the first time in Patna. The outlook of the worshop was presented by Dr.A.K.Sinha, Centre Director, UGC-DAE CSR, Kolkata Centre.

The technical session started with a motivating talk on Facilities & Research Programs at UGC-DAE CSR, Indore Centre, by Prof.Ajay Gupta, Centre Director, UGC-DAE CSr Indore Centre. He highlighted some of the major facilities at the Indore Centre and also spoke on some of the types of Research being carried out at the Centre. Dr.N.P. Lalla from Indore Centre of the consortium gave a detailed talk on the principle and applications of TEM. Dr.S.K.Deshpandey gave a very interesting talk on the various facilities at Mumbai Centre. The facilities at the Variable Energy Cyclotron Centre, Kolkata wee highlighted by Dr.Chandana Bhattacharjee, while details of some material science research being carried out at VECC using ion beams was presented by Dr.Gayatri Banerjee. Dr.R.J.Choudhury from UGC-DAE CSR Indore Centre spoke on Electronic structure studies of magnetic thin films using synchrotron. The Scientists of the Kolkata Centre also highlighted the various facilities and the type of research being carried out at the Centre. The technical sessions ended with two bringt talks by students of Patna womens college. Overall, this workshop was very highly appreciated, specially because of the multi disciplinary nature of the talks.

7.7 National Workshop on Radiation – A Powerful Tool for Research in Physical, Chemical and Life Sciences.

A National workshop was held on application of radiation for research in physical, chemical and life sciences at Central University of Jharkhand (CUJ), Ranchi during February 13-15, 2013. The workshop was jointly organized by the Centre for Applied Physics, CUJ, Ranchi and UGC DAE CSR Kolkata Centre. The aim of the workshop was to highlight the role of radiation in as a unique tool in studying problems of academic and technological importance in various areas of science. Since this was the first such worskhop in this region of the country it was felt that it would spread the awareness of the potential of various kinds of radiations in carrying out novel research programs in physical, chemical and life sciences. The idea was to motivate the faculty of various universities and colleges around Ranchi, who participated in the workshop, to come forward with some collaborative research proposals which could be supported by the Centre.

The workshop was attended by around 130 delegates which included 15 invited speakers. The selected participants were from different universities and adjoining colleges around Ranchi like Birla Institute of Technology, Mesra, Ranchi Univesity, Jubilee college Ranchi, Cooperative college, Jamshedpur, Silkworm

Physiology Laboratory, Central Tasar Research & Training Institute (Central Silk Board), Ranchi, Bhagalpur University, St. Xaviers college, Ranchi and also from universities and colleges from other parts of the country like Andhra University, Sambalpur University, Utkal University, NEHU, Shillong, Govt.TD Medical College, Alappuzha, Kerala

The workshop started with a welcome note by Prof.S.Medhekar, Head of Department, Centre for Applied Physics, CUJ Ranchi. The workshop was inaugurated by the Vice Chancellor, CUJ, Prof. D.T.Kathing. Dr.A.K.Sinha, Centre Director UGC-DAE CSR Kolkata Centre gave the outlook of the workshop highlighting the role of the Consortium in reaching out to the Universities and colleges through such workshops resulting collaborative research programs in areas of overlapping interest. This was followed by a kenote address by Dr.D.K.Srivastava, Director VECC, Kolkata who gave a very motivating talk on why we should pusue basic research in science.

The technical sessions started out with talks by senior scientists from the various Centres of the consortium regarding the various facilities open to the universities and colleges for carrying out research in different fields of science. Dr.Alok Banerjee from the Indore Centre gave two talks in which he described the facilities avaialble at the Indore centre and also at RRCAT Indore which were being used by the faculty of the Centre and also various universities to carry out international level research in the area of materials science. Dr. Gautam Ghosh of Mumbai Centre described the facilites available at the Mumbai Centre and also the Dhruva reactor where neutron scaterring experiments were being carried out in collaboration with a large number of univeristies for studying fundamental problems of materials science. Dr.Sujit Bandopadhyay from Variable Energy Cyclotron Centre spoke on the Ion beam facilities at VECC and particle irradiation studies of super conductors. Scientists of UGC-DAE CSR, Kolkata Centre made presentations highlighting the various facilities and research programs of the Centre. There were also presentations by the faculty of some colleges in Ranchi and Bihar where the work carried out using radiation was presented. The talk by Dr. J.P.Pandey, Silk Worm Physiology Laboratory, CTRTI Ranchi on “Applications of Radiation in Tasar Silk Culture to Provide Livelihood Sequarity to the Commons“ particularly appeared to be a new area in which some efforts could be made to have viable projects. The workshop ended with a valedictory session conducted by the senior faculty of Centre for Applied Physics, CUJ Ranchi, followed by distribution of certificates.

7.8 Thematic Orientation Workshop on Trace Element Analysis and Radiological Sciences, March 12 – 14, 2013

UGC-DAE Consortium for Scientific Research, Kolkata Centre and Manipur University, Imphal jointly organized a Thematic Orientation Workshop on “Trace Element Analysis and Radiological Sciences” during March 12-14, 2013 at the premises of Court Room, Manipur University. The workshop aimed to encourage and familiarize potential collaborators from universities and institutions in the use of various techniques involved in trace elemental research. The workshop also aimed to exploit the cross disciplinary potential of trace element studies including physicists, chemists, biologists, geologists, environmentalists, etc. We received more than 180 applications for the workshop. Unfortunately, we were able to select only 130 participants with a view to match the accommodation facility available in Manipur University. Participants from various disciplines including agriculture, physics, chemistry, biology, biotechnology, environmental sciences, forensic sciences, etc. and from various universities, institutes and Government agencies attended the workshop. In number, 9 colleges, 11 institutes, 15 Universities, 3 medical sciences centres and 3 Government agencies took part in the workshop. The 3 medical sciences centre are – (i) Regional Institute of Medical Sciences, Imphal (ii) Cachar Cancer

Hospital and Research Centre, Silchar (iii) Tata Memorial Centre, Advance Centre for Treament, Research and Education in Cancer, Navi Mumabi; and the 3 Government agencies are – (i) Directorate of Environment, Govt. of Manipur (ii) Department of Forensic Science, Govt. of Manipur (iii) Department of Horticulture and Soil Conservation, Govt. of Manipur. The workshop was formally inaugurated by Prof. H. N. K. Sarma, Vice-Chancellor, Manipur University as Chief Guest along with Prof. R. K. Gartia, Dean of Mathematical and Physical Sciences, Manipur University as the Guest of Honour. Prof. L. Warjeet Singh, Head, Department of Chemistry, Manipur University presided over the inaugural function. In the inaugural function, Dr. A. K. Sinha, Centre Director, UGC-DAE, CSR, Kolkata Centre highlighted the theme and outlook of the workshop.

The technical session had eight sub-sessions and a poster session. Sessions I – VI were comprised of 15(fifteen) invited lectures, sessions VII – VIII were comprised of 10 (ten) oral presentations from participants. In the poster session, there were 8 (eight) presentations. The Technical session was initiated with the invited lecture delivered by Prof. A. K. Das, Former Vice-Chancellor of Kalyani University on "Green Strategies in Trace Analysis and Speciation" which is indeed a very crucial task for sustainable resource utilization and environment friendly. Among the invited speakers, Dr. M. K. Tiwari, Dr. Sushanta Lahiri and Dr. M. Sudarshan presented illuminating talks on the principles and applications of certain techniques such as X-Ray Fluorescence, Synchrotron X-ray Fluorescence, Inductively Coupled Plasma Optical Emission Spectroscopy. Dr. Anindita Chakraborty, Prof. S. N. Kalkura and Prof. M.L. Garg delivered fascinating lectures on the essentials of trace elements in health issues such as carcinogenesis, biomineralization, protein specific metal ion binding, etc. Prof. S.C. Santra gave a lecture on the threats of metal ions and micronutrients to the environment as well as remedies. Prof. A. R. Thakur, former Vice-Chancellor, Techno India University and Dr. S. R. Chaudhuri also gave lectures on biosorption and bioremediation of trace elements with the help of microbes which is a very effective approach in reducing quantity and toxicity to the environment. Prof. S.K. Sarkar delivered a lecture on the distribution and toxicity of arsenic in the marine environment, especially oriented to arsenic speciation in sediments and representative biota of Sundarban Mangrove Wetland, India. Prof. S. Chattopadhyay presented an update on the use of radioisotope Technetium-99m in nuclear medicine along with the chemical separation strategies and technology. Last but not the least, Prof. G. J. Sharma have clearly opened the world of radiation highlighting how living beings are frequently exposed to the realm of radiation, its benefits and harmfulness as well as the remediation strategies.

8. Theses and Student Projects

8.1 Ph.D Theses

1. Mr Devdutta Misra has been awarded the Ph D degree for his thesis entitled "*Elemental Homeostasis and associated oxidative stress in chemical carcinogenesis"* from University of Calcutta. The work was carried out under the supervision of Dr.Anindita Chakraborty and Prof. Maitree Bhattacharya of University of Calcutta.

2. Ms Shaoli Majumdar: has been awarded the Ph D degree for her thesis entitled "*Elemental profile and physiological response f epiphytic lichen parmelia caparata exposed to air pollutants: an approach towards passive monitoring of air polution in Kolkata"*from University of Kalyani. The work was carried out under the supervision of Prof. S.C Santra, University of Kalyani and Prof. N.K.Jana, Charudhandra College, Kolkata

3. Mr. S. Vinodh Kumar has been awarded the Ph.D. Degree from Jadavpur University for thesis entitled "Some Aspects of Physico-Chemical Modification of Selective Organic Polymers" under the supervision of Dr. Abhijit Saha. Ms. Pallavi Kushwaha has been awarded Ph.D. degree from DAVV, Indore. Her thesis title was, "Study of phase separation and metastability across first order magnetic transitions." The work was carried out under the supervision of Dr. R.Rawat.

4. Ms. Deepti Kothari awarded PhD. The title of her thesis work is "Preparation and characterization of bismuth ferrite based multiferroic materials". The work was carried out under the supervision of Dr.V.R.Reddy

8.2 Student Projects

A number of M.Sc., M.Tech. and M.Phil students from various universities do their project work using the facilities of the Consortium. Short term summer projects are also done by some of the students.

At Indore Centre

MPhil Projects:

1. Ms Pooja Parmar, Department of Computer Science, Govt. Holkar Science College, affiliated to DAVV, Indore (2012) on Automation of I-V characteristics measurement setup at various temperatures. Supervisor: Dr. G. S. Okram

M.Sc. Project

1. Ms. Rajshree Pandey, Devi Ahilya University, Indore on "Preparation and Characterization of Nanocrystalline Fe doped CdS thin films". Supervisor: Dr.V.Ganesan

2. Ms. Shanu Sharma from Govt. Girls Post Graduation College, Indore. Supervisor: Dr.A. Lakhani
3. Ms. Trapti Sharma from Govt. Girls Post Graduation College, Indore. Dr.A. Lakhani
4. Ms. Versha Chauhan of SOP,DAVV on "In-situ stress measurement during growth of Ag film Dr.Dileep Kumar Gupta
5. Ms. Akita Pal: "Synthesis and Characterisation of ZnO/TiO_2 bilayer film deposited on Si (100) substrate Supervisor: T. Shripathi
6. Ms Nivedita Pandey, Govt. Holkar Sci. College, Indore, M.P. (2012) did her M.Sc project: Superpara-magnetism of nanocrystalline nickel of nearly 1 nm. Supervisor: Dr. G. S. Okram
7. Ms. Kanika, School of Physics, D.A.V.V., Indore project in Raman laboratory in 2012 . Supervisor: Dr.Vasant Sathe
8. Shri Sonu Yadav, from School of Physics, D.A.V.V., Indore, project in Raman laboratory in 2012 . Supervisor: Dr.Vasant Sathe

M. Tech. Project

9. Ms. Shakti Sanago, M. Tech. (Nanotechnology), RGPV, Bhopal on "Study on Nanocrystalline ZnO Microstructure and its transport properties". Supervisor: Dr.V.Ganesan
10. Aarti Sirsat,DAVV, Indore, one : development of resistivity measurement set up for thin films. Supervisor: Dr.D.M.Phase
11. Ms. Sania Ayaz, RGPV, Bhopal, on "Photoconductive Properties of Nano Dots of Cadmium Sulphide (CdS)". Supervisor: Dr.V.Ganesan
12. Mr. Pawan Kumar of RGPV,Bhopal, "Development and utilization of MOKE interface software for in-situ study of magnetic ultra-thin film structures" Dr.Dileep Kumar Gupta
13. Mr. Manish Gupta,, ITM University, Gurgaon on "Heat capacity study on YMnO3". Supervisor: Dr.V.Ganesan

B. Tech Project:

14. Mr. Ankit Potdar,., Amity University, Noida, on "Preparation of Nanocrystalline Co doped CdS thin films and its AFM Analysis". Supervisor: Dr.V.Ganesan
15. Mr. Amandeep Singh of Panjab Technical University, Panjab, "Design and development of the computer controlled four terminal relay scanner for in-situ resistivity measurement". Supervisor: Dr.Dileep Kumar Gupta

At Kolkatta Centre

M.Phil Project:

16. Mr Sanjay Kumhas "Photon & Neutron induced nuclear reactions of actinides at intermediate energies", under the co-supervision of Dr D N Basu, from VECC.

M.Sc Project

17. Mr. Jijo Abraham, Centre for Nanoscience and Nanotechnology, Mahatma Gandhi University. Supervisor: Dr. Abhijit Saha
18. Ms. Barnita Makhal, Department of Chemistry, IIT, Roorke. Supervisor: Dr. Abhijit Saha
19. Ms. Hemalatha Bhojan, Department of Nanoscience and Nanotechnology, Bharathiar University Supervisor: Dr. Abhijit Saha

Summer projects

20. Ms. Pallabi Bhowmick of Deptt of Env Science Calcutta University "Effect of ionizing radiation and pH change on some metabolic aspect of *Penicillium Sp*" Supervisor: Dr.Anindita Chakraborty
21. Ms. Devlina Paul from Deptt of Home Science Food and Nutrition Section J.D.Birla Institute completed a project entitled "Fortification of yoghurt using Ferrous lactate and doing the sensory evaluation to judge its acceptability" Supervisor: Dr.M.Sudarshan
22. Ms Deblina Ghosh from Deptt of Home Science Food and Nutrition Section J.D.Birla Institute completed a project entitled "Iron fortification of puffed rice by using *spirulina plapensis* powder" Supervisor: Dr.M.Sudarshan

At Kalpakkam Node

Four students have carried out their summer project at the Kalpakkam Node of UGC-DAE CSR during June-July, 2012. Two students from Harishchandra Research Institute, Allahabad, have worked on the XRD as a tool of characterisation under Dr. Sujay Chakravarty of the Node. Two students from the Chennai Mathematical Institute have carried out their project under Dr. Shamima Hussain on the applications and use of scanning electron microscopy.

9. Seminar/Lectures delivered by UGC-DAE CSR Scientists/Personnel

1. A. K. Sinha: "Future experiments using RIB facility – Barrier Distribution Studies using quasi-elastic Scattering with ^{32}Mg Beam", International workshop on Future plans with Radioactive Ion beam, SINP Kolkata, April, 2012
2. A. K. Sinha: "Frontiers in Gamma Spectroscopy: Spectroscopy near the Island of Inversion", One-Day National Seminar on New Frontiers in Physics, Physics Department, Gauhati University, May, 2012
3. Dr. G.S. Okram: Tapping electricity from waste heat, Physics Department, Tezpur University, Tezpur, May 3, 2012.
4. Dr.S.K.Deshpande: "X-ray Analysis of Thin Films" at the Workshop on Powder X-ray Diffraction and Small Angle Scattering held at IISER Pune, during May 15-16, 2012.
5. Dr. P.D. Babu: "study of magnetic materials through neutron diffraction" at the workshop on powder x-ray diffraction and small angle scattering held at IISER, Pune, organized jointly by IISER and NCL Pune, May 15-16, 2012.
6. Dr. G.S. Okram: Harvesting electricity from waste heat: A material's aspect, Physics and chemistry Departments, Manipur University, Imphal, May 16, 2012.
7. Dr. G.S. Okram: Electricity from waste heat: A Perspective, National Seminar cum Workshop on Physics for Cultural Heritage, DM College of Science, Imphal, May 25, 2012.
8. Ajay Gupta: "Study of interfaces in magnetic multilayers", invited talk at 12th International Conference on Surface X-ray and Neutron Scattering, Kolkata, 25th to 28th July, 2012.
9. Vasant Sathe: "Probing spin, orbital and domain orders in highly correlated oxides by polarized Raman spectroscopy" Invited talk in 23rd International conference on Raman spectroscopy held at Bangalore August 12-17, 2012
10. Dr.R.J.Choudhary : "Magnetic Semiconductors: Problems and Prospects" at C.M. Science College, Darbhanga, Bihar on 18th August 2012
11. R Rawat: "Magnetotransport and MFM studies in LPCMO film" at Physics department, Pune University, Pune, August 25, 2012.
12. D.Das: "Defects in ZnO nanostructure: an evaluation by positron annihilation and photoluminescence spectroscopy" at Condensed Matter Days 2012 , BIT Mesra, Jharknand , August 29-31, 2012.
13. V. Ganesan: **"**Visualization and Measurements at Nano-scales – Role of SPM" at the Kerala University, Trivandrum, Sept 10, 2012.
14. A Saha: "Optical Spectroscopic Techniques for Characterization of Nanomaterials" in 'Workshop on Frontiers of Spectroscopy and Microscopy', held at Mahatma Gandhi University, September 10-12, 2012.
15. V. Ganesan: "Scanning Probe Microcopy – Applications ranging from Physics–to Biology" during the National workshop "Frontiers of Spectroscopy & Microscopy" at the Mahatma Gandhi University, Kottayam, Sept 11, 2012.
16. V. Ganesan: "Role of SPM in semiconductors" at National Conference on Indian Development in Recent and Ideal Semiconductors for Novel Applications NC-IDRIS 2012 at Agrawal Sci. College, Navapur, Nandurbar, Maharashtra, Oct 6, 2012.
17. Ajay Gupta: "X-ray study of Swift Heavy Ion Induced interface modifications in Multilayer nanostructures" at International conference on 'Swift Heavy Ions in Materials Engineering and Characterization (SHIMEC 2012)', New Delhi, 9th October to 12th October 2012.
18. DM Phase: "Growth and properties of pulse laser deposited transition metal oxide thin films" at Department of Physics, University of Pune, refresher Course, October 16, 2012.
19. Dr.R.J.Choudhary : "Thin films of dilute magnetic semiconductors" in the refresher course at Department of Physics, University of Pune on 22nd October, 2012.

20. S. Rayaprol: “Understanding Structure-Property Correlations using Neutron Diffraction” during refresher Course in Physics at University of Pune, October 26, 2012.
21. V. Ganesan: Invited talk at “Inspire” program of DST at Swami Vivekanand College, Seshore, MP, Oct 27-31, 2012.
22. S. S. Ghugre: “Hybrid Gamma ray detectors”, invited talk at the Nustar Week 2012, at Variable Energy Cyclotron Centre, Kolkata October 2012
23. V. Ganesan: “AFM/STM Analysis of thin films and Coatings” in the STEM-2012 conference on Challenges and issues in surface modification, thin films and coatings held at IGCAR, Kalpakkam, Nov 6, 2012.
24. V. Siruguri: "In-field neutron diffraction evidence for kinetic arrest in some magnetic functional materials", MI-1 Semina, Helmholtz Zentrum Berlin, November 7, 2012.
25. V. Ganesan: “Basics of Liquefaction of Gases” during the inauguration of their low temperature facilities at the IPS Academy, Indore, Nov 24, 2012.
26. S. S. Ghugre: “Spectroscopy near the Island of Inversion : An Indian Perspective”, invited talk at Workshop on Science with rare Ion Beams SCRIBE-2012, at Variable Energy Cyclotron Centre, Kolkata November 2012.
27. S. S. Ghugre: “Spectroscopy near the Island of Inversion”, invited talk at the Third International Symposium on Frontiers in Nuclear Physics November 2012 at Beihang University in Beijing, China.
28. S. S. Ghugre: “Gamma-ray spectroscopic data: Indian perspective”, BRNS workshop on Evaluation of Nuclear Structure and Decay Data, at Variable Energy Cyclotron Centre, Kolkata November 2012.
29. R. Raut: “Gamma Induced Cross-Section Measurements at HIGS: Addressing theAstrophysical Context”, at School on Low Energy Nuclear Astrophysics, November, 2012,at Saha Institute of Nuclear Physics.
30. P Chaddah: “Exploring the tunable coexistence of magnetic phases” at DAE_SSP Symposium, IIT Bombay, Mumbai, Dec 3-7, 2012.
31. P. D. Babu: “Rotational Tunneling States of NH 4^{+} ions and Specific Heat of (NH4)xRb1-xBr” at DAE Solid State Physics Symposium held at IIT Bombay, Dec 3- 7, 2012.
32. R Raut: “Photodisntigration Studies at HI□S: Addressing the Few and the Many”, DAE Nuclear Physics Symposium, held at Delhi University, Delhi, Dec 3-7, 2012.
33. A K Sinha: “Nuclear Physics with Indian National Gamma Array (INGA)”, DAE Nuclear Physics Symposium, held at Delhi University, Delhi, Dec 3-7, 2012.
34. Mukul Gupta: “Silver Surfactant Mediated Growth of Magnetic Multilayers”, at 1st Winter Workshop on Engineering at Nanoscale: From Materials to Bio-sensors, held at Indian Institute of Technology, Indore. 10-12 December, 2012
35. Dr.R.J.Choudhary : “Growth of Fe3O4 films and modification in its electronic property due to Nanostructure” at National conference on Physics of Nanomaterials and Applications’ on 14th and 15th December 2012 at Department of Physics, Dayanand College of Arts & Science, Solapur.
36. V. Ganesan: Invited talk at “Inspire” program of DST at Helios College, Ujjain, Dec 17, 2012,
37. V. Ganesan: Invited talk at “Inspire” program of DST at Avantika College Ujjain, Dec 25, 2012.
38. R. Raut: “Nuclear Photodisintegration Studies at HIGS: Addressing the Few and the Many, **,** Symposium Invited Talk, DAE Symposium on Nuclear Physics, December, 2012, Department of Physics and Astrophysics, University of Delhi
39. Vasant Sathe: “Orientational order and domain structure analysis using Raman spectroscopy” Workshop on “Exotic materials: synthesis, Characterization and Application” Department of Physics, Banaras Hindu University, Varanasi 1-3 Jan. 2013-01-04.
40. V. Siruguri: "In-field neutron diffraction and the CHUF protocol: A novel way of probing metastabilities across first order phase transitions" at the 2nd International Symposium on Neutron Scattering at Bhabha Atomic Research Centre, Mumbai during January 14-17, 2013.
41. P. D. Babu: “Effect of Magnetic Field and Temperature on the Magnetic Structure of Rare-Earth rich intermetallic compounds” at the International Symposium on Neutron Scattering (ISNS-2013) held in Mumbai during Jan 14-17, 2013.

42. V.Ganesan: National Seminar on, "Advances in Nano-structured Materials and Their Applications" on 22nd - 23rd January 2013 C.H.C. Arts, S.G.P. Commerce and B.B.J.P. Science College, Taloda, Dist. Nandurbar, (M.S.) India.
43. V.Ganesan: "SPM analysis of Nano-structures – Imaging and Quantification Part 1" at the Second International Symposium on Semiconductor Materials and Devices (ISSMD-2)" held at Jammu University, Jammu, during January 31st and 1st February 2013
44. Mukul Gupta: "Depth Profiling in Thin Films using X-Ray Reflectivity (XRR), Neutron Reflectivity (NR) and Secondary Ion Mass Spectroscopy (SIMS), Part I", at Refresher course, School of Physics, DAVV Indore, 9 January 2013.
45. Mukul Gupta: "Depth Profiling in Thin Films using X-Ray Reflectivity (XRR), Neutron Reflectivity (NR) and Secondary Ion Mass Spectroscopy (SIMS), Part II", at Refresher course, School of Physics, DAVV Indore, 10 January 2013.
46. T. Shripathi: "Electron Spectroscopy for Chemical Analysis Part I" UGC Refresher course at DAVV university, Jan, 2013 Indore
47. T. Shripathi: "Electron Spectroscopy for Chemical Analysis Part II" UGC Refresher course at DAVV university, Jan, 2013 Indore
48. D.M.Phase."Growth and properties of pulse laser deposited transition metal oxide thin films" by Dr.D.M.Phase at DAVV, Indore , refresher Course Jan.2013.
49. D.M.Phase "Photoelectron studies using laboratory and synchrotron sources" UGC Refresher course at DAVV university, Jan, 2013 Indore
50. R.J.Choudhary : "Growth and Properties of Thin Films" in the refresher course at Department of Physics, DAVV, Indore on 15th January, 2013.
51. R.J.Choudhary : "Thin Films of Functional Magnetic Oxides" in the refresher course at Department of Physics, DAVV, Indore on 16th January, 2013.
52. Vasant Sathe: Raman spectroscopy and application Part I" in refresher course held at school of physics, D.A.V.V., Indore on 16 and 17th of January 2013
53. Vasant Sathe: Raman spectroscopy and application Part II" in refresher course held at school of physics, D.A.V.V., Indore on 16 and 17th of January 2013
54. V.Ganesan: "SPM analysis of Nano-structures – Imaging and Quantification Part 2" at the Second International Symposium on Semiconductor Materials and Devices (ISSMD-2)" held at Jammu University, Jammu, during January 31st and 1st February 2013
55. Ajay Gupta:."X-ray study of interfaces in magnetic multilayers," at 6t India - Singapore Joint Physics Symposium (ISJPS - 2013), Kharagpur,February 25 -27, 2013.
56. V. Siruguri: "Metastabilities across first order phase transitions in magnetic functional materials", at the Indo-Singapore Joint Physics Symposium, held at IIT Kharagpur during Feb 25-27, 2013.
57. R. Raut: "Knocking on the Heaven's Door: Nuclear Astrophysics Endeavours usingGamma-ray Beams" at National Conference on Nuclear Dynamics andAstrophysics, February, 2013.
58. Mukul Gupta: "Depth Profiling in Thin Film Multilayers using x-ray, neutron reflectivity and Secondary Ion Mass Spectroscopy (SIMS)", at Nanomaterials: Synthesis and Applications, held at Government Autonomous Post Graduate College Chhindwara (M.P.), March 4-6, 2013
59. D.Das: "Tailoring thermal , magnetic and optical properties of BiFeO3nanoparticles by alkaline earth metals" at Third National Seminar on Recent Ttrends in Condensed Matter Physics including Laser application , March 5-7, 2013, Centre of Advanced Study,Burdwan University, W B
60. Ajay Gupta: "Tailoring surfaces, thin films and multilayers using heavy ions," at National Workshop on Ion Beams in Materials Research (IBMR-2013), Jaipur, 22 -23 March 2013.
61. V.Ganesan: "SPM techniques in standardization" at the 1st National Seminar on Standardization for Nanoscience and Nanotechnology" held at NPL, New Delhi, during March 25-26, 2013

10 Other Activities

Annual Day 2012

The Annual day of UGC-DAE Consortium for Scientific Research (CSR) was celebrated on December 14, 2012. Prof. Dhananjai Pandey, Director, Indian Institute of Technology (BHU), Varanasi, was the Chief Guest.

The function started with Dr. P. Chaddah, Director, UGC-DAE CSR, welcoming the guests. He informed the achievements of the Consortium such as utilization and development of various facilities and its research activities, specifically the role of Consortium in providing many state-of-art in-house experimental facilities & big science facilities of the country to University researchers of the country. He mentioned that a total of about 1000 researchers have utilized the facilities of Consortium in the last year and resulted in about 200 journal publications, so far with the Consortium by-line. He mentioned about the addition of the chemistry wing at IGCAR, Kalpakkam Node. He also appreciated the vibrant interaction of CSR students with the University students during their visit to CSR, which resulted in the scientific growth of the Consortium. He then introduced the Chief Guest to the gathering, highlighting his scientific achievements, recognitions and awards.

In his inaugural address, Prof. Pandey commended the achievement of CSR in providing access to state of art research facilities to the University researchers. He also recalled his association with the Consortium at various capacities from the inception and mentioned that he witnessed a substantial progress of CSR. He spoke on "Isostructural Phase Transitions", where he discussed emerging applications of the multiferroic materials and many fascinating physical properties of these materials. He also discussed his research work and elaborated on the use of diffraction methods such as x-ray and neutron in the fundamental understanding of these materials. He mentioned that his results are the first of its kind to demonstrate the linear magneto-electric coupling in $BiFeO_3$ based multiferroic systems. The observed magneto-electric coupling is explained in terms of Isostructural Phase Transitions.

After the Chief Guest address, the CSR award for Scientific Excellence was presented to Dr Abhijit Saha of the Kolkata Centre for his sustained contribution towards the mandate of the Consortium and carrying out internationally impact making research work.

Prof. Ajay Gupta, Centre-Director, UGC DAE CSR, Indore Centre, proposed vote of thanks. The function was attended by scientists and academicians from RRCAT, DAVV and other institutions and Scientists and students of CSR. The address of Prof. Pandey was followed by a poster session highlighting the research activities / facilities of the three Centres at Indore, Kolkata, Mumbai and the Kalpakkam Node and the thesis presentations by the research students of the CSR in the afternoon session. Ms. Ridhi Master received the first prize for her presentation.

The day ended with a musical program by Shri. Vilas Khargonkar and Shri. Ambrish Kalele.

National Science Day 2013

National Science day 2013 was celebrated at the consortium on 28th February 2013. This year the event was well attended by the students from different schools and colleges along with scientific staff and research students of the consortium. Two lectures were arranged on this occasion followed by laboratory visit to different laboratories for the school/college students conducted by Dr. Ganesan. The event started with Dr. Vasant Sathe, Scientist at Indore centre of the Consortium giving his first lecture on "Polarized Raman Spectroscopy: A tool to investigate domain structure in epitaxial films". He started the lecture at a popular level describing the Raman Effect in a very simple way along with historical events and excitement of discovery of Raman Effect. The sharp scientific insight shown by Raman excited the school children present in the audience. He emphasized the importance of Lasers and current Raman set-ups in brief. He then showed by examples how Raman spectroscopy is presently used in solving complex problems in condensed matter physics. He focused on the use of polarization analysis of the scattered photon and how it can give information on the orientation of a single crystal. The intensity of a Raman mode depends on the Polarization of incident and scattered photon, Raman tensor matrix and orientation of unit cell axis of the material being investigated. Dr. Sathe showed that by doing some algebraic calculations a simpler relationship can be obtained that can give information of the orientation of the crystal axis in a plane unambiguously and in a non-destructive manner. He gave example of finding orientation of unit cell orientation in the epitaxial films of $CaCu_3Ti_4O_{12}$ compound. The epitaxy of the film was also confirmed by polarization analysis. Further developing the formulation involving the geometry of the system and Raman tensor they could analyze the absence of twin domain structure in these epitaxial films. This is an important issue as presence of twin domain structure was considered as one of the essential factor giving internal barrier layer capacitance in $CaCu_3Ti_4O_{12}$ compound showing extra ordinarily high dielectric constant. He ended his lecture by giving summary of the talk and usefulness of the invention of Raman effects in present scientific world.

The second lecture was given by Dr. Rajeev Rawat, Scientist at Indore centre of the Consortium on "Supercooling and superheating in a disorder broadened first order magnetic transition". With a brief introduction to first order transition and its broadening due to quench disorder, speaker recalled the Science Day Talks of previous year (i.e. 2012) which were also related to supercooling and superheating. One of these talk (by Dr. Banerjee) dealt with the analogue of counterintuitive age old observation of "hot water freezes faster than the cold" i.e. Mpemba effect, in magnetic material. Later that year Royal Society of Chemistry offered £1000 prize for eye-catching and scientifically sound explanation of Mpemba Effect, which was awarded to Nikola Bregović, University of Zagreb, Croatia in Jan 2013. Supercooling is believed to be one of the reasons for this effect and the cooling curves of water invariably showed warming at the ice to water transformation. However, such signatures of the transformation of supercooled states, i.e. warming when heat is extracted from the system, are rarely observed across first order magnetic transitions. The only magnetic material where similar effect has been observed is by Gschneidner et al. (Phys. Rev. Lett. 78 (1997) 4281) in ultra-high purity rare earth elements Dy and Er. Dr. Rawat then showed similar effect in magnetic compound Ta doped HfFe2 prepared with commercially available constituent elements. He showed that the first order antiferromagnetic (AFM) to ferromagnetic (FM) transition in this system during cooling is accompanied by rise in temperature though rate of heat extraction was almost constant. Opposite effect was observed during warming i.e. when system is warmed by supplying a constant heat per unit time it showed cooling for FM to AFM transition. These two counterintuitive effects were taken as the signature of the transformation of metastable supecooled AFM state to stable FM state and metastable superheated FM state to stable AFM state, respectively. He then discussed the role of quench disorder broadening and influence of magnetic field on supercooling and superheating in this system.

हिंदी पखवाड़ा 2012

हिंदी पखवाड़ा के अवसर पर दिनांक 29 सितम्बर 2012 को निम्न–सारांषित व्याख्यानों का आयोजन किया गया।

पदार्थों के चुम्बकीय गुणों पर आयन प्रतिरोपण का प्रभाव

रत्नेष गुप्ता : स्कूल आफ इंस्ट्रूमेन्टेषन, देवी अहिल्या विष्वविद्यालय, इन्दौर

आयन प्रतिरोपण से हम किसी पदार्थ के गुण–धर्म को प्रभावित कर सकते हैं तथा इन्हें इच्छानुसार बदल सकते हैं जिससे उस पदार्थ का इच्छित उपयोग किया जा सकता है । इस व्याख्यान में आयन प्रतिरोपण के चुम्बकीय गुणधर्मों की विवेचना की गई है । मुख्यतः हमने इसमें कोबाल्ट धातु की तनु फिल्म पर आयन प्रतिरोपण से होने वाले प्रभाव का अध्ययन किया जिसमें तीव्र ऊर्जा तथा कम ऊर्जा वाले आयनों के प्रतिरोपण से पदार्थ के चुम्बकीय गुण–धर्म में हुए परिवर्तन का भी अध्ययन किया गया । आयनों के कारण तनु कोबाल्ट फिल्म की क्रिस्टलीय–संरचना परिवर्तन, HCP से FCC में होता है, जिसके कारण फिल्म का चुम्बकीय आघूर्ण कम हो जाता है । कम ऊर्जा वाले आयनों का प्रभाव चुम्बकीय गुणधर्म पर अधिक पाया गया। आयन प्रतिरोपण के कारण चुम्बकीय एनाइसोट्रापी चार–गुणा से दो गुणा हो गई । व्याख्यान में Co/Fe कपल्ड फिल्म पर आयनिक प्रभाव का भी वर्णन किया गया। सिंक्रोट्रान किरणों से इन फिल्मों के अध्ययन की भी विवेचना की गई ।

<u>अवस्था परिवर्तन पर भौतिकीय कारकों का प्रभाव</u>

देवेन्द्र कुमार: विष्वविद्यालय अनुदान आयोग – परमाणु ऊर्जा विभाग वैज्ञानिक अनुसंधान संकुल

इस वयाख्यान में अवस्था की स्थिरता, अवस्था परिवर्तन के क्रम, और प्रथम-क्रम अवस्था-परिवर्तन के दर पर विभिन्न वाह्य कारकों (जैसे चुम्बकीय क्षेत्र) के प्रभाव के बारे में चर्चा करेंगे | प्रथम क्रम अवस्था परिवर्तन के दौरान, उच्च ताप अवस्था के अंश, अवस्था परिवर्तन के तापमान के नीचे, सुपरकूल अल्प-स्थिर अवस्था में रह सकते है | सुपरकूल अल्प-स्थिर अवस्था में स्थिर अवस्था का निर्माण दोनों अवस्थाओं के मुक्त उर्जा में अंतर के द्वारा संचालित होता है, जबकी इन अवस्थाओं की बीच अंतरफलक के निर्माण के लिए आवश्यक तनाव ऊर्जा और अनुपयुक्त आयतन तनाव ऊर्जा इसका विरोध करते हैं | आबाधित स्थिति (Unarrested state) में, सुपरकूल अल्प-स्थिर अवस्था से स्थिर अवस्था में परिवर्तन की दर सुपरकूल अवस्था में उपस्थित पदार्थ के अंश और स्थिर अवस्था के स्थाई नाभिक के न्यूकलिऐसन (Nucleation) की उर्जा पर निर्भर करती है | सुपरकूल अल्प-स्थिर अवस्था से स्थिर अवस्था में परिवर्तन ताप और वाह्य क्षेत्र की कुछ परिस्थितयों में बाधित हो जाता है | $NdNiO_3$ बल्क और थिन फिल्म, $Pr_{0.5}Ca_{0.5}Mn_{0.975}Al_{0.025}O_3$, और $La_{0.5}Ca_{0.5}MnO_3$ में अवस्था परिवर्तन की दर पर क्रिस्टल दोष, ताप, और वाह्य चुम्बकीय क्षेत्र के प्रभावों की चर्चा की गयी ||

Awards and Recognitions

1. Dr. A. Saha, Scientist F, CSR Kolkata Centre received the *CSR award for Scentific Excellence, 2012.*

2. Mr. Akhil Tayal got the First prize in 'Research Scholar Presentation' at the 12th Indian Society of Mass Spectrometry- Triennial International Conference on Mass Spectrometry held at Cidade-de-Goa, Dona Paula, Goa during March 3-8, 2013.

New Appointments:

Mr. Neeraj Shukla joined the Kalpakkam Node as Scientist-D in Sep. 2012. He is in-charge of high-field low-temperature magnetic characterization laboratory. He did his M.Sc. (Phys) from IIT Kanpur and recently submitted his PhD thesis titled "Ion Beam Induced Nano Structuring and Magnetic Ordering" at IIT Kanpur under supervision of late Prof V.N. Kulkarni and Prof. H.C. Verma. His Research work dealt with nano structuring by focused ion beam (FIB) as a result of ion beam induced adhesion of thin gold film to non conducting substrates (useful as novel metamaterial plasmonic structures), comprehensive analysis of the deposition caused by scattered Ga ions during FIB-induced deposition. His work also included inducing magnetic ordering in HOPG by high energy carbon ions (utilizing 1.7 MeV Tandetron accelerator) and analyzing the samples by means of vibration sample magnetometer and magneto-resistance studies. His current interests are utilizing ion beams for inducing magnetism based on s- and p- shell electrons and using FIB as a nano fabrication tool for transport measurements and related studies.

Dr. Kiran Singh did his M. Sc. (Physics) and Ph. D. from Barkatullah University Bhopal in year 2002 and 2008, respectively. He has completed his Ph. D. on superconductivity entitled "Studies on the effect of doping on the crystal structure and superconductivity of MgB_2" under the supervision of Dr. N. K. Gaur, Reader, Department of Physics, Barkatullah University Bhopal. During his Ph. D., he was a recipient of 22nd M. P. Young Scientist Award in Physics given by M. P. Council of Science and Technology, Govt. of M. P., India, in 2007. He did his post doctoral research (Jan. 2009 to Dec. 2011) in CNRS Lab. CRISMAT, Caen, France with Dr. Charles Simon and Dr. Antoine Maignan. There he has explored the multiferroics and magnetoelectric properties of different materials. In March 2012, he joined Prof. E. V. Sampathkumaran group in Tata Institute of Fundamental Research, Mumbai as a visiting fellow. There he has developed multiferroics and magnetoelectric properties measurement facilities at wide range of temperature (1.8-350K) and magnetic field (0-14T).

Dr. Sudip Mukherjee joined CSR Mumbai Centre in November, 2012 as Scientist-D

Dr. Mukherjee obtained his Ph.D. (Sc.) degree in 2006 from Jadavpur University in the area of magnetic nanostructured materials. After that, he joined as postdoctoral researcher in the surface nanoscience group at the Center for Condensed Matter Sciences, National Taiwan University, Taipei, Taiwan. During two year stay from 2007 – 2009, he conducted high-resolution scanning probe microscopy (SPM) and spectroscopy study on complex transition oxide surfaces [single crystal sodium cobaltate (Na_xCoO_2)]. Later, he worked as postdoctoral fellow in low temperature physics group at the Department of Physics and Center for Nanoscience and Nanotechnology, National Sun Yat-Sen University, Kaohsiung 804, Taiwan. His work here involved fabrication of new class of high-*k* materials in which their dielectric constant could be modified by application of both electric and magnetic field. His current research interests are on studying the effects of spin fluctuations, magnetic ordering, and external magnetic field on the dielectric properties of the nanomagnetic materials, strongly correlated systems.

Foreign Visits by Faculty and Students of CSR:

S No	Name	Place visited	Date	Purpose
1.	Dr.D.M.Phase	Photon Factory, Japan	April 20-23, 2012	To perform experiments at the Indian Beamline
2.	Ms. Komal Bapna	Photon Factory, Japan	April 20-23, 2012	To perform experiments at the Indian Beamline
3.	Dr. S.K. Deshpande	Elettra Synchrotron Facility, Trieste, Italy,	April 29-May 6, 2012	To carry out XAFS experiments under ICTP-Elettra Users Programme
4.	Mr. Gagan Sharma	ILL, Grenoble, France and DESY, Germany	May 3-10, 2012 and May 10-17, 2012	To carry out Neutron Reflectivity and Nuclear Forward Scattering Experiments.
5.	Prof. Ajay Gupta	ILL, Grenoble, France and DESY, Germany	May 4-10, 2012 and May 12-16, 2012	To carry out Neutron Reflectivity and Nuclear Resonance Scattering Experiments.
6.	Dr. Dileep Kumar	DESY, Germany	May 12 16, 2012	Utilization of the synchrotron radiation at PETRA-III,
7.	Mr. Sunil W. D'Souza	PSI, Switzeland	June 10-13, 2012	To attend Conference
8.	Dr. S. Rayprol	ILL, Grenoble, France	July 1-6, 2012	To carry out Neutron Diffraction Experiments.
9.	Dr. V. Siruguri	ILL, Grenoble, France	July 1-6, 2012	To carry out Neutron Diffraction Experiments.
10.	Dr. S.R. Barman	Fritz Haber Institute, Berlin DESY, Germany	July 26-29 & Aug. 4-15, 2012 July 28 - Aug. 4, 2012	For discussions & Data evaluation To perform experiments at PETRA-III.
11.	Ms. Jayata Nayak	DESY, Germany	July 28 - Aug. 4, 2012	To perform experiments at PETRA-III.
12.	Mr. M. Maniraj	DESY, Germany	July 30 - Aug. 3, 2012	To perform experiments at PETRA-III.
13.	Dr. Mukul Gupta	DESY, Germany & PSI Switzerand	Aug. 26 – Sept. 14, 2012	To perform experiments at PETRA-III and PSI
14.	Mr. Akhil Tayal	DESY, Germany & PSI Switzerand	Aug. 26 – Sept. 14, 2012	To perform experiments at PETRA-III and PSI
15.	Prof. Ajay Gupta	DESY, Germany & ILL, Grenoble, France	Aug. 28 – Sept. 3 & Sept. 4- 10, 2012	To perform experiments at PETRA-III and ILL
16.	Mr. Gagan Sharma	ILL, Grenoble, France	Sept. 3- 110, 2012	To perform experiments at ILL
17.	Mr. SS Samatham	Rugen, Germany	Sept. 30 - Oct. 12, 2012	To attend and make oral presentation at 3rd EuroMagNET Summer School 2012
18.	Mr. SC Das	Institut for Physik, Greifswald, Germany	Oct. 1-31, 2012	Research work on deposition of functional thin solid films using HiPIMS
19.	Dr. V. Siruguri	Helmholtz Zentrum Berlin Germany	Nov. 6-8, 2012	Invited Talk
20.	Dr. P. D. Babu	ILL, Grenoble, France	Nov. 9-12, 2012	To perform experiments at ILL
21.	Dr. V. Siruguri	ILL, Grenoble, France	Nov. 9-12, 2012	To perform experiments at ILL
22.	Mr. UP Deshpande	KEK Japan	Dec. 9-13, 2012	To perform experiments at Indian Beamline at Photon Factory
23.	Dr. T. Shripathi	KEK Japan	Dec. 9-13, 2012	To perform experiments at Indian Beamline at Photon Factory
24.	Prof. Ajay Gupta	DESY, Germany	Feb. 8-14, 2013	To perform experiments at PETRA III
25.	Dr. Mukul Gupta	DESY, Germany	Feb. 10-13, 2013	To perform Nuclear Resonance Reflectivity Experiments.

11. List of Collaborative Research Schemes

11.1 Kolkata Centre

Utilizing VECC, Kolkata

1. Prof. S.C. Bhattacharya, Department of Chemistry, Jadavpur University,Effect on biomolecules by synthesized nanoparticles using ionizing radiations.
2. Dr. C.T. Aravinda Kumar, Department of Chemical Sciences, Mahatma Gandhi University Radiation Induced Modification of DNA and Some Pyrimidine Nucleosides and Nucleotides.
3. Prof. Kalyan Kumar Mukherjee, Department of Chemistry, Jadavpur University.Protection of radiation and chemical induced DNA damage by chemicals and nano materials.
4. Dr.Geeta K Sharma, Department of Chemistry, University of Pune.Radiation Induced synthesis of Metal Clusters: Effect of dose rate and LET.
5. Dr. Prabitra Chattopadhyay, Department of Chemistry, Burdwan University Study of the effects of radiation dose and ion beam on the structure and ion-exchange property of polyoxometallates".
6. Dr. Dilip Kumar Kakati, Department of Chemistry, Gauhati University.Studies on Ion-Beam Induced Modification and Gamma-Radiation Induced Graft Copolymerisation of N-vinyl pyrollidone and Glycidyl methacrylate on Polyurethane ".
7. Prof.. Jag Mohan Keller, Macromolecular Research Centre, Rani Durgawati University "Study of Effect Radiation on the Metalloid/ Oxide Incorporated Polymeric high Temperature Resistive Flexible Nano-Composite Thin Films for Microelectronics Application".
8. Dr. R. Dhanasekaran, Crystal Growth Centre, Anna University, Effect of ion implantation in GaN and ZnSe semiconductors for the fabrication of electornic and photonic devices.
9. Dr. Sunita Keshri (Shaw), Birla Institute of Technology.Effect of ion implantation and gamma irradiation on wide band gap semiconductors ".
10. Dr. Nandakumar Kalarikkal, School of Pure & Applied Physics, Mahatma Gandhi University, Ion beam Irradiation effects on the structural and ferroic properties of selected sol-gel derived films of nanomultiferroics".
11. Prof. S.C. Santra, Dept. of Environmental Science, University of Kalyani Comprehensive study on radiation induced metal tolerance in fungal strain".
12. Dr. Sanjit Dey, Dept. of Physiology, Calcutta University, Radiation Protection using Moringa oleifera principles.
13. Dr. Sarmistha Raychaudhuri, Department of Biophysics Molecular Biology & Bioinformatics, University Of Calcutta, Radiation induced alterations in DNA, RNA and Polyamine levels in plants.
14. Prof. Tapas Dasgupta, Department of Genetics & Plant Breeding, University Of Calcutta Radiation mediated Restructureing of new plant type in sesame adaptable to agro-climatic condition of West Bengal.
15. Dr.Sukhendusekhar Sarkar, Deparment of Physics, Bengal Engineering and Science Univeristy, Study of shape co-existence in ^{153}Ho and few-valence particle nuclei around ^{146}Gd Core".
16. Dr. Suresh Kumar, Deparment of Physics, University of Delhi Magnetic Rotational bands crossing and role of the proton and neutron orbitals in magnetic rotation (MR) phenomena near A = 135".
17. Dr. P.V.Madhusudhana Rao, Deparment of Nuclear Physics, Andhra University, Search for anti-magnetic rotation in A ~ 100 nuclei.
18. Prof. L. Chaturvedi, Guru Ghasidas University, Search for highly deformed structures in A ~ 130 region".
19. Dr. Sourav Ganguly, Department of Physics, Chandernagore College Study of Magnetic Rotation in odd-A Rb isotopes from lifetime measurement.

20. Dr. T.R. Routray, Department of Physics , Sambalpur University, The finite range effective nuclear interaction: A complete nuclear model .

Utilizing 3 MV Pelletron at IOP, Bhubaneswar

21. Dr. (Mrs.) Shanti Lata Sahoo, P. G. Dept. of Botany, Utkal University, Bhubaneswar, Regulation and Expression of Antioxidant Enzymes and Comparative Study on Metal Detection of Withania Somnifera L. and Abutilon indicum L. in Response to Various Metal Stresses.
22. Dr. Madhumita Manna, Dept. of Zoology, Bethune College, Kolkata, Influences of Trace Elements in Immune Funtion in Visceral Lesishmaiasis and post kala-azar Bermal Leishamaniasis of India.
23. Prof. S. C. Santra, Dept. of Environmental Science, University of Kalyani, Studies on trace element distribution and their role in salt stress adaptation in halophytic plants of mangrove vegetation of West Bengal.
24. Dr. R K Dutta, Dept. of Chemistry, IIT Roorkee, Roorkee, Ion Beam Assisted Synthesis and Chracterization.
25. Dr. Anup Kumar Talukdar, Dept. of Chemistry, Gauhati University, Guwahati, Studies on Effect of Ion Beam Irradiation on the Nanostructured TiO2 prepared by Nanocasting Replication Method.
26. Dr. Shaon Ray Chaudhuri, Dept. of Biotechnology West Bengal Univesity of Technology, Developing a laboratory scale biofilm based metal removal system using heavy metal tolerant radioresistant marine coastal microbes.
27. Dr. A K Sen, Dept. of Earth Sciences, IIT Roorkee, Roorkee, Investigation of Potential Metalliferous Nature of Coal from India.
28. Dr. Ansuman Chattopadhyay, Dept. of Zoology, Siksha Bhavana, Visva-Bharti, Santiniketan , Arsenic induced genotoxicity and modulation of trace elements in mammalian cells.
29. Dr. S Narayana Kalkura, Crystal Growth Centre, Anna University, Chennai, Ion Implantation and trace element analysis of materials of importance in Biology and Medicine.
30. Dr. M L Garg, Dept of Biophysics, Panjab University, Chandigarh, Characterization of MT isolated from As treated rats for toxicity and sensor application.
31. Dr. H.M.Agarwal, Department of Physics G.B. Pant University of Ag. & Tech., Pantnagar, Multielemental analysis of soil & plant samples of GBPUAT Research Centres in Uttarakhand.
32. Dr. Debasis Das, Department of Chemistry, University of Burdwan, Studies on chemical speciation and metal ion separation by some newly synthesized chelating ligands with N, S and / O donor sites: Applications to environmental samples.
33. Dr. H. N. Thatoi, Department of Biotechnology, CET, Bhubaneswar, Bioremediation of hexavalent chromium using stress tolerant microbes isolated from chromite mine environments of Orissa.

Collaborative research program utilising EDXRF facility of Kolkata Centre

34. Dr. S. Santhosh Kumar ,Mahatma Gandhi Govt. Arts College,Elemental Analysis of Traditional Medicinal Plants used in Keraleeya-ayurveda-chikitsa
35. Prof. N. Rajmuhon Singh, Dept. of Chemistry, Manipur University, Trace Element Analysis and Biological Activities of Some Selected Medicinal Plants of Manipur

Utilizing 14 UD BARC-TIFR Pelletron facility at TIFR Mumbai.

36. Dr Bivash Behra, Dept. of Physics, Panjab, University Spin distribution measurement a probe to understand the reaction mechanizm of medium mass systems.
37. Dr. Aloke De, Dept of Physics, Raniganj Girls College Burdwan, Study of orbiting anomalies in $^{12}C + ^{89}Y$ and $^{16}O + ^{89}Y$.
38. Dr. Surjit Mukherjee, Dept. of Physics MS University, Vadodara, Nuclear structure ffects on breakup and multi-nucleon transfer reaction.
39. Prof N L Singh, Dept. of Physics MS University, Vadodara, Effect of projectile spin on fission fragement angular distribution for the system ^{13}C , $^{14}N + ^{238}U$.

11.2 Indore Centre

40. Dr. Prakash Nath Vishwakarma, Asst. Professor, Low Temperature Condensed Matter Physics, Dept. of Physics, NIT – Rourkela - Magneto-electric study of doped rare earth cobaltites.
41. Dr. N. Lakshmi, Associate Professor, Department of Physics, M.L. Sukhadia University, Udaipur - Magnetic properties in Co-based multilayer systems.
42. Dr. Shankar I. Patil Professor, Interdisciplinary School of Science, Department of Physics University of Pune, Pune - Investigation of physical parameters in the context of VBS for 3d elements doping at Mn site in hole doped pervskite
43. Dr. Ratnesh Gupta, School of Instrumentation, Devi Ahilya University- To investigate the electronic structure of nitride and carbirused of thick films using AIPES beamline of Indus-I.
44. Prof. Ashok Rao, Professor & Head, Physics Department, Manipal Institute of Technology, Manipal - Electrical and thermal properties of some doped manganites
45. Dr. Venkata Rama Rao Medicherla, Asst. Professor, Department of Physics, Institute of Technical Education and Research, Siksha 'O' Anusandhan University, Jagamohan Nagar, Jagamara, Bhubaneshwar - Electronic properties of disordered transition metal alloys.
46. Dr. Pratima Sen, Professor, School of Physics, Devi Ahilya University - Electronic and Optical properties of ZnO based multilayered thin films
47. Dr. M. Umadevi, Associate Professor, Dept. of Physics, Mother Teresa Women's Univ., Kodaikanal- Synthesis and characterisation and surface enhanced raman spectral activity of metal nanoparticles
48. Dr. Anil Vithal Ghule, Asistant Professor, Dept. of Nanotechnology, Dr.B.A.M. University, Aurangabad - Simple and economic biosynthesis of SnO2 nanoparticles thin films for gas sensor applications.
49. Dr. T.K. Chaudhuri, Professor & Head, Dr.K.C. Patel Research and Development Centre, Charotar Univ. of Science & Tech Changa- Solution grown Cu2SnS3 thin films for solar cells
50. Prof. A. Kumar, Dept. of Physics, Tezpur University, Napaam- Electrical and thermal transport in conducting polymer nanostructures
51. Dr. S.N. Kane, School of Physics, Devi Ahilya University - Study of ferrite thin films prepared by pulsed laser deposition
52. Prof. P.B. Joshi, Dept. of Physics, Solapur University, Kegaon, Solapur - Synthesis and characterisation of ferroelectric hetrostructures

53. Dr. Tapan Guha, Professor, Modern Dental College and Research Centre, Gandhi Nagar, Airport Road, Indore- AFM investigations of effect of some important drugs on red blood cells in physiological condition and hemoglobinopathy like sickle cell anaemia

54. Dr. Ramphal Sharma, Reader, Dept. of Physics, Dr. Babasaheb Ambedkar Marathwada University, Aurangabad- Effect of Ag incorporation in nanostructured CdS thin films grown by cost effective chemical technique for photovoltaic applications

55. Dr. P.S. Gupta, Professor, Dept. of Applied Physics Indian School of Mines, Dhambad - Preparation and charactersation of oxide and fatty acid thin films

56. Prof. M.S.M. Rawat, Dean, Dept. of Chemistry, H.N.B. Garhwal University, Srinagar, Garhwal - Effect of solvent system on the stabilty of fluorescence crown ether complexes of metal ions

57. Prof. Dhananjai Pandey, School of Materials Science and Technology, Institute of Technology, Banaras Hindu University Varanasi - Low temperature magnetic transitions in Disordered BiFeO3.

58. Prof. Mandira Banerjee, School of Physics, Devi Ahilya University - Study of the melting behaviour of soft condensed matter thin films

59. Prof. B.L. Ahuja, Head (Chairman), Dept. of Physics Univ. College of Science, M.L. Sukhadia University, Udaipur- Study of electronic structure of spinal ferrites by resonant photoemission and compton spectroscopic

60. Dr. A.K. Bajpai, Dept. of Chemistry, Govt. Medical Science College, Jabalpur - Synthesis and characterisation of controllable size magnetic nanoparticles of metal oxides containing biopolymers and evaluation of their drug release potential

61. Dr. D.G. Kuberkar, Dept. of Physics, Saurashtra University, Rajkot- Electronic structure and valance band studies on functional oxides

62. Dr. O.P. Pandey, Sr. Professor, School of Physics and Matrls Science, Thapar University, Patiala- Synthesis and characterisation of vanadium carbide nanoparticles

63. Dr. B.N. Dole, Reader, Dept. of Physics, Dr.B.A.M. University, Aurangabad - Development and different property studies of Co doped ZnS nanowires

64. Prof. Dinesh Varshney, School of Physics, Devi Ahilya University - Structural and Physical properties of pure and doped BiFeO3 multife

65. Dr. Archana Tiwari, Assistant Professor in Physics, Sikkim University, 6th Mile, Tadong, Gangtok - Synthesis and optical readout of potential fullerenes for quantum information processing

66. Dr. Rajesh Kumar, Assistant Professor, Bhilai Institute of Technology, Durg - Synthesis and characterization of doped nanocrystalline CdSe and CdS thin films suitable for sensor applications

67. Dr. S.K. Sharma, Associate Professor, Department of Applied Physics, Indian School of Mines, Dhanbad - Synthesis and characterization of nanocomposite thin films for optoelectronic applications

68. Dr. R. Thirumurugan, Associate Professor, Department of Animal Science, School of Life Sciences, Bharathidasan University, Tiruchirapalli - Synthesis and characterization of metal nanoparticles using selective plants from kolli hills: applications on human health and environmental remediation

69. Prof. Ashutosh Mishra, Head, School of Physics, Devi Ahilya University - Effect of doping on structural, magnetic, electrical and dielectric properties of Sol-Gel prepared nanoparticles and pulse laser deposited thin films of $BaTiO_{3.}$

11.3 Mumbai Centre

Collaborative Research Schemes on neutron scattering at Dhruva Reactor, Mumbai

70. Dr. R. V. Upadhyay, Charotar Institute of Applied Sciences, Size dependent magnetic properties of Co-Zn spinel ferrite nanoparticles using diffraction technique
71. Prof. Kabir-ud-Din, Aligarh Muslim University, Interaction between serum albumins and drugs
72. Prof. J.A.E. Desa, University of Goa, Studies of porous materials by SANS
73. Prof. J.A.E. Desa, University of Goa, Structural studies of gels by light scattering and SANS
74. Dr. S. Ravi, IIT Guwahati, Neutron powder diffraction studies in charge ordered and double exchange ferromagnetic samples of Nd-Mn-O series.
75. Dr. Sanjeev Kumar, M. S. University- Baroda, Stimuli responsive solution behavior of surfactants: A SANS study.
76. Dr. Sugata Ray, IACS, Probing the 4d and 5d magnetism in prototypical using neutron diffraction.
77. Dr. R.K. Mahajan, Guru Nanak Dev University, Structural and interactional behavior of mixed micelles of twin tail surfactants and with triblock copolymers
78. Prof. A. K. Raychaudhuri, SNBCBS, Neutron diffraction studies of collapse of charge ordering in narrow band half doped manganite $Y_{0.5}Ca_{0.5}MnO_3$.
79. Dr. Atul Khanna, Guru Nanak Dev University, Structural investigations of binary borate and tellurite glasses by high-Q neutron diffraction and small angle neutron scattering techniques
80. Dr. Puyam Singh, Central Salt & Marine Chemicals Research Institute (CSMCRI), SANS investigation of the silicon rubber membranes
81. Dr. Bragadish Iyer, Charotar Institute of Applied Sciences, Studies on structure of microbial exopolysaccharide (EPS) solutions and hydrogels using SANS
82. Dr. A. V. Mahajan, IIT Bombay, Magnetism in low-dimension and/or frustrated magnetic systems
83. Dr. Basavaraj Angadi, Bangalore University, Synthesis and studies on Magneto-Electric and Spin-Lattice Coupling in $Pb(Fe_{1/2}Nb_{1/2})O_3$ based multiferroic systems
84. Dr. N. V. Sastry, Sardar Patel University, Studies on Aggregation behavior of Pyridinium based amphiphilic ionic liquids in water and in presence of aggregate growth parameters
85. Dr. M. S. Jogad, Sharnbasveshwar College of Science, Gulbarga, Structural study of Pb-glass by Neutron Diffraction
86. Dr. Babita Sehgal, M. S. University of Baroda, Use of SANS in preparation of doped transition metal hollow spheres using carbon as template and its photo catalytic activity under visible light
87. Dr. Michael Anjello Jothi Rajan, Arul Anandar College, Karamathur, Light Scattering Investigations on Bio-Macro molecule assisted synthesis / assembly of metal nanoparticles.
88. Dr. C. Peter Sebastian, JNCASR, Structure-property relations in RE_2TGe_3 (RE = rare earths; T=transition metals) compounds.
89. Dr. Niharika Mohapatra, IIT-Bhubaneswar, Neutron Diffraction studies of field induced magnetic transitions in Er_5Si_3
90. Dr. R. Nirmala, IIT-Madras, Study of magnetic ordering and magnetic field-induced effects in rare earth intermetallic compounds and oxides by powder Neutron Diffraction
91. Dr. Alok Srivastava, Punjab University, Study of Kidney Stones from Belt of India using Neutron Activation Analysis.
92. Prof. J. A. E. Desa, Goa University, Structural and optical properties of Rare Earth Doped Borate Glasses.

93. Dr. G. Harikrishnan, IIT-Kharagpur, Probing urea phase separation in polyurethane foams made from bio-renewable castor oil.
94. Dr. S. S. Soni, Sardar Patel University, Influence of Micellar Morphology on Conductivity of Polymer Gel Electrolytes
95. Dr. Sarathi Kundu, IASST, Self-assembly in Nanomaterials and Biomaterials : An SANS and SAXS study
96. Prof. P. Bahadur, V. N. South Gujarat University, Self-assembly of Stimuli-responsive Amphiphilic Block Copolymers
97. Dr. Basavaraj Gurappa, IIT-Madras, SANS investigation of Sponge to Lamellar Transition in Surfactant – Protic Ionic Liquid Mixture
98. Dr. R. Perumal Ramasamy, Anna University, Investigation of the effects of nanoparticles in polymers using Neutrons and Dielectric Spectroscopy
99. Dr. Saurav Giri, IACS, Magnetic Ordering and magneto-elastic effects in materials
100. Prof. Sundararaman, University of Hyderabad, Influence of doping on the multiferroic properties of $YbMnO_3$
101. Dr. N. E. Rajeevan, Z. G. College, Calicut, Study of Magnetic structure in multiferroic materials by Neutron Diffraction
102. Dr. S. Srinath, University of Hyderabad, Multiferroic properties in Rare earth doped $BiFeO_3$
103. Dr. N. Narsimulu, Osmania University, Studies on Core-Shell Structured Metal Oxide / PANI Nanocomposites
104. Prof. N. Lakshmana Das, GITAM University, Studies on Archaeological artifacts using Nuclear Analytical techniques
105. Prof. H. Bohidar, Jawaharlal Nehru University, Structure of DNA-Protein (Gelatin) coacervates in ionic liquid environment.
106. Dr. Saket Asthana, IIT-Hyderabad, To investigate the magnetoelectric coupling in site specific substituted NBT ($Na_{0.5}Bi_{0.5-x}R_xTi_{1-y}Mn_yO_3$).
107. Prof. Pragnesh Dave, K. S. K. V. Kuchh University, Synthesis of silica oxide photonic crystals by using water soluble polymers as self-assembled templates.
108. Dr. Pritam Deb, Tezpur University, Study on the controlled self-assembly of magnetic nanostructures using neutron scattering.
109. Dr. Anil Kumar Singh, NIT-Rourkela, Search for multiferroicity and its microscopic origin in $BiPbSr_2XO_6$ (X = Mn, Fe, Co).
110. Dr. S. Patnaik, Jawaharlal Nehru University, Correlation between magneto-electric coupling and exotic magnetic structure in some oxide multiferroics
111. Dr. B. B. Nanda, Biju Patnaik University of Technology, Determination of Aluminium contents in foodstuffs and medicines using nuclear analytical techniques.

11.4 Kalpakkam Node

112. Prof. S. Thomas, School of Chemical Sciences, M.G. University, Kottayam - Carbon nanotube filled natural rubber latex nano-composites.
113. Prof. Anand P. Pathak, School of Physics, Universityof Hyderabad - Ion beam synthesis of semiconductor nanocrystals and modifications of III-V semiconductor multi quantum wells under SHI irradiation.
114. Dr. Prasanna Ghalsasi, Department of Chemistry, M.S. University of Baroda - Designing Chiran Molecular Magnets.
115. Dr. Lisa Sreejit Soft Materials Res. Lab. Dept. of Science & Humanities, National Institute of Technology, Calicut - Temperature dependent optical switch from organised assemblies.
116. Prof. V. Rajendran, Director, R&D Centre for Nano Science and Technology, KSR Colege of Technology, Tiruchendogu - Development and characterisation of nano metal oxides for biomedical applications.
117. Prof. N. Rajendran, Madras Inst. Of Technology, Anna University Campus, Chennai - Development of TiO2 nanotubes for biomedical applications.

118. Dr. G.D. Janaki Ram, Met. & Mat. Engg., IIT, Chennai - A rapid manufacturing approach to facilitate joining of stainless steel pipes to Titaniu Pipes.

119. Prof. S. Vasanth, Associate Professor, In-organic Chemistry, Head, Department of Chemistry, Lady Doak College, Madurai - Super hydrophobic coating for enhancing corrosion resistance.

120. Prof. V. Srinivas, IIT Madras, Chennai - Studies on giant electrical transport anomalies induced by magnetic instability in Fe-Rich intermetallics.

121. Dr.K.Suresh Babu, Centre for Nanoscience and Technology, Pondicherry University - Engineering, Mechanical and Electrical Properties of Nanostructured oxide materials.

122. Dr. P. Thangadurai, Pondicherry University - Correlation of electrical properties with microstructure of nanostructured oxide materials.

123. Dr. R. Nirmala, IIT Madras, Chennai - Studies of size effect on the physical properties of phase separated electron doped manganites and other novel oxides.

124. Dr. S. Kaleemulla, VIT University, Vellore - Investigations for Room temp ferromagnetism in Cr,Fe,Ni and Cu-doped In2O3 thin films for spintronic applications.

125. Prof. V.S. Chakravarthy, IIT Chennai - Investigating the neutral substrates for motor preparation using high density Electroencehalogram and Magnetoencephalogram.

126. Prof. Thomas Muthaiah, Bharatidasan University, Trichy.- Synthesis, supramolecular interactions and properties of Uranyl complexes.

127. Dr. J. Jayapriya, Anna University, Chennai - Detection and analysis of Microbiologically influenced corrosion on stainless steel in seawater using electrochemical noise technique (EN).

128. Dr. N. Ponpandian, Bharathiar University, Coimbatore - Ion beam synthesis and characterization of nanocomposite exchange spring magnets.

129. Dr. Basavaraj Angadi, Bangalore University - Synthesis and studies on magnetic properties of doped Zinc Oxide nano powdeers and thin films.

130. Prof. K. Venkataramaniah, Sri Sathya Sai Institute of Higher Learning, Prasanthinilayam - Studies on thermoelectric performance of nanostructured Bismuth Teluride and Lead Telluride Nanocomposites grown via novel solvothermal nanoplating technique.

131. Prof. Dilip R. Peshwe, Dept. of Metallurgical & Materials Engineering, VNIT., Nagpur - Characterisation of creep properties of Grade 92 steel using small punch creep testing method.

132. Prof. A.R. Ballal, Dept. of Metallurgical & Materials Engineering, VNIT., Nagpur - Characterisation of tensile and fracture properties of Grade 92 steel using ball identation technique.

133. Dr. Mary George, Department of Chemistry, Stella Maris College, 17, Cathedral Road, Chennai - Synthesis and humidity sensing properties of nanocomposites of lanthanum mixed metal oxide.

134. Dr.K.R. Balasubramanian, Assistant Professor, Dept.of Mechanical Engg, National Institute of Technology, Tiruchirapalli - Modeling of A-TIG welding of austenitic stainless steels and prediction of residual stresses.

135. Dr. Sudakar Chandran, Department of Physics, Indian Institute of Technology, Chennai - Defect controlled properties in indium oxide- investigations on defect free and defect - incorporated In2O3 single crystals and epitaxial thin films.

136. Dr. S. Kalainathan, Vellore Institute Of Technology University, School of Advanced Sciences, Vellore - Growth and characterization of oxide single crystals using optical floating zone technique.

137. Dr. Anuradha M. Ashok, PSG Institute of Advanced Studies, Peelamedu, Coimbatore - Synthesis, characterization, proton and oxide ion conduction in doped nanocrystalline LaTiO3-$ perovskites.

138. Prof. R. Bhar/Prof. Pal, Dept. of Instrumentation Science, Jadavpur university, Kolkata - Studies on grain in CdTe thin films by pulsed laser deposition technique and realizing a ZnO/CdS/CdTe solar cell structure.

139. Dr. B. Sundrakannan, Department of Physics, Manonmanian Sundranar University, Tirunelveli - Electric field control of magnetization in FM/FE hybrid structures.

140. Dr. K.R. Ravi, PSG Institute of Advanced Studies, Coimbatore - Synthesis and characterization of ultra high strength and ductile NiAl-Al2O3 nanocomposites.

141. Prof . S.R. Koteswara Rao, Department of Mechanical Engg., Tagore Engineering College, Ratinamangalam, Chennai - Activated flux GTA welding of duplex stainless steels - addition of nitrogen to weldmetal.

142. Dr. R. Rajendran, Dept. of Mechanical Engineering, School of Mechanical &Building Sciences, Vandalur Chennai - Wear behaviour of duplex coated steels.

143. Dr. Ramesh Gardas, IIT Madras, Chennai - Experimental measurement and prediction of thermo physical and electrochemical properties of ionic liquids useful for metal ions separation.

144. Dr. A.N. Paul Angelo, St. Joseph's College, Trichy - Design, microwave assisted synthesis characterization and electrochemical investigation of potential sequestrands for the isolation of radioactive lanthanide and actinide metal ions.

145. Dr. P. Balaji Bhargav, SSN College of Engineering Kalavakkam (OMR), Chengalpattu - Invaestigations on various doped ZnO films as front contact TCO in fexible amorphous silicon solar cells.

146. Dr. S. Muthukumaran, Dept of MME, National Institute of Technology, Trichy - Welding of titanium tube to steel tube plate/tube by using an improved FWTPET process.

147. Dr. Muthupandi, Deptt. Of Metallurgical & Materials Engineering, National Institute of Technology, Tiruchirapalli - A study on the properties of dissimilar weldments between P92-S304H materials for power plant applications.

148. Prof. M.S. Rama Chandra Rao, Department of Physics and Nano Functional Materials Technoloty Centre, IIT Madras, Chennai - Electrical transport and spectroscopy studies on doped ZnO thin films.

149. Dr. T.M.R. Panicker, Professor in Radiology & Dean-Research Faculty, K.J. Research Foundation, Chennai - Application of nanotechnology on prosthetic heart value material to prevent clot formation and infection.

150. Dr. Ajith Kulangara Madam, National Institute of Technology, NITK, Srinivasanagar - Computational studies of thermodynamic and mechanical properties of boron carbide.

12. Utilisation of in-house facilities of UGC-DAE CSR: User List

12.1 Indore Centre

Indore centre has been attracting large number of users, and its state of art instruments have been widely used by the university researchers. The number of users is less for the more advanced facilities because of the time required and also because the usage is more specialized.

AFM/SPM

1.	Mr. Naveen Agrawal, Dr. Mitesh Sarkar	MS University of Baroda, Varodara, (Gujarat)
2.	Mr. Hysen Thomas, Prof. Anantharaman	Cochin University, Cochin, Kerala
3.	Mrs. Sumathi, Dr.Jothirajan Arockiam	Mother Terasa University, Periyakulam, TN
4.	Ms. Kachilakshmi, Dr.Jothirajan Arockiam	Mother Terasa University, Periyakulam, TN
5.	Mr. Ratnesh Sharma, Dr. S.B. Shrivastava	Vikram University, Ujjain
6.	Mr. Mahesh Hedaoo, Dr. Navin Chand	University Institute of Technology, RGPV, BPL
7.	Mr. Vikalp Pachori, Dr. Navin Chand	University Institute of Technology, RGPV, BPL
8.	Mrs. Durgesh Nandini,	RDVV, Jabalpur
9.	Mr. Ankit Poddar,	Amity University , Noida
10.	Miss. K. Geetha, Dr. M. Umadevi	MTW University, Kdaikanal
11.	Miss. Ambika,	DAVV, Indore
12.	Mr. Ashish Ravalia, Prof. D.K. Kuberkar	Saurastra University Rajkot
13.	Dr. Nitin M. Shah	AS College, Kamraj charrasta,Surat (GJ)
14.	Ms. Mega Vagadia, Prof. D.K. Kuberkar	Saurastra University Rajkot
15.	Mr. Sajid Babu N., Dr. M. Abdul Khadar	University of Kerala, Trivendrum, Kerala
16.	Mr. Dhrubojyoti Roy, Prof. P.S. Gupta	ISM, Dhanbad, (Jharkahand)
17.	Mr. S. Ramakrishnan, Dr. Nikhil K. Kothurkar	Amrita Vishwa Vidhyapeetam, Coimbatore
18.	Mr. Savan Mankadia, Dr. J.A. Bhalodia	Saurastra University, Rajkot (GJ)
19.	Mr. Maneesha Mishra, Dr. P. Kuppusami	IGCAR, Kalpakkam (TN)
20.	Ms. Deepshikha Rathore, Dr.Rajnish K	Barkatullah University, Bhopal (MP)
21.	Mr. Vijay Kumar , Dr. Y.C. Goswami	ITM University, Gwalior (MP)
22.	Mr. Akash Singh, Dr. P. Kuppusami	IGCAR, Kalpakkam (TN)
23.	Dr. Saravana Kumar	Kongunadu Art and Science College (TN)
24.	Mr. Prasannan G., Dr. Mahadevan Pillai	University of Kerala, Trivendrum, Kerala
25.	Mr. Dhanu Krishana G., Dr. Mahadevan P	University of Kerala, Trivendrum, Kerala
26.	Dr. Neha Bhadoria, Dr. N.D. Shashiriran	Peoplis college of Dental science, BPL
27.	Mr. Tejas Tank, Prof. S.P. Sanyal	Barkatullah University, Bhopal (MP)
28.	Mr. Ramesh Babu, Dr. S. Kalainathan	VIT University, Vellore, (TN)
29.	Mr. Nimma Naresh, Dr. R.N. Bhawnik	Pondicherry University, Pondicherry
30.	Ms. Swati Mehra, Dr. A.K. Singh	Dr. C.V. Raman Univ. Bilaspur (CG)

31.	Mr. Piyush Solanki, Dr. D.G. Kuberkar	Saurastra University, Rajkot (GJ)
32.	Mr. Ratnesh Sharma, Dr. S.B. Shrivastav	Vikram University, Ujjain (MP)
33.	Dr. K. Tamilarasan,	Kongu Engineering College, Perundurai,(TN)
34.	Ms. Megha Vagadia, Dr. D.G. Kuberkar	Saurastra University Rajkot (GJ)
35.	Ms. Chalana S.P., Dr. Mahadevan Pillai	University of Kerala, Trivendrum, Kerala
36.	Ms. Urmila K.S., Dr. B. Pradeep	CUSAT, Cochi, Kerala
37.	Mr. BT Rao/Sweta Verma , Dr. L.M. Kukreja	LMPD, RRCAT, Indore (MP)
38.	Mr. Unnikrishnan T.E., Dr. Abdul Khadar	University of Kerala, Trivendrum, Kerala
39.	Mr. Yasir Beevan, Dr. Abdul Khadar	University of Kerala, Trivendrum, Kerala
40.	Mr. Gund Girish Sambhaji, Prof. Lokhande	Shivaji University, Kolhapur (MS)
41.	Mr. Ashiq Hussain Shan, Dr. Basheer Ahmad	B.S. Abdul Rahman University, Chennai (TN)
42.	Mr. Mahesh Chand Sharma, Prof. Y.K. Vijay	University of Rajasthan, Jaipur (RJ)
43.	Mr. Nishant J. Barot, Dr. P.K. Mehta	M.S. University of Baroda, Vadodara (GJ)
44.	Mr. JayaKumar, Dr. V. Dharuman	Alagappa University, Karaikudi, Tamilnadu
45.	Ms. Compesh, Dr. D.K. Avasthi	IUAC, New Delhi
46.	Ms. Annu P., Dr. Mahadevan Pillai	University of Kerala, Trivendrum, Kerala
47.	Mr. Mahadik Abasabeb, Prof. C.H. Bhosale	Shivaji University, Kolhapur (MS),
48.	Mr. Vinod Kumar, Prof. V.N. Mishra	Indian Institute of Tech. BHU, Varanasi (UP)
49.	Mr. Irshad Ahmad Bhat, Dr. Shanid Hussain	Aligarh Muslim University, Aligarh (UP)
50.	Mr. Khalid Sultan, Dr. M. Ikram	NIT, Srinagar, J & K
51.	Mr. Hiremya K. Moha, Dr. Mahadevan Pillai	University of Kerala, Trivendrum, Kerala
52.	Ms. Rajani Jawb, Dr. Rachel Reena Philip	Union Christon College, Aluva, Cochin
53.	Ms. Kavitha V, Dr. Mahadevan Pillai	University of Kerala, Trivendrum, Kerala
54.	Mr. Neeraj Sharma, Dr. Alka Tiwari	Govt. V.Y.T. PG Auto College, Durg (CG)
55.	Mr. Savan V Katba, Prof. D.G. Kuberkar	Saurastra University, Rajkot (RJ)
56.	Mr. Mohit Vijay Sampat, Prof. C.H. Bhosale	Shivaji University, Kolhapur (MS)
57.	Mr. Nayan Mani Das, Prof. P.S. Gupta	Indian School of Mines, Dhanbad
58.	Mr. Vinay Jaiswal, Prof. R.B. Rastogj	Indian Institute of Tech., BHU, Varanasi (UP)
59.	Mr. P. Nagaraju, Dr. M.V. RamanaReddy	Osmania University, Hyderabad
60.	Mr. M. Earnest Stephen, Dr. M.A. Jothirajan	St. Joseph's College, Trichy
61.	Mr. S. Thiruvenkadam, Dr. Leo Rajesh	St. Joseph's College, Trichy
62.	Mr. Vishal Jain, Prof. N. Lakshmi	Mohanlal Sukhadia University, Udaipur (RJ)
63.	Mr. Jaison Joseph, Prof. R.B. Tangsali	Goa University, Goa
64.	Ms. Archana S. Kamble, Dr. Pramod S. Patil	Shivaji Univesity, Kolhapur (MS)
65.	Mr. Amol Singh, Dr. M.H. Modi	RRCAT, Indore
66.	Mr. M.K. Agrawal, Prof. N.S. Panwar	GBPEC, Pauri, Garhwal (UK)
67.	Mr. Kamal K. Kushwaha, Prof.Meera R	RDVV, Jabalpur (M.P.)
68.	Mr. Jolly Bose R., Dr. Mahadevan Pillai	University of Kerala, Trivendrum, Kerala

Low Temperature measurements (14T/0.3K PPMS)

69.	Ms. Mamatha Daivajana	Manipal Institute of Technology, Manipal
70.	Dr. Kalyanalakshmi Yanapu	Osmania University, Hyderabad
71.	Dr. Yakhmi	BARC, Mumbai
72.	Mr. Kumaraswamy N	ITM University, Gurgoan
73.	Dr. Chandana Rath	Banaras Hindu University
74.	Dr. Deepti Jain	ITM University, Gwalior
75.	Dr. Souvik Chatterjee	IUAC, Kolkata
76.	Mr. Nimma Naresh	School of of Physics, Pondicherry University
77.	Mr. Manish Gupta	ITM University, Gurgaon
78.	Dr. Piyush Solanki	Sourashtra Universtiy
79.	Mr. N. Kumaraswamy	ITM University, Gurgaon
80.	Mr. Devendra Sharma	Jaipur University
81.	Dr. Kalyanalakshmi	Osmania University
82.	Ms. Meenakshi	G.B.Pant University
83.	Mr. Shankar Kekade	Pune Universtiy
84.	Mr. Nageswararao	Osmania University, Hyderabad

Thermopower/Resistivity

85.	Y.K. Lakshmi, Prof. V. Reddy,	Osmania Univ., Hyderabad
86.	T. Diana, Prof. H. N. K. Sharma	
87.	Pooja Parmar,	Holkar Sci. College, Indore
88.	C. Urmila, Prof. B. Pradeep,	CUSAT,Kochi, Kerala
89.	R. Thakur, N. K. Gaur,	Barkatullah U, Bhopal
90.	C. Nath, Prof. A. Kumar,	Tezpur Univ. Assam
91.	P.Chutia, Prof A. Kumar,	Tezpur Univ. Assam
92.	R. Bhatt, Dr.D. K. Aswal,	BARC, Mumbai
93.	M.E. S. Gnanadoss, Dr. J. Rajan,	A. A. College, Karumathur, TN
94.	S. Thiruvenkadam, Dr. A. L. Rajesh,	St. Joseph College, Trichy, TN
95.	Ms M Verma, S. Kumar, Prof. B. Das,	BHU, Varanasi

Resistivity/Magnetoresistance

96.	Ms. Lalitha Reddy	Osmania Univ., Hyderabad
97.	Ms. Sheetal Soni/ Dr. Ratnesh Gupta	School of Physics, DAVV, Indore
98.	Ms. Laliths Reddy	Osmania University, Hyderabad
99.	Ms. Vibhooti Khaira/ Dr. Dinesh Varshney	DAVV, Indore
100.	Mr. Pankaj Mohanty/ Dr. Chandana Rath	Banaras Hindu University, Varanasi
101.	Mr. S. S. Kekede/ Prof. S.I. Patil	Pune University, Pune
102.	Ms. Mamtha D Daivajna	Manipal University, Karnataka
103.	Mr. Hilal Ahmed/ Dr. Shakeel Khan	Zakir Hussain College of Engg. & Tech., Aligarh

104.	Mr. T. Kannan/ Dr. P. Pradeep	NIT, Calicut, Kerala
105.	Dr. Vilash Shelke	Barkhatullha Univ., Bhopal
106.	Mr. Raju Mimicry/ Dr. Rama Reddy	Osmania Univ., Hyderabad
107.	Mr. Tanveer Ahmad Dhar/ Dr. Pratima Sen	DAVV, Indore
108.	Mr. Anchit Modi/ Dr. N.K. Gaur	Barkhatullha Univ., Bhopal
109.	Ms. K.S. Urmila./ Dr B. Pradeep	Cochin University of Sc. and Tech, Kochi, Kerala
110.	Mr. Mankadia Savan/ Dr. J.A. Bhalodia	Saurastra University, Rajkot
111.	Ms. G. Lalitha	Osmania University, Hyderabad
112.	Ms. Priyanka/ Dr. D.G. Kuberkar	Saurastra University, Rajkot
113.	Dr. A. Venimadhav	IIT, Kharagpur
114.	Mr. Masroor Ahamad Bhat/ Dr. N.K. Gaur	Barkhatullha Univ., Bhopal
115.	Ms. K.S. Urmila/ Dr. B Pradeep	Cochin University of Sc. and Tech, Kochi, Kerala
116.	Ms. Lija K Joy/ Prof. M.R. Anantharaman	Cochin University of Sc. and Tech, Kochi, Kerala
117.	Dr. A. Jaiswal	RRCAT, Indore
118.	Mr. Masroor Ahmed Bhatt/Dr. N. K. Gaur	Barkatullah University Bhopal
119.	Mr. Yogesh Kumar/ Prof. Ravi Kumar	IUAC, New Delhi
120.	Mr. Tarale Arjun Naganath/ Prof. P.B. Joshi	Solapur University, Solapur
121.	Mr. Shailendra Singh Rajput/ Dr. Sunita Keshri	BIT, Mesra, Ranchi
122.	Dr. Vilas Shelke	Barkatullah University Bhopal
123.	Dr. Y. Kayanalakshmi/ Prof. P. Venugopal Reddy	Osmania University, Hyderabad
124.	Dr. G. D. Verma	IIT, Roorkee
125.	Mr. Paragjoyti Chutia/ Prof. Ashok Kumar	Tezpur University, Assam
126.	Mr. T. Kannan	NIT, Calicut, Kerala
127.	Mr. Khalid Sultan	NIT, Srinagar
128.	Mr. Shankar Kekade/ Prof. S.I. Patil	University of Pune, Pune
129.	Mr. Vishal Jain/ Prof. N. Lakshmi	Mohanlal Sukhadia University,Rajasthan

Heat capacity

130.	Mr. Pavan Kumar	Osmania University, Hyderabad

Raman Spectroscopy

131.	Mr. Pradip SahuC/o Dr. D. Varshney,	School of Physics, DAVV
132.	Ms. Ayushi Paliwal	RRCAT, Indore
133.	Mr. N. Raju	Osmania University,Hydrabad
134.	Jyoti Prakash Dwivedi	School of Physics, DAVV
135.	Ms. Supriya Bisen	School of Physics, DAVV
136.	Ms. Poonam Rani	Dept. of Physics, Banaras Hindu University, Varanasi-
137.	Ms. Mayuri Srivastava	Dept. of Physics, Banaras Hindu University, Varanasi
138.	Mr. Gowrinaidu B.	RRCAT, Indore
139.	Mr. T. KannaC/o Prof. P. Predeep,	NITC, Kerala
140.	Mr. Sandip Bhatt C/o Prof. M. P. Deshpande,	Sardar Patel University, Vallabh Vidynagar

141.	Mr. Sajio Babu N	Centre for Nanoscience and Nanaotechnology, Univ. of Kerala.
142.	Mr. S. Ramkrishnan C/o Dr. Nikhil K.	Kothurkar, Amrita Vishwavidhyapeetham, Coimbatore, TN.
143.	Mr. Dhrubojyoti RoyC/o Prof. P. S. Gupta,	Dept. of Applied Physics, ISM, Dhanbad, Jharkhand
144.	Ms. Akrati Verma	School of Chemical Science, DAVV,Indore
145.	Mr. Imran Khan	Dept. of Applied Physics, Aligarh Muslim University,
146.	Dr. Deepa Dey	IIT Indore, Dept. of Chemistry, Indore
147.	Mr. Anil Tomar,C/o Dr. Shyam Kumar,	Dept of Physics, Kurukshetra, University of
148.	Mr. Manish Dixit,Prof. Manish K. Mishra,	Dharm Sinh Desai University, Nadiad, Gujrat
149.	Mr. Srinibas Satapathy	RRCAT, Indore
150.	Rajendra Sharma	School of Instrumentation, DAVV, Indore
151.	Mr. Anoop Chandran,C/o Dr. K. C. George,	S. B. College, Changenessery, Kerala
152.	Dr. Suman Mahendia,	Department of Physics, K. U. Kurukshetra
153.	Mr. Japaram. P	Depart. of Physics, University of Calicut,
154.	Naresh Nima	
155.	Prabhakar	
156.	Mrs. Janita Saji	NIT, Raipur
157.	Mrs. Deepika Tripathi	Department of Physics, Barkatulla University,
158.	Mr. Thombare Jagannath,C/o Dr. Fulalari V. J.,	Shivaji University, Kolhapur
159.	Mr. A. H. Shah,C/o Dr. M. B. Ahamed, B. S.	Abdur Rahman University, Vandalur, Chennai
160.	Mr. Yasir Beeran P. T.	University of Kerala, Trivandram, Kerala
161.	Mr. Unnikrishnan T. E.	
162.	Mr. Gund G. S.,C/o Prof. C. D. Lokhande,	Dept. of Physics, Shivaji University, Kolhapur
163.	S. Premkumar,C/o Dr. A Milton Franklin,	Dept. of Phy. N.M.S.S.V.N College,Madurai,TN
164.	Dr. T. S. Dhami	RRCAT, Indore
165.	Mr. Bharat B. Gabhale,C/o Prof. S. R. Jadkar,	School of Energy Studies, University of Pune,
166.	Mr. Shashikant D. Gunjal ,C/o Prof. S. R. Jadkar,	School of Energy Studies, University of Pune,
167.	Mr. Kinjal Patel,C/o Dr. Vipul Kheraj,	S.V.N.I.T, Surat, Gujrat
168.	Mr. Irshad Ahmad Bhat,C/o Dr. Shahid Husain,	Aligarh Muslim University, Aligarh-202002
169.	Mr. Kamal Kumar Gupta	Dept. of Chemical Engg, IIT, BHU Varanasi
170.	Mr. R. Sharma	School of Instrumentation, DAVV, Indore
171.	Mr. Khalid Sultan,C/o Dr. Ikram,	A.P. N. T. Sringar
172.	Dr. Gurvinderjit Singh	RRCAT, Indore
173.	Dr. Avneesh Anshul	National Physical Lab, Delhi
174.	Mr. Shrikant R. Naik,C/o Prof A.V. Salker,	Dept. of Chemistry, Goa University
175.	Ms. Tulshi Shiyani,C/o Dr. Abhijit Ray,	School of Solar Energy, PDP University, Gandhinagar
176.	Mr. Rajiv Ranjan	I.I.Sc, Bangalore.
177.	Mr. Harish Chandra Singh,C/o Dr. A. K. Sinha,	RRCAT, Indore.
178.	Mr. Mahesh Patange,C/o Dr. Somnath Biswas,	The LNM Institute of info. Technology, Jaipur
179.	Dr. Umadevi	Dept. of Physics, MTW University, Kodaikanal
180.	Mr. Nilesh Kanhe,C/o Dr. S. Karmakar,	Dept.of Physics, University of Pune
181.	Mr. Masroor Ahmad Bhat,C/o Dr. N.K. Gaur,	Dept. of Physics, Barkatullah University, Bhopal

182.	P. Nagaraju,Dr. M.V. Ramanareddy,	Dept. of Physics, Osmania University, Hyderabad
183.	Mr. A. H. Shah,C/o Dr. E. Manikandan,	B.S. Abdul Rahaman University, Chennai.
184.	Ms. Deepti K Sethia,C/o Dr. P. M. Rade,	Institute for Plasma Researceh, Gandhinagar.
185.	Mr. Sohanlal,C/o Dr. Suman Mehandiya,	NIT, Kurukshetra
186.	Mr. Chiranjit Debnath,C/o Dr. K. S. Bartwal,	RRCAT
187.	Mr. S. Thrvenkadam,C/o Dr. A. Leo Rajesh,	Dept. of Physics, Bharathidasan University,Trichy, Tamilnadu.
188.	Mr. Saurabh Pandy	Electrical Engg. Dept, PACL Campus, IIT, Indore.
189.	Mr.Mahadit Mahadeo,C/o Prof. C.H. Bhosak,	Shivaji Univesity, Kolhapur.
190.	Mr. Nikita H Patil,C/o Prof. M. P. Deshpande,	Dept. of Physics, Sardar Patel University, V. V. Nagar, Gujarat.
191.	Mr. Sanket Kumar Shrivastava,C/o Mr. Vijay Kumar Sharma	LKCT, Indore
192.	Mr. Mahesh D Choudhury,C/o Prof. Sunil Chaki,	Dept. of Physics, Sardar Patel University, Vallabh Vidyanagar,

Magnetism

193.	Dr. S.A. Acharya	Nagpur University, Maharastra
194.	Prof. D.G. Kuberkar	Saurashtra University, Rajkot
195.	Dr. Gopalakrishnan	SRM University Chennai
196.	Prof. P. Pradeep	NIT Calicut
197.	Dr. K. C. George	M.G. University Kerla
198.	Dr. C. Gopalkrishnan	SRM University
199.	Dr. Kaustubh Priolkar	Goa University
200.	Prof. A. Mishra	DAVV University, Indore
201.	Prof. D Suresh Babu	Osmania University Hyderabad
202.	Prof. K.G. Suresh	IIT, Mumbai
203.	Prof. V.B. Singh	Banaras Hindu University, Varanasi
204.	Prof. S. Meenakshisundar	MS University Tamilnadu
205.	Prof. A. K. Singh	BHU, Varanasi UP
206.	Dr. Sandeep Chaterjee	BHU, Varanasi UP
207.	Dr. P. Venugopal Reddy	Osmania University Hyderabad
208.	Prof. N S Gajbhiye	IIT, Kanpur
209.	Dr. Biswas Somnath	LNMIIT, Jaipur
210.	Dr. D. Pandey	IIT-BHU, Banaras
211.	Prof. Arun V. Salker	Goa, University
212.	Dr. M. Ikram	NIT, Srinagar
213.	Dr. N.K. Gaur	B.U. University Bhopal
214.	Prof. Ashu Rani	Kota University Rajasthan
215.	Dr. Mohd. Ikram	NIT, Srinagar
216.	Dr. Balasubramanium	IPR, Gandhinagar, Gujrat
217.	Dr. M.P. Deshpandey	S.P. University, Gujrat
218.	Prof. H.M. Agrawal	GBPANT University Uttarakhand

DSC

219.	Dr. Ajay Semalty	HNB Univ, Garhwal
220.	Dr. P.P. Pradyumnan	Calicut University
221.	Dr. Rakesh Bajpai	RDVV, Jabalpur
222.	Prof. M. Roy	MLS Univ., Udaipur
223.	Prof. R. Prasad	DAVV, Indore
224.	Dr. S.N. Reddy	PG College of Science, Osmania Univ.
225.	Dr. A.K. Sinha	RRCAT, Indore
226.	Dr. S.P. Mahapatra	NIT, Riapur
227.	Dr. V.J. Fulazi	Shivaji University, Kolhapur
228.	Prof. M. Roy	MLS Univ., Udaipur
229.	Dr. S.P. Singh	DAVV, Indore
230.	Dr. A. Rawat	MSJ Gov. Col., Bharatpur (Raj.)
231.	Prof. S.P. Sanyal	Barkatullah Univ., Bhopal
232.	Dr. V.V.S. Murty	Holkar Science College, Indore
233.	Dr. Bartwal	RRCAT, Indore
234.	Dr. N.P. Singh	Udai Pratap College, Varanasi
235.	Dr. Deepti K. Sethia	IPR, Gandhinagar
236.	Dr. M.A. Jothirajan	St. Joseph's College, Trichy

Dielectric Permittivity

237.	Prof. Meera Ramrakhini	RDVV, Jabalpur
238.	Prof. A. Mishra	DAVV, Indore
239.	Dr. S.N. Reddy	PG College of Science, Osmania Univ.
240.	Dr. B.D. Shrivastav	Govt. PG College, Dhar (MP)
241.	Dr. Vilas Shelke	Barkatullah Univ., Bhopal
242.	Dr. Deepti K. Sethia	IPR, Gandhinagar
243.	Dr. S. Acharya	RTM Nagpur University
244.	Prof. D.G. Kuberkar	Saurashtra University, Rajkot
245.	Dr. N. Sridharan	IGCAR, Kalpakkam
246.	Dr. H.M. Agrawal	GBPU of A. & T., Pantnagar (UA)
247.	Dr. A.K. Sinha	RRCAT, Indore

Cryogenics

248.	Dr.A.Jajoo	DAVV,Indore
249.	Dr.Ritu Jain	DAVV,Indore
250.	Dr.Anil Kumar	DAVV,Indore
251.	Dr.S.V.Sai Prasad	DAVV,Indore
252.	Dr.Meeta Jain	DAVV,Indore

253.	Dr.V.S.Bhatia	Soyabean Research Centre,Indore
254.	Dr.Nineet Kumar	Soyabean Research Centre,Indore
255.	Dr.M.M.Ansari	Soyabean Research Centre,Indore
256.	Dr.S.K.Gupta	Soyabean Research Centre,Indore
257.	Dr.G.R.Kumawat	Soyabean Research Centre,Indore
258.	Dr.Ramesh	Soyabean Research Centre,Indore
259.	Dr.R.Prasad	SCS, DAVV, Indore
260.	Dr.A.N.Mishra	Indian Agricultural Research Inst.,

TEM

261.	Mr.Rishi Pal	Kurukshetra Univ.
262.	Prof.Ashu Rani Sahay	Kota Univ., Kota
263.	Mr.Arunendra K Tiwari	DIMAT,Raipur
264.	Mrs. Tehmina Khan	Govt. Madhav Sci.P.G. College, Ujjain
265.	Dr. Umadevi	Mother Teresa Women's Univ., Kodaikanal
266.	Mr.Thombare J. Vishnu C\o.Dr. V.J.Fulari	Shivaji Univ., Kolhapur
267.	Ms.Neeru Tiwari	DRDO,Kanpur
268.	Dr.S.G.Deshmukh	Solapur Univ.
269.	Mr.A.S.Ganeshraja C\o.Dr.K.Anbalagan	Dept. of Chemistry,Pondicherry Univ.
270.	Mr.R.Varadhaseshan C\o.Dr.S.M Sunder	Parama Kalyani Collage, Tirunelueli, TN
271.	Ms.Sushma Sharma C\o.Prof.Uma Sharma	Dept. of Chemistry,Vikram Univ.,Ujjain
272.	Mr.Bhaskar Soni C\o.Dr.Somnath Viswash	LNMIIT, Jaipur
273.	Dr.H.B.Patil	NHU, Jalgao
274.	Mr.Ashiq Husain Shah C\o.Dr.Manikandan	BSAR Univ., Channai
275.	Mr.Shrikant Naik C\o.Prof.A.V.Salkes	Dept. of Chemistry, Goa Univ.
276.	Ms.Rashmi C\o.Dr.Seema Sharma	A.N. Collage Patna, Magadh Univ.Bihar
277.	Mr.Vinod Kumar C\o.Dr.S.K.Singh	Dept.of Physics, DCR Univ. Sc. Tech., Sonepat
278.	Dr.Naheed Ahmed	Patna Women's college Patana Univ. Bihar
279.	Mr.Karanan	VHSN Collage, M.K.Univ., TN
280.	Mr.Stephen	St.Joshef Collage,Trichy M.K.Univ., TN
281.	Mr.S.Tmruvenkadam C\o.Dr.A.L.Rajesh	St.Joshef Collage,Trichy M.K.Univ., TN
282.	Dr.Debmalya Roy	DRDO,Kanpur
283.	Mr.Rangawar Rajendra C\o. Dr.Nirmalya Ballav	IISER, Pune
284.	Mr.G.G.Sambhaji,C\o.Prof.C.D.Lokhande	Shivaji Univ., Kolhapur

D8 Advanced XRD

285.	A.H. Shah	B.S.A.R. Univ., Chennai
286.	A.K. Tiwari	DIMAP, Raipur
287.	A. Jain	SOP, DAVV, Indore
288.	Abhishek Dwivedi	B.H.U., Varanasi
289.	Akruti Verma	SCS, DAVV, Indore

290.	Alveera Khan	M.V.M. Collg., Bhopal
291.	Amit Ku. Verma	SOP, DAVV, Indore
292.	Anand Rawat	M.S.J. Collg., Bharatpur
293.	Anirudha Bahadur Yadav	I.T.B.H.U., Varanasi
294.	Anjali Jain	SOP, DAVV, Indore
295.	Anjali Maurya	Sagar Univ., M.P.
296.	Anju Pathak	SCS, DAVV, Indore
297.	Ankita Pal	SOP, DAVV, Indore
298.	Annapurna Mehta	SCS, DAVV, Indore
299.	Arati Sharma	SOP, DAVV, Indore
300.	Arjun Mehra	S.G.S.I.T.S., Indore
301.	Arjun N. Tarale	Solapur Univ.
302.	Arpana Agrawal	SOP, DAVV, Indore
303.	Arvind Sharma	MLSU, Udaipur
304.	Ashiq Hussain Shah	P.N.T.C.,Vandalur, Chennai
305.	Ashish Ravalia	Saurashtra Univ., Rajkot
306.	Ashutosh Kumar	BIT, Meshra, Ranchi
307.	Ashwini kumar	SOP, DAVV, Indore
308.	Avinash Shrivastav	Univ. of Kota, Rajasthan
309.	Balakrishnan C.	IPR, Gujrat
310.	Bharat Singh	Barkatulla Univ., Bhopal
311.	Bhaskar Soni	LNM Institute of IT, Jamdoli, Jaipur
312.	Biju Majumdar	IIT, Indore
313.	Bindhu M.R.	M.T.W. Univ., Kodaikanal, T.N.
314.	D.S. Rane	D.D.N.B. Collg., Bhusawal
315.	Debabrata Saha	RRCAT, Indore
316.	Deepshikha Rathore	Barkatulla Univ., Bhopal
317.	Deepti K. Sethia	IPR, Gujrat
318.	Devendra Meda	S.G.S.I.T.S., Indore
319.	Devendra Sharma	Univ. of Rajasthan, Jaipur
320.	Dhaval Modi	M.S. Univ., Baroda
321.	Dhrubojyoti Roy	ISM, Dhanbad
322.	Dnyanesh Rasale	IIT, Indore
323.	Dr. Arindam Ghosh	SOP, DAVV, Indore
324.	Dr. D. Varshney	SOP, DAVV, Indore
325.	Dr. Deepa Dey	IIT, Indore
326.	Dr. Kumar Bhalse	S.G.S.I.T.S., Indore
327.	Dr. Manavendra Kumar	Allahabad Univ.
328.	Dr. Nitin Shah	V.N.S.G.Univ., Surat
329.	Dr. Rajendra Prasad	SCS, DAVV, Indore
330.	Dr. S.N. Kane	SOP, DAVV, Indore
331.	Fozia Aziz	IIT, Indore

332.	G. Sumathi	J.A.C., Periyakulam, Tamil Nadu
333.	G.S. Gund	Shivaji Univ., Kolhapur, Maharastra
334.	Garima Jain	SOP, DAVV, Indore
335.	Gautam Sheel Thool	Govt. V.Y.T.P.G. Auto. Collg., Durg
336.	Hafsa Siddiqui	MANIT, Bhopal
337.	Harinath Arreddy	IIT, Khargpur
338.	Harsha Patil	SOP, DAVV, Indore
339.	Hemant Kumar	G.B. Pant Univ. of Ag. & Tech., Uttarakhand
340.	Hilal Ah. Rashi	Barkatulla Univ., Bhopal
341.	I.N. Bhatti	SOP, DAVV, Indore
342.	Imtiaz Bhatti	SOP, DAVV, Indore
343.	Indrajit Maity	IIT, Indore
344.	Jaishree Bhale	S.C.M.I.P.S., Indore
345.	Jaison Joseph	Goa Univ., Goa
346.	Jashashree Ray	NIT, Rourkela, Odisha
347.	Jaswant Carpenter	SCS, DAVV, Indore
348.	Jayram P.	Univ. of Calicut, Kerala
349.	Jyoti Prakash Dwivedi	IIT, Indore
350.	K. Geetha	Mother Teresa Women's Univ., Kodaikanal
351.	K. Karnan	VHNSN Collg., Virudhunagar, TN
352.	Kamal Kushwaha	Govt. Engg. Collg., Jabalpur
353.	Kamal Shah	G.L.A. Univ., Mathura, U.P.
354.	Khalid Sultan	NIT, Srinagar
355.	Khushboo Purohit	Holker Science Collg., Indore
356.	Kinjal Patel	S.V.N.I.T., Surat
357.	Kirti Sahu	Holker Science Collg., Indore
358.	Kumar Mohit	BIT, Meshra, Ranchi
359.	Lal Singh Chongad	SOP, DAVV, Indore
360.	Laxmi Tomar	M.S. Univ., Baroda
361.	M. Earnest Stephen	St. Joseph's Collg., Tirchy, TN.
362.	M. K. Agarwal	G.B. Pant Univ. of Ag. & Tech., Uttarakhand
363.	M. Kalyau Raju	Andhra Univ.
364.	Mahesh Chaudra	IIT, Indore
365.	Mahesh D. Choudhary	S.P. Univ., Gujrat
366.	Mahesh Vikalp	R.G.P.V., Bhopal
367.	Manish Gupta	I.T.M. Univ. Gurgaon, Haryana
368.	Manoj Ku. Manna	IIT, Indore
369.	Manoj Kumar Tripathi	B.H.U., Varanasi
370.	Mansi Satlakar	SOP, DAVV, Indore
371.	Maruti Kunda	IIT, Indore
372.	Megha Vagudia	Saurashtra Univ., Rajkot
373.	Mitali Panchpuri	HNBGU, Srinagar, Garhwal

374.	Mitali Swain	BARC, Mumbai
375.	N. Naresh	Pondichery Univ., Pondichery
376.	N. Rajeswara Rao	NIT, Warangal, Andhra Pradesh
377.	N. Raju	Osmania Univ., Hyderabad
378.	Nayan Mani Das	ISM, Dhanbad
379.	Neeru Tiwari	DMSRDE, Kanpur
380.	Nikita Gour	SOP, DAVV, Indore
381.	Nimesh Patel	M.S. Univ., Baroda
382.	Niraj Sharma	Govt. V.Y.T.P.G. Auto. Collg., Durg
383.	Nishant J. Barot	M.S. Univ., Baroda
384.	Nivedita Pandey	Holker Science Collg., Indore
385.	Niyati Mishra	SOP, DAVV, Indore
386.	Pallavi Saxena	SOP, DAVV, Indore
387.	Pankaj Mohanty	B.H.U., Varansi
388.	Payal Soni	Holker Science Collg., Indore
389.	Pooja Shrivastava	DRDE, Gwalior
390.	Poorva Sharma	SOP, DAVV, Indore
391.	Prabhakar Sharma	SCS, DAVV, Indore
392.	Pradeep Ku. Sahu	SOP, DAVV, Indore
393.	Pragya Ojha	Deptt. Of Physics, MANIT, Bhopal
394.	Pramod Ku. Malviya	SOP, DAVV, Indore
395.	Pranay Rameshrao Bagde	Smt. Kishoritai Bhoyar Collg. Of Pharmacy,
396.	Prasannan G.	Univ. of Kerala, Kerala
397.	Prerna Kathane	Govt. V.Y.T.P.G. Auto. Collg., Durg
398.	Priti Shrivastava	SCS, DAVV, Indore
399.	Priyanka Trivedi	Saurashtra Univ., Rajkot
400.	Prof. Shaibal	IIT, Bombay
401.	Puja Dey	Vikram Univ., Ujjain
402.	Puneet Negi	G.B. Pant Univ. of Ag. & Tech., Uttarakhand
403.	R. Varadhaseshan	Sri Paramakalyani Collg.,Tirunelveli, TN
404.	Rajesh Kumar	BIT, Meshra, Ranchi
405.	Ramachandran	Calicut Univ., Kerala
406.	Ramkanya Ratidar	Vikram Univ., Ujjain
407.	Rashmi Nagar	Vikram Univ., Ujjain
408.	Rashmi Yadav	Bhopal Univ., Bhopal
409.	Ratnesh Sharma	Vikram Univ., Ujjain
410.	Renu Hada	Univ. of Kota, Rajasthan
411.	Ricky Anthony	IIT, Indore
412.	Rinne Singh	SOP, DAVV, Indore
413.	Rishi Pal	Kurukshetra University, Kurukshetra
414.	Rishikesh Yadav	R.G.P.V., Bhopal
415.	Ruchi Gupta	Jiwaji Univ., Gwalior

416.	S. Thiruvenkadam	SJC, Tirchy, Tamil Nadu
417.	S. Thiruvenkadam	SJC, Tirchy, Tamil Nadu
418.	Sajad Ahmed	NIT, Srinagar
419.	Sajid Babu	Univ., of kerala
420.	Sameer Kulkarni	BIT, Meshra, Ranchi
421.	Sandeep Ku. Gohar	Holker Science Collg., Indore
422.	Sandeep Ranjan	Amity Univ., Haryana
423.	Sangeeta Kalal	MLSU, Udaipur
424.	Sanjeet Srivastava	LKCT, Indore
425.	Saurabh Ku. Pandey	IIT, Indore
426.	Savan V. Katba	Saurashtra Univ., Rajkot
427.	Shailendra Sing Rajput	BIT, Meshra, Ranchi
428.	Shakti Sanago	R.G.P.V., Bhopal
429.	Shashank Agrawal	Smmriti Collg. Of Pharma, Indore
430.	Sheetal Soni	SOI, DAVV, Indore
431.	Shweta Rajawat	MANIT, Bhopal
432.	Smrath Ninama	SOP, DAVV, Indore
433.	Smt. D. N. Nagwanshi	RDVV, Jabalpur
434.	Sonam Dwivedi	SOP, DAVV, Indore
435.	Sonam Mandani	IIT, Indore
436.	Stuti Katra	Univ. of Kota, Rajasthan
437.	Sunita Keshari	BIT, Meshra, Ranchi
438.	Supriya Bisen	SOP, DAVV, Indore
439.	Sushil Ku. Pandey	IIT, Indore
440.	T. Kannaan	N.I.T.C., Kerala
441.	Tamalika Bhattacharya	IIT, Indore
442.	Tanveer Ahmed	SOP, DAVV, Indore
443.	Tehmina Khan	Govt. Madhab Sci. P.G. Collg., Ujjain
444.	Tejas Tank	Barkatulla Univ., Bhopal
445.	Thombare J.V.	Shivaji Univ., Kolhapur, Maharastra
446.	Tulshi Shiyani	P.D.P.Univ., Gandhinagar
447.	Vijay Kumar	I.T.M. Univ., Gwalior, M.P.
448.	Vinaya Jaiswal	IIT-BHU, Varanasi
449.	Vishakha Vibhute	SOP, DAVV, Indore
450.	Vishal Jain	MLSU, Udaipur
451.	Vishnu Awasthi	IIT, Indore
452.	Yasir Beeran	Univ. of Kerala, Kerala
453.	Yogesh Patidar	S.G.S.I.T.S., Indore

SIMS

454.	Dr. C Das	BARC Trombay, Mumbai (MS)
455.	Dr. C. David	IGCAR, Kalpakam, T.N.
456.	Dr. D. Bhattacharya	BARC Trombay, Mumbai (MS)
457.	Dr. Pujara	IGCAR, Kalpakam, T.N.
458.	Dr. Pusan Banerjee	Vidya Sagar Engineering Collg., Kolkata
459.	Dr. Ratnesh Gupta	School of Electronics, DAVV Indore (MP)
460.	Dr. T. D. Das	University of Calcutta, Kolkata
461.	Jaya Kumar	Alagappa University, T.N.
462.	Miss Mitali Swain	BARC Trombay, Mumbai (MS)
463.	Mr. Hysen Thomas	Cochin University, Cochin, (Kerala)
464.	Mr. Pranab Biswas	IIT, Kharagapur.
465.	Mr. Rajani Jacob	Cochin University, Cochin, (Kerala)
466.	Mr. Sushil Ku. Pandey	IIT, Indore
467.	Mrs. Geeta Phookat	Cochin University, Cochin, (Kerala)
468.	Dr. S. Sarkar	IIT Bombay (MS)

PES

469.	Mr. Jaison Joseph	Goa University, Goa
470.	Niyati Mishra/ Prof.A.Mishra	DAVV, Indore
471.	Dr.S.N.Kane	DAVV, Indore
472.	Ch.Nageshwar Rao	DIAT Pune
473.	M.V.R.Naidu	IIT, Chennai
474.	Priyanka Yadaw/ Prof.S.I.Patil	Pune University, Pune
475.	Bharat Singh	Barkatullah Univ. Bhopal
476.	Megha Vagadia/Prof.Kuberkar	Saurashtra University, Rajkot
477.	Arvind Shrivastav/ Pragya Tiwari	RRCAT, Indore
478.	Rohini Bhalerao	Pune University, Pune
479.	Anjali Jain/ Dr.R.V.nandedkar	IPS Academy, Indore
480.	Sheetal Soni/ Ratnesh Gupta	DAVV, Indore
481.	Mr.Gulbag Singh	IIT, Mumbai
482.	Pankaj Sagdeo	BARC, Vizag
483.	Shashi Shinde/ Dr.K.P.Adhi	Pune University, Pune
484.	Dr.S.N.Jha	BARC, Mumbai
485.	Madhusmita/ T.Ganguli	RRCAT, Indore
486.	Dr.Archana Sagdeo	RRCAT, Indore
487.	Dr.Pooja Gupta/ T.Ganguli	RRCAT, Indore
488.	Dr.Shailja Tiwari/ Prof.Ahuja	M.LSU, Udaipur
489.	Aparna Agarwal/ Prof.P.Sen	DAVV, Indore

248nm, KrF Excimer Pulsed Laser Deposition System

490.	Dr.Prashant S. Vachhani	University of Hyderabad
491.	Mr.Nimma NareshC/o Dr.R.N.Bhomik	Pondicherry University
492.	Mr.Jayaram PC/o Dr. P.P.Pradyumnan	University of Calicut
493.	Ms.Arpana AgrawalC/o Prof.Pratima Sen	School of physics ,DAVV University
494.	Dr.Arvindam GhoshC/o Dr.S.N.Kane	School of physics ,DAVV University
495.	Mr.Anshul Jain,C/o Dr.R.S.Chauhan	R.B.S.College Agra(U.P.)
496.	Ms.Megha Vagadia,C/o Prof.U.G.Kuberkar	Saurashtra University, Rajkot
497.	Dr.Manvendra Kumar	University of Allahabad
498.	Mr.Ashiq Hussain Shah,C/o Dr.M.Basheer Ahmad	B.S.A.Rahaman University, Chennai
499.	Mr. Jaison Joseph,C/o Prof.R.B.Tangsali	Goa University, Goa
500.	Mr.Irshad Ahmad Bhatt C/o Dr.Shahid Hussain	Aligarh muslim university, Aligarh
501.	Mr.Khalid Sultan,C/o Dr.M.Ikram	NIT,Srinagar
502.	Mr.Savan V.Katba C/o Prof.D.G.Kuberkar	Saurashtra University, Rajkot
503.	Ms.Priyanka G.Trivedi C/o Prof.D.G.Kuberkar	Saurashtra University, Rajkot
504.	Mr.Tarale Arjun Nagarath C/o Prof.P.B.Joshi	Solapur University, Solapur
505.	Mr.Sajad Ahmad Mir,C/o Dr.Mohd. Ikram	NIT,Srinagar (J&K)
506.	Mr.P.Nagaraju C/o Dr.M.V.Ramana Reddy	Osmania University, Hyderabad
507.	Mr.Harinath Aireddy,C/o Dr.Amal Kumar Das	IIT, Kharagpur
508.	Ms.Mitali Chaudhary,C/o Dr.S.K.Sharma	ISM, Dhanbad (Jharkhand)
509.	Mr.Arup Kumar Kunti,C/o Dr.S.K.Sharma	ISM, Dhanbad (Jharkhand)

7 Tesla Quantum Design SQUID VSM System

510.	Mr. Arvind Sharma c/o Prof. B. L. Ahuja	M. L. Sukhadiya Univ., Udaipur
511.	Ms. Reshma c/o Dr. R Jotania & Prf. H Virk	Gujarat University, Ahmedabad
512.	Ms. Priyanka c/o Prof. S.I. Patil	Pune University, Pune
513.	Mr. Pankaj Mohanti c/o Dr. Chandna Rath	B.H.U. Varanasi
514.	Dr. S. N. Kane	SOP, DAVV, Indore
515.	Dr. Ratnesh Gupta	SOI, DAVV, Indore
516.	Ms. Megha c/o Prof. D. G. Kuberkar	Saurashtra University, Rajkot
517.	Ms. Pratibha Agarwaal c/o Dr. S. Bhagwat	Garware College Pune University
518.	Mr. Aashish c/o Prof. D. G.Kuberkar	Saurashtra University, Rajkot
519.	Dr. Prashant c/o Prof. A.K.Bhatnagar	University of Hydrabaad
520.	Dr. Avneesh Anshul	NPL, Delhi
521.	Mr. Nishad c/o Dr. R.K.Pandey	Barkattula university, Bhopal
522.	Ms. Lisha Raghvan c/o Prof. M R Anantharaman	Cochin university, Kerla
523.	Dr. Yogesh c/o Dr.K.Ashokan	IUAC, Delhi
524.	Dr. H. B. Patil	RC Patel ASC College, Shirpur
525.	Dr. S. Satpati	RRCAT, Indore
526.	Mr. Irshad c/o Dr. S. Husain	AMU, Aligarh

527.	Mr. Khalid c/o Dr. M. Ikram	NIT Shrinagar
528.	Remya K.P C/O Dr. S. Amirthapandian	IGCAR Kalpakkam
529.	Minakshi Sharma C/O Prof. Ravi Kumar	NIT Hamirpur
530.	Priyanka B.Kashil C/O Dr.Vijaya Puri	Shivaji university Kolhapur, Maharashtra
531.	Anar Singh C/O Prof Dhananjai Pandey	IIT, BHU
532.	Shankar c/o Prof. S.I. Patil	Pune university
533.	Harinath Aireddy C/O Amal Kumar Das	IIT Kharagpur
534.	Dr.Anju Ahalawat	RRCAT Indore
535.	Sawan C/O Prof.D.G.Kuberkar	Saurashtra University Rajkot
536.	Pawanpreet C/O Prof.Ravi Kumar	NIT Hamirpur
537.	Lisha Raghwan c/o Prof. M R Anantharaman	Cochin university, Kerla
538.	R. Vettumperumal c/o Dr. S. Kalyanaraman	Sri Paramakalyani College, Alwarkurichi, Tamilnadu
539.	Anupam Sharma	DOP, Manipal University Jaipur
540.	Manoj Kumar Jaiswal C/O Dr.Rajesh Kumar	GGSIP University ,New Delhi

Room temperature Mossbauer spectroscopy

541.	Ms D.Rathore,	B.U.University, Bhoapl
542.	Dr.Ratnesh Gupta,	DAVV, Indore
543.	Mr.Hemant Kumar,	PantNagar Univ.,
544.	Mr.Girish Chandra,	PantNagar University
545.	Mr.T. Ghosh,	S.N.Bose Centre, Kolkota
546.	Dr.D.Vashney,	DAVV indore
547.	Mr.M.Siddaling,	Banglore University
548.	Mr.Hashim,	AMU Aligrah
549.	Dr Jocob Methew,	Kerala University
550.	Dr.Bharthi,	IGCAR kalpakkam
551.	Dr.Sebastian,	JNCSR, Bangalore
552.	Dr.S.N.Kane,	DAVV indore
553.	Mr.Vishal,	MLS Univ., Udaipur

Low temperature and high field Mossbauer spectroscopy

554.	Mr.T.Ghosh,	S.N.Bose Centre, Kolkatta
555.	Mr.Durgesh Kumar,	IIT BHU
556.	Dr Bharthi,	IGCAR,Kalkappam
557.	Mr.Devendra Sharma,	Rajasthan University, Jaipur
558.	Mr.Ramesh Babu,	VIT,Vellore
559.	Dr.S.Rayaprol,	CSR, Mumbai
560.	Dr.N.Laxmi,	MLSU, Udaipur
561.	Ms.Rabia Pandit	NIT Hamirpur
562.	Dr.R.C.Shrivastwa	PantNagar University

Magneto optical Kerr effect (MOKE)

563.	Ms.Alphonsha,	IPR Gujarat
564.	Dr.Ratnesh Gupta,	DAVV, Indore
565.	Ms.Lisha Raghvan,	CUSAT,Kerala
566.	Mr.Sagar Sen,	SOI,DAVV Indore

GIXRD and XRR

567.	Mr.Dhurbo Roy,	ISM dhanbad
568.	Ms. Manisha,	IGCAR
569.	Ms.Lisha Raghvan,	CUSAT,Kerala
570.	Mr.Naresh,	Pondichery University
571.	Mr.Tarale Arjun.N,	Solapur University
572.	Mr.Dhanu Krishna,	Kerala University
573.	Mr.Chalana,	Kerala University
574.	Dr.S.N.Kane,	SOP,DAVV Indore
575.	Dr.Manvendra,	Allahabad University
576.	Dr.Ratnesh Gupta,	SOI,DAVV Indore
577.	Mr.Yasir,	Kerala University
578.	Mr.UnniKrishana,	Kerala University
579.	Mr.Girish Gund,	Shivaji University, Kolhapur
580.	Mr.Ashiq Hussian, B.	Rahman Univ., Chennai
581.	Mr.Irshad,	AMU aligragh
582.	Ms.Sheetal Soni,	DAVV, Indore
583.	Ms.Archana Kamble	Shivaji University , Sholapur
584.	Mr.Shaibal Sarkar,	IIT Bombay
585.	Ms.Priyanka Kashid,	Shivaji University , Sholapur
586.	Mr.Khalid,	NIT Shrinagar
587.	Mr Vishal,	MLSU Udaipur
588.	Mr. Harinath Reddy,	IIT Kharagpur
589.	Prof S.I.Patil,	Pune University
590.	Mr.Arjun Tarale,	Solapur University
591.	Mr.Amol singh,	RRCAT indore
592.	Mr.Vinod Kumar,	IT BHU
593.	Mr P. Naagraj,	Osmania University
594.	Mr.Stephen,	MKU ,TamilNadu
595.	Mr.Jaisan,	Goa University
596.	Dr. Arindham Ghosh,	DAVV Indore
597.	Mr. Jolly Bose,	Kerala University
598.	Mr.Arup Kumar,	ISM Dhanbad

Ferroelectric (P-E) loop tracer

599.	Prof.P.B.Joshi,	Solapur Univ.,
600.	Prof.Kuberkar,	Rajkot
601.	Dr.Basavaraj Angadi,	Bangalore Univ.,
602.	Ms.Oroosa Subohi,	MANIT, Bhopal
603.	Dr.M.M.Malik,	MANIT, Bhopal
604.	Prof. D.Varshney,	DAVV, Indore ,
605.	Dr.Seema Sharam,	Patna

ESCA

606.	Mr. Puneet Negi	GB Pant Univ., Pantanagar
607.	Mr. Pankaj Mohanty	IT-BHU, Varansai
608.	Mr. Devendra Tiwari	CHARUSAT, Anand
609.	Dr. Smita Acharya	Nagpur Univ. Nagpur
610.	Mr. Heman Dave	IPR, Gandhinagar
611.	Prof. Milind Deshpande,	S.V. Univ., Vidyanagar
612.	Dr. Chandana Rath	BHU, Varanasi
613.	Ms. Urmila K.S.	CUSAT, Cochin
614.	Ms. Namitha Ashokan	CUSAT, Cochin
615.	Mr. Neelabh Shrivastava	BHU, Varanasi
616.	Mr. Arvind Kumar Rastogi	BHU, Varanasi
617.	Mr. Jaykumar P.	Univ. of Calicut, Calicut
618.	Dr. Suman Mahendia	Kurukshetra Univ, Kurukshetra
619.	Dr. Ranu Bhatt	TPD, BARC, Mumbai
620.	Ms. Vishakha Kaushik	IIT, Delhi
621.	Mr. Chethan Pai	Mangalore Univ., Mangalore
622.	Ms. Lisha Raghwan	Cochin Univ., Cochin
623.	Ms. Niyati Mishra	DAVV, Indore
624.	Dr. Adarsh K.V.	IISER, Bhopal
625.	Mr. Sandeep Rajan	Amity Univ., Gurgaon
626.	Mr. Manish Dixit	Dharamsingh Desai Univ., Nadiad
627.	Mr. Shrikant Gunjal	Pune Univ., Pune
628.	Ms. Shreeja Pillai	Barkatullah Univ., Bhopal
629.	Mr. Bhaskar Soni	LNMIIT, Jaipur
630.	Mr. Rajesh T.	NCL, Pune
631.	Dr. Pravin Siwach	NPL, Delhi
632.	Mr. Dhrubajyoti Roy	ISM, Dhanbad
633.	Dr. O.P. Pandey	Thapar Univ., Patiala
634.	Dr. Manish Mishra	Dharamsingh Desai Univ., Nadiad
635.	Ms. Rajani Jacob	CUSAT, Cochin

636.	Mr. Shrikant Naik	Goa Univ., Goa
637.	Dr. Arnab Biswas	IIT, Kharagpur
638.	Mr. Irshad Ahmed Bhatt	AMU, Aligarh
639.	Dr. Neeru Tiwari	DRDO, Kanpur
640.	Prof. S.K. Sandalshi	Tezpur Univ., Tezpur
641.	Mr. R. Varadaseshan	Paramakalyani College, Thirunelveli
642.	Dr. Kanwaljitsingh Sokhi	RRCAT, Indore
643.	Dr. Jai Khare	RRCAT, Indore
644.	Ms. Rashmi Singh	RRCAT, Indore
645.	Dr. Ajimsha	RRCAT, Indore
646.	Dr. Chintamani Das	BARC, Mumbai
647.	Dr. Deepa Dey	IIT, Indore
648.	Ms. Manavi Satalkar	DAVV, Indore

UV-Vis NIR

649.		
650.	Dr. Atul Khanna	G.N.D. Univ., Amritsar
651.	Ms. Rajani Jacob	Union Cristian College, Cochin
652.	Ms. Purnima Hazra	IT-BHU, Varanasi
653.	Mr. Abhishek Dwivedi	BHU, Varanasi
654.	Mr. Anupam Selot	Sadhuvaswani College, Bhopal
655.	Ms. Anjali Jain	IPS Academy, Indore
656.	Mr. Punit Negi	G.B. Pant Univ., Pantanagar
657.	Mr. Anil Kumar	Amity Univ., Noida
658.	Mr. Devendra Tiwari	CHARUSAT, Anand
659.	Dr. Smita Acharya	Nagpur Univ., Nagpur
660.	Mr. P. Jayaram	Univ. of Calicut, Calicut
661.	Mr. Naresh Nima	Pondichery Univ., Pondichery
662.	Mr. varadaseshan	M.S. Univ., Thirunelveli
663.	Dr. D.S. Rane	North Maharashtra Univ., Jalgaon
664.	Mr. Ashq Hussain	B.S. Abdul Rehman Univ., Chennai
665.	Mr. Prem Kumar	S.V.N. College, Madurai
666.	Ms. Compesh Pannu	IUAC, New Delhi
667.	Mr. Khalid Sultan	NIT, Shrinagar
668.	Mr. Nayanmani Das	ISM, Dhanbad
669.	Mr. P. Nagaraju	Osmania Univ., Hyderabad
670.	Mr. Thiruvcenkatalam	St. Joseph College, Trichi
671.	Mr. Maneesh Choudhari	Sardar patel Univ., Vidyanagar
672.	Ms. Durgesh Nandini	RDVV, Jabalpur
673.	Mr. Ratnesh Sharma	Vikram Univ., Ujjain
674.	Ms. Tehmina Khan	Vikram Univ., Ujjain

675.	Mr. Rajendra Sharma	DAVV, Indore
676.	Ms. Ankita Pal	DAVV, Indore
677.	Ms. Sonam Dwivedi	DAVV, Indore
678.	Ms. Arpana Agrawal	DAVV, Indore
679.	Dr. Deepa Dey	IIT, Indore
680.	Ms. Anuradha Gupta	Holkar Science College, Indore
681.	Ms. Kirti Sahu	Holkar Science College, Indore
682.	Ms. Payal Soni	Holkar Science College, Indore
683.	Ms. Preeti Jain	Holkar Science College, Indore
684.	Ms. Priyanka Makhija	Modern Dental College, Indore
685.	Ms. Vishakha Vibhute	Acropolis Institute, Indore
686.	Jaiveer Singh	IPS Academy, Indore

FTIR

687.	Ms. Sumati Shiva	Mother Teresa Univ., Kodaikanal
688.	Mr. N. Rajeshwar Rao	NIT, Warangal
689.	Ms. Durgesh Nandini	RDPB, Jabalpur
690.	Dr. Smeeta Acharya	Nagpur Univ., Nagpur
691.	Mr. Sajid Babu	Univ. of Kerla, TVM
692.	Mr. Nayanmani Das	ISM, Dhanbad
693.	Mr. Dhrubajyoti Roy	ISM, Dhanbad
694.	Ms. Sangeeta Kalal	MLS Univ., Udaipur
695.	Mr. Yogesh Kumar	IUAC, New Delhi
696.	Dr. Suman Mahendia	Kurukshetra Univ., Kurukshetra
697.	Mr. naresh Nima	Pondichery Univ., Pondichery
698.	Mr. Punit Negi	G.B. Pant Univ., Pantanagar
699.	Mr. Bhaskar Soni	LNMIIT, Jaipur
700.	Ms. Archana Kamble	Shivaji Univ, Kolhapur
701.	Mr. Neeraj sharma	VVPGT College, Durg
702.	Mr. Sohan Sani	Kurukshetra Univ., Kurukshetra
703.	Mr. Karnan	VHNSN College, Virudhunagar
704.	Mr. P. Nagaraju	Osmania Univ., Hyderabad
705.	Mr. Ashique Hussain	BSAR Univ., Chennai
706.	Dr. Deepti Kothari	IPR, Gandhinagar
707.	Mr. Abhishek Dwivedi	BHU, Varanasi
708.	Ms. Preeti Jain	Holkar Science College, Indore
709.	Mr. varadaseshan	M.S. Univ., Thirunelveli
710.	Ms. Richi Gupta	Jivaji Univ., Gwalior
711.	Ms. Anju Jain	MANIT, Bhopal
712.	Mr. Anupam Selot	Sadhuvaswani College, Bhopal
713.	Ms. Hafsa Siddiqi	MANIT, Bhopal

714.	Mr. Mohd. Ramzan	MANIT, Bhopal
715.	Ms. Tanuja Kadre	Vikram Univ., Ujjain
716.	Ms. Disha Acharya	Vikram Univ., Ujjain
717.	Shakuntala Solanki	Vikram Univ., Ujjain
718.	Mr. Nilesh patel	Maharaja Ranajeet Singh College, Indore
719.	Ms. Vaishali Giyakwad	GSITS, Indore
720.	Ms. Vishakha Vibhute	DAVV, Indore
721.	Mr. Pavan Kumar sharma	DAVV, Indore
722.	Mr. Prabhakar sharma	DAVV, Indore
723.	Mr. Rajendra Sharma	DAVV, Indore
724.	Ms. Sanchita Nag	DAVV, Indore
725.	Ms. Preeti Shrivastava	DAVV, Indore

Surface Physics Lab

726.	Nimma Naresh	Pondicherry Unv.
727.	M. Baral	RRCAT
728.	S. D. Singh	RRCAT
729.	Navneet Singh	IIT, Mandi
730.	Subhasis Ghosh	JNU, Delhi
731.	S. Ramakrishnan	Amrita Vishwa Vidyapeetham, Coimbatore
732.	K. Jayakumar	Alagappa Unv, Tamil Nadu
733.	Maneesha Gupta	AMU, Alighar
734.	Jitendra Panwar	Dept. of Biotechnology, BITS, Pilani
735.	KVANPS Kumar	UHV Technology, RRCAT, Indore
736.	Saibal Mukherjee	IIT, Indore

12. 2 Kalpakkam Node

TEM

737.	Mr. P. Kannappan	Anna University,Chennai
738.	Dr. Amiya Priyam	BIT Mesra, Ranchi
739.	Miss. Radhamani, Dr. Sudakar Chandran	IITM, Chennai
740.	Mr. Thiruvenkadam	St. Joseph College, Trichy
741.	Mr. Jastin, Dr. A. Mukharjee	VIT, Vellore
742.	Miss Dipika	VNIT, Nagpur
743.	Mr. Vasu, Dr. Sudakar Chandran	IITM, Chennai
744.	Dr. R. Ramesh, Dr. Muttamizhselvan	SRM Univ, Chennai

XRD

745.	M. Divya,	IGCAR, Kalpakkam
746.	Niranjan Kumar,	IGCAR, Kalpakkam
747.	Deepalekshmi P.,	MG University.Kottayam
748.	Akash Singh,	IGCAR, Kalpakkam

FESEM-EDX

749.	Jesi Arul	Govt. Arts College, Madurai
750.	Prof. R. Manoharan	PSG-IAS, Coimbatore
751.	Geetha Kumary	IGCAR, Kalpakkam
752.	Dr.Partho Ganguly	IGCAR, Kalpakkam
753.	Aditya Kela	CMI, Chennai
754.	Hari Babu	HBNI, Kalpakkam.
755.	Dibyendu Ghosh	Jadavpur University, Kolkata
756.	K. P. Remya	Bharathidasan Univ
757.	Anindita Ghosh	Jadavpur University, Kolkata
758.	Shubhajyoti Chowdhury	Jadavpur University Kolkata
759.	Dr. Sachindra Nath Das	Raj College ,Burdwan
760.	Kalaivani D	IGCAR, Kalpakkam
761.	Dr. Abani Mohan Rudra	Raj College ,Burdwan
762.	Md. Basith	Loyola College, Chennai
763.	Diganta Gogoi	IGCAR, Kalpakkam
764.	P.Suresh	Loyola College,Chennai
765.	Barun Ghosh	Jadavpur University, Kolkata
766.	N. Srinatha	Bangalore University
767.	P. Deepalekshmi	MG University.Kottayam
768.	Vinod K	IGCAR, Kalpakkam
769.	Dr. Judith Vijaya	Loyola College, Chennai
770.	R. Raja Madhavan	IGCAR, Kalpakkam
771.	Prof. Sabu Thomas	MG University.Kottayam
772.	K. Vinod	IGCAR,Kalpakkam
773.	Anindita Ghosh	Jadavpur University, Kolkata
774.	Tanuka Banerjee	Jadavpur University, Kolkata
775.	Pintu Pole	Presidency University, Kolkata
776.	Shibsanker	Presidency University, Kolkata
777.	R. Madhavan	IGCAR, Kalpakkam
778.	E. Prabhu	IGCAR, Kalpakkam
779.	Dipika Barbadikar	VNIT, Nagpur
780.	Velu Nirmal Kumar	Anna University.,Chennai
781.	Sanjay	UGC-DAE CSR,Indore

782.	Saoni Rudra	CGCRI, Kolkata
783.	Nayan Mani Das	ISM, Dhanbad
784.	Dhanya Chandran	M.G. College,Trivandrum
785.	Dhrubojyoti Roy	ISM, Dhanbad
786.	Nihar Ranjan Panda	Sambalpur Univ., Sambalpur
787.	Dr. S Deshmukh	SKN Singhad College,Solapur,
788.	Prof. P. Nayak	Sambalpur Univ. Sambalpur

XPS

789.	Prof Amitava Mookerjee	VIT,Vellore
790.	Dibyendu Ghosh	Jadavpur University, Kolkata
791.	Barun Ghosh	Jadavpur University, Kolkata
792.	Shubhajyoti Chowdhury	Jadavpur University, Kolkata

12.3 Kolkata Centre

Flow Cytometer

793.	Dipanwita Das	University of Kalyani
794.	Dipesh Kumar Das	University of Calcutta
795.	Krishnendu Manna	University of Calcutta
796.	Amitava Khan	University of Calcutta
797.	Ujjal Das	University of Calcutta
798.	Sayan Ghosh	University of Calcutta
799.	Ritu Srivastava	Visvabharati

Cell / Tissue Culture Facilities

800.	Dipanwita Das	Kalyani University
801.	Ujjal Das	Calcutta University
802.	Mahua Sinha	Calcutta University
803.	Amitava Khan	Calcutta University
804.	Dipesh Das	Calcutta University
805.	R. Srivastava	VB, Santiniketan
806.	Krishnendu Manna	Calcutta University
807.	Sangeeta Lahiri	Barasat Govt College

Fluorescence Microscope

808.	Anulipi Aich	GCELT, Kolkata

809.	Nirmalya Ghoshal	University of Calcutta
810.	Dipesh Kumar Das	University of Calcutta
811.	Krishnendu Manna	University of Calcutta
812.	Ujjal Das	University of Calcutta
813.	Sayan Ghosh	University of Calcutta

Centrifuges /Sonicator

814.	Pallabi Bhowmick	Calcutta University
815.	Satarupa Pattanayak	BIT, Meshra
816.	Sudip Biswas	Jadavpur University
817.	Sushma Sharma	Vikram University

UV-Vis Spectrophotometer

818.	Dr. M. Ghosh	Bengal Engineering & Science University
819.	Prof. P.S. Gupta,	Indian School of Mines, Dhanbad
820.	Shri. Jijo Abraham	M.G. University, Kottayam, Kerala
821.	Ms. Barnita Makhal	I.I.T. Roorkee
822.	Dr. Amiya Priyam	B.I.T. Meshra
823.	Dr. Ujjal Kumar Sur	Nagpur University
824.	Prof. Rajib Bandyopadhyay	Jadavpur University
825.	Dr. S. Kumar	Jadavpur University
826.	Prof. Amarjyoti Choudhury	Tezpur University
827.	Dr. S.K. Das	Variable Energy Cycltron Centre
828.	Dr. Bidhan Mohanto	Assam University, Silchar
829.	Ms. Hemlatha Bhojan	Bharathiar University
830.	Dr. P.K. Bag	Calcutta University
831.	Prof. S. C. Bhattacharyya	Jadavpur University
832.	Prof. A. Dutta	S.I.N.P. Kolkata

Luminiscence Spectrometer

833.	Prof. Amitava Datta	Jadavpur University
834.	Dr. M. Ghosh	B.E.S.U.
835.	Dr. A. Basumallik	B.E.S.U.
836.	Dr. Sarat Chandra Babu	Gitam University
837.	Prof. K.K. Mukherjea	Jadavpur University
838.	Prof. S. Bhattacharyya	S.I.N.P. Kolkata
839.	Dr. S. Jana	S.I. N. P. Kolkata
840.	Mr. Jijo Abraham	M.G. University, Kottayam, Kerala
841.	Ms. Barnita Makhal	I.I.T. Roorkee
842.	Dr. Ujjal Kumar Sur	Behala College

843.	Prof. Amarjyoti Choudhury	Tezpur University
844.	Dr. Sarat Chandra Babu	Gitam University
845.	Dr. S. Kumar,	Jadavpur University
846.	Dr. Amiya Priyam	B.I.T. Meshra
847.	Dr. Bidhan Mohanto	Assam University, Silchar
848.	Ms. Hemlatha Bhojan	Bharathiar University
849.	Dr. Kamalika Sen	University of Calcutta
850.	Dr. P. Nayak	Sambalpur University
851.	Prof. B. Ghosh	Jadavpur University
852.	Dr. P.K. Bag	Calcutta University
853.	Dr. S.K. Das	V.E.C.C. Kolkata
854.	Prof. S.C. Bhattacharyya	Jadavpur University, Kolkata

Gamma Chamber

855.	Dr. S.K. Das	V.E.C.C.
856.	Dr. S. Dey	Calcutta. University
857.	Prof. K.K. Mukherjea	Jadavpur University
858.	Prof. S.K. Dey	W.B.U.T.
859.	Ms. P. Bhowmik	Calcutta University
860.	Dr. Manas Kumar Pandit	Bidhan Chandra Krishi Viswavidyalaya
861.	Prof. Sarmistha Raychoudhuri	Calcutta University
862.	Dr. Amiya Priyam	B.I.T. Meshra
863.	Dr. C. Saha	W.B.U.T. Kolkata
864.	Ms. B. Makhal	I.I.T. Roorkee
865.	Dr. N. Kalarikkal	M.G. University, Kottayam, Kerala
866.	Dr. R. Sadhukhan	Bidhan Chandra Krishi Vishwavidyalaya
867.	Prof. A. Choudhury	Tezpur University
868.	Dr. S. Ray Choudhuri	W.B.U.T. Kolkata
869.	Dr. S.C. Santra	University of Kalyani
870.	Prof. S. Tarafdar	Jadavpur University
871.	Prof. S. K. Dey	W.B.U.T. Kolkata
872.	Dr. S. Kundagrami	Univ. of Calcutta
873.	Ms. H. Bhojan	Bharathiar University
874.	Dr. T. Dalal	Burdwan University
875.	Dr. G. K. Sharma	Pune University
876.	Dr. M. Mandal,	I.I. T. Kharagpur
877.	Prof. M. Radhakrishna	I.I.I.T. Allahabad
878.	Prof. S.C. Bhattacharyya	Jadavpur University, Kolkata

Dynamic Light Scattering

879.	Prof. Amitava Datta	Power Engg. Jadavpur University, Kolkata

880.	Dr. P. K. Chakraborty	Burdwan University
881.	Shri. S. P. Paik	Calcutta University
882.	Dr. S. K. Paul	S.N. Bose, Kolkata
883.	Dr. K. Sen	University of Calcutta
884.	Dr. A. Goswami	Indian Statistical Institute
885.	Dr. S. K. Paul	S. N. Bose National Centre for Basic Sciences
886.	Dr. S. Halder	Jadavpur University
887.	Dr. S.K. Das	V.E.C.C
888.	Shri. Jijo Abraham	M.G. University, Kottayam, Kerala
889.	Dr. C. Saha,	W.B.U.T. Kolkata
890.	Prof. S K. Dey	W.B.U.T. Kolkata
891.	Dr. U. K. Sur	Behala College
892.	Dr. P. Chattopadhyay	Burdwan University
893.	Prof. Amarjyoti Choudhury	Tezpur University
894.	Dr. N. Kalarikkal	Mahatma Gandhi University
895.	Dr. S. De	Kalyani University
896.	Dr. R. Biswas	S.N. Bose National Centre for Basic Sciences
897.	Ms. Hemlatha Bhojan	Bharathiar University
898.	Dr. (Mrs.) Uma Sharma	Vikram University, Ujjain
899.	Prof. S.C. Bhattacharyya	Jadavpur University

Fourier Transform Infrared Spectrometer

900.	Dr. M. Ghosh	B.E.S.U.
901.	Prof. P.S. Gupta	Indian School of Mines, Dhanbad
902.	Dr. D. Mondal	Jadavpur University
903.	Prof. A. Datta	Jadavpur University
904.	Shri. Jijo Abraham	M.G. University, Kottayam, Kerala
905.	Prof. Rajib Bandyopadhyay	Jadavpur University
906.	Dr. Ujjal Kumar Sur	Nagpur University
907.	Ms. Hemlatha Bhojan	Bharathiar University
908.	Prof. S.C. Bhattacharyya	Jadavpur University, Kolkata
909.	Dr. S.K. Das	V.E.C.C
910.	Dr. C. Saha	W.B.U.T. Kolkata
911.	Prof. S. K. Dey	W.B.U.T. Kolkata
912.	Dr. P.K. Bag	Calcutta University

Laser Raman Spectrometer

913.	Prof. S.K. Dolui	Tezpur University
914.	Dr. S. Kumar	Jadavpur University
915.	Ms. H. Bhojan	Bharathiar University
916.	Dr. P. Nayak	Sambalpur University

917.	Prof. S.C. Bhattacharyya	Jadavpur University, Kolkata
918.	Dr. S.K. Das	V.E.C.C
919.	Dr. D. Mohanta	Tezpur University
920.	Dr. A. Priyam	B.I.T. Meshra
921.	Shri. Jijo Abraham	M.G. University, Kottayam, Kerala
922.	Prof. Sabu Thomas	M.G. University, Kottayam, Kerala
923.	Dr. Sudipto Bandopadhya	Calcutta University
924.	Dr. Nandakumar Kalarikkal	Mahatma Gandhi University
925.	Dr. C. Saha,	W.B.U.T. Kolkata
926.	Prof. S. K. Dey	W.B.U.T. Kolkata
927.	Dr. P.K. Bag	Calcutta University
928.	Prof. D. Banerjee	BESU

Isothermal Calorimeter

929.	Dr. P.K. Bag	Calcutta University
930.	Prof. S.C. Bhattacharyya	Jadavpur University, Kolkata
931.	Dr. C. Saha,	W.B.U.T. Kolkata
932.	Dr. S.K. Dey	W.B.U.T. Kolkata

Sample Preparation Facilities, (Freeze drier, Pelletiser, Vacuum Filtration

933.	Prof. S.C Santra	Kalyani Univesity
934.	Dr. A. Chattopadhyay	Visva Bharti University
935.	Deblina Ghosh	JD Birla College, Kolkata
936.	Devlina Paul	JD Birla College, Kolkata
937.	Prof. Sarmistha Raychoudhuri	Calcutta University
938.	Dr. H.N. Thatoi	BPTU, Bhubaneswar
939.	Dr.Shantilata Sahoo	Utkal University
940.	Jijo Abraham	Mahatma Gandhi University
941.	Ankhi haldar	Calcutta University
942.	Samraggi saha chowdhury	JD Birla College, Kolkata
943.	Debanjali jairam	JD Birla College, Kolkata
944.	Dr. Uma Sharma	Vikram University
945.	Hemalatha Bhojan	Bharathiar University
946.	Dr. Shaon Raychaudhuri	WBUT, Kolkata
947.	Prof. Anjana Dewanji	ISI, Kolkata
948.	Dr. M. Manna	Barasat Govt College
949.	Dr. N. K. Sharat Singh	Manipur University
950.	Kamalesh Kumar	Jadavpur University

Energy Dispersive X-Ray Fluorescence

951.	Prof. S.C Santra	Kalyani Univesity
952.	Dr. A. Chattopadhyay	Visva Bharti University
953.	Deblina Ghosh	JD Birla College, Kolkata
954.	Devlina Paul	JD Birla College, Kolkata
955.	Prof. Sarmistha Raychoudhuri	Calcutta University
956.	Dr. H.N. Thatoi	BPTU, Bhubaneswar
957.	Dr.Shantilata Sahoo	Utkal University
958.	Samraggi saha chowdhury	JD Birla College, Kolkata
959.	Debanjali jairam	JD Birla College, Kolkata
960.	Dr. Shaon Raychaudhuri	WBUT, Kolkata
961.	Prof. Anjana Dewanji	ISI, Kolkata
962.	Dr. M. Manna	Barasat Govt College
963.	Dr. N. K. Sharat Singh	Manipur University

High Magnetic Field (SQUID & 15 tesla Magnet

964.	Dr Trilochan Swain	Utkal University, Bhubaneswar
965.	Dr Sunita Keshri	BIT,Mesra , Ranchi
966.	Prof. B.K Das	ITM University , Haryana
967.	Dr Kalyan Mondal	S N Bose National Centre
968.	Dr. Aritra Banerjee	Calcutta University
969.	Prof S K De	IACS Kolkata
970.	Prof Saurav Giri	IACS,Kolkata
971.	Prof Alok Ghosh	NIST, Orissa
972.	Prof Khaja Atlaf Hussain	Kakatia University ,Warangal
973.	Dr S K Pradhan	Burdwan University
974.	Dr P K Mukhopadhyay	S N Bose National Centre
975.	Dr Barnali Ghosh	S N Bose National Centre
976.	Dr Ranjana Gosawami	B P Poddar Eng College
977.	Dr S Pal	Kalyani University
978.	Dr P K Chakraborty	Burdwan University
979.	Prof A K Raychudhuri	S N Bose National Centre
980.	D S C Bhattacharaya	Jadavpur University
981.	Dr Chandan Mukherjee	IIT Guhawati
982.	Dr Kalyan Mondal	S N Bose National Centre
983.	Dr Sanjay Kumar	Jadavpur University
984.	Prof. B.K Das	ITM Haryana
985.	Dr P K Chakraborty	Burdwan University
986.	Prof S Arumugam	Bharathi Dasan University
987.	Prof Khaja Atlaf Hussain	Kakatia University ,Warangal

988.	Dr S K Pradhan	Burdwan University
989.	Dr Nandakumar Kalarikkal	M G University ,Kottayam, Kerala
990.	Dr Sujit Bandhapadya	VECC, Kolkata
991.	Dr D Jana	Calcutta University
992.	Dr Kuntal Chaterjee	Vidyasagar University
993.	Dr B R Rudraswami	Bangalore University
994.	Dr Vijaylaxmi Dayal	MIT Mysore

X-Ray Diffraction

995.	Dr. S K Pradhan	Burdwan University
996.	Dr. S Bandopadhyay	Calcutta University
997.	Dr. Alok Ghosh	NIST, Orissa
998.	Dr. S K Das	VECC
999.	Dr. Bhavya Bhushan	Centrl University of Jharkhand, Ranchi
1000.	Dr. Anjan Das	Burdwan University
1001.	Dr. Nandakumar Kalarikkal	M G University Kottayam
1002.	Dr. Rajib Bandopadhyay	Jadavpur University
1003.	Dr. Binay Pratap Singh	BHU, Varanasi
1004.	Dr. S Giri	IACS, Kolkata
1005.	Dr. Subham Majumdar	IACS, Kolkata
1006.	Dr. Pushan Banerjee	Jadavpur University
1007.	Dr. Sudipta Bandoradhyay	Calcutta University
1008.	Dr. Samarat Mukherjee	BIT Mesra
1009.	Dr. Amiya Priyam	BIT Mesra
1010.	Dr. Sudipta Pal	Kalyani University
1011.	Dr. Chandana Banerjee	Kalna College
1012.	Dr. Sanjay Kumar	Jadavpur University
1013.	Dr. Manojit Ghosh	Bengal Engineering and Science University, Shibpur
1014.	Dr. P.K.Chakraborty	Burdwan University
1015.	Dr. Atish Mandal	Burdwan University

Indian National Gamma Array

1016.	Dr R Palit	Tata Institute of Fundamental Reserach.
1017.	Dr Ashok Kumar	Panjab University
1018.	Prof U D Pramanik	Saha Institute of Nuclear Physics
1019.	Prof Polash Banejee	Saha Institute of Nuclear Physics
1020.	Prof A Goswami	Saha Institute of Nuclear Physics
1021.	Dr S Shirota	Panjab University
1022.	Dr H P Sharma	Banaras Hindu University
1023.	Dr Ajay Singh	Indian Institute of Technology, Kharagpur.
1024.	Dr Sukalyan Chattopadhyay	Saha Institute of Nuclear Physics

1025.	Dr P V Madusoodanan Rao	Andhra University
1026.	Dr D C Biswas	Bhaba Atomic Research Centre
1027.	Dr S Mukhopadhyay	Bhaba Atomic Research Centre
1028.	Dr U Garg	University of Notre Dame

Detector Laboratory

1029.	Dr T R Routray	P G Department of Physics, Sambalpur University
1030.	Prof Amitav Gupta	School of Nuclear Studies & Applications,

12.4 Mumbai Centre

Light Scattering

1031.	Prof. S. Umapathy	Madurai Kamaraj Univ., Madurai
1032.	Dr. H.S. Misra	Molecular Biol. Div., BARC, Mumbai.
1033.	Dr. Debasis Sen	SSPD, BARC, Mumbai.
1034.	Biswajit Manna	WSCD, BARC, Mumbai.
1035.	Dr. A. G. Kumbhar	WSCD, BARC, Mumbai
1036.	Dr. Indrajit Sinha	IIT-BHU, Varanasi.
1037.	Dr. R. K. Gopalkrishnan	RSSD, BARC, Mumbai.

Impedance Analyzer

1038.	Dr. A .K. Tyagi	Chemistry Division, BARC
1039.	Dr. S. N. Achary	Chemistry Division, BARC
1040.	Dr. V. Grover	Chemistry Division, BARC
1041.	Dr. P. K. Pujari	RCD, BARC
1042.	Dr. V. Dayal	Maharaja Institute of Technology, Mysore
1043.	Dr. B. Angadi	Department of Physics, Bangalore.
1044.	Mrs. V. V. Soman	Priyadarshini College of Engineering, Nagpur

Material Preparation Lab

1045.	Dr. A. Biswas	BARC
1046.	Dr. A. K. Tyagi*	BARC
1047.	Dr. S. N. Achary*	BARC
1048.	R. Shukla*	BARC
1049.	Dr. V. Grover	BARC
1050.	Vinod Kumar	NIT, Hamirpur
1051.	Ms. Vasundara	BARC

1052.	B. P. Mandal	BARC
1053.	Ms. N. Farheen*	BARC
1054.	Ashish Tyagi*	BARC
1055.	Ms. Anitha	BARC
1056.	Sidique Patwe	BARC
1057.	M. Jafar	BARC

*used multiple times

High Energy Planetary Ball Mill

1058.	Dr. A. V. Mahajan	IIT-Bombay
1059.	Dr. S. Bhattacharya	TPD, BARC
1060.	Dr. K. P. Muthe	TPD, BARC

Vibrating Sample Magnetometer

1061.	Dr. Aniruddha Biswas	GAMD, BARC
1062.	Bikas Maji	GAMD, BARC
1063.	Dr. N. Goswami	Jaypee Institute of Information Technology
1064.	Dr. B. N. Dash	Jadavpur University
1065.	Dr. S. Srinath	University of Hyderabad, Hyderabad
1066.	Dr. N. Harish Kumar	IIT-Madras, Chennai
1067.	Dr. P. K. Mishra	TPD, BARC
1068.	Prof. A. K. Raychowdhury	SNBCSE, Kolkata
1069.	Prof. D. Pandey	IIT-BHU, Varanasi
1070.	Dr. Mainak Roy	Ch.D, BARC
1071.	Dr. S. K. Ghosh	MPD, BARC
1072.	Dr. S. N. Acharya	Ch.D, BARC
1073.	Dr. M. C. Rath	RPCD, BARC
1074.	Dr. A. Dogra	NPL, New Delhi
1075.	Dr. B. Angadi	Bangalore University, Bengaluru
1076.	Dr. Sebastian C. Peter	JNCASR, Bengaluru
1077.	Dr. Saket Asthana	IIT-Hyderabad, Hyderabad
1078.	Dr. Niharika Mohapatra	IIT-Bhubaneswar, Bhubaneswar
1079.	Prof. R. V. Upadhyay	CHARUSAT, Changa

FCD Neutron Diffractometer

1080.	Dr. K. Madangopal	BARC, Mumbai
1081.	Dr. D. Bhattacharya	CGCRI, Kolkata
1082.	Dr. A. Biswas	BARC, Mumbai
1083.	Dr. Keka Chakraborty	BARC, Mumbai
1084.	Dr. V. R. Reddy	UGC-DAE CSR, Indore

1085.	Dr. C. P. Sebastian	JNCASR, Bengaluru
1086.	Dr. D. Das	UGC-DAE CSR, Kolkata
1087.	Dr. R. Nirmala	IIT-Madras, Chennai
1088.	Dr. N. Mohapatra	IIT-Bhubaneswar, Bhubaneswar
1089.	Dr. R. Rawat	UGC-DAE CSR, Indore
1090.	Dr. Saket Asthana	IIT-Hyderabad, Hyderabad
1091.	Prof. R. Upadhyay	CHARUSAT, Changa (Gujarat)
1092.	Dr. P. Vishwakarma	NIT, Rourkela
1093.	Dr. S. B. Patnaik	JNU, New Delhi
1094.	Dr. Chandana Rath	IIT-BHU, Varanasi
1095.	Dr. P. U. Sastry	BARC, Mumbai
1096.	Dr. A. M. Awasthi	UGC-DAE CSR, Indore
1097.	Dr. N. E. Rajeevan	Z. G. College, Calicut (Kerala)
1098.	Prof. A. V. Mahajan	IIT-Bombay, Mumbai
1099.	Dr. Anjana Dogra	NPL, New Delhi
1100.	Dr. Pramod Bhatt	BARC, Mumbai
1101.	Dr. V. Sathe	UGC-DAE CSR, Indore
1102.	Dr. Dilip Pal	IIT-Guwahati, Guwahati
1103.	Dr. Basavaraj Angadi	Bangalore University, Bengaluru
1104.	Prof. A. K. Raychaudhuri	SNBCSE, Kolkata

13. General information on staff position (as on March 31, 2013)

Sl. No.	Designation	A	B
Director Office and Indore Centre			
01	Director of the Consortium	1	1
02	Centre-Director	1	1
03	Scientist	24	22
04	Engineer	4	4
05	Junior Engineer / Scientific Assistant	25	21
06	AO – II	1	1
07	AO – I	3	3
08	PS (to Director)	1	1
09	PA (to Centre-Director)	1	1
10	Assistant II	1	1
11	Assistant	3	3
12	Typist/Clerk/StenoTypist/ Steno-Clerk/Stenographer	4	3
13	Scientific Assistant (Library)	1	1
14	Caretaker	1	1
15	Driver/Driver-cum-Aux.Staff	3	3
16	Helper / Lab. Attendant / Aux.Staff	9	9
Kolkata Centre			
01	Centre-Director	1	1
02	Scientist	6	6
	Engineer	1	1
03	Junior Engineer / Scientific Assistant	14	14
04	Scientific Assistant (Library)	1	1
05	AO - I (Personnel)	1	1
06	AO – I (Accounts)	1	1
07	AO - I (Pur. & Stores)	1	1
08	PA (to Centre-Director)	1	1
09	Stenographer, Clerk/Typist	2	2
10	Guest House Attendant	1	1
11	Driver	2	2
12	Lab Attendant/Auxiliary Staff	4	4
Mumbai Centre			
01	Centre-Director	1	1
02	Scientist	5	5
03	Engineer	1	1
04	Junior Engineer / Scientific Assistant	5	5
05	AO – I	2	1
06	P.A. (to Centre-Director)	1	0
07	Steno-Typist	1	1
08	Driver	1	1
09	Attendant-cum-Auxiliary Staff	1	1

A: Number of posts approved till 2012-2013
B: Existing manpower as on 31.03.2013.

14. Specializations and research facilities of our Scientists/Engineers

Name, Designation	Specialization	Facility
P. Chaddah Director	Condensed Matter Physics, Low Temperature Physics, Superconductivity	Director and overall in-charge of Head Office and facilities at the Centres
A. Gupta, Centre-Director	Nanostructured materials including nanocrystalline soft magnetic alloys, thin films and multilayers.	In-charge of facilities at Indore Centre
A. K. Sinha, Centre-Director	Experimental nuclear and accelerator physics	In-charge of facilities at Kolkata Centre
V. Siriguri, Centre-Director	Structure and magnetism of strongly correlated electron systems, disordered systems; neutron and high pressure X-ray diffraction	In-charge of facilities at Mumbai Centre
A. M. Awasthi, Scientist-G	Multiferroics. Colossal Dielectrics. Magnetic Superconductors.	Modulated Differential Scanning Calorimeter (-150 °C to 550 °C), Dielectric & Impedance Analyzer (mHz-MHz, 20-300K, RT-800 °C), Thermal Conductivity (5-330K)
P.D. Babu, Scientist-F	Magnetism and magnetic materials, Chemical and Magnetic structures	Focusing Crystal Powder Neutron Diffractometer (FCD), Vibrating Sample Magnetometer (VSM)
Alok Banerjee, Scientist-G	Electron transport and magnetic properties of materials, synchrotron radiation	Ac-susceptibility setup, vibrating sample magnetometer, dielectric measurement setup, SQUID magnetometer.
S. R. Barman, Scientist-F	Surface electronic structure	Photoemission and low energy electron diffraction (LEED) experimental station
G.M. Bhalerao Scientist-D	Nanomaterials, electron and x-ray crystallography techniques	TEM
A. Chakraborty, Scientist-F	Radiation biology	Fluorescent microscope, ultra centrifuge, electrophoresis set up, ultra freezer, CO_2-incubator, Flow Cytometer
Sujoy Chakravorty Scientist-D	Thin film Deposition and Characterization using X-Ray and Neutrons, Atomic Diffusion in Thin Films.	XRD
Souvik Chatterjee Scientist -D	Magnetic investigation of 3d transition metal based intermetallic alloys, phase separated manganites and iron based super conductors.	High Magnetic and Low Temperature facility, X Ray Diffraction
R.J. Choudhary Scientist – E	Thin Films, Pulsed Laser Deposition, Functional Magnetic Materials	PLD, SQUID-VSM
D. Das, Scientist-G	Condensed matter physics, magnetic materials,	Mössbauer spectrometer, positron annihilation spectrometer, Low Temperature High Magnetic Field Facility, XRD, DLTS
S.K. Deshpande, Scientist-F	Dielectric and X-ray characterization of materials	Broadband Dielectric Spectroscopy and X-ray diffractometer

Uday P. Deshpande, Scientist-D	Optical properties, X-ray photoelectron spectroscopy, metal oxide nanomaterials	UV-VIS spectrometer, FTIR spectrometer, X-ray photoelectron spectroscopy.
V. Ganesan, Scientist-H	Low temperature physics, cryogenics and microscopy, ultra low temperature measurement system for T< 1K and also at high magnetic fields	14T PPMS for Resistivity and Heat capacity, Thermoelectric Power, Scanning Probe Microscopy AFM/MFM, Laser Scanning Confocal Optical Microscopy
G. Ghosh, Scientist-E	Soft matter and nanomaterials	Static and dynamic light scattering
S. S. Ghugre, Scientist-G	In-beam gamma ray spectroscopy, nuclear physics	Clover array, radiation detectors and associated nuclear instrumentation, computational laboratory
Dileep Kumar Gupta Scientist –E	Condensed Matter Physics, magnetic ultra thin films and multilayers	In-situ MOKE set up
Mukul Gupta Scientist –E	Thin films and multilayer deposition, study ofsurface, interfaces and depth profiling in thin film multilayers	XRD, SIMS, Soft x-ray absorption and polarization beamline on Indus-2 SR
Shamima Hussain Scientist-D	Thin Film Synthesis and characterisations,Nanomaterials, Photoluminescence	FESEM and the material synthesis facilities
Bhushan Jain Engineer D	Electrical Engineer	
Som Datta Kaushik Engineer – D	Magnetic Materials and magnetic structures	FCD, Cryocooler, Material synthesis
Devendra Kumar, Scientist D	Condensed Matter Physics, Low Temperature Physics	Magnetization measurements by PPMS and MPMS, AC susceptibility setup.
Archana Lakhani Scientist – E	Condensed Matter Physics, Low Temperature Physics, Imaging techniques	Low temperature and High Field Magnetisation.
N.P. Lalla, Scientist-F	Stucturalcharacterisation of materials using XRD and TEM, sysnthesis, phase transformation,quasicrystals and perovskites	TEM facility (with low and high temperature attachments), Powder XRD facility (with low-temperature-90K and high-temperature-1400K attachments).
T. K. Mishra, Engineer F	Mechanical engineer, heat and mass transfer simulations	Mechanical workshop, vacuum systems
Sudip Mukherjee Scientist – D	Strongly correlated electron systems, Nanomagnetism , Impedance spectroscopy	Low temperature resistivity, Material synthesis
G. S. Okram, Scientist/Engineer – E	Low Temperature Thermoelectricity	Dc electrical resistivity and thermoelectric power set up (5-300K).
D. M. Phase, Scientist –G	Synchrotron beamline design, thin films, bilayers and multilayers, low and high energy implantation, surface and interface physics, vacuum technology	PLD, SEM-EDX Beamline for photoelectron spectroscopy at INDUS-1 and MCD on INDS-II
V. Raghavendra Reddy, Scientist-F	Experimental condensed matter physics	Mössbauer Spectroscopy: transmission geometry(7 Tesla, 4.2 1000 K) and conversion electron, thin film x-ray diffraction, MOKE, Ferroelectric loop tracer

R. Raut Scientist – D	Experimental Nuclear Structure	Indian National Gamma Array
R. Rawat, Scientist-F	Magneto-transport and magnetocaloric properties of magnetic materials at low temperature. Microscopic studies of magnetic material at low temperature and magnetic field	Resistivity / magnetoresistance set up (1.5-325 K, 0-8 Tesla), heat capacity set up (3-300 K, 0-8 Tesla), Low temperature high field scanning probe microscope (5-300 K, 0-9 Tesla)
S. Rayaprol Scientist –E	Structure-property correlations in quasi 1D spin-chain systems, novel mixed oxide compounds	FCD, VSM, Material Synthesis lab
A. Saha, Scientist-F	Radiation Chemistry, Macromolecular chemistry	Luminiscence Spectrometer,FTIR spectrometer, Radio-chemistry, micro – Raman, Calorimetry, DLS, UV-VIS-NIR
P. Saravanan, Engineer-F	Electronics and communications Cryogenics	Cryogenic Facilities and Instrumentation
V. G. Sathe, Scientist-F	X-ray and neutron diffraction, EXAFS spectroscopy, synchrotron radiation and data analysis, superconductors and thin films and nano-materials	Raman spectrometer
T. Shripathi, Scientist-H	Crystal growth, electronic structure at surfaces, thin films, oxides, semiconductors, nanostructured materials	Electron spectroscopy for chemical analysis, UV-Vis-NIR, FTIR and Computer Centre.
Neeraj Shukla Scientist – D	Ion Matter Interaction, Low Temperature physics	15 T Cryofree Magneto-resistance Measurement and 7 T SQUID VSM Magnetometer
Kiran Singh Scientist – D	Multiferroics and Magnetic materials	
M. Sudarshan, Scientist-F	Trace elements Studies	Proton Induced X-ray Emission, Energy dispersive X-ray fluorescence spectrometer, atomic absorption spectrometer, Target Preparation facilities - freeze drier, vacuum coating system, pelletiser, vacuum filtration
S. S. Thakur, Engineer-E	Civil engineer	

15. List of staff at UGC-DAE CSR

Sl.No.	Name	Designation
1.	Dr. P. Chaddah	Director
2.	Prof. Ajay Gupta	Centre-Director
3.	Dr. A.K. Sinha	Centre-Director
4.	Dr. Vasudeva Siruguri	Centre-Director
5.	Dr. V. Ganesan	Scientist – H
6.	Dr. T. Shripathi	Scientist – H
7.	Dr. Alok Banerjee	Scientist – G
8.	Dr. D.M. Phase	Scientist – G
9.	Dr. A.M. Awasthi	Scientist – G
10.	Dr. N.P. Lalla	Scientist – F
11.	Dr. S.R. Barman	Scientist – F
12.	Dr. Dipankar Das	Scientist – G
13.	Dr. S. S. Ghughre	Scientist – G
14.	Dr. P.D. Babu	Scientist – F
15.	Dr. Abhijit Saha	Scientist – F
16.	Dr. S.K. Deshpande	Scientist – F
17.	Dr. Vasant Sathe	Scientist – F
18.	Dr. M. Sudarshan	Scientist – F
19.	P. Saravanan	Engineer – F
20.	Tapas Kumar Mishra	Engineer – F
21.	Dr. Rajeev Rawat	Scientist – F
22.	Dr. V.R. Reddy	Scientist – F
23.	Dr. (Mrs.) A. Chakraborty	Scientist – F
24.	Dr. G.S. Okram	Engineer-E/Scientist-E
25.	Dr. Gautam Ghosh	Scientist – E
26.	Sanjay Singh Thakur	Engineer – E
27.	Dr. Mukul Gupta	Scientist – E
28.	Dr. R.J. Chowdhary	Scientist – E
29.	Dr. S. Rayaprol	Scientist – E
30.	Dr. ArchanaLakhani	Scientist – E
31.	Dr. Dileep Kumar Gupta	Scientist – E
32.	Dr. S. Datta Kaushik	Engineer – D
33.	Bhushan Jain	Engineer – D
34.	Dr.G.M. Bhalerao	Scientist-D
35.	Dr. Sujoy Chakravorty	Scientist-D
36.	Dr. Shamima Hussain	Scientist-D
37.	Dr. Devendra Kumar	Scientist-D
38.	Dr. Rajarshi Raut	Scientist-D
39.	U.P. Deshpande	Scientist-D

40.	Dr. Souvik Chatterjee	Scientist-D
41.	Dr. Neeraj Shukla	Scientist-D
42.	Dr. Kiran Singh	Scientist-D
43.	Dr. Sudip Mukherjee	Scientist-D
44.	Dr. J.B.M. Krishna	SA-F/JE-F
45.	Suresh Bhardwaj	SA-F/JE- F
46.	J.V. Joshi	SA-F/JE-F
47.	S.C.Das	SA-F/JE-F
48.	Nandkishore L. Ghodke	SA-F/JE-F
49.	Avinash Wadikar	SA-F/JE-F
50.	Satish R. Potdar	SA-F/JE-F
51.	B.R. Mendole	SA-F
52.	P.V. Rajesh	SA-F/JE-F
53.	Pinaki Das	SA-E/JE-E
54.	M.K. Verma	SA-E/JE-E
55.	N. Vijayakumar	JE-F
56.	Aparna Datta/Basu	SA-E
57.	S. Selvaraj	SA-E
58.	Kranti Kumar Sharma	JE-E
59.	Vinay K. Ahire	JE-D
60.	Mohd. Imran	JE-D
61.	Munshi Venugopal	JE-D
62.	Kaushik Basu	SA-D
63.	Mohan Kumar Gangrade	SA-D
64.	Mukesh Kumar	SA-D
65.	A.K. Rathore	SA-D
66.	Vinod Savaner	SA-C
67.	Jagnmoy Biswas	SA-C
68.	Rakesh Kumar Sah	SA-C
69.	Layanta Behera	SA-C
70.	S.Thilakaraj Kumar	SA-C
71.	C.K Modak	JE-C
72.	Preeti Mahajan/Bhradwaj	JE-D
73.	Anil Gome	JE-D
74.	Sachin Kumar	JE-D
75.	Manoj Kumar	JE-D
76.	B.K. Behra	JE-D
77.	Ms. M. Pal	Technician-H
78.	Rakesh Kumar	Technician-D
79.	Ms. Mahua Kar (Ghosh)	Scientific Assistant-D (Library)
80.	Mrs.Madhulika Sinha	Scientific Assistant-B (Library)
81.	Nitin Patil	Technician – H
82.	Sanjay Srivastava	Technician – F
83.	K. Dey	Technician – H

84.	D.H. Raju	Technician – F
85.	Prabir Kumar Das	Technician – G
86.	M.C. Gupta	Administrative Officer –II
87.	M. K. Chakraborty	Administrative Officer –I (Personnel)
88.	R.P. Chattopadhyay	Administrative Officer-I (Accounts)
89.	Sanjay Kumar Sinha	Administrative Officer-I (Pur. & Stores)
90.	S.S. Narayanan	Administrative Officer –I
91.	Ashish Upadhyay	Administrative Officer – I
92.	Rajeev Bhagwat	Administrative Officer – I
93.	Devendra Singh	Administrative Officer – I
94.	Arjun R. Sanap	PS (to Director)
95.	J. Viswanadha Sarma	PA (to Centre-Director)
96.	A.K. Sen	PA (to Centre-Director)
97.	Mrs. Rugma Menon	Steno-Typist
98.	Utpal Sarkar	Assistant-II
99.	Ramesh Babu	Assistant-I
100.	Mrs. Radhika Tare	Assistant –I
101.	C.L. Dwivedi	Assistant – I
102.	S.C. Chaudhury	Clerk-cum-Typist
103.	T.K. Gangopadhyay	Clerk-cum-Typist
104.	Smt. Sunita Chaudhari	Clerk-Typist
105.	Vishnu Kaushal	Clerk-Typist
106.	Ms. Meenakshi Gupta	Clerk-Typist
107.	Bireswar Pradhan	Guest House Attendent
108.	Ambrose Joseph	Caretaker
109.	Arun Yadav	Driver
110.	Joyanta Dhar	Driver
111.	Khokan Mitra	Driver
112.	Dilip Kaushal	Driver-cum-Aux. Staff
113.	Anil Rao Jadhav	Driver-cum-Aux. Staff
114.	Namdev Suryavanshi	Driver
115.	T.B. Thapa	Helper
116.	Iqbal Hussain	Lab Attendent
117.	Ram Chandra Baniya	Lab Attendent
118.	Kapil Nayak	Lab Attendent
119.	N.K. Reddy	Lab Attendent
120.	Ram Chandra Maity	Lab Attendent
121.	Deepak Yadav	Aux-Staff
122.	Ravindra Bhimgade	Attendent/Aux-Staff I
123.	Prafulla Chandra Das	Aux. Staff
124.	Nitin J. Patil	Attendent/Aux.Staff
125.	B.R.Behra	Attendent
126.	Manoj Kumar Sarwan	Attendent
127.	Sushil Kumar Sharma	Attendent
128.	Prakash Shinde	Attendent

16. Committees

Governing Council

(As on 31st March, 2013)

1	Prof. Ved Prakash, Chairperson, University Grants Commission, New Delhi 110 002	**President**
	Ex-Officio Members:	
2	Prof. S.K. Joshi Chairman, UGC-DAE CSR Governing Board	Member
3	Vice-Chairman, University Grants Commission, New Delhi – 110 002.	Member
4	Dr. R.K. Sinha, Secretary,Department of Atomic Energy, and Chairman, Atomic Energy Commission Government of India, Mumbai – 400 039. or his/her nominee	Member
5	Secretary, University Grants Commission, New Delhi – 110 002.	Member
6	Secretary, Department of Science & Technology, or his/her nominee Government of India, New Delhi 110 016	Member
7	Director General, Council for Scientific & Industrial Research, or his/her nominee Government of India, New Delhi 110 001.	Member
8.	Director General, Indian Council for Medical Research, or his/her nominee New Delhi 110 029	Member

9.	Director General, Indian Council for Agricultural Research, or his/her nominee New Delhi 110 001.	Member
10.	Prof. D.P. Singh Vice-Chancellor, Devi Ahilya University, Indore – 452 001.	Member
11	Dr. Sikhar Basu Director, Bhabha Atomic Research Centre Or his/her nominee Mumbai – 400 085.	Member
12.	Dr. P.D. Gupta, Director, R.R. Centre for Advanced Technology, Indore – 452 013.	Member
13.	Dr. D.K. Shrivastava, Director, Variable Energy Cyclotron Centre, Kolkata – 700 064.	Member
14.	Shri N.K. Sinha Joint Secretary (DL) Ministry of Human Resource Development, New Delhi – 110 001.	Member
15.	Prof. A.K. Sood, Chairman, Scientific Advisory Committee, UGC-DAE CSR, Indian Institute of Science, Bangalore 560012.	Member
16.	Dr. P. Chaddah, Director, UGC-DAE Consortium for Scientific Research, INDORE – 452 001.	Member-Secretary
17	Bureau Head (IUC), UGC	Member

Nominated Members:

Two eminent scientists
(nominated by UGC)

18	Prof. N. Mukunda, Indian Institute of Science, Bangalore 560012.	Member

19.	Prof. E. Krishnakumar, Department of Nuclear and Atomic Physics TIFR, Mumbai 400005	Member
	Member of UGC (nominated by Chairperson, UGC)	
20	Prof. Shivajirao Kadam, Vice-Chancellor, Bharti Vidyapeeth Deemed University, Pune.	Member
	Two Vice-Chancellors of Universities/Directors of Institute of higher learning and research (nominated by President of the Council)	
21.	Prof. P.B. Sharma, Vice-Chencellor, DTU, New Delhi.	Member
22.	Prof. N.S. Gajbhiye Vice-Chancellor, Dr. Hari Singh Gaur University, Sagar.	Member
	One Director of an I.I.T. (nominated by President of the Council)	
23	Prof. Devang V. Khakhar, Director, Indian Institute of Technology, Mumbai	Member
	Two eminent Scientists from Physical Sciences (nominated by President of the Council)	
24	Prof. G.K. Mehta New Delhi	Member
25.	Prof .Lakshman Chaturvedi Vice-Chancellor, GG University, Bilaspur	Member

One Agricultural Scientist
(nominated by President of the Council)

26.	Prof. P.K. Joshi, Director, NAARM, Rajendra Nagar. Hyderabad. (Vacant since 14-Sep-2012)	Member

One Medical Scientist
(nominated by President of the Council)

27.	Prof. T.P. Singh, Distinguished Biotechnology Research Professor AIIMS New Delhi	Member

Scientist
(nominated by MHRD)

28.	Prof. G. Baskaran, Sr. Professor, Institute of Mathematical Sciences, Chennai	Member

Governing Board

(As on 31st March, 2013)

1	Prof. S.K. Joshi JNCAR Vikram Sarabhai Professor NPL, New Delhi	**Chairman**

Ex-Officio Members:

2	Nominee of Secretary, Department of Atomic Energy, Government of India, Mumbai – 400 039.	Member
3	Secretary, University Grants Commission, New Delhi – 110 002.	Member
4.	Prof. D.P. Singh, Vice-Chancellor, Devi Ahilya University, Indore – 452 001.	Member
5.	Dr. Sikhar Basu, Director, Bhabha Atomic Research Centre, Mumbai – 400 085. Or his/her nominee	Member
6.	Dr. P.D.Gupta, Director, R.R. Centre for Advanced Technology, Indore – 452 013.	Member
7.	Dr. D.K.Srivastava, Director, Variable Energy Cyclotron Centre, Kolkata – 700 064.	Member
8.	Shri N.K. Sinha Joint Secretary (DL) Ministry of Human Resource Development, Government of India, New Delhi – 110 001.	Member

9.	Prof. A.K. Sood, Chairman, Scientific Advisory Committee, UGC-DAE CSR, Indian Institute of Science, Bangalore 560012.	Member
10	Dr. P. Chaddah Director, UGC-DAE Consortium for Scientific Research, INDORE – 452 001 .	Member-Secretary
11	Bureau Head (IUC), UGC	Member

Nominated Members:

Member of UGC
(nominated by Chairperson, UGC)

12.	Prof. Shivajrao Kadam Vice-Chancellor BhartiVidyapeeth Deemed University Pune	Member

Two Vice-Chancellors of Universities/Directors of Institute of higher learning and research
(nominated by President of the Council)

13.	Prof. P.B. Sharma, Vice-Chancellor, DTU, New Delhi. (Vacant since 14-Sep-2012)	Member
14	Prof. N.S. Gajbhiye Vice-Chancellor, Dr. Hari Singh Gaur University, Sagar (Vacant since 14-Sep-2012)	Member

One Director of an I.I.T.
(nominated by President of the Council)

15	Prof. Devang V. Khakhar, Director, Indian Institute of Technology Mumbai Mumbai. (Vacant since 14-Sep-2012)	Member

Two eminent Scientists from Physical Science
(nominated by President of the Council)

16.	Prof. G.K. Mehta New Delhi	Member
17.	Prof. Lakshman Chaturvedi Vice-Chancellor, GG University, Bilaspur	Member

One Agricultural Scientist
(nominated by President of the Council)

18.	Prof. P.K. Joshi, Director, NAARM, Rajendra Nagar, Hyderabad. (Vacant since 14-Sep-2012)	Member

One Medical Scientist
(nominated by President of the Council)

19.	Prof. T.P. Singh, Distinguished Biotechnology Research Professor AIIMS New Delhi	Member

Scientist
(nominated by MHRD)

20.	Prof. G. Baskaran, Sr. Professor, Institute of Mathematical Sciences, Chennai	Member

Finance Committee

(As on 31st March, 2013)

1	Prof. S.K. Joshi Chairman, Governing Board, UGC-DAE CSR	**Chairman**

EX- OFFICIO

2.	Secretary, University Grants Commission, New Delhi – 110 002.	Member
3.	Financial Advisor, University Grants Commision, New Delhi – 110 002.	Member
4.	Bureau Head, Plan Budget Section, University Grants Commission, New Delhi – 110 002.	Member
5.	Dr. P. Chaddah, Director, UGC-DAE Consortium for Scientific Research, Indore – 452 001	Member
6.	Prof. Ajay Gupta Centre-Director, UGC-DAE CSR, Indore Centre, Indore – 452 001.	Member
7.	Dr. V. Siruguri, Centre-Director, UGC-DAE CSR, Mumbai Centre, Mumbai – 400 085.	Member
8.	Dr. A.K. Sinha Centre-Director, UGC-DAE CSR, Calcutta Centre, Kolkata	Member
9.	Bureau Head (IUC), UGC	Member

NOMINATED:

Member of GB, UGC-DAE CSR

10.	Dr. P.D. Gupta Director, Raja Ramanna Centre for Advanced Technology, Indore	Member

External Member
(nominated by UGC)

11.	Prof. V.K. Jain Jawaharlal Nehru University, New Delhi	Member
12.	Shri M.C. Gupta, Administrative Officer-II, UGC-DAE CSR, Indore.	Non-Member Secretary

Scientific Advisory Committee

(As on 31st March, 2013)

1.	Prof. Ajay K. Sood, Indian Institute of Science, Bangalore.	**Chairman**
	EX-OFFICIO	
2	Director (or his nominee), Bhabha Atomic Research Centre, MUMBAI – 400 085	Member
3	Director (or his nominee), Variable Energy Cyclotron Centre, Kolkata – 760 064	Member
4	Director (or his nominee) R.R. Centre for Advanced Technology, INDORE – 452 013	Member
5	Dr. A. K. Sinha, Centre-Director, UGC-DAE CSR-Kolkata Centre, Kolkata.	Member
6.	Prof. Ajay Gupta, Centre-Director, UGC-DAE CSR-Indore Centre, INDORE	Member
7.	Dr. V. Siruguri, Centre-Director, UGC-DAE CSR-Mumbai Centre, MUMBAI.	Member
8.	Dr. P. Chaddah, Director, UGC-DAE CSR, Univ. Campus Khandwa Road, INDORE – 452 001.	Member - Secretary
	NOMINATED	
9	Dr. C.S. Sundar, Head, Materials Science Division, Indira Gandhi Centre for Atomic Research, Kalpakkam – 603 102.	Member

10	Prof. E.V. Sampathkumaran, Tata Institute of Fundamental Research, Mumbai – 400 005.	Member
11	Prof. Dhananjai Pandey, School of Materials Science and Technology, Indian Institute of Technology (BHU), Varanasi – 221 005.	Member
12	Prof. S.N. Kaul, Central University, Hyderabad.	Member
13	Dr. V.M. Datar, BARC, Mumbai.	Member
14	Dr. S.K. Deb, RRCAT, Indore	Member